



Durham E-Theses

Metal imido-catalyzed ethylene and 1-hexene dimerization

MESSINIS, ANTONIOS, MARINOU

How to cite:

MESSINIS, ANTONIOS, MARINOU (2013) *Metal imido-catalyzed ethylene and 1-hexene dimerization*, Durham theses, Durham University. Available at Durham E-Theses Online: <http://etheses.dur.ac.uk/9449/>

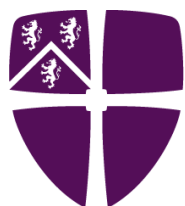
Use policy

The full-text may be used and/or reproduced, and given to third parties in any format or medium, without prior permission or charge, for personal research or study, educational, or not-for-profit purposes provided that:

- a full bibliographic reference is made to the original source
- a [link](#) is made to the metadata record in Durham E-Theses
- the full-text is not changed in any way

The full-text must not be sold in any format or medium without the formal permission of the copyright holders.

Please consult the [full Durham E-Theses policy](#) for further details.



Durham
University

**Metal imido-catalyzed ethylene
and 1-hexene dimerization**

Thesis submitted for the Degree of Doctor of
Philosophy

By

Antonios M. Messinis, M.Sc. (Durham)

Department of Chemistry
Durham University

October 2013

Statement of copyright

This thesis is based on work conducted by the author, in the Department of Chemistry at Durham University, during the period January 2010 to September 2013.

All work described in this thesis is original, unless otherwise acknowledged in the text or in the references. None of this work has been submitted for another degree in this or any other University.

The copyright of this thesis rests with the author. No quotation from it should be published without the author's prior written consent and information derived from it should be acknowledged.

Signed: _____

Date: _____

Antonios M. Messinis

Abstract

This thesis investigates the development of well-defined ethylene and 1-hexene dimerization pro-initiators related to the industrially important SASOL α -olefin dimerization system, which consists of $WCl_6/RNH_2/Et_3N$ activated by $EtAlCl_2$. The role of Et_3N in the SASOL system is to remove HCl generated from the reaction of the amine with WCl_6 , something that is suggestive of the possible *in situ* formation of tungsten imido complexes. To probe the potential role of tungsten imido species, here a range of ethylene and 1-hexene dimerization experiments are described using discrete tungsten, niobium, and tantalum imido complexes in combination with an alkyl aluminum activator (usually $EtAlCl_2$). In order to better understand the possible dimerization mechanisms, selected reactions of the aforementioned imido complexes with alkyl aluminum reagents are also explored.

Chapter 1: the industrial importance of olefins and the olefin oligomerization processes are introduced with emphasis on the SASOL α -olefin dimerization system. Mechanistic aspects of the olefin oligomerization process are outlined giving examples of previously reported ethylene and 1-hexene dimerization systems. The aims of this PhD thesis are summarized.

Chapter 2: the synthesis and structural characterization of a range of tungsten bis(imido) complexes $W(NR)(NR')Cl_2(DME)$ ($R, R' = \text{alkyl or aryl}$) is presented. The activity of such complexes as pro-initiators in the dimerization of ethylene and 1-hexene is detailed and the effects of ethylene pressure, temperature, activator, pro-initiator concentration, pro-initiator:activator ratios, and use of additives explored; pro-initiator structure-catalytic activity correlations are established. Preliminary mechanistic studies of tungsten bis(imido)-mediated dimerization are described.

Chapter 3: tungsten mono(imido) complexes, $W(NR)Cl_4(THF)$ and $[W(NR)Cl_4]_2$ ($R = \text{alkyl or aryl}$), are tested in the dimerization of ethylene and 1-hexene. Studies similar to those in Chapter 2 are described, demonstrating that such mono(imido) complexes are reasonably active and selective ethylene and 1-hexene dimerization pro-initiators. Reactions between the tungsten mono(imido) complexes and alkyl aluminum reagents are detailed, providing insight into the role of the aluminum activator in the dimerization process; these suggest that reduction of the tungsten centre is an important part of the initiation process. Hence, discrete $W(IV)$ and $W(V)$ mono(imido) complexes were tested for olefin dimerization, with the latter being active. The beneficial effect of additives (chloride anions, amines) in catalytic dimerization reaction is demonstrated and their mode of action probed.

Chapter 4: the use of niobium and tantalum imido complexes, $M(NR)Cl_3(DME)$, as pro-initiators is explored. In contrast to their tungsten counterparts these group V imido complexes were able to both polymerize and/or dimerize ethylene, but were inactive towards 1-hexene.

Chapter 5: full experimental details are presented.

Chapter 6: supplementary information including - reactivity of the alkyl aluminum reagents employed for the activation of the pro-initiators; definitions used in the analysis of catalysis test data (TON, etc); and development and validation of methods for the analysis of olefin dimerization products.

Acknowledgements

During my time in Durham I met a multitude of interesting people who have contributed to the work presented herein and I would like to apologize in advance if I have omitted someone.

First I would like to thank my supervisor at Durham University, Dr Phil Dyer whose knowledge of chemistry combined with his experience in teaching, his kindness, gentle nature, and patience set the foundations for this work.

My supervisor in Sasol, Dr Martin Hanton for his help with the ethylene and 1-hexene dimerization experiments along with his industrial chemistry knowledge, organization skills (which hopefully have rubbed off on me), direct attitude, and the great conversations we had during my visits in St. Andrews.

Durham University and Sasol technology UK for financial support (Dr Martin Hanton and Dr Robert Tooze) and everyone in Sasol for creating a wonderful working environment and especially Dr William Gabrielli and Dr David Smith for their practical help and the pleasant conversations.

Special thanks also go to everyone in Lab 101 during these three years for creating a very pleasant working environment: Kate Appleby, Mathew Barker, Simon Beaumont, Ben Coombs, Mathew Gibbins, Eddie Leslie, Li Li, Owen Metters, Pippa Monks, Louise Parkes, Andreas Phanopoulos James Radcliffe, Jack Rowbotham, and Luke Tuxworth. I would also like to thank Prof. Paul Low and everyone in Lab 100 for being great lab neighbours and sharing their sink and chemicals with us.

The NMR service (Dr Alan Kenright, Dr Juan Aguilar, Mr Ian McKeag, and Mrs Catherin Heffernan), the X-ray crystallography service (Dr Andrei Batsanov), the thermal analysis service for DSC data (Mr Douglas Carswell), the Glassblowers (Mr Peter Coyne, Mr Malcolm Richardson, and Mr Aaron Brown) and the engineers and electricians in the mechanical and electrical workshops (Mr Neil Holmes, Mr Omer Ekinoglu) are also warmly acknowledged.

My Tai Ji teacher, Joe Harte for his valuable teaching on refining oneself through the practice and his positive emotional influence and support, as well the rest of my Tai Ji training partners.

I am also thankful to Andreas Pantazatos, Matthias Verbeet, Waika Jik, Kevin Vincent and Hannah Kerr for being great friends and hence indirectly contributing to the creation of the present work.

Additionally, Andreas once said about PhDs: "One must take the decision to start them and then decide to finish them". Hence, I would like to thank Young Zoe (Ue Nam) Liu for helping to make this decision of finishing this work and for her patience and support in the critical last months of writing.

Lastly, I want to thank my father Marinos, my mother Eleftheria, and my brother Yiorgis for obvious reasons, which cannot be outlined only in a few sentences.

Antonios Marinou Messinis

October 2013

Dedication

This work is dedicated to my father, Marinos Messinis.

Table of contents

	Table of abbreviations	i
1	Literature review	1
1.1	Industrial importance of olefins	1
1.2	Commercial importance of the olefin oligomerization process	3
1.2.1	The SHOP process	3
1.2.2	The Fischer-Tropsch process	3
1.3	Industrial homogeneous transition metal olefin oligomerization systems	6
1.3.1	The IFP Dimersol olefin oligomerization system	6
1.3.2	The Goodyear olefin oligomerization system	6
1.3.3	The Sasol olefin oligomerization system.....	8
1.4	Mechanisms of olefin oligomerisation	9
1.4.1	The step-wise addition mechanism (Cossee-Arlman)	9
1.4.2	The Metallacycle mechanism.....	12
1.5	Processes that compete with oligomerization	15
1.5.1	Substrate-oligomer co-dimerization	15
1.5.2	Olefin metathesis.....	16
1.5.3	Olefin isomerization.....	17
1.6	Determining the mechanism of an oligomerization process	18
1.6.1	Isomerization of starting olefin substrate and olefinic products	18
1.6.2	Selectivity of the catalytic oligomerization reaction.....	19
1.6.3	Deuterium labeling experiments.....	19
1.7	A comparison of selected well-defined transition metal-catalyzed homogeneous olefin dimerization systems.....	22
1.7.1	Nickel-, cobalt-, and iron-based olefin dimerization	23
1.7.1.1	Ethylene dimerization using nickel-, cobalt-, and iron-based pro-initiators.....	23
1.7.1.1.1	Nitrogen-based ligands	23
1.7.1.1.1.1	Pyrazole-based ligands.....	23
1.7.1.1.1.2	2-(1-Aryliminoethylidene)pyridine-based ligands (N [^] N)	25
1.7.1.1.1.3	8-Benzoxazolyl- or 8-benzothiazolyl-2-alkylquinoline ligands	27
1.7.1.1.1.4	2-Arylimino-9-phenyl-1,10-phenanthroline ligands	27
1.7.1.1.1.5	Imino-imidazole-chelating ligands.....	28
1.7.1.1.1.6	Tridentate O [^] N [^] X ligands	29
1.7.1.1.2	Phosphorus-containing ligands	30
1.7.1.1.2.1	Bi-dentate P [^] N ligands.....	30
1.7.1.1.2.2	Phosphino-borate ligands	31
1.7.1.1.2.3	Phosphinooxazoline ligands	31
1.7.1.1.3	Summary of the basic characteristics of the nickel-, iron-, and cobalt-based ethylene dimerization systems.....	32

1.7.1.2	Nickel-, cobalt-, and iron-based higher α -olefin dimerization.....	32
1.7.1.2.1	Nickel-based pro-initiators.....	33
1.7.1.2.2	Cobalt- and iron-based pro-initiators.....	34
1.7.2	Palladium- and platinum-catalyzed olefin dimerization.....	36
1.7.3	Olefin dimerization based on titanium and zirconium pro-initiators.....	36
1.7.3.1	Ethylene dimerization mediated by titanium and zirconium systems.....	36
1.7.3.2	Higher α -olefin dimerization mediated by titanium and zirconium systems.....	38
1.7.4	Vanadium-based olefin dimerization systems.....	38
1.7.5	Dimerization of olefins <i>via</i> molybdenum- and tungsten-based pro-initiators.....	39
1.7.5.1	Discovery of tungsten and molybdenum imido-based ethylene dimerization systems..	39
1.7.5.2	Mechanistic aspects of tungsten imido-based ethylene dimerization.....	41
1.8	Objectives of the present work.....	43
1.9	References.....	45
2	Understanding ethylene and 1-hexene dimerization mediated by tungsten bis(imido) pro-initiators.....	48
2.1	Introduction.....	48
2.2	Synthesis of tungsten bis(imido) complexes.....	48
2.2.1	Synthesis of bis(imido) complexes of the type $W(NR)_2Cl_2(DME)$	48
2.2.2	Synthesis of mixed bis(imido) complexes of the type $W(NDipp)(NR)Cl_2(DME)$	49
2.2.2.1	Synthesis of tungsten mixed bis(imido) complexes.....	49
2.2.2.2	Limitations to the synthesis of tungsten mixed bis(imido) complexes.....	49
2.2.3	Synthesis of $W(NDipp)_2Cl_2py_2$ (39) and $W(NDipp)_2Cl_2(PMe_3)$ (40).....	51
2.3	Crystallographic study of complexes $W(NR)_2Cl_2(DME)$ (R = Dipp (27), Tfp (28), Pfp (29), Mes ^F (30), Tpp (31)) and $W(NDipp)(NR)Cl_2(DME)$ (R = ⁱ Pr (32), ^t Bu (33), Mes (34), Tfp (35), Tpp (36), Dnp (37)).....	52
2.3.1	General remarks.....	52
2.3.2	Crystallographic study of symmetric tungsten bis(imido) complexes: $W(NR)_2Cl_2(DME)$ (R = Dipp (27), Tfp (28), Pfp (29), Mes ^F (30), Tpp (31)).....	52
2.3.3	Crystallographic study of tungsten mixed bis(imido) complexes: $W(NDipp)(NR)Cl_2(DME)$ (R = ⁱ Pr (32), ^t Bu (33), Mes (34), Tfp (35), Tpp (36), Dnp (37)).....	54
2.4	Ethylene and 1-hexene dimerization mediated by tungsten bis(imido) pro-initiators	55
2.4.1	Ethylene dimerization mediated by tungsten bis(imido) pro-initiators.....	56
2.4.1.1	Tungsten(VI) bis(imido)-based ethylene dimerization testing (40 bar, 60 °C): effect of the imido ligands on activity and TON.....	56
2.4.1.1.1	Influence of imido ligand steric effects on catalytic activity.....	58
2.4.1.1.2	Effect of electron withdrawing imido ligands on catalytic activity.....	59
2.4.1.1.3	Catalytic potential of bis(alkylimido) tungsten complexes in the dimerization of ethylene.....	59
2.4.1.1.4	Activation of the ethylene dimerization reaction with $MeAlCl_2$ instead of $EtAlCl_2$	60
2.4.1.1.5	Pre-activation of $W(NDipp)(N^tBu)Cl_2(DME)$ (33) in the absence of ethylene.....	60

2.4.1.2	Tungsten(VI) bis(imido) complex-mediated ethylene dimerization (45 bar, 70 °C)	60
2.4.1.2.1	Effect of temperature on the catalytic activity of the tungsten bis(imido) ethylene dimerization systems.....	62
2.4.1.2.2	Ethylene dimerization using $WCl_2(NDipp)(N^iBu)(DME)/EtAlCl_2$ at 50 bar and 80 °C ...	63
2.4.1.2.3	Catalytic ethylene dimerization tests in a 1.2 L autoclave	63
2.4.1.3	Selectivity of the tungsten bis(imido) ethylene dimerization systems	64
2.4.1.4	Tungsten bis(imido)-based ethylene dimerization using lower tungsten loading (5-10 μ mol vs. 20 μ mol).....	66
2.4.1.5	Exploring tungsten(IV)-initiated ethylene dimerization.....	67
2.4.1.6	Mechanistic considerations for tungsten bis(imido)-mediated ethylene dimerization....	67
2.4.1.6.1	Two possible mechanistic pathways available for the tungsten imido/ $EtAlCl_2$ systems	67
2.4.1.6.2	Proposed metallacycle-mediated mechanism for the tungsten imido/15 $EtAlCl_2$ systems	69
2.4.1.6.3	Proposed step-wise addition mechanism for the tungsten imido/15 $EtAlCl_2$ systems...	70
2.4.1.6.4	Comparison of predicted and experimentally-observed products from metallacyclic and step-wise addition oligomerization pathways	71
2.4.1.7	Effect of additives in the bis(imido) tungsten-mediated ethylene dimerization	72
2.4.1.7.1	Effect of Et_3N , Oct_4NCl , and Et_3NHCl on the activity of $W(NDipp)_2Cl_2(DME)$ (27)	73
2.4.1.7.2	Effect of Et_3N , Oct_4NCl , and Et_3NHCl on the selectivity of $W(NDipp)_2Cl_2(DME)$ (27)....	74
2.4.1.7.3	Effect of the imido substituent and type of additive on the catalytic activity and selectivity	75
2.4.1.7.4	Large-scale ethylene dimerization with $W(NDipp)_2Cl_2(DME)$ (27)/2 Oct_4NCl /15 $EtAlCl_2$ or $W(NDipp)(NTpp)Cl_2(DME)$ (36)/2 Oct_4NCl /15 $EtAlCl_2$: attempts to develop a highly active and selective dimerization system.....	76
2.4.2	1-Hexene dimerization mediated by tungsten bis(imido) pro-initiators	77
2.4.2.1	Comments on the activity of the tungsten bis(imido)-based 1-hexene dimerization systems	77
2.4.2.2	Selectivity of the tungsten bis(imido)-based 1-hexene dimerization systems.....	79
2.4.2.3	Examination of the dimerization potential of the system $W(NDipp)_2Cl_2(DME)/15 EtAlCl_2$ with different olefinic substrates	81
2.4.2.4	Study of the effect of $W:EtAlCl_2$ ratio on the dimerization of 1-hexene.....	82
2.4.2.5	Use of various alkyl and hydride sources for the activation of $W(NDipp)_2Cl_2(DME)$ (27)	83
2.4.2.6	Additive effects on the catalytic dimerization of 1-hexene mediated by $W(NDipp)Cl_4(THF)/15 EtAlCl_2$ and $[W(NDipp)Cl_4]_2/15 EtAlCl_2$	84
2.4.2.7	Reactions of $W(NDipp)_2Cl_2(DME)$ (27) with $Me_nAlCl_{(3-n)}$ reagents and catalytic testing of the isolated products in 1-hexene dimerization.....	86
2.5	Future investigations	89
2.6	Chapter Summary	89
2.7	References	90

3	Tungsten mono(imido) complex-mediated ethylene and 1-hexene dimerization .	92
3.1	Introduction.....	92
3.2	Synthesis of tungsten mono(imido) complexes	92
3.2.1	Tungsten(VI) complexes	92
3.2.2	Tungsten(V) complexes	93
3.2.3	Tungsten(IV) complexes	93
3.3	Crystallographic study of complexes $[W(NR)Cl_4]_2$ ($R = Et, ^iPr, Ph^{Me}, Ph^F, Tfp,$ and $Dipp$), $[[W(NDipp)Cl_2]_2(\mu-Cl)_3][Et_4N]$, and $W(NDipp)Cl(H)(PMe_3)_3$	94
3.3.1	Comparison of the structural properties of complexes 48-51	94
3.3.2	Molecular structures of $[[W(NDipp)Cl_2]_2(\mu-Cl)_3][Et_3NH]$ and $W(NDipp)Cl(H)(PMe_3)_3$	96
3.4	Tungsten mono(imido) complexes as pro-initiators for ethylene and 1-hexene dimerization	97
3.4.1	Ethylene dimerization studies	97
3.4.1.1	Ethylene dimerization testing using tungsten(VI) mono(imido) pro-initiators.....	97
3.4.1.1.1	General remarks.....	97
3.4.1.1.2	Effect of the imido substituent on the ethylene dimerization catalytic activity.....	99
3.4.1.1.2.1	Beneficial effect of electron withdrawing imido ligands on catalysis.....	99
3.4.1.1.2.2	Effect of imido ligand steric bulk on the catalytic activity of the mono(imido) tungsten-based dimerization systems	100
3.4.1.1.3	Effect of temperature on ethylene dimerization activities of mono(imido) pro-initiators.....	100
3.4.1.1.4	Effect of imido substituent and reaction conditions on ethylene dimerization selectivity with mono(imido) tungsten-based systems.....	101
3.4.1.1.5	Mechanistic implications of the C_6 fraction composition	102
3.4.1.2	Reactions of $[W(NR)Cl_4]_2$ ($R = Dipp, Et, Tfp$) and $W(NDipp)Cl_4(THF)$ with $R_nAlCl_{(3-n)}$ reagents	102
3.4.1.2.1	Reactions of mono(imido) tungsten complexes with $Et_nAlCl_{(3-n)}$	102
3.4.1.2.2	Reactions of mono(imido) tungsten complexes with Me_3Al	104
3.4.1.2.2.1	Reaction of $[W(NDipp)Cl_4]_2$ with Me_3Al : isolation and characterization of $W(NDipp)Me_3Cl \cdot AlCl_3$ (64).....	104
3.4.1.2.2.2	Reaction of $[W(NDipp)Cl_4]_2$ with excess Me_3Al	105
3.4.1.2.2.3	Reaction of $W(NDipp)Cl_4(THF)$ with excess Me_3Al	106
3.4.1.2.3	Reactions of mono(imido) tungsten complexes with $MeAlCl_2$	107
3.4.1.2.3.1	Reaction of $[W(NDipp)Cl_4]_2$ and $W(NDipp)Cl_4(THF)$ with $MeAlCl_2$	108
3.4.1.2.3.2	Reaction of $[W(NEt)Cl_4]_2$ with six equivalents of $MeAlCl_2$	111
3.4.1.3	Tungsten(IV) mono(imido)-initiated dimerization of ethylene	111
3.4.1.4	Ethylene dimerization initiated by the $[[W(NDipp)Cl_2]_2(\mu-Cl)_3][Et_4N]$ (60)/15 $EtAlCl_2$ system	112
3.4.1.4.1	Rationale for choosing complex 60 as a tungsten(V) pro-initiator and preliminary catalysis results.....	112

3.4.1.4.2	Effect of chloride addition on catalysis with pro-initiator $[\text{W}(\text{N-Dipp})\text{Cl}_2)_2(\mu\text{-Cl})_3][\text{Et}_4\text{N}]$ (60)	114
3.4.1.4.3	Activation of $[\text{W}(\text{NDipp})\text{Cl}_2]_2(\mu\text{-Cl})_3][\text{Et}_4\text{N}]$ (60) with 7.5 equivalents of EtAlCl_2	114
3.4.1.4.4	Activation of $[\text{W}(\text{NDipp})\text{Cl}_2]_2(\mu\text{-Cl})_3][\text{Et}_4\text{N}]$ (60) at high dilution	115
3.4.2	1-Hexene dimerization studies	115
3.4.2.1	Influence of the imido group on the dimerization of 1-hexene using mono(imido) tungsten pro-initiators activated with 15 eq. EtAlCl_2	116
3.4.2.2	Effect of the EtAlCl_2 loading and the presence of THF in the dimerization of 1-hexene	117
3.4.2.3	Activation of $\text{W}(\text{NDipp})\text{Cl}_4(\text{THF})$ and $[\text{W}(\text{NDipp})\text{Cl}_4]_2$ with various alkyl and hydride sources	119
3.4.2.4	Additive effects on the catalytic dimerization of 1-hexene mediated by $\text{W}(\text{NDipp})\text{Cl}_4(\text{THF})/15 \text{EtAlCl}_2$ and $[\text{W}(\text{NDipp})\text{Cl}_4]_2/15 \text{EtAlCl}_2$ systems.....	120
3.4.2.5	Exploring the interactions of mono(imido) tungsten complexes with Et_3N and ammonium chlorides	122
3.4.2.5.1	Reaction of $\text{W}(\text{NDipp})\text{Cl}_4(\text{THF})$ and $[\text{W}(\text{NDipp})\text{Cl}_4]_2$ with Et_3NHCl	122
3.4.2.5.2	Chloride effect on the catalytic activity of the tungsten mono(imido) systems.....	123
3.4.2.5.3	Reaction of $\text{W}(\text{NDipp})\text{Cl}_4(\text{THF})$ (59) , $[\text{W}(\text{NDipp})\text{Cl}_4]_2$ (53) with Et_3N	124
3.5	A proposed mechanism for the mono(imido) tungsten-based dimerization systems ..	125
3.6	Future investigations	127
3.7	Chapter Summary	128
3.8	References	130
4	Exploring ethylene polymerization and ethylene and 1-hexene dimerization with Ta and Nb imido complexes.....	132
4.1	Introduction – Niobium- and tantalum-based olefin oligomerization and polymerization	132
4.1.1	Ethylene dimerization	132
4.1.2	Ethylene trimerization	133
4.1.3	Ethylene polymerization	134
4.1.3.1	Niobium-based ethylene polymerization	134
4.1.3.2	Tantalum-based ethylene polymerization catalysis	135
4.1.4	Difficulties in rationalizing differences in catalytic activity of ethylene polymerization systems.....	137
4.1.5	Niobium and tantalum imido-only ethylene oligomerization systems	138
4.2	Synthesis of niobium and tantalum imido complexes: $\text{M}(\text{NR})\text{Cl}_3(\text{DME})$ ($\text{M} = \text{Nb}$, $\text{R} = \text{Ph}$ (70) , $\text{R} = \text{Mes}$ (71) , $\text{R} = \text{Dipp}$ (72) , $\text{R} = \text{}^t\text{Bu}$ (73) ; $\text{M} = \text{Ta}$, $\text{R} = \text{Ph}$ (74) , $\text{R} = \text{Mes}$ (75) , $\text{R} = \text{Dipp}$ (76) , $\text{R} = \text{}^t\text{Bu}$ (77))	138
4.3	Crystallographic study of $\text{M}(\text{NR})\text{Cl}_3(\text{DME})$ complexes ($\text{M} = \text{Nb}$ and Ta , $\text{R} = \text{Ph}$, Mes , Dipp , $\text{}^t\text{Bu}$)	139

4.3.1	Niobium imido complexes: Nb(NR)Cl ₃ (DME), R = Ph (70), Mes (71), Dipp (72), ^t Bu (73)	139
4.3.2	Tantalum complexes: TaCl ₃ (NR)(DME), R = Ph (74), Mes (75), Dipp (76), ^t Bu (77)...	141
4.4	Niobium and tantalum imido-based oligomerization/polymerization of ethylene and 1-hexene.....	143
4.4.1	General considerations	143
4.4.1.1	Choice of catalytic conditions.....	143
4.4.1.2	Effect of cyclopentadienyl ligands in niobium and tantalum imido-catalyzed ethylene oligomerization/polymerization.....	143
4.4.2	Niobium imido-based ethylene oligomerization and polymerization testing	144
4.4.2.1	General remarks.....	144
4.4.2.2	Simultaneous dimerization and polymerization catalysis by niobium imido pro-initiators	144
4.4.2.3	Effect of the imido substituent on the catalytic activity of niobium imido/EtAlCl ₂ systems	145
4.4.2.4	Dilution effect on the performance of the Nb(NDipp)Cl ₃ (DME)/15 EtAlCl ₂ system	147
4.4.2.5	Niobium imido/EtAlCl ₂ -mediated polymerization: polyethylene analysis	147
4.4.2.6	Mechanistic complexity of the niobium imido/EtAlCl ₂ systems	149
4.4.2.7	Future investigations	151
4.4.3	Tantalum-based ethylene oligomerization	152
4.4.3.1	General remarks.....	152
4.4.3.2	Effect of the imido group on the catalytic activity of the tantalum imido/EtAlCl ₂ systems	153
4.4.3.3	Analysis of the polyethylene produced by the tantalum imido/EtAlCl ₂ systems	153
4.4.3.4	Comparison of the tantalum imido systems with previously reported tantalum-based ethylene oligomerization systems	154
4.4.3.5	Mechanistic considerations for tantalum imido-mediated ethylene oligo-/poly-merization	154
4.4.3.6	Future investigations	155
4.4.4	Dimerization of 1-hexene using tantalum- and niobium-imido/EtAlCl ₂ systems	156
4.4.4.1	General remarks.....	156
4.4.4.2	Niobium and tantalum imido-mediated 1-hexene isomerization: mechanistic implications	157
4.5	Chapter Summary	159
4.6	References	160
5	Experimental details	162
5.1	General details	162
5.2	Synthesis.....	163
5.2.1	Bis-imido tungsten complexes	164
5.2.1.1	W(NDipp) ₂ Cl ₂ (DME) (27) from W(NDipp)Cl ₄ (THF) (59) and DABCO.....	164

5.2.1.2	W(NTfp) ₂ Cl ₂ (DME) (28)	164
5.2.1.3	W(NPfp) ₂ Cl ₂ (DME) (29)	164
5.2.1.4	W(NMes ^F) ₂ Cl ₂ (DME) (30)	165
5.2.1.5	W(NTpp) ₂ Cl ₂ (DME) (31)	165
5.2.1.6	W(NDipp) ₂ Cl ₂ (PMe ₃) (40)	165
5.2.1.7	W(NDipp) ₂ Cl ₂ (py) ₂ (39)	166
5.2.1.8	W(NDipp)(N ^t Bu)Cl ₂ (DME) (33)	166
5.2.1.9	W(NDipp)(NMes)Cl ₂ (DME) (34)	167
5.2.1.10	W(NDipp)(N ⁱ Pr)Cl ₂ (DME) (32)	167
5.2.1.11	W(NDipp)(NTpp)Cl ₂ (DME) (36)	167
5.2.1.12	W(NDipp)(NTfp)Cl ₂ (DME) (35)	168
5.2.1.13	W(NDipp)(NDnp)Cl ₂ (DME) (37)	169
5.2.2	Mono(imido) tungsten complexes	169
5.2.2.1	[W(NTfp)Cl ₄] ₂ (52) and W(NTfp)Cl ₄ (THF) (58)	169
5.2.2.2	W(NDipp)(H)(Cl)(PMe ₃) ₃ (62)	170
5.2.2.3	[[W(NDipp)Cl ₂] ₂ (μ-Cl) ₃][Et ₄ N] (60)	170
5.2.3	Tantalum and niobium imido complexes	170
5.2.3.1	Nb(NMes)Cl ₃ (DME) (71)	170
5.2.3.2	Ta(NMes)Cl ₃ (DME) (75)	171
5.3	Reactions	171
5.3.1	Reactions of aluminum-based reagents	171
5.3.1.1	Reaction of PhNO ₂ with Me ₃ Al	171
5.3.1.2	Reaction of THF with Me ₃ Al	171
5.3.1.3	Reaction of THF with AlCl ₃	171
5.3.1.4	Reaction of DME with Me ₃ Al	172
5.3.1.5	Reaction of PhCl with Me ₃ Al and 1-hexene	172
5.3.1.6	Reaction of PhCl with Et ₃ Al and 1-hexene	172
5.3.1.7	Reaction of PhCl with MeAlCl ₂ and 1-hexene	172
5.3.1.8	Reaction of PhCl with EtAlCl ₂ and 1-hexene	172
5.3.1.9	Reaction of Et ₃ N with AlCl ₃ : formation of Et ₃ N-AlCl ₃	173
5.3.1.10	Reaction of Et ₃ N with EtAlCl ₂ : formation of Et ₃ N-AlEtCl ₂	173
5.3.1.11	Reaction of Et ₃ N with MeAlCl ₂ : formation of Et ₃ N-AlMeCl ₂	173
5.3.1.12	Reaction of [Et ₃ NH]Cl with AlCl ₃ : formation of [Et ₃ NH][AlCl ₄]	173
5.3.1.13	Reaction of [Et ₃ NH]Cl with Me ₃ Al: formation of methane and Et ₃ N-AlMe ₂ Cl	174
5.3.1.14	Reaction of [Et ₃ NH]Cl with Et ₃ Al: formation of ethane and Et ₃ N-AlEt ₂ Cl	174
5.3.1.15	Reaction of [Et ₃ NH]Cl with EtAlCl ₂ : formation of [Et ₃ NH][EtAlCl ₃]	174
5.3.1.16	Reaction of [Et ₃ NH]Cl with MeAlCl ₂ : formation of [Et ₃ NH][MeAlCl ₃]	175
5.3.2	Reactions of mono-imido tungsten complexes	175
5.3.2.1	Reaction of [W(NDipp)Cl ₄] ₂ (53) with 1-hexene	175

5.3.2.2	Reaction of $W(NDipp)Cl_4(THF)$ (59) or $[W(NDipp)Cl_4]_2$ (53) with $[Et_3NH]Cl$: formation of $[W(NDipp)Cl_5][Et_3NH]$ (66)	176
5.3.2.3	Reaction of $[W(NDipp)Cl_4]_2$ (53) with Et_3Al	176
5.3.2.4	Reaction of $[W(NDipp)Cl_4]_2$ (53) with $MeAlCl_2$	176
5.3.2.5	Reaction of $W(NDipp)Cl_4(THF)$ (59) with one equivalent of $MeAlCl_2$	177
5.3.2.6	Reaction of $[W(NEt)Cl_4]_2$ (48) with $MeAlCl_2$	177
5.3.2.7	Reaction of $[W(NTfp)Cl_4]_2$ (52) with $MeAlCl_2$	177
5.3.2.8	Reaction of $[W(NDipp)Cl_4]_2$ (59) with Me_3Al : formation of $W(NDipp)Me_3Cl \cdot AlCl_3$ (64) .	177
5.3.2.9	Reaction of $W(NDipp)Me_3Cl \cdot AlCl_3$ (64) with Et_4NCl : formation of $W(NDipp)Me_3Cl$ and $[Et_4N][AlCl_4]$	178
5.3.2.10	Reaction of $W(NDipp)Cl_4(THF)$ (59) with Me_3Al : formation of $W(NDipp)Me_3Cl$	178
5.3.2.11	Reaction of $[W(NEt)Cl_4]_2$ (48) with Me_3Al : formation of $W(NEt)Me_3Cl \cdot AlCl_3$	179
5.3.2.12	Reaction of $[W(NTfp)Cl_4]_2$ (52) with Me_3Al : formation of $W(NTfp)Me_3Cl \cdot AlCl_3$	179
5.3.2.13	Reaction of $[W(NDipp)Cl_4]_2$ (53) or $W(NDipp)Cl_4(THF)$ (59) with Et_3N	179
5.3.2.14	Reaction of $[W(NDipp)Cl_4]_2$ (53) with $W(NDipp)Cl_2(PMe_3)_3$ (61)	180
5.3.3	Reactions of bis-imido tungsten complexes.....	180
5.3.3.1	Reaction of $W(NDipp)_2Cl_2(DME)$ (27) with Et_3N	180
5.3.3.2	Conversion of $W(NDipp)(NTfp)Cl_2(DME)$ (35) to a mixture of $W(NDipp)(NTfp)Cl_2(DME)$ (35), $W(NDipp)_2Cl_2(DME)$ (27) and $W(NTfp)_2Cl_2(DME)$ (28).....	180
5.3.3.3	Reaction of $W(NDipp)_2Cl_2(DME)$ (27) with one equivalent of Me_2AlCl : Synthesis of $W(NDipp)_2Me_2$ (44) and $[AlCl_2(DME)_2][AlCl_4]$ (43)	180
5.3.3.4	Reaction of $W(NDipp)_2Cl_2(DME)$ (27) with two equivalents of Me_3Al : Synthesis of $W(NDipp)_2Me_2 \cdot AlClMe_2$ (45).....	181
5.3.3.5	Reaction of $W(NDipp)_2Cl_2(DME)$ (27) with two equivalents of $MeAlCl_2$: Synthesis of $W(NDipp)_2Me_2 \cdot AlCl_3$ (47) and $[AlCl_2(DME)_2][AlCl_4]$ (43) .	181
5.3.3.6	Reaction of $W(NDipp)_2Me_2 \cdot AlClMe_2$ (45) with one equivalent of Et_4NCl : formation of $W(NDipp)_2Me_2$ (44)	182
5.4	Attempted syntheses.....	182
5.4.1	$W(NPh^F)(N^tBu)Cl_2(DME)$	182
5.4.2	$W(NDipp)(NMe_s^F)Cl_2(DME)$	182
5.4.3	$W(NDipp)(NPh^F)Cl_2(DME)$	182
5.4.4	$W(NPh)(N^tBu)Cl_2(DME)$	183
5.4.5	$W(NDipp)(NPh)Cl_2(DME)$	183
5.4.6	$W(NPh)_2Cl_2(DME)$	183
5.4.7	$W(NDipp)(NTtp)Cl_2(DME)$	184
5.5	Catalysis protocols	185
5.5.1	Catalysis protocol: 1-hexene dimerisation	185
5.5.2	Catalysis protocol: 1-hexene dimerisation in NMR tubes	185
5.5.3	Catalysis protocol: ethylene	186
5.6	References	186

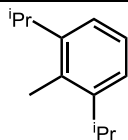
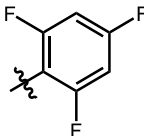
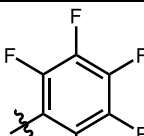
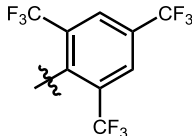
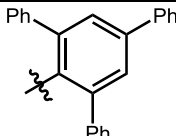
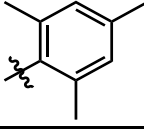
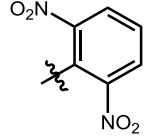
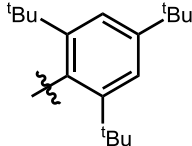
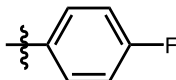
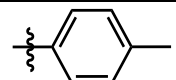
6	Appendices	188
6.1	Appendix I: exploring the interaction of $R_nAlCl_{(3-n)}$ reagents with DME, THF, and Et_3NHCl	188
6.1.1	NMR spectroscopic data for Me_3Al , Et_3Al , Me_2AlCl , $MeAlCl_2$, and $EtAlCl_2$ in C_6D_6	188
6.1.2	Reactions of $R_nAlCl_{(3-n)}$ reagents with DME and THF.....	189
6.1.3	Reactions of aluminum-containing reagents with Et_3NHCl	193
6.2	Appendix II: definitions used in the analysis of catalysis test data	194
6.2.1	Definition of the performance parameters for catalytic ethylene dimerization	195
6.2.1.1	Productivity (TON) and activity.....	195
6.2.1.2	Percentage of liquid and polymer fractions in the catalysis products	195
6.2.1.3	Percentage of 1-alkene in corresponding alkene product fraction.....	196
6.2.1.4	Determination of weight and mole percentage product compositions	196
6.2.1.5	Hexenes fraction branching selectivity.....	196
6.2.2	Definition of the performance parameters for catalytic 1-hexene dimerization.....	197
6.2.2.1	Productivity (TON) and activity for the dimers fraction.....	197
6.2.2.2	Productivity and activity.....	198
6.2.2.3	Determination of weight and mole percentage product compositions	198
6.2.2.4	Percent Conversion (Conv%).....	199
6.2.2.5	Percentage Substrate Isomerized (Isom%)	199
6.2.2.6	Branching selectivity in the dimer fraction.....	199
6.3	Appendix III: analysis of olefin dimerization products: analytical method validation	200
6.3.1	Analysis of olefinic hydrocarbons using gas chromatography	200
6.3.1.1	Use of the analyte's FW as its response factor.....	201
6.3.1.2	Determination of the relative response factors <i>via</i> a calibration curve.	203
6.3.2	Evaluation of the quantification errors resulting from 1-hexene evaporation.....	206
6.3.3	Gas chromatographic analysis of ethylene dimerization products.....	207
6.3.4	NMR spectroscopic analysis of 1-hexene dimerization products	207
6.4	Appendix IV: crystallographic data.....	214
6.5	Appendix V: numbering scheme for compounds referred to in the text	221
6.6	References	224

Table of Abbreviations

General abbreviations

Bu = ⁿbutyl
 Cp = cyclopentadienyl
 Cp* = pentamethylcyclopentadienyl
 DABCO = 1,4-Diazabicyclo[2.2.2]octane
 DCM = Dichloromethane
 DFT = Density functional theory
 DME = 1,2-Dimethoxyethane
 dmpe = 1,2-Bis(dimethylphosphino)ethane
 DSC = Differential scanning calorimetry
 EASQ = Ethylaluminum sesquichloride
 Et = Ethyl
 GC = Gas chromatography
 GPC = Gel Permeation Chromatography
 HDLPE = High density linear polyethylene
 HP-LDPE = High pressure low density polyethylene
 LLDPE = Linear low density polyethylene
 Me = Methyl
 NMR = Nuclear magnetic resonance
 Oct = n-octyl
 PE = Polyethylene
 py = pyridine
 RedAl = [Na][Al(OCH₂CH₂OCH₃)₂(H)₂]
 THF = Tetrahydrofuran
 TM = Transition metal
 TMS = Trimethyl silyl
 TON = Turnover number
 Tp = *Tris*(pyrazolyl)borate

Abbreviations of imido ligand substituents

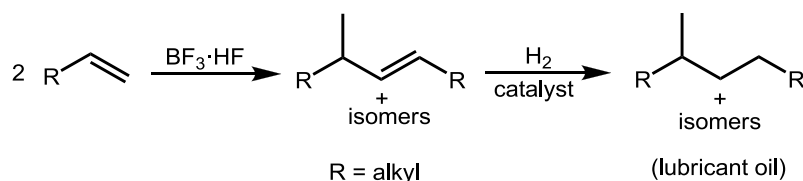
Ph	Phenyl
Dipp	
Tfp	
Pfp	
Mes ^F	
Tpp	
ⁱ Pr	Isopropyl
^t Bu	<i>Tert</i> -butyl
Mes	
Dnp	
Ttbp	
Ph ^F	
Ph ^{Me}	

1 Literature review

In the present work the catalytic dimerization of ethylene and 1-hexene using pre-formed tungsten, tantalum, and niobium imido complexes as pro-initiators is explored. In order to establish the rationale behind and the context of the work described in this thesis, the following chapter outlines the commercial importance of olefin dimerization catalysis and of the resulting products.

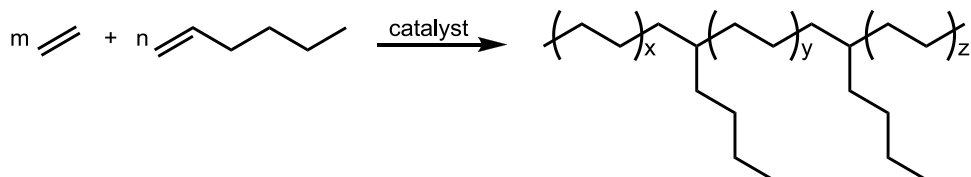
1.1 Industrial importance of olefins

Olefins and especially α -olefins are compounds of significant industrial importance due to their synthetic versatility and their applicability in materials' synthesis. In particular, olefins can be converted into various products such as synthetic lubricants, plasticizer alcohols, detergent alcohols, and synthetic fatty acids.^{1,2} For example, the oligomerization of C_6 - C_{12} α -olefins over an acid catalyst such as $BF_3 \cdot HF$ yields heavier olefins that, after hydrogenation, form high quality lubricants (Scheme 1.1).³ These lubricants can be used in high performance automotive and diesel crankcase applications, gear and axle grease bases, hydraulic fluids, and heat transfer media.



Scheme 1.1 Synthesis of lubricant oils from α -olefins.³

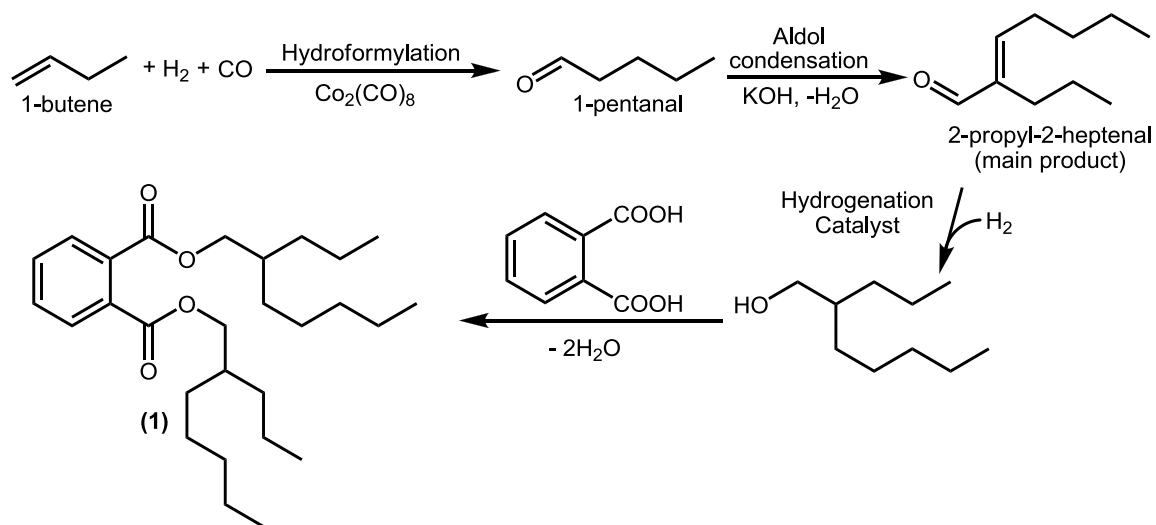
Additionally, olefins such as 1-butene, 1-hexene, 1-octene, and 1-decene are widely used as co-monomers in polymerization reactions. Incorporation of the co-monomer unit in the polymer chain results in polymeric macromolecules with short side chains (Scheme 1.2).⁴ The presence of side chains in the polymer macromolecules prohibits their effective packing, which in turn affects the physical properties of the produced co-polymer. For example, co-polymerization of ethylene with 1-hexene results in polymers with a lower average molecular weight, lower density, lower melting point, and lower crystallinity compared to homopolymeric polyethylene.⁴ The synthesized co-polymers can be used as adhesives, compatibilizers, or additives to other polymeric materials.⁴



Scheme 1.2 The copolymerization of ethylene with 1-hexene⁴

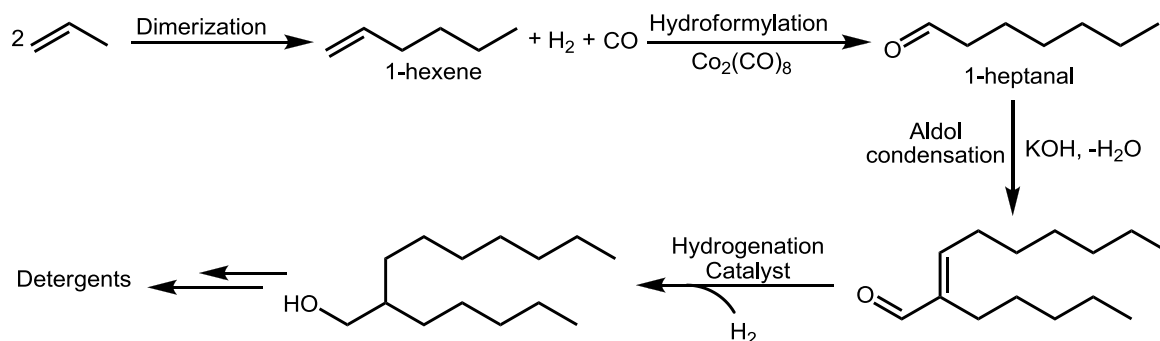
As already stated, olefins are important starting materials for the synthesis of plasticizer and detergent alcohols. For example, 1-butene is converted into 1-pentanal *via* a hydroformylation reaction using $Co_2(CO)_8$ as the pro-catalyst (Scheme 1.3).⁵ An aldol condensation of the resulting 1-pentanal over

KOH results in the formation of 2-propyl-2-heptenal as the major product, which is further hydrogenated to the desired plasticizer alcohol (2-propyl-2-heptanol). The resulting alcohol can then be converted to the desired plasticizer *via* an esterification reaction with phthalic acid.



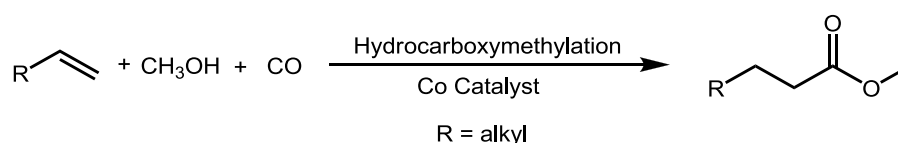
Scheme 1.3 Synthesis of plasticizer 1 from 1-butene.⁵

Similarly, detergent alcohols can be synthesized from the dimerization of propene to 1-hexene followed by hydroformylation to yield 1-heptanal (Scheme 1.4). Furthermore, 1-heptanal is converted to 2-pentyl-2-nonenal *via* a self-aldol condensation. Hydrogenation of 2-pentyl-2-nonenal yields the desired nonanol derivative.⁵



Scheme 1.4 Synthesis of detergent alcohols from 1-propene.⁵

From the chemistry described in Scheme 1.3 and Scheme 1.4, it is evident that olefins can be the starting materials for the synthesis of fatty acids, since the aldehydes produced by hydroformylation can be oxidized to their corresponding carboxylic acids. Nevertheless, it is also possible to synthesize the fatty acid methylesters directly from olefins through hydrocarboxymethylation (also known as methoxycarbonylation), a process analogous to hydroformylation (Scheme 1.5).^{6,7}



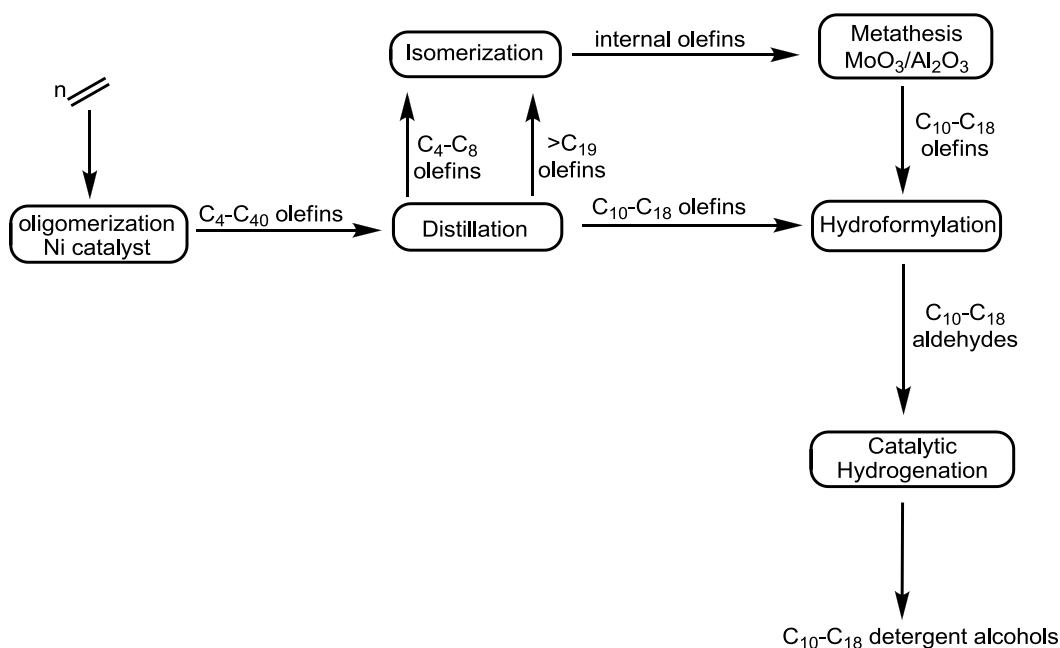
Scheme 1.5 The hydrocarboxymethylation process.⁶

1.2 Commercial importance of the olefin oligomerization process

The importance of the olefin oligomerization process becomes evident by considering that there are several industrial processes that produce mixtures of olefins, with a high C₂-C₄ olefinic content, from various low cost starting materials. These, C₂-C₄ olefins can be further oligomerized to afford more valuable higher olefins. A summary of the most important industrial processes using this type of oligomerisation strategy is given below.

1.2.1 The SHOP process

Oligomerization is the first step in the Shell Higher Olefins Process (SHOP) in which ethene is converted into linear α -olefins (LAOs) using a nickel catalyst (see also section 1.7.1), Scheme 1.6.^{1,8} The result is a mixture of C₄-C₄₀ α -olefins (with a Schulz-Flory-type distribution⁹), which is fractionated to give C₄-C₈, C₁₀-C₁₈, and >C₁₉ fractions. The olefins isolated from the middle C₁₀-C₁₈ fraction are used as starting materials for the synthesis of various other products as described in section 1.1. The heavier and lighter fractions are isomerized towards internal alkenes, which are then converted to a statistical mixture of linear C₁₀-C₁₈ internal alkenes *via* a catalytic metathesis reaction over MoO₃/Al₂O₃. These latter olefins can be used as starting materials for the manufacture of detergent alcohols or alkylates.

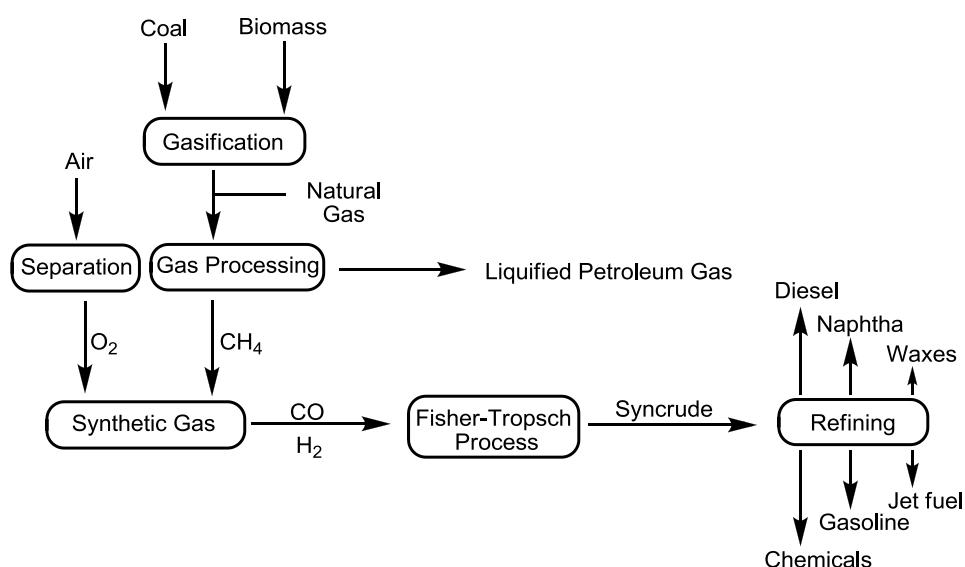


Scheme 1.6 The Shell Higher Olefins Process (SHOP).⁸

1.2.2 The Fischer-Tropsch process

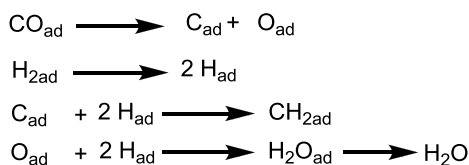
The Fischer-Tropsch process is industrially important since transportation fuels (high energy density/unit volume) are currently produced mainly from the refining of crude oil. Since oil deposits are finite (peak oil production estimated to be 2020¹⁰), other carbon sources must be considered. Amongst the most

important alternatives are natural gas, coal, and biomass. Arguably, natural gas, a gas mixture consisting of mainly methane, is potentially the most important of these feedstocks, not only due to its diverse uses (power generation, domestic use, methanol, and syngas manufacture *via* steam-methane reforming (SMR), *etc.*), but also due to its vast deposits in nature.^{11,12} It is estimated that the amount of natural gas stored around the globe amounts to 156 trillion m³.^{11,12} Nevertheless, only 20% of this amount can be used directly as a gas, use being limited, in part, by issues surrounding its transfer *via* pipelines. In order to circumvent this problem, processes that convert natural gas to liquid fuels (physical compression to liquefied natural gas or chemical transformation to liquid compounds) are necessary. Ultimately, the same technologies can be applied to coal and biomass since they can be converted to methane *via* a gasification process.^{11,12} The resulting methane can then be converted to a mixture of carbon monoxide and hydrogen that is known as synthetic gas (syngas). In turn, syngas is the starting material of the Fischer-Tropsch process, which converts it to “syncrude”, a mixture of organic compounds similar to crude oil.^{11,12} These processes are summarized in Scheme 1.7.



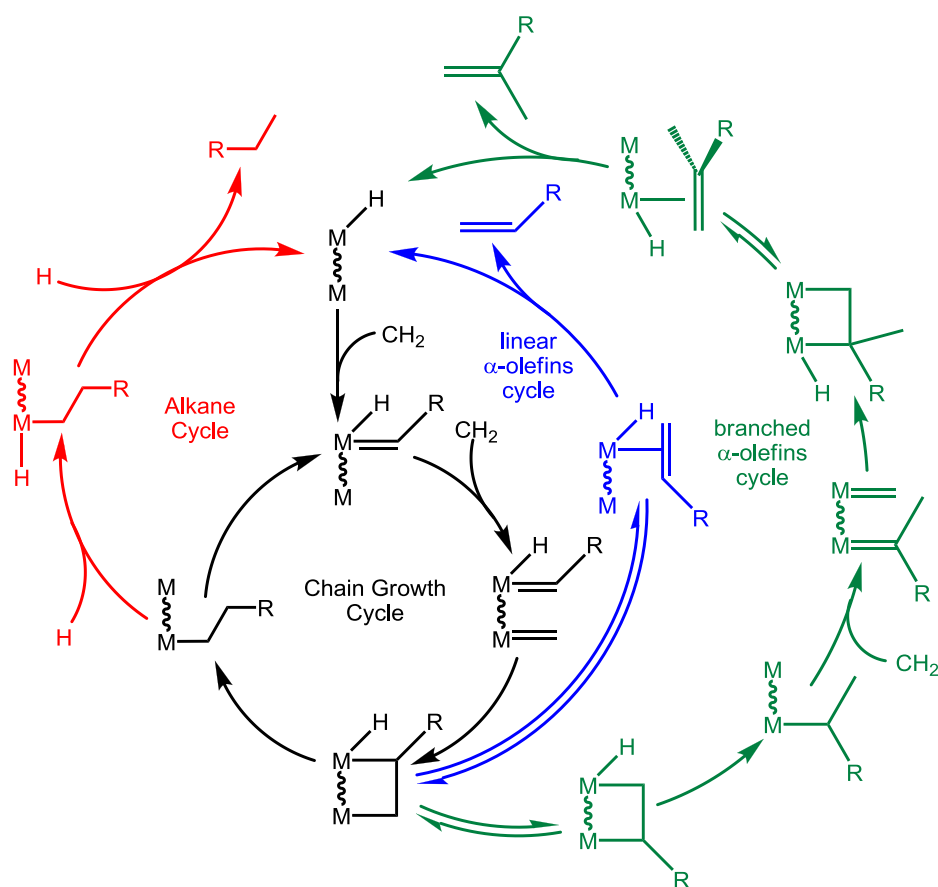
Scheme 1.7 Industrial processes for the conversion of natural gas, coal or biomass to liquid hydrocarbons.^{11,12}

The products of the Fischer-Tropsch process are gaseous C₂-C₄ olefins (25% of the total syncrude production), heavier olefins, paraffins, waxes and a small amount of oxygenates (aldehydes, alcohols, *etc.*).¹² The possible mechanisms by which these products are formed are outlined in Scheme 1.8, and start from adsorption of CO and H₂ on the catalyst's active centers, which react to yield surface-bound CH_{2ad} and H_{ad} moieties.



Scheme 1.8 Formation of surface-bound CH_{2ad} species during the Fischer-Tropsch process.¹²

Subsequently, the adsorbed $\text{CH}_{2\text{ad}}$ species participate in various insertions and α - and β -hydride elimination reactions forming alkanes, linear α -olefins, and branched α -olefins, as described in the catalytic cycle in Scheme 1.9.¹³



Scheme 1.9 Proposed Fischer-Tropsch mechanism for the formation of higher hydrocarbons.¹³

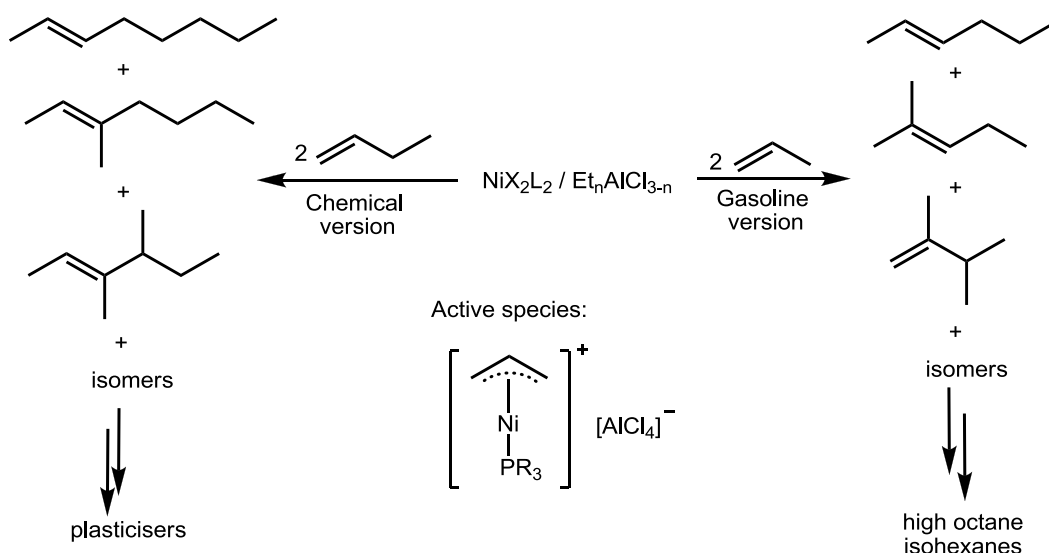
Although the resulting “syncrude” from Fischer-Tropsch resembles crude oil, it can not be refined in the same way due to its quite different chemical composition and, hence physical properties, which make purification very inefficient, both economically and in terms of waste production.¹² Thus, processes that are able to convert syncrude into more useful products are necessary. Since linear α -olefins are one of the main components of syncrude, it is evident that an efficient olefin dimerization/oligomerization process would integrate very effectively with the Fischer-Tropsch process. For example, utilizing the gaseous C_2 - C_4 olefins produced (~25% of the total syncrude) in an oligomerization process will afford liquid products that can be used in diesel or gasoline fuel. In addition, the quality of the produced fuel can be improved by controlling the degree of chain branching of the oligomerization products. For example, in diesel fuel a high cetane number is desired. The cetane number, which is a measure of the speed at which a compound will burn inside an engine, increases by decreasing the degree of branching of the olefin.¹² On the other hand for production of high quality gasoline, a high octane number (measure of a fuel’s auto-ignition characteristics) is desired. Internal olefins with a high degree of branching have higher octane numbers.¹²

1.3 Industrial homogeneous transition metal olefin oligomerization systems

From the discussions presented in sections 1.1 and 1.2 it is evident that the olefin oligomerization process is important, not only for synthesizing useful materials (section 1.1), but also for converting the products of various industrial processes into useful compounds. In this section three characteristic industrial olefin oligomerization systems are described.

1.3.1 The IFP Dimersol olefin oligomerization system

The IFP (Institute Française du Pétrole) Dimersol catalytic system uses nickel organometallic complexes of the type NiX_2L_2 , where X is a halide (e.g. Cl) and L is a phosphine such as P^iPr_3 .^{14,15} When these nickel complexes are combined with a chloro(ethyl)aluminum compound they become dimerization-active. There are two versions of the Dimersol process (Scheme 1.10): the gasoline version, where propylene is dimerized to a mixture of high octane isohexenes, and the chemical version, where 1-butenes are converted to isooctenes that can be used in the manufacture of plasticizers. The catalytically active species in both processes are thought to be cationic nickel phosphine species as illustrated in Scheme 1.10.^{14,15} The ionic character of the initiator led to the development of the related Difasol system, which uses ionic liquids as the reaction medium in which the active species were found to be more stable, hence increasing the efficiency of the process. In addition, the isolation of the oligomerization products is easier since they are immiscible with the ionic liquid phase.^{14,15}



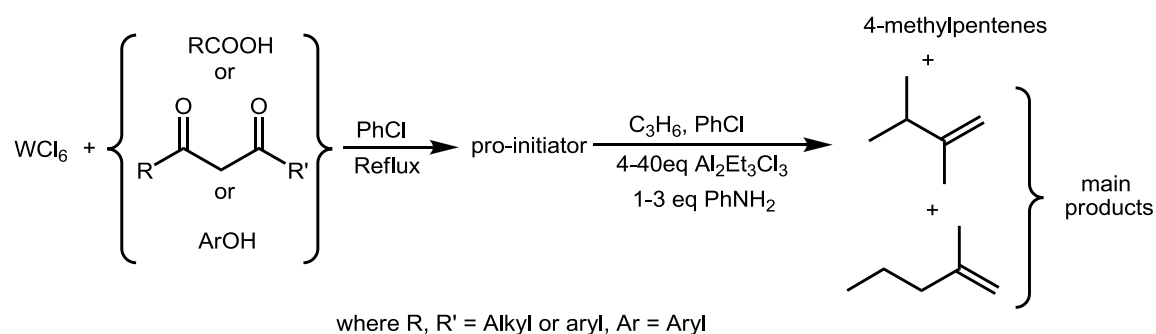
Scheme 1.10 The Dimersol dimerization system.^{14,15}

1.3.2 The Goodyear olefin oligomerization system

In 1974 the Goodyear Company conducted extensive research into olefin dimerization processes. Most notably, they used a mixture of WCl_6 , an amine, an oxo compound (e.g. a carboxylic acid, a phenolic compound or a diketone), and an organometallic aluminum reagent as the catalytic system. Various

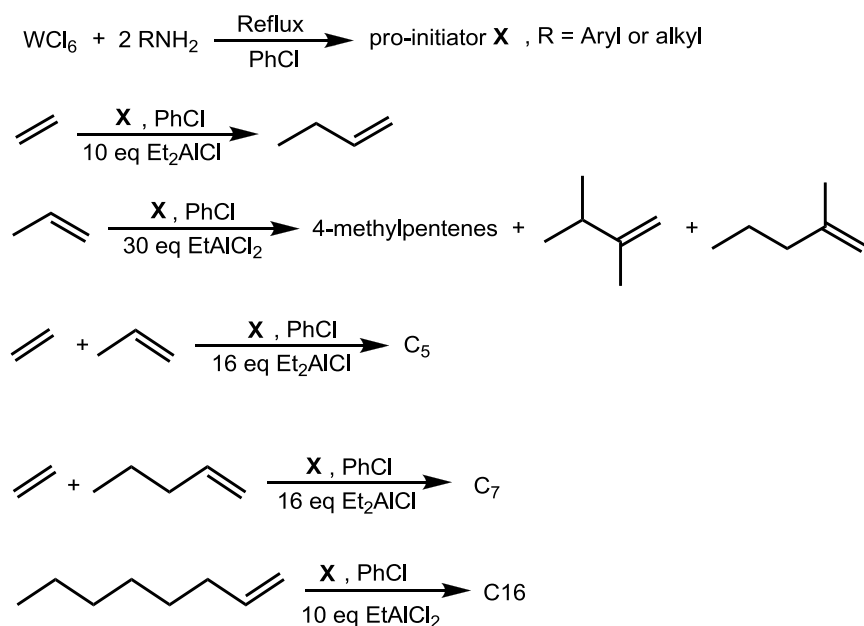
reaction conditions were tested with different olefins, oxo compounds, amines, aluminum reagents, reaction temperatures, and order of mixing or reacting the catalytic systems' components.¹⁶⁻²¹ A short summary of these experiments follows.

During initial studies, WCl_6 was pre-reacted with one of the various different oxo compounds at reflux in chlorobenzene.¹⁶⁻²¹ The product of this reaction was then treated with 10 equivalents of $Al_2Et_3Cl_3$ and 2 equivalents of aniline, which gave a system active for dimerizing propylene in chlorobenzene. Subsequently, various other amines and aluminum reagents were also found to be viable, with reaction temperatures between 30 and 60 °C being commonly employed. The general Goodyear dimerization process is summarized in Scheme 1.11, with the main products being 2,3-dimethyl-1-butene and 2-methyl-1-hexene.¹⁶⁻²¹ It was also determined that propylene conversion and the selectivity towards dimerization in these reactions strongly depends on the nature of the oxo compound, which was used to pre-react with the WCl_6 during initiator preparation.¹⁶⁻²¹



Scheme 1.11 The WCl_6 /oxo compound Goodyear olefin dimerization system.¹⁶⁻²¹

Although in the initial experiments both an oxo compound and an amine were used in the formation of the catalytic systems, as described in Scheme 1.11, in subsequent studies it was found that the oxo compound could be omitted. In this alternative approach, WCl_6 was pre-reacted with the amine to form a pro-initiator, which could be activated on addition of an alkylaluminum chloride compound. Scheme 1.12 describes the dimerization reactions of various olefins over the "oxo"-free catalytic systems activated with various ethylaluminumchloride reagents.¹⁶⁻²¹

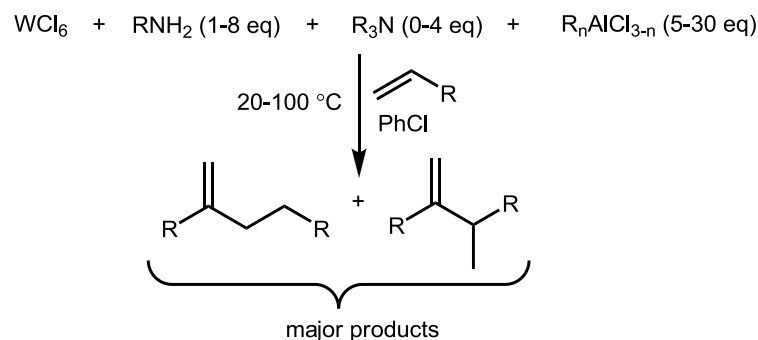


Scheme 1.12 The WCl_6 /amine Goodyear olefin dimerization system.¹⁶⁻²¹

The conversion and selectivity of each of the systems (Scheme 1.12) depends on the type of amine and olefin used. The results obtained using the WCl_6 /amine/ $\text{R}_n\text{AlCl}_{3-n}$ systems were more promising in terms of their selectivity towards dimerization, olefin conversion, and activity, compared to the results obtained from the systems with the oxygen-containing additives, or those in which the amine was not pre-reacted with the WCl_6 . It must be highlighted that pre-reacting the amine with the WCl_6 is a key step in achieving high catalytic activities, something that suggests that the initiator is formed *in situ* from the reaction of WCl_6 with the amine.¹⁶⁻²¹ This proposal is also supported by further research conducted by the Exxon Chemicals Inc., where evolution of HCl was observed during the pre-reaction process of WCl_6 with aniline, as described in the next section.²²

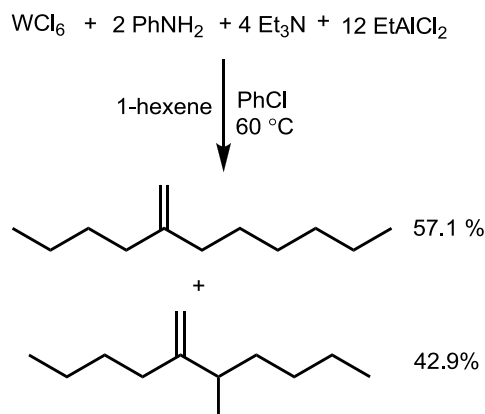
1.3.3 The Sasol olefin oligomerization system

In 1991 an improved version of the Goodyear olefin oligomerization system was patented by Exxon, in which the HCl evolved following treatment of WCl_6 with aniline is removed from the reaction mixture by means of an inert gas stream sparge. This methodology has the benefit that a much smaller quantity of alkylaluminum chloride reagent is required to initiate the dimerization process.²² This, subsequently led Sasol to improve this system further by adding a base, such as triethylamine, to remove the hydrogen chloride evolved during the formation of the initiator. Hence, in this modification, the catalyst is formed *in situ* from reaction of WCl_6 and, preferably, an amine although a variety of other compounds can also be employed (carboxylic acids, diketones, alcohols, N^-N or N^-O bidentate amines, etc.) in the presence of the base, followed by addition of an alkyl- or alkoxy-aluminum chloride co-initiator.²³ Each of these modified Sasol systems was found to be active for the dimerization of C_2 - C_7 α -olefins. However, systems of the type $\text{WCl}_6/\text{RNH}_2/\text{R}_3\text{N}/\text{R}_n\text{AlCl}_{3-n}$ (Scheme 1.13) stand out in terms of activity and selectivity towards the monomethyl-branched dimer and in achieving the best olefin conversion.^{23,24}



Scheme 1.13 *The WCl₆/amine Sasol olefin dimerization system.*^{23,24}

A characteristic example of olefin dimerization using a Sasol system of the type WCl₆/RNH₂/R₃N/R_nAlCl_{3-n} is presented in Scheme 1.14. Starting with 1-hexene the system is selective for the formation of mono- and di-methyl-branched dimers with a conversion of 1-hexene of 43.2%.^{21,22} The selectivity towards the dimer fraction is 95.3%, while the selectivity for the mono-methyl branched alkenes is 57.1% and for the di-methyl branched alkenes 42.9%.^{23,24}



Scheme 1.14 *The dimerization of 1-hexene over WCl₆/PhNH₂/EtAlCl₂.*^{23,24}

1.4 Mechanisms of olefin oligomerisation

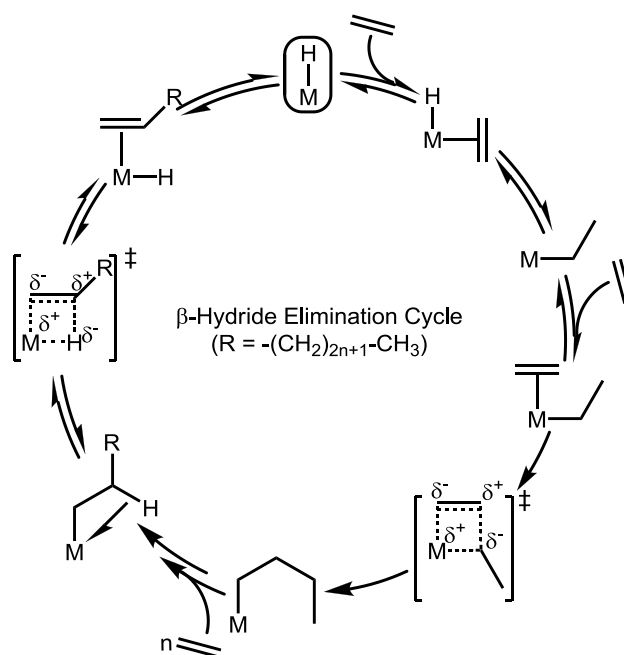
In this section the two most common olefin oligomerization mechanisms will be examined. In addition, other considerations relevant to the oligomerization mechanisms will be discussed. These include the potentially competitive olefin metathesis and isomerization processes, together with methods employed in order to probe the nature of the mechanism operative for a specific oligomerization system.

1.4.1 The step-wise addition mechanism (Cossee-Arlman)

When a step-wise addition (or Cossee-Arlman-type) mechanism is operative for an oligomerization process, the organic products can be dimers, oligomers, or even polymers. The catalytically active species in step-wise addition processes can be either a metal hydride (Scheme 1.15) or a metal alkyl species (Scheme 1.16), something that leads to two different mechanistic pathways.²⁵⁻²⁷ Below, each of

these mechanisms will be examined in terms of the oligomerization of ethylene; note that the same mechanisms can also be potentially operative for the dimerization of higher olefins.

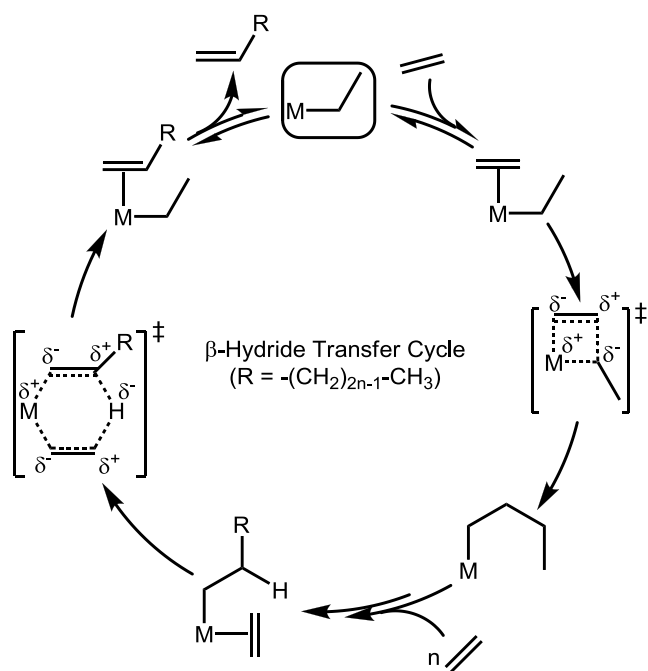
Starting from a metal-hydride, oligomerisation proceeds *via* initial olefin coordination to the metal, followed by migratory insertion, forming a metal alkyl, and subsequent chain propagation through coordination, followed by coordination and migratory insertion of the olefin into the metal-carbon bond (Scheme 1.15).²⁵⁻²⁷ The transition state for the chain propagation step is a polar four-centered intermediate with a positive charge on the metal. After n olefin molecules have reacted, β -hydride elimination occurs through a polar four-centered transition state, which releases the dimer, oligomer or polymer, and regenerates the metal hydride.



Scheme 1.15 Mechanism for the oligomerization of olefins initiated via a metal hydride species.²⁵⁻²⁷

When a metal alkyl is the catalytically active species/resting state, the process by which chain propagation takes place is largely identical to that described above for a metal hydride-based system. However, in contrast to the metal hydride mechanism, in the metal alkyl case chain termination occurs with a β -hydride transfer process from the oligomer chain to the monomer, *via* a polar six-membered transition state as described in Scheme 1.16.²⁵⁻²⁷

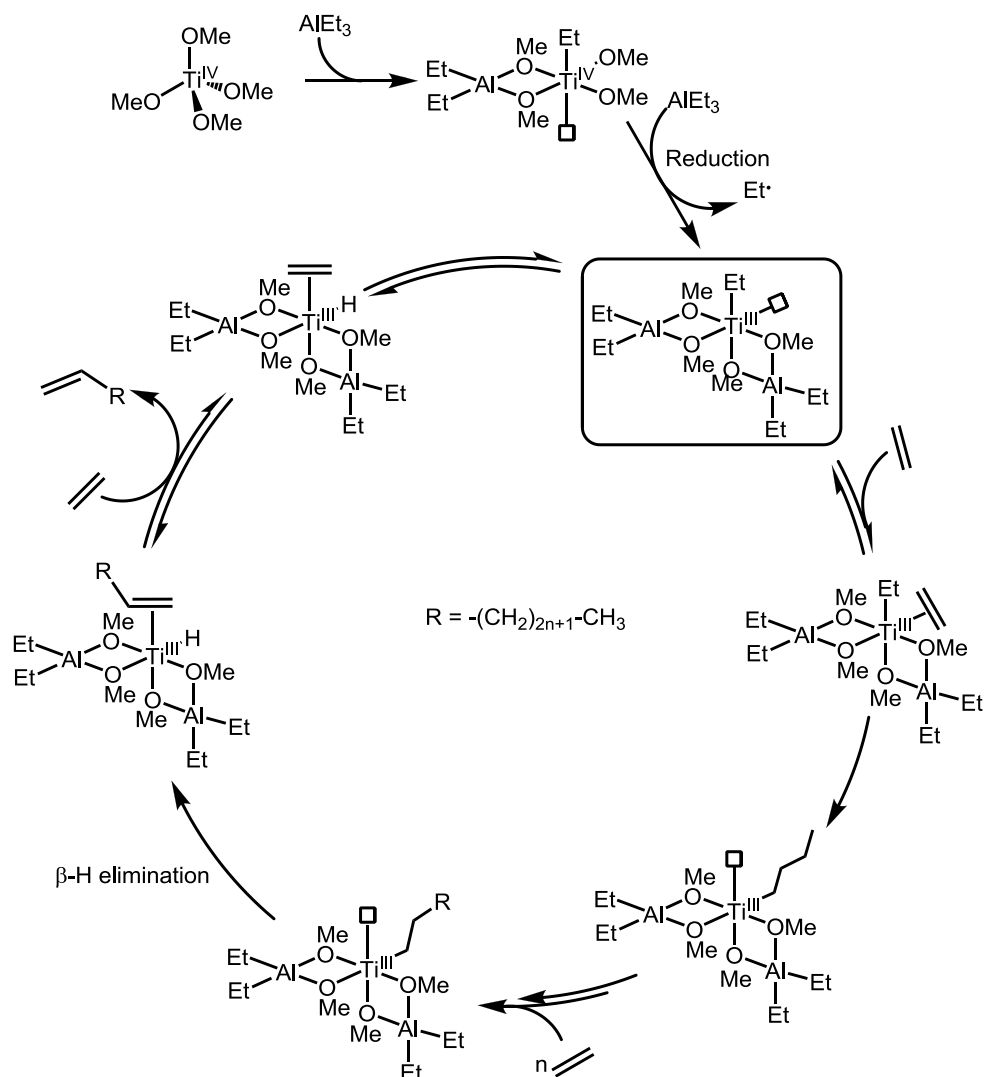
Distinguishing between the two chain propagation mechanisms is difficult, since both have similar characteristics. However, it is argued that at high olefin concentrations, which are typical in the ethylene oligo/polymerization experiments (for examples see section 1.7), a metal hydride species is unlikely to be present.²⁸ Additionally, DFT computational studies on nickel-, palladium-, and platinum-based ethylene dimerization systems have demonstrated that the metal alkyl-mediated mechanism is energetically more favorable than its metal hydride counterpart.²⁸ Hence, it can be concluded that during olefin oligo-/poly-merization *via* a stepwise addition mechanism, the true catalytic species is more likely to be a metal alkyl than a metal hydride.



Scheme 1.16 Mechanism for the oligomerization of olefins initiated via a metal alkyl species.²⁵⁻²⁷

The relation between the rate of the chain propagation and the chain termination (e.g. β -hydride elimination or β -hydride transfer) steps determines whether the products of the reaction are a dimer, an oligomer, or a polymer. If the rate of the chain propagation step is much higher than that of the β -hydride elimination or transfer steps, then a polymer will result. On the other hand, if the β -hydride elimination or transfer step occurs faster than the chain propagation, then the product will be a dimer. It must be noted that the rates of the chain propagation and chain termination steps will depend on the stabilization of their transition states under the conditions of the oligomerization (solvent, type of metal, type of ligands on the metal, oxidation state, *etc.*), which together provide a potential means of controlling product selectivity.²⁵⁻²⁷

Lastly, a characteristic example of a step-wise addition mechanism for the oligomerization of ethylene with the Ziegler Natta-type titanium-based system $\text{Ti}(\text{OMe})_4/\text{AlEt}_3$ is presented in Scheme 1.17.²⁹ Note that the alkyl aluminum co-initiator is of utmost importance, generating a titanium alkyl species from the catalytically inactive titanium tetra(alkoxide), while also simultaneously reducing the metal centre from Ti(IV) to what is believed to be the catalytically active species, namely Ti(III). This reduction is a key feature of many systems that use alkyl aluminum reagents as co-initiators.²⁹



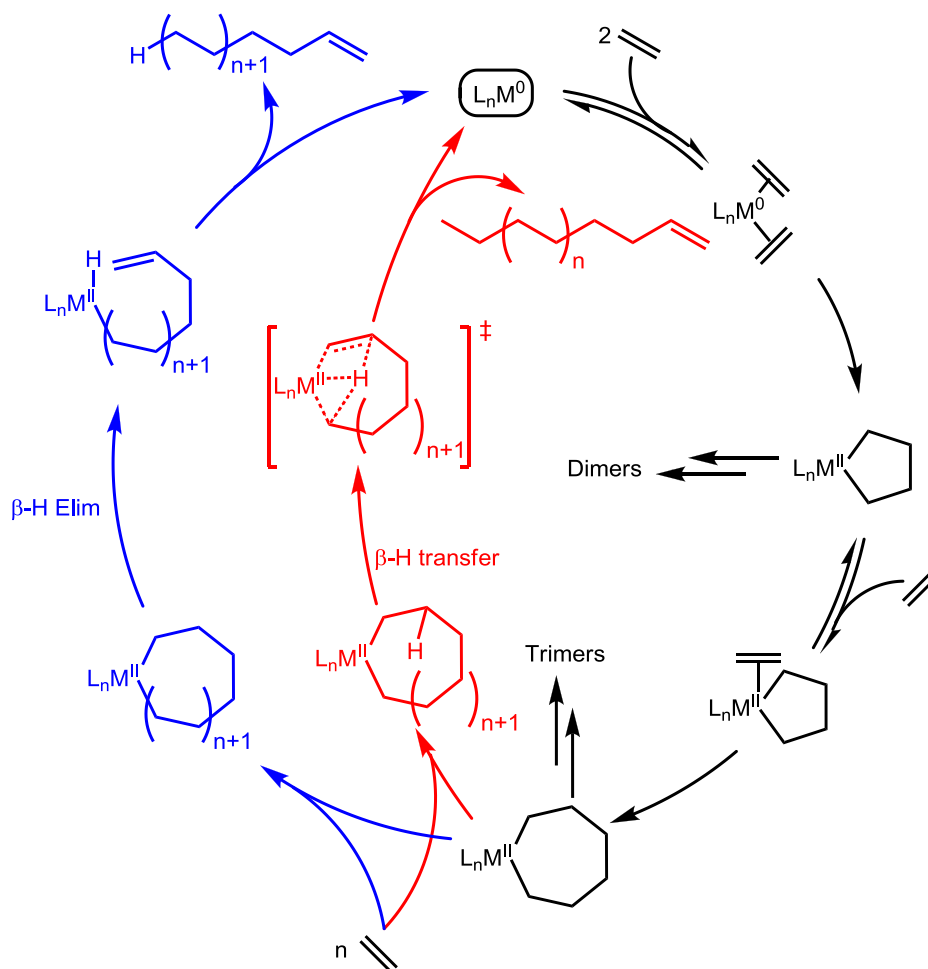
Scheme 1.17 Ziegler Natta-type process for the oligomerization of ethylene over $\text{Ti}(\text{OMe})_4/\text{AlEt}_3$.²⁹

1.4.2 The Metallacycle mechanism

Olefin oligomerization *via* a process involving the formation of a metallacycle is described in Scheme 1.18 and usually leads to the formation of dimers or trimers, although the formation of higher oligomers,^{30,31} or even polymers,³² has also been observed. Kinetic experiments indicate that the metallacycle-mediated catalytic reaction is second order with respect to ethylene, suggesting that this process starts with the coordination of two ethylene molecules to the metal centre followed by formation of a metallacyclopentane and, hence, an increase of the oxidation state of the metal by two units (Scheme 1.18).^{32,33} The metallacyclopentane formed can then incorporate another ethylene molecule to form a metallacycloheptane species. The olefin incorporation process can be repeated with n ethylene molecules generating a metallacycle with $2n+6$ carbon atoms (chain propagation).^{32,33} Chain termination can occur either *via* β -hydride elimination (Scheme 1.18, blue path) or *via* an agostic assisted β -hydride transfer process (Scheme 1.18, red path), releasing the dimer (for the case of a metallacyclopentane), trimer (for the case of a metallacycloheptane), or oligomer.³² It must also be noted that in addition to the oligomerization of ethylene, olefin initiators that proceed *via* a metallacyclic

pathway can also oligomerize higher alkenes or even co-oligomerize ethylene with other α -olefins such as 1-octene.^{34,35}

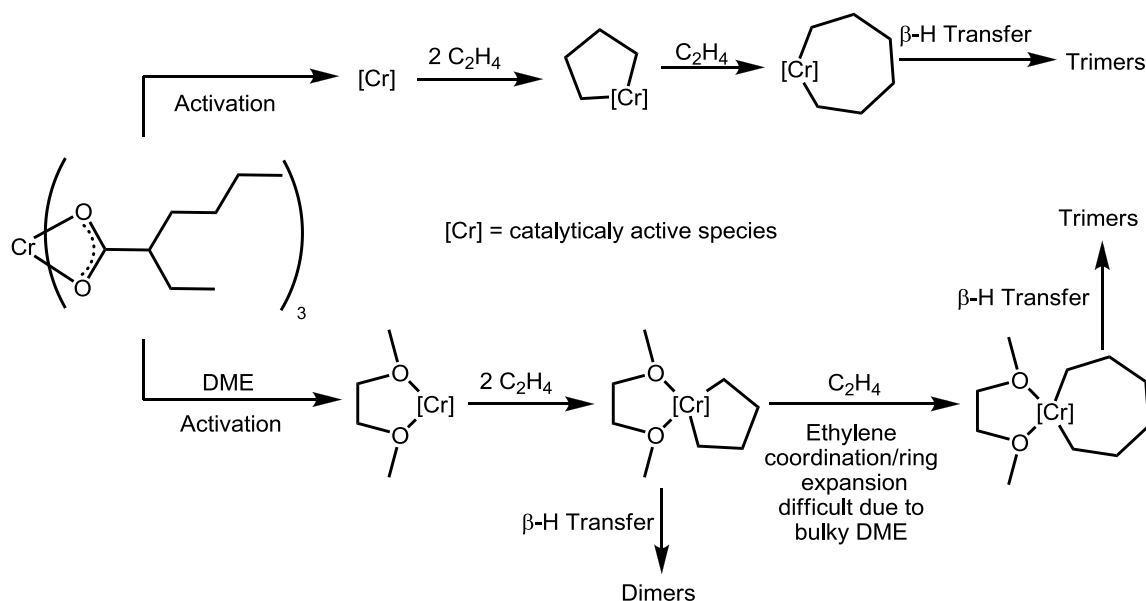
Computational studies on tantalum-based systems (such as TaCl_3Me_2) have shown that a β -hydride transfer process is a more favorable pathway compared to that of β -hydride elimination.³³ Of course, for systems other than those utilizing tantalum this may not be the case. Additionally, in the same study on TaCl_3Me_2 it was calculated that the β -hydride transfer step is more likely to occur from a metallacycloheptane, rather than a metallacyclopentane, due to geometric constraints in the latter. It is due to this increased tendency of the metallacycloheptane intermediate to easily undergo β -hydride transfer that makes metallacycle-mediated ethylene oligomerization systems selective towards trimers instead of dimers or oligomers.³³



Scheme 1.18 The metallacyclic mechanism for the oligomerization of alkenes.³³

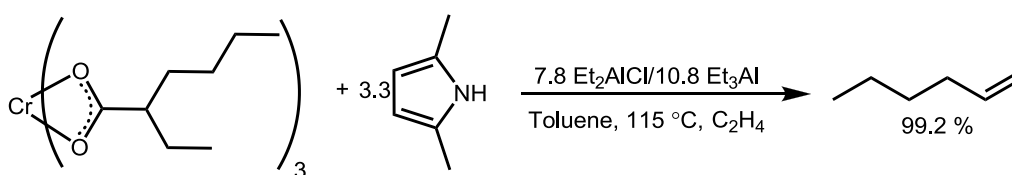
Similar computational results to those for the TaCl_3Me_2 system have also been obtained for the chromium-based ethylene trimerization system: chromium *tris*(2-ethylhexanoate)/partially hydrolyzed *tri*-isobutyl aluminum, which gives rise to trimers as the main products.³⁶ However, when DME is added to the same chromium *tris*(2-ethylhexanoate)/partially hydrolyzed $\text{Al}(i\text{-Bu})_3$ system, ethylene dimerization also occurs along with ethylene trimerization.³⁶ This change in selectivity has been attributed to DME coordination to the metallacyclopentane, as described in Scheme 1.19, which increases the steric demands about the metal centre, and disfavors coordination of a third ethylene molecule. Hence, it

must be born in mind that the ligands around the metal centre can significantly influence the course of these types of catalytic reaction.



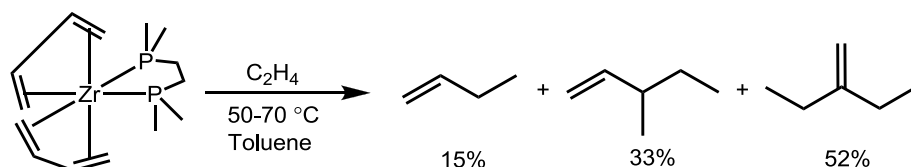
Scheme 1.19 Effect of DME on the oligomerization of ethylene initiated by chromium tris(2-ethylhexanoate)/ partially hydrolyzed tri-isobutyl aluminum.³⁶

It has generally been proposed that complexes that initiate olefin oligomerization through a metallacyclic pathway exhibit high catalytic activities and selectivities in olefin oligomerization. A typical example that demonstrates these characteristics is the ethylene trimerization process developed by Phillips in 1991.³⁴ This system, comprising chromium(III) 2-ethylhexanoate, a pyrrole, triethylaluminum, and diethylaluminum chloride, has been shown to trimerize ethylene with activities exceeding $88.5 \text{ kg C}_2\text{H}_4 (\text{mol Cr})^{-1} \text{ h}^{-1} \text{ bar}^{-1}$. Notably, this system has very high selectivity, 99.85% of the ethylene was converted to hexanes, of which 99.2% was 1-hexene (Scheme 1.20).



Scheme 1.20 The Phillips ethylene trimerization system.³⁴

In addition to the Phillips system, there are a wide variety of other catalyst packages that are able to oligomerize olefins and thought to operate *via* a metallacyclic pathway. Many of these systems are chromium-based, something that is an area that has been reviewed recently by J. T. Dixon *et al.*³⁴ Nevertheless, other metals can also achieve the oligomerization of ethylene *via* a metallacyclic pathway. For example, the butadiene complex $\text{Zr}(\eta^4\text{-C}_4\text{H}_6)_2(\text{dmpe})$ was found to dimerize ethylene with a conversion of 96% (Scheme 1.21).³⁷ Here, the ethylene trimers are thought to originate not from the direct, sequential trimerization of ethylene, but rather from the co-dimerization of ethylene with the resulting 1-butene. It is suggested that this process proceeds *via* a metallacyclic intermediate since the formation of 3-methyl-2-pentene or isomerized products have not been observed (Scheme 1.21).



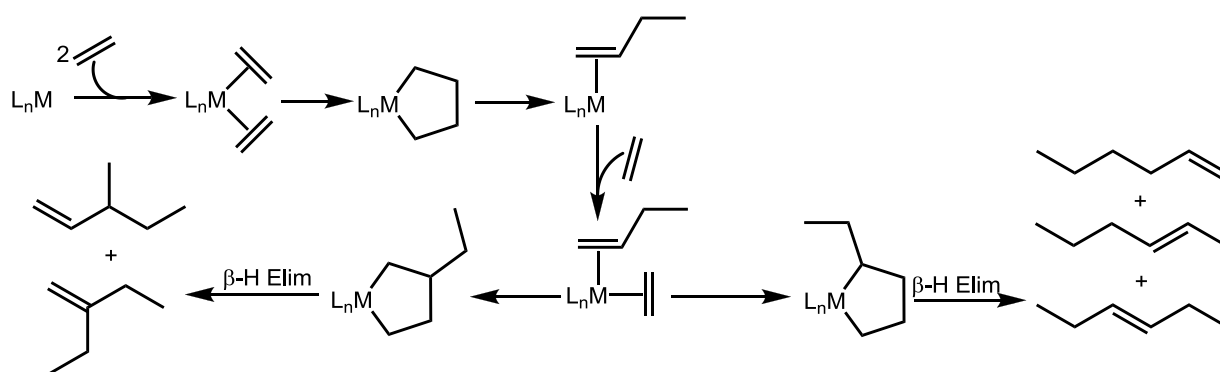
Scheme 1.21 The oligomerization of ethylene via $Zr(\eta^4-C_4H_6)_2(dmpe)$.³⁷

1.5 Processes that compete with oligomerization

One of the most important characteristics of an oligomerization catalyst (and catalysts more generally) is its selectivity towards the desired product. A catalyst with high selectivity not only produces greater amounts of the desired oligomer, but also results in a simple mixture of products that is easier to separate/purify. Unfortunately, during catalytic olefin oligomerization reactions, other processes can occur that decrease the catalytic selectivity. The most common processes of this type include: 1) co-dimerization of the starting olefin with higher olefins produced by the catalyst, 2) olefin metathesis, and 3) olefin isomerization.

1.5.1 Substrate-oligomer co-dimerization

Oligomerization, as well as dimerization and polymerization catalysts, are sometimes able to co-dimerize different olefins.³⁸⁻⁴⁰ Thus, the higher olefins produced during dimerization can also act potentially as substrates, resulting in their co-dimerization with the desired monomer olefin. This type of process can dramatically decrease the selectivity of the system, forming more than one product. For example, in the dimerization of ethylene *via* a metallacyclic mechanism the only product would be 1-butene if no isomerization occurs. Nevertheless, if the 1-butene produced co-dimerizes with the remaining ethylene, then formation of five additional olefins becomes theoretically possible as described in Scheme 1.22; this is also the case for the system described in Scheme 1.21.

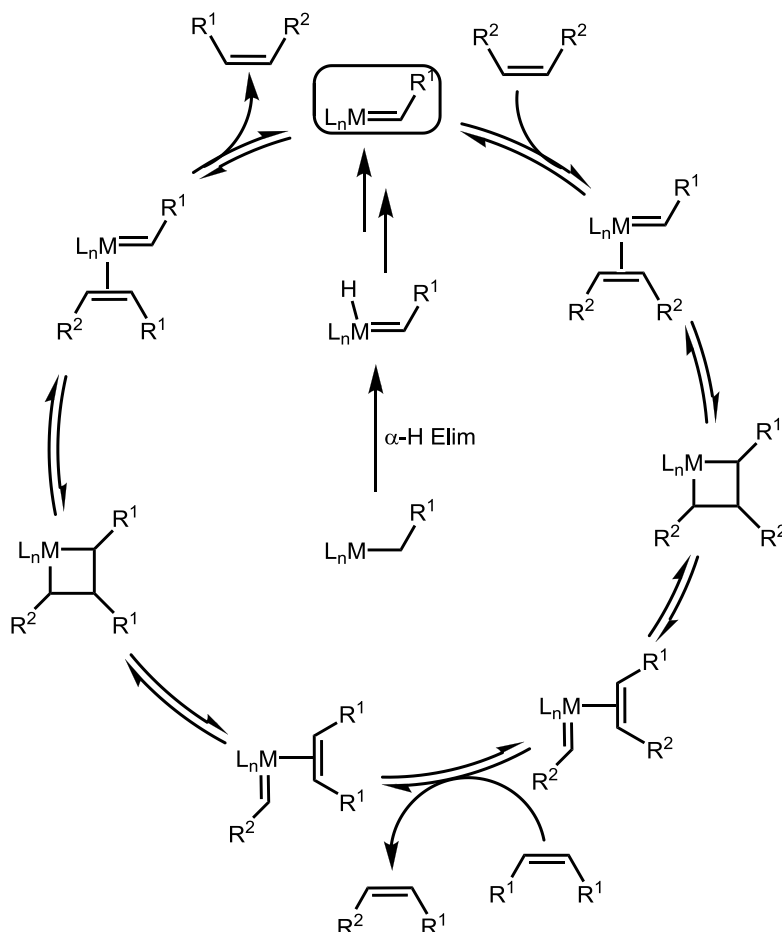


Scheme 1.22 The co-dimerization of ethylene with 1-butene.

Since the products of this type of “monomer-dimer” dimerization process are formally trimers of the starting monomer, this type of behavior can sometimes be mistaken with genuine trimerization. One way of distinguishing between the two pathways is to repeat the catalysis experiment with ethylene in the presence of an odd-numbered olefin, which is of a similar molecular weight to the dimers such as 1-pentene. The absence of odd numbered oligomers in the products resulting from catalysis indicates that genuine trimerization takes place.³⁰

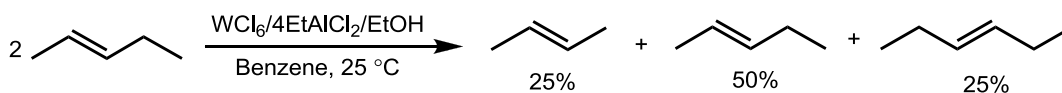
1.5.2 Olefin metathesis

Olefin metathesis is a process that interchanges alkylidene fragments between two olefins. Transition metal-catalyzed olefin metathesis has been extensively studied over the years, but its detailed description is beyond the scope of this project.^{41,42}



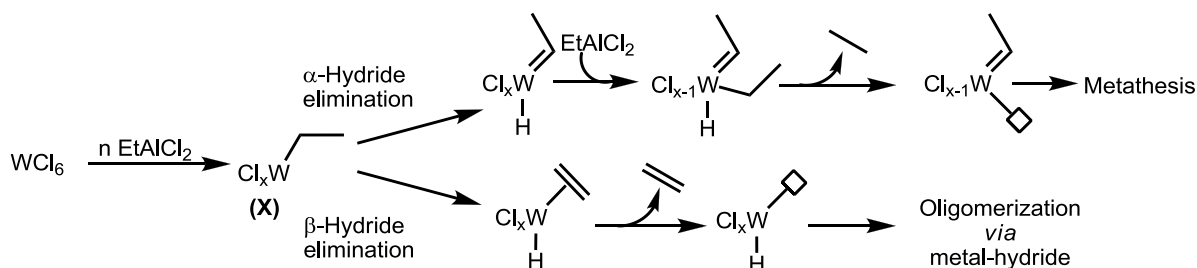
Scheme 1.23 A typical catalytic olefin metathesis mechanism.^{41,42}

Extensive mechanistic studies have led to the development of the mechanism shown in Scheme 1.23, for which the key element is the role of a metal carbene. Importantly, metal carbene species may be generated during olefin oligomerization processes, since metal carbenes can be formed from a metal alkyl species *via* an α -hydride elimination reaction,⁴³ with the necessary metal alkyl species commonly encountered during step-wise oligomerization (see for example section 1.4.1). A typical example of a system that can promote both olefin metathesis and oligomerization was developed by the Goodyear Co.^{44,45} This initiator package is based on $WCl_6/EtAlCl_2$, identical to that of the oligomerization systems described in section 1.3.2. The main difference between the Goodyear *olefin oligomerization* and the Goodyear *olefin metathesis* system is that the aniline used in the former is replaced with ethanol in the latter. The metathesis of 2-pentene by the Goodyear system is described in Scheme 1.24.



Scheme 1.24 The Goodyear olefin metathesis system.^{43,44}

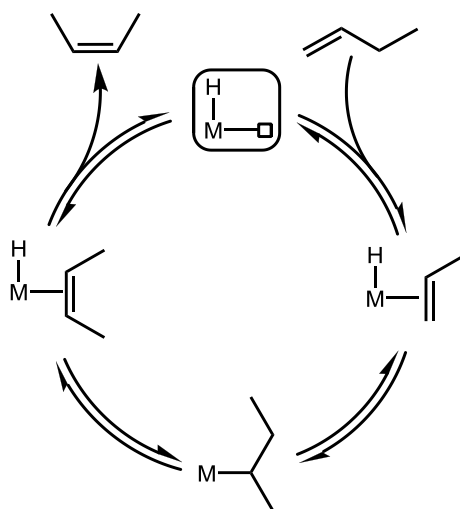
An important characteristic of the Goodyear olefin metathesis system is that when a higher concentration of the initiator is used, olefin oligomerization occurs, resulting in an attenuation of olefin metathesis. This clearly highlights the potential connection between the oligomerization and metathesis processes.^{44,45} Drawing on previously reported work, a mechanism can be proposed that demonstrates the connection between the olefin oligomerization and metathesis processes, *i.e.* a mechanism by which the species invoked in the Goodyear dimerization system initiate olefin metathesis (Scheme 1.25). Depending on the reaction conditions, such as the concentration of the W-containing component, the resulting tungsten alkyl species **X** in Scheme 1.25 could be envisaged to undergo either/both an α -hydride or β -hydride elimination process, which could subsequently result in the formation of species that are capable of initiating olefin metathesis or oligomerization, respectively.



Scheme 1.25 A proposed mechanism for the Goodyear olefin metathesis system.

1.5.3 Olefin isomerization

Olefin isomerization is a process in which the olefinic double bond of the substrate is “moved” along the carbon chain, usually to form the thermodynamically more stable internal olefin. Such olefin isomerization reactions occur readily in the presence of a coordinatively-unsaturated metal hydride, as described in Scheme 1.26.⁴⁶



Scheme 1.26 General mechanism for the isomerization of 1-butene to 2-butene via a metal hydride.

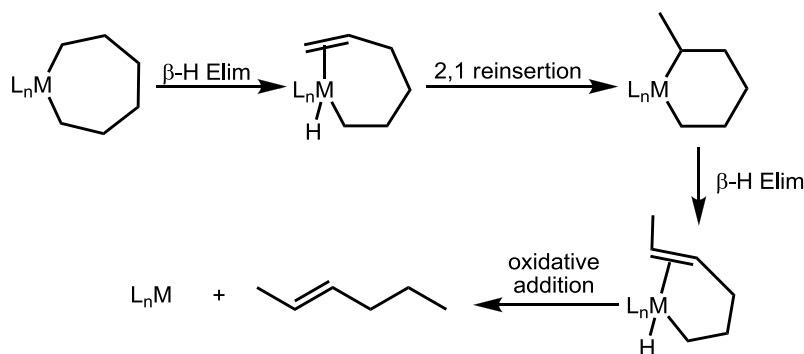
This mechanistic interpretation implies that isomerization is an easily accessible pathway during step-wise oligomerization, since the catalytically-active species of both processes is a coordinatively-unsaturated metal hydride. Hence, if no isomerization occurs, the only products of the step-wise dimerization of 1-butene will be the 1-butene dimers. However, if isomerization does take place (which is usually the case for step-wise oligomerization), some of the starting 1-butene will be converted to the more thermodynamically stable 2-butene, which is not readily dimerized, Scheme 1.26.⁴⁶ In addition, a quantity of the C₈ α -olefins formed will also be isomerized towards the more stable internal C₈ olefins. Together, access to this type of pathway, makes olefin isomerization an undesirable competitive process, not only because it decreases the selectivity of the catalyst and converts the desired α -olefin dimers to the less useful internal isomers, but also because it decreases the conversion of the starting α -olefin through its isomerization to the internal olefin. Note that when a metallacycle-mediated mechanism is active, isomerization is less likely to occur compared to the case where a step-wise addition mechanism is in operation, since in the metallacyclic mechanism the olefin is more likely to be released *via* a β -hydride transfer rather than a β -hydride elimination reaction.³³ Hence, metal hydride species are less likely to form during metallacycle-mediated oligomerization processes, which reduces the possibility for olefin isomerization to occur.³³

1.6 Determining the mechanism of an oligomerization process

1.6.1 Isomerization of starting olefin substrate and olefinic products

The ability of an olefin oligomerization catalytic system to mediate olefin isomerization can provide some insight about the oligomerization mechanism in operation. In section 1.5.3 it was mentioned that olefin isomerization and step-wise addition oligomerization are related processes. Hence, if isomerization of the olefinic substrate is observed, it is likely that a step-wise addition mechanism is in operation since isomerization of the starting olefin is most commonly encountered when the active species is a coordinatively-unsaturated metal hydride (see section 1.5.3). The same argument can be used in the case where isomerization of the catalysis products is observed.⁴⁷

Nevertheless, it must be highlighted that the isomerization of the starting olefin or of the dimerization products is not the only criterion needed in order to determine the mechanism of the process since isomerization could theoretically occur even as a part of processes operative *via* a metallacycle mechanism. For example, the starting olefin could bind to the metal hydride generated after a metallacyclic species undergoes β -hydride elimination. This would result in the isomerization of the starting olefin, just as in the step-wise addition case. For example, in the trimerization of ethylene *via* a metallacyclic pathway the chromium alkenyl hydride species could perform a 2,1-reinsertion into the Cr-H bond, generating a metallacyclohexane. In turn, the metallacyclohexane can then undergo a β -hydride elimination followed by a reductive elimination, resulting in the formation of 2-hexene (Scheme 1.27).⁴⁸



Scheme 1.27 Isomerization during ethylene trimerization via a metallacyclic process.⁴⁸

Another instance where isomerization can occur when a metallacycle mechanism is in operation is when multiple catalytically active sites are generated during the initiation of the oligomerization reaction. Hence, it is possible that some of these sites form metallacycles, which produce dimers and some others are active only in the isomerization of α -olefins producing internal alkenes.

1.6.2 Selectivity of the catalytic oligomerization reaction

In order to gain further insight into the mechanism of a catalytic dimerization process, the selectivity of the process must also be considered. It has already been mentioned that metallacycle-mediated oligomerization is potentially more selective than the comparable step-wise addition oligomerization due to the geometric constraints imposed by the variously-sized metallacycle rings (section 1.4.2). Additionally, a step-wise addition mechanism is more likely to lead to formation of a larger variety of isomers compared to a metallacyclic pathway, due to the potential for chain walking* that the former creates.²⁶ Hence, highly selective oligomerization processes point towards a metallacycle mechanism. Again, this doesn't exclude the existence of a selective step-wise addition oligomerization mechanism.

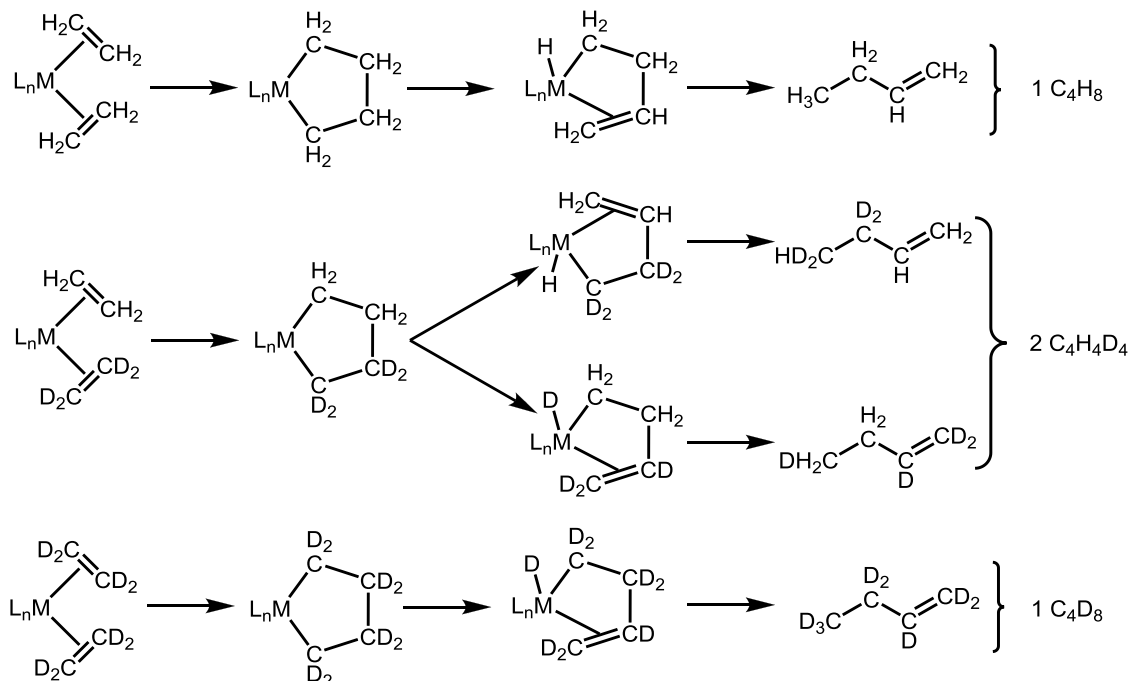
1.6.3 Deuterium labeling experiments

To date, one of the most informative methods for distinguishing between a system operating through a step-wise addition versus that involving a metallacyclic pathway is to conduct deuterium labeling experiments, a strategy developed initially by Bercaw and co-workers.⁴⁹ In such an experiment, the oligomerization products from a 1:1 mixture of the monomer and its deuterated analogue are examined. The weight distribution of the resulting isotopomer dimers will depend on the mechanism of the oligomerization.

Consider, for example, the dimerization of a 1:1 mixture of ethylene and ethylene- d_4 . If the dimerization occurs *via* a metallacyclic mechanism, then two ethylene molecules, deuterated or not, will be coordinated to the metal centre to form the metallacycle. Subsequently, the metallacycle will undergo β -hydride elimination, resulting in the transfer of a proton or deuterium atom onto the metal. However, during the reductive elimination step this proton or deuterium will be moved back to the alkenyl chain it

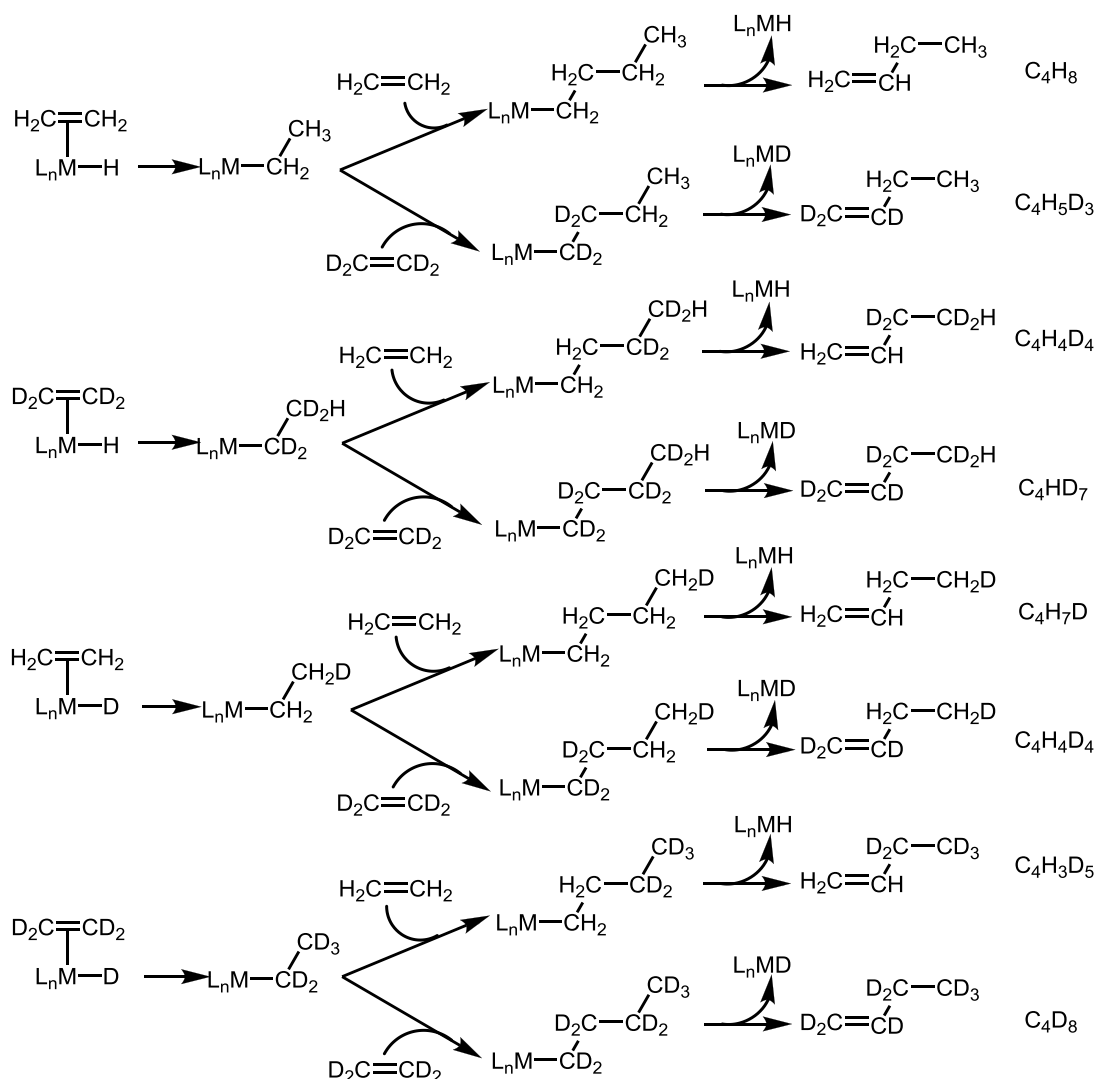
* Chain walking is a process where the metal on a metal alkyl chain moves by one carbon atom *via* a β -hydride elimination process followed by reinsertion with a different topology. This process can be repeated multiple times resulting in the formation of internal metal alkyls.

originated from. Thus, in the case of a metallacyclic mechanism, no deuterium scrambling between butene molecules will occur. As a consequence, the resulting butene isotopomers will contain only an even number of deuterium atoms (*i.e.* multiples of four). The various possible processes are described in Scheme 1.28.⁴⁹ Thus, it is evident that the dimerization of a 1:1 mixture of ethylene and ethylene-d₄ via a metallacyclic pathway will result in a 1:2:1 mixture of C₄H₈:C₄H₄D₄:C₄D₈.



Scheme 1.28 The dimerization of a 1:1 mixture of ethylene:ethylene-d₄ via a metallacyclic pathway.

Contrastingly, if a step-wise addition mechanism is operative, then the product distribution will deviate from the 1:2:1 ratio of C₄H₈:C₄H₄D₄:C₄D₈. This departure will occur as a result of the β-hydride or β-deuteride elimination steps in the step-wise addition process, which releases butene leaving the eliminated proton on the metal. This results in the separation of the proton or the deuterium from the originating alkyl chain, leading to deuterium scrambling as described in Scheme 1.29. Note that in contrast to the metallacyclic mechanism, in a step-wise addition dimerisation process butene isotopomers with an odd number of deuterium atoms are formed. Furthermore, the distribution of the isotopomers is wider since a 1:1:1:2:1:1:1 mixture of C₄H₈:C₄H₅D₃:C₄HD₇:C₄H₄D₄:C₄H₇D:C₄H₃D:C₄D₈ results.⁴⁹ It must be noted that the above deuterium labeling experiment can also be used for determining the mechanism in trimerization or even in oligomerization processes.^{48,50}



Scheme 1.29 The dimerization of a 1:1 mixture of ethylene:ethylene-d₄ via a step-wise addition mechanism.

Despite the potential of the H/D labeling experiments described above, complete agreement between the theoretically calculated isotopomer distributions and those obtained experimentally is not always observed. Such deviations from ideality can occur in a number of ways. Firstly, the process described in Scheme 1.29 must be reconsidered. When oligomerization occurs, the rate of propagation is similar to the rate of termination. This implies that many ethylene insertions into an M-H or M-D bond followed by β-hydride eliminations from the metal alkyl species will have taken place before oligomerization. This will result in a complete deuterium scrambling leading to a statistical distribution of the isotopomer molecular weights.⁵⁰ Secondly, processes other than those described above could be operative during the oligomerization process (*i.e.* trimerization or isomerization). For example, in many ethylene dimerization systems small amounts of trimers or higher oligomers are inevitably formed (see for example the systems described in section 1.7). This can cause some deviation from the theoretically calculated deuterium distribution in the labeling experiment due to deuterium leaching into the heavier fraction. Lastly, the kinetic isotope effect can change the deuterium distribution of the oligomerization products. The β-hydride elimination process is expected to be subject to a large primary isotope effect,

with β -deuteride elimination being slower than β -hydride elimination. This means that the β -deuterated metal alkyl intermediate will be more likely to undergo insertion of an additional olefin instead of β -deuterium elimination, compared to its β -protonated metal alkyl analogue. This creates a tendency for deposition of deuterium atoms in the higher olefins, which in turn leads to deviations from the theoretically calculated deuterium distribution in the oligomerization products.⁴⁸

1.7 A comparison of selected well-defined transition metal-catalyzed homogeneous olefin dimerization systems

Due to the commercial importance of α -olefins and their dimers (sections 1.1, 1.2, and 1.3), the field of α -olefin dimerization has attracted significant attention, something that has led to the study of a variety of transition metal complexes, together with a wide range of activators and reaction conditions. As a result of this extensive research effort, a detailed literature review of all these systems is outside the scope of this thesis. Hence, this overview will be restricted to a selection of the most recently reported, well-defined, ethylene and higher α -olefin dimerization initiator systems.

Throughout the following literature overview, it must be noted that direct comparison of the various initiator systems reported is not always straightforward, with comparisons of catalytic activity being particularly problematic. Specifically, many reports only cite catalytic activities, making it impossible to establish a true and full picture of catalytic performance in terms of activity. Consequently, the true catalyst activity profile as a function of time remains unclear (see Figure 1.1). Additionally, the catalytic reactions presented in the literature are often conducted under different conditions (temperature, ethylene pressure, solvent, concentration, amount and type of activator used, etc.), which have not been thoroughly optimized and again makes comparisons between the various systems difficult.

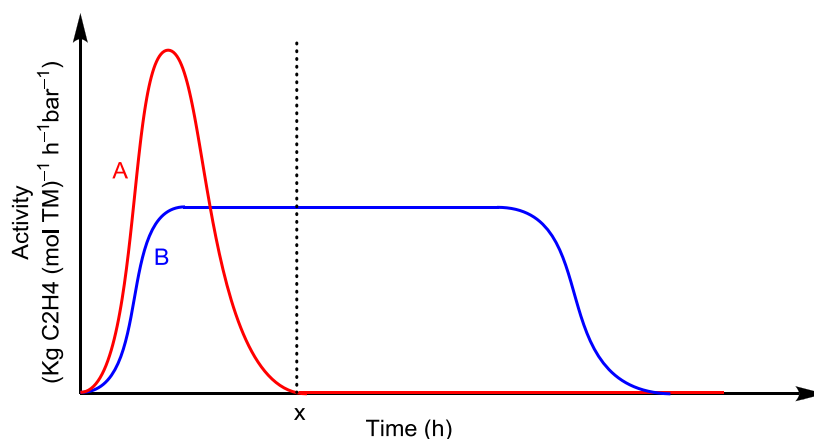


Figure 1.1 Comparison of activity versus time profiles for two different catalysts A (red) and B (blue). x = Time at which reaction was quenched and catalyst activity determined, a methodology that underestimates the performance of B.

1.7.1 Nickel-, cobalt-, and iron-based olefin dimerization

Historically, ethylene oligomerization initiator systems based on nickel were the first to be developed, but they remain important to this day. The original nickel-based ethylene oligomerization systems were developed in the 1970s, something that subsequently led to the development of the SHOP process (section 1.2.1), which uses κ^2 -P \wedge O-chelated complexes such as $(\eta^3\text{-C}_8\text{H}_{13})(\kappa^2\text{-P}\wedge\text{O-Ph}_2\text{PCH}_2\text{COO})\text{Ni}$.^{51,52} These types of nickel complex oligomerize ethylene to mixtures of C₄-C₂₄ olefins with activities of up to 3 kg C₂H₄ (mol Ni)⁻¹ h⁻¹ bar⁻¹.⁵³ These encouraging results formed the basis for the development of a plethora of nickel-based systems with a range of activities and product selectivities.⁵⁴⁻⁵⁷

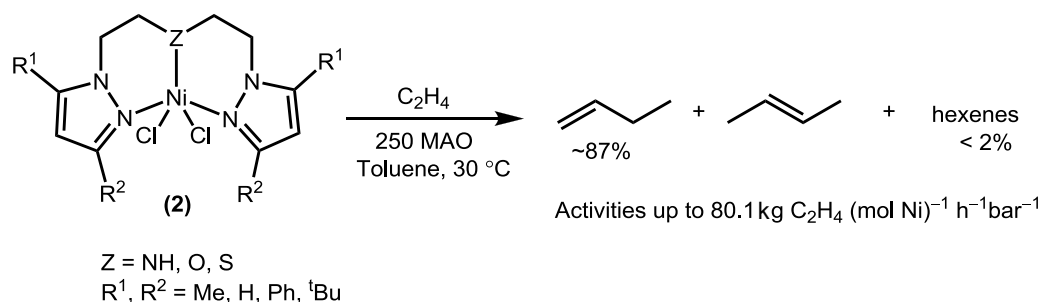
Following the success of nickel complexes in the oligomerization and polymerization of ethylene, cobalt- and iron-based pro-initiators were developed. The majority of these latter types of system reported give rise to products from both oligomerization and polymerization of ethylene. However, some examples of iron and cobalt systems that demonstrate high selectivity towards dimerization have also been reported.

1.7.1.1 Ethylene dimerization using nickel-, cobalt-, and iron-based pro-initiators

1.7.1.1.1 Nitrogen-based ligands

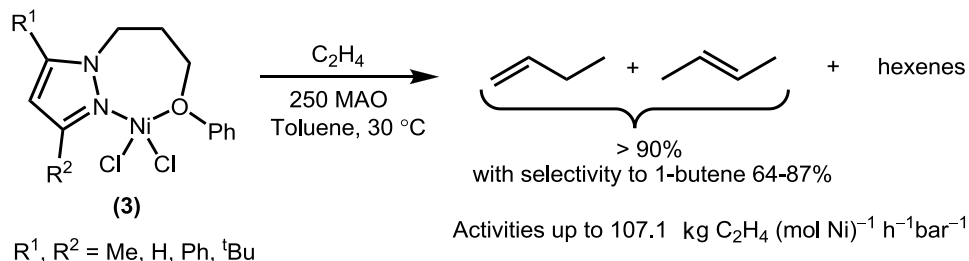
1.7.1.1.1.1 Pyrazole-based ligands

Complexes of nickel with tridentate *bis*(pyrazolyl)-containing ligands (e.g. **2**, Scheme 1.30) have been found to be active in the dimerization of ethylene. For example, in combination with 250 equivalents of MAO, these systems achieve activities of up to 80.1 kg C₂H₄ (mol Ni)⁻¹ h⁻¹ bar⁻¹ (activity intimately linked to the nature of the substituents R¹, R², and Z) with very good selectivities towards 1-butene (~ 87% of the product fraction), Scheme 1.30.⁵⁶ Importantly, pro-initiator **2** gives rise to product selectivities, which are strongly linked to ethylene pressure and reaction temperature. It was found that increasing reaction temperature increases the extent of 1-butene isomerization, while increasing ethylene pressure has the opposite effect, presumably by favoring chain transfer processes over chain propagation.⁵⁶



Scheme 1.30 Selective ethylene dimerization using nickel *bis*(pyrazolyl) complexes as pro-initiators.⁵⁶

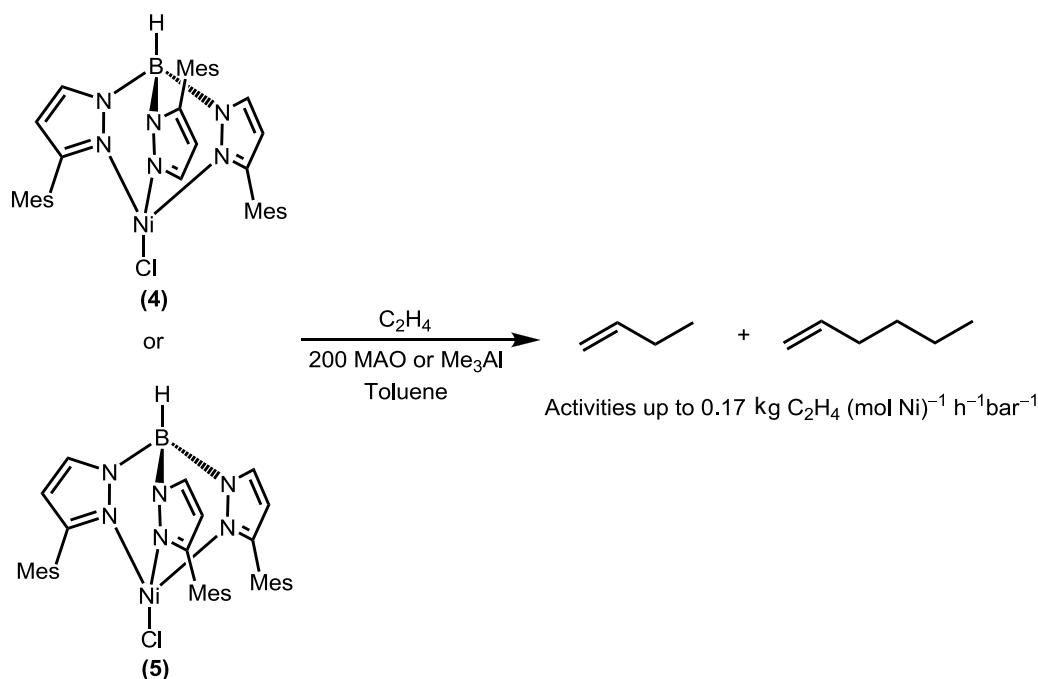
More recently, nickel complexes of unsymmetrical, bidentate ether-pyrazolyl ligands **3** have been reported to demonstrate ethylene oligomerization activities reaching $107.1 \text{ kg C}_2\text{H}_4 (\text{mol Ni})^{-1} \text{ h}^{-1} \text{ bar}^{-1}$, with selectivities of over 90% towards the dimer fraction, 64-87% of which typically consisted of 1-butene (Scheme 1.31).⁵⁵



Scheme 1.31 Performance of ether-pyrazolyl-ligated nickel complexes in the dimerization of ethylene.⁵⁵

Increasing the steric bulk of the substituents of the pyrazolyl component of **3** led to a decrease in the catalytic activity of these systems, while leaving the selectivity practically unchanged, an effect that has been attributed to a hindering of the coordination of ethylene at nickel. However, in contrast, raising the reaction temperature ($> 30 \text{ }^\circ\text{C}$) led to increased production of 2-butene, although this was accompanied by catalyst decomposition. Extending catalysis reaction times for **3** ($R^1 = R^2 = \text{Me}$), from 10 minutes to 40 minutes, resulted in an attenuation of the catalytic activity, which decreased from $107.1 \text{ kg C}_2\text{H}_4 (\text{mol Ni})^{-1} \text{ h}^{-1} \text{ bar}^{-1}$ to $53.8 \text{ kg C}_2\text{H}_4 (\text{mol Ni})^{-1} \text{ h}^{-1} \text{ bar}^{-1}$, suggesting that the catalyst life time of systems **3** is relatively short.⁵⁵ Furthermore, it was demonstrated that the activity of pro-initiator **3** ($R^1 = R^2 = \text{Me}$) in combination with MAO (250 equivalents) was found to increase by a factor of 2.6 in the presence of 1 equivalent of PPh_3 , compared to the PPh_3 -free system, something accompanied by a drop in selectivity towards 1-butene from 69% to 15% on addition of phosphine. No explanation of the role of PPh_3 was reported.⁵⁵

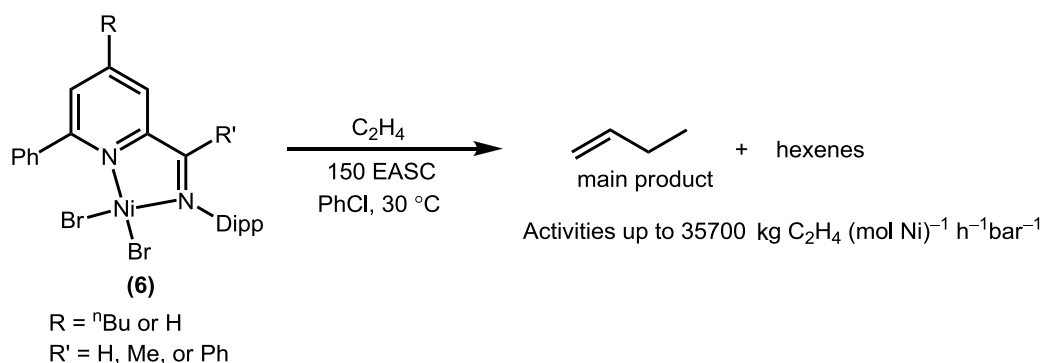
tris(Pyrazolyl)borate (Tp') complexes have been employed very effectively in the polymerization of ethylene.⁵⁸⁻⁶⁰ Much of their success has been attributed to their significant steric bulk, which can potentially improve catalysis by preventing the catalyst from participating in deactivation reactions.⁶¹ Consequently, the use of *tris*(pyrazolyl)borate ligands was extended to nickel, with complexes **5** and **4** subsequently being found to be active in the dimerization of ethylene in the presence of 200 equivalents of MAO or Me_3Al (Scheme 1.32). Activities up to $0.17 \text{ kg C}_2\text{H}_4 (\text{mol Ni})^{-1} \text{ h}^{-1} \text{ bar}^{-1}$ were achieved, with selectivities towards the dimer fraction of $> 80 \%$ in most cases, depending on the specific reaction conditions used. Interestingly, complex **5**, in which the steric hindrance on the nickel is greater due to the presence of the Mes groups, was found to be 16 times more active than **4**, suggesting that increased steric constraints on the ligand increase the activity of the catalytic system.⁶²



Scheme 1.32 Dimerization of ethylene initiated by Tp^*NiCl complexes **4** and **5**.⁶²

1.7.1.1.1.2 2-(1-Aryliminoethylidene)pyridine-based ligands (N[^]N)

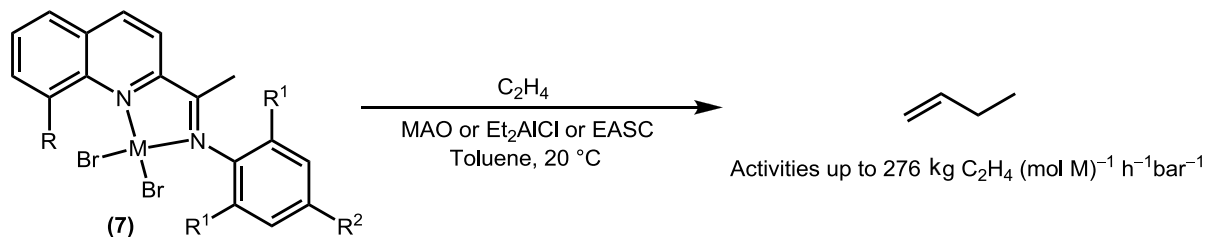
Ligands based on an (iminoethylidene)-pyridine backbone have demonstrated excellent performance in nickel-based ethylene dimerization. Notably, it has been reported that complexes **6** (Scheme 1.33) gave quite remarkable activities of up to $35700 \text{ kg C}_2\text{H}_4 (\text{mol Ni})^{-1} \text{ h}^{-1} \text{ bar}^{-1}$ for the dimerization of ethylene under the relatively mild conditions of 1.3 bar ethylene pressure and 30°C .⁵⁷ Additionally, these complexes were selective towards formation of the desirable 1-butene (81-88%) along with small amounts of 1-hexene (3-9%). From a structural point of view the most active pro-initiators **6** were those where $R = ^n\text{Bu}$ and $R' = \text{Ph}$, suggesting that again bulky groups on the ligand increases the activity of the ethylene dimerization systems.⁵⁷



Scheme 1.33 Ethylene dimerization with 2-(1-aryliminoethylidene)pyridinato nickel(II) pro-initiators.⁵⁷

In an extension of the work utilizing complexes **6**, the related nickel(II) system bearing 2-(1-aryliminoethylidene)quinoline ligands **7** (Scheme 1.34) were found to be reasonably active ethylene dimerization pro-initiators (activities of up to $276 \text{ kg C}_2\text{H}_4 (\text{mol Ni})^{-1} \text{ h}^{-1} \text{ bar}^{-1}$ were achieved) with

selectivities to 1-butene of > 80%.⁶³ These systems were activated with 200 equivalents of Et₂AlCl, which was found to be a more efficient activator than MAO, MMAO, or EASC. Studies revealed that pro-initiators **7** perform better at low temperatures, *i.e.* 20 °C, since it appears that catalyst deactivation occurs when the temperature of the catalytic reaction medium rises over 30 °C.⁶³

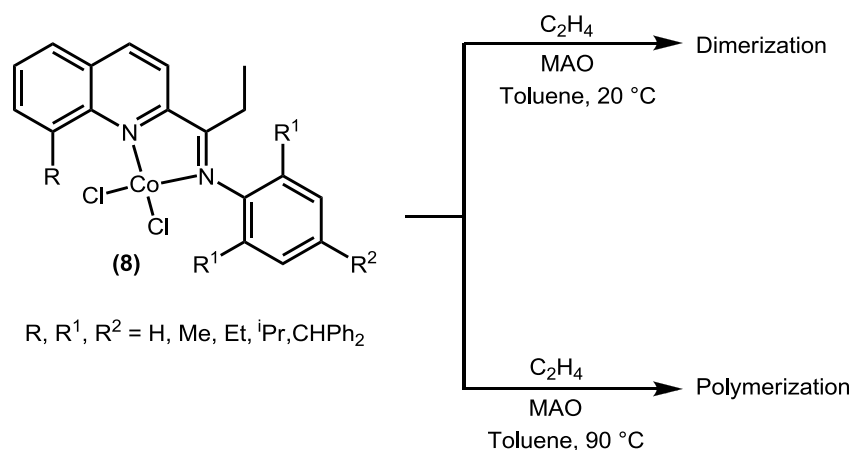


R, R¹, R² = H, Me, Et, ⁱPr, CHPh₂
M = Ni, Co, Fe

Scheme 1.34 2-(1-Aryliminoethylidene)quinolynickel(II) dibromide-mediated dimerization of ethylene.⁶³

Following the use of 2-(1-aryliminoethylidene)pyridine nickel complexes, the cobalt and iron analogues were synthesized and their catalytic reactivity towards ethylene explored under similar conditions to those used for their nickel analogues.⁶⁴ The catalytic dimerization activities obtained with the cobalt and iron systems, 182 kg C₂H₄ (mol Ni)⁻¹ h⁻¹ bar⁻¹ and 58.9 kg C₂H₄ (mol Ni)⁻¹ h⁻¹ bar⁻¹ respectively, were lower than those obtained using the related nickel systems. As with nickel, it was found that for both the iron and cobalt pro-initiators increasing the ligand's steric bulk improved catalytic activity, with both Fe- and Co-based systems exhibiting essentially quantitative conversion of ethylene to butenes, albeit with only moderate selectivity to 1-butene (61-69%). Again, as for the nickel system **7**, the individual catalytic performance of the iron and cobalt systems was intimately linked to the number of equivalents and the nature of the aluminum-based activator. While the best performance for the nickel complexes was achieved with 200 equivalents of Et₂AlCl, the cobalt systems required 1000 equivalents of MAO, and the iron analogues 2500 equivalents of MMAO.⁶⁴ These differences in the aluminum activator requirements of these complexes have not been rationalized, but demonstrate the complexity of the interplay between the transition metal component and the aluminum activator in catalytic olefin oligomerisation systems.

Interestingly, in a different report, cobalt complexes similar to **7**, *i.e.* **8** (Scheme 1.35), were found to be active in the dimerization of ethylene in combination with MAO at 20 °C, giving activities of up to 97 kg C₂H₄ (mol Ni)⁻¹ h⁻¹ bar⁻¹, but were found to produce only polyethylene (activities of up to 4.6 kg C₂H₄ (mol Ni)⁻¹ h⁻¹ bar⁻¹) when the catalysis temperature was increased to 90 °C.⁶⁵ This different response of systems **7** at increased temperature was attributed to the formation of a different catalytically active species. However no details about the nature of these species was provided.⁶⁵

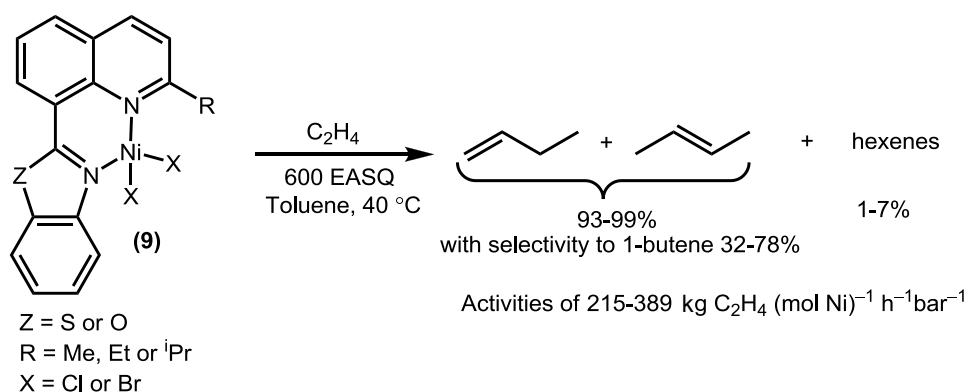


Scheme 1.35 Temperature-dependent ethylene dimerization or polymerization mediated by 2-(1-aryliminoethylidene)quinolincobalt(II) dichloride pro-initiators.⁶⁵

1.7.1.1.1.3 8-Benzoxazolyl- or 8-benzothiazolyl-2-alkylquinoline ligands

After the success of the 2-(1-aryliminoethylidene)pyridine-based complexes in the dimerization of ethylene, the structurally similar 8-benzoxazolyl- or 8-benzothiazolyl-2-alkylquinolinylnickel(II) **9** complexes were developed and tested (Scheme 1.36). Pro-initiators **9** proved to be slightly more active than **7**, displaying activities in the range of 215-389 kg C₂H₄ (mol Ni)⁻¹ h⁻¹bar⁻¹, with the exact activity being found to be dependent on the nature of the substituent R.⁶⁶ Irrespective of the identity of R, the selectivities towards 1-butene obtained were relatively low (32-78%).

In contrast to the behavior of complexes **4-7**, an increase of the bulk of the substituent R of **9** led to an attenuation in dimerization activity, something that was attributed to the ability of bulky groups to hinder ethylene coordination.⁶⁶

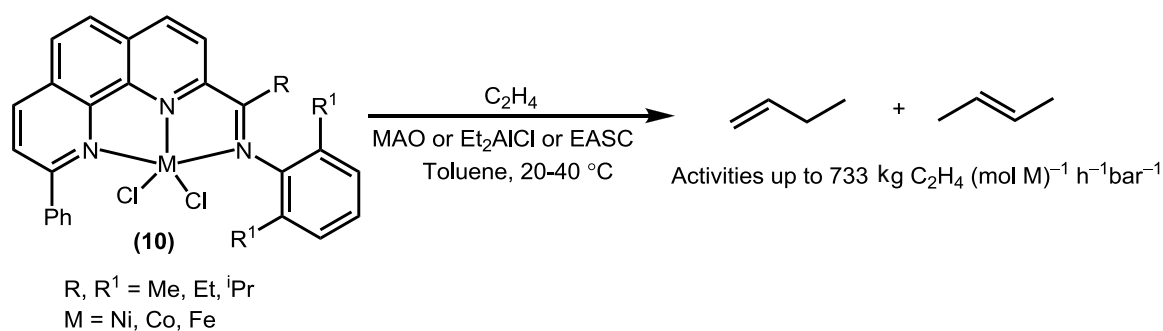


Scheme 1.36 8-Benzoxazolyl- or 8-benzothiazolyl-2-alkylquinolinylnickel(II) complexes as pro-initiators in ethylene dimerization.⁶⁶

1.7.1.1.1.4 2-Arylimino-9-phenyl-1,10-phenanthroline ligands

In an extension to the work employing 2-(1-aryliminoethylidene)pyridine ligands, related tridentate 2-arylimino-9-phenyl-1,10-phenanthroline analogues have been used in combination with nickel, cobalt, and iron in the dimerization of ethylene (**10**, Scheme 1.37).⁶⁷ As was observed with complexes **7**, the

iron analogues were more successfully activated with MAO, while the cobalt and nickel systems demonstrated better performance in combination with MAO and Et₂AlCl, respectively. Interestingly, the catalytic activities obtained with systems **10** were significantly higher for cobalt (up to 733 kg C₂H₄ (mol Ni)⁻¹ h⁻¹bar⁻¹) and, to a lesser extent with iron (264 kg C₂H₄ (mol Ni)⁻¹ h⁻¹bar⁻¹), rather than for nickel (22.6 kg C₂H₄ (mol Ni)⁻¹ h⁻¹bar⁻¹), although the reasons behind these differences remain unknown. Additionally, it was found that in contrast to systems 6 (section 1.7.1.1.2), the presence of bulky R¹ substituents on the metal scaffold led to a decrease in the catalytic activity of these systems.⁶⁷

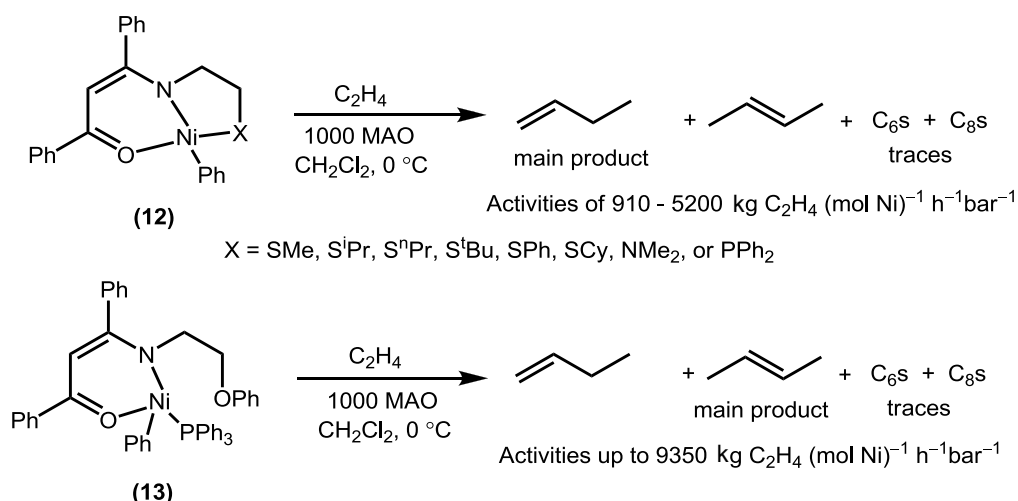


Scheme 1.37 2-Arylimino-9-phenyl-1,10-phenanthroline complexes of nickel, cobalt and iron **10** and their reactivity towards ethylene.⁶⁷

Notably, 100% selectivity towards 1-butene for the iron-containing variants of **10** was established. In contrast, the cobalt pro-initiators exhibited lower selectivities towards the dimer fraction (47-96%), which consisted mainly of 1-butene (> 95% of the dimer fraction). Subsequently, the impact of adding PPh₃ to the nickel pro-initiator systems **10** was studied in detail. It was found that the activity of complexes **10** (M = Ni, R = Ph, R¹ = Et) increased from 22.6 kg C₂H₄ (mol Ni)⁻¹ h⁻¹bar⁻¹ to 682 kg C₂H₄ (mol Ni)⁻¹ h⁻¹bar⁻¹ when 20 equivalents of PPh₃ were added prior to activation, with the expense of 1-butene selectivity, which dropped to only 8.5%.⁶⁷ Again, the PPh₃ additive effect was not rationalized.

1.7.1.1.1.5 Imino-imidazole-chelating ligands

A range of nickel(II) imino-imidazole pro-initiator complexes in which the terminal metal binding motif L has been varied have been prepared and tested for ethylene dimerization (Scheme 1.38).⁶⁸ Each of the nickel complexes **11** was found to be active in combination with 15 equivalents of EtAlCl₂ or 500 equivalents of MAO (Scheme 1.38 and Scheme 1.39). Specifically, activation with EtAlCl₂ proved to be superior to that achieved with MAO, with the former resulting in activities of up to 1033 kg C₂H₄ (mol Ni)⁻¹ h⁻¹bar⁻¹.⁶⁸



Scheme 1.40 Dimerization of ethylene using nickel complexes bearing O^NX tridentate ligands.⁶⁹

1.7.1.1.2 Phosphorus-containing ligands

1.7.1.1.2.1 Bi-dentate P^N ligands

A large variety of bidentate P^N ligands have been used to synthesize nickel-based ethylene dimerization pro-initiators, a selection of which has been reviewed by Braunstein *et al.*⁵⁴ The activities reported for this family of pro-initiators presented in Figure 1.2 strongly depend on the functionalization and type of the ligand used, but are typically around 170 kg C₂H₄ (mol Ni)⁻¹ h⁻¹ bar⁻¹, with selectivities towards butenes in the range 55-94%. Nevertheless, the selectivities towards 1-butene were very poor (< 35%) in all cases, greatly decreasing the industrial importance of these systems.⁵⁴ Interestingly though, in contrast to the nitrogen-based systems examined in section 1.7.1.1.1, where high MAO, MMAO, and Et₂AlCl loadings were used for activation, only 2-14 equivalents of EtAlCl₂ were used to activate most of these phosphorus-containing systems, making them financially and industrially more attractive.⁵⁴

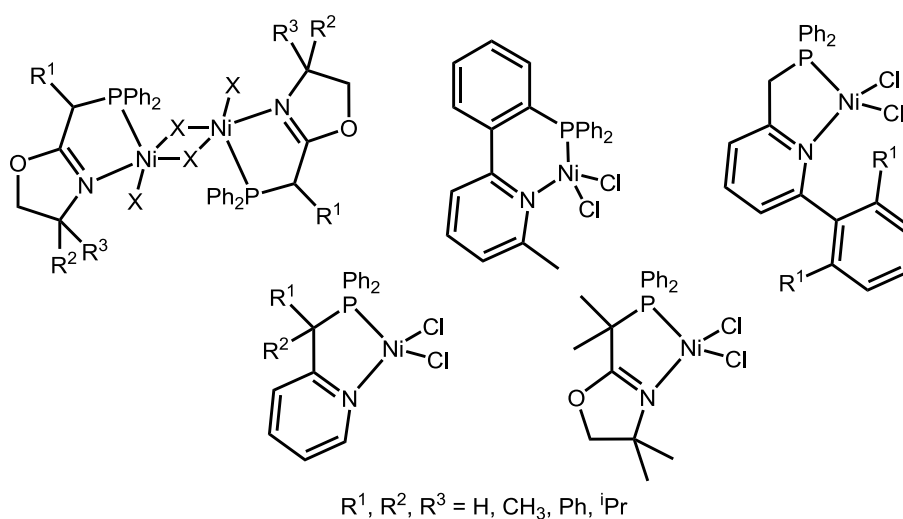
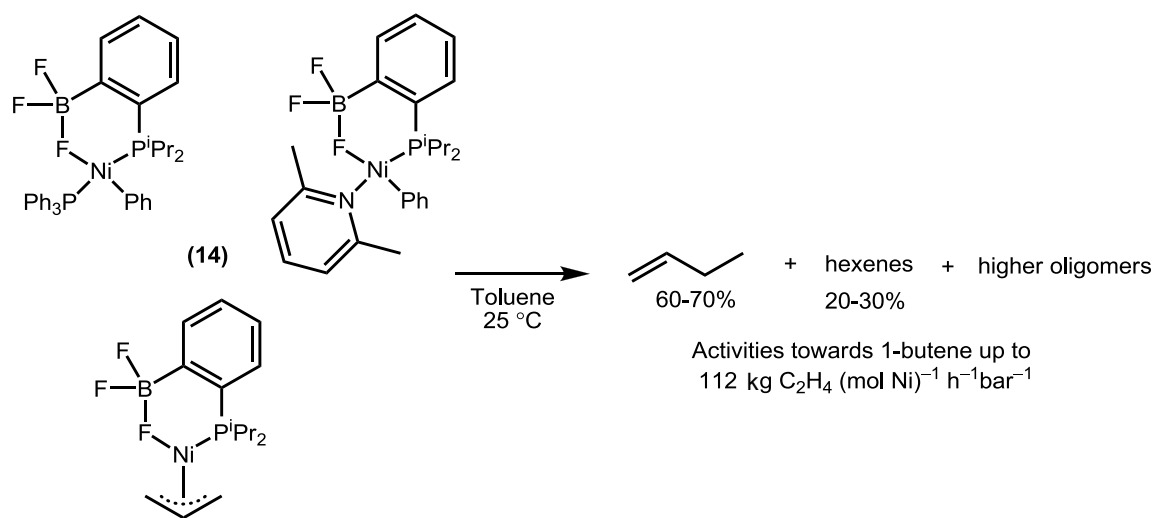


Figure 1.2 A selection of bidentate P^N nickel-based ethylene dimerization pro-initiators.⁵⁴

1.7.1.1.2.2 Phosphino-borate ligands

An interesting class of initiator system based around nickel phosphino borate complexes **14** has been developed, which are able to dimerize ethylene without the use of an activator (Scheme 1.41), with activities towards 1-butene of up to $112 \text{ kg C}_2\text{H}_4 (\text{mol Ni})^{-1} \text{ h}^{-1} \text{ bar}^{-1}$ having been achieved.⁷⁰ Although these activities can be considered relatively low compared to those for nickel-based pro-initiators such as **11-13**, the fact that no aluminum activator is required presents significant safety and economic benefits. However, the selectivities towards butenes achieved using **14** were moderate, in the range 60-70%.

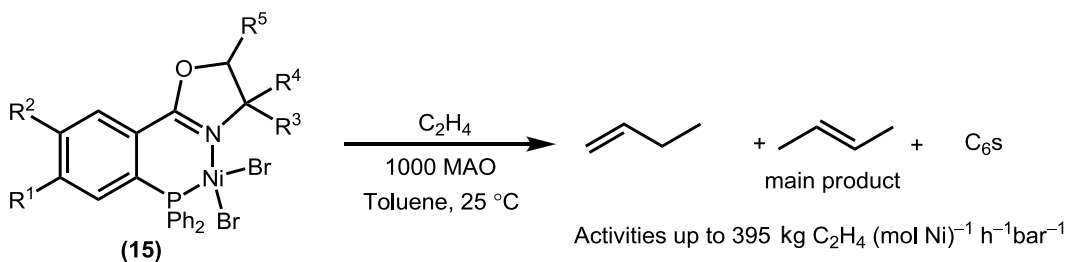


Scheme 1.41 Phosphino borate complexes as activator-free ethylene dimerization systems.⁷⁰

Another interesting feature of the ethylene dimerization reaction mediated by **14** is that once consumption of ethylene is complete, the 1-butene produced is isomerized to the thermodynamically more stable 2-butene, something that does not occur in the presence of ethylene, suggesting preferential ethylene binding over 1-butene.⁷⁰

1.7.1.1.2.3 Phosphinooxazoline ligands

Phosphinooxazoline complexes **15**, Scheme 1.42, achieve reasonable dimerization activities of up to $395 \text{ kg C}_2\text{H}_4 (\text{mol Ni})^{-1} \text{ h}^{-1} \text{ bar}^{-1}$ when activated with MAO. However, although the selectivities towards dimer were good (>74% of the products), the selectivities to 1-butene were low (8.5-52.6%), which in combination with the high aluminum loadings required (1000 equivalents per nickel), limits the industrial value of these systems.⁷¹



R groups = H, Me, Et, OCH₃, Ph

Scheme 1.42 Dimerization of ethylene by phosphinoxazoline pro-initiators activated with 1000 equivalents MAO.⁷¹

Variation of the various R substituents about the metal scaffold of complexes **15** alters catalytic activities, although no clear trends were observed. Furthermore, like most of the nickel systems described here (*vide supra*), catalysis is attenuated at temperatures over 30 °C or by longer reaction times.⁷¹ Again, as was shown for systems **3**, addition of PPh₃ (1 equivalent) to **15** brought about an increase in the systems' catalytic activity, along with an increase in the isomerization of 1-butene. Furthermore, the presence of PPh₃ increased the catalyst lifetime and introduced an induction period prior to the onset of catalysis.⁷¹

1.7.1.1.3 Summary of the basic characteristics of the nickel-, iron-, and cobalt-based ethylene dimerization systems

From the descriptions of the various nickel-, iron-, and cobalt-based ethylene dimerization systems presented above, some common characteristics become apparent for these systems and are summarized below:

- Activity of these systems is optimal at low temperatures (< 30 °C); at higher temperatures the catalytic activity and selectivity to 1-butene decrease.
- Higher ethylene pressures increase activity and selectivity towards 1-butene.
- Generally, the nickel-, iron-, and cobalt-based systems have short catalytic lifetimes, with increased run times resulting in a decrease in activity.
- Addition of PPh₃ before activation results in an increase in catalytic activity at the expense of selectivity towards 1-butene.
- Most of nickel-, iron-, and cobalt-based pro-initiators require activation with 100-2000 equivalents of MAO. However, examples of successful activation with lower loadings of EASQ and Et₂AlCl have also been reported (*e.g.* pro-initiators **11**)

1.7.1.2 Nickel-, cobalt-, and iron-based higher α -olefin dimerization

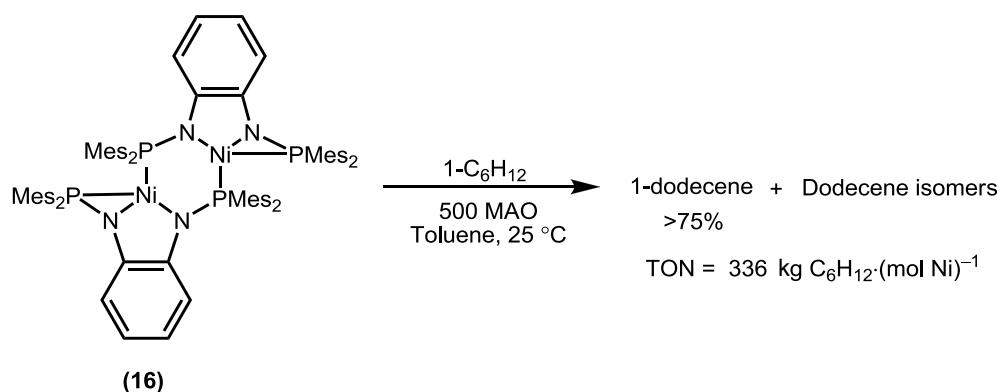
Compared to ethylene, α -olefins are more difficult to dimerize selectively since they are more bulky and can participate in isomerization reactions, with the resulting internal olefins being inert towards dimerization (see section 2.4.2.3). Additionally, the longer-chain dimerization products increase the viscosity of the catalytic reaction mixture, which attenuates catalysis due to mass transport effects. For these reasons, relatively few reports on the selective dimerization of higher α -olefins are available in the

literature compared to those utilising ethylene; selected examples of the catalytic dimerization of α -olefins are presented in this section.

1.7.1.2.1 Nickel-based pro-initiators

A large variety of nickel-based catalytic systems that can selectively dimerize ethylene have been reported to date (see section nickel). However, a search in the literature revealed only a few nickel-based higher α -olefin dimerization systems. One of the oldest was reported in 1971 and uses $\text{Ni}(\text{acac})_2$ which, upon activation with one equivalent of $\text{Et}_2\text{Al}(\text{OEt})$, selectively dimerizes 1-hexene to a mixture of C_{12} products with a high linear dodecene content (81%).⁶² However, the TON^\dagger associated with the formation of the dimer fraction by this system is very low ($6.3 \text{ kg C}_6\text{H}_{12} \cdot (\text{mol Ni})^{-1}$), with significant 1-hexene isomerization being observed (70% of the 1-hexene is converted to internal hexenes), making this system inappropriate for any industrial application.^{72,73}

More recently, however, complex **16** was reported to selectively dimerize 1-hexene with a TON of $336 \text{ kg C}_6\text{H}_{12} \cdot (\text{mol Ni})^{-1}$ (Scheme 1.43).⁷⁴ The most interesting feature of this system is that the main product of the catalytic reaction is 1-dodecene instead of the internal/branched olefins usually observed to originate from the majority of the high α -olefin dimerization systems described in section 1.7.1.2. The selective production of 1-dodecene from **16**/500 MAO is curious, since only internal dodecenes usually result from the dimerization of 1-hexene *via* both metallacyclic and a step-wise addition mechanisms; this unusual selectivity was not commented on by the authors.

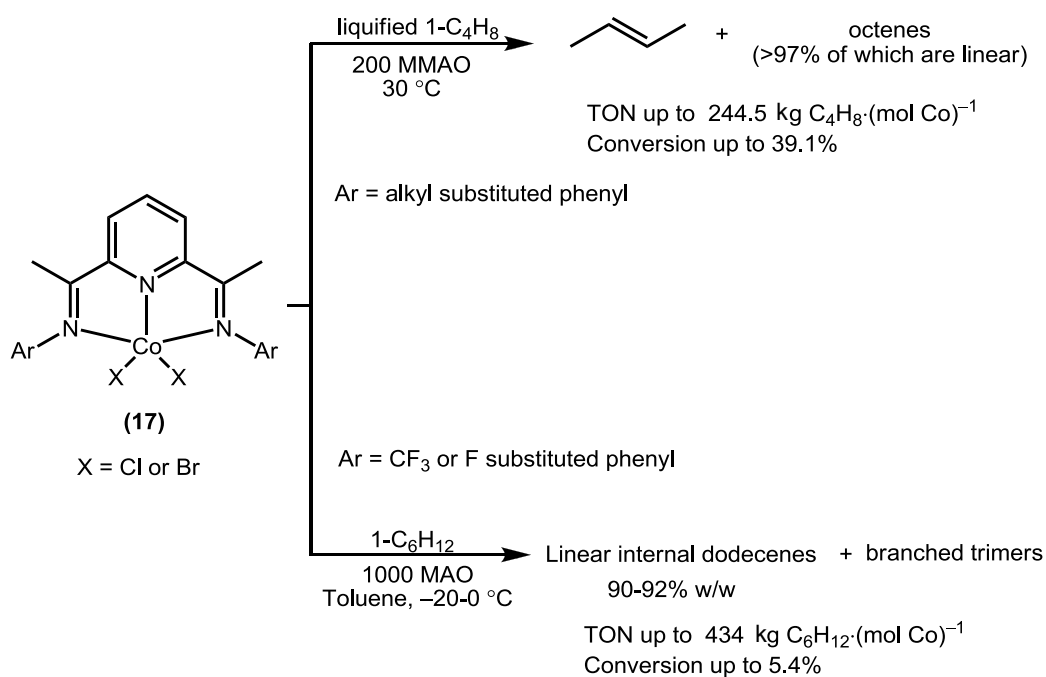


Scheme 1.43 Selective dimerization of 1-hexene to 1-dodecene by the nickel bis(amido) complex **16** activated with 500 MAO.⁷⁴

[†] The performance of ethylene oligomerization systems, in which ethylene is generally supplied at a constant feed rate until no further C_2H_4 uptake is observed, is measured in terms of their activity ($\text{kg C}_2\text{H}_4 \cdot (\text{mol Ni})^{-1} \text{ h}^{-1} \text{ bar}^{-1}$). In contrast, for the oligomerization of higher α -olefins (e.g. 1-hexene) the use of TON ($\text{kg olefin} \cdot (\text{mol Ni})^{-1}$) is more appropriate, (providing a better comparison) since a single aliquot of substrate is typically added at the start of the reaction and consumed as catalysis proceeds. As consumption of the substrate is rarely monitored during reactions, tests are generally left for a specified time before analyses, rather than the time at which catalysis stops.

1.7.1.2.2 Cobalt- and iron-based pro-initiators

The *bis(imino)pyridine* complexes **17**, bearing alkyl-substituted phenyl groups (Scheme 1.44), when activated with 200 equivalents of MMAO, generate systems that can dimerize 1-butene almost exclusively to linear dimers with a TON of $244.5 \text{ kg C}_4\text{H}_8 \cdot (\text{mol Co})^{-1}$.⁶⁵ A step-wise addition mechanism was assumed to be in operation for **17**/MMAO, based on the type of dimers and trimers produced from the oligomerization of propene.^{75,76}

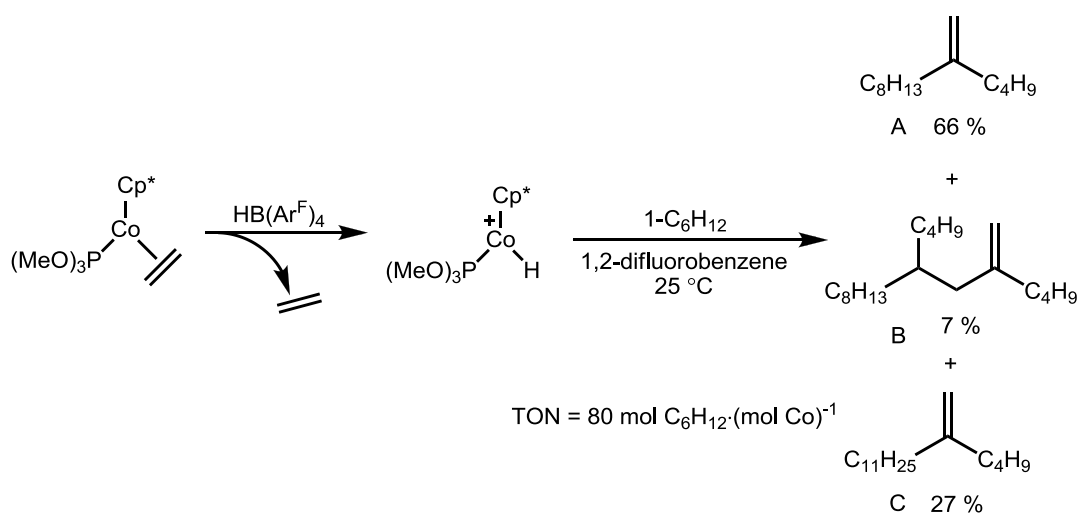


Scheme 1.44 Dimerization of 1-butene and 1-hexene to linear octenes and dodecenes, respectively, using *bis(imino)pyridine* complexes as pro-initiators.⁷⁵⁻⁷⁷

The greatest disadvantage of systems **17** is that they induce extensive isomerization of the substrate, producing 2-butene, which is inert to dimerization, resulting in the low conversions obtained (< 39.1%).⁷⁵ Isomerization occurs exclusively when systems **17** are activated with Et₂AlCl, which subsequently convert 1-hexene almost quantitatively to a mixture of *trans*- and *cis*-2-hexene.⁷⁵ The iron analogues of complexes **17** were also tested in the dimerization of 1-butene and 1-hexene providing similar results to the cobalt complexes, but with slightly higher activities.⁷⁶

Fluoro-substituted pro-initiators of the type **17** have also been synthesized and tested in the oligomerization of olefins (Scheme 1.44).⁷⁷ It appears that the fluoro substitution of the *bis(imino)pyridine* ligand enhances the activity of these cobalt pro-initiators giving systems that are comparable to their usually more active fluorine-free iron analogues.⁷⁷ Hence, complexes **17** activated with 1000 MAO achieved TONs with 1-hexene of up to $434 \text{ kg C}_4\text{H}_8 \cdot (\text{mol Co})^{-1}$ at low reaction temperatures. Notably, pro-initiators **17** do not isomerize the substrate under the described reaction conditions and are highly selective towards linear dodecenes.⁷⁷

From a mechanistic point of view, as was the case for their non-fluorinated analogues, a step-wise addition mechanism was proposed to be operative for **17** (M=Co), involving a cobalt hydride species as the active catalyst.⁷⁷ A similar mechanistic pathway is proposed for a well-defined cobalt-based initiator, reported by Brookhart *et al.*⁷⁸ After activation with HBAr^{F} , the complex $\text{Cp}^*\text{CoP}(\text{OMe})_3(\text{C}_2\text{H}_4)$ was able to dimerize and trimerize 1-hexene selectively towards the dimer **A** and the trimers **B** and **C** (Scheme 1.45), with a TON of $6.7 \text{ kg C}_6\text{H}_{12} \cdot (\text{mol Co})^{-1}$ after 10 days of reaction.⁷⁸ Usually, although well-defined initiators exhibit low activities due to their stability, it is exactly this stability that makes them suitable for mechanistic studies. Hence, it was demonstrated that a stepwise addition mechanism is in operation for the $\text{Cp}^*\text{CoP}(\text{OMe})_3(\text{C}_2\text{H}_4)/\text{HBAr}^{\text{F}}$ system *via* the *in situ* formation of the cationic cobalt hydride $[\text{Cp}^*\text{CoP}(\text{OMe})_3(\text{H})]^+$.⁷⁸



Scheme 1.45 Selective di- and tri-merization of 1-hexene by the well defined cobalt catalyst $[\text{Cp}^*\text{CoP}(\text{OMe})_3(\text{H})][\text{BAr}^{\text{F}}]$.⁷⁸

1.7.2 Palladium- and platinum-catalyzed olefin dimerization

After the successful development of nickel-based dimerization systems, analogues based on palladium and platinum naturally followed. It has been reported that the palladium-containing equivalent of complexes **14**, **18**,^{79,80} along with a variety of palladium complexes with N^N ligands **19**,⁸¹ and the carbene complexes **20**,⁸² Figure 1.3, were synthesized and found to be active in the dimerization of ethylene without the need for an activator.

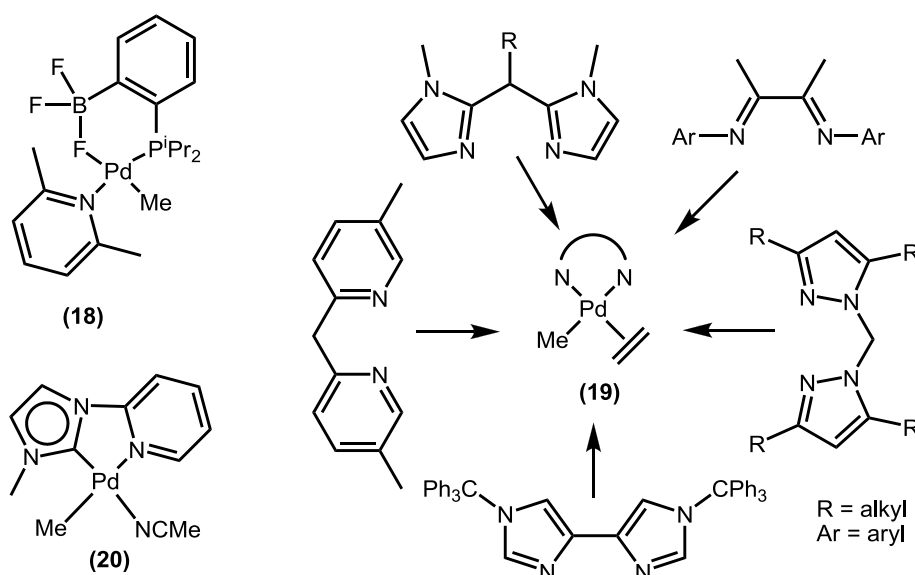


Figure 1.3 Examples of palladium complexes active in the dimerization of ethylene without the use of activators.^{69,70,81,82}

Complexes **18-20** are modest pro-initiators (specific values for activities were not reported in these studies) in the dimerization of ethylene with the dimerization reactions being performed on an NMR scale. Nevertheless, the ability of systems **18-20** to dimerize ethylene without the use of an activator, which significantly simplifies the reaction, allowed the mechanistic study of the dimerization process, revealing that a palladium hydride species is responsible here for dimerization;^{79,81,82} similar results were also obtained for platinum.^{83,84} However, it must be mentioned that neither palladium nor platinum is ideal for developing an industrial dimerization process due to their high cost, especially when the less expensive nickel is able to produce reasonably active ethylene dimerization systems (section 1.7.1).

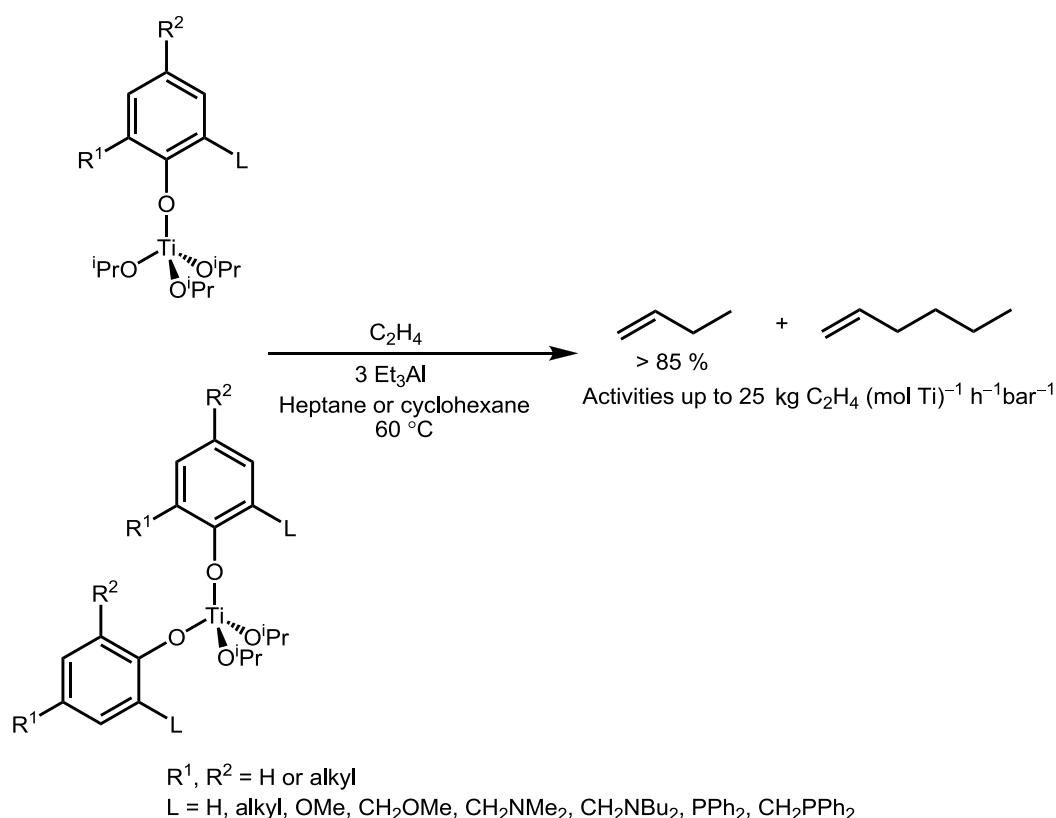
1.7.3 Olefin dimerization based on titanium and zirconium pro-initiators

1.7.3.1 Ethylene dimerization mediated by titanium and zirconium systems

Following the development and success of the Ziegler-Natta ethylene polymerization catalysts, their titanium-based ethylene dimerization equivalents appeared soon after. Hence, the Alphabutol process was born, which is one of the most important industrial processes for the production of 1-butene.⁸⁵ The most efficient of the Alphabutol systems is that using $\text{Ti}(\text{O}i\text{Bu})_4/\text{Et}_3\text{Al}$, which can achieve activities of

approximately 28000 kg C₂H₄ (mol Ti)⁻¹ h⁻¹ with a 1-butene selectivity of ~93%.⁷⁶ The equivalent zirconium alkoxide-based systems have also been examined, but although they exhibit similar selectivities, their activities are much lower compared to those for their titanium analogues.^{49,86}

More recently, titanium(IV) aryloxy-derived ethylene dimerization pro-initiators were reported (Scheme 1.46).^{87,88} However, although the selectivities towards 1-butene obtained were good, these systems proved to have very low activities in the dimerization of ethylene of just over 5 kg C₂H₄ (mol Ti)⁻¹ h⁻¹ bar⁻¹.^{87,88} This is somewhat surprising since the aforementioned very successful Alphabutol process is based on the very similar titanium(IV) alkoxides, and is presumed to reflect a very delicate influence of the ligands' steric and electronic effects.

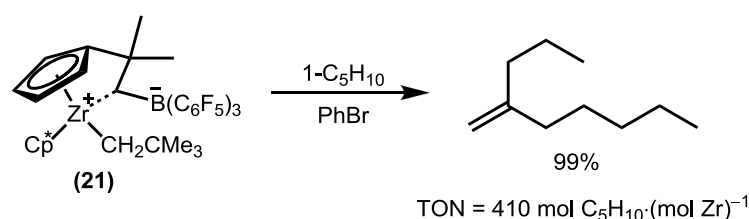


Scheme 1.46 Titanium(IV) aryloxy complexes as pro-initiators for the dimerization of ethylene.^{78,79}

Lastly, an interesting example of titanium-based ethylene dimerization systems is based on the family of titanium(II) complexes CpTiMe(dmpe)₂, CpTiH(dmpe)₂, CpTiCl(dmpe)₂.⁸⁹ These complexes are able to dimerize ethylene without the need of an aluminum activator, reaching activities of up to 25 kg C₂H₄ (mol Ti)⁻¹ h⁻¹ bar⁻¹.⁸⁹ However, the most important aspect of this study is that it suggests that the catalytically active titanium species could be a titanium(II) species, possibly originating from the reduction of Ti(IV) by the aluminum co-initiator.⁸⁹ Additionally, based on the detected organic products and NMR spectroscopic studies of the reaction between CpTiH(dmpe)₂ and ethylene, it is argued that the dimerization mechanism proceeds *via* a metallacyclic pathway, rather than through step-wise addition.⁸⁹

1.7.3.2 Higher α -olefin dimerization mediated by titanium and zirconium systems

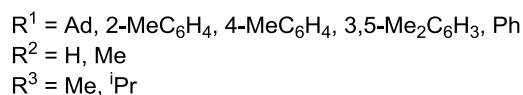
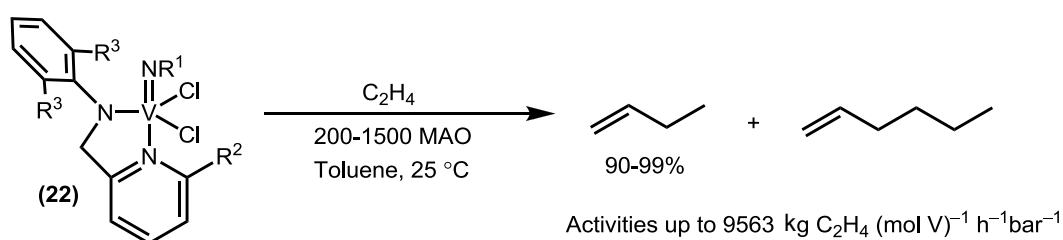
In the field of selective higher α -olefin dimerization, few zirconium-based systems have been reported. For example, it was found that the zirconocene complex **21** (Scheme 1.47) can dimerize 1-pentene to 2-propyl-1-heptene selectively (> 99% selectivity) without the need of an activator.⁹⁰ However, the TON recorded for the **21**-based system is low (410 mol C₅H₁₀·(mol Zr)⁻¹), something ascribed to fast deactivation of this catalyst.⁹¹ Additionally, the system Cp₂ZrCl₂/MAO has been reported to dimerize 1-butene, 1-pentene, 1-hexene and 1-heptene without significant amounts of higher oligomers being formed and a TOF of 6.1·min⁻¹, although little detail is provided.⁹⁰



Scheme 1.47 Highly selective dimerization of 1-pentene by complex **21**.⁹⁰

1.7.4 Vanadium-based olefin dimerization systems

Only recently have complexes of vanadium been used as ethylene dimerization pro-initiators, with only three reports being available from the group of Nomura.⁹²⁻⁹⁴ It should be noted that these imido-bearing vanadium systems have a number of similarities with the Group 6 imido systems described later in this thesis.



Scheme 1.48 Highly selective ethylene dimerization to 1-butene using vanadium imido pro-initiators.⁹²⁻⁹⁴

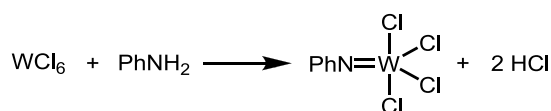
Various vanadium imido complexes bearing (2-anilidomethyl)pyridine ligands have been found to be highly active in the selective dimerization of ethylene to 1-butene with activities of up to 9563 kg C₂H₄ (mol V)⁻¹ h⁻¹bar⁻¹ for complex **22** (R¹ = Ad, R² = H, R³ = Me)⁹² and excellent selectivities towards 1-butene of over 90% for all tested pro-initiators (Scheme 1.48).⁹²⁻⁹⁴ The most interesting feature of these vanadium imido systems is the extreme dependence of their catalytic behavior towards ethylene on the nature of the activator, on the imido substituent, and on the nature of the (2-anilidomethyl)pyridine scaffold. For example, no activity was observed when the pyridine ring of the (2-anilidomethyl)pyridine

ligand was substituted in the *ortho* position ($R^2 \neq H$, Scheme 1.48), while, complexes **22** performed better when $R^3 = \text{Me}$ rather than when $R^3 = \text{iPr}$.⁹² Varying the substituent on the imido ligand has a dramatic effect, specifically, it was found that $R^1 = \text{adamantyl}$ gave the best activities ($\leq 9563 \text{ kg C}_2\text{H}_4 (\text{mol V})^{-1} \text{ h}^{-1} \text{ bar}^{-1}$), while $R^1 = \text{aryl groups with no } ortho \text{ substituents (e.g. 4-MeC}_6\text{H}_4, 3,5\text{-Me}_2\text{C}_6\text{H}_3, \text{Ph})$ resulted in an attenuation of the catalytic activity ($1800 \text{ to } 2300 \text{ kg C}_2\text{H}_4 (\text{mol V})^{-1} \text{ h}^{-1} \text{ bar}^{-1}$).⁹⁴ Interestingly, methyl substitution on one *ortho* position of the aryl imido ligand results in improved activity (of $6250 \text{ kg C}_2\text{H}_4 (\text{mol V})^{-1} \text{ h}^{-1} \text{ bar}^{-1}$) compared to the un-substituted systems,^{92,94} but methyl substitution in both *ortho* positions leads to polymerization.⁹⁵ In terms of activator dependence, polyethylene was obtained when ethylene was reacted with systems **22** activated with Et_2AlCl or Me_2AlCl instead of MAO.

1.7.5 Dimerization of olefins *via* molybdenum- and tungsten-based pro-initiators

1.7.5.1 Discovery of tungsten and molybdenum imido-based ethylene dimerization systems

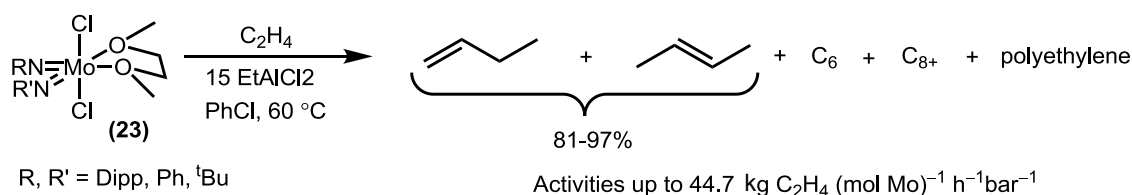
From the studies of the WCl_6 *in situ* olefin oligomerization systems developed by the Goodyear Company¹⁶⁻²¹ and Sasol technology UK²¹ (sections 1.3.2 and 1.3.3), it was found that when WCl_6 is treated with two equivalents of an aryl amine to form the pro-initiator, evolution of HCl occurred, suggesting *in situ* formation of tungsten mono-imido complexes (Scheme 1.49).⁹⁶



Scheme 1.49 Evolution of HCl during the reaction of WCl_6 and PhNH_2 implying formation of a mono-imido complex.⁹⁶

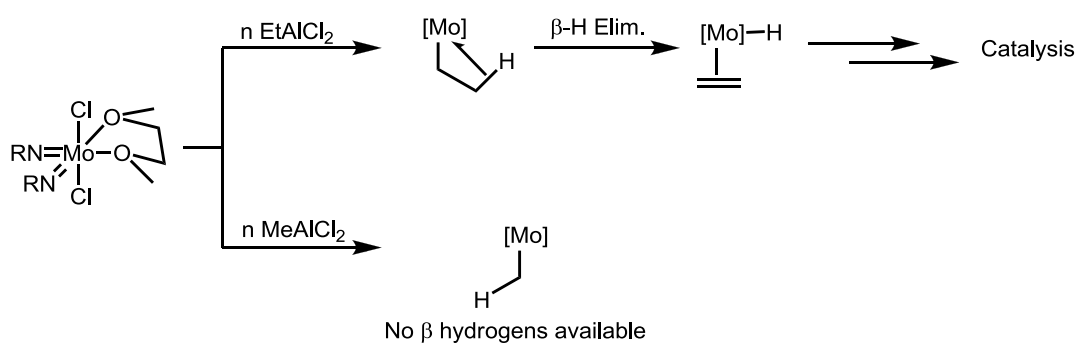
In order to probe the possibility that tungsten imido complexes are indeed responsible for the olefin dimerization activity by the *in situ* WCl_6 /aniline mixture when activated with EtAlCl_2 in the Goodyear and Sasol dimerization systems, the well-defined mono-imido complex $[\text{W}(\text{NPh})\text{Cl}_4]_2$ was tested. Significantly, it was found that $[\text{W}(\text{NPh})\text{Cl}_4]_2$ activated with 40 equivalents of EtAlCl_2 in PhCl solvent does initiate ethylene dimerization with an activity of $0.87 \text{ kg C}_2\text{H}_4 (\text{mol W})^{-1} \text{ h}^{-1} \text{ bar}^{-1}$ and selectivity towards 1-butene of 62%.⁹⁶

Following this successful demonstration, the potential of the somewhat related molybdenum *bis*(imido) complexes was examined in detail by Dyer *et al.*⁹⁷ It was found that complexes of the type **23** are able to dimerize ethylene, upon activation with EtAlCl_2 or MeAlCl_2 , with activities of up to $44.7 \text{ kg C}_2\text{H}_4 (\text{mol W})^{-1} \text{ h}^{-1} \text{ bar}^{-1}$ (Scheme 1.50).



Scheme 1.50 Ethylene dimerization using molybdenum bis(imido) pro-initiators.⁹⁷

Note that the activities of pro-initiators **23** are strongly dependent on the nature of the imido substituents and aluminum activator used during initiation.⁹⁷ For example, it was found that EtAlCl_2 was a much better activator compared to MeAlCl_2 , possibly due to the ability of the former to readily allow access to a metal hydride species *via* a β -hydride elimination reaction, assuming that dimerization occurs *via* a step-wise addition mechanism (Scheme 1.51). Additionally, the sterically demanding Dipp (2,6- $^i\text{Pr}_2\text{-C}_6\text{H}_3$) imido substituent was found to improve the activity for dimerization, presumably due to its ability to protect the imido complex from adopting bridging coordination modes in contrast to the ^tBu and Ph groups.⁹⁸



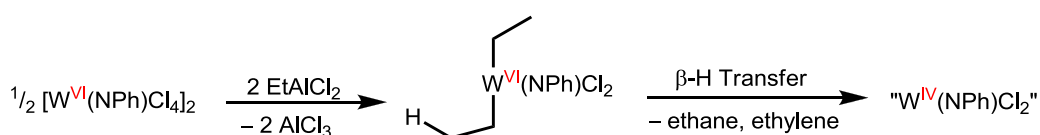
Scheme 1.51 Comparison between MeAlCl_2 and EtAlCl_2 as activators, with the latter allowing formation of a metal hydride species *via* β hydride elimination, which possibly facilitates catalysis.

In an analogous fashion to their impact on catalytic activity, the selectivities observed for these molybdenum pro-initiators also depend strongly on the nature of the imido ligands. For example, $\text{Mo}(\text{NDipp})_2\text{Cl}_2(\text{DME})$ exhibits a high selectivity towards butenes of 97.5% and a selectivity to 1-butene of 78.6% upon activation with EtAlCl_2 . In contrast, $\text{Mo}(\text{NPh})_2\text{Cl}_2(\text{DME})$ is a polymerization rather than a dimerization pro-initiator when activated with EtAlCl_2 with 69.6% of the products being polyethylene.⁹⁸

In addition to the above studies on the dimerization of ethylene with well defined imido pro-initiators, the potential of the Sasol *in situ* system (section 1.3.3) was examined in the dimerization of higher α -olefins such as 1-pentene and 1-hexene by Hanton *et al.*²⁴ In this detailed study, the influence of a multitude of parameters on dimerization performance was examined, including solvent, reaction temperature, olefinic substrate, as well as the amount and type of the primary amine, co-initiator, and tertiary amine used to bind the HCl evolved from the reaction between WCl_6 and PhNH_2 . From this study, it was found that this $\text{WCl}_6/2\text{PhNH}_2/4\text{Et}_3\text{N}$ *in situ* system performed well at 60°C in chlorobenzene with EtAlCl_2 as the co-initiator ($\text{W}:\text{Al} = 1:12$) with TONs of up to $55 \text{ kg C}_6\text{H}_{12} (\text{mol W})^{-1}$ and selectivities towards the dimer fraction of $>99.9\%$.²⁴ Additionally, in the dimer fraction only mono- and di-branched dodecenes were formed, which demonstrates the high selectivity of this system.²⁴

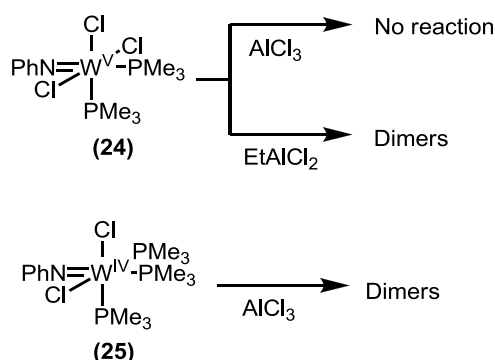
1.7.5.2 Mechanistic aspects of tungsten imido-based ethylene dimerization

In section 1.7.5.1 it was shown that tungsten(VI) imido complexes can dimerize ethylene in combination with an appropriate alkyl aluminum reagent. It is speculated that one of the roles of the aluminum co-initiator is to reduce the tungsten from W(VI) to W(IV) via a double alkylation followed by a β -hydride transfer (Scheme 1.52).⁹⁶ Hence, it is possible that the oxidation state of the active species might be lower than VI. This notion is also supported by studies of the Ziegler-Natta titanium oligomerization systems discussed in section 1.4.1, where reduction of the titanium from Ti(IV) to Ti(III) is proposed,²⁹ and also from the findings of You *et al.* where the Ti(II) complexes CpTiMe(DMPE)₂, CpTiH(DMPE)₂, and CpTiCl(DMPE)₂ were found active in the dimerization of ethylene without the need of an activator.⁸⁹



Scheme 1.52 Generation of a tungsten(IV) species from the reaction between $[W(NDipp)Cl_4]_2$ and $EtAlCl_2$.

In order to probe if a similar reduction does indeed occur in these tungsten imido systems, and thus to investigate the oxidation state of the catalytically active species, complexes **24** and **25** were tested in catalysis (Scheme 1.53). As described in Scheme 1.53, compound **24** is active in the dimerization of ethylene when treated with $EtAlCl_2$, but inactive when treated with $AlCl_3$. In contrast, complex **25** is active for the dimerization of ethylene when treated with $AlCl_3$ with an activity of $0.30 \text{ kg C}_2\text{H}_4 (\text{mol V})^{-1} \text{ h}^{-1} \text{ bar}^{-1}$.⁹⁶ Together, these results suggest that the active catalyst in the Goodyear-/Sasol-type systems is a W(IV) species since $AlCl_3$, lacking alkyl groups, is incapable of bringing about reduction of the W(VI) starting complex (through sequential Al-to-W *trans*-alkylation and subsequent β -hydride elimination and reductive elimination).⁹⁶



Scheme 1.53 Ethylene dimerization with W(VI) and a W(IV) mono-imido complexes.⁹⁶

Apart from the aforementioned ability of $EtAlCl_2$ to possibly reduce the tungsten centre from W(VI) to W(IV), there remains significant speculation around the role of the aluminum co-initiator in the tungsten imido catalyzed oligomerization of olefins. Moreover, computational studies have shown that, depending on whether the active species is a mono- or a bis-(imido) tungsten complex, the aluminum

co-initiator can bind along the W-Cl or W=NPh bonds, respectively.^{47,99} The proposed binding mode of Me₂AlCl in the case of a mono(imido) and a bis(imido) species is depicted in Figure 1.4.

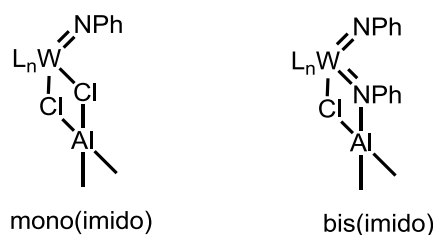
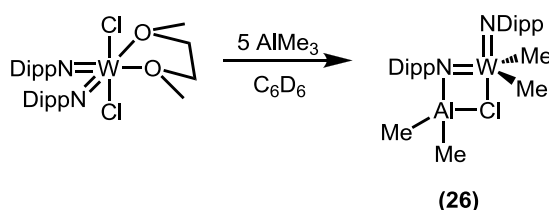


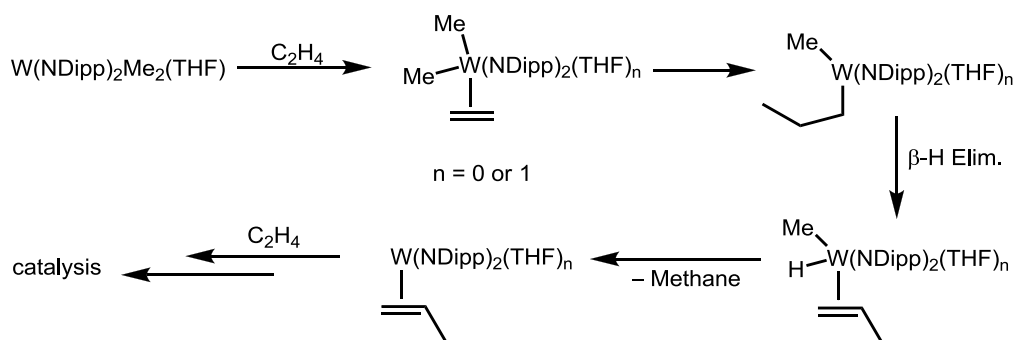
Figure 1.4 Computationally-derived binding modes of Me₂AlCl on imido complexes.^{47,99}

It is speculated that the aluminum co-initiator, in the case of the mono(imido) tungsten systems (Figure 1.4, left), donates some electron density to the tungsten centre and thus stabilizes the catalytically active species making it accessible for the following steps of the dimerization process. Binding of the aluminum co-initiator across the mono(imido) W=NPh bond is unfavorable, since it removes electron density from the W centre, resulting in the formation of a kinetically inaccessible species.³⁸ On the other hand, in the case of a bis(imido) complex (Figure 1.4, right), the tungsten centre is electronically saturated due to the presence of two imido moieties. Thus, the aluminum co-initiator binds across the W=NPh bond removing some electron density from the tungsten centre, which facilitates the β -hydride elimination process.^{47,99} The formation of bis(imido) tungsten alkylchloroaluminate adducts has also been confirmed experimentally from the reaction of W(NDipp)₂Cl₂(DME) with five equivalents of AlMe₃, which yields compound **26** as described in Scheme 1.54. Interestingly, **26** was found to be inactive in the dimerization of ethylene.⁹⁷



Scheme 1.54 Formation of a bis(imido) tungsten alkylchloroaluminate adduct.⁹⁷

In contrast, the complex W(NDipp)₂Me₂(THF), produced by displacement of Me₂AlCl by THF, reacts with ethylene to generate a mixture of methane and but-1-ene.⁹⁷ This contrasts to the aforementioned computational calculations on these systems, which suggest that coordination of the aluminum on the catalyst is necessary for dimerization to occur.^{47,99} The methane evolved from this reaction suggests that ethylene insertion into a tungsten-methyl bond takes place, followed by β -hydride elimination, and subsequent reductive elimination leading to the active catalyst (Scheme 1.55).⁹⁷



Scheme 1.55 Possible mechanism for the formation of methane from the reaction between $W(NDipp)_2Me_2(THF)$ and ethylene.⁹⁷

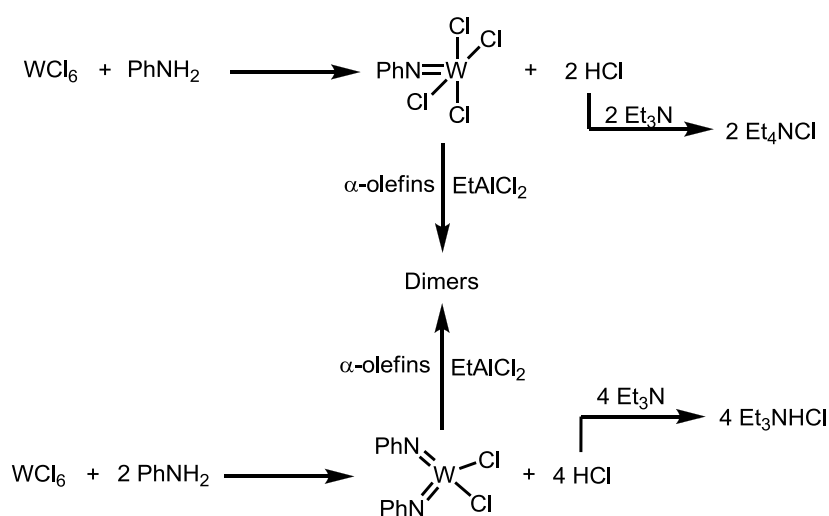
In addition to the above mechanistic studies with well-defined tungsten imido complexes,²⁴ analysis of the dimerization products resulting from reaction of 1-pentene with $WCl_6/2PhNH_2/4Et_3N/12EtAlCl_2$ revealed that this *in situ* system is highly selective since from the 57 possible $C_{10}H_{20}$ isomers, only 8 are formed.²⁴ Moreover, it was suggested that dimerization occurs *via* a step-wise addition mechanism rather than a metallacyclic process. This was supported by three arguments. Firstly, isomerization of 1-pentene to 2-pentene was observed. This can easily occur in the presence of a metal hydride species, something that is characteristic of a step-wise addition mechanism (section 1.4). Secondly, the formation of 4- and 5-decenes was observed, products that are characteristic of a step-wise addition mechanism. On the other hand, dimers that are formed *via* a metallacyclic mechanism, *i.e.* 3-decenes were absent.²⁴ Lastly, deuterium labeling experiments revealed full isotopic scrambling for the *in situ*²⁴ and the well-defined tungsten imido systems,³⁹ which is again supportive of a step-wise addition mechanism (section 1.6.3). However, it must be born in mind that considering the complexity of the *in situ* system, the possibility for simultaneous operation of both metallacyclic and step-wise (that can mediate isomerization) mechanisms form different tungsten species, which lead to the aforementioned characteristics of the *in situ* system, cannot be easily excluded.

1.8 Objectives of the present work

From the above observations (section 1.7.5) it is evident that the tungsten imido-based olefin dimerization systems are mechanistically complex and that additional studies are necessary in order to obtain a better understanding of their mode of operation. Additionally, in contrast to the work describing vanadium⁹²⁻⁹⁴ and molybdenum⁹⁸ imido-based systems, the potential of tungsten imido complexes in the catalytic dimerization of ethylene and 1-hexene has not been extensively studied. Hence, following the work of Dyer *et al.*,^{97,98,100} the objective of the work described in this thesis is to develop and optimize novel tungsten imido-based α -olefin dimerization systems with potential industrial applications. Additionally, attempts will be made to gain insight into the mechanistic aspects of the tungsten imido-based olefin dimerization processes, with the aim of further improving the activities and selectivities of these systems.

The emphasis on tungsten imido complexes as pro-initiators for olefin dimerization arises from the observation that in the Goodyear *in situ* dimerization system HCl is evolved when WCl_6 is mixed with

aniline to form the pro-initiator (section 1.3.2). Similarly, in the Sasol *in situ* dimerization system, a tertiary amine is necessary to bind the evolved HCl (section 1.3.3). Taking these observations together, it is likely that tungsten bis(imido) or/and mono(imido) species are formed in the Goodyear and Sasol ethylene dimerization systems (Scheme 1.56). Hence, an endeavor of this work is to synthesize well-defined tungsten bis(imido) complexes and test them in the dimerization of ethylene and 1-hexene under various different catalytic conditions (varying substrate, type of activator, W:activator ratio, temperature, pressure, and use of additives). Additionally, structure-catalytic activity correlations will be established by varying the nature of the imido substituents on the tungsten. As a final step, reactions of tungsten bis(imido) complexes with aluminum reagents will be explored in order to gain insight into the way in which these tungsten pro-initiators are activated and, potentially, into the nature of the catalytically active species.



Scheme 1.56 Possible formation of tungsten bis- and mono-(imido) complexes in the Goodyear and Sasol olefin dimerization systems.

Since the reaction between WCl_6 and $2 \text{PhNH}_2/4 \text{Et}_3\text{N}$ is complex leading to a multitude of products,¹⁰⁰ it is possible that apart from tungsten bis(imido) complexes, tungsten mono(imido) complexes are also formed (Scheme 1.56). For this reason, the studies on bis(imido) tungsten complexes will be extended to their mono(imido) counterparts, something that will allow a detailed comparison of the two systems.

Lastly, building on the work by Nomura *et al.*, which focused on the dimerization of ethylene using vanadium mono(imido) complexes,⁹²⁻⁹⁴ the use of tantalum and niobium imido complexes makes a logical extension. Hence, a selection of tantalum and niobium imido complexes have been synthesized and tested in the catalytic dimerization of ethylene and 1-hexene under similar conditions to those employed for their tungsten-based analogues.

1.9 References

- (1) Mol, J. C. *Journal of Molecular Catalysis a-Chemical* **2004**, 213, 39.
- (2) Kaminsky, W.; Arndt-Rosenau, M. In *Applied Homogeneous Catalysis with Organometallic Compounds*; Wiley-VCH Verlag GmbH: 2008, p 213.
- (3) Shubkin, R. L.; Baylerian, M. S.; Maler, A. R. *Industrial & Engineering Chemistry Product Research and Development* **1980**, 19, 15.
- (4) Bergemann, C.; Cropp, R.; Luft, G. *Journal of Molecular Catalysis a-Chemical* **1996**, 105, 87.
- (5) Barker, G. E.; Forster, D. In *United States Patent*, Co., M., Ed.; Monsanto Co.: United States 1984; Vol. 4,426,542.
- (6) Hofmann, P.; Kosswig, K.; Schaefer, W. *Industrial & Engineering Chemistry Product Research and Development* **1980**, 19, 330.
- (7) Robertson, R. A. M.; Cole-Hamilton, D. J. *Coordination Chemistry Reviews* **2002**, 225, 67.
- (8) Hartwig, J. *Organotransition Metal Chemistry*; University Science Books: California, 2010.
- (9) Flory, P. J. *Journal of the American Chemical Society* **1940**, 62, 1561.
- (10) BP Statistical Review of World Energy; https://www.google.com/url?q=http://www.bp.com/liveassets/bp_internet/globalbp/globalbp_uk_english/reports_and_publications/statistical_energy_review_2008/STAGING/local_assets/2010_downloads/statistical_review_of_world_energy_full_report_2010.pdf&sa=U&ei=SE0WUuHIDMOshQfZ3IG4DQ&ved=0CAcQFjAA&client=internal-uds-cse&usq=AFQjCNHHpt92mVKdxv312ujkWaryqYIkRq; 2010.
- (11) In *Oilfield Review* 2003; Vol. 15.
- (12) de Klerk, A. *Green Chemistry* **2008**, 10, 1249.
- (13) Gaube, J.; Klein, H. F. *Journal of Molecular Catalysis a-Chemical* **2008**, 283, 60.
- (14) Chauvin, Y.; Gilbert, B.; Guibard, I. *Journal of the Chemical Society-Chemical Communications* **1990**, 1715.
- (15) Gilbert, B.; Olivier-Bourbigou, H.; Favre, F. *Oil & Gas Science and Technology-Revue De L Institut Francais Du Petrole* **2007**, 62, 745.
- (16) Wideman, L. G. In *United States Patent Office*; Company, G. T. a. R., Ed. United States, 1974.
- (17) Menapace, R.; Benner, G. S.; Maly, N. A. In *United States Patent Office*; Company, G. T. a. R., Ed. United States, 1974.
- (18) Maly, N. A.; Menapace, R.; Benner, G. S. In *United States Patent Office*; Company, G. R. a. T., Ed.; United States Patent Office: United States, 1974.
- (19) Maly, N. A.; Menapace, R.; Benner, G. S. In *United States Patent Office*; company, G. t. a. r., Ed. United States Patent Office, 1974.
- (20) Maly, N. A.; Menapace, R.; Benner, G. S. In *United States Patent*; Company, T. G. T. a. R., Ed. United States, 1975.
- (21) Brown, M.; Menapace, H. R.; Maly, N. A. In *United States Patent*; Company, T. G. T. a. R., Ed. United States, 1975.
- (22) Hendriksen, D. E.; Exxon Chemical Patents: United States, 1991.
- (23) Tooze, R. P.; Hanton, M. J. In *World Intellectual Property Organization*; B01J 31/00 ed.; Limited, S. T. U., Ed. World Intellectual Property Organization, 2005.
- (24) Hanton, M. J.; Daubney, L.; Lebl, T.; Polas, S.; Smith, D. M.; Willemse, A. *Dalton Trans* **2010**, 39, 7025.
- (25) Pillai, S. M.; Ravindranathan, M.; Sivaram, S. *Chemical Reviews* **1986**, 86, 353.
- (26) Ittel, S. D.; Johnson, L. K.; Brookhart, M. *Chemical Reviews* **2000**, 100, 1169.
- (27) Skupinska, J. *Chemical Reviews* **1991**, 91, 613.
- (28) Roy, D.; Sunoj, R. B. *Organic & Biomolecular Chemistry* **2010**, 8, 1040.
- (29) Novaro, O.; Chow, S.; Magnouat, P. *Journal of Catalysis* **1976**, 41, 91.
- (30) Tomov, A. K.; Chirinos, J. J.; Jones, D. J.; Long, R. J.; Gibson, V. C. *Journal of the American Chemical Society* **2005**, 127, 10166.
- (31) Tomov, A. K.; Chirinos, J. J.; Long, R. J.; Gibson, V. C.; Elsegood, M. R. J. *Journal of the American Chemical Society* **2006**, 128, 7704.
- (32) Chen, Y.; Credendino, R.; Callens, E.; Atiqullah, M.; Al-Harhi, M. A.; Cavallo, L.; Basset, J.-M. *Acs Catal* **2013**, 1360.
- (33) Yu, Z. X.; Houk, K. N. *Angewandte Chemie-International Edition* **2003**, 42, 808.
- (34) Dixon, J. T.; Green, M. J.; Hess, F. M.; Morgan, D. H. *Journal of Organometallic Chemistry* **2004**, 689, 3641.
- (35) McGuinness, D. S. *Organometallics* **2009**, 28, 244.

- (36) Qi, Y.; Dong, Q.; Zhong, L.; Liu, Z.; Qiu, P.; Cheng, R.; He, X.; Vanderbilt, J.; Liu, B. *Organometallics* **2010**, *29*, 1588.
- (37) Datta, S.; Fischer, M. B.; Wreford, S. S. *Journal of Organometallic Chemistry* **1980**, *188*, 353.
- (38) Zhu, B.; Guo, C.; Liu, Z.; Yin, Y. *Journal of Applied Polymer Science* **2004**, *94*, 2451.
- (39) Komon, Z. J. A.; Bu, X.; Bazan, G. C. *Journal of the American Chemical Society* **2000**, *122*, 1830.
- (40) Frediani, M.; Piel, C.; Kaminsky, W.; Bianchini, C.; Rosi, L. *Macromolecular Symposia* **2006**, *236*, 124.
- (41) Connon, S. J.; Blechert, S. *Angewandte Chemie-International Edition* **2003**, *42*, 1900.
- (42) Sanford, M. S.; Love, J. A.; Grubbs, R. H. *Journal of the American Chemical Society* **2001**, *123*, 6543.
- (43) Rupprecht, G. A.; Messerle, L. W.; Fellmann, J. D.; Schrock, R. R. *Journal of the American Chemical Society* **1980**, *102*, 6236.
- (44) Calderon, N.; Ofstead, E. A.; Ward, J. P.; Judy, W. A.; Scott, K. W. *Journal of the American Chemical Society* **1968**, *90*, 4133.
- (45) Calderon, N.; Chen, H. Y.; Scott, K. W. *Tetrahedron Letters* **1967**, *8*, 3327.
- (46) Herrmann, W. A.; Prinzh, M. *Applied Homogeneous Catalysis with Organometallic Compounds*; Wiley-VCH: Weinheim, 2002.
- (47) Tobisch, S. *Organometallics* **2007**, *26*, 6529.
- (48) Agapie, T.; Labinger, J. A.; Bercaw, J. E. *Journal of the American Chemical Society* **2007**, *129*, 14281.
- (49) Suttill, J. A.; McGuinness, D. S. *Organometallics* **2012**, *31*, 7004.
- (50) Tomov, A. K.; Gibson, V. C.; Britovsek, G. J. P.; Long, R. J.; van Meurs, M.; Jones, D. J.; Tellmann, K. P.; Chirinos, J. J. *Organometallics* **2009**, *28*, 7033.
- (51) Keim, W.; Schulz, R. P. *Journal of Molecular Catalysis* **1994**, *92*, 21.
- (52) Keim, W.; Behr, A.; Limbacher, B.; Kruger, C. *Angewandte Chemie-International Edition in English* **1983**, *22*, 503.
- (53) Peuckert, M.; Keim, W. *Organometallics* **1983**, *2*, 594.
- (54) Speiser, F.; Braunstein, P.; Saussine, L. *Accounts of Chemical Research* **2005**, *38*, 784.
- (55) Ulbrich, A.; Campedelli, R. R.; Milani, J. L. S.; dos Santos, J. H. Z.; Casagrande, O. D. *Applied Catalysis a-General* **2013**, *453*, 280.
- (56) Ajellal, N.; Kuhn, M. C. A.; Boff, A. D. G.; Hörner, M.; Thomas, C. M.; Carpentier, J.-F.; Casagrande, O. L. *Organometallics* **2006**, *25*, 1213.
- (57) Chandran, D.; Lee, K. M.; Chang, H. C.; Song, G. Y.; Lee, J. E.; Suh, H.; Kim, I. *Journal of Organometallic Chemistry* **2012**, *718*, 8.
- (58) Murtuza, S.; Casagrande, O. L.; Jordan, R. F. *Organometallics* **2002**, *21*, 1882.
- (59) Gil, M. P.; dos Santos, J. H. Z.; Casagrande, O. L. *Macromol. Chem. Phys.* **2001**, *202*, 319.
- (60) Furlan, L. G.; Gil, M. P.; Casagrande, O. L. *Macromol. Rapid Commun.* **2000**, *21*, 1054.
- (61) Michiue, K.; Oshiki, T.; Takai, K.; Mitani, M.; Fujita, T. *Organometallics* **2009**, *28*, 6450.
- (62) Kunrath, F. A.; de Souza, R. F.; Casagrande, O. L.; Brooks, N. R.; Young, V. G. *Organometallics* **2003**, *22*, 4739.
- (63) Song, S. J.; Li, Y.; Redshaw, C.; Wang, F. S.; Sun, W. H. *Journal of Organometallic Chemistry* **2011**, *696*, 3772.
- (64) Song, S. J.; Zhao, W. Z.; Wang, L.; Redshaw, C.; Wang, F. S.; Sun, W. H. *Journal of Organometallic Chemistry* **2011**, *696*, 3029.
- (65) Xiao, T.; Lai, J.; Zhang, S.; Hao, X.; Sun, W.-H. *Catalysis Science & Technology* **2011**, *1*, 462.
- (66) Hao, P.; Song, S. J.; Xiao, T. P. F.; Li, Y.; Redshaw, C.; Sun, W. H. *Polyhedron* **2013**, *52*, 1138.
- (67) Jie, S.; Zhang, S.; Sun, W. H. *European Journal of Inorganic Chemistry* **2007**, 5584.
- (68) Boudier, A.; Breuil, P. A. R.; Magna, L.; Olivier-Bourbigou, H.; Braunstein, P. *Journal of Organometallic Chemistry* **2012**, *718*, 31.
- (69) Xu, C. J.; Shen, Q.; Sun, X. L.; Tang, Y. *Chinese Journal of Chemistry* **2012**, *30*, 1105.
- (70) Gutsulyak, D. V.; Gott, A. L.; Piers, W. E.; Parvez, M. *Organometallics* **2013**.
- (71) Tang, X.; Zhang, D.; Jie, S.; Sun, W.-H.; Chen, J. *Journal of Organometallic Chemistry* **2005**, *690*, 3918.
- (72) Jones, J. R.; Symes, T. J. *Journal of the Chemical Society C: Organic* **1971**, 1124.
- (73) daRosa, R. G.; deSouza, M. O.; deSouza, R. F. *Journal of Molecular Catalysis a-Chemical* **1997**, *120*, 55.
- (74) Majoumo-Mbe, F.; Lonneck, P.; Volkis, V.; Sharma, M.; Eisen, M. S.; Hey-Hawkins, E. *Journal of Organometallic Chemistry* **2008**, *693*, 2603.
- (75) Small, B. L. *Organometallics* **2003**, *22*, 3178.
- (76) Small, B. L.; Marcucci, A. J. *Organometallics* **2001**, *20*, 5738.

- (77) Tellmann, K. P.; Gibson, V. C.; White, A. J. P.; Williams, D. J. *Organometallics* **2004**, *24*, 280.
- (78) Broene, R. D.; Brookhart, M.; Lamanna, W. M.; Volpe, A. F. *Journal of the American Chemical Society* **2005**, *127*, 17194.
- (79) Gott, A. L.; Piers, W. E.; Dutton, J. L.; McDonald, R.; Parvez, M. *Organometallics* **2011**, *30*, 4236.
- (80) Kim, Y.; Jordan, R. F. *Organometallics* **2011**, *30*, 4250.
- (81) Burns, C. T.; Jordan, R. F. *Organometallics* **2007**, *26*, 6726.
- (82) Khlebnikov, V.; Meduri, A.; Mueller-Bunz, H.; Montini, T.; Fornasiero, P.; Zangrando, E.; Milani, B.; Albrecht, M. *Organometallics* **2012**, *31*, 976.
- (83) Sheng, Y.; Geng, Z. Y.; Wang, Y. C.; Wang, Y. Z.; Sun, X. J. *Chinese Journal of Chemistry* **2011**, *29*, 1084.
- (84) Shiotsuki, M.; White, P. S.; Brookhart, M.; Templeton, J. L. *Journal of the American Chemical Society* **2007**, *129*, 4058.
- (85) McGuinness, D. S. *Chemical Reviews* **2011**, *111*, 2321.
- (86) Al-Sa'doun, A. W. *Applied Catalysis A: General* **1993**, *105*, 1.
- (87) Grasset, F.; Cazaux, J. B.; Magna, L.; Braunstein, P.; Olivier-Bourbigou, H. *Dalton Transactions* **2012**, *41*, 10396.
- (88) Cazaux, J. B.; Braunstein, P.; Magna, L.; Saussine, L.; Olivier-Bourbigou, H. *European Journal of Inorganic Chemistry* **2009**, 2942.
- (89) You, Y. J.; Girolami, G. S. *Organometallics* **2008**, *27*, 3172.
- (90) Christoffers, J.; Bergman, R. G. *Journal of the American Chemical Society* **1996**, *118*, 4715.
- (91) van der Heijden, H.; Hessen, B.; Orpen, A. G. *Journal of the American Chemical Society* **1998**, *120*, 1112.
- (92) Zhang, S.; Nomura, K. *Journal of the American Chemical Society* **2010**, *132*, 4960.
- (93) Igarashi, A.; Zhang, S.; Nomura, K. *Organometallics* **2012**, *31*, 3575.
- (94) Nomura, K.; Igarashi, A.; Katao, S.; Zhang, W. J.; Sun, W. H. *Inorganic Chemistry* **2013**, *52*, 2607.
- (95) Onishi, Y.; Katao, S.; Fujiki, M.; Nomura, K. *Organometallics* **2008**, *27*, 2590.
- (96) Olivier, H.; Laurent-Grot, P. *Journal of Molecular Catalysis A: Chemical* **1999**, *148*, 43.
- (97) Wright, W. R. H.; Batsanov, A. S.; Howard, J. A. K.; Tooze, R. P.; Hanton, M. J.; Dyer, P. W. *Dalton Transactions* **2010**, *39*, 7038.
- (98) Wright, W. R. H.; Batsanov, A. S.; Messinis, A. M.; Howard, J. A. K.; Tooze, R. P.; Hanton, M. J.; Dyer, P. W. *Dalton Transactions* **2012**, *41*, 5502.
- (99) Tobisch, S. *Dalton Transactions* **2008**, 2120.
- (100) Wright, W. R. H., PhD Thesis, Durham University, 2009.

2 Understanding ethylene and 1-hexene dimerization mediated by tungsten bis(imido) pro-initiators

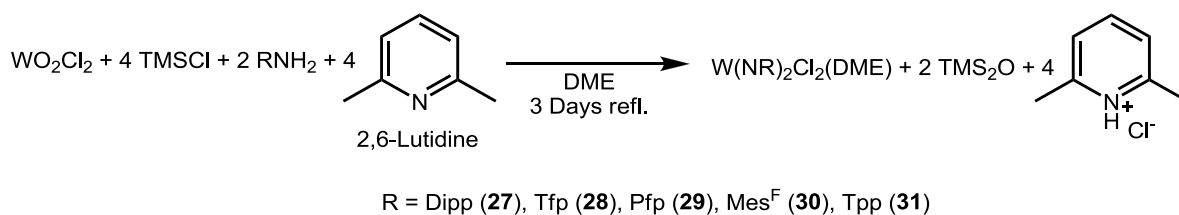
2.1 Introduction

In sections 1.3.3 and 1.8 it was highlighted that the reaction between WCl_6 , $PhNH_2$, and Et_3N results in a complex mixture of products, which after activation with $EtAlCl_2$, is able to dimerize α -olefins.¹ In this WCl_6 -based olefin dimerization system, the *in situ* formation of tungsten bis(imido) complexes has often been inferred or assumed, with such species then being intimately involved in catalysis following activation with $EtAlCl_2$.^{1,2} Indeed, preliminary experiments have confirmed that discrete tungsten bis(imido) complexes are able to catalyze the dimerization of ethylene in the presence of an appropriate aluminium-containing activator.^{3,4} Hence, in this chapter the potential of a variety of well-defined tungsten bis(imido) complexes in the dimerization of ethylene and 1-hexene under various conditions is examined in detail, with a view to further developing and increasing understanding of tungsten imido-based catalytic olefin dimerization.

2.2 Synthesis of tungsten bis(imido) complexes

2.2.1 Synthesis of bis(imido) complexes of the type $W(NR)_2Cl_2(DME)$

A selection of symmetric tungsten bis(imido) complexes was synthesized by modifying the synthetic methodology reported by Schrock *et al.* for the synthesis of $W(NDipp)_2Cl_2(DME)$ (**27**).⁵ Hence, WO_2Cl_2 was reacted with $TMSCl$, 2,6-lutidine, and the appropriate primary amine in DME, to give crude bis(imido) complexes **27-31**, which can be purified *via* recrystallization (Scheme 2.1). Note, the synthesis of complex **29** has, subsequently been reported recently using a different methodology.⁶

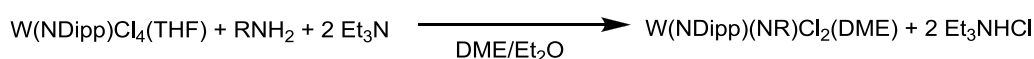
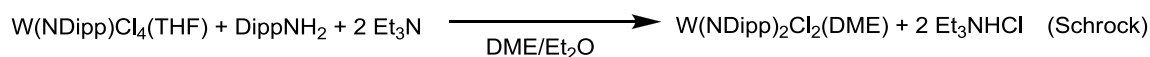


Scheme 2.1 Synthesis of complexes $W(NR)_2Cl_2(DME)$ ($R = Dipp$ (**27**)⁵, Tfp (**28**), Pfp (**29**)⁶, Mes^F (**30**), Tpp (**31**))

2.2.2 Synthesis of mixed bis(imido) complexes of the type W(NDipp)(NR)Cl₂(DME)

2.2.2.1 Synthesis of tungsten mixed bis(imido) complexes

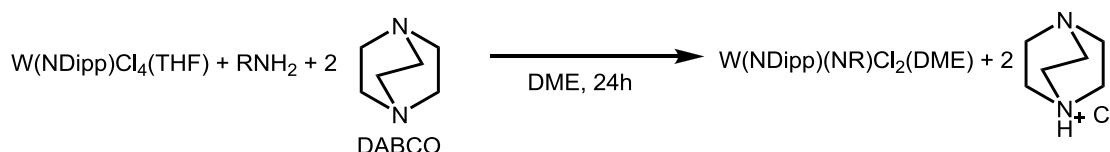
The synthesis of mixed imido complexes of the type W(NR)(NDipp)Cl₂(DME) (R = alkyl or aryl) was deemed necessary in order to broaden the range of electronic and steric tuning of the tungsten bis(imido) systems. For this reason, the reaction, reported by Schrock *et al.*, of W(NDipp)Cl₄(THF) and DippNH₂/2 Et₃N, which affords W(NDipp)₂Cl₂(DME) (**27**) was studied in greater depth, since replacing DippNH₂ with RNH₂ (R = alkyl or aryl) could lead to formation of the desired mixed imido complexes (Scheme 2.2).⁵ However, it was found that using Schrock's procedure, purification of the formed W(NDipp)₂Cl₂(DME) (**27**) is difficult due to the slight solubility of Et₃NHCl (which forms as a co-product from the reaction between Et₃N and the HCl released during formation of the imido bond), in the reaction medium. Similar problems were encountered in the synthesis of **27** from WO₂Cl₂, as described in section 2.2.1.⁴



R = alkyl or aryl

Scheme 2.2 Initial attempts to synthesise tungsten mixed bis(imido) complexes W(NR)(NDipp)Cl₂(DME), based on a synthetic methodology reported by Schrock *et al.*⁵

Consequently, a modification of the procedure described in Scheme 2.2 was used, in which Et₃N was replaced with DABCO and the solvent changed to DME alone. This allowed the synthesis of a variety of mixed bis(imido) complexes as described in Scheme 2.3. The use of DABCO here is crucial, since the significantly poor solubility of the resulting DABCO·HCl salt in DME, allows its efficient separation from the reaction mixture *via* simple filtration.



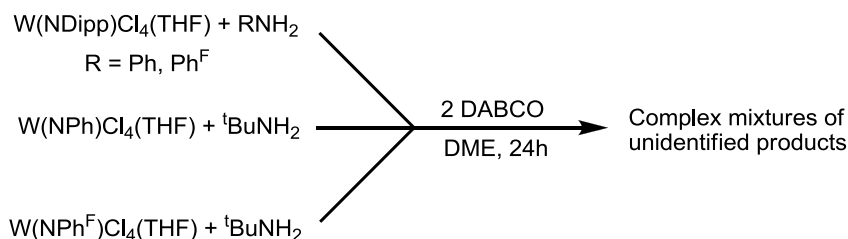
R = ⁱPr (**32**), ^tBu (**33**), Mes (**34**), Tfp (**35**), Tpp (**36**), Dnp (**37**)

Scheme 2.3 Synthesis of complexes W(NR)(NDipp)Cl₂(DME) (R = ⁱPr (**32**), ^tBu (**33**), Mes (**34**), Tfp (**35**), Tpp (**36**), Dnp (**37**))

2.2.2.2 Limitations to the synthesis of tungsten mixed bis(imido) complexes

It must be noted that the amine used in the synthesis of the mixed imido complexes (section 2.2.2.1) must have certain characteristics in order for the reaction to be successful. For example, attempts to

were all unsuccessful, with mixtures of products being formed instead of the well-defined bis(imido) complexes (Scheme 2.6).



Scheme 2.6 Attempted synthesis of bis(imido) tungsten complexes with 2,6-un-substituted aromatic imido ligands

It is proposed that the 2,6-substitution of the aromatic ring of the imido ligands is essential in order to prevent the NAr groups from adopting metal-bridging coordination modes; an example of a bridging NPh group in a tungsten imido complex is presented in Figure 2.1.⁷ Hence, it is possible that bridged imido complexes, similar to the known material **38** (Figure 2.1), could result from the reaction between $W(NPh)Cl_4(THF)$ and $^tBuNH_2/2$ DABCO (Scheme 2.6).

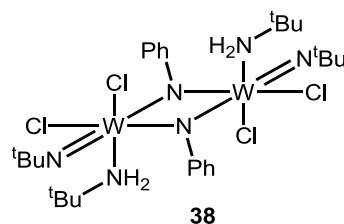
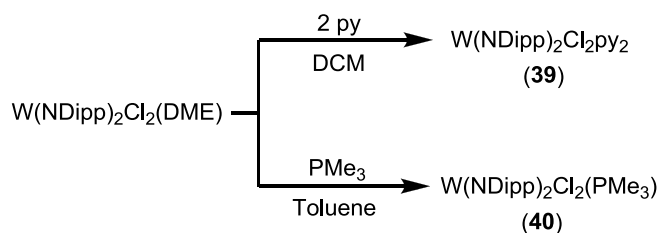


Figure 2.1 Example of an unsymmetrical tungsten bis(imido) complex with bridging NPh groups⁷

2.2.3 Synthesis of $W(NDipp)_2Cl_2(py)_2$ (**39**) and $W(NDipp)_2Cl_2(PMe_3)$ (**40**)

The study of complexes $W(NDipp)_2Cl_2(py)_2$ (**39**) and $W(NDipp)_2Cl_2(PMe_3)$ (**40**) as olefin dimerization pro-initiators was necessary for comparison purposes, as described in sections 2.4.1.1.3 and 2.4.1.5. Hence, complexes **39** and **40** were synthesized by adding four equivalents of pyridine or 1.3 equivalents of PMe_3 , respectively, to a solution of $W(NDipp)_2Cl_2(DME)$ (Scheme 2.7). Both complexes **39** and **40** were isolated and characterized using NMR spectroscopy and X-ray crystallography.



Scheme 2.7 Synthesis of complexes $W(NDipp)_2Cl_2(py)_2$ (**39**) and $W(NDipp)_2Cl_2(PMe_3)$ (**40**)

2.3 Crystallographic study of complexes $W(NR)_2Cl_2(DME)$ ($R = Dipp$ (27), Tfp (28), Pfp (29), Mes^F (30), Tpp (31)) and $W(NDipp)(NR)Cl_2(DME)$ ($R = iPr$ (32), tBu (33), Mes (34), Tfp (35), Tpp (36), Dnp (37))

2.3.1 General remarks

The crystal structure of complex $W(NDipp)_2Cl_2(DME)$ (27) has been reported previously,³ while selected structural parameters of the newly synthesized complexes 28-37 are provided here in Table 2.1 and Table 2.2. The molecular structures of selected symmetrical and unsymmetrical tungsten bis(imido) complexes are also presented in Figure 2.2 and Figure 2.3, respectively.

All complexes of the type $W(NR')(NR)Cl_2(DME)$ (with $R = R'$ or $R \neq R'$) examined herein adopt a distorted octahedral coordination with the chlorine atoms being *trans* to each other and bent away from the imido substituents, presumably as a result of steric constraints ($\Sigma_{ang} N(1)-W-X$ ($X = N(2), Cl, O(1)$) and $N(2)-W-Y$ ($Y = N(1), Cl, O(2)$) is between $389 - 395^\circ$). These observations are in accordance to those from previously-reported tungsten bis(imido) complexes.^{3,8-12} The W-N interatomic distances in each of the symmetrical and mixed bis(imido) complexes are in the range of 1.738(2)-1.787(3) Å, which is slightly longer than that for their mono(imido) analogues ($W-N = 1.685-1.727$ Å) examined in section 3.3, suggesting that the W-N bond order in the symmetrical and mixed bis(imido) complexes is between 2 and 3. This elongation of the W-N interatomic distances in the symmetrical and mixed bis(imidos) compared to their mono(imido) analogues is a result of the absence of available tungsten π -symmetry orbitals for π -bonding with all four p orbitals provided by the two imido substituents, making the symmetrical and mixed bis(imido) complexes electronically saturated.³

2.3.2 Crystallographic study of symmetric tungsten bis(imido) complexes: $W(NR)_2Cl_2(DME)$ ($R = Dipp$ (27), Tfp (28), Pfp (29), Mes^F (30), Tpp (31))

Following X-ray crystallographic analysis (Table 2.1), the W-N(1) and W-N(2) bond distances are identical within experimental error in each of the tungsten bis(imido) complexes, while each of the W-N(1)-C(1) and W-N(2)-C(2) angles differ slightly ($1.5-7^\circ$) within the series, depending on the nature of the imido substituent.

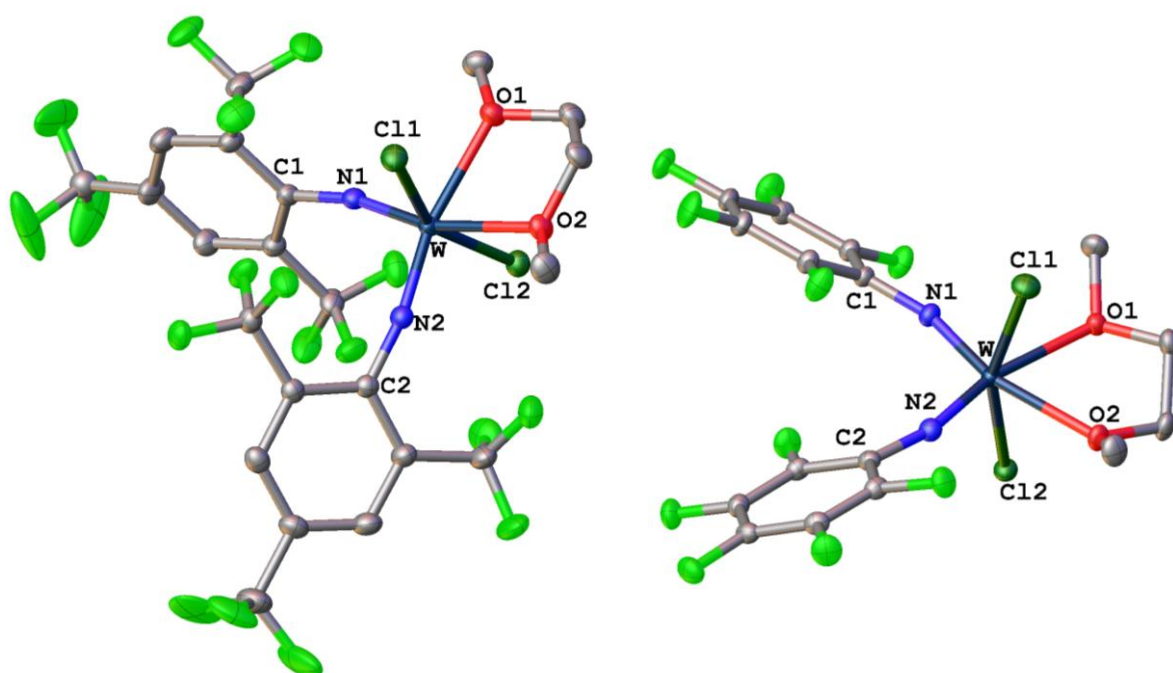


Figure 2.2 Molecular structures of $W(\text{NMes}^{\text{F}})_2\text{Cl}_2(\text{DME})$ (**30**) (left) and $W(\text{NPfp})_2\text{Cl}_2(\text{DME})$ (**29**) (right). H atoms are omitted for clarity and the thermal ellipsoids are shown at the 50% probability level.

Table 2.1 Selected interatomic distances (Å) and angles (°) for $W(\text{NR})_2\text{Cl}_2(\text{DME})$ (R = Dipp (**27**), Tfp (**28**), Pfp (**29**), Mes^F (**30**), Tpp (**31**))

	$W(\text{NDipp})_2\text{Cl}_2(\text{DME})^3$ (27)	$W(\text{NTfp})_2\text{Cl}_2(\text{DME})$ (28)	$W(\text{NPfp})_2\text{Cl}_2(\text{DME})$ (29)	$W(\text{NMes}^{\text{F}})_2\text{Cl}_2(\text{DME})$ (30)	$W(\text{NTpp})_2\text{Cl}_2(\text{DME})$ (31)
W-N(1)	1.7598(17)	1.755(19)	1.7593(16)	1.7749(16)	1.760(4)
W-N(2)	1.7599(17)	1.74(2)	1.7570(16)	1.7695(16)	1.768(5)
W-O(1)	2.3494(15)	2.320(15)	2.2901(13)	2.2918(14)	2.363(4)
W-O(2)	2.3446(15)	2.336(17)	2.3115(13)	2.3178(13)	2.362(9)
W-Cl(1)	2.3841(7)	2.369(5)	2.3791(5)	2.3516(5)	2.3623(15)
W-Cl(2)	2.3878(9)	2.380(5)	2.3663(5)	2.3589(5)	2.3749(14)
N(1)-C(1)	1.393(3)	1.40(3)	1.371(2)	1.377(2)	1.401(6)
N(2)-C(2)	1.395(3)	1.39(3)	1.371(2)	1.380(2)	1.387(5)
W-N(1)-C(1)	163.06(15)	162(2)	158.62(14)	165.22(14)	165.8(4)
W-N(2)-C(2)	161.47(15)	160.1(18)	165.55(14)	166.82(14)	161.7(3)
N(1)-W-Cl(1)	99.73(6)	97.3(7)	95.45(5)	99.38(5)	100.51(13)
N(1)-W-O(1)	89.35(7)	93.0(9)	91.24(6)	92.50(6)	95.28(19)
N(1)-W-Cl(2)	97.11(6)	96.3(6)	97.66(5)	98.84(5)	95.70(14)
N(1)-W-N(2)	103.89(8)	104.5(10)	104.91(7)	102.81(7)	104.55(19)
N(2)-W-Cl(2)	97.19(6)	97.3(6)	97.73(5)	97.48(5)	96.57(14)
N(2)-W-O(2)	96.69(7)	92.1(7)	93.26(6)	93.65(6)	91.57(17)
N(2)-W-Cl(1)	97.45(6)	97.6(6)	95.10(5)	98.38(5)	101.42(14)

Somewhat surprisingly, the W-N interatomic distances of complexes **27-29**, **31** were found to be the same within experimental error (~1.760 Å), despite the completely different electronic properties (electron withdrawing imido substituents would be expected to exhibit longer W-N bonds). Notably, only in complex **30** a slightly longer W-N bond (by ~0.01 Å) is observed. This similarity in the W-N bond lengths between complexes **27-31** is rationalized by considering the electronic saturation of the

tungsten centre in bis(imido) complexes.³ The lack of π -symmetry orbitals available in the *cis*-bis(imido) framework results in what can be regarded as a delocalized $[(R^1N)W(NR^2)]$ arrangement.

The W-O distances in the different symmetrical bis(imido) complexes vary in the order **31** > **27** > **28** > **29** = **30** (see Table 2.1). Hence, it can be inferred that the *trans* influence of the different imido ligands increases in the order $Mes^F = Pfp < Tfp < Dipp < Tpp$, which is approximately in line with the expected electron withdrawing character of the different substituents.

2.3.3 Crystallographic study of tungsten mixed bis(imido) complexes: $W(NDipp)(NR)Cl_2(DME)$ ($R = iPr$ (**32**), tBu (**33**), Mes (**34**), Tfp (**35**), Tpp (**36**), Dnp (**37**))

X-Ray crystallographic analysis reveals that the W-N(1) interatomic distances in complexes **32-34** lie in the range 1.738(2)-1.751(2) Å, with those for complexes **35** and **36** being slightly longer, 1.7680(16) and 1.771(2) Å, respectively, Table 2.2; the W-N(1) bond of the nitro complex **37** is longer still at 1.787(3) Å. Again, these results can reflect the electron withdrawing character of the imido substituents, with the strongly electron withdrawing Tfp, Tpp, and Dnp groups resulting in a lengthening of the W-N(1) imido. The effect of the strongly electron withdrawing imido groups on the structural parameters of the mixed imido complexes is also reflected in the W-NDipp (W-N(2)) bonds of complexes **35-37**, which are shorter than that for complex **33** (Table 2.2). This shortening of the W-N(2) bonds in complexes **35-37** results from significant N→W lone pair donation from the NDipp imido group, which dominates due to the poor nitrogen-to-tungsten donor character of the electron withdrawing imido groups NTfp, NTpp and NDnp in complexes **35-37**.

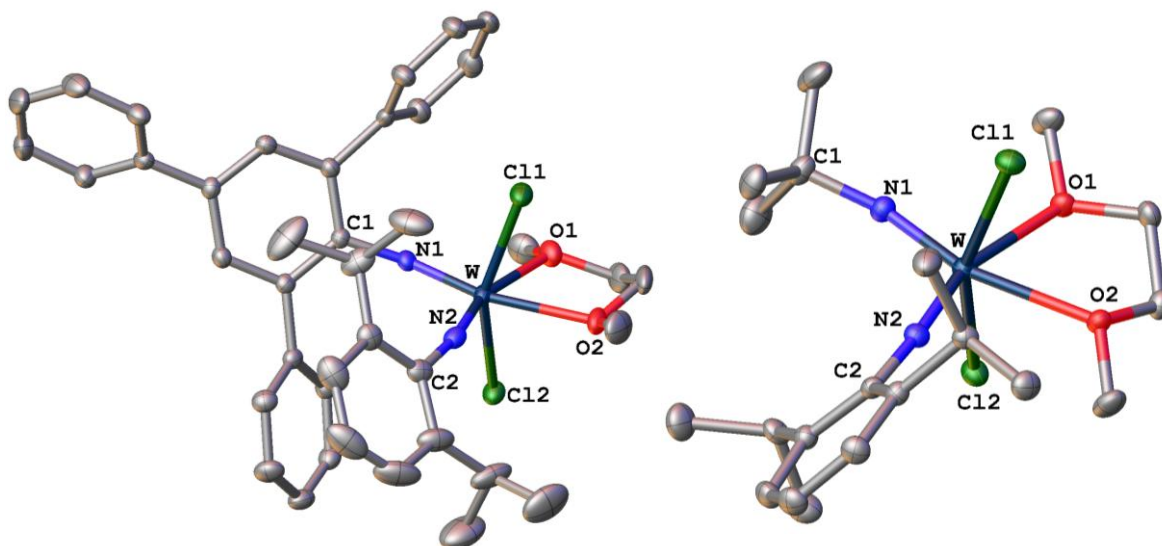


Figure 2.3 Molecular structures of $W(NDipp)(NTpp)Cl_2(DME)$ (**36**) (left) and $W(NDipp)(N^tBu)Cl_2(DME)$ (**33**) (right). H atoms are omitted for clarity and the thermal ellipsoids are shown at the 50% probability level.

The W-O(1) and W-O(2) bond distances in complexes **32-37** vary significantly with no readily apparent trend. Even the W-O(1) bond, which is *trans* to the NDipp group in all six mixed(imido) complexes and

that is hence expected to be similar for all **32-37**, assumes different values between 2.278(3) and 2.3499(18) Å (Table 2.2). It is suggested that slight variations in the WO₂C₂ chelate conformation of the DME ligand is responsible for this unexpected variation in the W-O(1) bond lengths.

Table 2.2 Selected interatomic distances (Å) and angles (°) for W(NR)(NDipp)Cl₂(DME) (R = ⁱPr (**32**), ^tBu (**33**), Mes (**34**), Tfp (**35**), Tpp (**36**), Dnp (**37**))

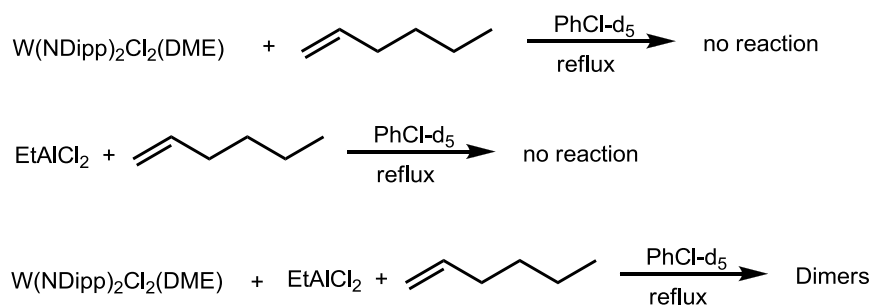
	R = ⁱ Pr (32)	R = ^t Bu (33)	R = Mes (34)	R = Tfp (35)	R = Tpp (36)	R = Dnp (37)
W-N(1)	1.738(2)	1.744(2)	1.751(2)	1.7680(16)	1.771(2)	1.787(3)
W-N(2)^a	1.757(2)	1.766(2)	1.760(2)	1.7500(15)	1.751(2)	1.745(3)
W-O(1)	2.304(2)	2.319(2)	2.3459(18)	2.3290(14)	2.3499(18)	2.278(3)
W-O(2)	2.405(2)	2.375(2)	2.3366(18)	2.3397(13)	2.3547(18)	2.317(2)
W-Cl(1)	2.3935(7)	2.3901(7)	2.4003(7)	2.3699(5)	2.3752(6)	2.3701(9)
W-Cl(2)	2.3882(7)	2.3917(7)	2.3905(6)	2.4003(5)	2.3703(7)	2.3889(8)
N(1)-C(1)	1.445(4)	1.450(4)	1.383(3)	1.375(2)	1.393(3)	1.369(5)
N(2)-C(2)	1.387(3)	1.387(4)	1.385(3)	1.388(2)	1.393(3)	1.389(5)
W-N(1)-C(1)	157.1(2)	159.4(2)	168.70(18)	154.52(14)	150.69(17)	152.3(3)
W-N(2)-C(2)	173.1(2)	173.5(2)	167.08(18)	169.75(13)	167.82(19)	174.0(3)
N(1)-W-Cl(1)	97.78(9)	98.68(8)	95.90(7)	98.59(5)	100.17(6)	98.78(10)
N(1)-W-O(1)	93.89(10)	92.32(10)	91.97(8)	91.68(6)	94.06(8)	92.29(12)
N(1)-W-Cl(2)	96.30(9)	95.26(9)	97.77(7)	95.85(5)	96.35(6)	96.51(10)
N(1)-W-N(2)	105.26(11)	106.34(12)	106.31(10)	104.39(7)	103.27(9)	103.89(14)
N(2)-W-Cl(2)	97.89(8)	97.68(8)	94.35(7)	96.66(5)	98.10(7)	95.05(10)
N(2)-W-O(2)	91.29(9)	92.14(9)	91.79(8)	93.62(6)	92.90(9)	92.70(13)
N(2)-W-Cl(1)	95.46(8)	98.68(8)	98.39(7)	97.17(5)	97.06(7)	98.16(10)

^a Across all complexes the W-NDipp bond distance is numbered as W-N(2).

2.4 Ethylene and 1-hexene dimerization mediated by tungsten bis(imido) pro-initiators

Before attempting any olefin dimerization experiments using the tungsten bis(imido) pro-initiators reported in section 2.2, the presumed catalytic inactivity of the separate components of the olefin dimerization systems was verified (Scheme 2.8). Thus, when a mixture of EtAlCl₂ and 1-hexene was heated at reflux in PhCl-d₅, no reaction occurred, based on a ¹H NMR spectroscopic analysis of the reaction mixture. However, when W(NDipp)₂Cl₂(DME) (**27**) was subsequently added to the above solution, formation of 1-hexene dimers was observed. Similarly, W(NDipp)₂Cl₂(DME) (**27**) is inert towards 1-hexene in the absence of an aluminium-based activator. Note, that in order to compare the performance of the various well-defined bis(imido) complexes, and to facilitate comparison with the Sasol *in situ* tungsten-based initiator system,¹ identical conditions were employed for all subsequent catalyst tests:^{1,13}

- Solvent: chlorobenzene
- Reaction temperature: 60 °C
- Activator: EtAlCl₂
- Al:W ratio: 15:1.



Scheme 2.8 Reactions demonstrating that the individual components of the tungsten bis(imido) based olefin dimerization systems are catalytically “silent”

It must also be mentioned that in the majority of the catalytic experiments described below, only 15 equivalents of aluminium activator are used. The use of low aluminium activator loadings compared to previously reported olefin dimerization systems, where the Al:transition metal ratio is typically 100-2500,¹⁴⁻¹⁷ is advantageous from both a safety and a financial point of view.

2.4.1 Ethylene dimerization mediated by tungsten bis(imido) pro-initiators

In this section the symmetrical and mixed bis(imido) complexes synthesized (as described in section 2.2) are used as pro-initiators for the catalytic dimerization of ethylene under various conditions. Notably, each of these tungsten complexes was found to be dimerization-active, although their specific activity strongly depends on the nature of the imido substituents. Although frequently regarded as “spectator ligands”,¹⁸ the pronounced influence upon the catalytic outcomes of the NR^{2-} fragments in these complexes is not surprising, especially when the significant influence the imido groups impose on the structural parameters of the complexes **27-37** (see section 2.3) is born in mind.

2.4.1.1 Tungsten(VI) bis(imido)-based ethylene dimerization testing (40 bar, 60 °C): effect of the imido ligands on activity and TON

When the tungsten bis(imido) complexes **27-37**, **39**, **41** were activated with EtAlCl_2 at 60 °C and treated with ethylene at a constant feed rate, moderate catalytic activities of $3.1\text{-}141.3 \text{ kg C}_2\text{H}_4 (\text{mol W})^{-1} \text{ h}^{-1} \text{ bar}^{-1}$ were obtained (Table 2.3), when compared to the activities for other ethylene dimerization systems reported in the literature, typically in the range $0.17^{19}\text{-}10000^{20-22} \text{ kg C}_2\text{H}_4 (\text{mol TM})^{-1} \text{ h}^{-1} \text{ bar}^{-1}$. Although the activities of these various tungsten bis(imido)-based pro-initiators **27-37**, **39**, **41** (Table 2.3) strongly depends on the nature of their imido substituents, it is difficult to determine the origins of their influence, since it is challenging to prepare a series of complexes in which the imido ligands’ steric properties are kept constant, but without significantly altering the electronics of the system and *vice versa*. A further complication arises from the fact that for the aryl-substituted imido complexes, 2,6-ring-disubstitution is required in order to prevent the ligands adopting a bridging rather than terminal coordination mode (see section 2.2.2.2). Nevertheless, despite these limitations, some general comments on the relationship between activity and the nature of the imido ligand can be made.

Table 2.3 Dimerization of ethylene at 40 bar ethylene and 60 °C using well defined tungsten(VI) bis(imido) pro-initiators ^{a,b}

Run #	Pro-initiator	Time (min)	TON ^e	Act. ^f	Mol % C ₄ (in liq. prod.)	% 1-C ₄ in C ₄	Mol % C ₆ (in liq. prod.)	% 1-C ₆ in C ₆	% Lin in C ₆	% MP in C ₆	% 3Me 1C ₅ in C ₆	% 2Et 1C ₄ in C ₆	wt % C ₈₊ (in prod.)
1	W(NTfp) ₂ Cl ₂ (DME) (28)	43	101.1	141.3	85.7	97.6	13.9	3.7	5.1	94.9	39.4	53.3	0.9
2	W(NPfp) ₂ Cl ₂ (DME) (29)	62.7	99.1	94.9	89.4	97.8	10.4	5.2	3.6	96.4	39.1	52.5	0.6
3	W(NDipp) ₂ Cl ₂ (DME) (27)	98	79.5	48.9	75.2	98.3	24.1	1.6	5.4	94.6	40.3	53.7	1.4
4	W(NTpp) ₂ Cl ₂ (DME) (31)	5.8	1.1	12.0	75.4	97.7	22.9	3.1	10.3	92.1	37.2	53.8	3.3
5	W(NMes ^F) ₂ Cl ₂ (DME) (30)	13.7	0.6	2.7	89.0	84.3	2.3	33.7	49.1	50.9	49.3	0.0	21.0
6	W(NDipp) ₂ Cl ₂ py ₂ (39)	9.5	2.9	18.5	69.7	97.3	27.1	2.0	4.3	95.7	47.9	44.1	7.0
7	W(N ⁱ Bu) ₂ Cl ₂ py ₂ (41)	9.8	0.5	3.1	67.6	95.9	26.6	3.4	4.9	95.1	46.6	23.9	11.9
8	W(NDipp)(NTpp)Cl ₂ (DME) (36)	72.9	101.5	83.5	81.6	98.4	17.7	1.8	4.1	95.9	40.4	53.6	1.3
9	W(NDipp)(NTfp)Cl ₂ (DME) (35)	67	88.3	79.3	75.7	98.1	23.5	1.6	3.8	96.2	40.2	54.1	1.7
10	W(NDipp)(NMes)Cl ₂ (DME) (34)	59	33.4	26.2	80.2	97.9	18.4	2.1	5.2	94.8	51.3	39.4	3.8
11	W(NDipp)(N ⁱ Bu)Cl ₂ (DME) (33)	166	69.6	25.2	76.2	98.0	22.4	1.6	3.7	96.3	42.8	49.0	2.6
12	W(NDipp)(N ⁱ Pr)Cl ₂ (DME) (32)	64	20.5	19.3	70.3	97.2	28.4	1.8	4.6	95.4	44.9	48.1	2.7
13	W(NDipp)(NDnp)Cl ₂ (DME) (37)	13	1.1	5.5	76.3	96.7	17.2	3.9	8.1	91.9	86.1	0.71	14.8
14 ^c	W(NDipp) ₂ Cl ₂ (DME) (27)	30.1	12.8	25.5	93.1	81.6	6.7	22.4	93.5	6.5	2.07	3.85	0.4
15 ^c	W(NDipp)(N ⁱ Bu)Cl ₂ (DME) (33)	10	1.1	6.5	81.0	97.4	19.0	5.5	92.0	8.0	4.01	3.94	0.0
16 ^d	W(NDipp)(N ⁱ Bu)Cl ₂ (DME) (33)	10	3.0	18.2	78.4	97.6	20.6	2.8	6.4	93.6	79.0	6.90	1.7

^a General conditions: 20 μmol W complex and 300 μmol EtAlCl₂; PhCl (solvent) 74 mL; 60 °C; ethylene pressure (40 bar); stirrer speed 1000 rpm; nonane standard (1.000 mL); catalytic runs were performed until consumption of C₂H₄ dropped below 0.2 g min⁻¹ or until the reactor was filled, at which time reaction was quenched by addition of dilute HCl. ^b Only traces of polyethylene were produced (0-0.6% of products fraction). ^c 300 μmol of MeAlCl₂ were used instead of EtAlCl₂. ^d The pro-initiator was pre-activated in a Schlenk. ^e TON is reported in (kg C₂H₄) (mol W)⁻¹ bar⁻¹. ^f Activity is reported in (kg C₂H₄) (mol W)⁻¹ h⁻¹ bar⁻¹ and is based on the total ethylene consumption.

Figure 2.4 presents the activities and TONs of obtained for ethylene dimerization using pro-initiators **27-37**. It has already been mentioned that it is difficult to completely separate the imido groups' steric and electronic influence on the tungsten centre. Nevertheless, an attempt is made by differentiating complexes **28-30**, **35**, and **37**, which bear the strongly electron withdrawing groups Mes^F, Pfp, Tfp, and Dnp (see right hand side of the chart in Figure 2.4) from the rest of the complexes that bear less electron withdrawing groups (left hand side of Figure 2.4). With this distinction made, the electron withdrawing and steric hindrance effects of the imido substituents on the activity are discussed separately in the following sections.

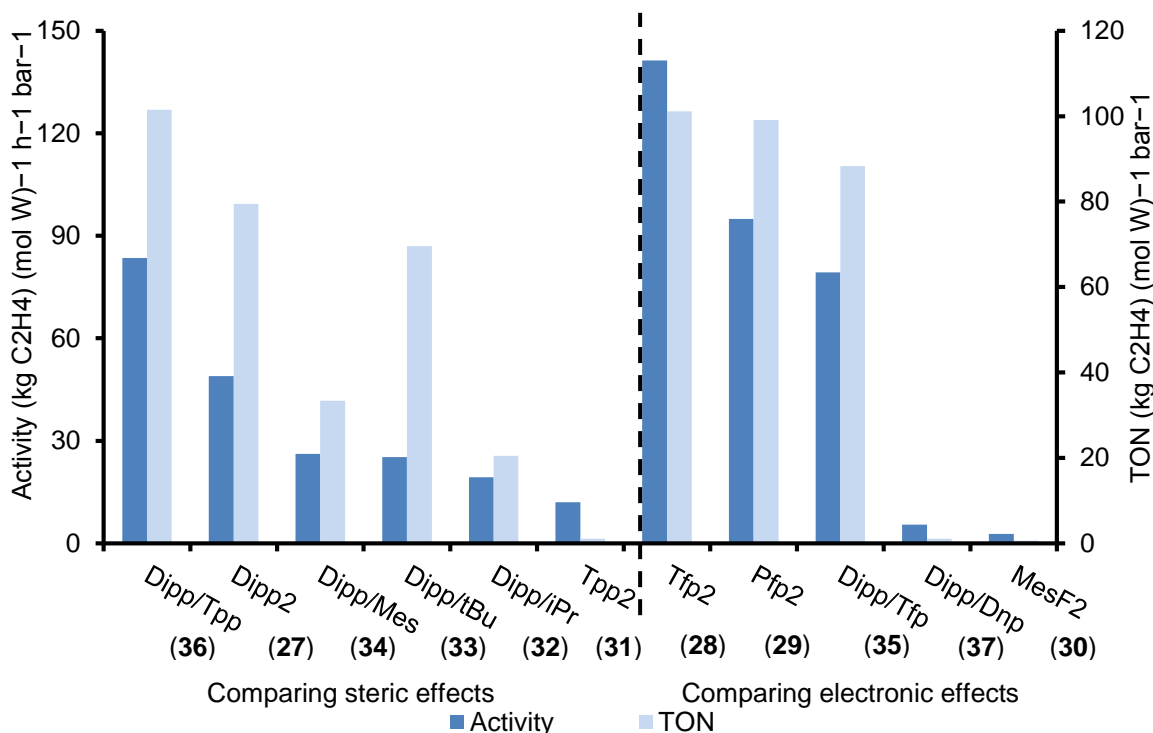


Figure 2.4 Summary of the catalytic activity ($\text{kg C}_2\text{H}_4 (\text{mol W})^{-1} \text{h}^{-1} \text{bar}^{-1}$) and TON ($\text{kg C}_2\text{H}_4 (\text{mol W})^{-1} \text{bar}^{-1}$) as a function of imido ligand substituents for the tungsten bis(imido) pro-initiators (**27-37**) tested at 40 bar ethylene /60 °C; data taken from Table 2.3, runs 1-16

2.4.1.1.1 Influence of imido ligand steric effects on catalytic activity

By comparing the catalytic activities achieved with pro-initiators **36**, **27**, and **34**, where the steric bulk of the imido ligand is varied systematically by replacing the bulky Tpp group in **36** with Dipp and then Mes, the more sterically-hindered imidos increase the activities and TONs of the catalytic system. Similar beneficial effects from sterically-demanding ligands on the catalytic activity of ethylene dimerization systems has also been reported in the literature for nickel-based ethylene dimerization systems.^{15,19}

The same trend applies when comparing the activities obtained using complexes $\text{W}(\text{NDipp})(\text{N}^i\text{Pr})\text{Cl}_2(\text{DME})$ (**32**) and $\text{W}(\text{NDipp})(\text{N}^i\text{Bu})\text{Cl}_2(\text{DME})$ (**33**) (Figure 2.4). The more sterically hindered ^tBu-bearing complex **33** (activity = 25.2 $\text{kg C}_2\text{H}_4 (\text{mol W})^{-1} \text{h}^{-1} \text{bar}^{-1}$), is slightly more active compared to its ⁱPr-substituted analogue **32** (activity = 19.3 $\text{kg C}_2\text{H}_4 (\text{mol W})^{-1} \text{h}^{-1} \text{bar}^{-1}$). More importantly, the TON value obtained using complex **33** is much larger than that achieved using complex **32** (Figure 2.4), implying that the catalytic system generated from complex **33** has a longer lifetime compared to that derived from **32**. This last observation is in line with the suggestion that sterically demanding ligands increase the catalytic systems' activities and TONs by protecting the catalyst from participating in deactivation reactions.²³

Based on the above findings relating to the effect of the imido ligands' steric bulk upon catalytic activity and, in order to further improve the tungsten bis(imido) based ethylene dimerization systems, complex $\text{W}(\text{NTpp})_2\text{Cl}_2(\text{DME})$ (**31**) bearing two bulky NTpp groups, was synthesized and its catalytic performance tested. Surprisingly, a very low activity and TON were obtained (Figure 2.4), in contrast to the expected

enhancement in catalytic activity. This apparent anomalous behavior can be rationalised since, although the increase in the steric hindrance provided by the ligands will beneficially attenuate catalyst deactivation, it will also have the detrimental effect of hindering efficient coordination of ethylene at the metal centre.²⁴ Furthermore, it must be mentioned that although the Tpp group is extremely sterically-demanding, it is also slightly more electron withdrawing compared to either the Mes or Dipp groups, something that also imposes an electronic influence on catalysis.²⁵⁻²⁷ However, this electronic effect is expected to be small judging by the small difference in the electron withdrawing character of the pendant organic groups about the aryl ligand periphery, Ph ($\chi = 2.52$), ⁱPr ($\chi = 2.25$), and Me ($\chi = 2.27$).²⁷

2.4.1.1.2 Effect of electron withdrawing imido ligands on catalytic activity

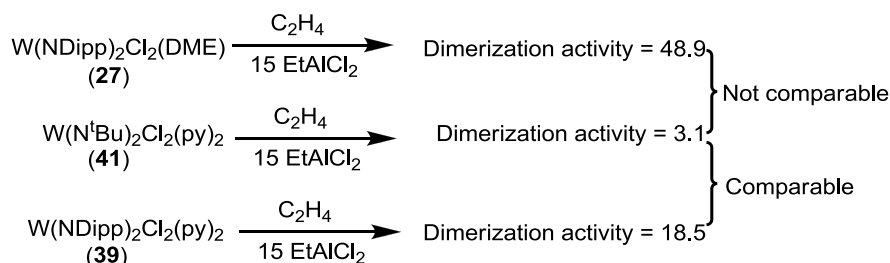
The ethylene dimerization activities obtained when the more electron deficient pro-initiators **28-30**, **35**, and **37** were employed (Figure 2.4) were the highest amongst complexes **27-37** with pro-initiators **28** and **29** exhibiting activities of 141.3 and 94.9 kg C₂H₄ (mol W)⁻¹ h⁻¹bar⁻¹, respectively. This suggests that electron withdrawing imido groups, such as NPfp and NTfp, increase the catalytic activities of the dimerization systems. However, on comparing the activities obtained using complexes **28**, **29**, and **35**, it appears that the incorporation of extremely electron withdrawing imido ligands, such as NPfp in complex **29**, results in lower catalytic activities, something that is hard to rationalize.

With these observations in mind, it was of interest to explore the behavior of the Dnp- and Mes^F-substituted imido complexes, **37** and **30** respectively, which bear the reasonably electron withdrawing groups NO₂ and CF₃.²⁵⁻²⁷ Although the two pro-initiators **37** and **30** would, thus, be predicted to perform well, the activities were in fact lower than 6 kg C₂H₄ (mol W)⁻¹ h⁻¹bar⁻¹ with TONs of only up to 1.1 kg C₂H₄ (mol W)⁻¹ bar⁻¹. The low catalytic activity found using complex **37** might be explained by possible side reactions of the pendant NO₂ group with the aluminum reagents used as activators. This was explored by treating PhNO₂ with Me₃Al in C₆D₆, which resulted in a mixture of unidentified products based on a ¹H NMR spectroscopic analysis. Hence, it is likely that in the presence of the EtAlCl₂ activator complex **37** undergoes a series of unwanted reactions, which lead to decomposition rather than to the formation of an active ethylene dimerization system. In contrast, no satisfactory explanation can be proposed to account for the low activity obtained when complex **30** was employed as pro-initiator.

2.4.1.1.3 Catalytic potential of bis(alkylimido) tungsten complexes in the dimerization of ethylene

Since the tungsten bis(imido) pro-initiators **27-37** contain at least one aryl imido substituent (NDipp), it was of interest to examine the catalytic behaviour of a bis(imido) complex bearing only alkyl imidos. Hence, the previously-reported complex W(N^tBu)₂Cl₂(py)₂ (**41**)¹² was synthesized and tested in the dimerization of ethylene (run 7, Table 2.3). Unfortunately, comparison of the performance of **41** with its DME-bearing analogues is not straightforward, since the pyridine ligands of **41** could influence the

outcome of the catalytic dimerization reaction (Scheme 2.9); see section 2.4.1.7 for a discussion of the role of Lewis bases upon catalysis. In order to circumvent this problem, the complex $W(\text{NDipp})_2\text{Cl}_2(\text{py})_2$ (**39**) was synthesized and tested (run 6, Table 2.3). Comparison of the results from runs 6 and 7 (Table 2.3) shows that complex $W(\text{N}^t\text{Bu})_2\text{Cl}_2(\text{py})_2$ (**41**) is a poor ethylene dimerization pro-initiator compared to **39**, which suggests that electron donating imido groups attenuate catalysis, something that is in line with the proposals made in section 2.4.1.1.2.



Scheme 2.9 Examination of the effect of alkyl imido ligands on catalysis for complexes **41** and **39**

2.4.1.1.4 Activation of the ethylene dimerization reaction with MeAlCl_2 instead of EtAlCl_2

During catalytic ethylene dimerization testing, complexes $W(\text{NDipp})_2\text{Cl}_2(\text{DME})$ (**27**) and $W(\text{NDipp})(\text{N}^t\text{Bu})\text{Cl}_2(\text{DME})$ (**33**) (Table 2.3: runs 14 and 15, respectively) were activated with MeAlCl_2 instead of EtAlCl_2 . From the activities of 6.5 and 25.5 $\text{kg C}_2\text{H}_4 (\text{mol W})^{-1} \text{h}^{-1} \text{bar}^{-1}$ achieved in these two runs, it is evident that MeAlCl_2 can also successfully activate the bis(imido) tungsten systems, suggesting that formation of a β -hydride-containing tungsten complex is not explicitly necessary for dimerization to occur. This observation has mechanistic implications, and is discussed in sections 2.4.1.6.4 and 2.4.2.5.

2.4.1.1.5 Pre-activation of $W(\text{NDipp})(\text{N}^t\text{Bu})\text{Cl}_2(\text{DME})$ (**33**) in the absence of ethylene

In an alternative test protocol, $W(\text{NDipp})(\text{N}^t\text{Bu})\text{Cl}_2(\text{DME})$ (**33**) was pre-activated in a Schlenk by dissolving an appropriate amount of **33** in PhCl , followed by addition of 15 equivalents of EtAlCl_2 with vigorous stirring at 60 °C (run 16, Table 2.3). The resulting solution was then injected into the reactor at 60 °C, which was immediately pressurized with 40 bar of ethylene. This alternative sequence gave a TON value of only 3.0 $\text{kg C}_2\text{H}_4 (\text{mol W})^{-1} \text{bar}^{-1}$, which is much lower than the TON of 69.6 $\text{kg C}_2\text{H}_4 (\text{mol W})^{-1} \text{bar}^{-1}$ achieved by the same pro-initiator when activated in the presence of ethylene (run 11, Table 2.3). Hence, it appears that during the activation of the tungsten bis(imido) pro-initiators the presence of ethylene is essential for the formation and stabilisation of the species responsible for dimerization.

2.4.1.2 Tungsten(VI) bis(imido) complex-mediated ethylene dimerization (45 bar, 70 °C)

In section 2.4.1.1 the performance of pro-initiators **27-37** was studied at 40 bar and 60 °C (Table 2.3), while here, the effect of increased temperature on the catalytic performance of the same pro-initiators

will be examined. For this purpose ethylene dimerization experiments with pro-initiators **27-37** were conducted at 45 bar ethylene pressure and 70 °C (Table 2.4). Note that these tests were carried out with an associated increase in ethylene pressure (45 bar rather than 40 bar) in order to ensure the same ethylene concentration in solution for the two different temperature regimes.[‡]

Table 2.4 Dimerization of ethylene at 45 bar ethylene, 70 °C using well defined W(VI) bis(imido) pro-initiators^{a,b}

Run #	Pro-initiator	Time (min)	TON ^c	Act. ^d	Mol % C ₄ (in liq. prod.)	% 1-C ₄ in C ₄	Mol % C ₆ (in liq. prod.)	% 1-C ₆ in C ₆	% Lin in C ₆	% MP in C ₆	wt C ₈₊ (in liq. prod.)	% (in liq. prod.)
1	W(NTfp) ₂ Cl ₂ (DME) (28)	21.2	88.3	255.2	87.1	97.6	12.6	3.8	5.2	94.9	0.8	
2	W(NDipp)(NTpp)Cl ₂ (DME) (36)	29.4	89.4	182.8	81.1	98.4	18.4	1.9	4.6	95.5	1.3	
3	W(NPfp) ₂ Cl ₂ (DME) (29)	29.0	87.5	181.3	89.1	97.6	10.6	5.2	3.7	96.3	0.5	
4	W(NDipp)(NTfp)Cl ₂ (DME) (35)	36.1	80.0	132.8	77.7	98.0	21.3	1.7	3.9	96.1	2.3	
5	W(NDipp) ₂ Cl ₂ (DME) (27)	39.6	82.4	128.9	80.4	98.1	18.9	1.3	7.0	93.0	1.5	
6	W(NDipp)(N ⁱ Bu)Cl ₂ (DME) (33)	34.5	62.0	107.8	71.3	98.2	27.7	1.9	4.2	95.8	2.0	
7	W(NDipp)(N ⁱ Pr)Cl ₂ (DME) (32)	57	61.7	65.3	81.2	97.7	18.1	1.7	4.6	95.4	1.6	
8	W(NDipp)(NMes)Cl ₂ (DME) (34)	81	77.5	57.7	78.5	97.7	20.9	1.5	4.1	95.9	1.1	
9	W(NTpp) ₂ Cl ₂ (DME) (31)	82.9	17.8	12.9	77.0	97.4	21.3	2.6	10.3	89.7	3.4	
10	W(NMes ⁻) ₂ Cl ₂ (DME) (30)	22.8	1.4	3.7	95.1	95.1	2.2	41.0	63.7	36.3	6.9	
11 ^e	W(NDipp) ₂ Cl ₂ (DME) (27)	4.2	2.7	39.2	72.1	98.0	23.5	2.2	5.1	94.9	10.1	
12 ^e	W(NDipp) ₂ Cl ₂ (DME) (27)	20.7	35.4	102.5	76.0	98.2	23.2	1.7	4.1	95.9	1.7	
13 ^f	W(NTfp) ₂ Cl ₂ (DME) (28)	104.6	225.7	129.5	88.9	97.5	10.8	4.5	5.7	94.3	0.5	
14 ^f	W(NDipp) ₂ Cl ₂ (DME) (27)	136.1	276.2	121.7	77.1	98.5	22.3	1.8	4.6	95.4	1.2	
15 ^f	W(NDipp)(NTpp)Cl ₂ (DME) (36)	65.0	244.6	225.7	83.2	98.7	16.4	2.0	5.2	94.8	0.9	
16 ^g	W(NDipp)(N ⁱ Bu)Cl ₂ (DME) (33)	7.8	53.9	370.6	78.5	95.8	20.7	2.2	4.8	95.2	1.5	

^a General conditions: 20 μmol W complex and 300 μmol EtAlCl₂; PhCl (solvent) 74 mL; 70 °C; ethylene pressure (45 bar); stirrer speed 1000 rpm; nonane standard (1.000 mL); catalytic runs were performed until consumption of C₂H₄ dropped below 0.2 g min⁻¹ or until the reactor was filled, at which time reaction was quenched by addition of dilute HCl. ^b No polyethylene was produced. ^c TON is reported in (kg C₂H₄) (mol W)⁻¹ bar⁻¹. ^d Activity is reported in (kg C₂H₄) (mol W)⁻¹ h⁻¹bar⁻¹ and is based on the total ethylene consumption. ^e Reaction was quenched at low or moderate TON. ^f Performed in a 1.2 L reactor with 40 μmol W complex and 600 μmol EtAlCl₂; PhCl (solvent) 148 mL; 70 °C; ethylene pressure (45 bar); stirrer speed 1000 rpm; nonane standard (2.000 mL). ^g Reaction started at 80 °C and 50 bar ethylene pressure with temperature rising at 163 °C due to loss of temperature control during the run.

However, it should be noted that it is well-established in the literature that increases in pressure enhance the catalytic activity of certain dimerization systems by increasing the concentration of ethylene in solution.¹⁴ Additionally, it must be mentioned that the reactions undertaken using pro-initiators **27-29, 35,**

[‡] According to calculations conducted in Sasol using aspen™ simulation software, the concentration of ethylene in chlorobenzene at 40 bar/60 °C, 45 bar/70 °C, and 50 bar/80 °C is 3.5570 M, 3.5853 M, and 3.6075 M respectively. For examples of such calculations see references: (28) Cozma, P.; Wukovits, W.; Mamaliga, I.; Friedl, A.; Gavrilescu, M. *Environmental Engineering and Management Journal* **2013**, 12, 147, (29) Lee, L. S.; Ou, H. J.; Hsu, H. F. *Fluid Phase Equilibria* **2005**, 231, 221, (30) Wu, J. L.; Pan, Q. M.; Rempel, G. L. *Journal of Applied Polymer Science* **2005**, 96, 645.

36 at 45 bar/ 70 °C resulted in the test autoclave ($V = 250$ mL or 1.2 L) being completely filled before the onset of catalyst deactivation could be observed (see runs 1-5 in Table 2.4). As a result, the total values of TON for these pro-initiators could not be determined since the catalytic systems did not reach their deactivation point (see section 6.2.2.2 for definition of TON).

2.4.1.2.1 Effect of temperature on the catalytic activity of the tungsten bis(imido) ethylene dimerization systems

The catalytic activities and TONs determined for the pro-initiators **27-36** at 45 bar C_2H_4 , 70 °C are presented and compared with the activities and TONs obtained at 40 bar, 60 °C in Figure 2.5. Inspection of the data presented in Figure 2.5, reveals that the effects of the various different imido substituents on the catalytic activities of the bis(imido) pro-initiators at 45 bar/70 °C are similar to the effects observed at 40 bar/60 °C, with pro-initiator **28** being the most active and systems **30**, **31** being the least active (Figure 2.5). The only exception is pro-initiator **33**, which was found to be ~50% more active compared to either complexes **32** or **34** at 45 bar/70 °C (Figure 2.5). Overall, the catalytic activities obtained at 45 bar/70 °C were found to be approximately two times greater (Figure 2.5, Table 2.4) than those from the same bis(imido) pro-initiators when tested at 40 bar/60 °C (Table 2.3), something that clearly demonstrates the beneficial effect of increased temperature on catalysis with bis(imido) tungsten complexes.

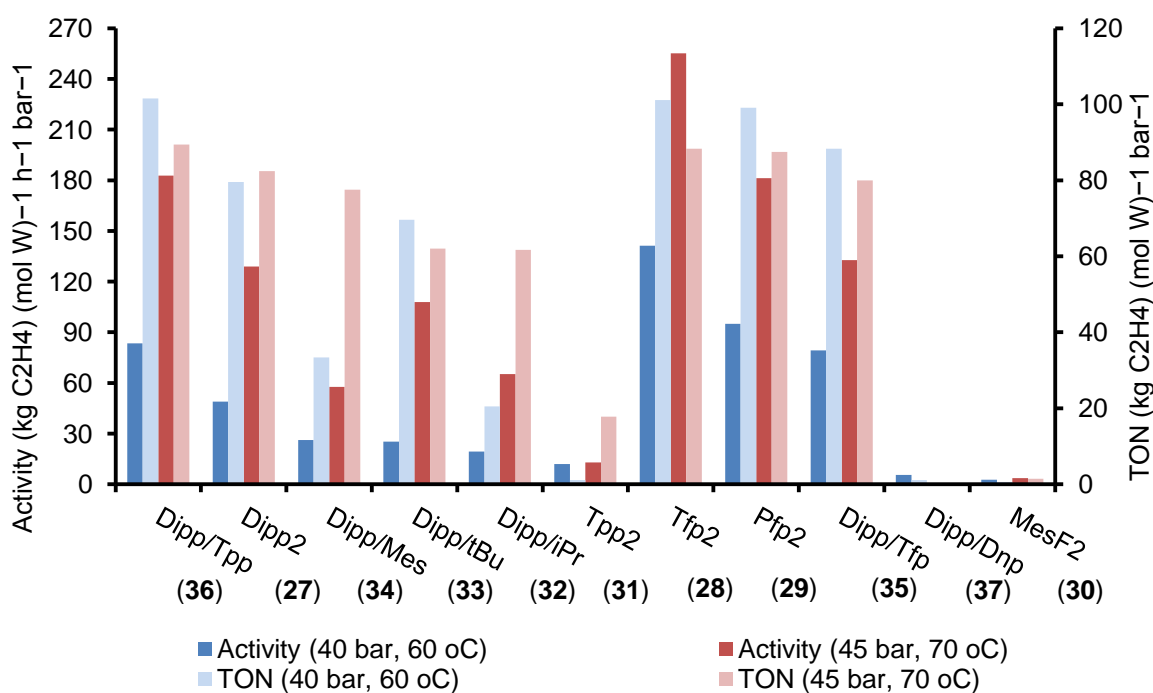


Figure 2.5 Comparison of catalytic activities of the tungsten bis(imido) pro-initiators (**27-36**) at 40 bar ethylene/60 °C and 45 bar ethylene/70 °C as a function of imido substituent; data taken from Table 2.3 runs 1-5, 8-13 and Table 2.4 runs 1-10

In contrast to certain previously-reported nickel-based dimerization systems (section 1.7.1.1.1) where attenuation of catalysis is observed at temperatures higher than 30 °C,^{24,31} the tungsten bis(imido) systems described here become significantly more active at higher temperatures. The increased

activities observed at these higher reaction temperatures could be attributed to purely kinetic effects (*i.e.* rate increases as temperature increases). Alternatively, it is possible that different, more active, catalytically-active species are formed when the pro-initiators are activated at a higher temperature. For example, a similar temperature effect has been observed with cobalt-based oligomerization pro-initiators, which mediates dimerisation at RT, but produces polyethylene on raising reaction temperature to 90 °C, something that was attributed to the formation of two different species (section 1.7.1.1.1.2, Scheme 1.35).³²

2.4.1.2.2 Ethylene dimerization using $WCl_2(NDipp)(N^tBu)(DME)/EtAlCl_2$ at 50 bar and 80 °C

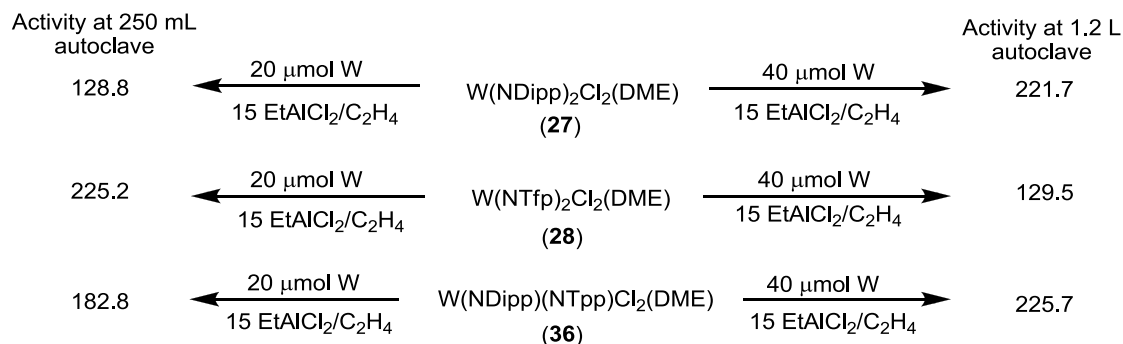
In order to examine the effect of a further increase in temperature (from 70 to 80 °C) on the catalytic activity of the various bis(imido) pro-initiators, an experiment was conducted at 50 bar/80 °C using pro-initiator $W(NDipp)(N^tBu)Cl_2(DME)$ (**33**) (run 16; Table 2.4). Soon (7.8 min) after activating $W(NDipp)(N^tBu)Cl_2(DME)$ (**33**) with $EtAlCl_2$ ($W:Al = 1:15$) and subsequent contact with C_2H_4 at 80 °C, a rapid rise in reaction temperature was observed, which could not be controlled with the available temperature control equipment, leading to the system reaching a temperature of 163 °C very quickly; consequently, the ethylene feed was shut off.[§] Analysis of the post catalysis organic products showed that an impressive activity of $370.6 \text{ kg } C_2H_4 (\text{mol } W)^{-1} \text{ h}^{-1} \text{ bar}^{-1}$ had been achieved, with a product distribution similar to that obtained when catalysis was conducted at 70 °C and 45 bar (run 16; Table 2.4). This preliminary experiment clearly highlights the further potential of these types of tungsten bis(imido) pro-initiators in catalytic olefin dimerization applications.

2.4.1.2.3 Catalytic ethylene dimerization tests in a 1.2 L autoclave

At the start of section 2.4.1.2 it was mentioned that the catalytic systems produced from pro-initiators **27-29**, **35**, and **36** (runs 1-5, Table 2.4) maintained steady ethylene consumption until the 250 mL autoclave was filled with products. Hence, in order to further examine the potential of the bis(imido) ethylene dimerization systems, pro-initiators **27**, **28**, and **36** were tested in a larger 1.2 L autoclave (runs 13-15, Table 2.4), something that potentially gives the advantage of being able to explore the performance of these initiators over longer periods of time before the reactor becomes filled. Interestingly, despite the increase in reactor volume the deactivation point for pro-initiators **27**, **28**, and **36** was still not reached, with the 1.2 L autoclave also becoming filled prior to the onset of catalyst deactivation; for note TONs of up to $276.2 \text{ kg } C_2H_4 (\text{mol } W)^{-1} \text{ bar}^{-1}$ were achieved when pro initiator $W(NDipp)_2Cl_2(DME)$ (**27**) was used, which corresponds to ~500 g of ethylene consumed. This value of ethylene up-take is by far the largest recorded amongst the various ethylene dimerization systems reported in this thesis. However, what is more interesting, is that for pro-initiators **27**, **28**, and **36** (runs 13-15, Table 2.4), the activity profiles obtained using the 1.2 L autoclave vessel differ significantly from those obtained using the 250 mL autoclave (Scheme 2.10, runs, 1, 2, 5). Specifically, in the 1.2 L vessel the activity of pro-initiator **28** decreased by 49% compared to that determined in the 250 mL

[§] Due to the difficulties in achieving good temperature control of the tungsten bis(imido) ethylene dimerization reaction at 50 bar and 80 °C only pro-initiator **33** was examined under these conditions.

reactor, the activity of **27** remained practically the same, while the activity of **36** increased by 23%. The increased catalytic activity of pro-initiator **36**, compared to that of **27** or **28**, at longer reaction times could be attributed to the increased steric bulk of **36** (compared to that of **27** and **28**), which provides additional protection from competing deactivation reactions, as suggested in section 2.4.1.1.1. Although the rate at which pro-initiator **36** generates dimeric products is somewhat slow when compared to **28**, the catalytic lifetime of **36** is significantly better.



Scheme 2.10 Dimerization of ethylene with pro-initiators **27**, **28**, and **36** in a 250 mL (left) and 1.2 L (right) autoclave; activities are reported in $(\text{kg C}_2\text{H}_4) (\text{mol W})^{-1} \text{h}^{-1} \text{bar}^{-1}$

2.4.1.3 Selectivity of the tungsten bis(imido) ethylene dimerization systems

The data presented in Figure 2.6 compare the selectivity of the tungsten bis(imido) systems as a function of the imido substituents for reactions performed at 40 bar/60 °C and 45 bar/70 °C. The selectivities obtained towards butenes from the bis(imido) pro-initiators are in the range of 70%-95% with a 1-butene content of over 95% (Table 2.3, Table 2.4, Figure 2.6). Additionally, only between 2.3-28.4 mol% of the products consisted of trimers, which are mainly branched in nature. The rest of the product fraction contained small amounts of heavier oligomers (typically less than ~3 %), with practically no polyethylene being produced (Table 2.3, Table 2.4, Figure 2.6). Together, these product selectivities compare very favorably with those reported for various different types of ethylene dimerization systems that have previously been reported in the literature (see section 1.7).

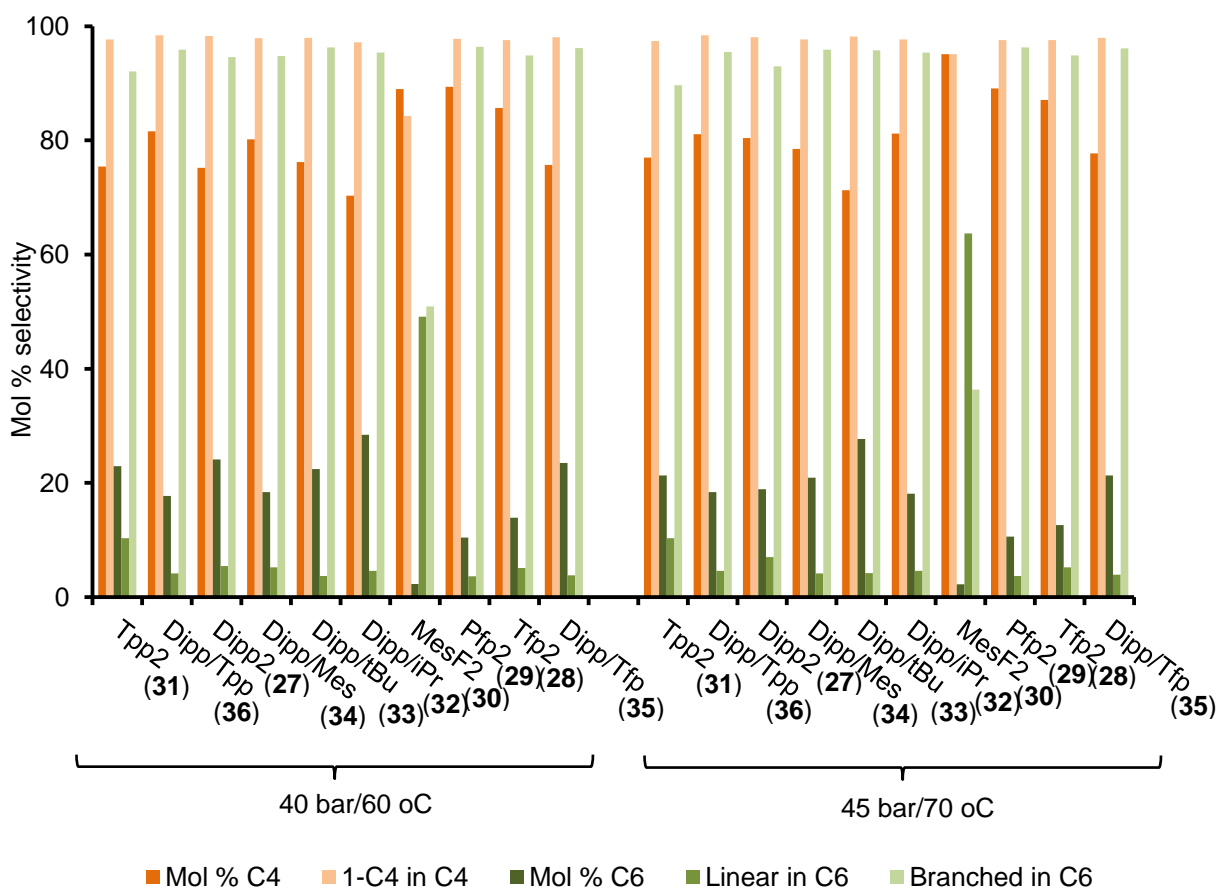


Figure 2.6 Product selectivities (expressed in mol %) obtained using the tungsten bis(imido) pro-initiators (**27-36**) at 40 bar ethylene/60 °C (left) and 45 bar ethylene/70 °C (right) versus imido substituent; data taken from Table 2.3 runs 1-5, 8-12 and Table 2.4 runs 1-10

Inspection of the data presented in Figure 2.6 shows that the selectivities of pro-initiators **27-36** do not change significantly as the nature of the imido substituents is varied. Even when the temperature at which catalysis is undertaken is raised, the selectivity profile of the bis(imido) systems remains practically unchanged, suggesting that a similar dimerization mechanism is in operation at 40 bar/60 °C and 45 bar/70 °C; formation of a different catalytically-active species is likely to alter the selectivity of the catalytic reaction.³² In contrast, when MeAlCl₂ is used instead of EtAlCl₂ as the activator (run 14 and 15, Table 2.3), a change in the selectivity of the trimers fraction is observed, with mainly linear products being produced. This suggests that formation of a different catalytically-active system occurs, which is reasonable since in contrast to EtAlCl₂, MeAlCl₂ cannot generate a W-H-type species due to its inability to undergo β-hydride elimination after Al-to-W transmetallation.

Lastly, it must be mentioned that the selectivity of the tungsten bis(imido) pro-initiators remains the same during the course of the catalytic reaction. This was concluded by comparing the product selectivities of run 5 with runs 11 and 12 in Table 2.4 where the ethylene dimerization reaction was deliberately quenched at lower TONs.

2.4.1.4 Tungsten bis(imido)-based ethylene dimerization using lower tungsten loading (5-10 μmol vs. 20 μmol)

In an attempt to increase the activities of the various tungsten bis(imido) ethylene dimerization systems, catalysis was attempted at lower tungsten loadings with pro-initiators **27** and **33** (Table 2.5). Surprisingly, a drop in the catalytic activity from 128.9 to 70.9 $\text{kg C}_2\text{H}_4 (\text{mol W})^{-1} \text{h}^{-1} \text{bar}^{-1}$ was observed on lowering the loading of the pro-initiator **27** from 20 μmol to 5 μmol (c.f. run 5 in Table 2.4 with run 1, Table 2.5, respectively). The mixed bis(imido) pro-initiator **33** behaved in a similar way with a decrease in activity from 107.8 to 48.4 $\text{kg C}_2\text{H}_4 (\text{mol W})^{-1} \text{h}^{-1} \text{bar}^{-1}$ (c.f. run 6 in Table 2.4 with run 3, Table 2.5, respectively) being determined. On increasing the tungsten loading of **27** from 5 μmol to 10 μmol (run 2, Table 2.5), no improvement in the catalytic activity was observed, although a better TON (111.7 $\text{kg C}_2\text{H}_4 (\text{mol W})^{-1} \text{bar}^{-1}$) was obtained.

Table 2.5 Dimerization of ethylene at 45 bar ethylene pressure and 70 °C using well defined W(VI) bis(imido) pro-initiators at tungsten loadings of 5 and 10 μmol .^{a,b}

Run #	Pro-initiator	W (μmol)	EtAlCl ₂ (eq.)	Time (min)	TON ^c	Act. ^d	Mol % C ₄ (in liq. prod.) ^e	Mol % C ₆ (in liq. prod.) ^f	% Lin in C ₆	% MP in C ₆	wt % C ₈₊ (in liq. prod.)
1	W(NDipp) ₂ Cl ₂ (DME) (27)	5	15	23.8	28.2	70.9	78.0	20.0	5.9	94.1	4.4
2	W(NDipp) ₂ Cl ₂ (DME) (27)	10	15	126.7	111.7	52.9	76.4	21.9	4.3	95.7	3.6
3	W(NDipp)(N ⁱ Bu)Cl ₂ (DME) (33)	5	15	190	48.4	15.3	75.4	21.3	5.0	95.0	7.4
4	W(NDipp)(N ⁱ Bu)Cl ₂ (DME) (33)	5	20	120	21.6	10.9	69.3	17.0	10.2	89.8	24.3
5	W(NDipp)(N ⁱ Bu)Cl ₂ (DME) (33)	5	60	50	5.8	6.9	80.0	17.7	11.9	88.1	4.4

^a General conditions: PhCl (solvent) 74 mL; 70 °C; ethylene pressure (45 bar); stirrer speed 1000 rpm; nonane standard (1.000 mL); catalytic runs were performed until consumption of C₂H₄ dropped below 0.2 g min⁻¹ or until the reactor was filled, at which time reaction was quenched by addition of dilute HCl. ^b No polyethylene was produced. ^c TON is reported in $(\text{kg C}_2\text{H}_4) (\text{mol W})^{-1} \text{bar}^{-1}$. ^d Activity is reported in $(\text{Kg C}_2\text{H}_4) (\text{mol W})^{-1} \text{h}^{-1} \text{bar}^{-1}$ and is based on the total ethylene consumption. ^e Over 96% of the C₄ fraction consists of 1-butene in all runs. ^f Less than 5.2% of the C₆ fraction consists of 1-hexene in all runs.

This attenuation in catalytic activity on lowering the tungsten loadings might be due to concentration effects, since this will give a more dilute pro-initiator solution *prior* to activation, which in turn, is something that could affect the reaction of the pro-initiator with the Al-based activator. In order to test this theory, samples containing 5 μmol of **33** were activated with 20 or 60 equivalents of EtAlCl₂ (runs 4, 5, respectively; Table 2.5), since it could be argued that use of a higher activator loading should compensate for the more dilute solution and hence, increase performance. However, disappointingly, the catalytic activity further decreased under these conditions.

2.4.1.5 Exploring tungsten(IV)-initiated ethylene dimerization

In section 1.7.5.2 the suggestion by Olivier *et al.* that a tungsten(IV) mono(imido) complex is responsible for the dimerization of ethylene rather than a tungsten(VI) imido was briefly outlined.² Hence, in order to examine whether tungsten(IV) species are also involved in the dimerization of ethylene using tungsten bis(imido) pro-initiators, the previously reported complex $W(NDipp)_2(PMe_3)_3$ (**42**) was synthesized and tested for ethylene dimerization,³³ alongside the PMe_3 -containing tungsten(VI) complex $W(NDipp)_2Cl_2(PMe_3)$ (**40**) (section 2.2.3). The results of these experiments are presented in Table 2.6.

Table 2.6 Dimerization of ethylene using $W(NDipp)_2(PMe_3)_3$ and $W(NDipp)_2Cl_2(PMe_3)$ as the pro-initiators^{a,b,c}

Run #	Pro-initiator	Time (min)	TON ^e	Act. ^f	Mol % C ₄ (in liq. prod.)	% 1-C ₄ in C ₄	Mol % C ₆ (in liq. prod.)	% 1-C ₆ in C ₆	% Lin in C ₆	% MP in C ₆	wt % C ₈₊ (in liq. prod.)
1	$W(NDipp)_2Cl_2(PMe_3)$ (40)	133	97.7	44.1	80.8	98.2	18.5	1.6	4.1	95.9	1.5
2	$W(NDipp)_2(PMe_3)_3$ (42)	10	0.4	2.1	82.7	100	17.3	0.0	0.0	100	0.0
3	$W(NDipp)_2(PMe_3)_3$ (42)	10.1	1.2	6.9	81.8	97.4	18.0	4.1	4.1	95.9	0.5

^a General conditions: 20 μ mol W complex and 300 μ mol $EtAlCl_2$; PhCl (solvent) 74 mL; 60 °C; ethylene pressure (40 bar); stirrer speed 1000 rpm; nonane standard (1.000 mL); catalytic runs were performed until consumption of C_2H_4 dropped below 0.2 g min^{-1} or until the reactor was filled, at which time reaction was quenched by addition of dilute HCl. ^b No polyethylene was produced. ^c No reaction occurred when $W(NDipp)_2(PMe_3)_3$ was activated with 10 eq. $AlCl_3$ or when no activator was used. ^d Performed at 70 °C and 45 bar of ethylene pressure. ^e TON is reported in $(kg C_2H_4) (mol W)^{-1} bar^{-1}$. ^f Activity is reported in $(kg C_2H_4) (mol W)^{-1} h^{-1} bar^{-1}$ and is based on the total ethylene consumption.

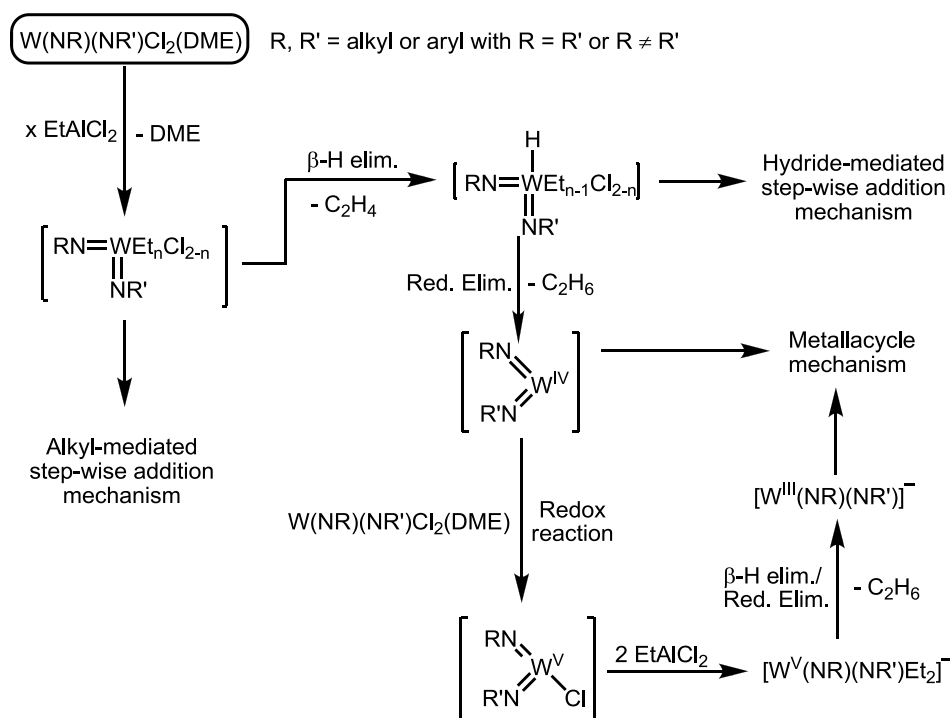
From the data presented in Table 2.6 it is clear that the tungsten(VI) complex $W(NDipp)_2Cl_2(PMe_3)$ is far superior in terms of ethylene dimerization activity (21 times more active and with a TON 244 times larger than with $W(NDipp)_2(PMe_3)_3$) compared to its tungsten(IV) counterpart (runs 1, 2; Table 2.6) even when the catalysis is performed at 45 bar/70 °C for the latter (run 3; Table 2.6). Additionally, no reaction was found to occur when ethylene dimerization mediated by **42** was attempted without the use of an activator or with 10 equivalents of $AlCl_3$. These results suggest that a tungsten(IV) compound is unlikely to be the main catalytically active species in the tungsten bis(imido)-mediated dimerization of ethylene.

2.4.1.6 Mechanistic considerations for tungsten bis(imido)-mediated ethylene dimerization

2.4.1.6.1 Two possible mechanistic pathways available for the tungsten imido/ $EtAlCl_2$ systems

The main mechanisms that lead to transition metal-catalyzed olefin dimerization, oligomerization, or polymerization (*i.e.* metallacycle-mediated and/or step-wise addition) have been examined in detail in section 1.4. Both these pathways could be accessed by the tungsten bis(imido) pro-initiators *via* the processes described in Scheme 2.11, where reaction of $W(NR)_2Cl_2(DME)$ with excess $EtAlCl_2$ removes DME, and alkylates the tungsten centre. The resulting tungsten alkyl species could be itself catalytically active, or could generate a tungsten hydride *via* β -hydride elimination. Alternatively, the tungsten alkyl species could undergo reductive elimination to give a tungsten(IV) species capable of forming

metallacycles *via* oxidative alkene coupling, or susceptible to oxidation by the starting material (see section 3.4.1.2.3.1) to form a W(V) species, which could lead to W(III) metallacycle-mediated dimerization (Scheme 2.11).



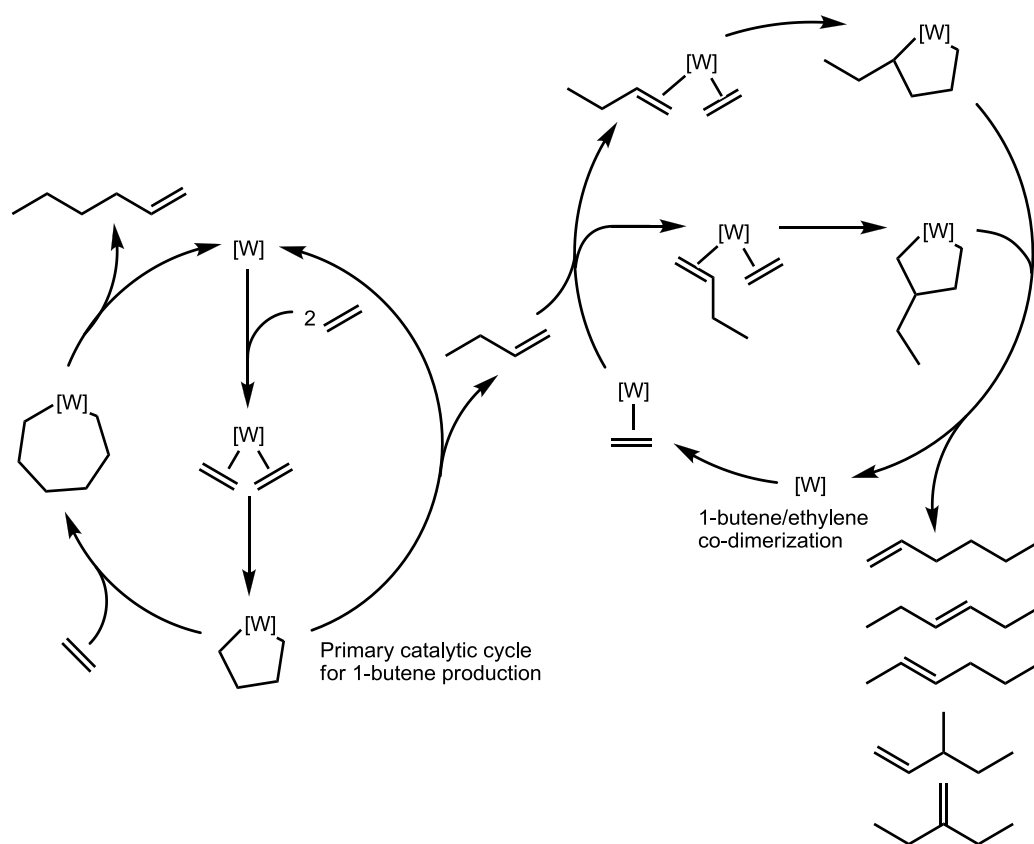
Scheme 2.11 Schematic representation of possible activation pathways for tungsten bis(imido) pro-initiators**

Deciding which of the possible mechanisms is actually operative is a complex procedure, and is something that has been discussed in section 1.6. However, in section 1.6 it was also mentioned that the nature of the organic products produced from a catalytic dimerization reaction can sometimes provide information about the catalytic mechanism in operation;^{1,34} different combinations of butenes and C₆ isomers will result from a metallacyclic or a metal hydride-centred mechanism. For example, from the catalysis results presented in Table 2.3, 1-butene is the major product (>70 % of liquid fraction) when EtAlCl₂ was used as an activator. Moreover, in addition to 1-butene and 1-hexene, production of methyl pentenes is also observed during catalysis with the activated tungsten bis(imido) systems (Table 2.3). If a metallacyclic mechanism is operative, then the only way that 3-methyl-1-pentene (3Me-1-C₅) and 2 ethyl-1-butene (2Et-1-C₄) can be formed is through the co-dimerization of the 1-butene with ethylene. Alternatively, if a step-wise addition mechanism is operating, branched alkenes can be produced *via* chain walking or/and from the co-dimerization of ethylene with 1-butene. These two mechanisms are described in sections 2.4.1.6.2 and 2.4.1.6.3 (Scheme 2.12 and Scheme 2.13, respectively).

** A specific proposal as to the nature of the counter cation for the proposed species [W(NR)(NR')Et₂]⁻ has not been made in the scheme, due to the complexity of the catalytic reaction. It is possible, however, that the cation is aluminum-based, such as [AlCl₂L_n]⁺ (L = neutral 2 electron donor ligand; see section 2.4.2.7) or could be an ammonium species when ammonium chloride additives are used (see section 2.4.1.7)

2.4.1.6.2 Proposed metallacycle-mediated mechanism for the tungsten imido/ η^5 -EtAlCl₂ systems

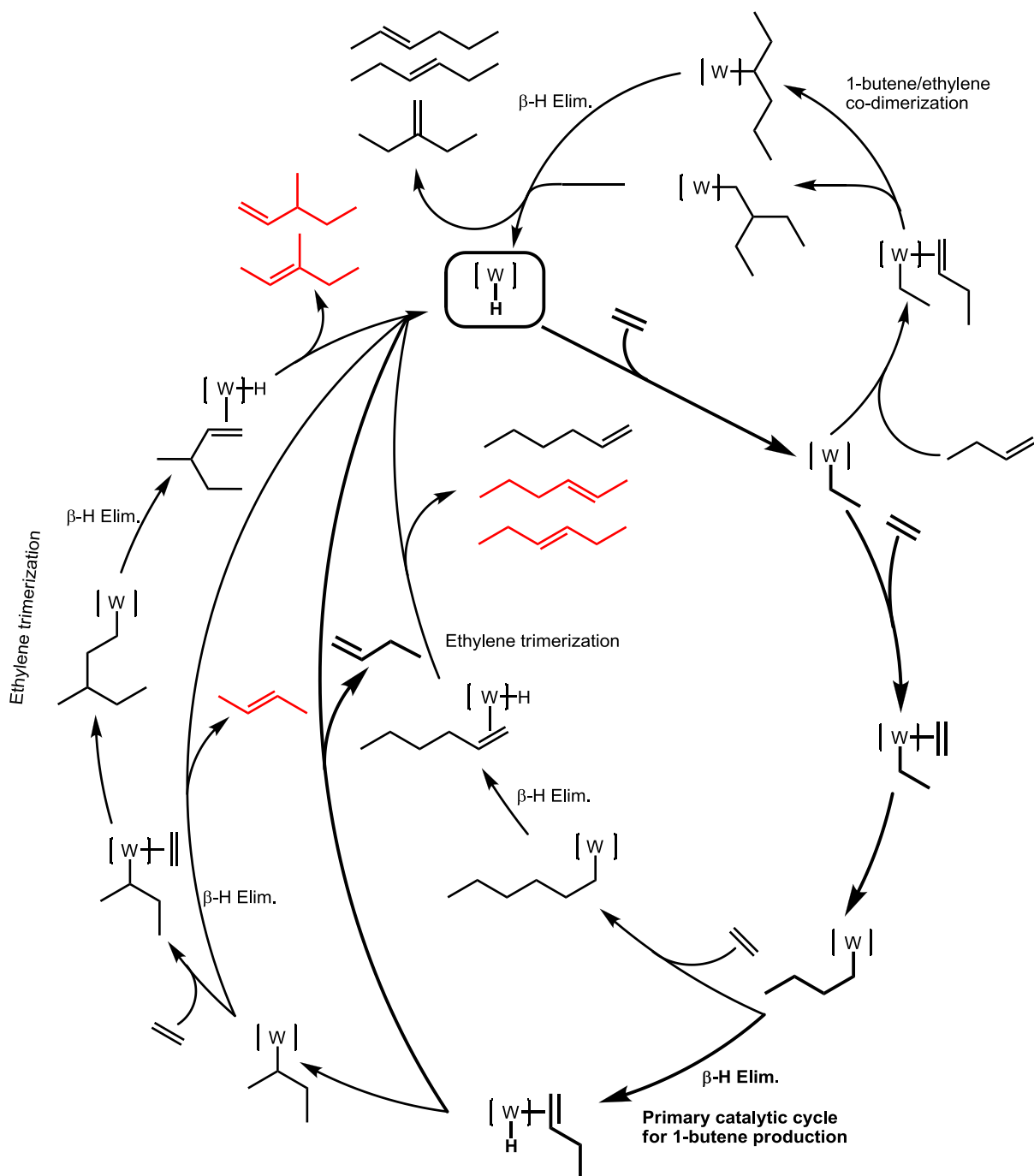
It is possible to use a tungsten-centered metallacyclic mechanism (Scheme 2.12) to rationalize the formation of ethylene, dimers, and trimers from the bis(imido) dimerization systems. Oxidative coupling of ethylene on a W(IV) or W(III) centre would afford a W(VI) or W(V) tungstenacyclopentane, respectively, which could then undergo agostic-assisted β -hydride transfer, resulting in the production of 1-butene. Alternatively, the tungstenacyclopentane could incorporate another ethylene molecule to form a tungstenacycloheptane, which would lead to production of 1-hexene. Coupling of one ethylene and one 1-butene molecule can lead to formation of two isomeric metallacycles, which can β -hydride eliminate to give 1-hexene, 3-hexene, 3 methyl-1-pentene, and 2 ethyl-1-butene (see catalysis cycle in the right hand side of Scheme 2.12).



Scheme 2.12 Proposed tungsten imido metallacycle-mediated mechanism for the selective dimerization and trimerization of ethylene

2.4.1.6.3 Proposed step-wise addition mechanism for the tungsten imido/15 EtAlCl₂ systems

In contrast to the proposed metallacyclic mechanism (Scheme 2.12), a more complicated tungsten-hydride mechanism can be envisaged (Scheme 2.13), in which the metal hydride could “chain walk” *via* successive β -hydride elimination/olefin re-insertion processes;³⁵ products that would result from chain walking are highlighted in red. According to the proposal described in Scheme 2.13, the tungsten hydride could incorporate ethylene, which then gives a tungsten ethyl species following hydride transfer.



Scheme 2.13 Proposed tungsten-hydride mediated mechanism for the selective dimerization and trimerization of ethylene (the products resulting from chain walking processes are highlighted in red)

Coordination of a second ethylene molecule would lead to a tungsten butyl species, which could either β -hydride eliminate to give 1-butene (main product), or incorporate another ethylene forming 1-hexene. Note, that in the case where 1-hexene remains bound or reinserts into the tungsten hydride, chain walking would again be likely, something that could lead to formation of both 2- and 3-hexene. Chain walking could also occur with 1-butene, giving rise to a tungsten-sec butyl intermediate, potentially allowing for 2-butene generation. Reaction of ethylene with such a tungsten *sec*-butyl intermediate could lead to formation of 3-methyl-1- and 3-methyl-2-pentene. Alternatively, trimers could form *via* reaction of 1-butene with a tantalum ethyl species, leading to the formation of 2- and 3-hexene and 2-ethyl-1-butene.

2.4.1.6.4 Comparison of predicted and experimentally-observed products from metallacyclic and step-wise addition oligomerization pathways

The data presented in Table 2.7 compare the main alkene products detected following tungsten imido-mediated ethylene oligomerization experiments against the alkenes theoretically produced *via* catalytic cycles involving i) a metallacycle, ii) a metal hydride with chain walking, and iii) a metal hydride without chain walking. Based on this analysis, it is proposed that a metallacyclic mechanism (*e.g.* Scheme 2.12) provides the best fit to the experimental results (Table 2.3). Specifically, the operation of a metallacyclic pathway is in agreement with the absence of 2-butene, and 3-methyl-2-pentene, as well as the formation of 3-methyl-1-pentene and 2 ethyl-1-butene, which form the majority of the C_6 fraction (> 85% in most runs, Table 2.3).

Table 2.7 Comparison of the theoretical and experimentally-observed organic products produced from various oligomerization mechanisms

	1-butene	2-butene	1-hexene	Internal hexenes	3 methyl-1-pentene	3 methyl-2-pentene	2 ethyl-1-butene
M-H with chain walking	✓	✓	✓	✓	✓	✓	✓
M-H without chain walking	✓		✓	✓			✓
Metallacycle	✓		✓	✓	✓		✓
Experimentally observed	✓		✓	✓	✓		✓

Furthermore, test runs 14 and 15 in Table 2.3, in which $MeAlCl_2$ was used instead of $EtAlCl_2$ as activator, clearly demonstrated catalytic dimerization. For both $EtAlCl_2$ and $MeAlCl_2$, Al-to-W *trans*-alkylation is likely. However, the resulting W-Et and W-Me species are likely to behave quite differently, with only the former being susceptible to β -hydride elimination, and hence to the formation of a W-H intermediate. The observed ability of $MeAlCl_2$ to initiate dimerization demonstrates that the presence of a β -hydride and hence, a metal hydride-mediated stepwise mechanism is, however, not absolutely necessary for dimerization to occur. Together, these results are in line with a metallacycle mechanism being active in the tungsten bis(imido)-mediated dimerization of ethylene.

However, it must be borne in mind that, in addition to the main products resulting from ethylene dimerization and trimerization, small amounts of heavier C_{8+} liquid olefins and traces of polyethylene are

also produced, along with traces of unidentified C₆ isomers. Although formation of polyethylene can occur *via* a metallacycle mechanism,³⁶ the presence of tungsten species able to promote a metal hydride-centered mechanism cannot be completely excluded. Hence, the most likely mechanistic scenario for the tungsten imido-mediated ethylene oligomerization described herein is that, following activation with EtAlCl₂, a dominant metallacyclic pathway is operative, but that a less favored secondary metal hydride process can also take place, generating traces of polyethylene and heavier C₈₊ alkenes.

2.4.1.7 Effect of additives in the bis(imido) tungsten-mediated ethylene dimerization

The use of additives that can improve the catalytic ethylene dimerization performance, in terms of activity and/or selectivity, has been reported previously. For example, it has been found that the addition of PPh₃ as an auxiliary ligand greatly enhanced the activity of certain nickel-based ethylene dimerization systems (section 1.7.1.1.1.1).^{24,37,38} Building on this work, a series of experiments was undertaken in order to probe the effects additives have on bis(imido) tungsten-mediated catalytic olefin dimerization. Et₃N was considered to be a good place to start since it has been successfully used as a component of the Sasol *in situ* olefin dimerization system (section 1.3.3). Additionally, the use of chloride as an additive in TaCl₅/Et₃Al-mediated ethylene oligomerization reactions has been reported to favor the formation of low molecular weight oligomers.⁴⁰ Similarly, the ethylene oligomerization system Cp₂ZrMe₂/LiCl/MAO produces dimers while the chloride-free Cp₂ZrMe₂/MAO system produces oligomers.³⁹ Hence, it was of interest to also examine whether the catalytic performance of the tungsten bis(imido) systems could also be influenced on addition of a chloride source. Consequently, in this section, a study of the effects resulting from addition of Et₃N, Oct₄NCl, and Et₃NHCl, prior to activation, on the performance of the tungsten bis(imido) ethylene dimerization systems is examined; the results are summarized in Table 2.8. Note, ammonium salts were chosen not only for their solubility, but also as their formation is implicit in the Sasol *in situ* initiator system (see section 1.3.3).

Table 2.8 Dimerization of ethylene at 45 bar ethylene/70 °C, using well-defined W(VI) bis(imido) pro-initiators in combination with a range of additives ^{a,b}

Run #	Pro-initiator	Additive (eq)	Time (min)	TON ^c	Act. ^d	Mol % C ₄ (in liq. prod.)	% 1-C ₄ in C ₄	Mol % C ₆ (in liq. prod.)	% 1-C ₆ in C ₆	% Lin in C ₆	% MP in C ₆	wt % C ₈ (in liq. prod.)
1	W(NDipp) ₂ Cl ₂ (DME) (27)	None	39.6	82.4	128.9	80.4	98.1	18.9	1.3	7.0	93.0	1.5
2	W(NDipp) ₂ Cl ₂ (DME) (27)	Et ₃ N (2)	32.1	89.9	168.0	85.6	98.9	14.0	2.5	8.9	91.1	0.7
3	W(NDipp) ₂ Cl ₂ (DME) (27)	Et ₃ N (4)	23.55	89.45	228.4	87.4	99.1	12.3	3.1	8.45	91.6	0.55
4	W(NDipp) ₂ Cl ₂ (DME) (27)	Et ₃ N (5)	24.1	88.8	221.5	89.9	99.2	9.9	3.6	22.2	77.8	0.4
5	W(NDipp) ₂ Cl ₂ (DME) (27)	Et ₃ N (6)	23.8	89.9	227.1	90.6	99.2	9.2	3.9	22.6	77.4	0.4
6	W(NDipp) ₂ Cl ₂ (DME) (27)	Et ₃ N (10)	55	63.5	69.3	94.1	99.2	5.8	4.3	6.4	93.6	0.2
7	W(NDipp) ₂ Cl ₂ (DME) (27)	Oct ₄ NCl (2)	18.2	89.4	295.2	85.2	98.9	14.4	2.7	5.8	94.2	0.8
8	W(NDipp) ₂ Cl ₂ (DME) (27)	Oct ₄ NCl (4)	17.9	88.5	297.3	88.4	99.2	11.3	3.4	7.3	92.7	0.6
9	W(NDipp) ₂ Cl ₂ (DME) (27)	Oct ₄ NCl (6)	17.9	87.6	293.9	91.1	99.3	8.7	4.1	8.4	91.6	0.4
10	W(NDipp) ₂ Cl ₂ (DME) (27)	Oct ₄ NCl (10)	19.4	22.2	69.0	95.4	99.3	4.5	3.8	8.2	91.8	0.2
11	W(NDipp) ₂ Cl ₂ (DME) (27)	Et ₃ NHCl (2)	20.9	89.8	257.7	83.7	98.7	15.8	2.3	15.5	84.5	0.8
12	W(NDipp) ₂ Cl ₂ (DME) (27)	Et ₃ NHCl (4)	23.7	96.2	244.1	87.7	99.1	12.0	3.1	15.1	84.9	0.6
13	W(NDipp)(NTpp)Cl ₂ (DME) (36)	None	29.4	89.4	182.8	81.1	98.4	18.4	1.9	4.6	95.5	1.3
14	W(NDipp)(NTpp)Cl ₂ (DME) (36)	Et ₃ N (4)	14.9	88.6	357.7	85.8	99.1	13.8	3.1	6.4	93.6	0.7
15	W(NDipp)(NTpp)Cl ₂ (DME) (36)	Oct ₄ NCl (2)	14.8	88.0	357.8	85.2	98.9	14.4	2.7	5.9	94.1	0.8
16	W(NTfp) ₂ Cl ₂ (DME) (28)	None	21.2	88.3	255.2	87.1	97.6	12.6	3.8	5.2	94.9	0.8
17	W(NTfp) ₂ Cl ₂ (DME) (28)	Et ₃ N (4)	46.3	9.4	12.2	89.7	97.0	10.1	6.6	8.2	91.8	0.5
18	W(NTfp) ₂ Cl ₂ (DME) (28)	Oct ₄ NCl (2)	34.3	88.2	154.5	90.4	98.0	9.4	5.9	7.4	92.6	0.4
19	W(NTfp) ₂ Cl ₂ (DME) (28)	Et ₃ NHCl (2)	7.8	1.2	9.1	93.2	97.7	6.3	8.6	10.5	89.5	1.0
20 ^e	W(NDipp) ₂ Cl ₂ (DME) (27)	None	136.1	276.2	121.7	77.1	98.5	22.3	1.8	4.6	95.4	1.2
21 ^e	W(NDipp) ₂ Cl ₂ (DME) (27)	Oct ₄ NCl (2)	37.8	229.2	364.2	89.1	99.1	10.7	2.8	6.0	94.0	0.5
22 ^f	W(NDipp) ₂ Cl ₂ (DME) (27)	Oct ₄ NCl (2)	61.6	441.1	429.9	88.8	99.0	10.9	2.7	5.7	94.3	0.5
23 ^f	W(NDipp)(NTpp)Cl ₂ (DME) (36)	Oct ₄ NCl (2)	88.5	421.0	285.3	87.6	98.9	12.1	2.4	5.2	94.8	0.6

^a General conditions: 20 μmol W complex and 300 μmol EtAlCl₂; PhCl (solvent) 74 mL; 70 °C; ethylene pressure (45 bar); stirrer speed 1000 rpm; nonane standard (1.000 mL); catalytic runs were performed until consumption of C₂H₄ dropped below 0.2 g min⁻¹ or until the reactor was filled, at which time reaction was quenched by addition of dilute HCl. ^b No polyethylene was produced. ^c TON is reported in (kg C₂H₄) (mol W)⁻¹ bar⁻¹. ^d Activity is reported in (kg C₂H₄) (mol W)⁻¹ h⁻¹bar⁻¹ and is based on the total ethylene consumption. ^e Performed in a 1.2 L reactor with 40 μmol W complex and 600 μmol EtAlCl₂; PhCl (solvent) 148 mL; 70 °C; ethylene pressure (45 bar); stirrer speed 1000 rpm; nonane standard (2.000 mL). ^f Performed in a 1.2 L reactor with 20 μmol W complex and 300 μmol EtAlCl₂; PhCl (solvent) 148 mL; 70 °C; ethylene pressure (45 bar); stirrer speed 1000 rpm; nonane standard (2.000 mL).

2.4.1.7.1 Effect of Et₃N, Oct₄NCl, and Et₃NHCl on the activity of W(NDipp)₂Cl₂(DME) (27)

Inspection of the data presented in Table 2.8 and Figure 2.7 clearly demonstrates that the addition of 2-6 equivalents of Et₃N, Oct₄NCl, or Et₃NHCl brings about an almost doubling of the ethylene dimerization activity of **27**, when activated with EtAlCl₂, with the highest activity of 297.3 kg C₂H₄ (mol W)⁻¹ h⁻¹bar⁻¹ being achieved with Oct₄NCl (run 8; Table 2.8). Interestingly, the dimerization activity remains constant over a wide range of additive-to-tungsten ratios (4-6 equivalents for Et₃N and 2-4 equivalents for

Oct₄NCl). When the additive-to-tungsten ratio is raised to 10, catalyst deactivation occurs, possibly due to high occupation of free coordination sites of the catalytically active species by these Lewis basic additives.

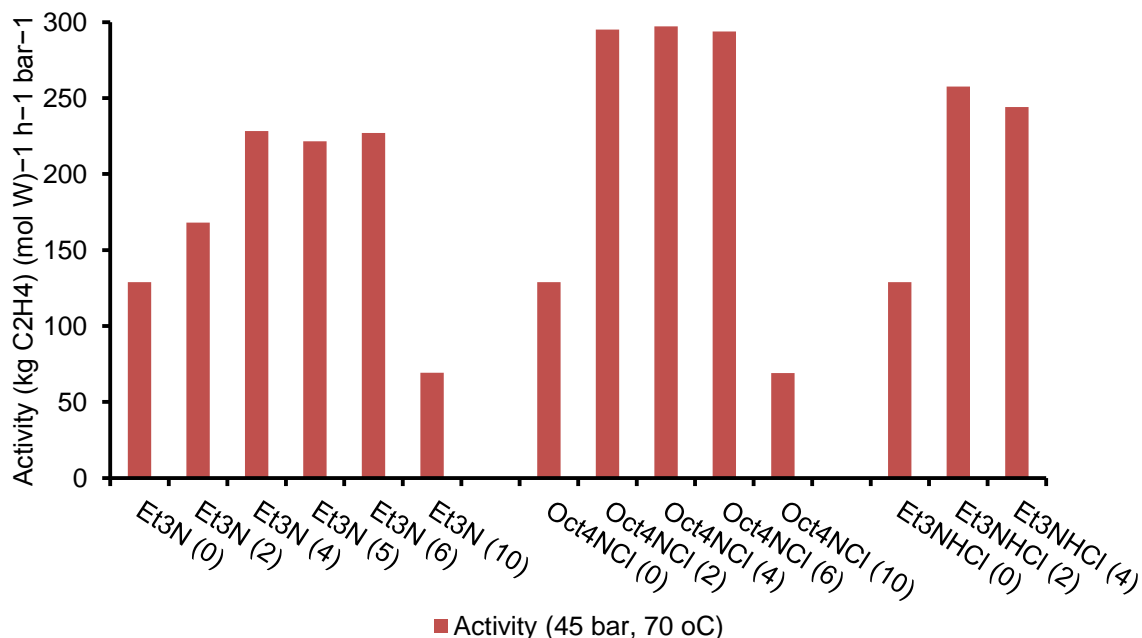


Figure 2.7 Activities achieved using $W(NDipp)_2Cl_2(DME)$ (**27**) in the dimerization of ethylene at 45 bar ethylene/70 °C as a function of additive (the amount of additive used in equivalents per tungsten is given in brackets); data taken from Table 2.8 (runs 1-12)

The different effect imparted on the catalytic performance by the ammonium chloride salts, compared with that from Et₃N, highlights the beneficial role of chloride ions. Nevertheless, the differences in performance of the additives Oct₄NCl and Et₃NHCl are hard to rationalize, especially due to the presence of an acidic proton for the latter.

2.4.1.7.2 Effect of Et₃N, Oct₄NCl, and Et₃NHCl on the selectivity of $W(NDipp)_2Cl_2(DME)$ (**27**)

The data presented in Figure 2.8 indicate how the product selectivity of pro-initiator **27** varies as a function of additive used. Comparison of the runs where an additive was used (runs 2-12; Table 2.8) with run 1 (Table 2.8) where no additive is employed, clearly demonstrate that the selectivity towards the dimers fraction increases as the tungsten to additive ratio is increased (see Figure 2.8), leading to an improvement in the selectivity towards butenes of 10% (compare run 1 with run 9 in Table 2.8), along with the aforementioned doubling of the catalytic activity (section 2.4.1.7.1). Within the dimers fraction the selectivity towards 1-butene remained excellent, at over 98.7%.

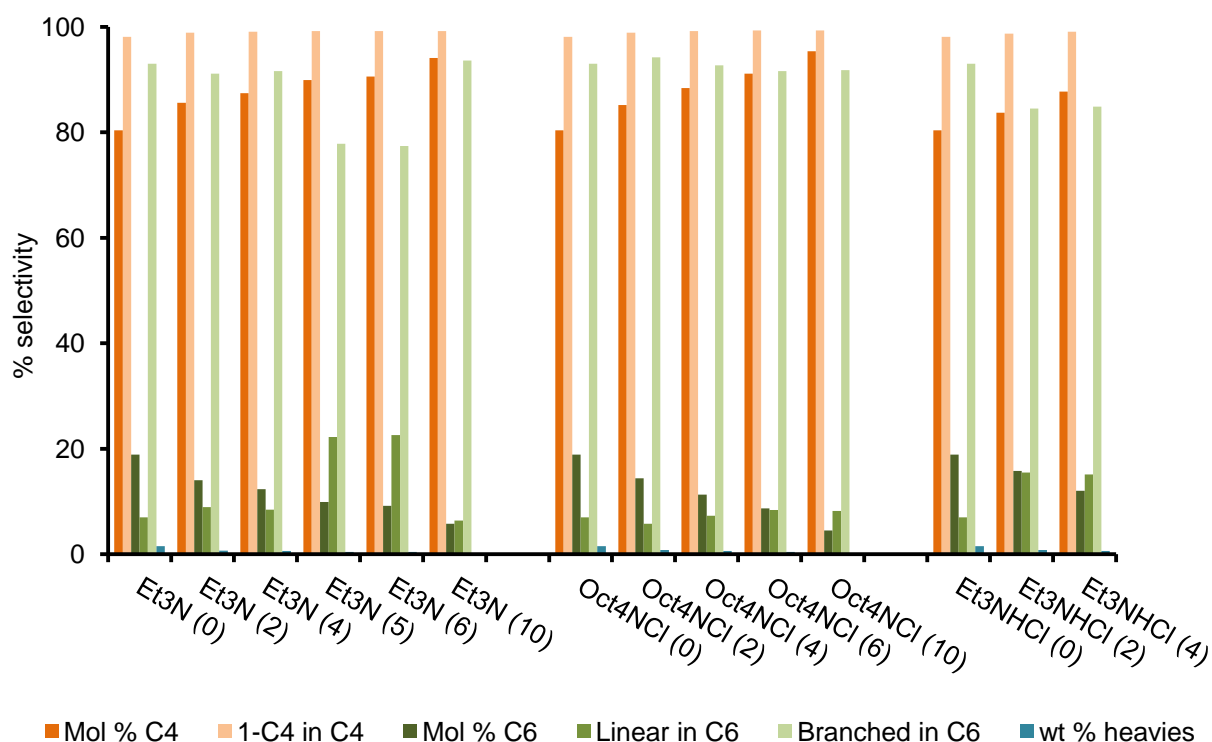


Figure 2.8 Product selectivities (expressed in mol % or wt%) obtained using $W(NDipp)_2Cl_2(DME)$ (**27**) in the dimerization of ethylene at 45 bar/70 °C as a function of additive (the amount of additive used in equivalents per tungsten is given in brackets); data taken from Table 2.8 (runs 1-12)

The selectivity towards trimers follows the opposite trend to the selectivity towards butenes, *i.e.* decreases as the tungsten to additive ratio increases without any significant changes being observed in the selectivity within the trimers fraction (Figure 2.8, Table 2.8). As was observed for the selectivity towards trimers, the amount of the heavier liquid olefins formed is also reduced, when additives are employed, further improving the selectivity profile of the tungsten bis(imido) based ethylene dimerization systems (Figure 2.8, Table 2.8).

2.4.1.7.3 Effect of the imido substituent and type of additive on the catalytic activity and selectivity

After the success of Et₃N (4 eqvs.), Oct₄NCl (2 eqvs.), and Et₃NHCl (2 eqvs.) in increasing the performance of ethylene dimerization pro-initiator $W(NDipp)_2Cl_2(DME)$ (**27**) in terms of activity and selectivity (sections 2.4.1.7.1 and 2.4.1.7.2), it was of interest to examine the effect of these additives on the activity and selectivity of the more active pro-initiators $W(NTfp)_2Cl_2(DME)$ (**28**) and $W(NDipp)(NTpp)Cl_2(DME)$ (**36**). The catalysis results from these studies are presented in Table 2.8 (runs 13-19), with a chart of the catalytic activity versus the type of additive and imido substituents being presented in Figure 2.9.

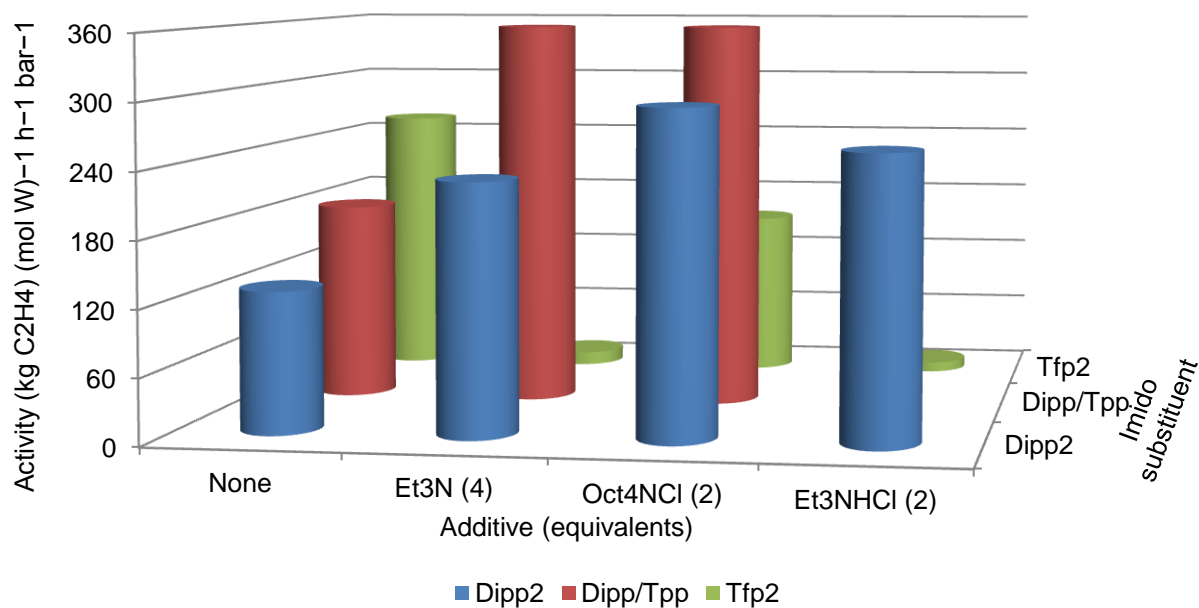


Figure 2.9 Activities achieved using $W(NDipp)_2Cl_2(DME)$ (**27**), $W(NTfp)_2Cl_2(DME)$ (**28**), and $W(NDipp)(NTpp)Cl_2(DME)$ (**36**) in the dimerization of ethylene at 45 bar ethylene pressure and 70 °C as a function of additive (the amount of additive used in equivalents per tungsten is given in brackets); data taken from Table 2.8 (runs 1, 3, 7, 11, 13-19)

From the data presented in Figure 2.9 it is evident that the catalytic activity of pro-initiator $W(NDipp)(NTpp)Cl_2(DME)$ (**36**) increases by approximately 100% when four equivalents of Et_3N or two equivalents of Oct_4NCl are added to the catalytic reaction *prior* to activation. As was observed for pro-initiator $W(NDipp)_2Cl_2(DME)$ (**27**) (section 2.4.1.7.1, Figure 2.9), there is a positive influence of the presence of additive on the activity of the system derived from pro-initiator **36**, although the magnitude of the effect is much higher, giving catalytic activities of up to 357.7 kg C₂H₄ (mol W)⁻¹ h⁻¹ bar⁻¹. Similarly, it was expected that the catalytic activity of the most active, additive-free, ethylene dimerization system, $W(NTfp)_2Cl_2(DME)$ (**28**)/15 EtAlCl₂ (see section 2.4.1.2), would also be enhanced using the aforementioned additives. Surprisingly, however, for this system a dramatic attenuation of catalysis was observed when complex **28** was used in combination with Et_3N , Oct_4NCl , or Et_3NHCl . To date, this unexpected result cannot be explained. Notably, as was the case with pro-initiator **27**, incorporation of additives with pro-initiators **36** and **28** again led to a slight increase in the selectivity towards 1-butene in the products fraction (Table 2.8; runs 1, 3, 7, 11, 13-19).

2.4.1.7.4 Large-scale ethylene dimerization with $W(NDipp)_2Cl_2(DME)$ (**27**)/2 Oct_4NCl /15 EtAlCl₂ or $W(NDipp)(NTpp)Cl_2(DME)$ (**36**)/2 Oct_4NCl /15 EtAlCl₂: attempts to develop a highly active and selective dimerization system

From the encouraging data obtained from the preliminary scoping studies made with the tungsten bis(imido)/additive-mediated ethylene dimerization systems, runs 1-19 (Table 2.8), the development of a highly active and selective ethylene dimerization system was attempted (runs 20-23; Table 2.8). To this

end, an initial baseline study was undertaken; 40 μmol of complex $\text{W}(\text{NDipp})_2\text{Cl}_2(\text{DME})$ (**27**) were activated with 15 equivalents EtAlCl_2 in the 1.2 L autoclave, which lead to an activity of 121.7 $\text{kg C}_2\text{H}_4 (\text{mol W})^{-1} \text{h}^{-1}\text{bar}^{-1}$ (run 20, Table 2.8). Repeating the same reaction by adding two equivalents of Oct_4NCl per tungsten *prior* to activation (run 21, Table 2.8) led to a tripling of the system's catalytic activity to 364.2 $\text{kg C}_2\text{H}_4 (\text{mol W})^{-1} \text{h}^{-1}\text{bar}^{-1}$. Subsequently, a further test was made with **27** at a lower tungsten loading of 20 μmol , which gave a further enhancement in activity to 429.9 $\text{kg C}_2\text{H}_4 (\text{mol W})^{-1} \text{h}^{-1} \text{bar}^{-1}$ (run 22, Table 2.8), which is the highest ethylene dimerization activity achieved in this thesis. The increase in catalytic activity observed here on lowering the pro-initiator loading from 40 to 20 μmol in the 1.2 L autoclave with an additive present, contrasts with the observations described in section 2.4.1.4 which demonstrated that lower tungsten loadings lead to an attenuation of the catalytic performance of system $\text{W}(\text{NDipp})_2\text{Cl}_2(\text{DME})$ (**27**) /15 EtAlCl_2 . A possible explanation for this increase in the catalytic activity at a lower tungsten loading in run 22 of Table 2.8 could be the presence of Oct_4NCl which can possibly stabilize the catalytic system in higher dilution. However, in contrast, when an identical test, this time employing 20 μmol $\text{W}(\text{NDipp})(\text{NTpp})\text{Cl}_2(\text{DME})$ (**36**) / 2 Oct_4NCl /15 EtAlCl_2 , was undertaken (run 23; Table 2.8), a lower activity of 285.3 $\text{kg C}_2\text{H}_4 (\text{mol W})^{-1} \text{h}^{-1} \text{bar}^{-1}$ was obtained. Together, these observations indicate that further studies are necessary in order to understand the exact role of ammonium chloride additives in the catalytic behavior of the tungsten bis(imido) systems towards ethylene.

2.4.2 1-Hexene dimerization mediated by tungsten bis(imido) pro-initiators

The importance of the oligomerization of heavier α -olefins has been outlined in section 1. Hence, it was of interest to explore the potential of the bis(imido) tungsten-based ethylene dimerization systems described herein, for the dimerization of 1-hexene. Importantly, the catalytic testing for 1-hexene dimerization can be easily conducted at 60 $^\circ\text{C}$, in contrast to the ethylene testing where the use of autoclaves is required.

It must be noted that, in contrast to the experiments where ethylene was used as a feedstock, 1-hexene consumption was not monitored during catalysis, hence the exact time when uptake of the olefinic substrate stops, due to catalyst deactivation, has not been determined for these systems. Consequently, only the TONs and 1-hexene conversions were determined for the 1-hexene dimerization systems, rather than the catalytic activity.

2.4.2.1 Comments on the activity of the tungsten bis(imido)-based 1-hexene dimerization systems

The results from the dimerization of 1-hexene mediated by a range of tungsten bis(imido) pro-initiators are presented in Table 2.9. The TONs obtained are in the range 14.0-239.3 $\text{kg C}_6\text{H}_{12} (\text{mol TM})^{-1}$, which compare well to the TONs determined for other 1-hexene dimerization systems previously reported.⁴⁰⁻⁴² However, the conversion of 1-hexene to oligomers is at best, moderate, in all cases (5.8-65.8%), something presumably due to the isomerization of 1-hexene to internal hexenes (of up to 63.0%), which

are inert towards dimerization (see section 2.4.2.3). Substrate isomerization is commonly encountered in the dimerization of heavier α -olefins and reduces the industrial value of the process, since it converts the useful terminal olefin to internal.^{40,41,43} Notably, the 1-hexene TON obtained using the well-defined tungsten bis(imido) complexes is comparable to that achievable with the Sasol *in situ* dimerization system.¹

Table 2.9 1-Hexene dimerization using well-defined tungsten bis(imido) pro-initiator complexes with EtAlCl₂ co-catalyst^a

Run #	Pro-initiator	TON ^b	Isom. ^c (%)	Conv. of C ₆ ^d (%)	Mol % in total fraction		
					C ₆	C ₁₂	C ₁₈
1	W(NDipp) ₂ Cl ₂ (DME) (27)	168.7	41.6	47.1	69.2	29.8	0.94
2	W(NTfp) ₂ Cl ₂ (DME) (28)	85.6	63.0	23.9	86.5	13.3	0.20
3	W(NTpp) ₂ Cl ₂ (DME) (31)	67.5	23.3	18.5	90.3	8.7	1.05
4	W(NPfp) ₂ Cl ₂ (DME) (29)	51.8	56.0	16.0	91.4	8.2	0.33
5	W(NMes ^F) ₂ Cl ₂ (DME) (30)	14.0	21.8	5.8	97.3	2.3	0.47
6	W(NDipp)(N ⁱ Bu)Cl ₂ (DME) (33)	239.3	30.2	65.8	51.2	47.7	1.02
7	W(NDipp)(NTpp)Cl ₂ (DME) (36)	221.4	30.4	59.7	57.8	40.8	1.38
8	W(NDipp)(NTfp)Cl ₂ (DME) (35)	149.8	52.4	40.9	74.6	24.5	0.92
9	W(NDipp) ₂ Cl ₂ (py) ₂ (39)	223.2	28.0	60.3	57.2	41.6	1.24
10	W(NtBu) ₂ Cl ₂ (py) ₂ (41)	235.8	33.2	65.2	51.7	47.7	0.54

^a General conditions: 0.40 μ mol tungsten and 6.0 μ mol EtAlCl₂; PhCl (solvent) 190 μ L; 60 °C; 1-hexene 250 μ L (2.00 mmol); nonane standard (40.0 μ L) and *p*-anisaldehyde standard (97.4 μ L) added after quenching; reaction time 300 min after which quenching followed by addition of wet d₆-acetone. The selectivity towards dimers was 95-100% for all runs. The branching selectivity of the dimers fraction in each run was found to be: mono branched dimers = 85%-95%, di-branched dimers = 5% - 15%, and linear < 0.5%. ^b Reported in (kg C₆H₁₂) (mol TM)⁻¹ and refers to the amount 1-hexene converted to oligomers. ^c Defined as the fraction of terminal alkene that is isomerized to internal alkenes at the end of a run. ^d Defined as the mass% of hexenes converted to oligomers at the end of a run and does not include isomerized 1-hexene.

In Figure 2.10 the TONs determined for pro-initiators **27-31** and **33, 35, 36** are presented as a function of the imido substituent; no obvious trends between the TON and the nature of the imido groups are evident. However, it appears that complexes containing the group NDipp, such as **27, 33, 35,** and **36,** exhibit higher TONs compared to the rest of the complexes, an observation that is not easy to rationalize. Additionally, the catalytic profiles obtained using pro-initiators **27-31** and **33, 35, 36** with respect to the dimerization of 1-hexene compared to ethylene (sections 2.4.1.1 and 2.4.1.2) are completely different. For example complex W(NDipp)(NⁱBu)Cl₂(DME) (**33**) was found to be the most effective pro-initiator for the dimerization 1-hexene, achieving a TON of 239.3 kg C₆H₁₂ (mol TM)⁻¹ (run 6, Table 2.9), although its ethylene dimerization activity was one of the lowest within the series (sections 2.4.1.1 and 2.4.1.2). In contrast, complex W(NTfp)₂Cl₂(DME) (**28**), which is one of the best ethylene dimerization pro-initiators (sections 2.4.1.1 and 2.4.1.2), exhibited a lower TON of 85.6 kg C₆H₁₂ (mol W)⁻¹ (run 2, Table 2.9) compared to that using **33**.

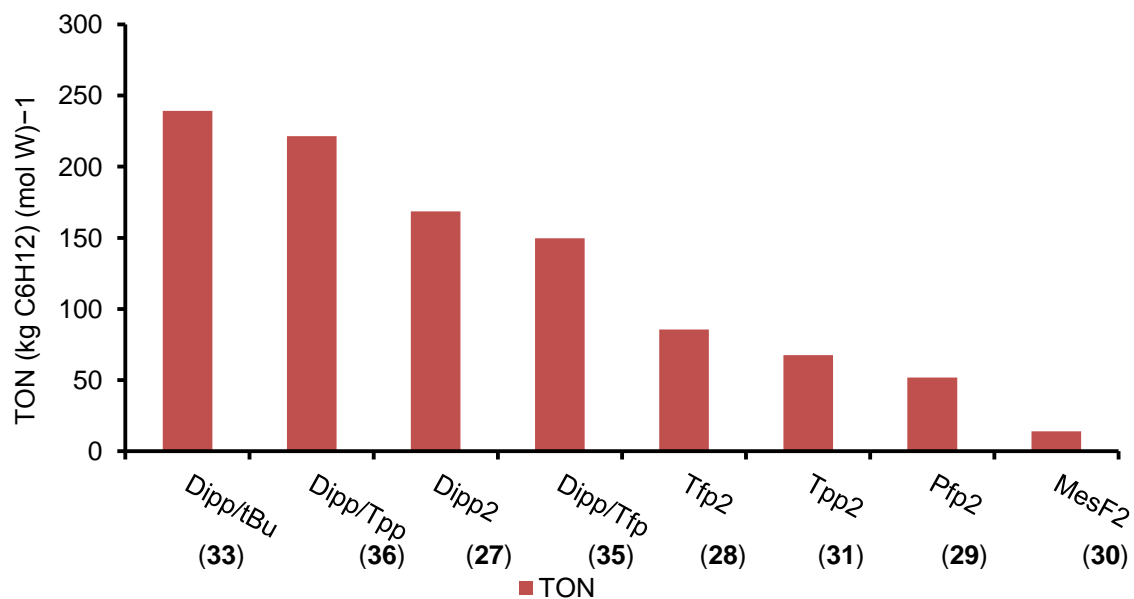


Figure 2.10 Summary of the TON versus imido ligand substituent of the tungsten bis(imido) pro-initiators in the dimerization of 1-hexene; data taken from Table 2.9

The observed difference in activity profile of the bis(imido) pro-initiators in the dimerization of 1-hexene compared to those for ethylene is not unexpected. In contrast to ethylene, substrate isomerization is possible with 1-hexene, a process that competes with the dimerization process, generating oligomerisation-inactive internal hexenes (see section 2.4.2.3). Hence, it is likely that the best catalytic system for the dimerization of 1-hexene is that which is not only stable and highly active, but also does not isomerize the substrate. This second requirement for the dimerization system to be inert towards substrate isomerization is enough to radically alter the catalytic profile of the bis(imido) pro-initiators in the dimerization of 1-hexene compared to ethylene.

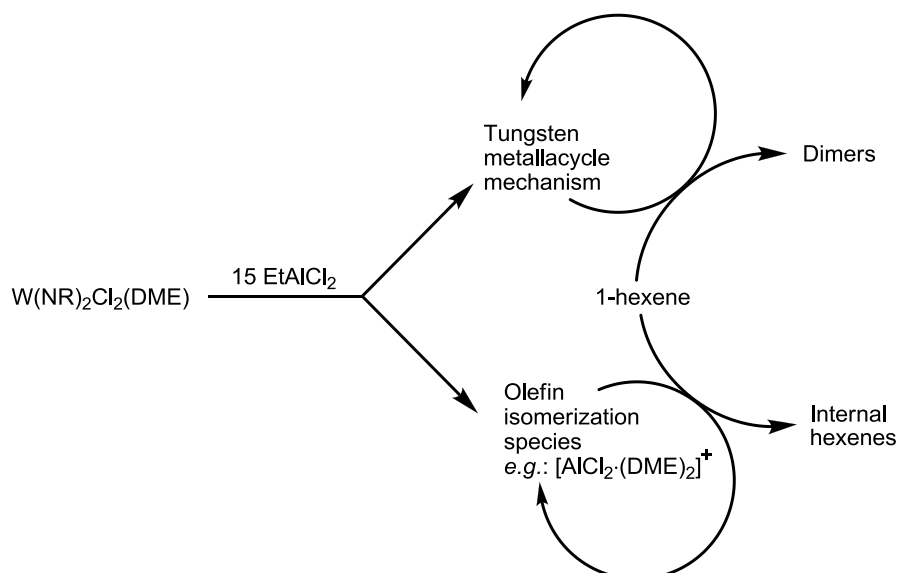
As was undertaken for the ethylene dimerization experiments (section 2.4.1.1.3), the TONs arising from the use of complexes $W(NDipp)_2Cl_2(py)_2$ (**39**) and $W(N^iBu)_2Cl_2(py)_2$ (**41**) in the dimerization of 1-hexene were compared, in order to probe the effect of alkyl versus aryl imido substituents. From the TONs presented in Table 2.9, runs 9 and 10, it is clear that the alkyl-substituted imido system is more effective for 1-hexene dimerization, a situation that is the reverse of that determined for the dimerization of ethylene using **39** and **41**. It must be noted that the TON achieved using complex **39** of $223.2 \text{ kg C}_6\text{H}_{12} (\text{mol TM})^{-1}$ is ~30% greater than that achieved using its DME-bearing counterpart $W(NDipp)_2Cl_2(DME)$ (**27**). This difference is attributed to the presence of pyridine, which similar to Et_3N (section 2.4.1.7) improves catalysis (see sections 2.4.1.7 and 2.4.2.6 describing additive effects on catalysis).

2.4.2.2 Selectivity of the tungsten bis(imido)-based 1-hexene dimerization systems

The selectivity of the tungsten bis(imido) pro-initiators for the dimers fraction is high, with the oligomers fraction consisting of 95-100% dimers, with only 0-5% trimers being produced, regardless of the bis(imido) complex pro-initiator employed (Table 2.9). Additionally, the branching selectivity within the dimers fraction is also high, with mono-branched dimers being the primary products (85-95% of the

dimers fraction), with much smaller quantities of di-branched dimers being generated (5-15% of the dimers fraction), together with traces of linear dodecenes (< 0.5% of the dimers fraction). Interestingly, the branching selectivity achieved using the *in situ* Sasol system for dimerization of 1-hexene is different to that obtained here with the well-defined pro-initiators; the *in situ* Sasol system produces larger amounts of di-branched dimers, comprising up to 48% of the dimers fraction. This difference in the branching selectivity between the Sasol *in situ* system and the well-defined mono(imido) systems examined herein, suggest that different dimerization mechanisms may be in operation for the two systems.¹

At this point it must be mentioned that in section 2.4.1.6.4, it is argued that the tungsten bis(imido)-based systems dimerize olefins *via* a metallacyclic mechanism rather than a step-wise addition pathway. Although olefin isomerization is possible *via* a metallacyclic mechanism, which undergoes β -hydride elimination (see section 1.6.1), computational studies suggest that the tungsten metallacycles generated here are more likely to degrade *via* a β -hydride transfer process, which does not support olefin isomerization.⁴⁴ Hence, the suggestion that a metallacyclic mechanism is operative for tungsten imido-mediated olefin dimerization is at odds with the observed isomerization when 1-hexene is used as the substrate. However, this apparent contradiction can be resolved by suggesting that both dimerization- and isomerization-active species are formed (Scheme 2.14). This idea is supported by the generation of compounds such as $[\text{AlCl}_2(\text{DME})_2][\text{AlCl}_4]$ (**43**) from the reaction of tungsten bis(imido) complexes with aluminum reagents (section 2.4.2.7), which were found active in the isomerization of 1-hexene.^{††}



Scheme 2.14 Formation of a metallacycle-mediated olefin dimerization species along with an olefin isomerization species after activation of a bis(imido) complex with 15 EtAlCl_2

^{††} For the case of ethylene dimerization, these potentially formed olefin isomerization species will be coordinatively saturated with ethylene due to the high ethylene pressures employed in these experiments preventing them in that way from isomerizing 1-butene to 2-butene. This is the reason why formation of mainly 1-butene is observed when ethylene is dimerized using tungsten bis(imido) pro-initiators (section 2.4.1.3).

2.4.2.3 Examination of the dimerization potential of the system W(NDipp)₂Cl₂(DME)/15 EtAlCl₂ with different olefinic substrates

In **Table 2.10** the catalytic behaviour of the system W(NDipp)₂Cl₂(DME) (**27**)/15 EtAlCl₂ is reported for various different olefinic substrates. Initially, it was of interest to examine the effect that the use of an increased amount of 1-hexene would have on the TON of the catalytic reaction. Hence, when 10,000 equivalents of 1-hexene were employed (run 2, Table 2.10), instead of the usual 5000 equivalents (run 1, Table 2.10), the TON almost doubled from 168.7 to 297.4 kg C₆H₁₂ (mol W)⁻¹, while the product selectivity remained almost the same. This increase in TON when a larger amount of substrate is used suggests that, in contrast to the dimerization of ethylene, the dimerization reaction of 1-hexene using the tungsten bis(imido) based systems stops not necessarily due to catalyst deactivation, but due to the insufficient/low concentration of 1-hexene in the reaction mixture towards the end of the dimerization suggesting that even higher TONs could be achieved by appropriately tuning the reactions conditions (e.g. by increasing the amount of substrate used).

Table 2.10 Dimerization of various olefinic substrates using W(NDipp)₂Cl₂(DME) (**27**) activated with 15 equivalents of EtAlCl₂^a

Run #	Pro-initiator	Substrate	TON ^b	Isom. ^c (%)	Conv. of monomer ^d (%)	Mol % in total fraction		
						Monomer	Dimer	Trimer
1	W(NDipp) ₂ Cl ₂ (DME) (27)	1-C ₆ H ₁₂	168.7	41.6	47.1	69.2	29.8	0.94
2 ^e	W(NDipp) ₂ Cl ₂ (DME) (27)	1-C ₆ H ₁₂	297.4	25.7	41.6	74.1	25.1	0.85
3 ^f	W(NDipp) ₂ Cl ₂ (DME) (27)	1-C ₁₂ H ₂₄	153.1	38.8	50.5	66.2	33.8	0.00
4	W(NDipp) ₂ Cl ₂ (DME) (27)	<i>trans</i> -3-C ₆ H ₁₂	0.0	0.0	0.0	100	0.0	0.00
5	W(NDipp) ₂ Cl ₂ (DME) (27)	2-Me-1-C ₅ H ₁₀	0.0	0.0	0.0	100	0.0	0.00

^a General conditions: 0.40 μmol tungsten; PhCl (solvent) 190 μL; 60 °C; 2.00 mmol of substrate; nonane standard (40.0 μL) and *p*-anisaldehyde standard (97.4 μL) added after quenching; reaction time 300 min after which quenching followed by addition of wet d₆-acetone. The selectivity towards dimers was 95-100% for all runs. The branching selectivity of the dimers fraction in each run was found to be: mono branched dimers = 85%-95%, di-branched dimers = 5% - 15%, and linear < 0.5%. ^b TON is reported in (kg C₆H₁₂) (mol TM)⁻¹ and refers to the amount of 1-hexene converted to oligomers. ^c Defined as the fraction of terminal alkene that is isomerized to internal alkenes at the end of a run. ^d Defined as the mass% of substrate converted to oligomers at the end of a run and does not include isomerized substrate. ^e 4.00 mmol (10000 eq) of 1-hexene were used. ^f GC chromatography was used to determine the composition of the final reaction mixture instead of ¹H NMR spectroscopy.

In order to examine the potential of the tungsten bis(imido) dimerization systems towards heavier α-olefins, an experiment was undertaken in which 1-dodecene was used in the place of 1-hexene (run 3, Table 2.10). The TONs and product selectivities between this run and that for 1-hexene (runs 1 and 3, Table 2.10) are comparable, indicating that that use of these tungsten bis(imido)-based pro-initiators can be extended to the dimerization of heavy α-olefins.

Lastly, an important finding is that the tungsten bis(imido) dimerization systems described here are inert towards internal olefins such as *trans*-3-hexene (run 4, Table 2.10) or terminal olefins, which are di-substituted on the β-olefinic carbon such as 2-methyl-1-pentene (run 5, Table 2.10). This inability of the bis(imido) systems to dimerize internal olefins is the reason for the observed moderate conversions of

1-hexene to oligomers (section 2.4.2.1) and confirms that the substrate isomerization that occurs during catalysis is an undesirable process that competes with oligomerization.

2.4.2.4 Study of the effect of W:EtAlCl₂ ratio on the dimerization of 1-hexene

In the introduction to section 2.4 it was stated that the pro-initiator-to-activator ratio used for the majority of the catalytic dimerization reactions undertaken during this work is 1:15. This choice was made based on the previous studies of the *in situ* Sasol dimerization system, where it was found that a W:Al ratio of 1:15 gave rise to a reasonably active dimerization system.¹ Nevertheless, the *in situ* Sasol system differs quite significantly in its behavior to that of the well-defined tungsten complexes examined herein. Hence, it is possible that 15 equivalents of EtAlCl₂ is not optimal for the dimerization of 1-hexene. In this section, a short study on the effect of varying the W:Al ratio on higher α -olefin dimerisation is performed, with the results given in Table 2.11 and summarised in Figure 2.11.

Table 2.11 Activation of W(NDipp)₂Cl₂(DME) (**27**) with various EtAlCl₂ loadings for the dimerization of 1-hexene^a

Run #	Pro-initiator	EtAlCl ₂ loading (eq)	TON ^b	Isom. ^c (%)	Conv. of C ₆ ^d (%)	Mol % in total fraction		
						C ₆	C ₁₂	C ₁₈
1	W(NDipp) ₂ Cl ₂ (DME)	1	0.0	0.0	0.0	0.0	0.0	0.00
2	W(NDipp) ₂ Cl ₂ (DME)	2	0.0	0.0	0.0	0.0	0.0	0.00
3	W(NDipp) ₂ Cl ₂ (DME)	4	16.4	18.1	4.5	97.7	2.3	0.03
4	W(NDipp) ₂ Cl ₂ (DME)	8	231.6	28.6	62.9	54.4	44.4	1.19
5	W(NDipp) ₂ Cl ₂ (DME)	15	168.7	41.6	47.1	69.2	29.8	0.94
6	W(NDipp) ₂ Cl ₂ (DME)	20	222.8	29.1	61.1	56.4	42.2	1.38

^a General conditions: 0.40 μ mol tungsten; PhCl (solvent) 190 μ L; 60 °C; 1-hexene 250 μ L (2.00 mmol); nonane standard (40.0 μ L) and *p*-anisaldehyde standard (97.4 μ L) added after quenching; reaction time 300 min after which quenching followed by addition of wet d₆-acetone. The selectivity towards dimers was 95-100% for all runs. The branching selectivity of the dimers fraction in each run was found to be: mono branched dimers = 85%-95%, di-branched dimers = 5% - 15%, and linear < 0.5%. ^b TON is reported in (kg C₆H₁₂) (mol TM)⁻¹ and refers to the amount of 1-hexene converted to oligomers. ^c Defined as the fraction of terminal alkene that is isomerized to internal alkenes at the end of a run. ^d Defined as the mass% of hexenes converted to oligomers at the end of a run and does not include isomerized 1-hexene.

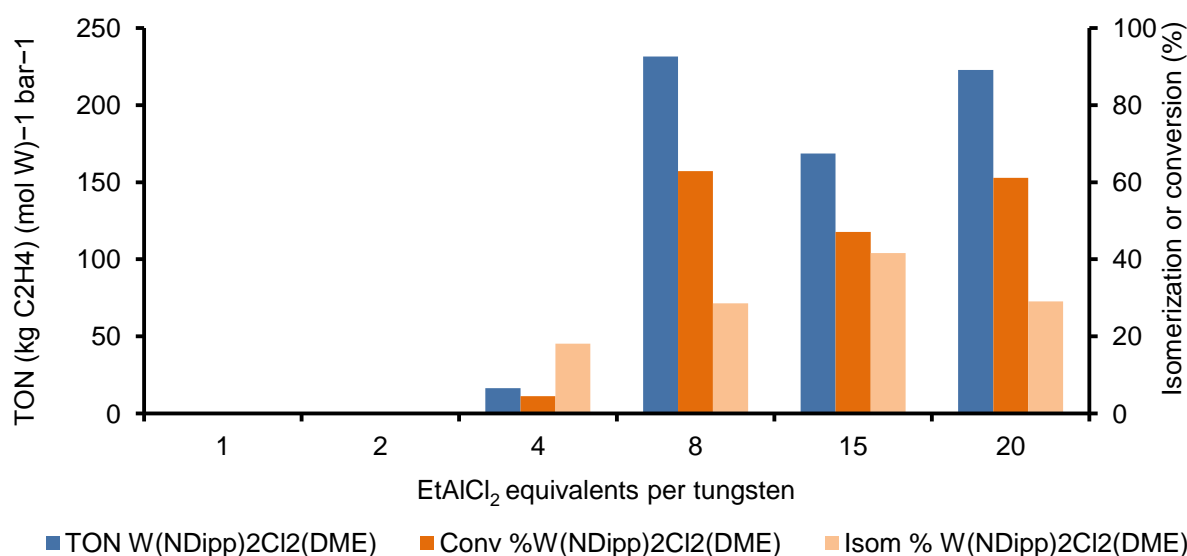


Figure 2.11 TONs, conversion, and extent of substrate isomerization mediated by W(NDipp)₂Cl₂(DME) (**27**) in the dimerization of 1-hexene versus the number of equivalents of EtAlCl₂ per tungsten used for activation; data taken from Table 2.11

Analyses of the catalytic test data show that when $W(NDipp)_2Cl_2(DME)$ (**27**) is activated with one or two equivalents of $EtAlCl_2$, no catalytic activity is observed, although a low TON is obtained when the W:Al ratio reaches 1:4. Here, the use of 15 equivalents of $EtAlCl_2$ (run 5, Table 2.11) is not optimal in the case of pro-initiator **27**, with the use of 8 or 20 equivalents of $EtAlCl_2$ resulting in higher TONs. The % conversion changes in a similar way to the TON while the % isomerization seems to achieve its maximum value at 15 equivalents of $EtAlCl_2$. This increase of the catalytic systems tendency towards isomerization when 15 equivalents of $EtAlCl_2$ are used could possibly explain the observed drop in TON at 15 equivalents of $EtAlCl_2$ since the dimerization and isomerization are competing processes (section 2.4.2.3). Hence, if no isomerization occurred it would be possible for the TON to achieve its maximum value at 15 equivalents of $EtAlCl_2$.

2.4.2.5 Use of various alkyl and hydride sources for the activation of $W(NDipp)_2Cl_2(DME)$ (**27**)

In section 2.4.1.1.4 the initiation of the ethylene dimerization reaction by **27** and $W(NDipp)(N^iBu)Cl_2(DME)$ (**33**) using $MeAlCl_2$ was briefly discussed (Table 2.3, runs 14 and 15). This is an interesting result since it suggests that the presence of a β -hydride on the tungsten is not always necessary in order to initiate catalysis. Hence, it was of interest to explore a wide range of potential activators in the $W(NDipp)_2Cl_2(DME)$ -mediated dimerization of 1-hexene in order to probe the essential characteristics of an efficient activator (Table 2.12).

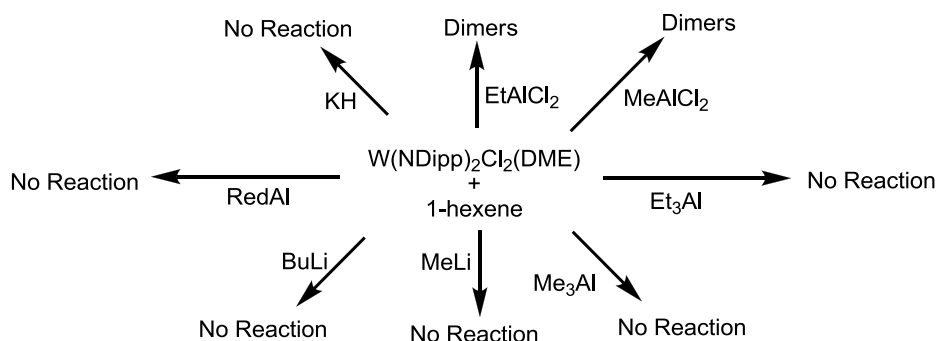
Table 2.12 Effect of the activator on the dimerization of 1-hexene over $W(NDipp)_2Cl_2(DME)$ (**27**)^a

Run #	Pro-initiator	Activator (eq)	Additive (eq)	TON ^b	Isom. ^c (%)	Conv. of C_6^d (%)	Mol % in total fraction		
							C_6	C_{12}	C_{18}
1	$W(NDipp)_2Cl_2(DME)$	$EtAlCl_2$ (15)	None	168.7	41.6	47.1	69.2	29.8	0.94
2	$W(NDipp)_2Cl_2(DME)$	$MeAlCl_2$ (15)	None	8.1	46.9	2.5	98.8	1.1	0.13
3	$W(NDipp)_2Cl_2(DME)$	Me_3Al (15)	None	0.0	0.0	0.0	100	0.0	0.00
4	$W(NDipp)_2Cl_2(DME)$	Me_3Al (15)	Oct_4NCl (4)	0.0	0.0	0.0	100	0.0	0.00
5	$W(NDipp)_2Cl_2(DME)$	Et_3Al (15)	None	0.0	0.0	0.0	100	0.0	0.00
6	$W(NDipp)_2Cl_2(DME)$	Et_3Al (15)	Oct_4NCl (4)	0.0	0.0	0.0	100	0.0	0.00
7	$W(NDipp)_2Cl_2(DME)$	$RedAl$ (15)	None	0.0	0.0	0.0	100	0.0	0.00
8	$W(NDipp)_2Cl_2(DME)$	$RedAl$ (2)	None	0.0	0.0	0.0	100	0.0	0.00
9	$W(NDipp)_2Cl_2(DME)$	KH (2)	None	0.0	0.0	0.0	100	0.0	0.00
10	$W(NDipp)_2Cl_2(DME)$	$MeLi$ (2)	None	0.0	0.0	0.0	100	0.0	0.00
11	$W(NDipp)_2Cl_2(DME)$	$BuLi$ (2)	None	0.0	0.0	0.0	100	0.0	0.00

^a General conditions: 0.40 μ mol tungsten; $PhCl$ (solvent) 190 μ L; 60 °C; 1-hexene 250 μ L (2.00 mmol); nonane standard (40.0 μ L) and *p*-anisaldehyde standard (97.4 μ L) added after quenching; reaction time 300 min after which quenching followed by addition of wet d_6 -acetone. The selectivity towards dimers was 95-100% for all runs. The branching selectivity of the dimers fraction in each run was found to be: mono branched dimers = 85%-95%, di-branched dimers = 5% - 15%, and linear < 0.5%. ^b TON is reported in $(kg C_6H_{12}) (mol TM)^{-1}$ and refers to the amount 1-hexene converted to oligomers. ^c Defined as the fraction of terminal alkene that is isomerized to internal alkenes at the end of a run. ^d Defined as the mass% of hexenes converted to oligomers at the end of a run and does not include isomerized 1-hexene.

According to the results presented in Table 2.12 and Scheme 2.15, only $EtAlCl_2$ and $MeAlCl_2$ were successful in initiating dimerization. The inability of Et_3Al and Me_3Al to activate the catalytic system is quite interesting since metal alkyls are thought to be either active catalysts or their precursors in various olefin oligo-/poly-merization reactions.^{35,45} Both these aluminum alkyl compounds are strong alkylating agents (see sections 6.1.3 and 3.4.1.2) and can easily produce tungsten alkyl species, as has indeed been demonstrated by the reaction between $[W(NDipp)Cl_4]_2$ and Me_3Al , which results in formation of

$W(NDipp)(Cl)Me_3$ (section 3.4.1.2.2). Similarly, the alkylating agents MeLi and BuLi both failed to activate $W(NDipp)_2Cl_2(DME)$ (**27**) towards olefins (runs 10 and 11; Table 2.12). This inability of the alkylating reagents Me_3Al , Et_3Al , MeLi, and BuLi to generate species active in catalytic olefin dimerization reactions suggests that just the presence of an alkyl on the tungsten bis(imido) framework is not sufficient for successful subsequent catalysis.



Scheme 2.15 Summary of attempted 1-hexene dimerization experiments using $W(NDipp)_2Cl_2(DME)$ (**27**) with various activators

Since metal hydrides are often considered to be involved in catalytic oligo-/poly-merization processes (see section 1.4.1), the possibility of directly introducing a hydride moiety using **27** was explored using RedAl and KH. Neither reaction of **27** with RedAl nor KH afforded a dimerization-active species (runs 7-9; Table 2.12).

The obvious main difference between the successful activators, $MeAlCl_2$ and $EtAlCl_2$, and those that do not generate a dimerisation-active system, e.g. Me_3Al and Et_3Al , is the presence of chloride. Notably, in section 2.4.1.7, it was shown that the addition of chloride to the tungsten bis(imido)-mediated ethylene dimerization systems improves catalytic performance, both in terms of activity and selectivity. Hence, the dimerization of 1-hexene was again attempted with pro-initiator **27**, but this time using Et_3Al and Me_3Al in the presence of a chloride source such as Oct_4NCl (runs 4, 6; Table 2.12). However, once again, the aluminum alkyls failed to initiate catalysis even in the presence of Oct_4NCl , presumably as a result of the formation of unreactive Lewis acid/base adducts.

In section 6.1.3 it was demonstrated that trialkyl aluminum reagents are strong alkylating agents, while the aluminum alkyl chlorides primarily behave as strong Lewis acids and, secondarily, as alkylating agents. Hence, it appears that it is both the strong Lewis acidity of $MeAlCl_2$ and $EtAlCl_2$, in combination with their ability to alkylate, which enables them to initiate dimerization catalysis.

2.4.2.6 Additive effects on the catalytic dimerization of 1-hexene mediated by $W(NDipp)Cl_4(THF)/15 EtAlCl_2$ and $[W(NDipp)Cl_4]_2/15 EtAlCl_2$

In section 2.4.1.7 it was shown that additives such as Et_3N , Et_3NHCl , and Oct_4NCl can enhance the catalytic activity and improve the selectivity of the tungsten bis(imido)-based ethylene dimerization

systems. In this section of the thesis, the use of additives is expanded to the tungsten bis(imido)-mediated dimerization of 1-hexene using the optimum W:additive ratios, determined in section 2.4.1.7.

Table 2.13 Additive effects on the dimerization of 1-hexene using $W(NDipp)_2Cl_2(DME)$ (**27**) activated with $EtAlCl_2$.^a

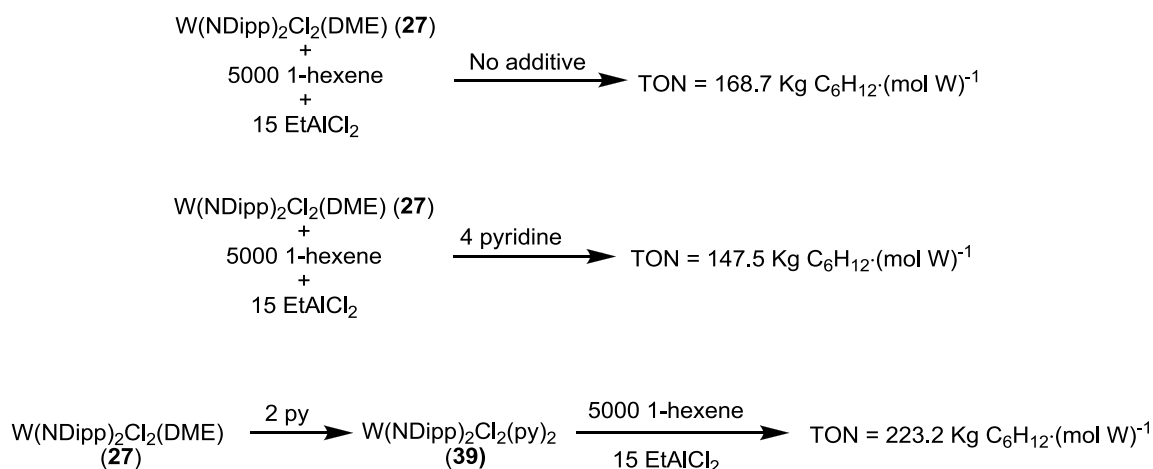
Run #	Pro-initiator	Additive (eq)	TON ^b	Isom. ^c (%)	Conv. of C ₆ ^d (%)	Mol % in products		
						C ₆	C ₁₂	C ₁₈
1	$W(NDipp)_2Cl_2(DME)$ (27)	None	168.7	41.6	47.1	69.2	29.8	0.94
2	$W(NDipp)_2Cl_2(DME)$ (27)	Et ₃ NHCl (2)	198.5	32.1	54.8	62.4	37.1	0.49
3	$W(NDipp)_2Cl_2(DME)$ (27)	Lutidine (4)	191.5	24.6	52.3	64.6	35.2	0.17
4	$W(NDipp)_2Cl_2(DME)$ (27)	Et ₃ N (4)	162.9	30.8	45.6	70.7	28.6	0.64
5	$W(NDipp)_2Cl_2(DME)$ (27)	pyridine (4)	147.5	37.4	43.2	72.6	27.0	0.44
6	$W(NDipp)_2Cl_2(DME)$ (27)	DABCO (4)	109.1	27.0	33.9	79.8	19.8	0.43
7	$W(NDipp)_2Cl_2(DME)$ (27)	Oct ₄ NCl (4)	63.2	19.0	18.2	90.1	9.8	0.16
8	$W(NDipp)(NTpp)Cl_2(DME)$ (36)	None	221.4	30.4	59.7	57.8	40.8	1.38
9	$W(NDipp)(NTpp)Cl_2(DME)$ (36)	Et ₃ NHCl (2)	200.9	33.5	56.3	60.9	38.8	0.32
10	$W(NDipp)(NTpp)Cl_2(DME)$ (36)	Et ₃ N (4)	187.3	28.5	51.5	65.4	34.2	0.31
11	$W(NDipp)(NTpp)Cl_2(DME)$ (36)	pyridine (4)	169.1	34.1	47.8	68.9	30.3	0.83
12	$W(NDipp)(NTpp)Cl_2(DME)$ (36)	Lutidine (4)	105.7	32.0	31.3	81.5	18.3	0.16
13	$W(NDipp)(NTpp)Cl_2(DME)$ (36)	Oct ₄ NCl (4)	97.1	22.3	27.5	84.1	15.9	0.07
14	$W(NDipp)(NTpp)Cl_2(DME)$ (36)	DABCO (4)	47.1	19.0	13.3	93.0	6.9	0.16

^a General conditions: 0.40 μmol tungsten and 6.0 μmol $EtAlCl_2$; PhCl (solvent) 190 μL; 60 °C; 1-hexene 250 μL (2.00 mmol); nonane standard (40.0 μL) and *p*-anisaldehyde standard (97.4 μL) added after quenching; reaction time 300 min after which quenching followed by addition of wet *d*₆-acetone. The selectivity towards dimers was 95-100% for all runs. The branching selectivity of the dimers fraction in each run was found to be: mono branched dimers = 85%-95%, di-branched dimers = 5% - 15%, and linear < 0.5%. ^b TON is reported in (kg C₆H₁₂) (mol TM)⁻¹ and refers to the amount 1-hexene converted to oligomers. ^c Defined as the fraction of terminal alkene that is isomerized to internal alkenes at the end of a run. ^d Defined as the mass% of hexenes converted to oligomers at the end of a run and does not include isomerized 1-hexene.

Table 2.13 presents the results from the catalytic dimerization of 1-hexene using a combination of complexes $W(NDipp)_2Cl_2(DME)$ (**27**) and $W(NDipp)(NTpp)Cl_2(DME)$ (**36**) with Et₃N, pyridine, 2,6-lutidine, DABCO, Et₃NHCl, and Oct₄NCl. Only for the case of **27** combined with 2,6-lutidine (run 3, Table 2.13) and Et₃NHCl (run 2, Table 2.13) an increase in the TON is observed from 168.7 kg C₆H₁₂ (mol TM)⁻¹ for the system with no additive (run 1, Table 2.13), to 198.5 kg C₆H₁₂ (mol TM)⁻¹ (run 2, Table 2.13) and 191.5 kg C₆H₁₂ (mol TM)⁻¹ (run 3, Table 2.13), respectively. Surprisingly, all of the other tests undertaken demonstrated an attenuation in the catalytic activity compared to that for the additive-free system (e.g. compare run 1 with runs 4-7 and run 8 with runs 9-14) Table 2.13. Again, since the precise mode of action of these additives is unclear, no further conclusions may be drawn from this study.

According to the above observations, the use of additives attenuated the catalytic dimerization of 1-hexene in most cases. This seems to be at odds with the observations made concerning the

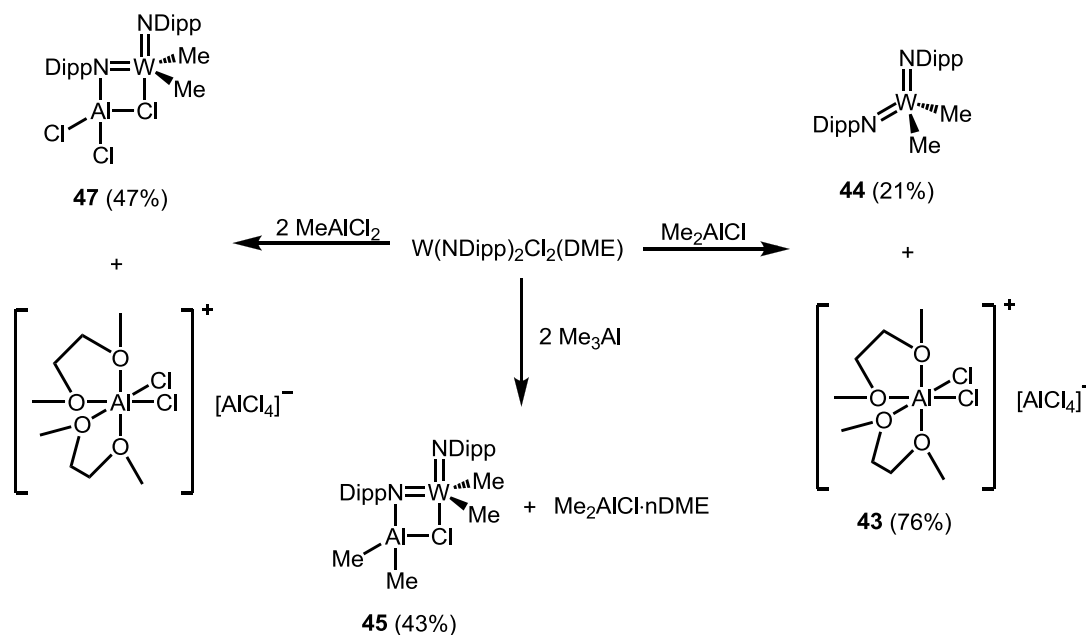
performance of the tungsten bis(imido)-based ethylene dimerization systems which improved when additives were employed (section 2.4.1.7). However, it must be highlighted that complex $W(NDipp)_2Cl_2(py)_2$ (**39**) (run 9, Table 2.9), mediated dimerization of 1-hexene with a TON of 223.2 kg C_6H_{12} (mol W)⁻¹ which is 32% higher compared to the TON obtained from the $W(NDipp)_2Cl_2(DME)$ (**27**) under the same conditions (Scheme 2.16). This suggests that in order to achieve an increase in the TON of the tungsten bis(imido) 1-hexene dimerization systems, the use of a W:additive ratio of two should be used instead of four. This means that it is possible that the W:additive ratio used in the ethylene dimerization experiments (section 2.4.1.7) is not suitable for the 1-hexene dimerization experiments suggesting that in the case of 1-hexene dimerization the optimal W:additive ratio must be re-determined.



Scheme 2.16 1-Hexene dimerization using pro-initiator $W(NDipp)_2Cl_2(DME)$ (**27**), **27/4 py**, and pro-initiator $W(NDipp)_2Cl_2(py)_2$ (**39**) demonstrating that use of two equivalents of pyridine as an additive rather than four improves dimerization

2.4.2.7 Reactions of $W(NDipp)_2Cl_2(DME)$ (**27**) with $Me_nAlCl_{(3-n)}$ reagents and catalytic testing of the isolated products in 1-hexene dimerization

The reactions of **27** with excess $Me_nAlCl_{(3-n)}$ reagents have been reported previously by Dyer *et al.* to generate tungsten methyl complexes such as $W(NDipp)_2Me_2$ (**44**), $W(NDipp)_2Me_2 \cdot AlMe_2Cl$ (**45**), $W(NDipp)_2Me_2 \cdot AlMeCl_2$ (**46**), and $W(NDipp)_2Me_2 \cdot AlCl_3$ (**47**), with each of these complexes having been characterized by both NMR spectroscopy and X-ray crystallography.^{3,4} Herein, complexes **44-47** were synthesized without the use of excess aluminium reagent, as described in Scheme 2.17. The yields of these complexes are moderate-to-low, in part due to the small scales on which the syntheses were conducted, but also due to the high solubility of **44**, **45**, **47** even in non-polar solvents such as pentane which prevented their efficient recrystallization. Interestingly, the previously-reported complex **43**,⁴⁶ was also formed along with **44** and **47** (Scheme 2.17), and isolated in the form of colourless crystals, which were found to be insoluble to all non-coordinating solvents and hence, the formation of **43** was confirmed only by an X-ray crystallographic study.



Scheme 2.17 Synthesis of complexes **44**, **45**, **47** and **43** using stoichiometric amounts of methyl aluminum reagents (isolated yields are given in brackets)

In section 2.4.1.1.4, it has been shown that the combination of $W(NDipp)_2Cl_2(DME)$ (**27**) with 15 equivalents of $MeAlCl_2$ results in a mixture that can dimerize alkenes (runs 2, Table 2.12 and 14, Table 2.3). Hence, the catalytic testing of complexes **44**, **45**, **47** for dimerization is imperative. For this reason, the discrete complexes **43**, **44**, **45**, and **47** were tested in the catalytic dimerization of 1-hexene in both the presence and absence of $EtAlCl_2$. The results from these tests are summarized in Table 2.14 below.

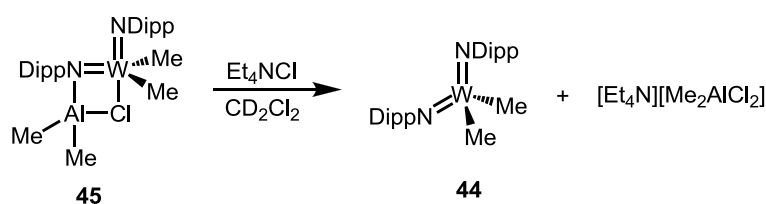
According to the results presented in Table 2.14, complexes **44**, **45**, and **47** were found to be catalytically silent when either no or one equivalent of $EtAlCl_2$ was used, something clearly demonstrating that **44**, **45**, and **47** are not the active catalysts in the tungsten bis(imido) olefin dimerization systems. Only in the presence of 15 equivalents of $EtAlCl_2$ did complexes **44**, **45**, and **47** initiate dimerization of 1-hexene, exhibiting TONs of 172.0, 118.3, and 109.0 $kg\ C_6H_{12}\ (mol\ TM)^{-1}$ respectively (runs 4, 9, 6; Table 2.14). Interestingly, according to the above results, the aluminum free pro-initiator **44** has a reasonably higher TON compared to the aluminum containing ones **45** and **47** when activated with 15 equivalents of $EtAlCl_2$ (runs 4, 9, 6; Table 2.14) suggesting that the presence of bound aluminum on the tungsten pro-initiator is detrimental for catalysis.

Table 2.14 Catalytic testing of products from the reactions of $W(NDipp)_2Cl_2(DME)$ (**27**) with aluminum reagents as pro-initiators in the dimerization of 1-hexene ^a

Run #	Pro-initiator	Activator (eq)	TON ^b	Isom. ^c (%)	Conv. of C ₆ ^d (%)	Mol % in total fraction		
						C ₆	C ₁₂	C ₁₈
1	$W(NDipp)_2Cl_2(DME)$ (27)	EADC (15)	168.7	41.6	47.1	69.2	29.8	0.94
2	$W(NDipp)_2Me_2$ (44)	None	0.0	0.0	0.0	100	0.0	0.0
3	$W(NDipp)_2Me_2$ (44)	EADC (1)	0.0	0.0	0.0	100	0.0	0.0
4	$W(NDipp)_2Me_2$ (44)	EADC (15)	172.0	25.6	47.6	69.1	29.9	1.01
5	$W(NDipp)_2Me_2 \cdot AlCl_3$ (47)	None	0.0	0.0	0.0	100	0.0	0.0
6	$W(NDipp)_2Me_2 \cdot AlCl_3$ (47)	EADC (15)	109.0	25.3	32.3	80.7	19.3	0.0
7	$W(NDipp)_2Me_2 \cdot AlClMe_2$ (45)	None	0.0	0.0	0.0	100	0.0	0.0
8	$W(NDipp)_2Me_2 \cdot AlClMe_2$ (45)	EADC (1)	0.0	0.0	0.0	100	0.0	0.0
9	$W(NDipp)_2Me_2 \cdot AlClMe_2$ (45)	EADC (15)	118.3	21.8	32.7	80.7	18.8	0.50
10	$[AlCl_2 \cdot 2(DME)][AlCl_4]$ (43)	EADC (15)	2.8	71.9	0.8	99.6	0.3	0.05

^a General conditions: 0.40 μmol tungsten; PhCl (solvent) 190 μL; 60 °C; 1-hexene 250 μL (2.00 mmol); nonane standard (40.0 μL) and *p*-anisaldehyde standard (97.4 μL) added after quenching; reaction time 300 min after which quenching followed by addition of wet *d*₆-acetone. The selectivity towards dimers was 95-100% for all runs. The branching selectivity of the dimers fraction in each run was found to be: mono branched dimers = 85%-95%, di-branched dimers = 5% - 15%, and linear < 0.5%. ^b Reported in (kg C₆H₁₂) (mol TM)⁻¹ and refers to the amount 1-hexene converted to oligomers. ^c Defined as the fraction of terminal alkene that is isomerized to internal alkenes at the end of a run. ^d Defined as the mass% of hexenes converted to oligomers at the end of a run and does not include isomerized 1-hexene.

Additionally, it was found that reaction of **45** with the chloride source Et₄NCl results in formation of the aluminum free **44** (Scheme 2.18). Taking the above observations into account, along with the fact that the presence of chloride in the appropriate W:Cl ratio improves the performance of the tungsten bis(imido) dimerization systems (section 2.4.1.7), it can be suggested that one of the ways that chloride benefits catalysis is by removing any aluminum species bound to tungsten.



Scheme 2.18 Reaction between $W(NDipp)_2Me_2 \cdot AlMe_2Cl$ (**45**) and Et₄NCl forming $W(NDipp)_2Me_2$ (**44**)

Lastly, the aluminum-containing complex **43**, which was formed as a byproduct of the reaction between $W(NDipp)_2Cl_2(DME)$ (**27**) and MeAlCl₂, was also tested in the dimerization of 1-hexene using 15 equivalents of EtAlCl₂ (run 10; Table 2.14) and was found to be dimerization silent. However, activation of **43** resulted in the isomerization of 71.9% of the substrate to internal hexenes. This is an interesting result, since it suggests that apart from olefin dimerization catalysts, formation of olefin oligomerization catalysts is also possible during the activation of the tungsten bis(imido) ethylene dimerization systems (Scheme 2.14). This formation of olefin isomerization catalysts during activation of the tungsten

bis(imido) olefin dimerization systems can explain the isomerization of 1-hexene observed in all of the tungsten bis(imido) mediated 1-hexene dimerization experiments (see section 2.4.2.2)

2.5 Future investigations

In this chapter the potential of the tungsten bis(imido) systems in the dimerization of olefins has been clearly demonstrated. However, these systems can be further developed. The following suggestions are made as the first steps towards this goal. Firstly, a thorough study of the tungsten:activator ratio is necessary in order to ensure that this is optimal. Additionally, the study of the ethylene dimerization catalytic reaction using tungsten bis(imido) complexes at a higher temperature is almost certain to produce impressive results, based on the data obtained from run 16 (Table 2.4), where pro-initiator W(NDipp)(N^tBu)Cl₂(DME) (**33**) was tested at 50 bar and 80 °C. Moreover, the role of additives should be further explored in order to improve the catalytic activities and to obtain a better understanding of the way(s) in which they improve catalysis. Lastly, the potential of the tungsten bis(imido)/15 EtAlCl₂ systems towards olefin isomerization should be further examined, with the aim of eliminating this side reaction, which is detrimental to dimerization, especially in the case of higher α -olefin dimerization.

2.6 Chapter Summary

In this Chapter a series of tungsten bis(imido) complexes of the type W(NR)(NR')Cl₂(DME) (R = R' = Dipp (**27**); R = R' = Tfp (**28**); R = R' = Pfp (**29**); R = R' = Mes^F (**30**); R = R' = Tpp (**31**); R = Dipp, R' = ⁱPr (**32**); R = Dipp, R' = ^tBu (**33**); R = Dipp, R' = Mes (**34**); R = Dipp, R' = Tfp (**35**); R = Dipp, R' = Tpp (**36**); R = Dipp, R' = Dnp (**37**)) along with complexes W(NDipp)₂Cl₂(py)₂ and W(NDipp)₂Cl₂(PMe₃) were synthesized and structurally characterized. The crystallographic studies of complexes **27-37** revealed that the nature of the imido substituent can influence their structural parameters but not always in a predictable way.

Following their characterization, the potential of complexes **27-37**, as well as W(NDipp)₂Cl₂(py)₂ (**39**) and W(NDipp)₂Cl₂(PMe₃) (**40**), in the dimerization of ethylene was explored under a wide variety of reaction conditions. Initially, complexes **27-37** were activated at 40 bar of ethylene pressure and 60 °C with 15 equivalents of EtAlCl₂ leading to the development of reasonably active and selective ethylene dimerization systems with activities of up to 141.3 kg C₂H₄ (mol W)⁻¹ h⁻¹bar⁻¹ (pro-initiator **28**) and selectivities towards 1-butene of over 70% mol. Additionally, from the above study it was found that bulky aryl imido ligands, such as Dipp and Tpp, and electron withdrawing aryl imido ligands, such as Tfp, favor catalysis leading to highly active pro-initiators such as complexes **27**, **28**, **36**, and **35**. Following the catalysis experiments conducted at 40 bar/60 °C, complexes **27-36** were tested at 45 bar/70 °C leading to a further increase in the catalytic activity without significant changes in the selectivity of the reaction. Hence, activities of up to 225.2 kg C₂H₄ (mol W)⁻¹ h⁻¹bar⁻¹ (pro-initiator **28**) and selectivities towards 1-butene of over 75% mol were achieved. The use of additives such as Oct₄NCl, added to the catalytic reaction mixture prior to activation, led to a further increase in the catalytic activity of up to 357.8 kg C₂H₄ (mol W)⁻¹ h⁻¹bar⁻¹ (for pro-initiator **36**) and improved the

selectivity towards 1-butene (> 80 % mol). Additionally, the use of pro-initiator **27** in combination with two equivalents of Oct₄NCl at a lower aluminum loading (20 μmol instead of 40 μmol) in a 1.2 L autoclave, led to formation of the most active ethylene dimerization system described in this theses with an activity of 429.9 kg C₂H₄ (mol W)⁻¹ h⁻¹ bar⁻¹ and a good selectivity towards 1-butene (87.9 % mol).

The ethylene dimerization studies with pro-initiators **27-31** and **33, 35, 36** were extended to the dimerization of 1-hexene where TONs of up to 239.3 kg C₆H₁₂ (mol TM)⁻¹ (pro-initiator **33**) were achieved with very good selectivities towards the dimers fraction of over 95% for all runs. Unfortunately, during dimerization, significant isomerization of the substrate also occurs, resulting in the formation of internal hexenes. These internal hexenes cannot be dimerized, something that limits the potential of the tungsten bis(imido)-based systems towards the dimerization of heavy α-olefins.

From a mechanistic perspective, it is suggested that a tungsten metallacycle mechanism could be in operation, based on the product selectivity obtained from the ethylene dimerization experiments, along with the observed ability of MeAlCl₂ to initiate catalysis. Additionally, it was suggested that during activation, apart from the aforementioned olefin dimerization catalysts, olefin isomerization catalysts are also formed, which are responsible for the isomerization of 1-hexene to internal hexenes when the latter is used as the substrate. However, the exact mechanism of the tungsten bis(imido)-mediated olefin dimerization systems is still not well understood, and hence an alternative stepwise addition mechanism cannot be easily excluded.

2.7 References

- (1) Hanton, M. J.; Daubney, L.; Lebl, T.; Polas, S.; Smith, D. M.; Willemse, A. *Dalton Trans* **2010**, *39*, 7025.
- (2) Olivier, H.; Laurent-Grot, P. *Journal of Molecular Catalysis A: Chemical* **1999**, *148*, 43.
- (3) Wright, W. R. H.; Batsanov, A. S.; Howard, J. A. K.; Tooze, R. P.; Hanton, M. J.; Dyer, P. W. *Dalton Transactions* **2010**, *39*, 7038.
- (4) Wright, W. R. H., PhD Thesis, Durham University, 2009.
- (5) Schrock, R. R.; Depue, R. T.; Feldman, J.; Yap, K. B.; Yang, D. C.; Davis, W. M.; Park, L.; Dimare, M.; Schofield, M.; Anhaus, J.; Walborsky, E.; Evitt, E.; Kruger, C.; Betz, P. *Organometallics* **1990**, *9*, 2262.
- (6) Yuan, J.; Schrock, R. R.; Müller, P.; Axtell, J. C.; Dobereiner, G. E. *Organometallics* **2012**, *31*, 4650.
- (7) Bradley, D. C.; Errington, R. J.; Hursthouse, M. B.; Nielson, A. J.; Short, R. L. *Polyhedron* **1983**, *2*, 843.
- (8) Bradley, D. C.; Errington, R. J.; Hursthouse, M. B.; Short, R. L.; Ashcroft, B. R.; Clark, G. R.; Nielson, A. J.; Rickard, C. E. F. *Journal of the Chemical Society-Dalton Transactions* **1987**, 2067.
- (9) Clegg, W.; Errington, R. J.; Hockless, D. C. R.; Redshaw, C. *Journal of the Chemical Society, Dalton Transactions* **1993**, 1965.
- (10) Dreisch, K.; Andersson, C.; StÅlhandske, C. *Polyhedron* **1993**, *12*, 1335.
- (11) Leung, W.-H.; Wu, M.-C.; Chim, J. L. C.; Wong, W.-T. *Polyhedron* **1998**, *17*, 457.
- (12) Rische, D.; Baunemann, A.; Winter, M.; Fischer, R. A. *Inorganic Chemistry* **2006**, *45*, 269.
- (13) Wright, W. R. H.; Batsanov, A. S.; Messinis, A. M.; Howard, J. A. K.; Tooze, R. P.; Hanton, M. J.; Dyer, P. W. *Dalton Transactions* **2012**, *41*, 5502.
- (14) Ajellal, N.; Kuhn, M. C. A.; Boff, A. D. G.; Hörner, M.; Thomas, C. M.; Carpentier, J.-F.; Casagrande, O. L. *Organometallics* **2006**, *25*, 1213.
- (15) Chandran, D.; Lee, K. M.; Chang, H. C.; Song, G. Y.; Lee, J. E.; Suh, H.; Kim, I. *Journal of Organometallic Chemistry* **2012**, *718*, 8.
- (16) Song, S. J.; Zhao, W. Z.; Wang, L.; Redshaw, C.; Wang, F. S.; Sun, W. H. *Journal of Organometallic Chemistry* **2011**, *696*, 3029.

- (17) Onishi, Y.; Katao, S.; Fujiki, M.; Nomura, K. *Organometallics* **2008**, *27*, 2590.
- (18) Lorber, C.; Choukroun, R.; Vendier, L. *European Journal of Inorganic Chemistry* **2006**, *2006*, 4503.
- (19) Kunrath, F. A.; de Souza, R. F.; Casagrande, O. L.; Brooks, N. R.; Young, V. G. *Organometallics* **2003**, *22*, 4739.
- (20) Zhang, S.; Nomura, K. *Journal of the American Chemical Society* **2010**, *132*, 4960.
- (21) Nomura, K.; Igarashi, A.; Katao, S.; Zhang, W. J.; Sun, W. H. *Inorganic Chemistry* **2013**, *52*, 2607.
- (22) Igarashi, A.; Zhang, S.; Nomura, K. *Organometallics* **2012**, *31*, 3575.
- (23) Michiue, K.; Oshiki, T.; Takai, K.; Mitani, M.; Fujita, T. *Organometallics* **2009**, *28*, 6450.
- (24) Ulbrich, A.; Campedelli, R. R.; Milani, J. L. S.; dos Santos, J. H. Z.; Casagrande, O. D. *Applied Catalysis a-General* **2013**, *453*, 280.
- (25) Clifford, A. F. *The Journal of Physical Chemistry* **1959**, *63*, 1227.
- (26) Huheey, J. E. *The Journal of Physical Chemistry* **1965**, *69*, 3284.
- (27) Huheey, J. E. *The Journal of Organic Chemistry* **1966**, *31*, 2365.
- (28) Cozma, P.; Wukovits, W.; Mamaliga, I.; Friedl, A.; Gavrilescu, M. *Environmental Engineering and Management Journal* **2013**, *12*, 147.
- (29) Lee, L. S.; Ou, H. J.; Hsu, H. F. *Fluid Phase Equilibria* **2005**, *231*, 221.
- (30) Wu, J. L.; Pan, Q. M.; Rempel, G. L. *Journal of Applied Polymer Science* **2005**, *96*, 645.
- (31) Song, S. J.; Li, Y.; Redshaw, C.; Wang, F. S.; Sun, W. H. *Journal of Organometallic Chemistry* **2011**, *696*, 3772.
- (32) Xiao, T.; Lai, J.; Zhang, S.; Hao, X.; Sun, W.-H. *Catalysis Science & Technology* **2011**, *1*, 462.
- (33) Ignatov, S. K.; Khalimon, A. Y.; Rees, N. H.; Razuvaev, A. G.; Mountford, P.; Nikonov, G. I. *Inorganic Chemistry* **2009**, *48*, 9605.
- (34) Small, B. L.; Marcucci, A. J. *Organometallics* **2001**, *20*, 5738.
- (35) Ittel, S. D.; Johnson, L. K.; Brookhart, M. *Chemical Reviews* **2000**, *100*, 1169.
- (36) Chen, Y.; Credendino, R.; Callens, E.; Atiqullah, M.; Al-Harhi, M. A.; Cavallo, L.; Basset, J.-M. *Acs Catal* **2013**, 1360.
- (37) Jie, S.; Zhang, S.; Sun, W. H. *European Journal of Inorganic Chemistry* **2007**, 5584.
- (38) Tang, X.; Zhang, D.; Jie, S.; Sun, W.-H.; Chen, J. *Journal of Organometallic Chemistry* **2005**, *690*, 3918.
- (39) Christoffers, J.; Bergman, R. G. *Inorganica Chimica Acta* **1998**, *270*, 20.
- (40) Jones, J. R.; Symes, T. J. *Journal of the Chemical Society C: Organic* **1971**, 1124.
- (41) daRosa, R. G.; deSouza, M. O.; deSouza, R. F. *Journal of Molecular Catalysis a-Chemical* **1997**, *120*, 55.
- (42) Majoumo-Mbe, F.; Lonneck, P.; Volkis, V.; Sharma, M.; Eisen, M. S.; Hey-Hawkins, E. *Journal of Organometallic Chemistry* **2008**, *693*, 2603.
- (43) Small, B. L. *Organometallics* **2003**, *22*, 3178.
- (44) Yu, Z. X.; Houk, K. N. *Angewandte Chemie-International Edition* **2003**, *42*, 808.
- (45) Suttill, J. A.; McGuinness, D. S. *Organometallics* **2012**, *31*, 7004.
- (46) Bury, W.; Chwojnowska, E.; Justyniak, I.; Lewinski, J.; Affek, A.; Zygadlo-Monikowska, E.; Bak, J.; Florjanczyk, Z. *Inorganic Chemistry* **2012**, *51*, 737.

3 Tungsten mono(imido) complex-mediated ethylene and 1-hexene dimerization

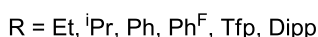
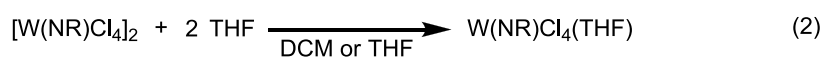
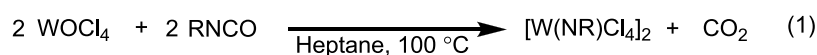
3.1 Introduction

In section 1.8 it was mentioned that when using the *in situ* olefin dimerization system developed by Sasol, it was possible that the formation of tungsten bis(imido) complexes could occur from the reaction of WCl_6 with $PhNH_2$ and Et_3N . However, what is less often discussed is the potential for the formation of tungsten mono(imido) complexes, which is possible under the same reaction conditions. Hence, it is possible that tungsten mono(imido) complexes could also be implicated in the dimerization of olefins using this Sasol *in situ* system. Since, as described in section 2, tungsten bis(imido) complexes have successfully been used as pro-initiators for the dimerization of ethylene and 1-hexene, then it is of interest to extend this study to appropriately-activated tungsten mono(imido) systems. Consequently, various tungsten mono(imido) complexes have been synthesized and structurally characterized. Subsequently, their ability to dimerize ethylene and 1-hexene has been assessed. Lastly, their reactivity towards selected reagents of relevance to the catalytic system, such as aluminum alkyls and alkyl chlorides, Et_3N , and ammonium chloride salts, is also examined in order to gain some mechanistic insight into their olefin dimerization abilities.

3.2 Synthesis of tungsten mono(imido) complexes

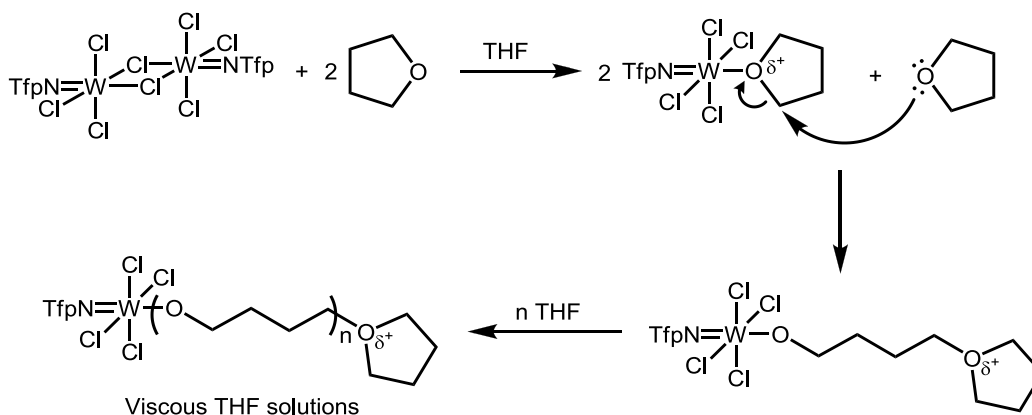
3.2.1 Tungsten(VI) complexes

The tungsten(VI) mono(imido) complexes **48-51**, **53** and **54-57**, **59** were synthesized using modifications of literature procedures, whereby $WOCl_4$ is reacted with the appropriate organic isocyanate in heptane, which leads to formation of dimeric mono(imido) complexes of the type $[W(NR)Cl_4]_2$ (Scheme 3.1, eq. 1).¹⁻⁶ These dimers have been reported as being insoluble in non-coordinating organic solvents.^{1,6} However, during the course of these studies, it was found that they can be dissolved and recrystallized from hot toluene, allowing their isolation in a highly pure form. Each dimeric imido complex can then be dissolved in THF to form the relevant mono-metallic THF adduct of general formula $W(NR)Cl_4(THF)$ (Scheme 3.1, eq. 2).



Scheme 3.1 Synthesis of complexes $[W(NR)Cl_4]_2$ ($R = Et$ (**48**),^{3,5} iPr (**49**),¹ Ph (**50**),⁵ Ph^F (**51**),⁴ Tfp (**52**), and $Dipp$ (**53**)^{1,6}) and $W(NR)Cl_4(THF)$ ($R = Et$ (**54**),^{3,5} iPr (**55**),¹ Ph (**56**),⁵ Ph^F (**57**),⁴ Tfp (**58**), and $Dipp$ (**59**)^{1,6}).

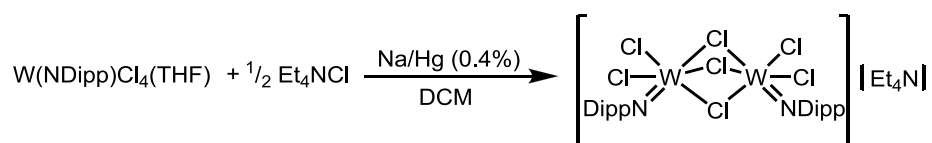
Apart from the previously reported complexes **48-51**, **53** complex **52** was also synthesized in a similar fashion (Scheme 3.1, eq. 1 and 2) using Tf_pNCO, and was isolated as a brown crystalline solid in 85% yield. However, it must be noted that in contrast to complexes **48-51**, **53**, the enhanced Lewis acidity of complex **52** (due to the presence of the electron-withdrawing Tf_pN imido moiety) results in the ring-opening and oligomerization of THF (Scheme 3.2), which leads to formation of viscous solutions that are difficult to handle. Hence, complex **58** was obtained by addition of one equivalent of THF to a suspension of **52** in DCM followed by filtration and removal of the volatile components *in vacuo*.



Scheme 3.2 Proposed mechanism for the $[W(NTfp)Cl_4]_2$ -initiated oligomerization of THF.

3.2.2 Tungsten(V) complexes

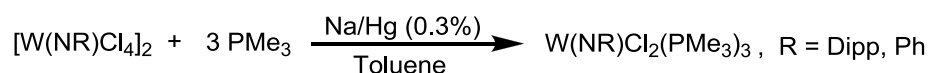
For comparative purposes, the W(V) mono(imido) complex $[W(NDipp)Cl_2]_2(\mu-Cl)_3[Et_4N]$ (**60**) was prepared in good yield (76 %) using a modification of the synthetic methodology reported by Bradley *et al.* for the synthesis of $[W(NPh)Cl_2]_2(\mu-Cl)_3[P(CH_2Ph)Ph_3]$.³ Hence, $W(NDipp)Cl_4(THF)$ was reacted with Et_4NCl in DCM over sodium/mercury amalgam, which resulted in a dark orange solution that, after recrystallization, gives pure **60** (Scheme 3.3).



Scheme 3.3 Synthesis of $[W(NDipp)Cl_2]_2(\mu-Cl)_3[Et_4N]$ (**60**).

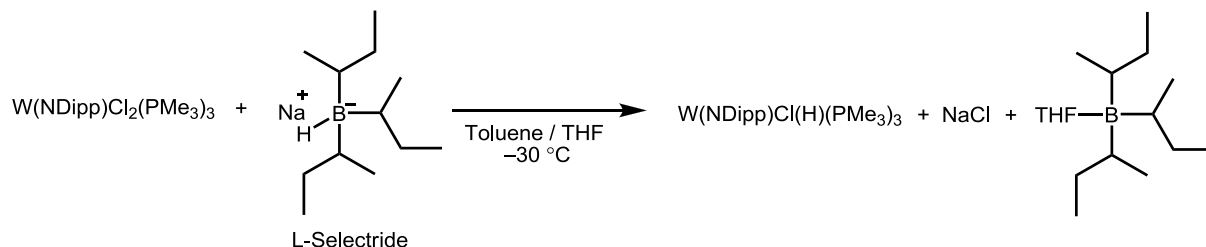
3.2.3 Tungsten(IV) complexes

Complexes $W(NR)Cl_2(PMe_3)_3$ (R = Dipp (**61**) and Ph (**25**)) were synthesized according to literature procedures by reacting $[W(NR)Cl_4]_2$ (R = Dipp and Ph) with sodium amalgam (0.3%) in the presence of PMe_3 (Scheme 3.4).⁷ This gave blue (R = Dipp) and brown (R = Ph) solids, which were used without further purification.



Scheme 3.4 Synthesis of complexes $W(NR)Cl_2(PMe_3)_3$ (R = Dipp (**61**) and Ph (**25**)).⁷

The new W(IV) hydride $W(NDipp)Cl(H)(PMe_3)_3$ (**62**) was prepared in moderate yield (55 %) by modifying the procedure reported by Nikonov *et al.* for the synthesis of $Mo(NDipp)Cl(H)(PMe_3)_3$.⁸ Hence, $W(NDipp)Cl_2(PMe_3)_3$ was reacted with *L*-selectride at -30 °C in toluene, forming a brown solution, which after recrystallization, gives pure **62** (Scheme 3.5).



Scheme 3.5 Synthesis of $W(NDipp)Cl(H)(PMe_3)_3$.

3.3 Crystallographic study of complexes $[W(NR)Cl_4]_2$ ($R = Et, iPr, Ph^Me, Ph^F, Tfp,$ and $Dipp$), $[[W(NDipp)Cl_2]_2(\mu-Cl)_3][Et_4N]$, and $W(NDipp)Cl(H)(PMe_3)_3$

The various mono(imido) pro-initiators used herein exhibit different catalytic behavior in the dimerization of ethylene and 1-hexene depending on the nature of the imido substituent (*vide infra*). Hence, it was of interest to examine complexes **48-53** via X-ray diffraction in order to probe the influence of the imido substituent on the structural properties of these pro-initiators.

3.3.1 Comparison of the structural properties of complexes **48-51**

The crystal structures of complexes **48-51** have been previously reported,^{2,3,9-11} while single crystals of complexes **52** and **53** were obtained by recrystallization from hot toluene solutions; their crystallographic characterization and their molecular structures are presented in Figure 3.2 and Figure 3.1, respectively. Selected interatomic distances and angles for complexes **48-51** are given in Table 3.1. Despite repeated efforts, complex **50** could not be crystallographically characterized, thus the molecular structure of the related, previously reported complex $[W(NPh^{Me})Cl_4]_2$ **63** is included for comparison.⁹ Note that although mainly the THF adducts of complexes **48-51** were used for catalysis (due to their greater solubility), their THF-free halide-bridged dimers were selected for this crystallographic study due to the availability of more extensive crystallographic data in the literature with which to make comparisons and does provide a self-consistent method for assessing the electronic and structural influences of the imido substituents.

In the solid state, complexes **48-53** are dimeric with an edge-shared bioctahedral structure, which is in accordance with previous reports on tungsten mono(imido) tetrachlorides, with a rhombohedral $[W_2-(\mu-Cl)_2]$ core (Figure 3.2, Figure 3.1).³ In contrast to the crystal lattice of complexes **48-51**, **53**, toluene was found in the unit cell of complex **52**, something is believed to occur as a result of weak

interactions between the *ortho* carbon of the Tfp and toluene rings (3.394 Å) in **52**. This type of interaction is commonly encountered with fluorinated aromatic rings.¹² The W-N interatomic distances are short (< 1.73(1) Å), in line with a W≡N triple bond, and are similar (within experimental error) for each complex in the series **48-53**, suggesting here that the substituent on the imido ligand has little effect on the imido bond length. The W-Cl(n) (n = 1-4) bond lengths were found to be equal for each of the complexes **48** to **53**, within experimental error. As expected, the interatomic distances for the tungsten-bridging chloride motif, W-Cl(1'), are longer than all the other W-Cl distances in each dimer, something due to the strong *trans* influence of the imido substituent. Furthermore, the W-Cl(1') interatomic distances are similar for complexes **48-51**, **53**, despite the presence of different imido groups located *trans* to the Cl(1') atom, suggesting that the *trans* influence of the NR moiety in these complexes is comparable. However, a shorter W-Cl(1') interatomic distance was observed in complex **52** compared to the rest of the complexes in the series, reflecting the weaker *trans* influence of the electron-withdrawing TfpN group.

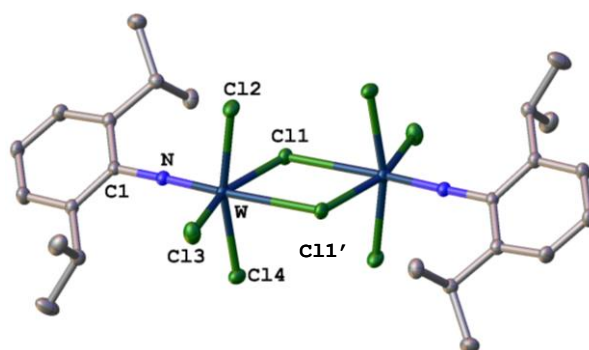


Figure 3.1 Molecular structure of $[W(NDipp)Cl_4]_2$ (**53**). H atoms are omitted for clarity and the thermal ellipsoids are shown at the 50% probability level.

Table 3.1 Selected interatomic distances (Å) and angles (°) for $[W(NR)Cl_4]_2$ (R = Et (**48**),³ iPr (**49**),² Ph^{Me} (**63**),⁹ Ph^F (**51**),^{10,11} Tfp (**52**), and Dipp (**53**)).

	$[W(NEt)Cl_4]_2^3$	$[W(N^iPr)Cl_4]_2^2$	$[W(NPh^{Me})Cl_4]_2^9$	$[W(NPh^F)Cl_4]_2^{10,11}$	$[W(NTfp)Cl_4]_2$	$[W(NDipp)Cl_4]_2$
W-N	1.685(13)	1.697(12)	1.712(18)	1.73(1)	1.7269(19)	1.727(3)
N-C(1)	1.440(18)	1.45(2)	1.411(27)	1.38(2)	1.361(3)	1.390(4)
W-Cl(1)	2.431(5)	2.418(4)	2.415(6)	2.440(5)	2.4381(8)	2.4168(9)
W-Cl(2)	2.305(5)	2.307(4)	2.307(7)	2.294(5)	2.2929(7)	2.3163(8)
W-Cl(3)	2.279(5)	2.285(4)	2.286(7)	2.284(6)	2.2701(8)	2.2858(10)
W-Cl(4)	2.307(5)	2.310(4)	2.298(7)	2.298(5)	2.3290(7)	2.3175(8)
W-Cl(1')	2.731(6)	2.736(5)	2.717(6)	2.709(4)	2.6725(6)	2.7119(7)
W-N-C(1)	176.3(9)	171.5(9)	177.3(15)	174(1)	173.69(17)	178.6(2)
Cl(1)-W-N	94.9(4)	95.6(4)	99.6(6)	94.9(5)	95.20((7)	98.31(10)
Cl(2)-W-N	97.7(4)	95.1(4)	93.4(6)	98.8(5)	97.87(6)	96.85(9)
Cl(3)-W-N	101.3(5)	101.4(4)	98.1(6)	99.7(5)	101.75(7)	101.76(10)
Cl(4)-W-N	96.6(5)	99.0(4)	99.2(6)	95.0(5)	94.12(6)	95.75(9)

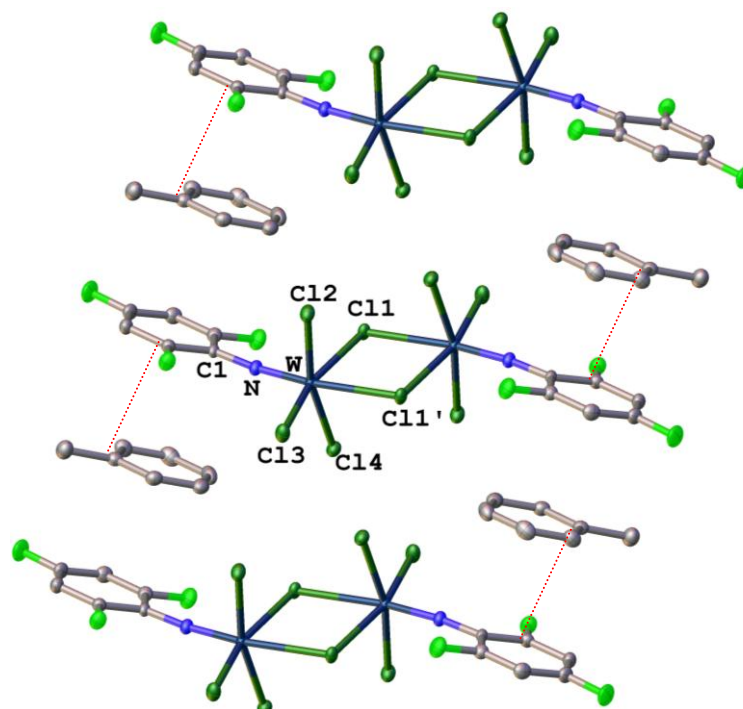


Figure 3.2 Molecular structure of $[W(NTfp)Cl_4]_2$ (**52**) showing π - π stacking interactions (dotted lines). H atoms are omitted for clarity and the thermal ellipsoids are shown at the 50% probability level.

The W-N_{imido}-C angles fall in the range 171.5 - 178.6° and are similar for each dimeric imido derivative, something that in combination with the short W-N interatomic distances, confirms the presence of an almost linear W≡N triple bond. Moreover, the sum of the angles N-W-Cl(n) (n = 1-4) is the same for each complex (~391°) suggesting that the steric pressure of the imido ligand on the four Cl(n) (n = 1-4) atoms, which displaces the tungsten centre out of the Cl(1)-Cl(2)-Cl(3)-Cl(4) plane, is independent of the imido substituent.

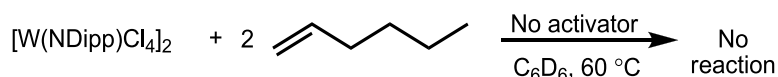
Taking the above observations together, it is clear that complexes **48-53** are structurally similar and that the substituent on the imido moiety does not influence significantly the structural parameters of the mono(imido) dimers examined herein. Nevertheless, it has been demonstrated that the nature of the imido substituent employed does have a critical impact on the catalytic dimerization of ethylene and 1-hexene using the THF complexes **54-59** as pro-initiators, something that is discussed in detail in the following sections.

3.3.2 Molecular structures of $[[W(NDipp)Cl_2]_2(\mu-Cl)_3][Et_3NH]$ and $W(NDipp)Cl(H)(PMe_3)_3$

Single crystals of **60** were obtained from DCM solution by slow evaporation, while **62** was recrystallized from a toluene/pentane solution at -30 °C. Following X-ray diffraction analyses, the resulting molecular structures, of complexes **60** and **62**, were obtained confirming in that way their successful synthesis.

3.4 Tungsten mono(imido) complexes as pro-initiators for ethylene and 1-hexene dimerization

In the following sections the catalytic dimerization of ethylene and 1-hexene using tungsten mono(imido) pro-initiators activated under various conditions is outlined. As was the case for the tungsten bis(imido) systems described in chapter 2, in the absence of aluminum activator the mono(imido) tungsten pro-initiators were found to be inert towards 1-hexene (Scheme 3.6).



Scheme 3.6 Attempted reaction of $[W(NDipp)Cl_4]_2$ with 1-hexene.

Additionally, in contrast to the majority of olefin oligomerization and polymerization systems, where a high aluminum to transition metal loading is required (> 100),¹³⁻¹⁶ it was found that only 15 equivalents of EtAlCl_2 per tungsten are necessary to efficiently activate these tungsten mono(imido) pro-initiators. The use of a lower EtAlCl_2 loading is advantageous since it lowers the cost and increases the safety of the catalytic process.

3.4.1 Ethylene dimerization studies

3.4.1.1 Ethylene dimerization testing using tungsten(VI) mono(imido) pro-initiators

3.4.1.1.1 General remarks

The conditions used for the catalytic dimerization studies performed in this section were chosen to be identical to those described in section 2.4. Specifically, the use of 15 equivalents of EtAlCl_2 to activate the mono(imido) pro-initiators is confirmed to be close to optimal in section 3.4.2.2. All of the examined mono(imido) pro-initiators were found to be active in the dimerization of ethylene, with the activity being strongly dependent on the nature of the imido substituent and catalytic reaction conditions.

Table 3.2 presents the results from the catalytic dimerization of ethylene for a range of mono(imido) complexes, activated with 15 equivalents of EtAlCl_2 at 40 bar of ethylene pressure and 60 °C. Table 3.3 describes results from a study of the most active pro-initiators based on the tests described in Table 3.2, undertaken at 45 bar/75 °C. The highest activity obtained in both sets of experiments was 167.8 kg C_2H_4 (mol W)⁻¹ h⁻¹bar⁻¹ for pro-initiators $W(\text{NTfp})\text{Cl}_4(\text{THF})$ (**58**) and $W(\text{NDipp})\text{Cl}_4(\text{THF})$ (**59**) at 45 bar/75 °C. This suggests that the tungsten mono(imido) complexes are moderate ethylene dimerization pro-initiators, when it is considered that the activities reported for other ethylene dimerization systems are between 0.17¹⁷ and 10000¹⁸⁻²⁰ kg C_2H_4 (mol TM)⁻¹ h⁻¹bar⁻¹ (see section 1.7). However, it must be mentioned that in most of the reports presented in the literature, the ethylene dimerization reaction is usually halted at an ethylene consumption of up to 10 g, thus providing information on only a small fraction of the true catalytic activity profile.^{13,14,17,21} In contrast, for the work undertaken in this thesis, the

catalytic reactions were run either a) until catalyst deactivation occurred or b) to the point that the reaction vessel was filled.

Table 3.2 Dimerization of ethylene using well-defined W(VI) imido complexes activated with 15 equivalents EtAlCl₂ at 40 bar ethylene pressure and 60 °C^{a,b}.

Run #	Pro-initiator	Time (min)	TON ^d	Act. ^e	Mol % C ₄ (in liq. prod.)	% 1-C ₄ in C ₄	Mol % C ₆ (in liq. prod.)	% 1-C ₆ in C ₆	% Lin in C ₆	% MP in C ₆	% 3Me 1C ₅ in C ₆	% 2Et 1C ₄ in C ₆	wt % C ₈₊ (in prod.)
1	W(NEt)Cl ₄ (THF) (54)	3.9	1.2	18.1	85.4	95.7	14.1	4.1	6.5	93.5	70.8	14.7	1.0
2	W(NiPr)Cl ₄ (THF) (55)	5.5	1.0	10.9	79.3	95.1	16.3	3.5	5.3	94.7	81.5	4.0	9.4
3	W(NPh)Cl ₄ (THF) (56)	61.7	15.0	14.6	90.0	74.5	10.0	8.1	10.9	89.1	40.5	43.2	4.0
4	W(NPh ^F)Cl ₄ (THF) (57)	125	81.0	38.9	81.6	97.5	18.0	3.3	5.7	94.3	40.9	49.3	0.8
5	W(NTfp)Cl ₄ (THF) (58)	94	87.5	55.9	81.5	97.0	16.5	3.3	4.3	95.7	44.8	42.6	4.8
6	W(NDipp)Cl ₄ (THF) (59)	95.6	98.7	61.9	80.2	98.0	18.7	1.5	4.0	96.0	41.9	51.3	2.6
7 ^c	W(NDipp)Cl ₄ (THF) (60)	24.3	10.7	26.6	93.4	80.8	6.4	22.6	89.3	10.7	1.2	21.2	0.3

^a General conditions: 20 μmol W complex and 300 μmol EtAlCl₂; PhCl (solvent) 74 mL; 60 °C; ethylene pressure (40 bar); stirrer speed 1000 rpm; nonane standard (1.000 mL); catalytic runs were performed until consumption of C₂H₄ dropped below 0.2 g min⁻¹ or until the reactor was filled, at which time reaction was quenched by addition of dilute HCl. ^b Only traces of polyethylene were produced (0-1% of products fraction). ^c 300 μmol of MeAlCl₂ were used instead of EtAlCl₂. ^d TON is reported in (kg C₂H₄) (mol W)⁻¹ bar⁻¹. ^e Activity is reported in (kg C₂H₄) (mol W)⁻¹ h⁻¹ bar⁻¹ and is based on the total ethylene consumption.

The main products from every catalytic run presented in Table 3.2 and Table 3.3 were butenes (>79% mol of the products), of which more than 75% consisted of 1-butene. Note, that a significant quantity of hexenes (10-20% mol of the product fraction) was also produced, along with heavier liquid olefins (although in most cases this only amounts to a small fraction of the products, < 6.2 % wt). Hence, the tungsten mono(imido) pro-initiators can be considered to be reasonably selective compared to previously-reported ethylene dimerization systems (see section 1.7). Additionally, under both sets of conditions (Table 3.2 and Table 3.3) only traces of polyethylene were produced (0-1% of products fraction) and, in most cases, no polyethylene at all was detected. The absence of polyethylene at the end of catalysis is advantageous, not only from selectivity and atom economy viewpoints, but also because it reduces the time required cleaning the reactor in between runs increasing the efficiency of the dimerization process.

Table 3.3 Dimerization of ethylene using well defined W(VI) imido complexes activated with 15 equivalents EtAlCl₂ at 45 bar ethylene pressure and 70 °C^{a,b}.

Run #	Pro-initiator	Time (min)	TON ^c	Act. ^d	Mol % C ₄ (in liq. prod.)	% 1-C ₄ in C ₄	Mol % C ₆ (in liq. prod.)	% 1-C ₆ in C ₆	% Lin in C ₆	% MP in C ₆	% 3Me 1C ₅ in C ₆	% 2Et 1C ₄ in C ₆	wt % C ₈₊ (in liq. prod.)
1	W(NPh)Cl ₄ (THF) (56)	53.6	101.2	113.2	87.0	96.9	12.2	2.7	4.2	95.8	41.8	46.9	1.7
2	W(NPh ^F)Cl ₄ (THF) (57)	46.2	100.1	130.0	87.8	96.9	11.1	3.0	4.8	95.2	43.9	45.0	2.6
3	W(NTfp)Cl ₄ (THF) (58)	30.8	86.0	167.4	84.7	97.0	12.9	3.8	5.2	94.8	49.9	38.9	6.2
4	W(NDipp)Cl ₄ (THF) (59)	35	97.8	167.8	78.9	97.9	20.2	1.6	4.1	95.9	41.1	52.0	2.0

^a General conditions: 20 μmol W complex and 300 μmol EtAlCl₂; PhCl (solvent) 74 mL; 70 °C; ethylene pressure (45 bar); stirrer speed 1000 rpm; nonane standard (1.000 mL); catalytic runs were performed until consumption of C₂H₄ dropped below 0.2 g min⁻¹ or until the reactor was filled, at which time reaction was quenched by addition of dilute HCl. ^b No polyethylene was produced. ^c TON is reported in (kg C₂H₄) (mol W)⁻¹ bar⁻¹. ^d Activity is reported in (kg C₂H₄) (mol W)⁻¹ h⁻¹ bar⁻¹ and is based on the total ethylene consumption.

3.4.1.1.2 Effect of the imido substituent on the ethylene dimerization catalytic activity

Although the mono(imido) pro-initiators **48-53** were found to be structurally similar (Section 3.3.1), their activities and TONs in the dimerization of ethylene vary considerably (Figure 3.3). From the data presented in Figure 3.3 it is evident that the alkyl-substituted imido systems (runs 1 and 2; Table 3.2) are extremely poor pro-initiators with limited lifetime (deactivation occurred within 5 minutes) and low TONs, compared to the rest of the imido systems examined herein. In contrast, complexes **57-59** filled the 250 mL reactor (runs 4-6; Table 3.2), achieving activities and TONs of up to 61.9 kg C₂H₄ (mol W)⁻¹ h⁻¹ bar⁻¹ and 98.7 kg C₂H₄ (mol W)⁻¹ bar⁻¹, respectively. Pro-initiator W(NPh)Cl₄(THF) (**56**) exhibited a moderate activity and TON placing its performance between that of the alkyl-substituted imido systems and that of the other aryl imidos. Taking these observations together, it appears that bulky imido groups such as NDipp or electron deficient imido groups such as NPh^F and NTfp favor catalysis. On the other hand electron-donating groups with a small steric hindrance, such as NEt and NⁱPr, result in the formation of poorly active ethylene dimerization systems after activation. Complex **56** bearing the NPh group, which can be considered as being in between the alkyl and aryl groups in terms of electron withdrawing character or steric bulk, leads to a catalytic system of intermediate activity.

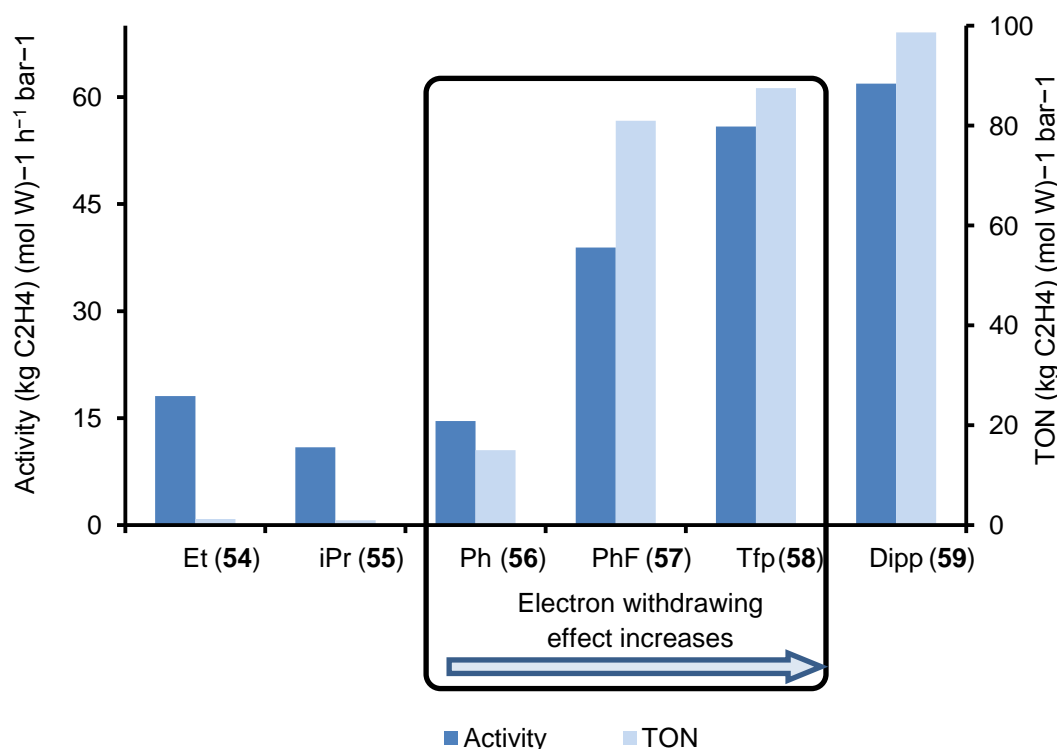


Figure 3.3 Summary of the catalytic activity and TON as a function of imido ligand substituent of the tungsten mono(imido) pro-initiators **54-59** at 40 bar ethylene/60 °C; data taken from Table 3.2

3.4.1.1.2.1 Beneficial effect of electron withdrawing imido ligands on catalysis

The beneficial effect that electron withdrawing imido ligands have on catalysis is demonstrated in Figure 3.3 (highlighted region), which compares the catalytic activities achieved by complexes **56-58** (runs 4-6;

Table 3.2) after activation. The electron withdrawing nature of the imido moieties in **56-58** increases in the order $\text{Ph} < \text{Ph}^{\text{F}} < \text{Tfp}$ due to the gradual substitution of protons by fluorine atoms on the aromatic ring, which mirrors the increase in their catalytic activity. It must be noted that the covalent radius of fluorine is two times larger compared to that for hydrogen (0.64 Å and 0.30 Å, respectively).²² Hence, it is possible that the NTfp group could impose a slightly greater steric hindrance on the imido complex compared to that of either NPh or NPh^{F} , due to the presence of fluoride on the *ortho* positions of the aromatic ring. Nevertheless, the differences observed in the catalytic activity of pro-initiators **56-58** is considered most largely to be due to their different electronic properties judging by the differences observed between pro-initiators **56** and **57**, which are sterically similar.

3.4.1.1.2.2 Effect of imido ligand steric bulk on the catalytic activity of the mono(imido) tungsten-based dimerization systems

In section 3.4.1.1.2.1 it was shown that electron withdrawing imido substituents such as NTfp increase the catalytic activity of the mono(imido) tungsten-based ethylene dimerization systems. Interestingly, complex **59** was found to be the most active pro-initiator examined in this chapter (with an activity of 61.9 kg C_2H_4 (mol W)⁻¹h⁻¹bar⁻¹), despite bearing the less electron-withdrawing NDipp group compared to NTfp. However, the Dipp group induces the greatest steric hindrance compared to the rest of the imidos examined in this chapter, due to the presence of the ⁱPr groups on the *ortho* positions of the aromatic ring. This suggests that imido substituents with greater steric bulk increase the catalytic activity of the mono(imido)-based dimerization systems. The beneficial effect of bulky imido ligands is also supported by comparing the data from run 6, Table 3.2 with that from run 3, Table 3.2, which shows that the NPh-containing pro-initiator exhibits a catalytic activity four times lower than that of its bulkier NDipp counterpart. Similar trends have also been recorded for the tungsten bis(imido) pro-initiators (section 2.4.1.1.1), as well as for previously-reported ethylene dimerization systems.^{14,17}

3.4.1.1.3 Effect of temperature on ethylene dimerization activities of mono(imido) pro-initiators

From the data presented in Table 3.3, the ethylene dimerization activities achieved when complexes **56-59** were activated and subsequently tested at 45 bar ethylene pressure, at 70 °C, and with 15 equivalents EtAlCl_2 , were at least three times greater compared to the activities recorded at 40 bar, 60 °C (Table 3.2).

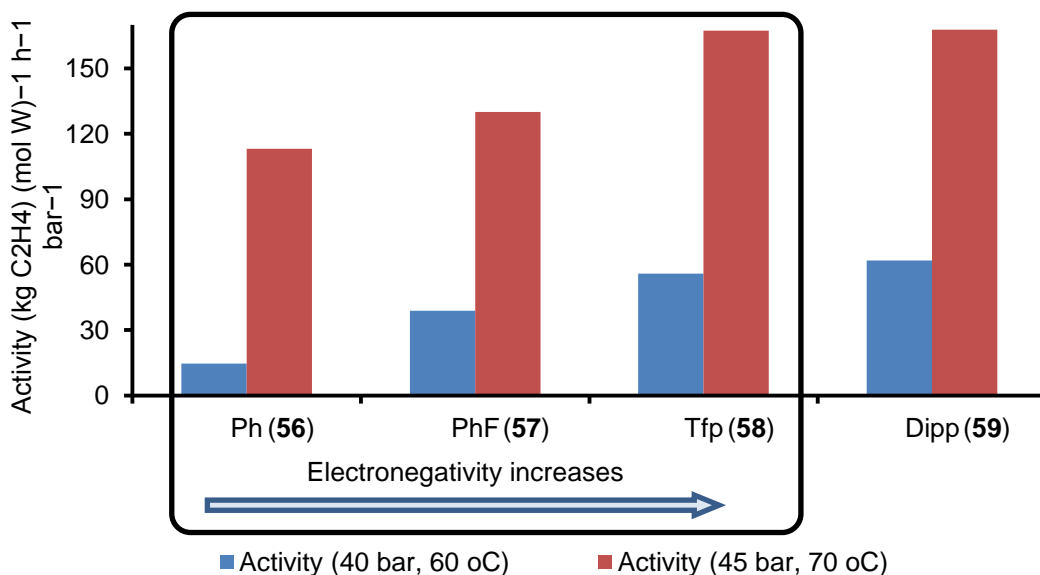


Figure 3.4 Comparison of catalytic activities of the tungsten mono(imido) pro-initiators (**56-59**) at 40 bar ethylene/60 °C and 45 bar/70 °C as a function of imido substituent; data taken from Table 3.2 and Table 3.3.

3.4.1.1.4 Effect of imido substituent and reaction conditions on ethylene dimerization selectivity with mono(imido) tungsten-based systems

As was the case for the tungsten bis(imido) ethylene dimerization systems (section 2.4.1.3), from the data presented in Figure 3.5 it is clear that the main product of the catalytic dimerization of ethylene mediated by the mono(imido) tungsten pro-initiators is 1-butene. In addition, the selectivity of the catalytic reaction towards 1-butene is independent of the nature of the imido substituent, and, generally of the reaction temperature and pressure. However, with pro-initiator $W(NPh)Cl_4(THF)$ (**56**) it was found that an increase in temperature and in pressure improved the selectivity towards 1-butene (Figure 3.5). A similar beneficial effect of increased ethylene pressure on the selectivity towards 1-butene has also been encountered in previously-reported ethylene dimerization systems, something that has been attributed to the chain transfer processes being favored over chain propagation under these conditions.¹³

Apart from butenes, trimers are also produced from the dimerization of ethylene mediated by the tungsten mono(imido) based systems. As can be seen from Figure 3.5, the selectivity of the catalytic reactions towards trimer formation does not vary significantly between the various runs. Additionally, since the composition of the trimers product fraction is very similar from catalytic tests using all of the mono(aryl imido) and bis(aryl imido) pro-initiators (see section 2.4.1.3), this suggests that the same mechanism of trimers formation is likely to be operative in each case.

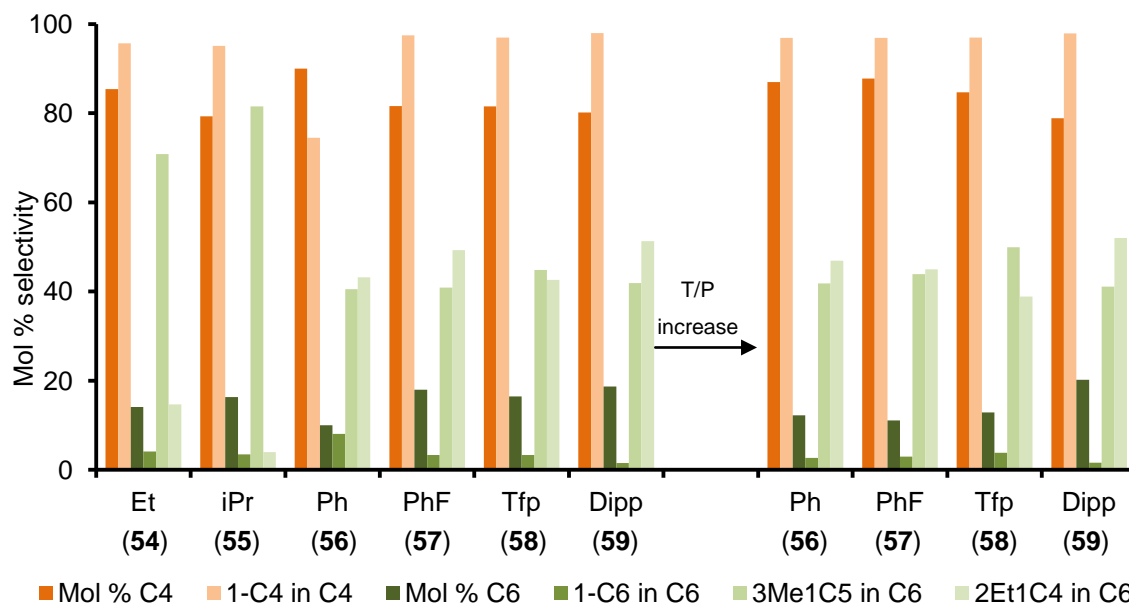


Figure 3.5 Product selectivities (expressed in mol %) from the tungsten mono(imido) pro-initiators (**54-59**) at $P = 40$ bar ethylene/ $T = 60$ °C (left) and $P = 45$ bar/ $T = 70$ °C (right) versus imido substituent; data taken from Table 3.2 and Table 3.3.

3.4.1.1.5 Mechanistic implications of the C₆ fraction composition

The nature of the products produced from a catalytic dimerization reaction can sometimes provide information about the catalytic mechanism in operation (see sections 1.6.2 and 2.4.1.6).^{23,24} For ethylene dimerization mediated by tungsten mono(imido) pro-initiators, the product selectivity is very similar to that observed for the tungsten bis(imido) ethylene dimerization systems (section 2.4.1.3), with the main products being 1-butene, 1-hexene, 3-methyl-1-pentene, and 2-ethyl-1-butene. Additionally, as was the case for the tungsten bis(imido) systems (section 2.4.1.1.4), the tungsten mono(imido) pro-initiators can also be successfully activated with MeAlCl₂ (run 7; Table 3.2). Hence, using the same argument employed in section 2.4.1.6, it is suggested that a metallacyclic mechanism is more likely to be operative here, rather than a step-wise addition mechanism.

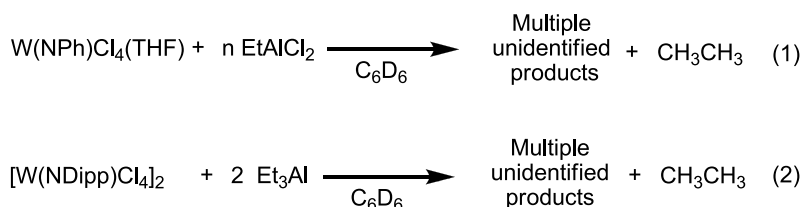
3.4.1.2 Reactions of [W(NR)Cl₄]₂ (R = Dipp, Et, Tfp) and W(NDipp)Cl₄(THF) with R_nAlCl_(3-n) reagents

In section 3.4.1.1 catalysis using pro-initiators **54-59** was initiated using 15 equivalents of EtAlCl₂, which afforded highly active ethylene dimerization systems. In order to gain insight into the mode of action of EtAlCl₂ during activation, discrete reactions of mono(imido) complexes with R_nAlCl_(3-n) reagents were studied.

3.4.1.2.1 Reactions of mono(imido) tungsten complexes with Et_nAlCl_(3-n)

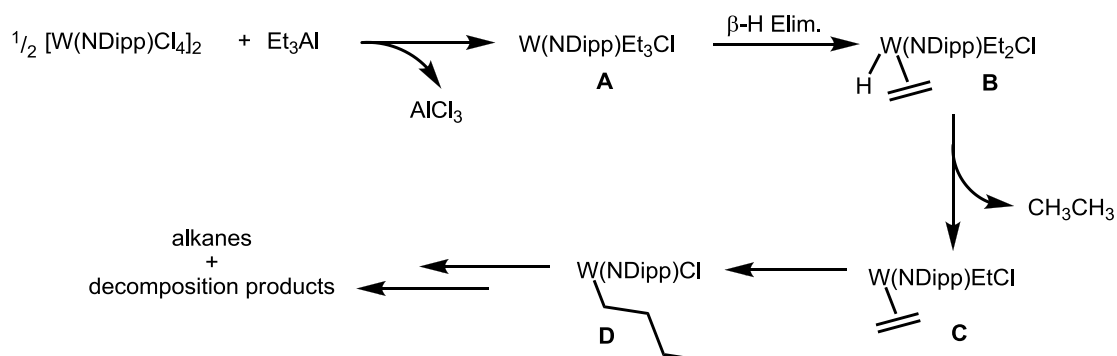
The reaction of W(NPh)Cl₄(THF) (**56**) with two or more equivalents of EtAlCl₂ has been previously reported by Wright *et al.*,^{25,26} and was shown to give a complex mixture of unidentified products, along

with the formation of ethane (Scheme 3.7, eq.1) (reaction of **56** with only one equivalent of EtAlCl_2 displaces the bound THF generating $\text{EtAlCl}_2 \cdot (\text{THF})_2$). The complexity of the reaction of **56** with EtAlCl_2 could be due to tungsten-bound THF and also to the presence of chlorine atoms on the aluminum reagent. Lewis basic THF is capable of coordination and can thus influence the reaction in unexpected ways (for example, in section 3.2.1 the ring-opening of THF caused complications in the synthesis of $\text{W}(\text{NTfp})\text{Cl}_4(\text{THF})$ (**58**)), while the presence of chloride atoms on EtAlCl_2 increases the aluminium's Lewis acidity (see section 6.1.3), giving the activator the dual character of a good Lewis acid and alkylating agent, something that opens at least two different reaction pathways. Thus, in an attempt to simplify the reaction between mono(imido) tungsten complexes with aluminum reagents, the THF-free complex $[\text{W}(\text{NDipp})\text{Cl}_4]_2$ (**53**) was reacted with one equivalent of chloride-free Et_3Al (Scheme 3.7, eq.2). When Et_3Al was added to a solution of **53** in C_6D_6 , evolution of ethane, along with formation of a complex mixture of products, was observed (based on ^1H and ^{13}C NMR spectroscopic analysis).



Scheme 3.7 Reaction of $\text{W}(\text{NPh})\text{Cl}_4(\text{THF})$ (**56**) and $[\text{W}(\text{NDipp})\text{Cl}_4]_2$ (**53**) with excess EtAlCl_2 and 2 eq. Et_3Al , respectively.

A suggested mechanism for the reaction of $[\text{W}(\text{NDipp})\text{Cl}_4]_2$ (**53**) with Et_3Al ($\text{W}:\text{Al} = 1:1$) is presented in Scheme 3.8. Formation of ethane suggests the following: Firstly, aluminium-to-tungsten transmetallation occurs, forming a tungsten ethyl complex **A**, which subsequently undergoes β -hydride elimination forming tungsten hydride **B**, which can undergo reductive elimination forming ethane and complex **C**. Since no olefins were detected in the final solution from the reaction between $[\text{W}(\text{NDipp})\text{Cl}_4]_2$ (**53**) and Et_3Al , it is suggested that complex **C** reacts further to form a tungsten butyl derivative **D**, which is highly coordinatively unsaturated and hence, likely to be extremely reactive, thus decomposing rather than undergoing a well-defined β -hydride elimination reaction.



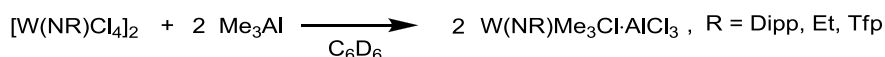
Scheme 3.8 Suggested mechanism for the reaction of $[\text{W}(\text{NDipp})\text{Cl}_4]_2$ with Et_3Al ($\text{W}:\text{Al} = 1:1$).

3.4.1.2.2 Reactions of mono(imido) tungsten complexes with Me₃Al

The results obtained from studying the reaction of [W(NDipp)Cl₄]₂ (**53**) with Et₃Al (section 3.4.1.2.1) suggest that the formation of W-Et species (generated *via* transmetallation) makes understanding the first stages of reaction between the aluminum activator and the tungsten mono(imido) pro-initiator complicated, due to the ability of the W-Et fragments to undergo β-hydride elimination. Consequently, a related reaction was performed, in which Et₃Al was replaced by Me₃Al, thus circumventing the issues surrounding β-hydride elimination.

3.4.1.2.2.1 Reaction of [W(NDipp)Cl₄]₂ with Me₃Al: isolation and characterization of W(NDipp)Me₃Cl·AlCl₃ (**64**)

Treatment of [W(NDipp)Cl₄]₂ (**53**) with two equivalents of Me₃Al in C₆D₆ (Scheme 3.9) resulted in the clean formation of W(NDipp)Me₃(Cl)·AlCl₃ (**64**). The presence of three tungsten-bound Me groups in **64** was confirmed by integration of the methyl resonance at 1.93 ppm against the imido protons in its ¹H NMR spectrum. Interestingly, what appears to be a singlet resonance is observed in the ¹H NMR spectrum for the aromatic protons of **64**, suggesting that the chemical shifts for these protons must be extremely similar.



Scheme 3.9 Reaction of [W(NR)Cl₄]₂ (R = Dipp, Et, Tfp) with two equivalents of Me₃Al

The presence of a potentially “W”-bound AlCl₃ moiety was inferred from detection of a broad resonance in the ²⁷Al NMR spectrum of **64** at 104 ppm, which is in the region characteristic of four-coordinate aluminum species such as AlCl₄⁻ (see section 6.1). However, it is possible to envisage that AlCl₃ could be bound to the W(NDipp)Me₃Cl fragment in four possible ways (Figure 3.6). Note that examples of each of the four different AlCl₃ modes have been recorded in the literature albeit in quite different complexes: i) *via* the tungsten-bonded Cl atom only,²⁷ ii) *via* two Cl atoms,²⁸ iii) *via* an imido bond,²⁶ and iv) as a discrete AlCl₄⁻ anion.²⁹ Hence, in order to further probe the nature of the AlCl₃ moiety in **64**, a crystallographic study was undertaken.

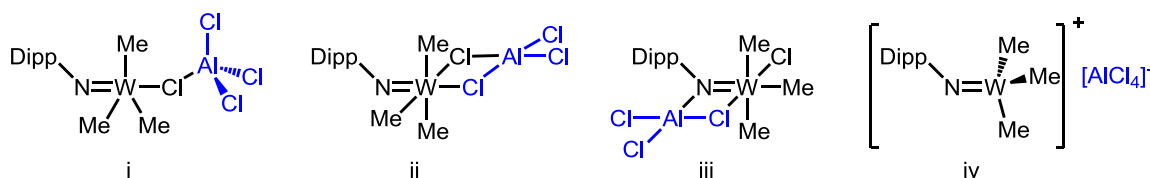


Figure 3.6 Possible arrangements of AlCl₃ on the W(NDipp)Me₃Cl fragment

To this end, single crystals of complex **64** were grown from a DCM solution after layering with hexane and were examined by X-ray diffraction. The molecular structure of **64**, along with selected interatomic distances and angles, are presented in Figure 3.7; the structure is in accordance with its NMR spectroscopic data. Complex **64** adopts a distorted trigonal bipyramidal geometry with the tungsten atom lying out of the C(1)-C(2)-C(3) plane due to steric pressure from the imido substituent ($\Sigma_n(W-N-C(n)) = 291.10(6)^\circ$). The AlCl₃ molecule is linked to the tungsten *via* the Cl(1) atom, with a W-Cl(1)-Al

angle of 123.807(19)°, *i.e.* mode i, Figure 3.6. The W-N interatomic distance and the W-N-C(4) angle measure 1.7243(11) Å and 170.94(10)°, respectively, values typical for a W≡N triple bond (see section 3.3). Notably, the imido W≡N interatomic distance in complex **64** is identical to that in complex **53**. The W-CH₃ interatomic distances of **64** are identical (2.0878(14) Å) and within the expected range for W-CH₃ single bonds (2.072-2.306 Å).³⁰ The W-Cl(1) bond (2.6512(3) Å) is elongated by 0.2314(9) Å compared to that of the W-Cl bond of the previously-reported W(NPh)Me₃Cl complex,²⁵ due to competition between the tungsten and aluminum for bonding with the Cl(1) atom. For the same reason, the Al-Cl(1) bond (2.2253(6) Å) is longer than the mean Al-Cl bond in the discrete AlCl₄⁻ anion (2.134(1) Å),³¹ by 0.091(1) Å. Hence, complex **64** can be regarded more as an ionic compound of the form [W(NDipp)Me₃][AlCl₄] rather than W(NDipp)Me₃Cl⋯AlCl₃ with a weak Cl(1)-Al interaction.

Selected interatomic distances (Å) and angles (°) for W(NDipp)Me₃Cl·AlCl₃ (**64**)

Interatomic Distances (Å)		Angles (°)	
W-N	1.7243(11)	W-Cl(1)-Al	123.807(19)
N-C(4)	1.3951(16)	C(4)-W-N	170.94(10)
W-C(1)	2.0869(14)	C(1)-W-N	96.57(5)
W-C(2)	2.0918(14)	C(2)-W-N	94.03(6)
W-C(3)	2.0878(14)	C(3)-W-N	100.05(6)
W-Cl(1)	2.6512(3)	C(1)-W-C(2)	120.91(6)
Al-Cl(1)	2.2253(6)	C(1)-W-C(3)	116.18(6)
Al-Cl(2)	2.1080(7)	C(3)-W-C(2)	118.70(7)

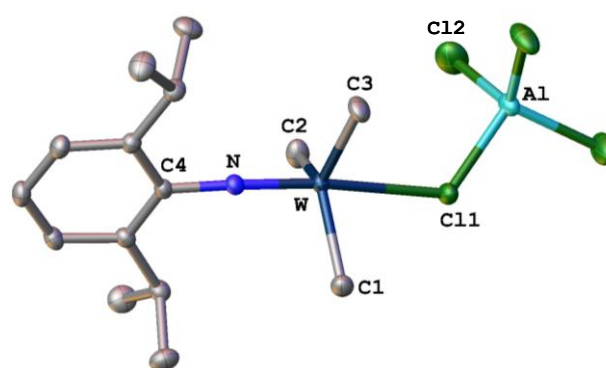
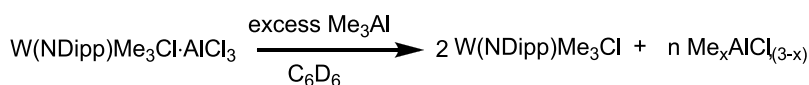


Figure 3.7 Selected interatomic distances (Å) and angles (°) for W(NDipp)Me₃Cl·AlCl₃ (**64**) and its molecular structure. H atoms are omitted for clarity and the thermal ellipsoids are shown at the 50% probability level.

In order to probe the effect of different imido substituents on the reaction between [W(NR)Cl₄]₂ and Me₃Al, analogous reactions of [W(NEt)Cl₄]₂ (**48**) and [W(NTfp)Cl₄]₂ (**52**) with two equivalents of Me₃Al were undertaken. Subsequent NMR spectroscopic analysis revealed the products from both reactions were analogous to that formed between [W(NDipp)Cl₄]₂ (**53**) and 2 Me₃Al (Scheme 3.9).

3.4.1.2.2.2 Reaction of [W(NDipp)Cl₄]₂ with excess Me₃Al

It has been shown that when an excess of Me₃Al (>5 equivalents) is reacted with [W(NDipp)Cl₄]₂, the aluminum-free complex W(NDipp)Me₃Cl is formed.²⁵ This is presumably due to formation of methylated aluminum chloride (Me_xAl_{3-x}) species during the reaction, which, in contrast to AlCl₃, are not Lewis acidic enough to bind efficiently to W(NDipp)Me₃Cl. To probe these differences, the reaction of [W(NDipp)Cl₄]₂ with 1 to 5 equivalents of Me₃Al (Scheme 3.10) was studied by ¹H NMR spectroscopy, with the resulting spectra following each Me₃Al addition being presented in Figure 3.8.



Scheme 3.10 Reaction of W(NDipp)Me₃Cl·AlCl₃ with excess Me₃Al

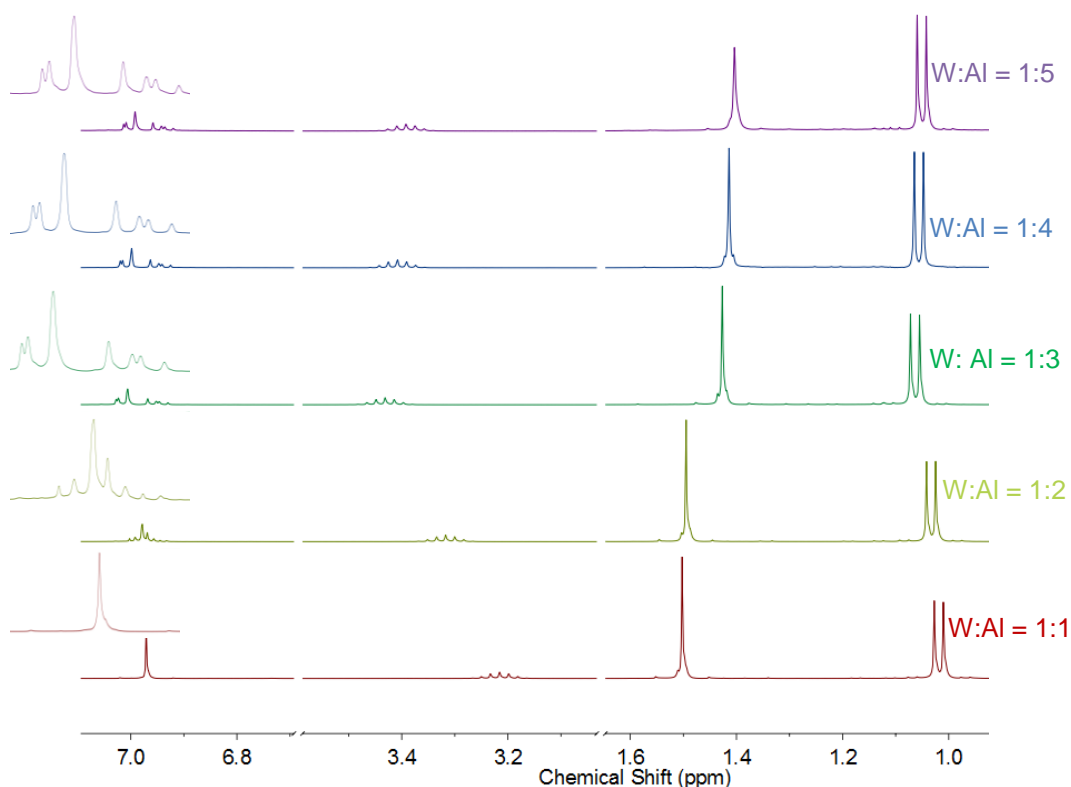


Figure 3.8 ^1H NMR (400 MHz, C_6D_6) spectroscopic study of the reaction of $[\text{W}(\text{NDipp})\text{Cl}_4]_2$ with Me_3Al at various $\text{W}:\text{Al}$ ratios (expansions shown for the region 7.03 - 6.92 ppm).

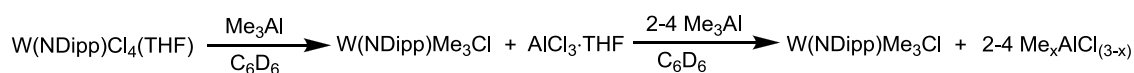
Upon addition of the second equivalent (per tungsten) of Me_3Al to the $[\text{W}(\text{NDipp})\text{Cl}_4]_2$ solution, a high frequency shift of the isopropyl CHCH_3 protons is observed, along with partial resolution of the broad singlet resonance at 6.97 ppm, corresponding to the aromatic Dipp protons. Further addition of Me_3Al (3 equivalents) causes a high frequency shift of 0.03 ppm for the CHCH_3 protons, a further 0.11 ppm high frequency shift of the CHCH_3 , and a low frequency shift of 0.07 ppm for the WCH_3 protons. The resonance from the aromatic protons after the addition of 3 equivalents of Me_3Al is split into a complex, second order, pattern. Addition of four or more equivalents of Me_3Al has no further effect on the ^1H NMR spectra.

As described (Figure 3.8), the ^1H NMR spectrum of $\text{W}(\text{NDipp})(\text{Cl})\text{Me}_3\cdot\text{AlCl}_3$ (**64**) is altered by the addition of one or more equivalents of Me_3Al . Since, previously it has been shown that reaction of $[\text{W}(\text{NDipp})\text{Cl}_4]_2$ (**53**) with excess Me_3Al yields $\text{W}(\text{NDipp})\text{Me}_3\text{Cl}$,²⁵ it is proposed that the changes in the ^1H NMR spectrum of **64** upon addition of Me_3Al result from the abstraction of the bound AlCl_3 from **64**. Hence, the ^1H NMR spectra presented in Figure 3.8 for a $\text{W}:\text{Al}$ ratio > 1:2 correspond to AlCl_3 -free $\text{W}(\text{NDipp})(\text{Cl})\text{Me}_3$ (Scheme 3.10).

3.4.1.2.2.3 Reaction of $\text{W}(\text{NDipp})\text{Cl}_4(\text{THF})$ with excess Me_3Al

In order to probe whether the presence of tungsten-bound THF has any effect on the reaction of the $\text{W}(\text{NDipp})\text{Cl}_4$ fragment with Me_3Al , $\text{W}(\text{NDipp})\text{Cl}_4(\text{THF})$ (**59**) was reacted with 1 to 4 equivalents of Me_3Al (Scheme 3.11). The ^1H NMR spectra from these reactions are presented in Figure 3.9. Comparison of

the spectra in Figure 3.9 with those in Figure 3.8 for a W:Al ratio > 1:2 indicates that the reaction of $W(NDipp)Cl_4(THF)$ (**59**) with Me_3Al always produces aluminum free $W(NDipp)Me_3Cl$ at any W:Al ratio instead of **64** probably due to the THF acting as a Lewis base which binds $AlCl_3$.



Scheme 3.11 Reaction of $W(NDipp)Cl_4(THF)$ (**59**) with 1 to 4 equivalents of Me_3Al

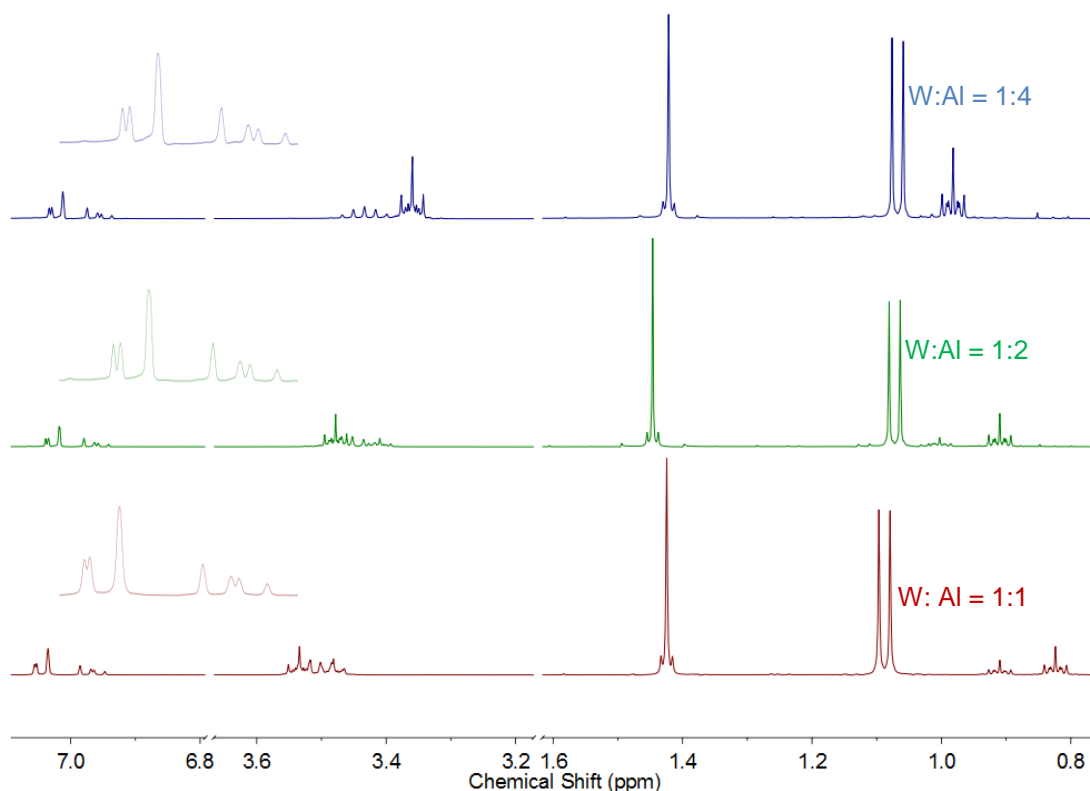


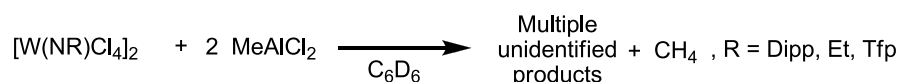
Figure 3.9 1H NMR (400 MHz, C_6D_6) spectroscopic study of the reaction of $W(NDipp)Cl_4(THF)$ (**59**) with Me_3Al at various W:Al ratios (expansions shown for the region 7.03-6.92 ppm).

3.4.1.2.3 Reactions of mono(imido) tungsten complexes with $MeAlCl_2$

In section 3.4.1.2.2 the reaction between $[W(NR)Cl_4]_2$ ($R = Dipp, Et, Tfp$) and Me_3Al was shown to result in the formation of well-defined tungsten complexes. However, Me_3Al is not a very good model for simulating the catalytic olefin dimerization reaction conditions, since it is significantly different to $EtAlCl_2$, which has been demonstrated to be the most effective activator. Unfortunately, reactions of tungsten mono(imido) complexes with $EtAlCl_2$ lead to mixtures of unidentified products (see section above) of low diagnostic value. Hence, in an attempt to gain some further insight about the way in which $EtAlCl_2$ interacts with the tungsten pro-initiators, reactions of $[W(NR)Cl_4]_2$ ($R = Dipp, Et, Tfp$) with $MeAlCl_2$ were performed.

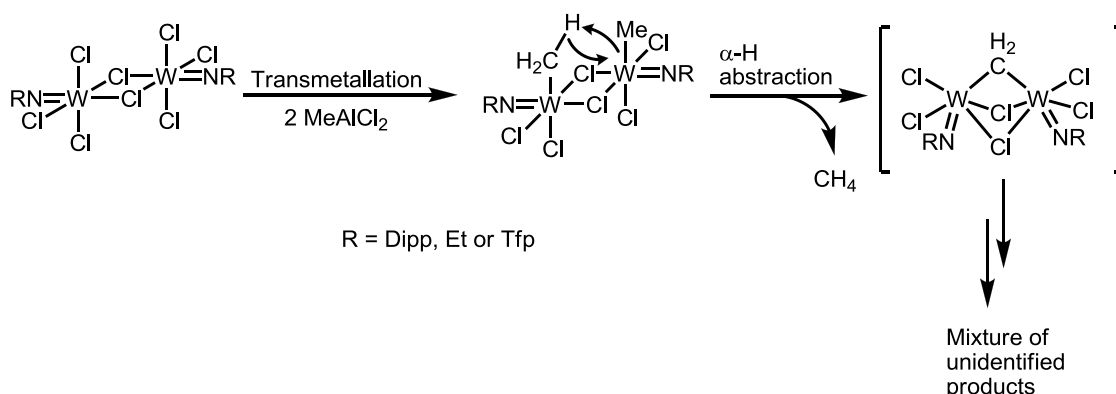
3.4.1.2.3.1 Reaction of $[W(NDipp)Cl_4]_2$ and $W(NDipp)Cl_4(THF)$ with $MeAlCl_2$

The complexes $[W(NR)Cl_4]_2$ ($R = Dipp, Et, Tfp$) were reacted with two equivalents of $MeAlCl_2$ ($W:Al = 1:1$) in C_6D_6 . Interestingly, a multitude of products were observed in the 1H NMR spectrum of the resulting reaction mixture; at least four Dipp environments were detected along with other by-products including methane (Scheme 3.12). Unfortunately, attempts to obtain crystals of the products formed in these reactions suitable for a crystallographic study were unsuccessful.



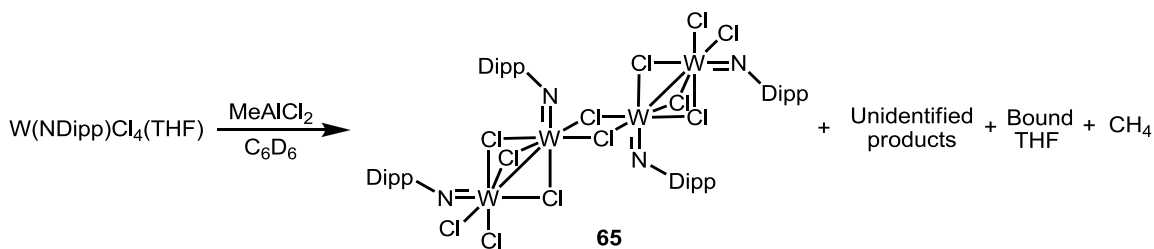
Scheme 3.12 Reaction of complexes $[W(NR)Cl_4]_2$ with two equivalents of $MeAlCl_2$

However, since methane is formed from the reaction of $[W(NR)Cl_4]_2$ ($R = Dipp, Et, Tfp$) with $MeAlCl_2$, it is likely that a tungsten methyl dimer species is formed, which is then subject to bimolecular α -hydride abstraction (α -hydride elimination cannot occur on a tungsten(VI) complex since it requires a two electron oxidation on the metal) leading to a μ - CH_2 -bridged tungsten dimer (Scheme 3.13), which can further react to give various unidentified products. Such μ - CH_2 -bridged tungsten dimers have been reported in the literature.³² These observations contrast to those made following the reaction of $[W(NDipp)Cl_4]_2$ (**53**) with two equivalents of Me_3Al (section 3.4.1.2.2), where stable tungsten methyl complexes were obtained.



Scheme 3.13 A suggested mechanism for the production of CH_4 from the reaction between $[W(NDipp)Cl_4]_2$ (**53**) with 2 $MeAlCl_2$

In an attempt to identify some of the products produced by the reaction between tungsten imido complexes and $MeAlCl_2$ ($W:Al = 1:1$), $W(NDipp)Cl_4(THF)$ (**59**) was reacted with $MeAlCl_2$ (Scheme 3.14). Complex **59** was selected for this reaction due to the presence of tungsten-bound THF, which can potentially prevent the coordination of $AlCl_3$ (by forming the $AlCl_3 \cdot THF$ adduct, section 3.4.1.2.2.3) to the resulting tungsten complexes, something that may limit the extent of side reactions.



Scheme 3.14 Reaction of $W(NDipp)Cl_4(THF)$ (**59**) with one equivalent of $MeAlCl_2$ ($W:Al = 1:1$)

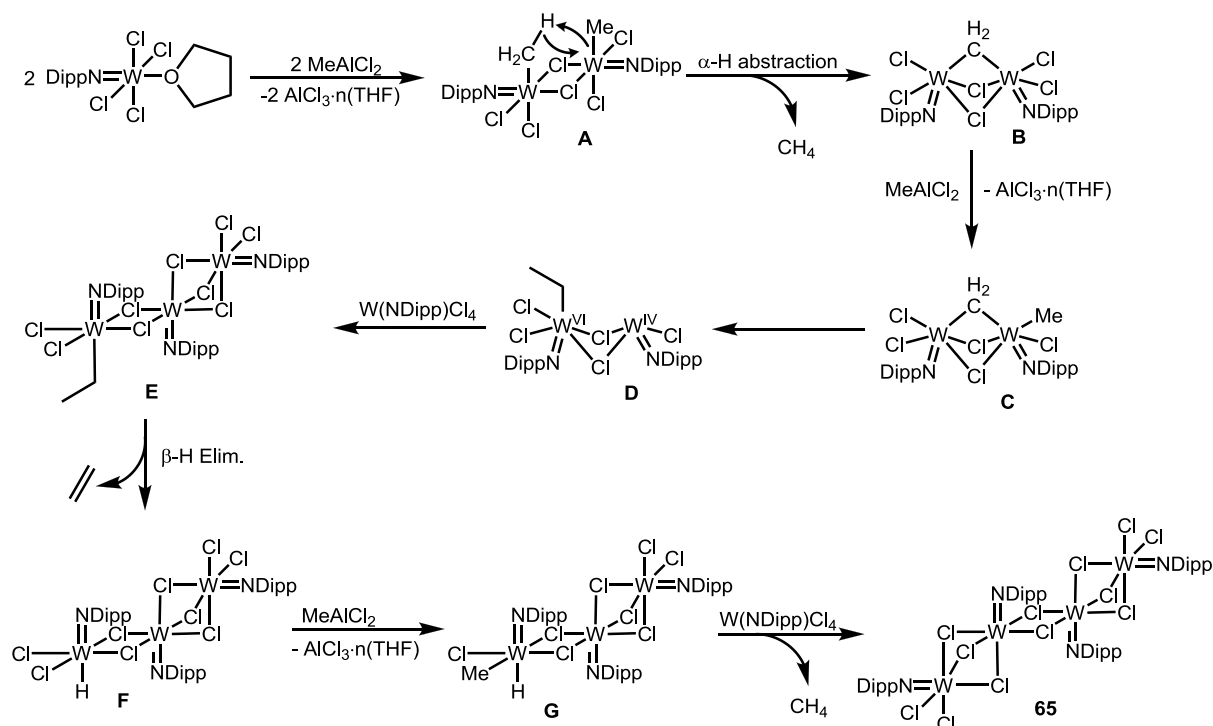
Indeed, the 1H NMR spectrum of the products from the reaction between (**59**) and $MeAlCl_2$ revealed two major Dipp resonances (1.09 and 1.24 ppm) of equal integration. However, these two Dipp resonances could not be attributed to any known imido complexes. A singlet resonance at 1.79 ppm with coupling to tungsten ($J_{WH} = 2.8$ Hz) was also detected, suggesting the presence of tungsten-bound methyl species, along with a single THF environment (3.56 and 0.88 ppm), corresponding to bound THF (free THF resonates at 3.57 and 1.40 ppm in C_6D_6 ³³). Interestingly, the presence of methane (0.16 ppm³³) and ethylene (5.25 ppm³³) were also detected in the 1H NMR spectrum, amongst various other species present in smaller quantities.

Since the identity of the products of the reaction between (**59**) and $MeAlCl_2$ could not be determined by 1H NMR spectroscopy, the resulting reaction mixture was layered with hexane, which resulted in the gradual formation of needle-like crystals (approximately 40 mg of crystals were isolated from 100 mg of starting material). The crystals were found to be insoluble to all non-coordinating solvents, which prevented their NMR spectroscopic characterization. Nevertheless, an X-ray crystallographic study of these crystals revealed that complex $[[W(NDipp)Cl_2](\mu-Cl)_3[W(NDipp)Cl]]_2(\mu-Cl)_2$ (**65**) was formed (Scheme 3.14).

The formation of complex **65** is intriguing and the exact mechanism of its formation cannot be deduced from the data available. Nevertheless, suggestions can be made based on the observation that ethylene and methane are produced when **59** is reacted with $MeAlCl_2$, along with the fact that during formation of **65** from **59**, reduction of W(VI) to W(V) must occur. Hence, the simplified mechanism presented in Scheme 3.15 is proposed for the formation of **65**.

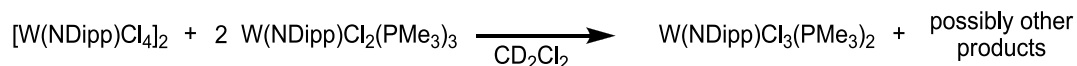
As outlined in Scheme 3.15, complex **59** is methylated by transmetalation with $MeAlCl_2$, something accompanied by simultaneous removal of THF by the $AlCl_3$ produced. It is suggested that the resulting product, $W(NDipp)Cl_3(Me)$, dimerizes leading to formation of complex **A**, which then eliminates methane *via* a bimetallic α -hydride abstraction pathway, forming complex **B**. Indeed, tungsten complexes with a bridging $\mu-CH_2$ group have been reported in the literature.³² Further alkylation of **B** by $MeAlCl_2$ leads to complex **C**. Migration of the tungsten-bound methyl group of **C** to the $\mu-CH_2$ group gives a mixed valence species **D**, in which a W(VI) centre is connected to a W(IV) centre *via* Cl bridges. Oxidation of **D** by a $W(NDipp)Cl_4$ fragment gives **E**. The ethyl group of **E** can then undergo β -hydride elimination, forming ethylene and **F**, which can further react with additional $MeAlCl_2$ to give **G**. Lastly, **G** is subject to reductive elimination producing methane followed by reaction with a $W(NDipp)Cl_4$ fragment to form **65**.

It must be noted that the mechanism presented in Scheme 3.15 is simplified and that the actual mechanism in operation is likely to be much more complicated.



Scheme 3.15 Proposed mechanism for the formation of complex **65** from the reaction between **59** and MeAlCl_2

The most important feature of the reaction between **59** and MeAlCl_2 is that the $\text{W}(\text{VI})$ species is reduced to $\text{W}(\text{V})$, possibly from the interaction between a $\text{W}(\text{VI})$ and a $\text{W}(\text{IV})$ species. In order to confirm that $\text{W}(\text{V})$ species can indeed be formed from the reaction between a $\text{W}(\text{IV})$ and a $\text{W}(\text{VI})$ species, $[\text{W}(\text{NDipp})\text{Cl}_4]_2$ (**53**) was treated with two equivalents of $\text{W}(\text{NDipp})\text{Cl}_2(\text{PMe}_3)_3$ (**61**) in CD_2Cl_2 (Scheme 3.16). As expected, only broad resonances were detected in the ^1H NMR spectrum of the resulting mixture, suggesting that a paramagnetic species was present. Layering this reaction mixture with hexane resulted in the formation of dark orange crystals of the previously reported paramagnetic $\text{W}(\text{V})$ complex $\text{W}(\text{NDipp})\text{Cl}_3(\text{PMe}_3)_2$,⁷ according to an X-ray crystallographic analysis.

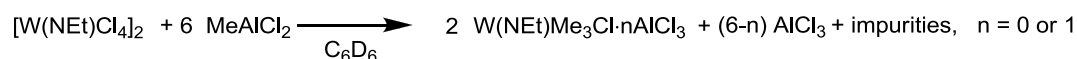


Scheme 3.16 Reaction of $[\text{W}(\text{NDipp})\text{Cl}_4]_2$ with $\text{W}(\text{NDipp})\text{Cl}_2(\text{PMe}_3)_3$ forming a $\text{W}(\text{V})$ complex

According to the results presented in this section, it appears that formation of $\text{W}(\text{IV})$ and $\text{W}(\text{V})$ species is possible under conditions analogous to those used for catalytic olefin dimerization (including for the *in situ* Sasol system). Hence, the active catalyst in such transformations could possibly be either a $\text{W}(\text{VI})$ or a $\text{W}(\text{V})$ species, originating from the reduction of the initial $\text{W}(\text{VI})$ pro-initiator during the activation stage with EtAlCl_2 . Consequently, well-defined $\text{W}(\text{IV})$ and $\text{W}(\text{V})$ complexes were tested in the catalytic dimerization of ethylene as described in the next sections (sections 3.4.1.3 and 3.4.1.4).

3.4.1.2.3.2 Reaction of $[W(NEt)Cl_4]_2$ with six equivalents of $MeAlCl_2$

Having undertaken the reaction of $[W(NR)Cl_4]_2$ ($R = Dipp, Et, Tfp$) with two equivalents of $MeAlCl_2$, complex $[W(NEt)Cl_4]_2$ (**48**) was reacted with six equivalents of $MeAlCl_2$ ($W:Al = 1:3$) in order to examine the effect of the $W:Al$ ratio on the reaction outcome (Scheme 3.17).

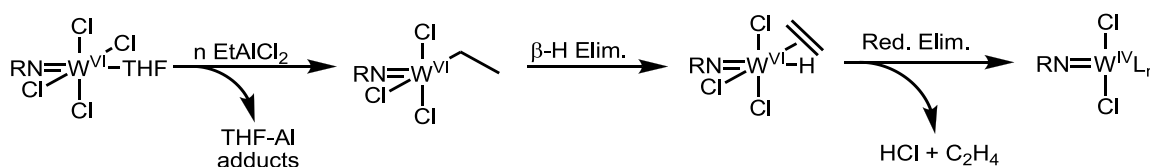


Scheme 3.17 Reaction of $[W(NEt)Cl_4]_2$ with six equivalents of $MeAlCl_2$ ($W:Al = 1:3$)

Thus, when $MeAlCl_2$ was added to a suspension of **48** in C_6D_6 , a white precipitate was formed (most likely $AlCl_3$) along with a dark orange solution. From the 1H NMR spectroscopic analysis of the dark orange solution, formation of $W(NEt)(Cl)Me_3$ or $W(NEt)Me_3(Cl) \cdot AlCl_3$ was inferred, along with the presence of small amounts of other unidentified products. These observations contrast those from the reaction between **53** and two equivalents of $MeAlCl_2$, where a mixture of unidentified products was obtained. This different behavior of **53** towards two and six equivalents of $MeAlCl_2$ demonstrates the significant impact of the $W:Al$ ratio on the reaction between tungsten(mono) imido complexes and alkyl aluminum chlorides, which is in agreement with the catalysis results presented in sections 2.4.2.4 and 3.4.2.2, where the $W:EtAlCl_2$ ratio was found to significantly influence the outcomes of the catalysis.

3.4.1.3 Tungsten(IV) mono(imido)-initiated dimerization of ethylene

In section 3.4.1.2.3 the results from the reaction between $W(NDipp)Cl_4(THF)$ (**59**) and $MeAlCl_2$ suggest that formation of $W(IV)$ species is possible. This could also be the case during activation of the mono(imido) pro-initiators with $EtAlCl_2$, since after transmetallation and ensuing β -hydride elimination, the resulting $W(VI)$ hydride could undergo reductive elimination of HCl to give a $W(IV)$ complex, as described in Scheme 3.18. This pathway is also supported by the results disclosed by Olivier *et al.*, which demonstrated that $W(IV)$ mono(imido) complexes can initiate ethylene dimerization.³⁴



Scheme 3.18 Suggested route for formation of a $W(IV)$ species during activation of a $W(VI)$ mono(imido) complex with $EtAlCl_2$ ($R = \text{alkyl or aryl}$ and L general ligand)

Hence, in order to examine if the dimerization catalyst that is produced after activation of the pro-initiators **54-59** with $EtAlCl_2$ is indeed a $W(IV)$ species, the previously reported well-defined $W(IV)$ complexes $W(NDipp)Cl_2(PMe_3)_3$ (**61**) and $W(NPh)Cl_2(PMe_3)_3$ (**25**), along with the novel $W(NDipp)(H)(Cl)(PMe_3)_3$ (**62**) complex, were synthesized and tested in the dimerization of ethylene. The results are presented in Table 3.4. From a comparison of the data presented in Table 3.2 and Table 3.4, it is clear that the $W(IV)$ pro-initiators, even when activated with 15 equivalents of $EtAlCl_2$, give poorly active, short-lived, dimerization systems of activities 60 times lower than those recorded for the tungsten(VI) pro-initiators.

Table 3.4 Dimerization of ethylene using well-defined W(IV) imido complexes^{a,b}

Run #	Pro-initiator	Time (min)	TON ^c	Act. ^d	Mol % C ₄ (in liq. prod.)	% 1-C ₄ in C ₄	Mol % C ₆ (in liq. prod.)	% 1-C ₆ in C ₆	% Lin in C ₆	% MP in C ₆
1	W(NDipp)Cl ₂ (PMe ₃) ₃ (61)	13.3	0.3	1.4	97.5	100	1.4	100	100	0.0
2	W(NPh)Cl ₂ (PMe ₃) ₃ (25)	10	0.5	3.2	98.6	98.1	1.4	100	100	0.0
3 ^e	W(NDipp)(H)(Cl)(PMe ₃) ₃ (62)	19.6	3.0	9.3	98.3	95.5	1.7	50.1	61.6	38.4

^a General conditions: 20 μmol W complex and 300 μmol EtAlCl₂; PhCl (solvent) 74 mL; 60 °C; ethylene pressure (40 bar); stirrer speed 1000 rpm; nonane standard (1.000 mL); catalytic runs were performed until consumption of C₂H₄ dropped below 0.2 g min⁻¹ or until the reactor was filled, at which time reaction was quenched by addition of dilute HCl. ^b Only traces of polyethylene were produced (0-0.5% of products fraction). ^c TON is reported in (kg C₂H₄) (mol W)⁻¹ bar⁻¹. ^d Activity is reported in (kg C₂H₄) (mol W)⁻¹ h⁻¹ bar⁻¹ and is based on the total ethylene consumption. PE = polyethylene. ^e Performed at 45 bar of ethylene pressure and 70 °C. No activity was recorded when run DU106 was repeated without EtAlCl₂ or with 10 equivalents of AlCl₃ in the role of the activator.

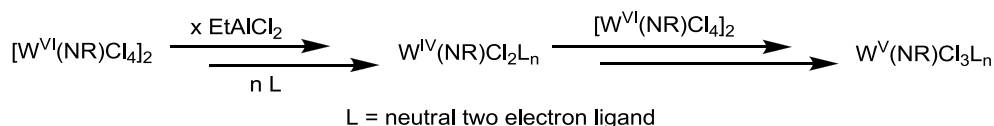
Additionally, since metal hydrides have been considered to be potentially the active intermediates for oligomerization and polymerization catalytic reactions, the tungsten(IV) hydride complex W(NDipp)(H)(Cl)(PMe₃)₃ (**62**) was synthesized (section 2.2.2) and tested in ethylene dimerization.^{23,35,36} Nevertheless, complex **62** was found not to react with ethylene by itself, or after having been treated with 10 equivalents of AlCl₃ as the activator, at 45 bar/70 °C (run 3; Table 3.4).[‡] Even when 15 equivalents of EtAlCl₂ were employed with complex **62** (run 3; Table 3.4), a species of only short-lived and low catalytic activity was obtained (deactivation occurred 19.6 min after addition of EtAlCl₂). Together, these results are in agreement with those reported by Olivier *et al.*, who showed that tungsten(IV) complexes were indeed found to be ethylene dimerization-active, but with very low activities of 0.30 kg C₂H₄ (mol V)⁻¹ h⁻¹ bar⁻¹, when activated with AlCl₃.³⁴ However, Olivier concludes that tungsten(IV) species are responsible for catalysis, which is clearly not the case according to the detailed studies presented herein, since the aforementioned tungsten(IV) complexes achieved much lower activities compared to their tungsten(VI) counterparts. Hence, the study of tungsten(IV) complexes was abandoned.

3.4.1.4 Ethylene dimerization initiated by the [[W(NDipp)Cl₂]₂(μ-Cl)₃][Et₄N] (**60**)/15 EtAlCl₂ system

3.4.1.4.1 Rationale for choosing complex **60** as a tungsten(V) pro-initiator and preliminary catalysis results

In Scheme 3.18 (section 3.4.1.3) a possible route for formation of W(IV) complexes during the activation of the mono(imido) pro-initiators with EtAlCl₂ was outlined, while in Scheme 3.16 it was shown that tungsten(V) complexes can be formed from the redox reaction between a tungsten(IV) and a tungsten(VI) complex. Hence, it is possible that during the activation of the tungsten(VI) mono(imido) complexes with EtAlCl₂, tungsten(V) species could form from the interaction of a tungsten(IV) species with the tungsten(VI) starting complex (Scheme 3.19).

[‡] AlCl₃ acts as a Lewis acid abstracting PMe₃ from the tungsten complex, providing a vacant coordination site for the coordination ethylene. Additionally, AlCl₃ is unable to change the oxidation state of the metal, since it lacks alkyl substituents and hence, if catalysis did occur, then it should result from an unreduced tungsten(IV) species.



Scheme 3.19 Proposed formation of W(V) complexes from the W(VI) starting material and EtAlCl₂

The potential for the formation of tungsten(V) species during activation is further supported by the reaction between W(NDipp)Cl₄(THF) (**59**) and MeAlCl₂, which is described in Scheme 3.15, where the tungsten(V) complex **65** was found to be one of the products. Additionally, the reduction of the pro-initiator by the aluminum-based activator is also thought to occur in various olefin polymerization and dimerization systems previously reported.^{37,38}

Unfortunately, complex **65** could not be tested as an ethylene dimerization pro-initiator due to problems encountered during attempts to isolate it in a sufficiently pure form (caused by **65** being insoluble in non-coordinating solvents). Nevertheless, the structurally similar complex **60** was synthesized and isolated in highly pure form (section 3.2.2). The similarity between **65** and **60** is evident in Figure 3.10, where the structurally identical fragments are highlighted in red. Hence, complex **60** can be regarded as being notionally-derived from complex **65** through cleavage of the central (μ-Cl)₂ bridge by two equivalents of Cl⁻; this is analogous to the formation of [W(NDipp)Cl₅][Et₄N] from [W(NDipp)Cl₄]₂ on addition of two equivalents of Et₄NCl (section 3.4.2.5.1, Scheme 3.20).

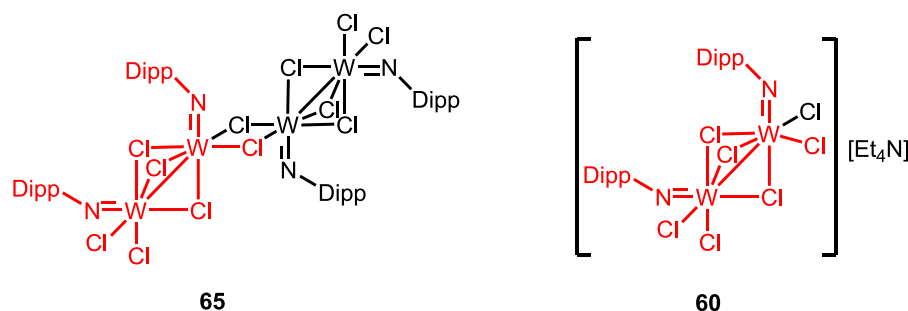


Figure 3.10 Structural similarity between complexes **65** and **60**.

Consequently, complex **60** was tested as a pro-initiator in the catalytic dimerization of ethylene under various conditions, with the results being summarized in Table 3.5. The high catalytic activity of 227.0 kg C₂H₄ (mol W)⁻¹ h⁻¹bar⁻¹ achieved in run 1 (Table 3.5), where **60** was activated with 15 equivalents of EtAlCl₂ under identical conditions to runs included in Table 3.3, along with the similarity of the product selectivities between these runs, further supports the possible formation of tungsten(V) species during the activation of the tungsten(VI) mono(imido) complexes with EtAlCl₂. Moreover, by comparing the activity of run 1 (Table 3.5) with run 4 (Table 3.3) it appears that complex **60** is a better pro-initiator compared to its tungsten(VI) counterpart, **59**. However, it must be borne in mind that complex **60** is an ammonium salt containing half an equivalent of Et₄NCl per tungsten. Taking into account the beneficial effect that addition of chloride salts has on catalysis (see section 2.4.1.7), it is expected that the activity of **60** will be slightly enhanced compared to its neutral form.

Table 3.5 Dimerization of ethylene using complex $[(W(N\text{-Dipp})Cl_2)_2(\mu\text{-Cl})_3][Et_4N]$ (**60**) under various conditions^{a,b}

Run #	Pro-initiator	Time (min)	TON ^g	Act. ^h	Mol % C ₄ (in liq. prod.)	% 1-C ₄ in C ₄	Mol % C ₆ (in liq. prod.)	% 1-C ₆ in C ₆	% Lin in C ₆	% MP in C ₆	% 3Me 1C ₅ in C ₆	% 2Et 1C ₄ in C ₆	wt % C ₈₊ (in liq. prod.)
1 ^c	$[(W(NDipp)Cl_2)_2(\mu\text{-Cl})_3][Et_4N]$ (60)	26.2	99.0	227.0	79.4	98.1	19.9	1.6	3.7	96.3	40.7	54.1	1.4
2 ^d	$[(W(NDipp)Cl_2)_2(\mu\text{-Cl})_3][Et_4N]$ (60)	39.3	98.4	150.1	80.0	97.8	19.0	1.5	3.6	96.4	41.7	52.7	2.2
3 ^e	$[(W(NDipp)Cl_2)_2(\mu\text{-Cl})_3][Et_4N]$ (60)	23.9	100.9	253.5	81.1	98.1	18.2	1.6	3.8	96.2	40.8	53.5	1.4
4 ^f	$[(W(NDipp)Cl_2)_2(\mu\text{-Cl})_3][Et_4N]$ (60)	34.4	9.6	16.6	72.6	96.8	18.3	3.1	6.6	93.4	76.0	11.9	17.0

^a General conditions: PhCl (solvent) 74 mL; 70 °C; ethylene pressure (45 bar); stirrer speed 1000 rpm; nonane standard (1.000 mL); catalytic runs were performed until consumption of C₂H₄ dropped below 0.2 g min⁻¹ or until the reactor was filled, at which time reaction was quenched by addition of dilute HCl. ^b No polyethylene was produced. ^c 10 μmol W complex and 300 μmol EtAlCl₂. ^d 10 μmol W complex and 150 μmol EtAlCl₂. ^e 10 μmol W complex, 300 μmol EtAlCl₂, and 20 μmol Oct₄NCl. ^f 2.5 μmol W complex and 75 μmol EtAlCl₂. ^gTON is reported in (kg C₂H₄) (mol W)⁻¹ bar⁻¹. ^h Activity is reported in (kg C₂H₄) (mol W)⁻¹ h⁻¹ bar⁻¹ and is based on the total ethylene consumption.

3.4.1.4.2 Effect of chloride addition on catalysis with pro-initiator $[(W(N\text{-Dipp})Cl_2)_2(\mu\text{-Cl})_3][Et_4N]$ (**60**)

In section 2.4.1.7 it has been shown that addition of chloride ions to the pre-catalytic mixture before initiation increases the activity of the tungsten bis(imido) ethylene and 1-hexene dimerization systems. Since complex **60** was found to be the best mono(imido) pro-initiator examined herein, the effect of the additional chloride ions on catalysis mediated by **60** was investigated. Addition of two equivalents of Oct₄NCl to complex **60** before activation (run 3; Table 3.5) resulted in a further increase in the catalytic activity, achieving the highest activity observed for the mono(imido) tungsten-based ethylene dimerization systems of 253.5 kg C₂H₄ (mol W)⁻¹ h⁻¹ bar⁻¹. Unfortunately, the exact way that Cl⁻ enhances catalysis remains unclear.

3.4.1.4.3 Activation of $[(W(NDipp)Cl_2)_2(\mu\text{-Cl})_3][Et_4N]$ (**60**) with 7.5 equivalents of EtAlCl₂

In sections 3.4.1.2.3.1 and 3.4.1.4.1 it was suggested that W(V) mono(imido) complexes are formed from a redox reaction between the W(VI) starting material and a W(IV) complex, the latter resulting from reaction of W(VI) with EtAlCl₂ (Scheme 3.19). Together, this implies that a certain amount of EtAlCl₂ added during the activation step may be consumed in order to form a tungsten(V) species. Hence, it is possible that when the pro-initiator is already in a reduced tungsten(V) form, less than 15 equivalent of EtAlCl₂ may be required to initiate catalysis (the reasons for using 15 equivalents of EtAlCl₂ for activation have been covered in section 2.4). Consequently, an ethylene dimerization experiment was conducted in which 7.5 equivalents of EtAlCl₂ per tungsten were used in combination with $[(W(N\text{-Dipp})Cl_2)_2(\mu\text{-Cl})_3][Et_4N]$ (**60**), (run 2; Table 3.5). This resulted in a catalytic activity of 76.9 kg C₂H₄ (mol W)⁻¹ h⁻¹ bar⁻¹, which is disappointingly lower than the activity obtained in (run 1; Table 3.5) where 15 equivalents of EtAlCl₂ were used (227.0 kg C₂H₄ (mol W)⁻¹ h⁻¹ bar⁻¹). Hence, it appears that the use of

15 equivalents of EtAlCl₂ is still necessary for efficient initiation,^{§§} although the exact reason why 15 equivalents of EtAlCl₂ is necessary for effective initiation remains unclear.

3.4.1.4.4 Activation of [[W(NDipp)Cl₂]₂(μ-Cl)₃][Et₄N] (60) at high dilution

In section 2.4.1.4 it was demonstrated that a significant decrease in the activity for the ethylene catalytic dimerization reaction occurs when it is performed at a high dilution (e.g. when 5 μmol of pre-catalyst were used instead of 20 μmol under the same conditions). It has also been suggested that the formation of tungsten(V) species could occur during catalysis (based on the reaction between the tungsten(VI) starting material and a tungsten(IV) species, section 3.4.1.4.1). Hence, a possible explanation for the decrease in catalytic activity upon dilution, is that the reaction between the tungsten(VI) pro-initiator and the tungsten(IV) species (formed from the interaction of the pro-initiator with EtAlCl₂) is slowed down, preventing the formation of the potentially catalytically active tungsten(V) (in section 3.4.1.3 it was shown that tungsten(IV) imidos are poor pro-initiators). In order to further investigate this suggestion, complex **60** was tested in the catalytic dimerization of ethylene using 2.5 μmol of **60** instead of 10 μmol (run 4; Table 3.5). Unfortunately, the low activity obtained in run 4 (Table 3.5) does not provide much insight into the nature of the catalytic reaction, since it does not support nor disprove the suggestion that a tungsten(V) species is formed during activation. Nevertheless, the results presented in this section suggest that the tungsten imido-based ethylene dimerization systems are extremely sensitive to concentration changes.

3.4.2 1-Hexene dimerization studies

In this section studies similar to the 1-hexene dimerization studies performed for the tungsten bis(imido) systems (section 2.4.2) are undertaken with the results from the catalytic dimerization of 1-hexene over the tungsten mono(imido) pro-initiators being presented in Table 3.6. The TONs obtained, 64-133.7 kg C₆H₁₂ (mol W)⁻¹, are comparable to those reported in the literature for other 1-hexene dimerization systems (6.3-434 kg C₆H₁₂ (mol W)⁻¹).³⁹⁻⁴¹ As is the case for the tungsten bis(imido) systems (section 2.4.2), moderate conversions to dimers are obtained (< 38.9%), with TONs of up to 133.7 kg C₆H₁₂ (mol W)⁻¹, something probably due to the isomerization of 1-hexene to internal hexenes (of up to 78.3%). The TONs obtained from these mono(imido) systems also compare relatively well to those obtained using the Sasol *in situ* system, which gives TONs approximately 2 times smaller.²³ In contrast to the TONs, the selectivity of the tungsten mono(imido) 1-hexene dimerization systems is practically identical to the one reported for the tungsten bis(imido) systems examined in section 2.4.1.3.

^{§§} The effect of the aluminum loading on catalysis is examined in detail in section 2.4.2.4 where it is demonstrated that 15 equivalents of EtAlCl₂ are required for the efficient activation of the mono(imido) dimerization systems.

Table 3.6 1-Hexene dimerization using well-defined tungsten mono(imido) pro-initiator complexes with EtAlCl₂ co-initiator^a

Run #	Pro-initiator	TON ^b	Isom. ^c (%)	Conv. of C ₆ ^d (%)	Mol % in total fraction		
					C ₆	C ₁₂	C ₁₈
1	W(NEt)Cl ₄ (THF) (54)	113.2	63.2	32.5	80.7	18.9	0.36
2	[W(NEt)Cl ₄] ₂ (48)	77.6	74.0	22.5	87.4	12.4	0.19
3	W(NPh)Cl ₄ (THF) (56)	96.0	69.0	27.6	84.2	15.5	0.38
4	W(NPh ^F)Cl ₄ (THF) (57)	64.3	77.0	18.5	90.0	9.7	0.34
5	W(NTfp)Cl ₄ (THF) (58)	93.9	69.5	29.0	83.4	15.9	0.73
6	[W(NTfp)Cl ₄] ₂ (52)	63.4	78.3	19.0	89.6	10.2	0.23
7	W(NDipp)Cl ₄ (THF) (59)	130.5	51.3	38.2	76.9	21.8	1.31
8	[W(NDipp)Cl ₄] ₂ (53)	133.7	44.2	38.9	76.5	21.9	1.60

^a General conditions: 0.40 μmol tungsten and 6.0 μmol EtAlCl₂; PhCl (solvent) 190 μL; 60 °C; 1-hexene 250 μL (2.00 mmol); nonane standard (40.0 μL) and *p*-anisaldehyde standard (97.4 μL) added after quenching; reaction time 300 min after which quenching followed by addition of wet d₆-acetone. The selectivity towards dimers was 95-100% for all runs. The branching selectivity of the dimers fraction in each run was found to be: mono branched dimers = 85%-95%, di-branched dimers = 5% - 15%, and linear < 0.5%. ^b Reported in (kg C₆H₁₂) (mol TM)⁻¹ and refers to the amount of 1-hexene converted to oligomers. ^c Defined as the fraction of terminal alkene that is isomerized to internal alkenes at the end of a run. ^d Defined as the mass% of hexenes converted to oligomers at the end of a run and does not include isomerized 1-hexene.

3.4.2.1 Influence of the imido group on the dimerization of 1-hexene using mono(imido) tungsten pro-initiators activated with 15 eq. EtAlCl₂

In Figure 3.11 the TONs resulting from use of the mono(imido) pro-initiators in the dimerization of 1-hexene are presented as a function of the imido substituent. In contrast to the ethylene dimerization experiments, where trends between the activities and the imido groups were clearly apparent (section 3.4.1.1.2), the TONs of the THF-containing pro-initiators in the dimerization of 1-hexene vary in a somewhat arbitrary fashion. For example, the most surprising result is the high TON obtained for complex **54**, which was previously found (section 3.4.1.1.2) to be one of the less active ethylene dimerization pro-initiators compared to complexes **56**, **57**. The surprisingly high activity of **54** compared to **56**, **57** could be due to the low steric bulk of the NEt imido group, which allows easier coordination of the bulkier 1-hexene. Nevertheless, complex **59** remains one of the most active dimerization pro-initiators for both ethylene and 1-hexene. The different activity profile of the mono(imido) pro-initiators in the dimerization of 1-hexene compared to ethylene was encountered also in the tungsten bis(imido) 1-hexene dimerization systems and is attributed to the isomerization of the olefinic substrate (see section 2.4.2.1).

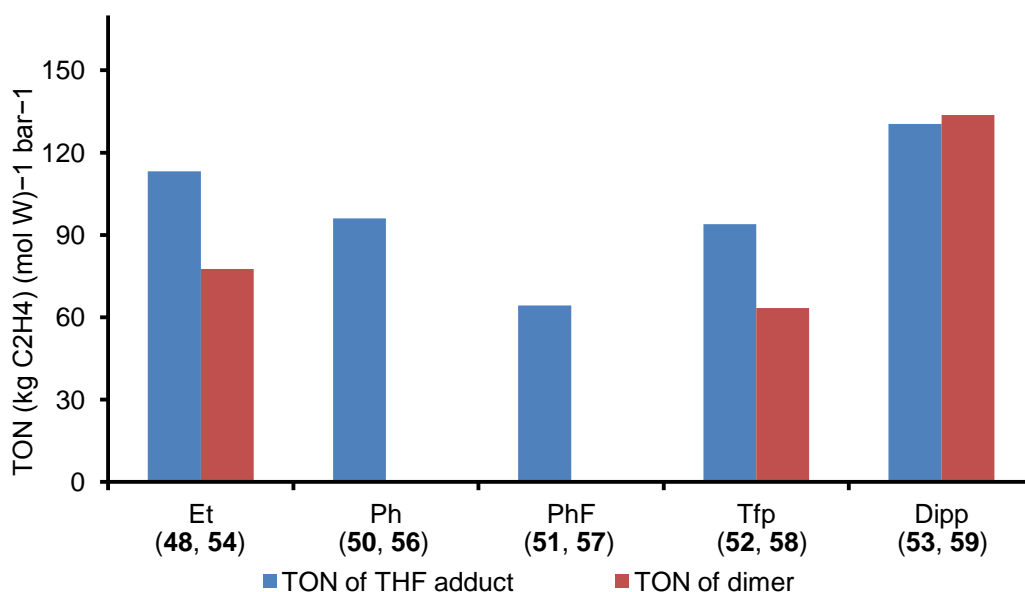


Figure 3.11 Summary of the change in TON as a function of imido ligand substituent of the tungsten mono(imido) pro-initiators in the dimerization of 1-hexene; data taken from Table 3.6

In Figure 3.11 the TONs of the THF-free imido dimers $[W(NR)Cl_4]_2$ (**48**, **50-53**) are also presented and compared to those from their THF-containing counterparts $W(NR)Cl_4(THF)$ (**54**, **56-59**). Interestingly, the TONs from complexes **54** and **58** are greater than those from the corresponding THF-free species, something that suggests that the presence of THF may influence the catalysis. Nevertheless, complexes **53** and **59** exhibit almost identical TONs. These seemingly contradictory observations can be rationalized by taking into account the low solubility of complexes **48** and **52** compared to that of **53**, **54**, **58**, and **59**, something that could attenuate the catalytic performance of **48** and **52**. Attributing the observed differences in TON found between pro-initiators **48** with **54** and **52** with **58** to solubility effects is also in line with the results described in section 3.4.2.2, where the effect of the presence of THF was found to have no influence upon catalysis.

3.4.2.2 Effect of the $EtAlCl_2$ loading and the presence of THF in the dimerization of 1-hexene

In section 2.4 the reasons for using 15 equivalents of $EtAlCl_2$ per tungsten to initiate the catalytic ethylene dimerization reactions were outlined. Consequently, in this section, the effect of $EtAlCl_2$ loading upon catalytic performance parameters for 1-hexene dimerization reactions is examined for pro-initiators **53** and **59**; results are presented in Table 3.7.

Table 3.7 Activation of W(NDipp)Cl₄(THF) (**59**) and [W(NDipp)Cl₄]₂ (**53**) with various EtAlCl₂ activator loadings^a

Run #	Pro-initiator	EtAlCl ₂ loading (eq)	TON ^b	Isom. ^c (%)	Conv. of C ₆ ^d (%)	Mol % in total fraction		
						C ₆	C ₁₂	C ₁₈
1	W(NDipp)Cl ₄ (THF)	2	0.0	0.0	0.0	100	0.0	0.00
2	W(NDipp)Cl ₄ (THF)	3	2.3	91.1	0.6	99.7	0.3	0.00
3	W(NDipp)Cl ₄ (THF)	4	19.7	78.7	5.5	97.2	2.8	0.00
4	W(NDipp)Cl ₄ (THF)	5	58.7	69.7	17.8	90.2	9.8	0.00
5	W(NDipp)Cl ₄ (THF)	6	74.8	64.4	23.1	86.9	13.1	0.00
6	W(NDipp)Cl ₄ (THF)	7	87.8	59.7	27.4	84.1	15.9	0.00
7	W(NDipp)Cl ₄ (THF)	8	84.4	65.3	27.2	84.3	15.7	0.00
8	W(NDipp)Cl ₄ (THF)	9	59.2	71.6	20.2	88.8	11.2	0.00
9	W(NDipp)Cl ₄ (THF)	15	130.5	51.3	38.2	76.9	21.8	1.31
10	W(NDipp)Cl ₄ (THF)	30	93.4	67.1	31.5	81.3	18.7	0.00
11	[W(NDipp)Cl ₄] ₂	2	0.0	29.4	0.0	100	0.0	0.00
12	[W(NDipp)Cl ₄] ₂	3	3.2	86.9	0.9	99.6	0.4	0.00
13	[W(NDipp)Cl ₄] ₂	4	25.5	76.2	7.7	96.0	4.0	0.00
14	[W(NDipp)Cl ₄] ₂	5	56.2	68.4	18.1	90.1	9.9	0.00
15	[W(NDipp)Cl ₄] ₂	6	68.9	63.3	23.4	86.7	13.3	0.00
16	[W(NDipp)Cl ₄] ₂	7	76.7	60.8	27.1	84.3	15.7	0.00
17	[W(NDipp)Cl ₄] ₂	8	83.2	61.9	29.4	82.7	17.3	0.00
18	[W(NDipp)Cl ₄] ₂	9	77.7	69.0	26.8	84.6	15.4	0.00
19	[W(NDipp)Cl ₄] ₂	15	133.7	44.2	38.9	76.5	21.9	1.60
20	[W(NDipp)Cl ₄] ₂	30	95.4	56.2	30.1	82.3	17.7	0.00

^a General conditions: 0.40 μmol tungsten; PhCl (solvent) 190 μL; 60 °C; 1-hexene 250 μL (2.00 mmol); nonane standard (40.0 μL) and *p*-anisaldehyde standard (97.4 μL) added after quenching; reaction time 300 min after which quenching followed by addition of wet d₆-acetone. The selectivity towards dimers was 95-100% for all runs. The branching selectivity of the dimers fraction in each run was found to be: mono branched dimers = 85%-95%, di-branched dimers = 5% - 15%, and linear < 0.5%. ^b TON is reported in (kg C₆H₁₂) (mol TM)⁻¹ and refers to the amount 1-hexene converted to oligomers. ^c Defined as the fraction of terminal alkene that is isomerized to internal alkenes at the end of a run. ^d Defined as the mass% of hexenes converted to oligomers at the end of a run and does not include isomerized 1-hexene.

From the data presented in Table 3.7 it is clear that the selectivities towards the dimers fraction are excellent for most runs. Notably, only when 15 equivalents of EtAlCl₂ are used, do small amounts of trimers form, something possibly due to the higher catalytic activity obtained under such conditions.

In Figure 3.12 the TONs and % substrate isomerization for W(NDipp)Cl₄(THF) (**59**) and [W(NDipp)Cl₄]₂ (**53**) are compared against the number of equivalents of EtAlCl₂ used for activation. Interestingly, the TONs of each system have two local maximum values: one between 7.0 and 8.0 equivalents of EtAlCl₂ and a second at 15 equivalents, something that confirms the use of 15 equivalents of EtAlCl₂ as an appropriate amount of activator for the initiation of the catalytic reactions. In contrast, the extent of substrate isomerization follows an opposite pattern, with two local minima: one between 7.0 and 8.0 equivalents and a larger one at 15 equivalents of EtAlCl₂. This inverse relationship between the TONs for dimerization and the degree of isomerization demonstrates the expected competition between the two processes, namely: the more active the dimerization initiator, the less isomerization is observed and *vice versa*. It must also be noted that these tungsten-based mono(imido) pro-initiators are converted to efficient 1-hexene isomerization systems (up to 91.1% isomerization) when three equivalents of EtAlCl₂ are used for activation (runs 2 and 12; Table 3.7).

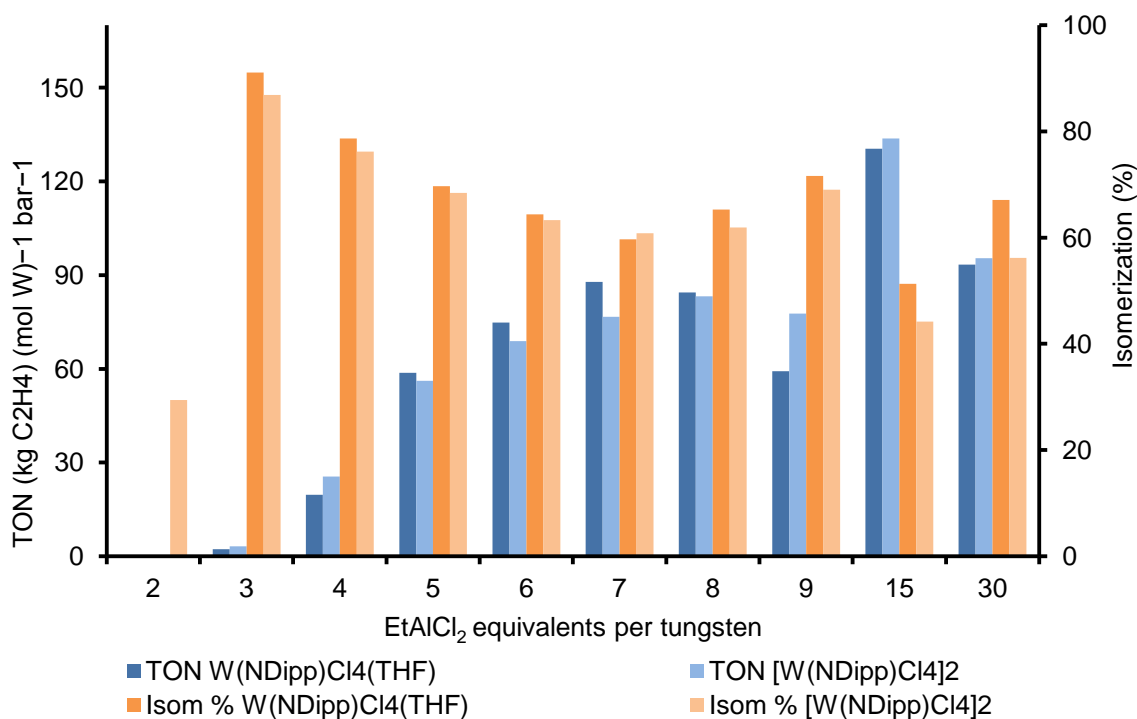


Figure 3.12 TONs and extent of substrate isomerization from $W(NDipp)Cl_4(THF)$ (**59**) and $[W(NDipp)Cl_4]_2$ (**53**) in the dimerization of 1-hexene versus the number of equivalents of $EtAlCl_2$ per tungsten used for activation; data taken from Table 3.7

Additionally, it has been argued (see section 3.4.2.1) that the presence of THF (and similarly DME) does not influence significantly catalysis, since these Lewis bases will be scavenged by the excess aluminum reagent used during activation (see section 6.1.2). From the data presented in Figure 3.12, it is clear that the TONs and extent of isomerization are similar for both $W(NDipp)Cl_4(THF)$ (**59**) and $[W(NDipp)Cl_4]_2$ (**53**) pro-initiators when activated with various amounts of $EtAlCl_2$, something that confirms that the THF bound to the pro-initiator does not have a significant impact on the dimerization reaction.

3.4.2.3 Activation of $W(NDipp)Cl_4(THF)$ and $[W(NDipp)Cl_4]_2$ with various alkyl and hydride sources

In section 2.4.2.5 pro-initiator $W(NDipp)_2Cl_2(DME)$ (**27**) was activated with a variety of alkylating reagents and hydride sources for the dimerization of 1-hexene. In this section, the same study is conducted with pro-initiators $W(NDipp)Cl_4(THF)$ (**59**) and $[W(NDipp)Cl_4]_2$ (**53**) with the results being summarized in Table 3.8. From Table 3.8 it is clear that pro-initiators **53** and **59** behave in the same way as pro-initiator $W(NDipp)_2Cl_2(DME)$ (**27**) (section 2.4.2.5), with only $EtAlCl_2$ and $MeAlCl_2$ successfully initiating catalysis.

Table 3.8 Effect of the activator on the dimerization of 1-hexene over W(NDipp)Cl₄(THF) (**59**) and [W(NDipp)Cl₄]₂ (**53**)^a

Run #	Pro-initiator	Activator (eq)	Additive (eq)	TON ^b	Isom. ^c (%)	Conv. of C ₆ ^d (%)	Mol % in total fraction		
							C ₆	C ₁₂	C ₁₈
1	W(NDipp)Cl ₄ (THF)	EtAlCl ₂ (15)	None	130.5	51.3	38.2	76.9	21.8	1.31
2	W(NDipp)Cl ₄ (THF)	MeAlCl ₂ (15)	None	17.2	74.4	5.8	97.2	2.40	0.40
3	W(NDipp)Cl ₄ (THF)	Me ₃ Al (15)	None	0.0	0.0	0.0	100	0.00	0.00
4	W(NDipp)Cl ₄ (THF)	Me ₃ Al (15)	Oct ₄ NCl (4)	0.0	0.0	0.0	100	0.00	0.00
5	W(NDipp)Cl ₄ (THF)	Et ₃ Al (15)	None	0.0	0.0	0.0	100	0.00	0.00
6	W(NDipp)Cl ₄ (THF)	Et ₃ Al (15)	Oct ₄ NCl (4)	0.0	0.0	0.0	100	0.00	0.00
7	W(NDipp)Cl ₄ (THF)	RedAl (15)	None	0.0	0.0	0.0	100	0.00	0.00
8	W(NDipp)Cl ₄ (THF)	RedAl (2)	None	0.0	0.0	0.0	100	0.00	0.00
9	W(NDipp)Cl ₄ (THF)	KH (2)	None	0.0	0.0	0.0	100	0.00	0.00
10	[W(NDipp)Cl ₄] ₂	KH (2)	None	0.0	0.0	0.0	100	0.00	0.00
11	W(NDipp)Cl ₄ (THF)	MeLi (2)	None	0.0	0.0	0.0	100	0.00	0.00
12	[W(NDipp)Cl ₄] ₂	MeLi (2)	None	0.0	0.0	0.0	100	0.00	0.00
13	W(NDipp)Cl ₄ (THF)	BuLi (2)	None	0.0	0.0	0.0	100	0.00	0.00
14	[W(NDipp)Cl ₄] ₂	BuLi (2)	None	0.0	0.0	0.0	100	0.00	0.00

^a General conditions: 0.40 μmol tungsten; PhCl (solvent) 190 μL; 60 °C; 1-hexene 250 μL (2.00 mmol); nonane standard (40.0 μL) and *p*-anisaldehyde standard (97.4 μL) added after quenching; reaction time 300 min after which quenching followed by addition of wet d₆-acetone. The selectivity towards dimers was 95-100% for all runs. The branching selectivity of the dimers fraction in each run was found to be: mono branched dimers = 85%-95%, di-branched dimers = 5% - 15%, and linear < 0.5%. ^b TON is reported in (kg C₆H₁₂) (mol TM)⁻¹ and refers to the amount 1-hexene converted to oligomers. ^c Defined as the fraction of terminal alkene that is isomerized to internal alkenes at the end of a run. ^d Defined as the mass% of hexenes converted to oligomers at the end of a run and does not include isomerized 1-hexene.

3.4.2.4 Additive effects on the catalytic dimerization of 1-hexene mediated by W(NDipp)Cl₄(THF)/15 EtAlCl₂ and [W(NDipp)Cl₄]₂/15 EtAlCl₂ systems

In section 2.4.1.7 the beneficial effect of additives such as Et₃N, Et₃NHCl, Oct₄NCl, pyridine, DABCO, and 2,6-lutidine for the tungsten bis(imido)-mediated catalytic dimerization of 1-hexene has been outlined. In this section, a similar study on the impact of such additives on tungsten mono(imido)-mediated 1-hexene dimerization systems is probed; the results are summarized in Table 2.13. The amount of additive used in each experiment was chosen based on the results from section 2.4.1.7.

From the TONs obtained (Table 3.9), the use of additives improves the activity of the tungsten mono(imido)-mediated 1-hexene dimerization in each case, with the exception of run 10 in Table 3.9. Overall, this contrasts to the observations made for the tungsten bis(imido)-based systems where the inclusion of the same additives generally lowered the 1-hexene dimerization activities obtained. This attenuation of the catalytic activity when additives were used with the tungsten bis(imido) pro-initiators was attributed to the use of a too high a additive:W ratio (see section 2.4.2.6). Unfortunately, the reasons why the tungsten mono(imido) complexes can tolerate a higher additive:W ratio compared to their tungsten bis(imido) counterparts remain unclear. Additionally, comparing the composition of the products from runs 1 and 2 (Table 3.9), where no additives were employed, with those from the other runs presented in Table 3.9, it is clear that the use of additives increases the selectivity of the 1-hexene dimerization system by producing less than half as much of the trimers compared to the additive-free systems. The same increase in the selectivity towards the dimers fraction was also observed when additives were employed in conjunction with the tungsten bis(imido) complexes (section 2.4.2.6).

Table 3.9 Additive effects on the dimerization of 1-hexene using W(NDipp)Cl₄(THF) (**59**) and [W(NDipp)Cl₄]₂ (**53**) pro-initiator complexes with EtAlCl₂ co-catalyst^a

Run #	Pro-initiator	Additive (eq)	TON ^b	Isom. ^c (%)	Conv. of C ₆ ^d (%)	Mol % in total fraction		
						C ₆	C ₁₂	C ₁₈
1	W(NDipp)Cl ₄ (THF)	none	130.5	51.3	38.2	76.9	21.8	1.31
2	[W(NDipp)Cl ₄] ₂	none	133.7	44.2	38.9	76.5	21.9	1.60
3	W(NDipp)Cl ₄ (THF)	Oct ₄ NCl (4)	179.1	37.8	51.0	65.9	33.7	0.40
4	[W(NDipp)Cl ₄] ₂	Oct ₄ NCl (8)	182.6	40.2	51.7	65.2	34.6	0.23
5	[W(NDipp)Cl ₄] ₂	Oct ₄ NCl (2)	179.0	42.2	51.6	65.6	33.3	1.11
6	W(NDipp)Cl ₄ (THF)	Et ₃ NHCl (2)	182.4	43.5	49.2	67.6	31.7	0.66
7	[W(NDipp)Cl ₄] ₂	Et ₃ NHCl (4)	165.5	47.4	46.8	69.6	29.7	0.67
8	W(NDipp)Cl ₄ (THF)	Et ₃ N (4)	197.4	35.2	53.3	63.8	35.8	0.44
9	[W(NDipp)Cl ₄] ₂	Et ₃ N (8)	151.0	48.5	44.3	71.7	27.8	0.50
10	W(NDipp)Cl ₄ (THF)	Pyridine (4)	118.8	52.6	35.7	78.4	21.2	0.39
11	[W(NDipp)Cl ₄] ₂	Pyridine (8)	206.4	33.1	56.0	61.4	37.9	0.72
12	W(NDipp)Cl ₄ (THF)	2,6-Lutidine (4)	191.9	33.5	53.7	63.3	36.4	0.25
13	[W(NDipp)Cl ₄] ₂	2,6-Lutidine (8)	193.1	36.9	54.6	62.5	37.2	0.34
14	W(NDipp)Cl ₄ (THF)	DABCO (4)	135.0	41.3	40.9	74.5	25.0	0.49
15	[W(NDipp)Cl ₄] ₂	DABCO (8)	173.4	38.0	51.6	65.2	34.8	0.00

^a General conditions: 0.40 μmol tungsten and 6.0 μmol EtAlCl₂; PhCl (solvent) 190 μL; 60 °C; 1-hexene 250 μL (2.00 mmol); nonane standard (40.0 μL) and *p*-anisaldehyde standard (97.4 μL) added after quenching; reaction time 300 min after which quenching followed by addition of wet d₆-acetone. The selectivity towards dimers was 95-100% for all runs. The branching selectivity of the dimers fraction in each run was found to be: mono branched dimers = 85%-95%, di-branched dimers = 5% - 15%, and linear < 0.5%. ^b TON is reported in (kg C₆H₁₂) (mol TM)⁻¹ and refers to the amount 1-hexene converted to oligomers. ^c Defined as the fraction of terminal alkene that is isomerized to internal alkenes at the end of a run. ^d Defined as the mass% of hexenes converted to oligomers at the end of a run and does not include isomerized 1-hexene.

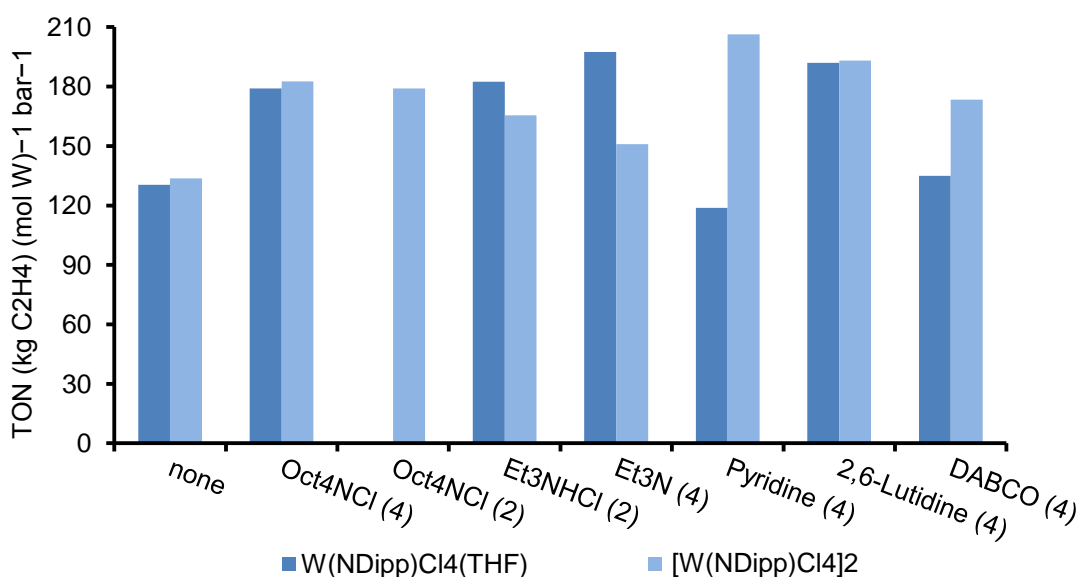


Figure 3.13 TONs achieved using W(NDipp)Cl₄(THF) (**59**) and [W(NDipp)Cl₄]₂ (**53**) in the dimerization of 1-hexene as a function of additive (the amount of additive used in equivalents per tungsten is given in brackets); data taken from Table 3.9

The TONs achieved when additives were used for the dimerization of 1-hexene using W(NDipp)Cl₄(THF) (**59**) and [W(NDipp)Cl₄]₂ (**53**) as the pro-initiator (Figure 3.13) vary with no obvious trends. Nevertheless, some general remarks can be made. Here, generally all of the additives lead to an increase in the TONs of the systems by 2.7-57%. Attenuation of catalysis was observed only in the case where **59** was combined with pyridine; the reasons behind this behavior remain unclear.

Additionally, as was the case for the tungsten bis(imido) ethylene dimerization systems (section 2.4.2.6), the 1-hexene dimerization reaction is not very sensitive to the amount of Oct₄NCl added per tungsten, since the same TON is achieved with two and four equivalents of the tertiary ammonium salt.

When amines are used as additives the situation is more complex, with the TONs of the 1-hexene dimerization systems being influenced by the specific nature of the amine and the presence of pro-initiator-bound THF. Only in the case where 2,6-lutidine was used as the additive are the TONs recorded for both **59** and **53** similar (runs 12 and 13 Table 3.9). When Et₃N was employed, an increase in the TON by 50% was observed for **59**, but only 15% for **53**. In contrast, when pyridine was used the **53** pro-initiator became 57% more active, while its THF adduct lost 10% of its activity. Lastly, DABCO, albeit being broadly similar to Et₃N in its structure and N-coordination ability, influences the dimerization of 1-hexene in a way comparable to pyridine by increasing the TON of **53**, while leaving the TON of **59** practically unchanged.

In conclusion, the way that additives (such as tertiary ammonium chlorides and amines) influence the tungsten mono(imido)-mediated dimerization of 1-hexene is complicated, making it difficult to determine the specific reasons behind the observed changes, based on the data available so far. Consequently, in order to gain a greater insight into the potential role of these additives, selected reactions between tungsten mono(imido) complexes and ammonium chlorides and amines were examined and are discussed in the following section.

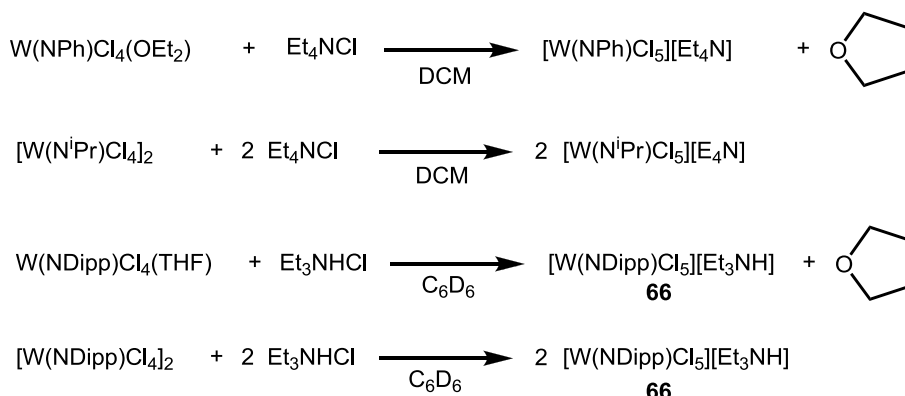
3.4.2.5 Exploring the interactions of mono(imido) tungsten complexes with Et₃N and ammonium chlorides

The catalysis results presented in section 2.4.2.6 demonstrate the beneficial effect of the addition of Et₃N, Et₃NHCl and Oct₄NCl on the tungsten bis(imido)-initiated dimerization of ethylene and 1-hexene. Hence, it was of interest to explore selected, discrete reactions between both W(NDipp)Cl₄(THF) (**59**) and [W(NDipp)Cl₄]₂ with Et₃NHCl and Et₃N to explore the origin(s) of this/these effect(s).

3.4.2.5.1 Reaction of W(NDipp)Cl₄(THF) and [W(NDipp)Cl₄]₂ with Et₃NHCl

Previously, it has been reported that the reactions of W(NPh)Cl₄(OEt₂) and [W(NⁱPr)Cl₄]₂ (**49**) with Et₄NCl produce the complexes [W(NPh)Cl₅][Et₄N]⁴² and [W(NⁱPr)Cl₅][Et₄N]⁴³ respectively (Scheme 3.20). Consequently, it has been assumed that identical types of reaction will also take place with Oct₄NCl. However, in this present study, the complexes W(NDipp)Cl₄(THF) (**59**) and [W(NDipp)Cl₄]₂ (**53**) were reacted with Et₃NHCl (a compound that is generated during the formation of the Sasol *in situ* catalyst system) in order to assess the influence of the weakly acidic proton of the ammonium salt upon any reactions (Scheme 3.20). From the data summarized in Scheme 3.20, it is evident that the presence of the Et₃NHCl proton has no influence on the course of the reaction, since generation of [W(NDipp)Cl₅][Et₃NH] (**66**) was observed in both cases, based on NMR spectroscopic and X-ray crystallographic analyses. Together, these results indicate that the formation of the pentachloro

tungstate anions is likely to occur in each case, and that it is these species that act as the pro-initiators in reactions with the various alkyl aluminium reagents necessary for catalysis.

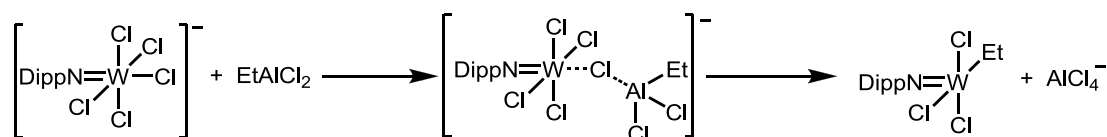


Scheme 3.20 Reactions of $\text{W(NPh)Cl}_4(\text{OEt}_2)$,⁴² $[\text{W(N}^i\text{Pr)Cl}_4]_2$ ⁴³ with Et_4NCl and $\text{W(NDipp)Cl}_4(\text{THF})$ (**59**), $[\text{W(NDipp)Cl}_4]_2$ (**53**) with Et_3NHCl

3.4.2.5.2 Chloride effect on the catalytic activity of the tungsten mono(imido) systems

According to the work outlined in section 3.4.2.5.1, when ammonium chloride salts are used as additives in the catalytic dimerization of 1-hexene, formation of $[\text{W(NR)Cl}_5][\text{Et}_3\text{NH}]$ or $[\text{W(NR)Cl}_5][\text{Et}_4\text{N}]$ (R = general group) will occur before activation with EtAlCl_2 . Taking into account the catalysis results presented in Table 3.9 (especially runs 1 and 5), it appears that formation of such ionic complexes increases the catalytic activity of the tungsten mono(imido)/15 EtAlCl_2 systems.

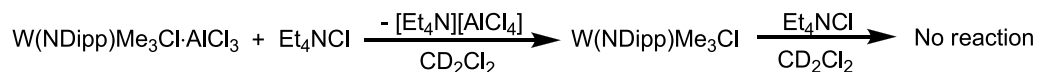
A possible rationale for this increased catalytic activity observed when an additional chloride source is present prior to activation, is that the excess chloride facilitates transmetallation between the EtAlCl_2 activator and the pro-initiator by acting as a bridge between the two molecules as illustrated in Scheme 3.21 (the affinity of EtAlCl_2 for chloride has been well established in section 6.1.3, where it was reacted with Et_3NHCl to produce $[\text{Et}_3\text{NH}][\text{EtAlCl}_3]$).



Scheme 3.21 Chloride anions facilitate transmetallation by acting as a bridge between the pro-initiator and the activator enhancing in that way the activity of tungsten(mono) imido olefin dimerization systems

Another possible explanation for the observed increase in catalytic activity when chloride-containing additives are used, is that the chloride anions can remove bound AlCl_3 from the alkylated tungsten complexes after activation. For example, when $\text{W(NDipp)Me}_3\text{Cl} \cdot \text{AlCl}_3$ is reacted with Et_4NCl in CD_2Cl_2 the W-Cl-bound AlCl_3 is removed forming AlCl_4^- , the discrete tetrachloroaluminate anion being readily observed in the ^{27}Al NMR spectra of the reaction products (Scheme 3.22). Further addition of Et_4NCl has no effect on the NMR spectra of the final mixture, implying that no additional reaction occurs. Abstraction of AlCl_3 from the active catalyst can potentially reduce the steric hindrance about the W

centre facilitating the binding of the olefinic substrate. Nevertheless, a definitive explanation for the reasons underlying the observation that the ionic complexes such as $[W(NR)Cl_5]^-$ ($R =$ general group) are more active, compared to their THF analogues, in the dimerization of 1-hexene (Table 3.9, runs 1 and 5) remains unavailable.



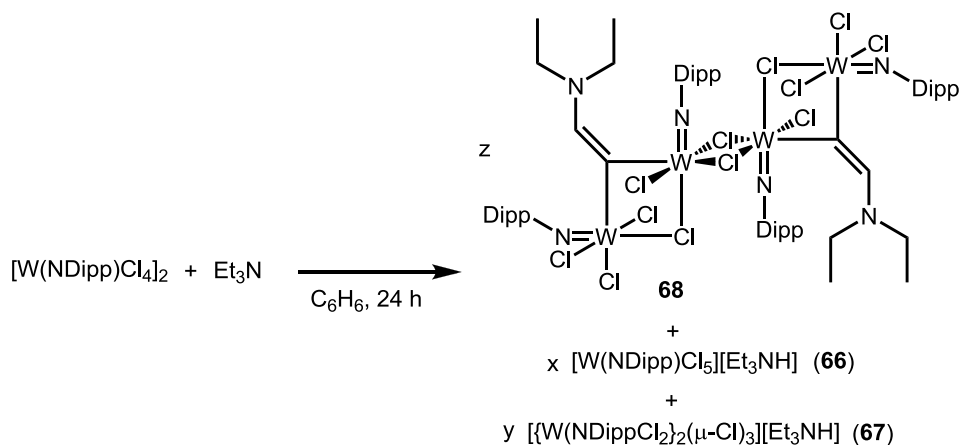
Scheme 3.22 Reaction between $W(NDipp)Me_3Cl \cdot AlCl_3$ with Et_4NCl

3.4.2.5.3 Reaction of $W(NDipp)Cl_4(THF)$ (**59**), $[W(NDipp)Cl_4]_2$ (**53**) with Et_3N

The beneficial effect of Et_3N on the activity of the tungsten bis(imido) olefin dimerization systems has been discussed in sections 2.4.2.6. Following this work, the reaction between tungsten mono(imido) complexes and Et_3N is examined herein. In contrast to there being no reaction between $W(NDipp)_2Cl_2(DME)$ (**27**) and Et_3N , when **53** was treated with one equivalent of Et_3N in C_6D_6 an instant color change of the solution occurred, along with formation of dark crystals which were isolated *via* filtration.

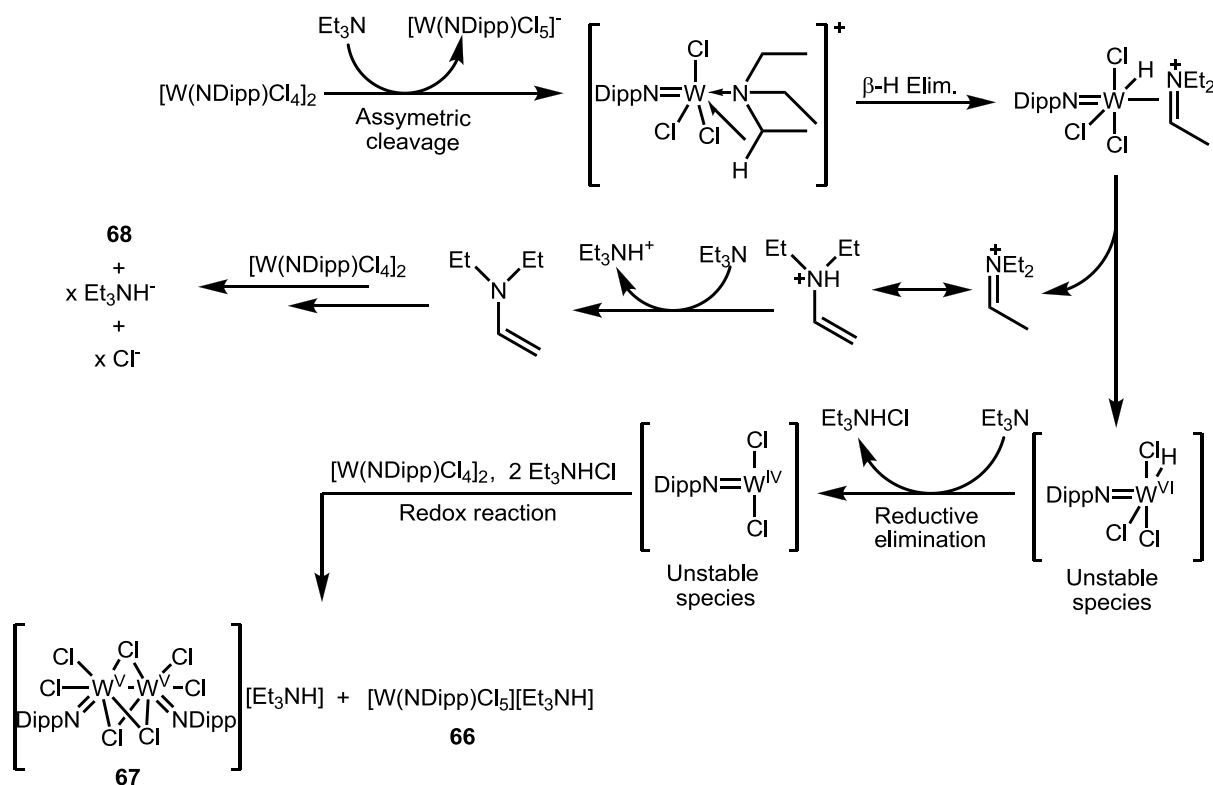
Firstly, a 1H NMR spectroscopic analysis of the resulting brown solution revealed the presence of two un-assignable Dipp environments. Following recrystallization, two types of crystals were isolated and found to be $[W(NDipp)Cl_5][Et_3NH]$ (**66**) and $[(W(NDipp)Cl_2)_2(\mu-Cl)_3][Et_3NH]$ (**67**) according to X-ray crystallographic analyses.

Secondly, the dark crystals isolated from the same reaction between $[W(NDipp)Cl_4]_2$ and Et_3N were insoluble to non-coordinating solvents, which prevented their NMR spectroscopic characterization. Nevertheless, they were partially characterized using crystallographic techniques (the collected diffraction data were of poor quality) as **68**, Scheme 3.23. The study of the structure of complex **68**, albeit interesting, is outside the scope of this work. However, its formation demonstrates the complexity and unpredictability of the reactions of tungsten imido complexes even before the addition of 15 equivalents of $EtAlCl_2$, which is expected to further increase the complexity of the system.



Scheme 3.23 Reaction of $[W(NDipp)Cl_4]_2$ with Et_3N

The reaction between $[W(NDipp)Cl_4]_2$ (**53**) and Et_3N is summarized in Scheme 3.23. Interestingly the formation of Et_3NH^+ suggests that a mechanism by which H^+ is generated must be operative. Additionally, reduction of tungsten(VI) to tungsten(V) occurs from the reaction between (**53**) and Et_3N (formation of **67**), which can be attributed to resulting from the reaction between tungsten(IV) and tungsten(VI) species (see section 3.4.1.2.3.1). Taking into account that tungsten(VI) can be reduced to tungsten(IV) *via* a β -hydride elimination reaction followed by reductive elimination of HCl, and that the only species available for β -hydride elimination in the reaction mixture is Et_3N , the mechanism presented in Scheme 3.24 is proposed for the formation of **66** and **67**.



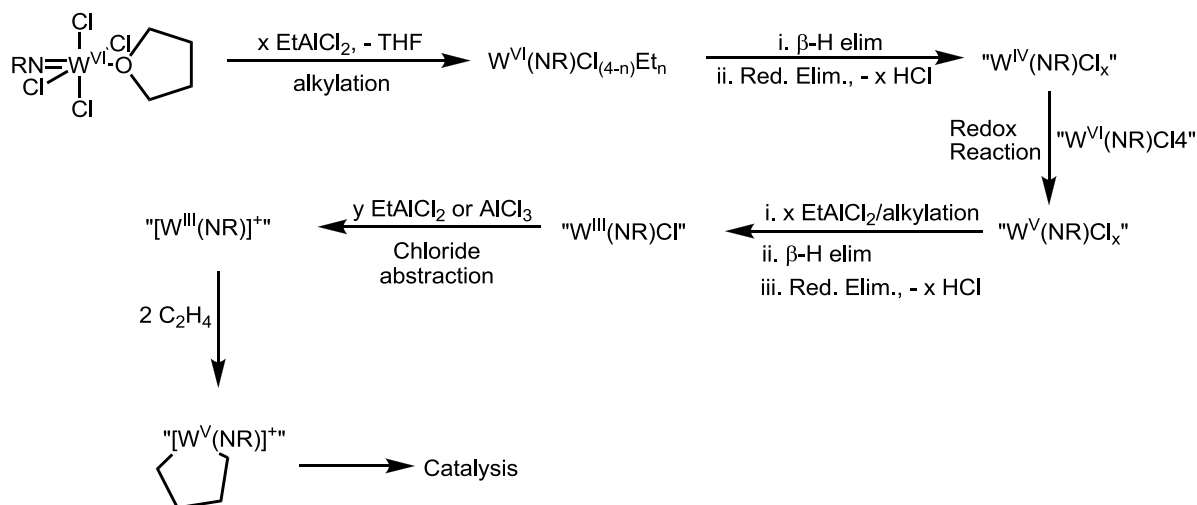
Scheme 3.24 Suggested mechanism for the reaction between $[W(NDipp)Cl_4]_2$ and Et_3N

From the above discussion, it appears that the interaction between Et_3N and the mono(imido) tungsten complexes can result in the generation of chloride anions along with formation of tungsten(V) species. Both of these processes have been proven to be beneficial for catalysis (see sections 2.4.2.6 and 3.4.1.4). Hence, it is suggested that the beneficial effect of Et_3N on dimerization could be attributed to its ability to convert $W(NDipp)Cl_4(THF)$ (**59**) to the more active $W(NDipp)Cl_5^-$ and $[[W(NDipp)Cl_2]_2(\mu-Cl)_3]^-$ anions before initiation.

3.5 A proposed mechanism for the mono(imido) tungsten-based dimerization systems

Based on the results presented in this chapter for the reactivity surrounding tungsten mono(imido)-based olefin dimerization pro-initiator systems, it is suggested that a tungsten(V) metallacycle is responsible for catalysis. This conclusion is based on the composition of the trimers product fraction

following dimerization of ethylene (section 3.4.1.1.5). In Scheme 3.25 a proposed mechanism is presented.



Scheme 3.25 Proposed mechanism for the dimerization of olefins mediated by tungsten mono(imido) / EtAlCl_2 -based systems

A step-wise addition mechanism, where a tungsten hydride or a tungsten alkyl is responsible for catalysis, is deemed less likely to be involved, since strong alkylating reagents and hydride sources did not initiate catalysis (section 2.4.2.5 and 3.4.2.3). Another factor that supports a metallacyclic mechanism is that EtAlCl_2 and MeAlCl_2 , which are strong Lewis acids with a strong affinity for chloride ions, but are weak alkylating agents (section 6.1.3), were the only efficient activators for the catalytic reaction. In contrast, the powerful alkylating aluminum reagents, Et_3Al and Me_3Al , were unable to initiate catalysis, suggesting that it is the strong Lewis acidity of the activator that is absolutely necessary for successful initiation. The observation that the Lewis acidity (which can also be expressed as an affinity towards chloride anions) is such an essential property of the activator, suggests that a chloride abstraction step occurs at some point during activation, something that creates vacant coordination sites available for binding the olefinic substrate towards formation of a metallacycle (Scheme 3.25).

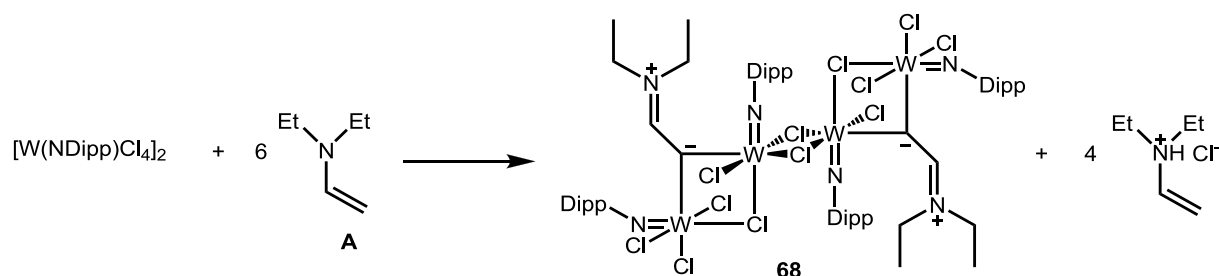
Formation of a tungsten(V) species during activation is proposed since complex **67** was found to be the most active pro-initiator examined herein (section 3.4.1.4), and since the formation of tungsten(V) complexes has been detected in the reaction products resulting from reaction of the tungsten(VI) imido complexes with the aluminum activators (section 3.4.1.2.3.1). Additionally, formation of tungsten(V) potentially explains the ability of EtAlCl_2 to activate the pro-initiators more efficiently than MeAlCl_2 , since EtAlCl_2 bearing a β -hydride-containing ethyl group will be able to reduce the tungsten(VI) to tungsten(IV) (Scheme 3.25). The resulting tungsten(V) complex can be further reduced to a tungsten(III) species *via* initial alkylation with EtAlCl_2 , followed by β -hydride elimination, and reductive elimination of HCl. Formation of tungsten(III) is necessary since a two electron oxidation is required to subsequently allow for the formation of a metallacyclopentane species (Scheme 3.25). This second reduction from tungsten(V) to tungsten(III) requires additional EtAlCl_2 and is thus in line with the

observed need for an excess of EtAlCl_2 (15 equivalents have been commonly used) to efficiently activate the tungsten mono(imido) pro-initiators.

3.6 Future investigations

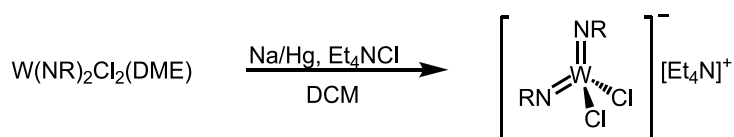
In section 3.4.1.1.2.2 the effect of the steric bulk of the imido ligand on the ethylene dimerization activity of the tungsten mono(imido) complexes was investigated by comparing the activities obtained from complexes $[\text{W}(\text{NPh})\text{Cl}_4]_2$ (**56**) and $[\text{W}(\text{NDipp})\text{Cl}_4]_2$ (**59**). However, in order to obtain a clearer view of the effect of the imido ligand's steric bulk on the catalytic activity, complex $\text{W}(\text{NMes})\text{Cl}_4(\text{THF})$, being in between complexes **56** and **59** from an imido steric bulk point of view (see section 4.4.2.3), should be synthesized and tested in the dimerization of ethylene.

The reaction of $\text{W}(\text{NDipp})\text{Cl}_4(\text{THF})$ or $[\text{W}(\text{NDipp})\text{Cl}_4]_2$ with Et_3N was described in section 3.4.2.5.3 and resulted in the isolation of complexes **66-68**. It was suggested that this reaction proceeds *via* a β -hydride elimination reaction from the Et_3N , forming amine **A** (Scheme 3.26), which further reacts with $[\text{W}(\text{NDipp})\text{Cl}_4]_2$ towards formation of **68** (Scheme 3.24). Complex **68** was partially characterized *via* an X-ray crystallographic study, revealing a complex molecular structure. Hence, in order to further examine the above suggestion, and to potentially fully characterize complex **68**, the reaction of $[\text{W}(\text{NDipp})\text{Cl}_4]_2$ with the amine **A** is proposed as describe in Scheme 3.26.



Scheme 3.26 Suggested reaction between $[\text{W}(\text{NDipp})\text{Cl}_4]_2$ and the amine **A** towards formation of **68**

From the high catalytic activities and selectivities towards 1-butene obtained using the tungsten(V) pro-initiators, it is clear that future work on the tungsten imido systems should concentrate in tungsten(V) systems. Specifically, complex $[\text{W}(\text{NTfp})\text{Cl}_2(\mu\text{-Cl})_3][\text{Et}_4\text{N}]$ should be synthesized and tested in catalysis, since in section 3.4.1.1.2 it was found that the Tfp imido substituent led to catalytic systems with high activity. Along the same lines, tungsten(V) bis(imido) complexes should be synthesized, as proposed in Scheme 3.27, and tested in the dimerization of ethylene and 1-hexene under various conditions.



Scheme 3.27 Suggested reaction for the formation of a $\text{W}(\text{V})$ bis(imido) complex

In addition, as suggested in section 3.5, the possibility of the formation and subsequent reaction of a tungsten(III) mono(imido) complex cannot be excluded. Hence, the synthesis of tungsten(III) imidos of the type $W(NR)Cl(L)_n$ (L = general two electron donor ligand) should be attempted, with the resulting complexes being tested as pro-initiators in the dimerization of ethylene and 1-hexene at various $EtAlCl_2$ loadings. Unfortunately, tungsten(III) imidos have never been reported before. Hence, their synthesis from tungsten(V) or tungsten(IV) complexes will not be trivial, possibly requiring the study of various different reducing agents under various conditions, until successful reduction can be achieved.

Lastly, reactions of the newly-synthesized tungsten(V) and tungsten(III) complexes with aluminum reagents should be conducted in a similar fashion to the reactions described in section 3.4.1.2, in order to reveal more information about the nature of the catalysts involved in these tungsten imido-based dimerization reactions. However it must be born in mind that tungsten(V) and tungsten(III) complexes will be paramagnetic as monomers reducing the diagnostic value of any attempted NMR spectroscopic studies.

3.7 Chapter Summary

In this chapter the tungsten(VI) mono(imido) complexes $[W(NR)Cl_4]_2$ (R = Et (**48**), i Pr (**49**), Ph (**50**), Ph^F (**51**), Tfp (**52**), Dipp (**53**)) and $W(NR)Cl_4(THF)$ (R = Et (**54**), i Pr (**55**), Ph (**56**), Ph^F (**57**), Tfp (**58**), Dipp (**59**)) were synthesized and characterized using NMR spectroscopic and X-ray crystallographic techniques. Complexes **48-53** were found similar in structure judging from their structural parameters although they bear considerably different imido groups. Hence, it appears that the group on the imido ligand does not influence significantly the structural parameters of **48-53**. Following the synthesis of tungsten(VI) mono(imido) complexes, the tungsten(V) complex $[W(NDipp)Cl_2]_2(\mu-Cl)_3[Et_4N]$ (**60**) and the tungsten(IV) complexes $W(NR)Cl_2(PMe_3)_3$ (R = Dipp (**61**) and Ph (**25**)) and $W(NDipp)Cl(H)(PMe_3)_3$ (**62**) were synthesized and characterized.

Complexes **54-59** were tested in the dimerization of ethylene at 40 bar of ethylene pressure and 60 °C using 15 equivalents of $EtAlCl_2$ as the activator resulting in the formation of reasonably active ethylene dimerization systems with activities of up to $61.9 \text{ kg C}_2\text{H}_4 (\text{mol W})^{-1} \text{ h}^{-1} \text{ bar}^{-1}$ (with pro-initiator **59**). The activity of the systems **54-59**/15 $EtAlCl_2$ strongly depends on the type of the imido substituent on the pro-initiator with bulky or electron withdrawing imidos favoring catalysis. When the reaction temperature and pressure was raised to 45 bar and 70 °C the catalytic activity of complexes **54-59** further increased achieving a new maximum of $167.8 \text{ kg C}_2\text{H}_4 (\text{mol W})^{-1} \text{ h}^{-1} \text{ bar}^{-1}$ (pro-initiator **59**). The product selectivity of the catalytic reaction was good both at 40 bar/60 °C and 45 bar/70 °C with more than 75% of the products consisting of 1-butene in each run. Additionally, based on the selectivity of the trimers fraction it was suggested that a metallocycle mechanism is more likely to be in operation for the tungsten mono(imido) mediated dimerization of ethylene although a step-wise addition mechanism cannot be completely excluded.

In order to gain further mechanistic insight on the activation process of the tungsten mono(imido) pro-initiators, reactions of selected tungsten mono(imido) complexes with $R_nAlCl_{(3-n)}$ reagents were

performed. Hence, well-defined tungsten mono(imido) alkyl complexes were isolated suggesting that alkylation of the pro-initiator occurs at the first stages of the alkylation process. However, the most important finding from the reactions between tungsten mono(imido) complexes and $R_nAlCl_{(3-n)}$ reagents was the formation of tungsten(V) complexes which suggests that a change in the oxidation state of the pro-initiator is possible after activation. For this reason, the tungsten(IV) complexes $W(NR)Cl_2(PMe_3)_3$ ($R = Dipp$ and Ph) and $W(NDipp)Cl(H)(PMe_3)_3$ (**62**) were tested as pro-initiators in the catalytic dimerization of ethylene exhibiting very low dimerization activities (up to $9.3 \text{ kg C}_2\text{H}_4 (\text{mol W})^{-1} \text{ h}^{-1} \text{ bar}^{-1}$). In contrast the W(V) complex $[[W(NDipp)Cl_2]_2(\mu-Cl)_3][Et_4N]$ (**60**) was found to be the best mono(imido) ethylene dimerization pro-initiator at 45 bar/70 °C with an activity of $227 \text{ kg C}_2\text{H}_4 (\text{mol W})^{-1} \text{ h}^{-1} \text{ bar}^{-1}$ suggesting that formation of tungsten(V) complexes is likely during the activation of the tungsten mono(imido) complexes with $EtAlCl_2$.

Following the ethylene dimerization experiments, the dimerization of 1-hexene using pro-initiators **54**, **56-59**, **48**, **52**, **53** was explored. Initiation of **56-59**, **48**, **52**, **53** with $EtAlCl_2$ led to 1-hexene dimerization systems with TONs of up to $133.7 \text{ kg C}_6\text{H}_{12} (\text{mol W})^{-1}$ (pro-initiator **53**) and selectivities towards the dimers fraction within the oligomerization products of over 95%. However, a completely different catalytic profile was obtained for the dimerization of 1-hexene compared to when ethylene was used without any trends between the TONs and the imido groups being observed. These differences in the dimerization profile between 1-hexene and ethylene were attributed to the ability of the tungsten mono(imido) based systems to isomerize higher α -olefins to internal ones. Additionally, it was found that a tungsten: $EtAlCl_2$ ratio of 15 is close to optimal not only for the dimerization of ethylene but also for the dimerization of 1-hexene.

Lastly, following the work on the tungsten bis(imido) complexes the effect of additives such as Et_3N , Et_3NHCl , Oct_4NCl , pyridine, DABCO, and 2,6-lutidine on catalysis was examined. It was found that the use of additives increases the TONs of the tungsten mono(imido) 1-hexene dimerization systems with TONs of up to $206.4 \text{ kg C}_6\text{H}_{12} (\text{mol TM})^{-1}$ (pro-initiator **53**/8 pyridine) being achieved. In order to shed some light on the way that these additives influence catalysis reactions between complexes **53** and **59** with Et_3NHCl and Et_3N were performed. The outcome of these reactions suggests that addition of Et_3NHCl or Et_3N to the catalytic mixture *prior* to activation either assists the transmetallation of the tungsten centre by the activator or leads to formation of the more active tungsten(V) species increasing in that way the catalytic activity of the tungsten mono(imido) systems.

3.8 References

- (1) Leny, J. P.; Osborn, J. A. *Organometallics* **1991**, *10*, 1546.
- (2) Ashcroft, B. R.; Clark, G. R.; Nielson, A. J.; Rickard, C. E. F. *Polyhedron* **1986**, *5*, 2081.
- (3) Bradley, D. C.; Errington, R. J.; Hursthouse, M. B.; Short, R. L. *Journal of the Chemical Society-Dalton Transactions* **1990**, 1043.
- (4) Bradley, D. C.; Hodge, S. R.; Runnacles, J. D.; Hughes, M.; Mason, J.; Richards, R. L. *Journal of the Chemical Society-Dalton Transactions* **1992**, 1663.
- (5) Bradley, D. C.; Hursthouse, M. B.; Malik, K. M. A.; Nielson, A. J.; Short, R. L. *Journal of the Chemical Society-Dalton Transactions* **1983**, 2651.
- (6) Schrock, R. R.; Depue, R. T.; Feldman, J.; Yap, K. B.; Yang, D. C.; Davis, W. M.; Park, L.; Dimare, M.; Schofield, M.; Anhaus, J.; Walborsky, E.; Evitt, E.; Kruger, C.; Betz, P. *Organometallics* **1990**, *9*, 2262.
- (7) Clark, G. R.; Nielson, A. J.; Rickard, C. E. F. *Journal of the Chemical Society, Dalton Transactions* **1995**, 1907.
- (8) Peterson, E.; Khalimon, A. Y.; Simionescu, R.; Kuzmina, L. G.; Howard, J. A. K.; Nikonov, G. I. *Journal of the American Chemical Society* **2008**, *131*, 908.
- (9) Clegg, W.; Errington, R. J. *Acta Crystallographica Section C-Crystal Structure Communications* **1987**, *43*, 2223.
- (10) Bruno, I. J.; Cole, J. C.; Edgington, P. R.; Kessler, M.; Macrae, C. F.; McCabe, P.; Pearson, J.; Taylor, R. *Acta Crystallographica Section B-Structural Science* **2002**, *58*, 389.
- (11) Hursthouse, M. B.; Howes, A. J.; Bradley, D. C.; Runnacles, J. D. *Private communication* **2004**, REFCODE FOBUY.
- (12) Marushima, Y.; Uchiumi, Y.; Ogu, K.; Hori, A. *Acta Crystallographica Section C* **2010**, *66*, o406.
- (13) Ajellal, N.; Kuhn, M. C. A.; Boff, A. D. G.; Hörner, M.; Thomas, C. M.; Carpentier, J.-F.; Casagrande, O. L. *Organometallics* **2006**, *25*, 1213.
- (14) Chandran, D.; Lee, K. M.; Chang, H. C.; Song, G. Y.; Lee, J. E.; Suh, H.; Kim, I. *Journal of Organometallic Chemistry* **2012**, *718*, 8.
- (15) Song, S. J.; Zhao, W. Z.; Wang, L.; Redshaw, C.; Wang, F. S.; Sun, W. H. *Journal of Organometallic Chemistry* **2011**, *696*, 3029.
- (16) Onishi, Y.; Katao, S.; Fujiki, M.; Nomura, K. *Organometallics* **2008**, *27*, 2590.
- (17) Kunrath, F. A.; de Souza, R. F.; Casagrande, O. L.; Brooks, N. R.; Young, V. G. *Organometallics* **2003**, *22*, 4739.
- (18) Zhang, S.; Nomura, K. *Journal of the American Chemical Society* **2010**, *132*, 4960.
- (19) Nomura, K.; Igarashi, A.; Katao, S.; Zhang, W. J.; Sun, W. H. *Inorganic Chemistry* **2013**, *52*, 2607.
- (20) Igarashi, A.; Zhang, S.; Nomura, K. *Organometallics* **2012**, *31*, 3575.
- (21) Ulbrich, A.; Campedelli, R. R.; Milani, J. L. S.; dos Santos, J. H. Z.; Casagrande, O. D. *Applied Catalysis a-General* **2013**, *453*, 280.
- (22) Speight, J. G. *Lange's Handbook of Chemistry*; 16 ed.; McGraw-Hill, 2005.
- (23) Hanton, M. J.; Daubney, L.; Lebl, T.; Polas, S.; Smith, D. M.; Willemse, A. *Dalton Transactions* **2010**, 39, 7025.
- (24) Small, B. L.; Marcucci, A. J. *Organometallics* **2001**, *20*, 5738.
- (25) Wright, W. R. H., PhD Thesis, Durham University, 2009.
- (26) Wright, W. R. H.; Batsanov, A. S.; Howard, J. A. K.; Tooze, R. P.; Hanton, M. J.; Dyer, P. W. *Dalton Transactions* **2010**, 39, 7038.
- (27) Albahily, K.; Gambarotta, S.; Duchateau, R. *Organometallics* **2011**, *30*, 4655.
- (28) Jabri, A.; Temple, C.; Crewdson, P.; Gambarotta, S.; Korobkov, I.; Duchateau, R. *Journal of the American Chemical Society* **2006**, *128*, 9238.
- (29) Holmes, S. J.; Schrock, R. R.; Churchill, M. R.; Wasserman, H. J. *Organometallics* **1984**, *3*, 476.
- (30) Orpen, A. G.; Brammer, L.; Allen, F. H.; Kennard, O.; Watson, D. G.; Taylor, R. *Journal of the Chemical Society, Dalton Transactions* **1989**, *0*, S1.
- (31) Gálvez-Ruiz, Juan C.; Guadarrama-Pérez, C.; Nöth, H.; Flores-Parra, A. *European Journal of Inorganic Chemistry* **2004**, *2004*, 601.
- (32) Chamberlin, R. L. M.; Rosenfeld, D. C.; Wolczanski, P. T.; Lobkovsky, E. B. *Organometallics* **2002**, *21*, 2724.
- (33) Fulmer, G. R.; Miller, A. J. M.; Sherden, N. H.; Gottlieb, H. E.; Nudelman, A.; Stoltz, B. M.; Bercaw, J. E.; Goldberg, K. I. *Organometallics* **2010**, *29*, 2176.
- (34) Olivier, H.; Laurent-Grot, P. *Journal of Molecular Catalysis A: Chemical* **1999**, *148*, 43.
- (35) Ittel, S. D.; Johnson, L. K.; Brookhart, M. *Chemical Reviews* **2000**, *100*, 1169.

- (36) Suttill, J. A.; McGuinness, D. S. *Organometallics* **2012**, *31*, 7004.
- (37) You, Y. J.; Girolami, G. S. *Organometallics* **2008**, *27*, 3172.
- (38) Novaro, O.; Chow, S.; Magnouat, P. *Journal of Catalysis* **1976**, *41*, 91.
- (39) Jones, J. R.; Symes, T. J. *Journal of the Chemical Society C: Organic* **1971**, 1124.
- (40) daRosa, R. G.; deSouza, M. O.; deSouza, R. F. *Journal of Molecular Catalysis a-Chemical* **1997**, *120*, 55.
- (41) Majoumo-Mbe, F.; Lonnecke, P.; Volkis, V.; Sharma, M.; Eisen, M. S.; Hey-Hawkins, E. *Journal of Organometallic Chemistry* **2008**, *693*, 2603.
- (42) Pedersen, S. F.; Schrock, R. R. *Journal of the American Chemical Society* **1982**, *104*, 7483.
- (43) Ashcroft, B. R.; Clark, G. R.; Nielson, A. J.; Rickard, C. E. F. *Polyhedron* **1986**, *5*, 2081.

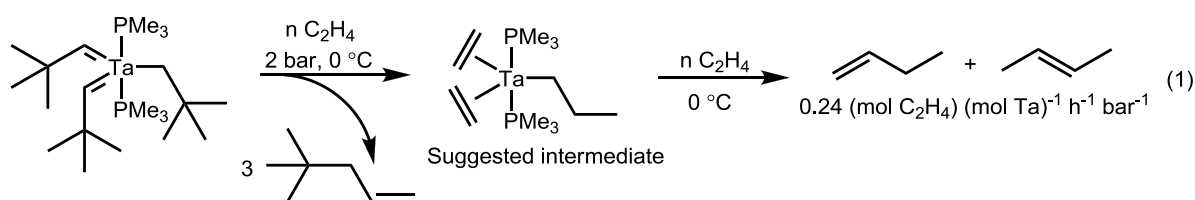
4 Exploring ethylene polymerization and ethylene and 1-hexene dimerization with Ta and Nb imido complexes

4.1 Introduction – Niobium- and tantalum-based olefin oligomerization and polymerization

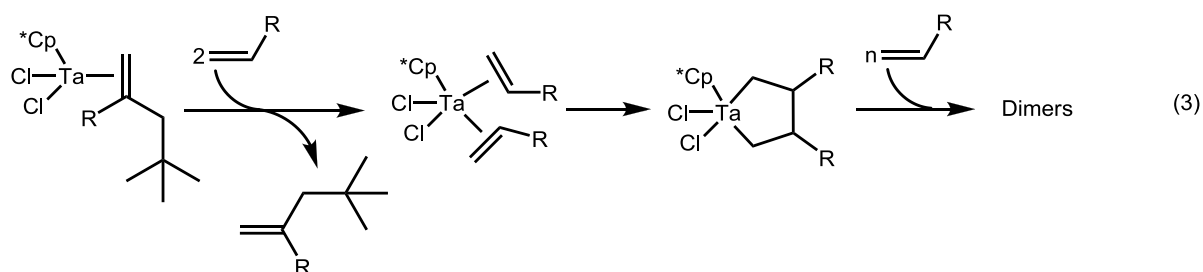
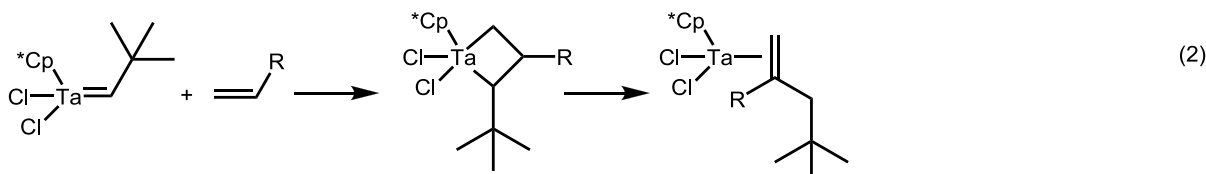
4.1.1 Ethylene dimerization

Tantalum- and niobium-mediated ethylene oligomerization/polymerization chemistry has only comparatively recently attracted significant attention.^{1,2} Indeed, to date, there are no reports of niobium-based ethylene or 1-hexene dimerization systems, while a search of the literature revealed only three reports of tantalum-based ethylene dimerization systems (Scheme 4.1). The first of these Ta-focussed reports by Schrock *et al.* in 1979, demonstrated that $\text{Ta}(\text{CHCMe}_3)_2(\text{PMe}_3)_2(\text{CH}_2\text{CMe}_3)$ reacts with ethylene to afford a species active for the catalytic dimerization of ethylene (activity of $0.0067 \text{ kg C}_2\text{H}_4 (\text{mol Ta})^{-1} \text{ h}^{-1} \text{ bar}^{-1}$ at $0 \text{ }^\circ\text{C}$), Scheme 4.1 (eq. 1).³ Later, the same group reported that $\text{Cp}^*\text{Ta}(\text{CHCMe}_3)\text{Cl}_2$ reacts with α -olefins to afford complexes of the general formula $\text{Cp}^*\text{TaCl}_2(\text{olefin})$ via a tantalacyclobutane species. Addition of excess olefin to $\text{Cp}^*\text{TaCl}_2(\text{olefin})$ lead to formation of a tantalacyclopentane species that, after rearrangement, produced dimers (Scheme 4.1, eq. 2 and 3).³⁻⁶ Subsequently, Chang *et al.* reported the use of polymer-supported CpTaCl_4 , in combination with neopentyl lithium, which forms a system that dimerizes ethylene with an activity of $0.09 \text{ kg C}_2\text{H}_4 (\text{mol Ta})^{-1} \text{ h}^{-1} \text{ bar}^{-1}$ at $100 \text{ }^\circ\text{C}$ and 5.5 bar ethylene pressure (Scheme 4.1, eq. 4).⁷ The final and most recent report of a tantalum-based ethylene dimerization system was described by Taoufik *et al.*,⁸ in which a silica-supported tantalum complex of formula $(\equiv\text{SiO})_2\text{TaH}(\text{PMe}_3)$ was employed and found to mediate the catalytic formation of butenes and heavier oligomers with an overall activity of $0.26 \text{ kg C}_2\text{H}_4 (\text{mol Ta})^{-1} \text{ h}^{-1} \text{ bar}^{-1}$ at $90 \text{ }^\circ\text{C}$ (Scheme 4.1, eq. 5).

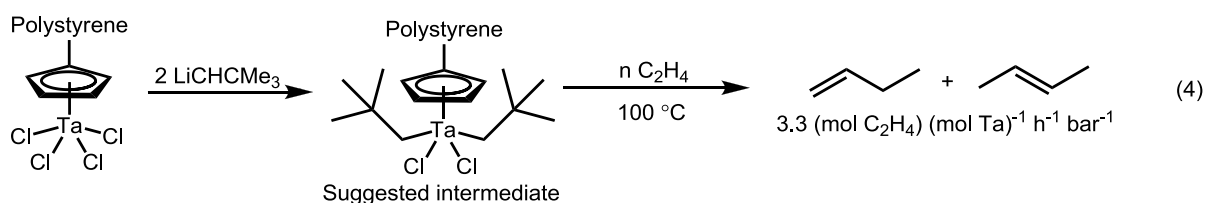
• Schrock *et al*, 1979:



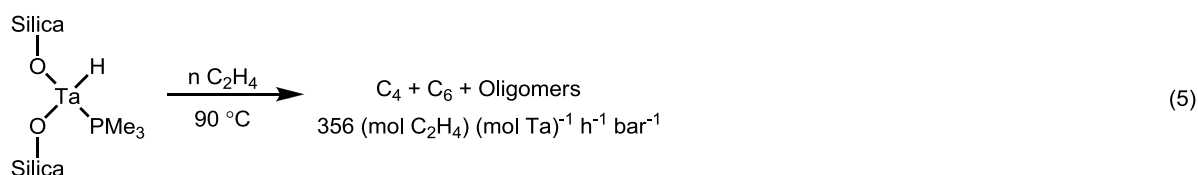
• Schrock *et al*, 1980:



• Chang *et al*, 1985:



• Taoufik *et al*, 2001:



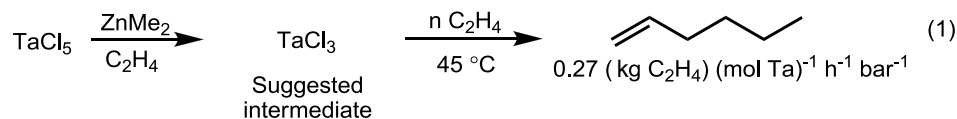
Scheme 4.1 Tantalum-mediated ethylene dimerization systems reported up to 2013

4.1.2 Ethylene trimerization

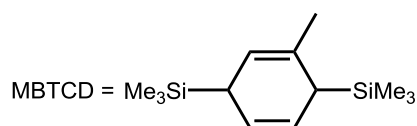
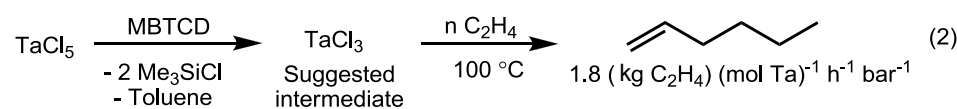
In the related area of ethylene trimerization, again very few tantalum-based systems have been reported (Scheme 4.2). For example, it has been shown that TaCl_5 in combination with one equivalent of ZnMe_2 gave a system that was capable of trimerizing ethylene with an activity of $0.27 \text{ kg C}_2\text{H}_4 (\text{mol Ta})^{-1} \text{ h}^{-1} \text{ bar}^{-1}$ at $45 \text{ }^\circ\text{C}$ and 48 bar of ethylene pressure (Scheme 4.2, eq. 1).⁹ In 2009 a similar, but somewhat more active, TaCl_5 -derived system was reported, which achieved activities of up to $1.8 \text{ kg C}_2\text{H}_4 (\text{mol Ta})^{-1} \text{ h}^{-1} \text{ bar}^{-1}$ at $100 \text{ }^\circ\text{C}$ and 48 bar of ethylene pressure (Scheme 4.2, eq. 2).¹⁰ The most

recent development in this area is the synthesis of the silica-supported reagent, $(\equiv\text{SiO})\text{TaCl}_2(\text{Me})_2$, which achieves activities reaching $0.21 \text{ kg C}_2\text{H}_4 (\text{mol Ta})^{-1} \text{ h}^{-1} \text{ bar}^{-1}$ at $100 \text{ }^\circ\text{C}$ and 50 bar of ethylene pressure (Scheme 4.2, eq. 3).¹¹ Notably, it is proposed that each of the above ethylene dimerization and trimerization systems is thought to operate *via* formation of a Ta metallacyclic species.¹²

- Andes *et al*, 2001:



- Arteaga-Muller *et al*, 2009:



- Basset *et al*, 2012:

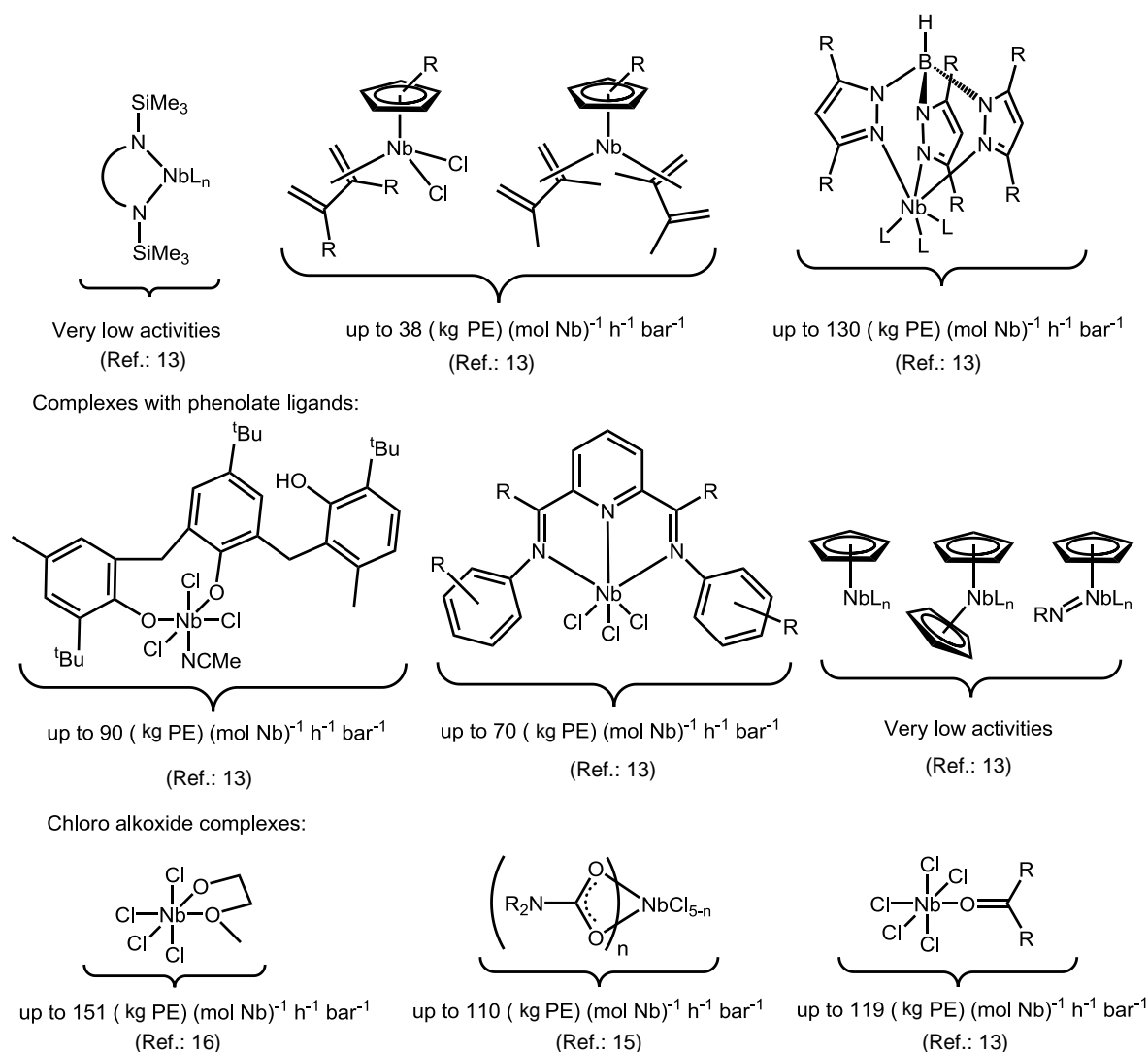


Scheme 4.2 Tantalum-mediated ethylene trimerization systems reported up to 2013

4.1.3 Ethylene polymerization

4.1.3.1 Niobium-based ethylene polymerization

In contrast to niobium- and tantalum-mediated ethylene dimerization and trimerization, the related polymerization reaction is more common. A recent review by Galletti *et al.* summarizes many of the Nb-based ethylene polymerization systems up to 2009.¹³ An overview of the various ligands employed, along with the highest activity towards polymerization achieved with each type of system, is presented in Scheme 4.3.¹³⁻¹⁶



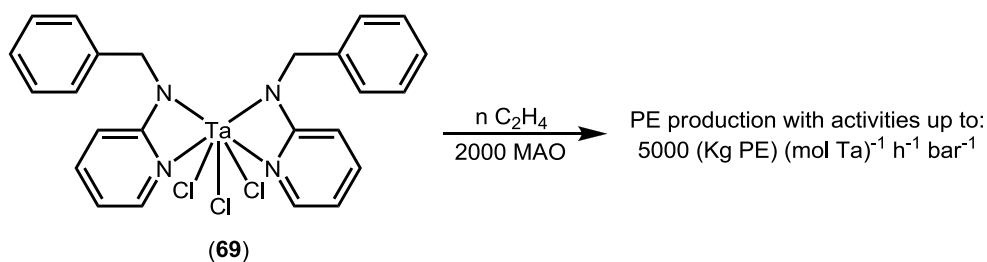
Scheme 4.3 Overview of ligands employed in Nb-mediated ethylene polymerization (R = general organic group or H; L = general ligand).

4.1.3.2 Tantalum-based ethylene polymerization catalysis

In the tantalum-based catalytic ethylene polymerization field, Schrock *et al.* again provided the first report. They demonstrated that the complex $\text{Ta}(\text{CHCMe}_3)(\text{H})(\text{PMe}_3)_3\text{I}_2$ is able to generate small amounts of ethylene oligomers (C_6 to C_{12}) when treated with two equivalents of ethylene at 0 °C in toluene. Mechanistic studies of this system showed that the active species was the complex $\text{Ta}[\text{CH}_2(\text{CH}_2\text{CH}_2)_n\text{CH}_3](\text{H})(\text{PMe}_3)_3\text{I}_2$.¹⁷

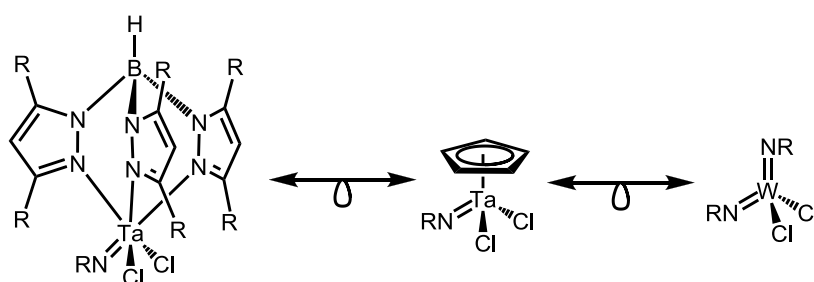
Following the above reports from Schrock, the corresponding tantalum derivatives of the cyclopentadienyl niobium butadiene and niobium phenolate complexes (Scheme 4.3) were also examined in ethylene polymerization. It was noted that the activities of the CpTa-containing complexes were lower than those of the Nb systems (up to 5.93 kg PE (mol Ta)⁻¹ h⁻¹ bar⁻¹),¹⁸ while similar activities were found for the Ta and Nb phenolate systems (up to 46 kg PE (mol Ta)⁻¹ h⁻¹ bar⁻¹).¹⁹ The simplest tantalum-based ethylene polymerization system to have been reported is based on TaCl_5 activated with one equivalent of EtAlCl_2 . This $\text{TaCl}_5/\text{EtAlCl}_2$ system produced hyper-branched liquid

polyethylene with an activity of $0.04 \text{ kg PE (mol Ta)}^{-1} \text{ h}^{-1} \text{ bar}^{-1}$.²⁰ However, the highest catalytic activities for the Nb- and Ta-mediated polymerization of ethylene were obtained by complexes such as **69** (Scheme 4.4) that, in combination with methylaluminoxane (MAO), exhibit activities of up to $5000 \text{ kg PE (mol Ta)}^{-1} \text{ h}^{-1} \text{ bar}^{-1}$.²¹ Lastly, the most recent tantalum-based ethylene polymerization system was reported by Basset *et al.* who used a well-defined silica-grafted catalyst of the type $(\equiv\text{SiO})_3\text{Ta}$, which exhibited ethylene polymerization activities of up to $1.7 \text{ kg PE (mol Ta)}^{-1} \text{ h}^{-1} \text{ bar}^{-1}$. One of the most interesting results from this latter study was that production of polyethylene proceeded *via* a metallacyclic species rather than through the much more common ethylene polymerization pathway involving a metal-hydride intermediate.²²



Scheme 4.4 Polymerization of ethylene using the highly active system **69**/MAO

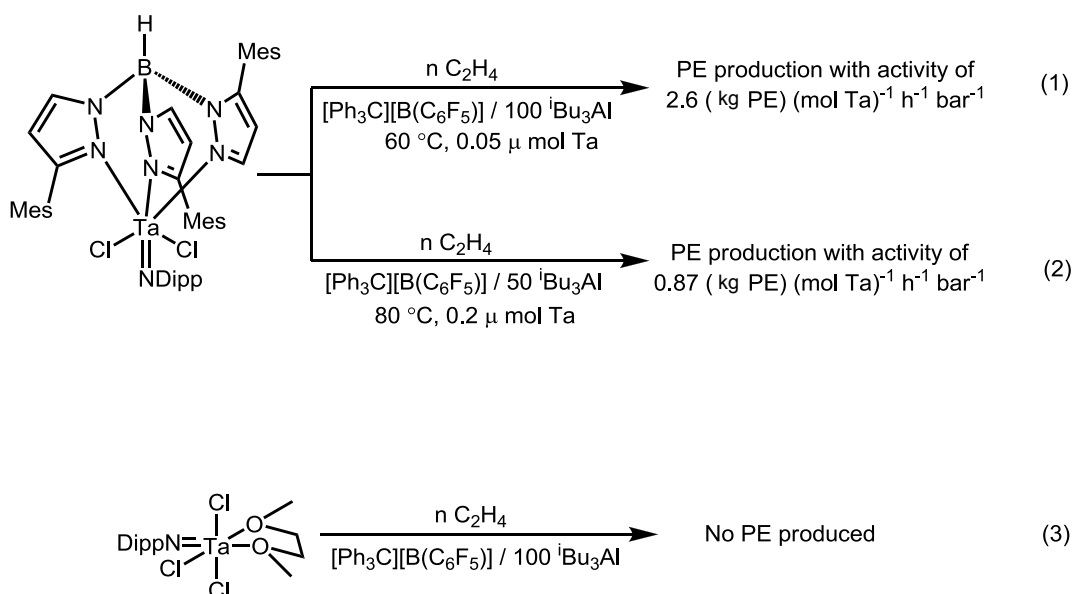
Once the potential of Cp tantalum-based ethylene polymerization systems had been established, examination of the Tp (*tris*(pyrazolyl)borate) analogues was inevitably undertaken, since there is a well-established isolobal and isoelectronic relationship between the Cp and Tp ligand frameworks (Scheme 4.5).^{23,24} Both the monoanionic Cp and Tp ligands adopt facial, *pseudo*-tridentate coordination modes at transition metal centres, each providing five valence electrons to the system's overall electron count. This coordination similarity has led to the use of Tp ligands as Cp mimics, with the *tris*(pyrazolyl)borates having the added benefit of the ready incorporation of substituents R (Scheme 4.5) in the 5-position of the pyrazolyl units, which upon coordination of the Tp moiety, lie close to the metal centre, providing additional steric constraints.



Scheme 4.5 *pseudo-isolobal relationships between Tp tantalum imido, Cp tantalum imido, and tungsten bis(imido) complexes*

The potentially greater steric demands imposed by Tp over Cp ligands has been explored with a view to using the bulkier ligands to favor polymerization over oligomerization. For example, the Tp-imido complexes of tantalum have been tested in the polymerization of ethylene by Michiue *et al.* (Scheme 4.6; eq. 1 and 2),²⁵ who concluded that the nature of the substituents on the Tp ligand are indeed crucial in determining the system's performance in ethylene polymerization. For example, the combination of a

bulky Mes-substituted Tp ligand with the bulky Dipp imido unit (Scheme 4.6; eq. 1 and 2) gave a system that was more active than the system in which a much less sterically encumbered methyl-substituted Tp ligand was employed.²⁵ Notably, the mono(imido) complex, Ta(NDipp)Cl₃(DME), was found to be polymerization-inactive under the same reaction conditions (Scheme 4.6, eq. 3), something presumed to arise due to the lack of a bulky Tp scaffold. However, again, it must be stressed that for these Tp-substituted systems even slight changes in the reaction conditions or the activation protocol employed can have a dramatic effect on the activity of the catalytic system (Scheme 4.6, eq. 1 and 2).²⁵

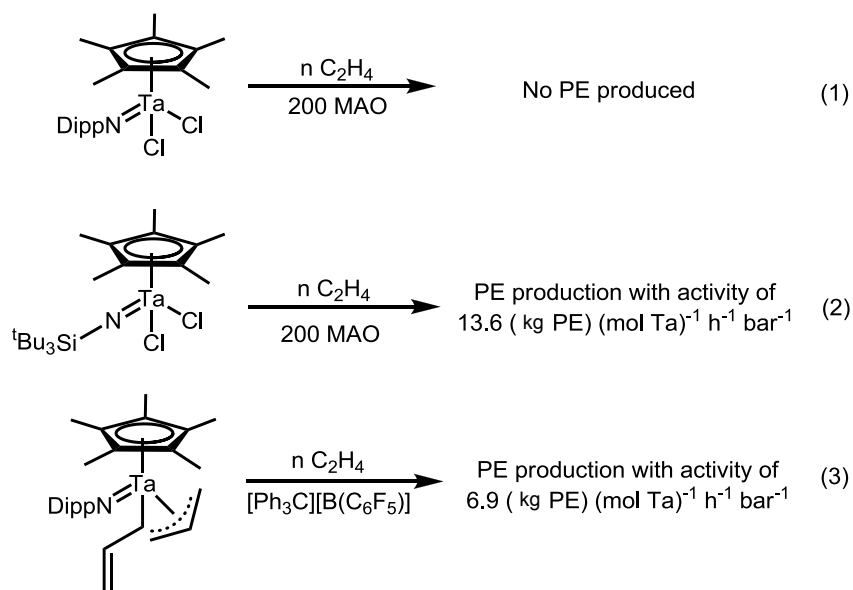


Scheme 4.6 An active tantalum Tp imido ethylene polymerization system (top) and an in-active mono(imido) derivative (bottom).²⁵

4.1.4 Difficulties in rationalizing differences in catalytic activity of ethylene polymerization systems

The significant differences between the catalytic activities observed for the various niobium- and tantalum-based ethylene polymerization systems described above are difficult to rationalize, largely as a consequence of the absence of mechanistic and systematic structure/activity correlation studies. An example of the types of problems encountered when comparing even similar complexes is given by a study of a series of Cp*Ta imido complexes (Scheme 4.7).²⁶ It has been shown that while the Cp*TaCl₂(NDipp) complex was not active for the polymerization of ethylene in the presence of MAO, its tributylsilylimido analogue exhibited reasonable activities (13.6 kg PE (mol Ta)⁻¹ h⁻¹ bar⁻¹) under identical reaction conditions (Scheme 4.7, eq. 1 and 2). The difference in behaviour between these two complexes has, somewhat arbitrarily, been attributed to the impact of the steric bulk of the silyl imido ligand in Cp*TaCl₂(NSi^tBu₃), which is believed to better inhibit deactivation *via* dimerization of the catalytically active species.²⁶ Nevertheless, the related *bis*(allyl) Dipp-imido complex (Scheme 4.7, eq. 3) did polymerize ethylene when activated with [Ph₃C][B(C₆F₅)], a result that was not rationalized in this study.²⁶ Clearly, the mode of activation and, as a result, the mechanism of polymerization is different for

systems described by eq. 1 and eq. 2 compared with that in eq. 3 (Scheme 4.7), with many factors having a subtle and additive effect upon catalytic activity.



Scheme 4.7 Half-sandwich tantalum imido complex-mediated polymerization of ethylene²⁶

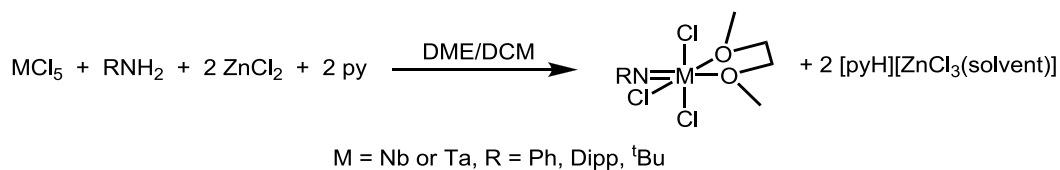
4.1.5 Niobium and tantalum imido-only ethylene oligomerization systems

Despite the potential utility of the initiator systems disclosed in previous studies, only the behavior of the Ta(NDipp)Cl₃(DME) / [Ph₃C][B(C₆F₅)₄] system has been examined.²⁵ Since work presented elsewhere in this thesis outlines the development of highly active ethylene and 1-hexene dimerization systems based on Cp- and Tp-free tungsten imido complexes and, recognizing the similarity between these tungsten and the related Nb/Ta systems, it was of interest to extend our work to include a more detailed study of these imido-only group V pro-initiators. Hence, a range of Nb and Ta imido complexes with different imido substituents (Dipp, Mes, ^tBu, and Ph) were synthesized and their potential in the EtAlCl₂-initiated dimerization of ethylene probed. This study aims at establishing a preliminary understanding of the behaviour of niobium and tantalum mono(imido) complexes towards ethylene under oligomerization/polymerization conditions and to establish structure-reactivity correlations by comparing the catalytic results with those of X-ray crystallographic studies of the various pro-initiator complexes.

4.2 Synthesis of niobium and tantalum imido complexes: M(NR)Cl₃(DME) (M = Nb, R = Ph (70), R = Mes (71), R = Dipp (72), R = ^tBu (73); M = Ta, R = Ph (74), R = Mes (75), R = Dipp (76), R = ^tBu (77))

Niobium and tantalum mono(imido) complexes are accessible from the respective pentahalides by extending methods described by Korolev *et al.* This synthetic approach is very convenient and involves

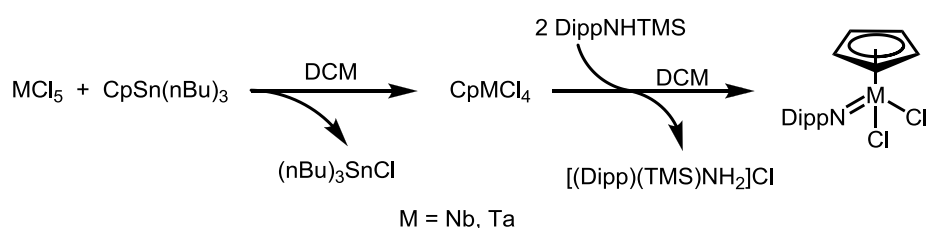
reaction of the appropriate metal(V) chloride with an amine and a combination of ZnCl₂ and pyridine (Scheme 4.8).²⁷



Scheme 4.8 Synthesis of Nb and Ta mono(imido) complexes MCl₃(NR)(DME) (**70-77**) reported by Korolev et al.²⁷

Using this strategy, the novel NMes derivatives, M(NMes)Cl₃(DME) (M=Nb (**71**), Ta (**75**)) were synthesized in reasonable yields (63 % and 72 %, respectively) in order to provide a comparison with the less bulky PhN systems. All of the new complexes were analyzed *via* ¹H and ¹³C NMR spectroscopy; the solution-state spectroscopic data obtained were in agreement with the results from the crystallographic studies presented in the next section.

To extend the structure/property correlation further, the previously reported half-sandwich imido complexes CpNb(NDipp)Cl₂ (**78**) and CpTa(NDipp)Cl₂ (**79**) were also synthesized (Scheme 4.9^{28,29}) and screened. Since the ethylene polymerization activity of these half-sandwich imido systems has been extensively probed in the literature, their ability to promote ethylene oligomerization, in combination with a suitable activator (e.g. EtAlCl₂), would provide a useful comparison.



Scheme 4.9 Synthesis of Nb and Ta cyclopentadienyl imido complexes (**78** and **79** respectively) as described by Williams et al. and Nikonov et al.^{28,29}

4.3 Crystallographic study of M(NR)Cl₃(DME) complexes (M = Nb and Ta, R = Ph, Mes, Dipp, ^tBu)

4.3.1 Niobium imido complexes: Nb(NR)Cl₃(DME), R = Ph (**70**), Mes (**71**), Dipp (**72**), ^tBu (**73**)

Crystals of **70** and **71** suitable for X-ray diffraction studies were grown and their molecular structures determined (Figure 4.1); selected interatomic distances and angles are given in Table 4.1. The unit cell determined for **71** contains two independent molecules, which differ in the conformation of the ligands about the Nb centre (A and B). As both conformers are similar, only conformation A will be discussed in detail. Since the molecular structures of **72** and **73** have been reported previously, their metric parameters are included in Table 4.1 for comparison.^{27,30} The molecular symmetry of all four of these niobium complexes **70-73** is C₁, with the niobium-bound substituents being arranged in a distorted

octahedral fashion. In each case, one of the DME O-donor atoms lies *trans* to the imido nitrogen, with the O-C-C-O fragment lying perpendicular to the *trans*-Cl-M-Cl axis. Based on NMR spectroscopy, the imido substituents are free to rotate in solution at ambient temperature.

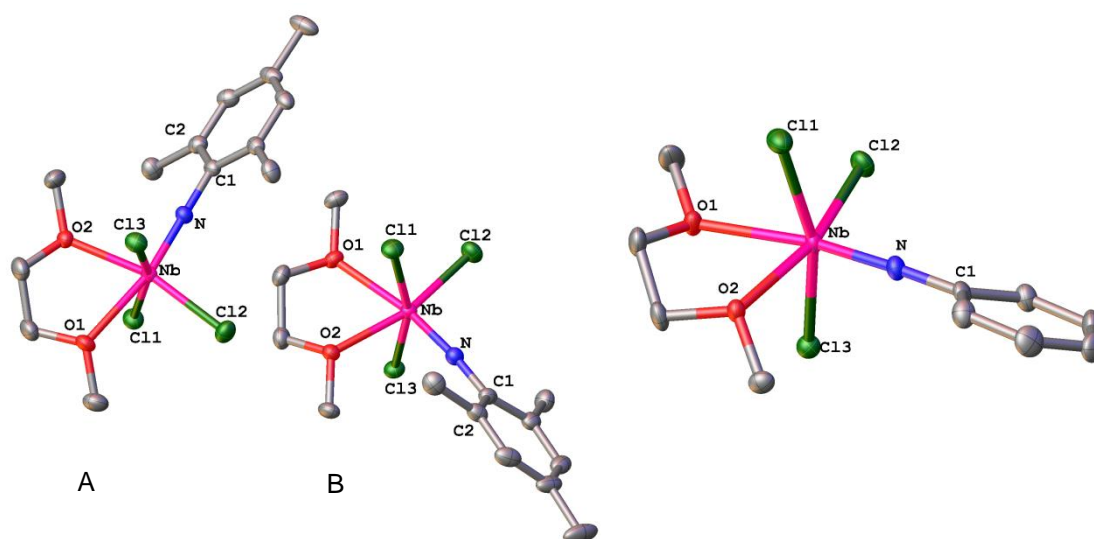


Figure 4.1 Molecular structures of $\text{Nb}(\text{NMes})\text{Cl}_3(\text{DME})$ (**71**) (left), showing both molecules in the unit cell, and $\text{Nb}(\text{NPh})\text{Cl}_3(\text{DME})$ (**70**) (right). H atoms are omitted for clarity and the thermal ellipsoids are shown at the 50% probability level.

In all four complexes **70-73** the Nb-N interatomic distances are short ($< 1.7647(17)$ Å), which is suggestive of a $\text{M}\equiv\text{N}$ triple bond.³¹ As expected, the Nb-N distance of the ^tBu derivative **73** is the shortest (1.722(2) Å), due to the strong electron-releasing character of the ^tBu group, which promotes donation of electron density from the imido nitrogen atom to niobium. The Nb-N distance of the Dipp derivative **73** is slightly longer (1.746(4) Å) than that of the ^tBu derivative **73**, while the Nb-N distances of the Ph and Mes derivatives were found to be the longest amongst complexes **70-73**. The imido N-C distances of the N-aryl-substituted complexes **70-73** are statistically indistinguishable from one another, while that for the ^tBu analogue **73** is 0.06 Å longer, the former reflecting some degree of conjugation between the nitrogen lone pair and the aromatic rings. In all of the niobium complexes **70-73**, the Nb-Cl(1) and Nb-Cl(3) distances are similar (~ 2.40 Å), while the Nb-Cl(2) distances are shorter (0.04 Å), something arising from the location of the Cl(2) atoms *trans* to the weakly-coordinated DME oxygen, O(2). The Nb-O distances are more than 0.4 Å longer than a formal Nb-O covalent single bond (e.g. in $\text{NbCl}_4(\text{OCH}_2\text{CH}_2\text{OCH}_3)$),¹⁶ consistent with dative coordination. As expected, the DME is bound in an unsymmetrical fashion, with the Nb-O(1) interatomic distances being between 0.12-0.20 Å greater than those of Nb-O(2) due to the strong *trans* influence of the imido ligand.³² By considering the variation in the Nb-O(1) distances, an assessment of the relative *trans* influences of the four imido groups can be derived, which lies in the order: NPh $<$ NMes $<$ NDipp $<$ N^tBu. This trend is in agreement with the findings of Clark *et al.* who demonstrated that the NPh imido group has a weaker *trans* influence compared to the NDipp group in complexes of the type $\text{W}(\text{NR})\text{Cl}_3(\text{PMe}_3)_2$ (R = Ph and Dipp).³³

Table 4.1 Selected interatomic distances (Å) and angles (°) for Nb(NPh)Cl₃(DME) (**70**), Nb(NMes)Cl₃(DME) (**71**), and for previously-reported Nb(NDipp)Cl₃(DME) (**72**),²⁷ and Nb(N^tBu)Cl₃(DME) (**73**).³⁰

	Nb(NPh)Cl ₃ (DME)	Nb(NMes)Cl ₃ (DME) ^a	Nb(NDipp)Cl ₃ (DME) ³⁰	Nb(N ^t Bu)Cl ₃ (DME) ²⁷
Nb-N	1.7561(16)	1.7647(17)	1.746(4)	1.722(2)
N-C(1)	1.397(2)	1.390(3)	1.403(5)	1.463(1)
Nb-Cl(1)	2.4015(6)	2.3952(6)	2.391(1)	2.400(3)
Nb-Cl(2)	2.3611(6)	2.3671(6)	2.355(2)	2.366(3)
Nb-Cl(3)	2.4070(5)	2.4121(5)	2.390(1)	2.424(3)
Nb-O(1)	2.3366(13)	2.3420(14)	2.352(4)	2.389(6)
Nb-O(2)	2.2047(14)	2.1980(14)	2.232(3)	2.187(6)
Nb-N-C(1)	176.23(15)	174.28(15)	177.7(3)	176.8(7)
Cl(1)-Nb-N	97.48(6)	96.38(6)	97.01(12)	95.8(3)
Cl(2)-Nb-N	100.37(6)	101.38(6)	100.15(12)	100.8(3)
Cl(3)-Nb-N	96.82(6)	96.98(6)	96.79(11)	98.4(3)
O(2)-Nb-N	97.23(7)	96.56(7)	98.1(2)	97.4(3)
O(1)-Nb-O(2)	72.14(5)	72.30(5)	71.9(2)	70.9(2)
Cl(2)-Nb-O(1)	90.24(4)	89.94(4)	89.89(11)	91.0(2)
Cl(1)-Nb-Cl(2)	93.78(2)	96.23(2)	93.81(5)	94.9(1)
Cl(2)-Nb-Cl(3)	92.122(19)	92.54(2)	94.08(5)	92.9(1)

^a Two independent molecules located in the unit cell that differ in the conformations about Nb; the data of conformer A only is discussed here (Figure 4.1).

For each of the Nb complexes **70-73** the Nb-N-C(1) angles are essentially linear (> 174°), which is formally in agreement with the presence of a Nb≡N triple bond. However, deviation of the Nb-N-C(1) imido unit from linearity is not indicative of weaker Nb-N bonding, since it can be influenced significantly by other factors such as crystal packing forces, and is hence, an unreliable indicator of M-N bond order.³⁴ In each of the Nb imido complexes **70-73**, the Nb atoms lie out of the N-Cl(2)-Cl(3)-O(2) plane, presumably as a result of steric constraints imposed by the imido ligands. It is argued that the N-Dipp ligand exerts a slightly larger steric pressure compared to that from the NPh ligand, due to the presence of the bulky isopropyl groups in the *ortho* positions of the Dipp fragment.³³ Hence, it might be expected that the sum of the N-Nb-X angles (X = O or Cl atom) will differ when different imido groups are employed. Nevertheless, in this study, varying the nature of the group on the imido doesn't significantly affect the sum of the N-M-X angles, which are the same (within experimental error) for all of the imido groups employed with a value of ~392°.

4.3.2 Tantalum complexes: TaCl₃(NR)(DME), R = Ph (**74**), Mes (**75**), Dipp (**76**), ^tBu (**77**)

In a related investigation, the molecular structures of **74-77** were determined by X-ray diffraction studies (Figure 4.2, selected interatomic distances and angles are given in Table 4.2); the interatomic distances and angles of the previously-reported complex Ta(NDipp)Cl₃(DME) (**76**) are also listed in Table 4.2.³⁰ Three independent, chemically equivalent molecules A-C were found in the unit cell of Ta(NPh)Cl₃(DME) (**74**), which differ only in the conformation about Ta; consequently, only A is discussed. A comparison of the structural parameters of the various tantalum complexes reveals a greater variation compared to that observed in the related Nb series (section 4.3.1). The Ta-N interatomic distances of the aryl-substituted tantalum imidos are identical within experimental error, while that for the ^tBu derivative is shorter. The Ta-O(1) bond lengths increase in the order NDipp < NPh

$< \text{NMe} < \text{N}^t\text{Bu}$, which implies that the Dipp group has the weakest *trans* influence within the series. This contrasts to the observation made previously for the niobium complexes, where the NDipp was found to exert the strongest *trans* influence after the N^tBu according to the observed Nb-O(1) interatomic distances. Taking these observations together, it is clear that a number of different factors contribute to the variations in the bond distances around the metal centres in these group V imido/DME complexes and hence, simple comparisons of bond distances cannot be used to assess reliably relative *trans*-influences.

The Ta-N-C(1) angles of each of the four tantalum-imido complexes are essentially linear ($> 169.2^\circ$). Summation of the N-Ta-X angles ($X = \text{O}$ or Cl) gives a value of $\sim 394^\circ$ (Table 4.2), for all tantalum imido complexes **74-77** suggesting that the steric pressure applied on the Cl1, Cl2, Cl3, and O2 atoms by the imido substituent is not significantly influenced by the imido functional group.

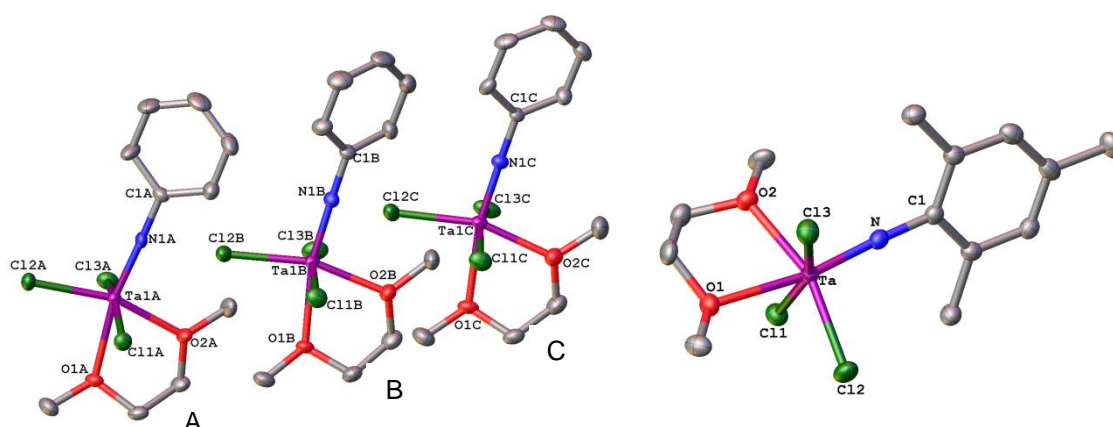


Figure 4.2 Molecular structures of $\text{Ta}(\text{NPh})\text{Cl}_3(\text{DME})$ (**74**) (left), showing all molecules A-C in the unit cell, and $\text{Ta}(\text{NMes})\text{Cl}_3(\text{DME})$ (**75**) (right). H atoms are omitted for clarity and the thermal ellipsoids are shown at the 50% probability level.

Table 4.2 Selected interatomic distances (Å) and angles ($^\circ$) for $\text{Ta}(\text{NPh})\text{Cl}_3(\text{DME})$ (**74**), $\text{Ta}(\text{NMes})\text{Cl}_3(\text{DME})$ (**75**), $\text{Ta}(\text{N}^t\text{Bu})\text{Cl}_3(\text{DME})$ (**76**), and previously-reported $\text{Ta}(\text{NDipp})\text{Cl}_3(\text{DME})$ (**77**).²⁷

	$\text{Ta}(\text{NPh})\text{Cl}_3(\text{DME})^a$	$\text{Ta}(\text{NMes})\text{Cl}_3(\text{DME})$	$\text{Ta}(\text{NDipp})\text{Cl}_3(\text{DME})^{30}$	$\text{Ta}(\text{N}^t\text{Bu})\text{Cl}_3(\text{DME})$
Ta-N	1.766(4)	1.774(3)	1.771(6)	1.747(3)
N-C(1)	1.387(6)	1.380(5)	1.390(9)	1.463(4)
Ta-Cl(1)	2.3861(11)	2.4051(10)	2.378(2)	2.4149(7)
Ta-Cl(2)	2.3353(12)	2.3508(11)	2.338(3)	2.3615(7)
Ta-Cl(3)	2.3879(12)	2.3709(9)	2.376(2)	2.3801(7)
Ta-O(1)	2.341(3)	2.362(3)	2.330(6)	2.384(2)
Ta-O(2)	2.183(3)	2.170(3)	2.208(6)	2.162(2)
Ta-N-C(1)	177.4(3)	177.4(3)	178.1(5)	169.2(2)
Cl(1)-Ta-N	97.01(13)	96.98(11)	97.8(2)	101.22(8)
Cl(2)-Ta-N	100.86(12)	101.16(11)	100.8(2)	99.81(8)
Cl(3)-Ta-N	98.63(12)	98.21(11)	97.2(2)	96.60(8)
O(2)-Ta-N	97.18(14)	97.62(13)	97.7(3)	99.35(10)
O(1)-Ta-O(2)	71.98(12)	72.73(11)	72.3(3)	71.98(7)
Cl(2)-Ta-O(1)	90.00(9)	88.56(8)	89.3(2)	88.82(5)
Cl(1)-Ta-Cl(2)	92.52(4)	92.13(4)	93.49(10)	92.29(3)
Cl(2)-Ta-Cl(3)	92.89(4)	94.58(4)	93.44(9)	92.29(3)

^a Three independent molecules located in the unit cell that differ in the conformations about Ta; the data of conformer A only is discussed here (Figure 4.2)

In conclusion, it is apparent from this crystallographic study that the niobium and tantalum imido complexes **70-77** adopt very similar structures, with only very subtle structural differences. Nevertheless, each of these complexes exhibits very different catalytic reactivity patterns towards ethylene, something detailed in the following sections.

4.4 Niobium and tantalum imido-based oligomerization/polymerization of ethylene and 1-hexene

4.4.1 General considerations

4.4.1.1 Choice of catalytic conditions

Identical reaction conditions were employed for the testing of the niobium- and tantalum-based ethylene and 1-hexene oligomerization/polymerization systems to those used for tungsten (section 2.4), so that direct comparisons between the group 5 and 6 systems could be made. It should be noted that, in contrast to the group 5 MAO-activated systems reported in the literature, which require high aluminum loadings to promote catalysis (typically over 500 equivalents of MAO per transition metal¹³), the systems described in this chapter require only 15 equivalents of EtAlCl₂ per transition metal in order to initiate the catalytic reaction.

The polymerization activity of the catalysts examined herein are classified according to the criteria set out by Gibson as summarized in Table 4.3.³⁵

Table 4.3 Gibson criteria for polymerization initiator classification based on their activity³⁵

Catalyst Classification	Activity in (kg PE) (mol M) ⁻¹ h ⁻¹ bar ⁻¹
very low activities	< 1
low activities	1-10
moderate activities	10-100
high activities	100-1000
very high activities	> 1000

4.4.1.2 Effect of cyclopentadienyl ligands in niobium and tantalum imido-catalyzed ethylene oligomerization/polymerization

It was found that CpNb(NDipp)Cl₂ (**78**) and CpTa(NDipp)Cl₂ (**79**) (Table 4.4, run 1 and Table 4.6, run 1, respectively) exhibited very low polymerization activities, which is in accordance with the activity recorded in the similar system CpNb(N-2-tBu-C₆H₄)Cl₂/30 Et₂AlCl examined by Gibson *et al.*³⁶ However, both the **78** and **79** complexes (in combination with Et₂AlCl) were found to initiate ethylene dimerization, producing almost exclusively 1-butene with an activity of 2.9 and 0.9 kg C₂H₄ (mol TM)⁻¹ h⁻¹bar⁻¹, respectively (Table 4.4, run 1 and Table 4.6, run 1, respectively). It is suggested that the low activities observed for **78** and **79** may be due to the presence of the η⁵-Cp ligand, which prevents access of the co-initiator and/or olefinic substrate. Indeed, in most literature reports where Cp-niobium or Cp-tantalum complexes have been employed as initiators for olefin oligomerization, very low activities

have been recorded (for examples see Scheme 4.3). Therefore, Cp-free imido complexes were employed here. For example, the activities observed for Nb(NDipp)Cl₃(DME) (**72**) and Ta(NDipp)Cl₃(DME) (**76**) were at least one order of magnitude larger compared to CpNb(NDipp)Cl₂ (**78**) (Table 4.4) and CpTa(NDipp)Cl₂ (**79**) (Table 4.6), respectively, which further demonstrates the negative effect of the Cp ligand in the oligomerization/polymerization of ethylene.

4.4.2 Niobium imido-based ethylene oligomerization and polymerization testing

4.4.2.1 General remarks

The results of the niobium imido-mediated oligo-/poly-merization of ethylene are summarized in Table 4.4. Low to moderate polymerization, along with considerable dimerization activities, were achieved in all cases. The organic products from all runs were mainly polyethylene, butenes, and small amounts of hexenes. Note, that the vast majority of the butenes and hexenes produced were the 1-isomers (over 86% of the butenes fraction and over 70% of the hexenes fraction) with the exception of Nb(NPh)Cl₃(DME) (**70**) where only 36% of the hexenes fraction consisted of 1-hexene. This indicates that little olefin isomerization occurs during catalysis using these niobium systems. Particularly, these niobium imido systems produce only very small amounts of heavy liquid olefins (>C₈), the only exception being Nb(NDipp)Cl₃(DME) (**72**), which is discussed in the next section.

Table 4.4 Ethylene oligomerization and polymerization using well-defined Nb imido complexes with EtAlCl₂ co-catalyst^a

Run #	Pro-initiator	Time (min)	TON ^b	Tot. Act. ^c	Act. to C ₄ ^d	% PE	Act. to PE ^e	Mol % C ₄ (in liq. prod.)	% 1-C ₄ in C ₄	Mol % C ₆ (in liq. prod.)	% 1-C ₆ in C ₆	% Lin in C ₆	wt % C ₈₊ (in liq. prod.)
1	CpNb(NDipp)Cl ₂ (78)	10	0.5	3.0	2.9	1.1	0.03	98.6	97.9	1.4	0.0	-	0.0
2	Nb(NMes)Cl ₃ (DME) (71)	2.3	1.6	42	29	25.1	11	96.2	94.7	3.0	69.6	90.7	2.1
3	Nb(N ⁱ Bu)Cl ₃ (DME) (73)	3.4	3.2	57	16	62.7	36	88.5	97.8	5.7	100	92.8	16.8
4	Nb(NPh)Cl ₃ (DME) (70)	7.5	6.0	48	42	5.2	2.5	95.3	85.6	4.3	35.6	85.1	0.9
5	Nb(NDipp)Cl ₃ (DME) (72)	7.9	9.6	73	1.9	70.7	52	27.9	98.6	8.9	92.0	85.0	87.0
6 ^f	Nb(NDipp)Cl ₃ (DME) (72)	7.8	6.6	51	13	60.2	30	83.0	98.0	4.7	88.1	100	32.0

^a General conditions: 20 μmol Nb complex and 300 μmol EtAlCl₂; PhCl (solvent) 74 mL; 60 °C; ethylene pressure (40 bar); stirrer speed 1000 rpm; nonane standard (1.000 mL); catalytic runs were performed until consumption of C₂H₄ dropped below 0.2 g min⁻¹, at which time reaction was quenched by addition of dilute HCl. ^b TON is reported in (kg C₂H₄) (mol Nb)⁻¹ bar⁻¹. ^c Total activity is reported in (kg C₂H₄) (mol Nb)⁻¹ h⁻¹bar⁻¹ and is based on the total ethylene consumption. ^d Activity towards butene formation is reported in (kg C₂H₄) (mol Nb)⁻¹ h⁻¹bar⁻¹. ^e Activity towards PE formation is reported in (kg PE) (mol Nb)⁻¹ h⁻¹ bar⁻¹. ^f 5 μmol Nb complex and 75 μmol EtAlCl₂. PE = polyethylene.

4.4.2.2 Simultaneous dimerization and polymerization catalysis by niobium imido pro-initiators

From the data presented in Table 4.4 it can be seen that the niobium imido pro-initiators **70-73** are all able to promote both the dimerization and polymerization of ethylene. Notably, in the liquid product fraction only trace quantities of oligomers heavier than butenes (namely trimers; less than 9% mol) were detected. Only in run 5 (Table 4.4) were significant amounts of octenes or heavier soluble oligomers detected (87.0 % w/w of the alkenes in the liquid fraction). Taking these data together (Figure 4.3), it is clear that the balance between oligomerization and polymerization is directly influenced by the nature of the imido N-substituent.

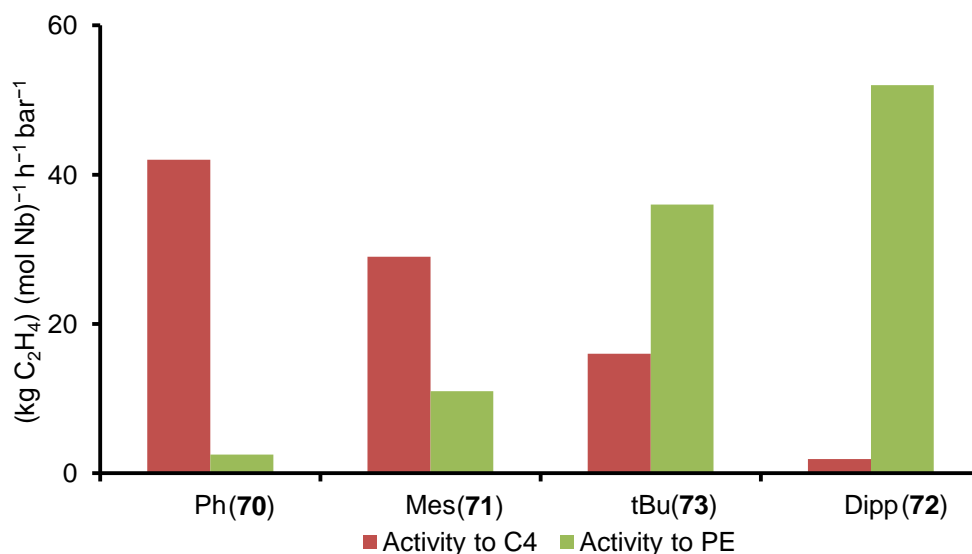


Figure 4.3 Summary of the catalytic activity versus imido ligand substituent of the niobium pro-initiators; data taken from Table 4.4

Complexes Nb(N^tBu)Cl₃(DME) (**73**) and Nb(NMes)Cl₃(DME) (**71**) favor both polymerization and dimerization (Table 4.4). In contrast, the complex Nb(NPh)Cl₃(DME) (**70**) is selective towards ethylene dimerization, exhibiting a low polymerization activity of 2.5 kg PE (mol Nb)⁻¹ h⁻¹ bar⁻¹ and a dimerization activity of 42 kg C₂H₄ (mol Nb)⁻¹ h⁻¹ bar⁻¹ (run 4; Table 4.4). Complex Nb(NDipp)Cl₃(DME)(**72**) (run 5; Table 4.4) on the other hand can be regarded as an ethylene polymerization pro-initiator with a moderate polymerization activity of 52 kg PE (mol Nb)⁻¹ h⁻¹ bar⁻¹. The polymerization activity of **72** is the highest observed amongst the niobium and tantalum (see also section 4.4.3) imido systems examined in this chapter, and is comparable to the activities of the niobium-based pro-initiators reported in the literature (Scheme 4.3).

4.4.2.3 Effect of the imido substituent on the catalytic activity of niobium imido/EtAlCl₂ systems

In order to correlate the catalytic performance of the various niobium imido pro-initiators **70-73** against structure, an assessment of both the electronic and steric demands of the imido substituents is required. It is reasonable to suggest that, at least qualitatively, the steric bulk of the aryl substituents increases in the order Ph < Mes < Dipp as may be seen in the space-filling molecular structure diagrams of the various complexes (Figure 4.4). The electronic influence of the aryl imido substituents may be probed, semi-quantitatively, by comparing the Nb-N bond lengths of the complexes **70-72** (section 4.3.1). These data suggest that the electron withdrawing ability of these three aryl substituents is similar, something that is supported from the similar pK_a values (in water) of the corresponding protonated anilines (PhNH₂, MesNH₂, and DippNH₂), which lie in the range between 4.0 and 4.6.³⁷ Hence, it is reasonable to suggest that the imido groups NPh, NMes, and NDipp may be regarded as being electronically similar.

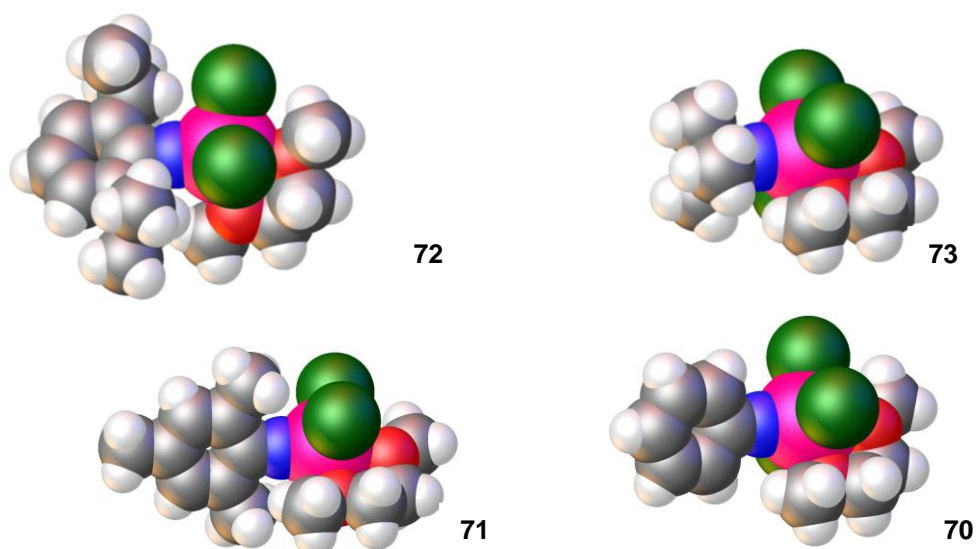


Figure 4.4 Space-filling representations of the molecular structures of $\text{Nb}(\text{NDipp})\text{Cl}_3(\text{DME})$ (**72**),²⁷ $\text{Nb}(\text{N}^t\text{Bu})\text{Cl}_3(\text{DME})$ (**73**),³⁰ $\text{Nb}(\text{NMes})\text{Cl}_3(\text{DME})$ (**71**), and $\text{Nb}(\text{NPh})\text{Cl}_3(\text{DME})$ (**70**)

The catalysis data presented in Figure 4.5 suggest that an increase in the steric hindrance of the imido substituents alone favours polymerization over dimerization, since the electronic character of the aryl imido ligands is comparable (*vide supra*). The beneficial effect of bulky ligands on the activities of ethylene polymerization catalysts is widely documented in the literature, and is attributed to their ability to prevent catalysts from both undergoing β -hydride elimination from the growing polymer chain (as a result of geometric constraints), and from undergoing detrimental deactivation reactions, such as dimerisation.^{15,25,38} Alternatively, it is also possible that different metal imido-containing fragments are formed depending on the bulk of the imido ligands, which are either more selective for dimerization or for polymerization.

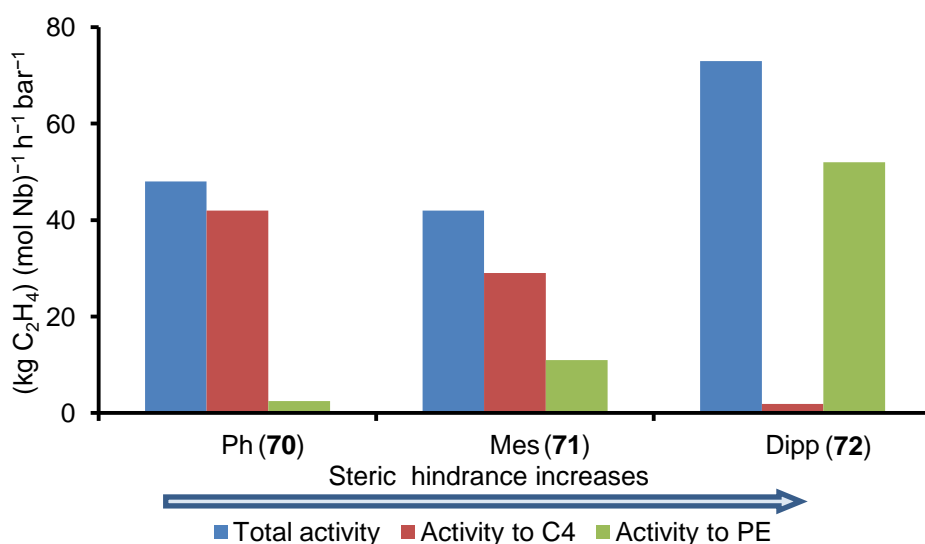


Figure 4.5 Catalytic activity as a function of aryl substituent on the imido ligand of the niobium pro-initiators of the type $\text{Nb}(\text{NR})\text{Cl}_3(\text{DME})$ ($R = \text{Ph}, \text{Mes}, \text{Dipp}$). Data were taken from Table 4.4

The catalytic behavior of the initiator system $\text{Nb}(\text{N}^t\text{Bu})\text{Cl}_3(\text{DME})$ (**73**)/ EtAlCl_2 towards ethylene was examined in order to explore whether introduction of a much more electron donating imido ligand would

have a significant impact on catalysis. In contrast to the aryl substituents, the ^tBu group has a much greater electron donating character, which is reflected to the shorter Nb-N bond length of **73** complex compared to its aryl analogues and to the much larger pK_a value of 10.6.³⁷ It was found that the catalytic activity of the **73**/EtAlCl₂ system towards both dimerization and polymerization lies in between the activities determined for the **71**/EtAlCl₂ and **72**/EtAlCl₂ systems (Table 4.4). Consequently, it is suggested that the electronic properties of the imido groups have little influence on the catalytic behavior of these Nb-based systems.

4.4.2.4 Dilution effect on the performance of the Nb(NDipp)Cl₃(DME)/15 EtAlCl₂ system

Since the tests performed with the pro-initiator Nb(NDipp)Cl₃(DME) (**72**) (run 5; Table 4.4) afforded significant amount of polyethylene, which will have significantly increased the viscosity of the reaction medium, it was of interest to probe the influence of any resulting mass transport effects on the organic product distribution. To this end, an experiment was performed at higher dilution, but with the same Nb:Al ratio (run 6; Table 4.4). This change led to a drop in the overall catalytic activity of this **72**/EtAlCl₂ system, with a decrease in the activity towards polyethylene and an increase in the dimerization activity from 1.9 kg C₂H₄ (mol Nb)⁻¹ h⁻¹ bar⁻¹ for run 5 (Table 4.4) compared to 13 kg C₂H₄ (mol Nb)⁻¹ h⁻¹ bar⁻¹ for run 6 (Table 4.4). This observed decrease in the activity of the niobium imido-based systems after dilution has also been observed for tungsten imido pro-initiators when activated under the same conditions in the dimerization of ethylene (section 2.4.1.4), and is difficult to rationalize. One possible explanation for the observed reduction in polymerization activity of **72** upon dilution, is that the catalytically active species could be a niobium dimer complex, which forms from the reaction between two niobium complexes during the activation step, something that will be concentration-dependent. Alternatively, the activation of **72** by EtAlCl₂ at a higher dilution could result in formation of completely different, less active and/or less selective catalytic species. Note, however, that simple catalyst decomposition effects cannot be ruled out.

4.4.2.5 Niobium imido/EtAlCl₂-mediated polymerization: polyethylene analysis

An understanding of the properties of the polyethylenes produced from the catalytic reactions mediated by the niobium imido pro-initiator systems **70-73** can provide some information on the mechanisms at work during catalysis. Unfortunately, access to high temperature GPC (Gel Permeation Chromatography) for analysis of these poorly soluble materials was not available. Hence, as a partial substitute, DSC (Differential Scanning Calorimetry) analyses of the various polymeric materials produced during catalysis were obtained; the resulting data are summarized in Table 4.5.

Table 4.5 Melting points (°C) and crystallinities (%) of the polyethylene produced by the niobium imido-based catalytic systems **70-73** determined by DSC^{a,b}

Run #	Pro-initiator	Melting point (°C)	Density ^d	Crystallinity (%)
1	Nb(NMes)Cl ₃ (DME) (71)	133.0	0.95	66
2	Nb(N ^t Bu)Cl ₃ (DME) (73)	130.9	0.95	81
3	Nb(NPh)Cl ₃ (DME) (70)	133.3	0.95	67
4	Nb(NDipp)Cl ₃ (DME) (72)	42.4–128.6	-	-
5 ^c	Nb(NDipp)Cl ₃ (DME) (72)	136.3	0.96	77

^a General conditions: 20 μmol Nb complex and 300 μmol EtAlCl₂; PhCl (solvent) 74 mL; 60 °C; ethylene pressure (40 bar); stirrer speed 1000 rpm; nonane standard (1.000 mL); catalytic runs were performed until consumption of C₂H₄ dropped below 0.2 g min⁻¹, at which time reaction was quenched by addition of dilute HCl. ^b For DSC analysis conditions see section 5.1. ^c 5 μmol Nb complex and 75 μmol EtAlCl₂. ^d Densities were calculated from the peak melting point values.³⁹

The polyethylenes produced by complexes **70-73**/Runs 1-5 (Table 4.5) show moderate crystallinity (> 50% crystallinity), with high melting points of over 130 °C and densities of ~0.95 g/cm³; these values are characteristic of high molecular weight, high density linear polyethylene (HDLPE); see Figure 4.6.^{19,22,40,41} In contrast, the polymer produced in run 4 (Table 4.5), gave rise to multiple broad peaks in the DSC thermogram, which is consistent with linear low density polyethylene, LDLPE (Figure 4.6).^{40,41}

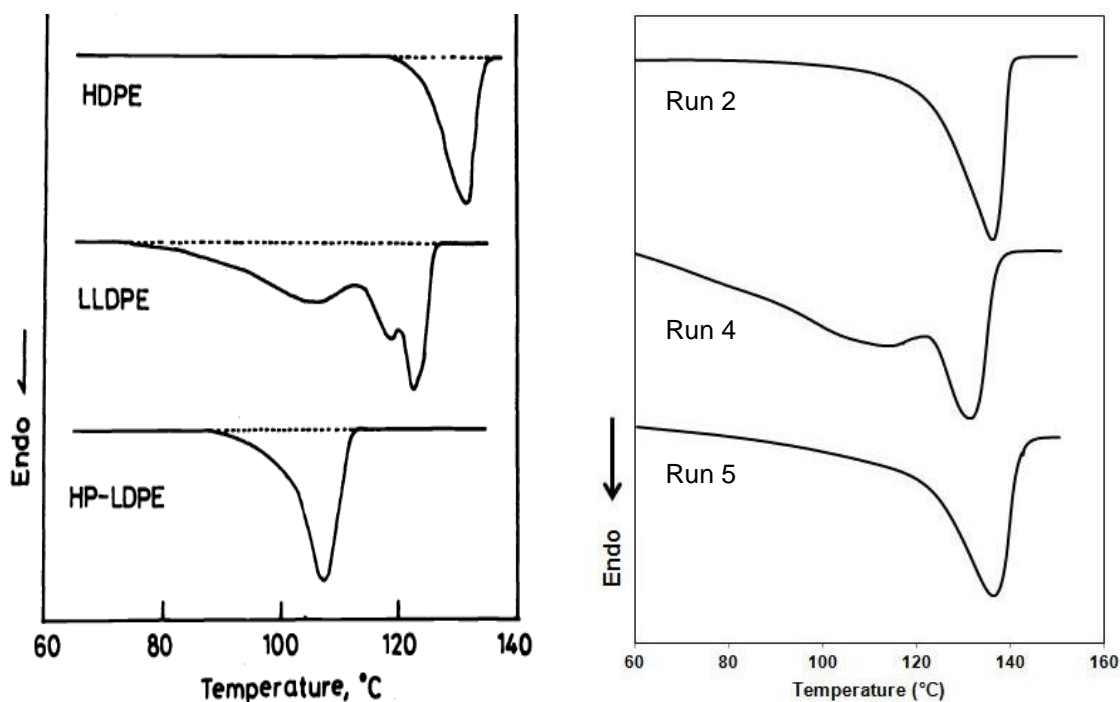


Figure 4.6 Previously-reported DSC thermograms of HDLPE, LLDPE, and HP-LDPE (left)⁴¹ and of the polyethylenes produced from runs 2, 4, and 5 (right) of Table 4.5

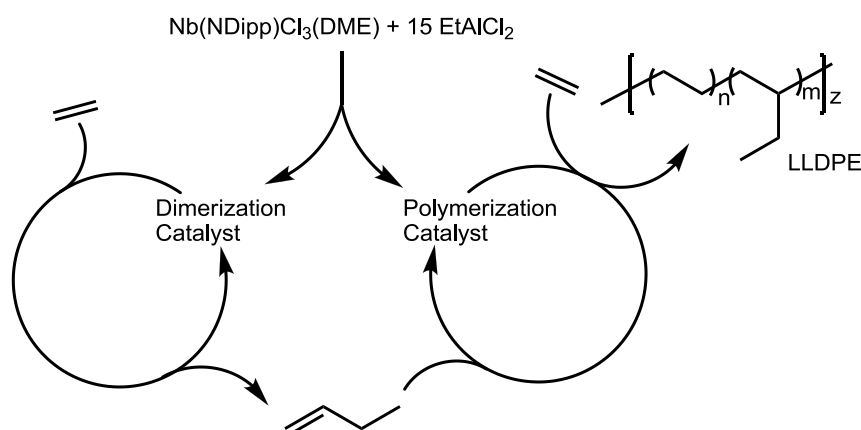
Notably, catalysis run 5 (Table 4.4) also gave rise to comparatively large amounts of heavy oligomers (87% wt) in the liquid product fraction (run 5, Table 4.4). Interestingly, when the same catalyst system as for run 5 (Table 4.4) was used under identical conditions, but at a higher dilution (Table 4.4 and Table 4.5 run 6 and run 5 respectively), both an attenuation in the catalytic activity (section 4.4.2.4) and the formation of a polymer of high crystallinity, melting point, and density were observed, consistent with high density polyethylene (Figure 4.6). The properties of the polyethylene formed under high dilution

conditions are in sharp contrast to those of the polyethylene produced by the same pro-initiator at higher concentration (run 4; Table 4.5), something that can have mechanistic implications (see section 4.4.2.6).

4.4.2.6 Mechanistic complexity of the niobium imido/EtAlCl₂ systems

Interestingly, for test runs 2-4 (Table 4.4), butene and polyethylene are the dominant products, with only very small amounts of other products being formed. Since it is unlikely that a single catalyst species will simultaneously produce both dimers and polymer, it is suggested that at least two different catalytically active systems are formed from the reaction between the niobium imido pro-initiators and EtAlCl₂: an ethylene dimerization system and an ethylene polymerization system.

The possibility that both ethylene dimerization and polymerization systems are formed upon activation of the niobium imido pro-initiators with EtAlCl₂ can also explain the changes in products obtained using Nb(NDipp)Cl₃(DME) (**72**)/15 EtAlCl₂ from production of LLDPE (run 5; Table 4.4) to production of HDPE (run 6; Table 4.4) when catalysis is performed at higher dilution (section 4.4.2.5). The ethylene polymerization system formed during run 5 (Table 4.4) is able to co-polymerize ethylene with the dimers produced *in situ* from the dimerization system, resulting in formation of LLDPE (Scheme 4.10). This type of *in situ* co-polymerization is also known as *concurrent tandem catalysis* and has been successfully used for the production of LLDPE.⁴²⁻⁴⁵ When catalysis with **72** is performed at lower dilution (run 5; Table 4.4) the concentration of the 1-butene produced from the dimerization system (which is formed after activation of **72** along with the polymerization system) will be lower compared to the concentration of ethylene, which is independent of dilution since the catalytic reaction is carried out at a constant ethylene pressure (40 bar). As a result, the incorporation of 1-butene to the polymerization system is attenuated at higher dilution due to its lower concentration and higher steric bulk compared to ethylene, resulting in production of HDLPE along with an increase of the ethylene dimerization activity and decrease in the activity towards ethylene polymerization (Table 4.4).



Scheme 4.10 Possible mechanism for formation of butene/ethylene co-polymers with niobium imido/EtAlCl₂ systems

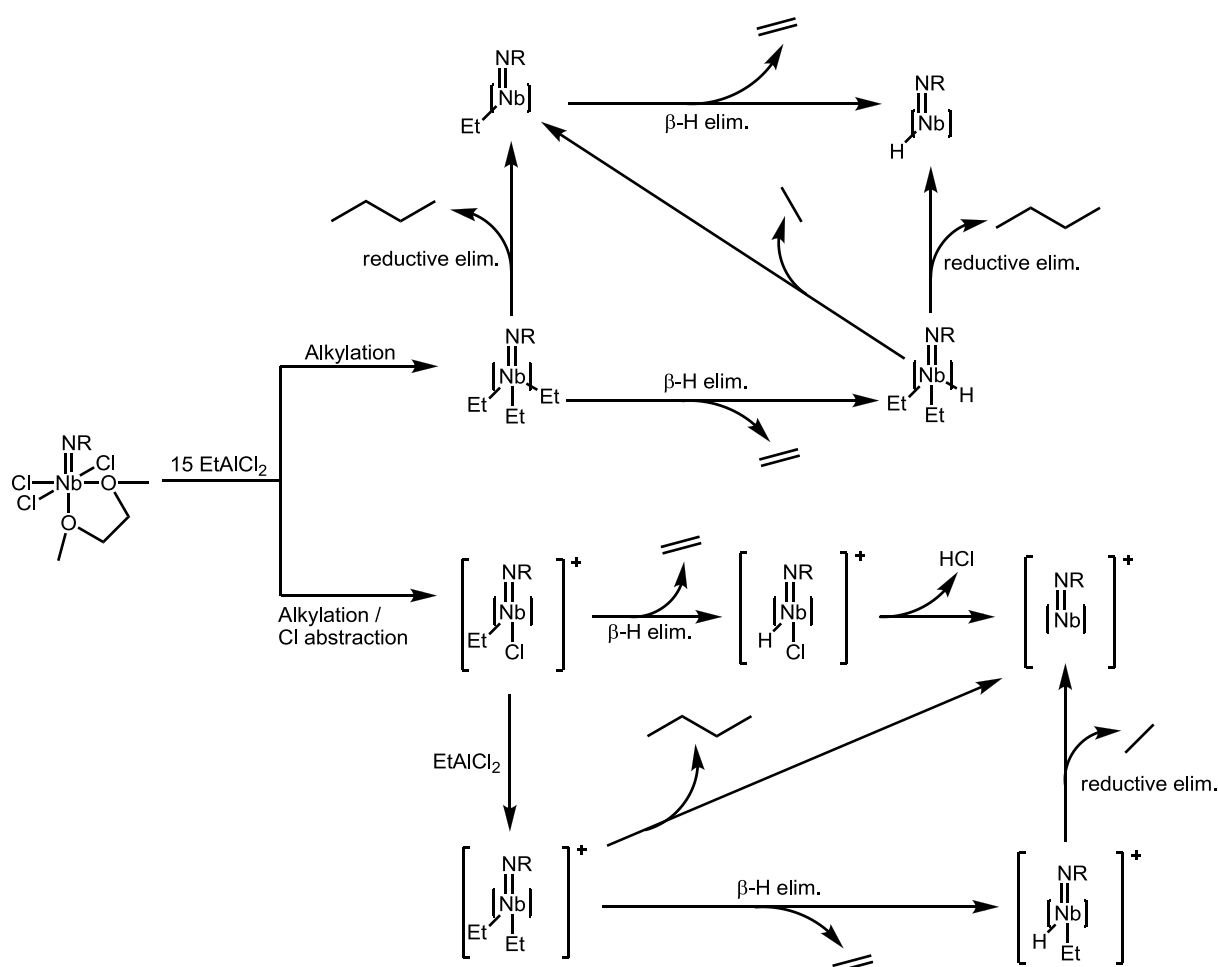
It must also be noted that, in contrast to **72**/EtAlCl₂, the systems Nb(NPh)Cl₃(DME) (**70**)/EtAlCl₂, Nb(N^tBu)Cl₃(DME) (**73**)/EtAlCl₂, and Nb(NMes)Cl₃(DME) (**71**)/EtAlCl₂ do not produce LLDPE under the

same conditions, instead producing only HDLPE and oligomers (section 4.4.2.5, Table 4.5). This suggests that the polymerization systems produced when **70**, **71**, and **73** are activated with EtAlCl_2 are less active compared to **72**/ EtAlCl_2 and thus unable to co-dimerize the bulkier 1-butene with ethylene, something that is in line with the lower ethylene polymerization activities observed in runs 2-4 (Figure 4.3, Table 4.4).

For the catalytic systems examined herein, the possible factors that could lead to this type of concurrent dimerization/polymerization behavior could include various factors such as:

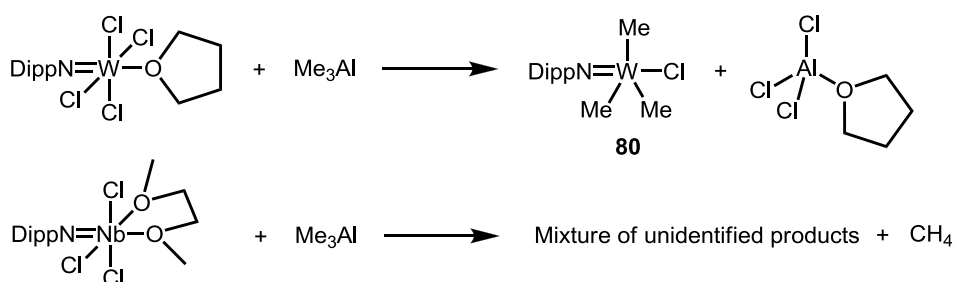
- Generation of species with different niobium oxidation states
- Formation of dimeric niobium complexes
- Coordination of the alkyl aluminum halide to the Nb imido-containing fragment
- Involvement of more than one mechanistic pathway

Furthermore, the ability of the EtAlCl_2 to act both as an alkylating and as a chloride abstracting agent (discussed in section 6.1.3),²⁰ further complicates a clear understanding of the niobium imido catalytic systems. This dual behaviour provides routes towards formation of cationic niobium(V) or niobium(III) species and neutral niobium(V) or niobium(III) ethyl complexes (Scheme 4.11).



Scheme 4.11 Possible pre-catalyst transformations occurring following activation of $\text{Nb}(\text{NR})\text{Cl}_3(\text{DME})$ with EtAlCl_2

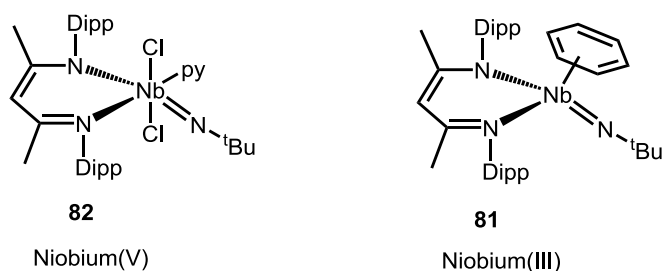
This reaction complexity makes it difficult to suggest a mechanism for the mode of operation of the niobium imido/EtAlCl₂ systems in the catalytic oligo-/poly-merization of ethylene based only on catalytic data. The intricacy of the reaction chemistry associated with these niobium imido systems is reflected even in their stoichiometric reaction with Me₃Al, which result in complicated mixtures of products, which are un-assignable using ¹H NMR spectroscopy. This contrasts to analogous reactions between tungsten mono(imido) complexes and Me₃Al, which give well defined, methylated tungsten complexes, e.g. **80**, as described in Scheme 4.12 (see also section 3.4.1.2.2).



Scheme 4.12 Reaction of *W*(NDipp)Cl₄(THF) (**59**) and *Nb*(NDipp)Cl₃(DME) (**72**) with one equivalent of Me₃Al

4.4.2.7 Future investigations

The first step towards gaining more information about the nature of the catalysts involved in the niobium imido-mediated ethylene oligo-/poly-merization is proposed to be the determination of the oxidation state of these catalytic species. In the experiments described herein, only niobium(V) complexes were used as pro-initiators. Nevertheless, it is possible that during activation with EtAlCl₂ the niobium(V) is converted to a niobium(III) complex *via* reductive elimination (see Scheme 4.11). The idea of a niobium(III) species being responsible for catalysis is attractive for two reasons. Firstly, examples of niobium(III) imidos are scarce in the literature, mainly due to their instability, which suggests that they are likely to be highly active species, which could initiate catalysis.⁴⁶ Secondly, it has been demonstrated that related tantalum(III) species, are able to trimerize olefins in the absence of an activator.^{9-12,22} Although niobium(III) imido complexes are rare, the synthesis of a mixed imido/(β-diketiminato)niobium(III)benzene complex **81** was recently reported (Scheme 4.13).⁴⁷ Therefore, comparing the potential catalytic activity of complexes such as the Nb(III) complex **81** and the related Nb(V) system **82** towards ethylene under various conditions might provide some information about the oxidation state of some of the catalytically active species present during catalysis.



Scheme 4.13 A niobium(V) imido complex **82**⁴⁶ and its niobium(III) counterpart **81**⁴⁷

Additionally, in order to unambiguously assess the way in which the electronic properties of the imido substituents influence catalysis, a second series of niobium imido complexes must be synthesized with similar steric demands and different electronic properties. One such series might include fluorophenyl N-substituents such as the ones described in Figure 4.7.³⁷ Comparison of the catalytic activities and product selectivities of these fluoroarylimido in the oligo-/poly-merization of ethylene should be able to provide a clear indication of the impact that the electronic properties of the imido ligand can have on catalysis.

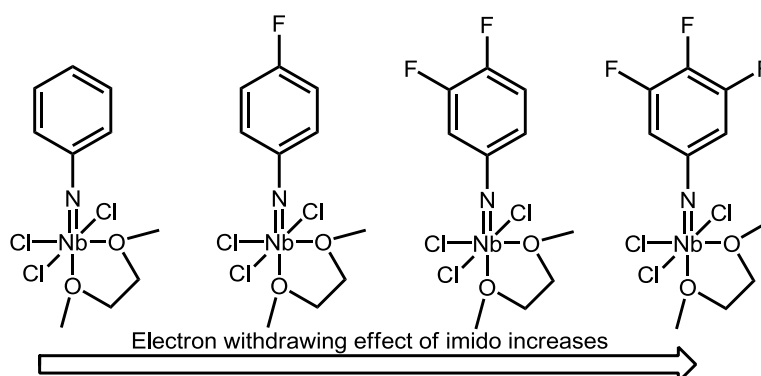


Figure 4.7 A series of niobium imido complexes where the steric hindrance of the imido ligand is kept constant, while their electron withdrawing character is varied

4.4.3 Tantalum-based ethylene oligomerization

4.4.3.1 General remarks

The catalytic behaviour of the tantalum imido pro-initiators **74-77** towards ethylene is presented in Table 4.6. The overall activities and TONs observed for the tantalum systems are ~50% lower than those from their niobium analogues (section 4.4.2). The poorer relative catalytic performance of the tantalum compared to the niobium imido systems is in line with a number of reports in the literature, which identify the same trend.^{18,19} Additionally, in contrast to the results obtained with the niobium imido pro-initiators (section 4.4.2), the analogous tantalum-containing systems afforded very little polymer; the products comprised 1-butene (the only C₄ product) and 1-hexenes (> 60 % of C₆ fraction), something indicative of little olefin isomerization.

Table 4.6 Ethylene oligomerization and polymerization using well-defined Ta imido complexes with EtAlCl₂ co-catalyst^a

Run #	Pro-initiator	Time (min)	TON ^b	Total Act. ^c	Act. to C ₄ ^d	% PE	Act. to PE ^e	Mol % C ₄ (in liq. prod.)	% 1-C ₄ in C ₄	Mol % C ₆ (in liq. prod.)	% 1-C ₆ in C ₆	% Lin in C ₆	wt % C ₈₊ (in liq. prod.)
1	CpTa(NDipp)Cl ₂ (79)	10.0	0.2	1.3	0.9	6.0	0.08	81.9	100.0	11.5	74.0	85.1	11.6
2	Ta(NMes)Cl ₃ (DME) (75)	5.0	1.7	20	14	7.0	1.4	84.0	99.8	15.3	75.6	80.7	1.2
3	Ta(NPh)Cl ₃ (DME) (74)	5.6	2.0	21	17	2.2	0.4	86.5	100.0	12.8	77.8	81.7	1.4
4	Ta(N ⁱ Bu)Cl ₃ (DME) (77)	6.5	2.7	25	19	2.7	0.7	85.7	100.0	13.8	67.4	72.4	0.9
5	Ta(NDipp)Cl ₃ (DME) (76)	7.6	3.2	25	18	8.8	2.2	85.7	100.0	12.4	64.1	68.9	3.5

^a General conditions: 20 μmol Ta complex and 300 μmol EtAlCl₂; PhCl (solvent) 74 mL; 60 °C; ethylene pressure (40 bar); stirrer speed 1000 rpm; nonane standard (1.000 mL); catalytic runs were performed until consumption of C₂H₄ dropped below 0.2 g min⁻¹, at which time reaction was quenched by addition of dilute HCl. ^b TON is reported in kg C₂H₄ (mol Ta)⁻¹ bar⁻¹. ^c Total activity is reported in kg C₂H₄ (mol Nb)⁻¹ h⁻¹ bar⁻¹ and is based on the total ethylene consumption. ^d Activity towards butene formation is reported in kg C₂H₄ (mol Nb)⁻¹ h⁻¹ bar⁻¹. ^e Activity towards PE formation is reported in kg PE (mol Ta)⁻¹ h⁻¹ bar⁻¹. PE = polyethylene.

4.4.3.2 Effect of the imido group on the catalytic activity of the tantalum imido/ EtAlCl_2 systems

According to the data in Table 4.6, all four tantalum imido pro-initiators are similar in terms of their overall activity, their activity towards dimerization, and product selectivity, something that suggests that the imido substituent has little affect. This contrasts to the niobium-based systems where the type of functional group on the imido ligand does considerably influence catalysis (section 4.4.2).

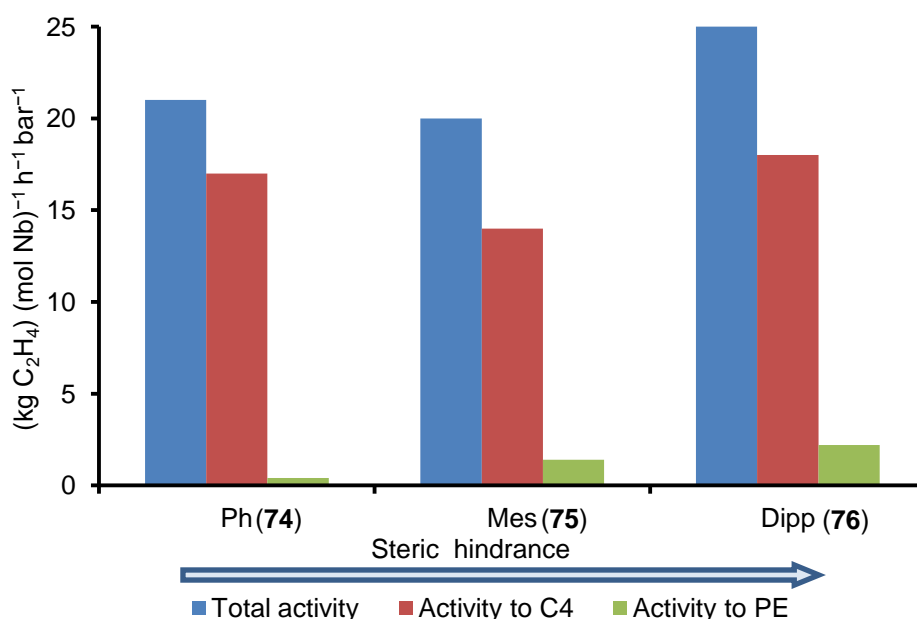


Figure 4.8 Comparison of catalytic activity versus imido ligand substituent of the tantalum pro-initiators based on data from Table 4.6

Figure 4.8 presents a comparison of the overall activity, the activity towards butenes, and the activity towards polymerization as a function of the N-imido substituent of the tantalum pro-initiator complexes **74-76**. These data indicate that the steric demands of the aryl imido ligand do not affect the total activity and the activity towards formation of butenes in a systematic way without any noticeable trends. Nevertheless, although the differences are very small, sterically-demanding ligands on Ta do show a slight preference for polymerization, something also observed for the niobium systems (section 4.4.2) albeit with an activity that is over a magnitude greater (Figure 4.8).

4.4.3.3 Analysis of the polyethylene produced by the tantalum imido/ EtAlCl_2 systems

The properties of the polyethylene produced from the tantalum-based initiator systems based on a DSC analysis are presented in Table 4.7. From the high melting points, densities, and crystallinities of each of the polyethylenes produced, each material has high molecular weight, with a linear structure and low polydispersity, data that together are indicative of HDLPE.^{16,3240,41} Note that the crystallinity is exceptionally high for the polyethylene material obtained from run 1 in Table 4.7 (approaching 100% crystalline).

Table 4.7 Melting points (°C) and crystallinities (%) of the polyethylene produced by the tantalum imido-based catalytic systems determined by DSC^a

Run #	Pro-initiator	Melting point (°C)	Density ^b	Crystallinity (%)
1	Ta(NMes)Cl ₃ (DME) (75)	130.6	0.95	94
2	Ta(NPh)Cl ₃ (DME) (74)	132.0	0.95	68
3	Ta(N ^t Bu)Cl ₃ (DME) (77)	129.6	0.94	77
4	Ta(NDipp)Cl ₃ (DME) (76)	128.7	0.94	80

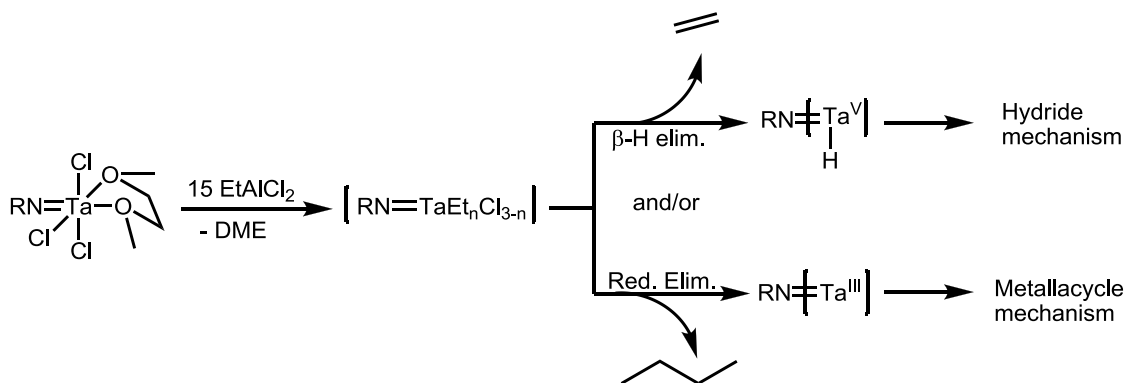
^a General conditions: 20 μmol Ta complex and 300 μmol EtAlCl₂; PhCl (solvent) 74 mL; 60 °C; ethylene pressure (40 bar); stirrer speed 1000 rpm; nonane standard (1.000 mL); catalytic runs were performed until consumption of C₂H₄ dropped below 0.2 g min⁻¹, at which time reaction was quenched by addition of dilute HCl. ^b Densities were calculated from the peak melting point values.³⁹

4.4.3.4 Comparison of the tantalum imido systems with previously reported tantalum-based ethylene oligomerization systems

The catalytic behavior of the tantalum imido-based ethylene oligo-/poly-merization systems described in this chapter differs to some extent from the trimerization systems previously reported (section 4.1.2).⁹⁻¹¹ Specifically, the imido systems exhibit much higher overall activities (up to 25 kg C₂H₄ (mol Ta)⁻¹ h⁻¹ bar⁻¹) compared to the ligand-free and silica-supported tantalum systems reported in the literature (up to 1.8 kg C₂H₄ (mol Ta)⁻¹ h⁻¹ bar⁻¹, see section section 4.1.2). This greater activity of the tantalum imido-based systems can be attributed partly to the presence of the organoimido ligands, which enhance the solubility of the resulting catalytically-active species formed during activation. Another difference between the imido-bound and ligand-free or silica-supported systems is reflected by their product selectivity. In most cases, the ligand-free trimerization systems produce almost exclusively 1-hexene (selectivities between 80%-99%) with small amounts of butenes or polyethylene being produced. Contrastingly, the imido systems **74-77** produce mainly 1-butene with significant amounts of trimer, and only small amounts of polyethylene (see Table 4.6).

4.4.3.5 Mechanistic considerations for tantalum imido-mediated ethylene oligo-/poly-merization

For analogous reasons to those outlined in section 4.4.2, it is difficult to comment on the precise mechanism or the nature of the actual initiator species involved in the catalytic oligo-/poly-merization of ethylene mediated by the tantalum imido systems **74-77**. However, the catalytic trimerization of ethylene initiated by somewhat related tantalum-based pro-initiators (see section 4.1.2) has been reported, allowing parallels to be drawn with the tantalum imido systems described herein.^{8-12,22} In particular, it has been disclosed that the tantalum-mediated oligomerization of ethylene is believed to proceed *via* a Ta(III) metallacyclic mechanism (see section 1.4.2).^{3-6,9-12} This type of pathway could also be accessed by the tantalum imido pro-initiators **74-77** *via* the process described in Scheme 4.14, where reaction of Ta(NR)Cl₃(DME) with excess EtAlCl₂ removes DME, and alkylates the Ta centre. The resulting tantalum alkyl species could then undergo reductive elimination to give a Ta(III) species capable of forming metallacycles *via* oxidative alkene coupling, or could generate a Ta-hydride *via* β-hydride elimination.



Scheme 4.14 Schematic representation of possible activation pathways for the tantalum imido pro-initiators **74-77**

As discussed in detail in section 2.4.1.6, careful examination of the post catalysis organic products can provide insight into which mechanism (step-wise or metallacycle) is dominant for the metal imido-mediated oligomerization of ethylene. For example, from the catalysis results obtained from the tantalum imido-mediated oligomerization of ethylene (Table 4.6), 1-butene is the major product (>81 % of liquid fraction). Additionally, 1-hexene and methyl pentenes are also produced during catalysis with the activated tantalum imido systems (Table 4.8). Hence, using the same rationale employed in section 2.4.1.6.4, a comparison of the predicted versus the experimentally-observed products (**Table 4.9**) indicates that a metallacyclic mechanism provides the best fit to the experimental results (Table 4.6 and Table 4.8). Together, these results are in line with literature reports in which a tantalacyclic mechanism is favored over a tantalum hydride-mediated process.²²

Table 4.8 Composition of the C₆ product fraction from tantalum imido-initiated ethylene oligomerization

Run #	Pro-initiator	% 1-C ₆ in C ₆	% 3Me-1-C ₅ in C ₆	% 2Et-1-C ₄	Others ^a
1	Ta(NMes)Cl ₃ (DME)	75.6	12.1	1.8	10.5
2	Ta(NPh)Cl ₃ (DME)	76.4	12.0	1.5	10.1
3	Ta(N ^t Bu)Cl ₃ (DME)	65.3	13.1	11.6	10.0
4	Ta(NDipp)Cl ₃ (DME)	64.1	14.0	15.9	6.0

^a Consists of at least four unidentified products in similar quantities

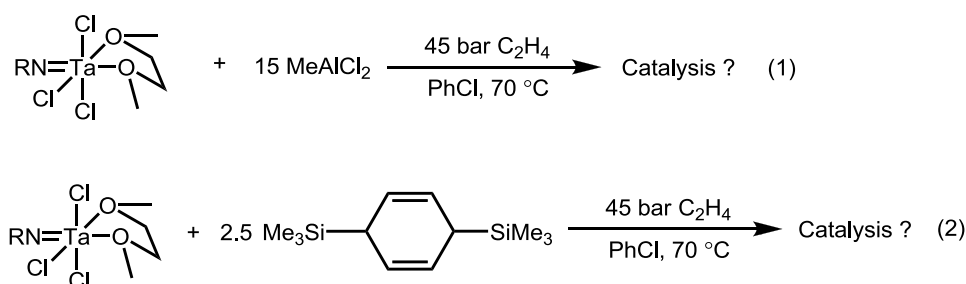
Table 4.9 Comparison of the theoretically- and experimentally-observed organic products produced from various oligomerization mechanisms.

	1-butene	2-butene	1-hexene	2-hexene	3-hexene	3 methyl-1-pentene	3 methyl-2-pentene	2 ethyl-1-butene
M-H with chain walking	✓	✓	✓	✓	✓	✓	✓	✓
M-H without chain walking	✓		✓	✓	✓			✓
Metallacycle	✓		✓	✓	✓	✓		✓
Experimentally observed	✓		✓			✓		✓

4.4.3.6 Future investigations

In order to further assess whether a metal hydride and/or a metallacyclic species is involved in the tantalum imido-mediated catalytic oligomerization of ethylene, two additional experiments are proposed: i) MeAlCl₂ activation of tantalum imido pro-initiators (Scheme 4.15, eq. 1) and ii) use of 3,6-

bis(trimethylsilyl)-1,4-cyclohexadiene (Scheme 4.15, eq. 2) as the activator instead of Al-containing reagents. Both of these activators disfavour the formation of tantalum hydrides, but both are able to reduce Ta(V) to Ta(III) species with simultaneous abstraction of Cl ligands.¹⁰ Thus, if the tantalum imido complexes can be successfully activated under the conditions described in Scheme 4.15, then it is likely that the tantalum imido pro-initiators would provide access to a metallacycle pathway, which could also be the case when they are activated with EtAlCl₂; this is in line with the suggestions made in section 4.4.3.5.



Scheme 4.15 Suggested catalysis experiments that could potentially provide further mechanistic insight on the tantalum imido-catalyzed ethylene oligomerization

4.4.4 Dimerization of 1-hexene using tantalum- and niobium-imido/EtAlCl₂ systems

4.4.4.1 General remarks

The importance of the oligomerization of heavier α -olefins has been outlined in section 1. Consequently, the ability of the tantalum- and niobium-imido/EtAlCl₂ systems described herein for 1-hexene oligomerization has been examined. The results from this set of catalytic experiments are presented in Table 4.10. Note that for reasons explained in detail in sections 1.7.1.2.1 and 2.4.2, only the TONs and 1-hexene conversions were determined for the 1-hexene dimerization systems, rather than catalytic activity.

Table 4.10 1-Hexene dimerization using well-defined Nb and Ta imido pro-initiator complexes with EtAlCl₂ co-catalyst^a

Run #	Pro-initiator	TON ^b	Isom. ^c (%)	Conv. of C ₆ ^d (%)	Mol % in products			Branching selectivity			
					C ₆	C ₁₂	C ₁₈	Linear	Mono-branched	Di-branched	Others
1	Ta(NDipp)Cl ₃ (DME) (76)	12	1.6	4.2	97.9	1.9	0.2	1.36	49.3	44.1	5.20
2	Ta(N ^t Bu)Cl ₃ (DME) (77)	11	5.9	3.0	98.5	1.3	0.1	1.65	50.9	41.6	5.84
3	Nb(N ^t Bu)Cl ₃ (DME) (73)	10	46.2	3.3	98.6	1.3	0.1	27.5	65.2	1.35	5.90
4	Nb(NDipp)Cl ₃ (DME) (72)	12	24.2	3.6	98.2	1.7	0.1	22.8	73.8	0.00	3.45
5	Nb(NPh)Cl ₃ (DME) (70)	44	15.7	12.4	93.7	5.8	0.5	36.6	60.6	0.17	2.63

^a General conditions: 20 μ mol Nb or Ta complex and 300 μ mol EtAlCl₂; PhCl (solvent) 8.50 mL; 60 °C; 1-hexene 12.4 mL (100 mmol); stirrer speed 1000 rpm; nonane standard (1.000 mL); reaction time 240 min after which quenching followed by addition of dilute HCl. ^b TON is reported in (kg C₆H₁₂) (mol TM)⁻¹. ^c Defined as the fraction of terminal alkene that is isomerized to internal alkenes at the end of a run. ^d Defined as the mass% of hexenes converted to oligomers at the end of a run and does not include isomerized 1-hexene.

From the results presented in Table 4.10 it is evident that the tantalum and niobium systems are poor pro-initiators for the dimerization of 1-hexene, giving rise to only low conversions (< 13%) and TONs (<

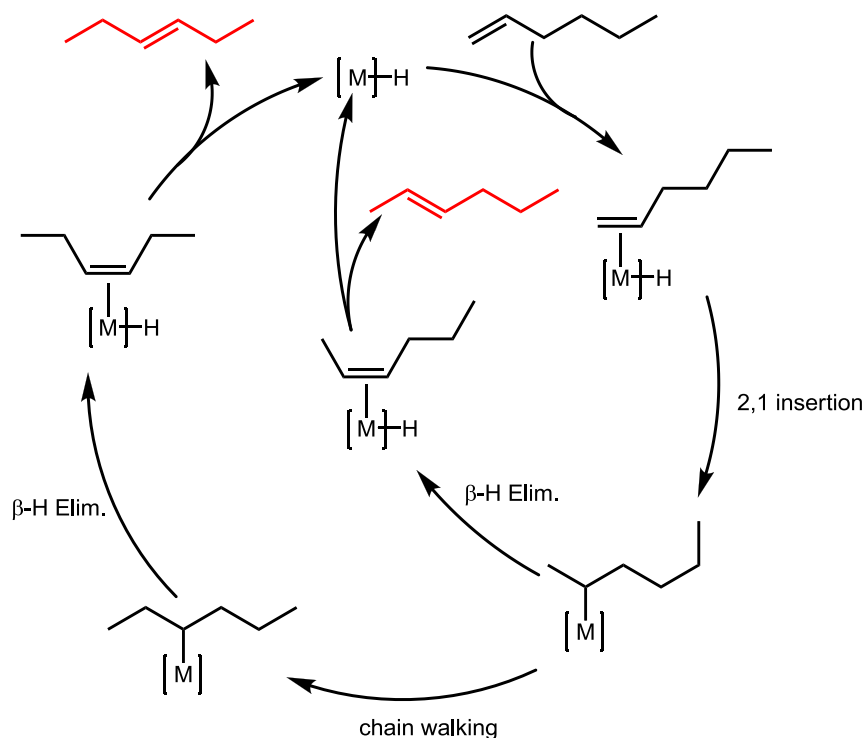
44 (kg C₆H₁₂) (mol TM)⁻¹), *c.f.* 1-hexene dimerization conversions of over 70% and TONs of 224 (kg C₆H₁₂) (mol TM)⁻¹ using *bis*(imino)-pyridine iron pre-catalysts have been reported to date.⁴⁹ The lower activities observed for 1-hexene compared with ethylene dimerization could be attributed to the greater steric bulk of 1-hexene, which prevents efficient metal coordination. It must also be noted that the TONs and conversions obtained for each pro-initiator are comparable, irrespective of the metal and/or imido substituent. The origin of this effect has been attributed to the steric bulk of 1-hexene, which dominates the catalytic efficiency. An exception to this trend are the results from studies involving Nb(NPh)Cl₃(DME) (**70**) (run 5; Table 4.10), a pro-initiator that was found to be four times more active compared to its other niobium and tantalum analogues. The reason for the enhanced activity of complex **70** remains unclear.

With regards to the branching selectivity achieved using the tantalum imido-mediated initiator systems with 1-hexene, approximately equal amounts of mono- and di-branched dodecenes were obtained, with only very small quantities (< 2% of the dimer fraction) of linear products observed. In contrast, the niobium systems mainly produce mono-branched dodecenes (60-70% of the dimers fraction) with significant amounts of linear dodecenes (27-37% of the dimers fraction), but traces of di-branched dimers. These differences in the branching selectivity between the tantalum and niobium systems suggest that the catalysts formed after activation with EtAlCl₂, and the mechanisms in operation, must differ significantly for the two metals. These observations are also in line with the different poly-/oligomerization mechanisms that have been suggested for the niobium and tantalum imido pro-initiators in the previous sections of this chapter (see for example sections 4.4.2.6 and 4.4.3.5).

4.4.4.2 Niobium and tantalum imido-mediated 1-hexene isomerization: mechanistic implications

In the analysis of the products from test runs 1-5 in Table 4.10, only small amounts of dodecenes were observed (< 6 mole%), along with traces of 1-hexene trimers (< 0.5 mole%). However, significant amounts of internal hexenes (up to 46 % of the initial substrate) were also detected in the post catalytic products of 1-hexene dimerization obtained using the niobium imido pro-initiators (runs 3-5; Table 4.10), implying that the systems Nb(NR)Cl₃(DME)/15 EtAlCl₂ are active in the isomerization of 1-hexene to internal hexenes. In contrast, the tantalum pro-initiators are weak 1-hexene isomerization catalysts, converting less than 6% of the substrate to internal hexenes.

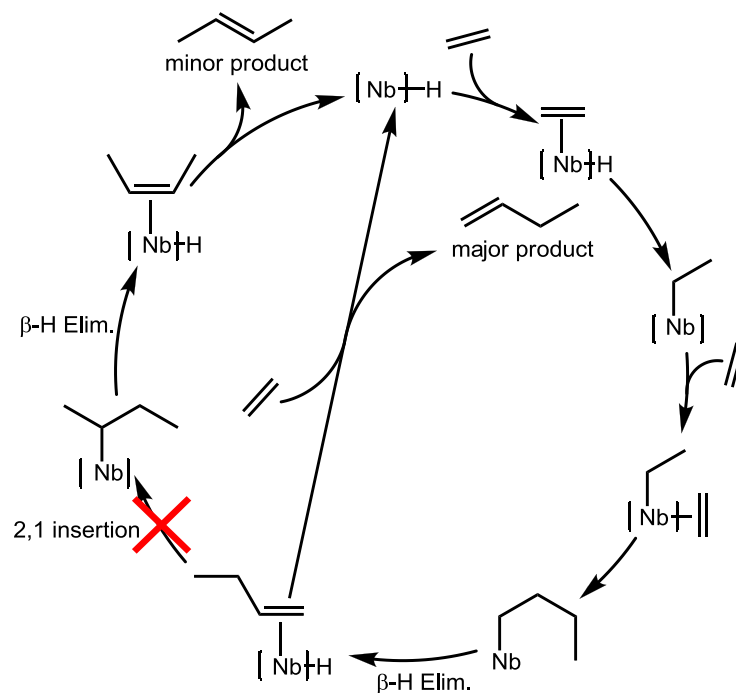
Together, these observations are in agreement with a metallacycle mechanism, as proposed in section 4.4.3.5 for tantalum imido-mediated catalysis, since 1-hexene isomerization is not observed in this case.^{9,10} In contrast, for the niobium imido pro-initiators a metal-hydride intermediate capable of 1-hexene isomerization could also be present. The catalytic cycle for the niobium hydride-mediated 1-hexene isomerization is presented in Scheme 4.16.



Scheme 4.16 Proposed catalytic cycle for the isomerization of 1-hexene to internal hexenes via a niobium hydride

Initial 2,1-insertion affords a niobium alkyl species, which could undergo β -hydride elimination producing 2-hexene, but if chain walking occurs, followed by β -hydride elimination, 3-hexene will be produced. Hence, it is clear that the niobium imido pro-initiators can isomerize α -olefins to internal olefins, possibly via a niobium hydride species. Nevertheless, when ethylene was dimerized by the activated niobium imido systems, the butenes produced consisted almost exclusively of 1-butene (Table 4.4). This apparent contrast can be rationalized by taking into account the high ethylene pressure at which the ethylene poly-/oligo-merization experiments were conducted, in combination with the ease of coordination of ethylene over 1-butene. These two factors will favour displacement of the niobium-bound 1-butene by ethylene, thus preventing a potential 2,1-insertion of 1-butene to the niobium hydride species, a process that can lead to formation of 2-butene (Scheme 4.17). Lastly, it must be noted that the low 1-hexene conversion to dimers obtained using the niobium imido pro-initiators can be partially attributed to the ability of these systems to isomerize the substrate to internal hexenes, which are inert towards dimerization.^{***,48,50}

^{***} The inert character of internal hexenes towards dimerization has also been demonstrated in section 2.4.2.3. For example, no dimerization of *trans*-3-hexene was achieved even in the presence of the highly active ethylene and 1-hexene dimerization system $W(NDipp)_2Cl_2(DME)$ (**27**) /15 $EtAlCl_2$.



Scheme 4.17 Proposed metal hydride catalytic cycle demonstrating the preferential formation of 1-butene over 2-butene in the niobium imido-mediated ethylene dimerization

4.5 Chapter Summary

In this chapter the niobium and tantalum complexes of general formula $M(NR)Cl_3(DME)$ ($M = Nb$, $R = Ph$ (**70**), $R = Mes$ (**71**), $R = Dipp$ (**72**), $R = ^tBu$ (**73**); $M = Ta$, $R = Ph$ (**74**), $R = Mes$ (**75**), $R = Dipp$ (**76**), $R = ^tBu$ (**77**)) were synthesized using variants of literature procedures. The crystallographic studies carried out for each of the new complexes revealed that all the complexes **70-77** were structurally similar, with their interatomic distances and angles being influenced only subtly by the imido substituent employed. Each of the niobium and tantalum imido complexes was found to be able to act as a pre-catalyst in the oligomerization and/or polymerization of ethylene and 1-hexene when activated with 15 equivalents of $EtAlCl_2$. The niobium imido/15 $EtAlCl_2$ systems were able to both dimerize and polymerize ethylene exhibiting moderate activities towards polymerization (based on the Gibson criteria) and reasonable dimerization activities of up to $42 \text{ kg C}_2\text{H}_4 (\text{mol Nb})^{-1} \text{ h}^{-1} \text{ bar}^{-1}$. Additionally, it was found that imido ligands with a greater steric bulk favour ethylene polymerization over dimerization, while the electronic properties of the niobium imido moiety do not influence catalysis significantly.

From a mechanistic perspective, the niobium imido-based ethylene oligo-/poly-merization reaction is complex. Hence, only general conclusions were drawn, such as the presence of two catalytically active systems in the niobium imido catalytic reaction mixture, which can be potentially combined to give rise to tandem catalysis. In contrast to the niobium systems, those employing tantalum displayed lower ethylene oligomerization activities (up to $19 \text{ kg C}_2\text{H}_4 (\text{mol Nb})^{-1} \text{ h}^{-1} \text{ bar}^{-1}$) and very low polymerization activities. Variation of the imido moiety for these tantalum pro-initiators didn't have a significant impact on catalysis. However, from an analysis of the type of oligomers obtained from the tantalum imido-

based catalytic oligomerization of ethylene, a metallacyclic mechanism is suggested to be the main mode of operation for these systems.

Lastly, complexes **70**, **72**, **73**, **76**, and **77** were tested in the dimerization of 1-hexene, but gave rise only to very low conversions of ~3- 2%. However, the low activities obtained using the tantalum pro-initiators towards isomerization of 1-hexene further supported the aforementioned assignment of a metallacyclic mechanism to the tantalum systems, while the high activities towards 1-hexene isomerization obtained for the niobium imido / 15 EtAlCl₂ systems suggest the presence of a niobium hydride species.

4.6 References

- (1) Li, Y. G.; Hong, M.; Zhang, G. B.; Li, Y. S. *Chin. J. Polym. Sci.* **2013**, *31*, 574.
- (2) Breslow, D. S.; Newburg, N. R. *Journal of the American Chemical Society* **1957**, *79*, 5072.
- (3) Fellmann, J. D.; Rupprecht, G. A.; Schrock, R. R. *Journal of the American Chemical Society* **1979**, *101*, 5099.
- (4) McLain, S. J.; Sancho, J.; Schrock, R. R. *Journal of the American Chemical Society* **1979**, *101*, 5451.
- (5) McLain, S. J.; Sancho, J.; Schrock, R. R. *Journal of the American Chemical Society* **1980**, *102*, 5610.
- (6) Schrock, R. R.; McLain, S. J.; Sancho, J. *Pure and Applied Chemistry* **1980**, *52*, 729.
- (7) Chang, B.-H.; Lau, C.-P.; Grubbs, R. H.; Brubaker Jr, C. H. *Journal of Organometallic Chemistry* **1985**, *281*, 213.
- (8) Taoufik, M.; de Mallmann, A.; Prouzet, E.; Saggio, G.; Thivolle-Cazat, J.; Basset, J. M. *Organometallics* **2001**, *20*, 5518.
- (9) Andes, C.; Harkins, S. B.; Murtuza, S.; Oyler, K.; Sen, A. *Journal of the American Chemical Society* **2001**, *123*, 7423.
- (10) Arteaga-Muller, R.; Tsurugi, H.; Saito, T.; Yanagawa, M.; Oda, S.; Mashima, K. *Journal of the American Chemical Society* **2009**, *131*, 5370.
- (11) Chen, Y.; Callens, E.; Abou-Hamad, E.; Merle, N.; White, A. J. P.; Taoufik, M.; Coperet, C.; Le Roux, E.; Basset, J. M. *Angewandte Chemie-International Edition* **2012**, *51*, 11886.
- (12) Yu, Z. X.; Houk, K. N. *Angewandte Chemie-International Edition* **2003**, *42*, 808.
- (13) Galletti, A. M. R.; Pampaloni, G. *Coordination Chemistry Reviews* **2010**, *254*, 525.
- (14) Marchetti, F.; Pampaloni, G.; Patil, Y.; Galletti, A. M. R.; Hayatifar, M. *Polymer International* **2011**, *60*, 1722.
- (15) Marchetti, F.; Pampaloni, G.; Patil, Y.; Galletti, A. M. R.; Renili, F.; Zacchini, S. *Organometallics* **2011**, *30*, 1682.
- (16) Marchetti, F.; Pampaloni, G.; Patil, Y.; Maria, A.; Galletti, R.; Zacchini, S. *Journal of Polymer Science Part a-Polymer Chemistry* **2011**, *49*, 1664.
- (17) Turner, H. W.; Schrock, R. R.; Fellmann, J. D.; Holmes, S. J. *Journal of the American Chemical Society* **1983**, *105*, 4942.
- (18) Mashima, K.; Fujikawa, S.; Tanaka, Y.; Urata, H.; Oshiki, T.; Tanaka, E.; Nakamura, A. *Organometallics* **1995**, *14*, 2633.
- (19) Redshaw, C.; Rowan, M.; Homden, D. M.; Elsegood, M. R. L.; Yamato, T.; Perez-Casas, C. *Chemistry-a European Journal* **2007**, *13*, 10129.
- (20) Murtuza, S.; Harkins, S. B.; Long, G. S.; Sen, A. *Journal of the American Chemical Society* **2000**, *122*, 1867.
- (21) Hakala, K.; Lofgren, B.; Polamo, M.; Leskela, M. *Macromol. Rapid Commun.* **1997**, *18*, 635.
- (22) Chen, Y.; Credendino, R.; Callens, E.; Atiqullah, M.; Al-Harhi, M. A.; Cavallo, L.; Basset, J.-M. *ACS Catal* **2013**, 1360.
- (23) Trofimenko, S. *Chemical Reviews* **1993**, *93*, 943.
- (24) Sundermeyer, J.; Putterlik, J.; Foth, M.; Field, J. S.; Ramesar, N. *Chemische Berichte* **1994**, *127*, 1201.
- (25) Michiue, K.; Oshiki, T.; Takai, K.; Mitani, M.; Fujita, T. *Organometallics* **2009**, *28*, 6450.
- (26) Antonelli, D. M.; Leins, A.; Stryker, J. M. *Organometallics* **1997**, *16*, 2500.
- (27) Korolev, A. V.; Rheingold, A. L.; Williams, D. S. *Inorganic Chemistry* **1997**, *36*, 2647.

- (28) Williams, D. N.; Mitchell, J. P.; Poole, A. D.; Siemeling, U.; Clegg, W.; Hockless, D. C. R.; Oneil, P. A.; Gibson, V. C. *Journal of the Chemical Society-Dalton Transactions* **1992**, 739.
- (29) Nikonov, G. L.; Mountford, P.; Ignatov, S. K.; Green, J. C.; Leech, M. A.; Kuzmina, L. G.; Razuvaev, A. G.; Rees, N. H.; Blake, A. J.; Howard, J. A. K.; Lemenovskii, D. A. *Journal of the Chemical Society-Dalton Transactions* **2001**, 2903.
- (30) Heinselman, K. S.; Miskowski, V. M.; Geib, S. J.; Wang, L. C.; Hopkins, M. D. *Inorganic Chemistry* **1997**, 36, 5530.
- (31) Wigley, D. E. In *Progress in Inorganic Chemistry*; John Wiley & Sons, Inc.: 2007, p 239.
- (32) Lyne, P. D.; Mingos, D. M. P. *Journal of Organometallic Chemistry* **1994**, 478, 141.
- (33) Clark, G. R.; Nielson, A. J.; Rickard, C. E. F. *Journal of the Chemical Society-Dalton Transactions* **1995**, 1907.
- (34) Wright, W. R. H., PhD Thesis, Durham University, 2009.
- (35) Britovsek, G. J. P.; Gibson, V. C.; Wass, D. F. *Angewandte Chemie-International Edition* **1999**, 38, 428.
- (36) Coles, M. P.; Dalby, C. I.; Gibson, V. C.; Little, I. R.; Marshall, E. L.; da Costa, M. H. R.; Mastroianni, S. *Journal of Organometallic Chemistry* **1999**, 591, 78.
- (37) Speight, J. G., *Lange's Handbook of Chemistry*; 16 ed., McGraw-Hill, 2005.
- (38) Jaffart, J.; Nayral, C.; Choukroun, R.; Mathieu, R.; Etienne, M. *European Journal of Inorganic Chemistry* **1998**, 425.
- (39) Chai, C. K.; Frye, C. J. 2003; Vol. US 6,642,339 B1.
- (40) Gelfer, Y.; Winter, H. H. *Macromolecules* **1999**, 32, 8974.
- (41) Furumiya, A.; Akana, Y.; Ushida, Y.; Masuda, T.; Nakajima, A. *Pure and Applied Chemistry* **1985**, 57, 823.
- (42) Zhu, B.; Guo, C.; Liu, Z.; Yin, Y. *Journal of Applied Polymer Science* **2004**, 94, 2451.
- (43) Komon, Z. J. A.; Diamond, G. M.; Leclerc, M. K.; Murphy, V.; Okazaki, M.; Bazan, G. C. *Journal of the American Chemical Society* **2002**, 124, 15280.
- (44) Komon, Z. J. A.; Bu, X.; Bazan, G. C. *Journal of the American Chemical Society* **2000**, 122, 1830.
- (45) Frediani, M.; Piel, C.; Kaminsky, W.; Bianchini, C.; Rosi, L. *Macromolecular Symposia* **2006**, 236, 124.
- (46) Tomson, N. C.; Arnold, J.; Bergman, R. G. *Organometallics* **2010**, 29, 5010.
- (47) Gianetti, T. L.; Nocton, G.; Minasian, S. G.; Tomson, N. C.; Kilcoyne, A. L. D.; Kozimor, S. A.; Shuh, D. K.; Tyliszczak, T.; Bergman, R. G.; Arnold, J. *Journal of the American Chemical Society* **2013**, 135, 3224.
- (48) Ittel, S. D.; Johnson, L. K.; Brookhart, M. *Chemical Reviews* **2000**, 100, 1169.
- (49) Small, B. L.; Marcucci, A. J. *Organometallics* **2001**, 20, 5738.
- (50) Christoffers, J.; Bergman, R. G. *Journal of the American Chemical Society* **1996**, 118, 4715.

5 Experimental details

5.1 General details

All operations were conducted under an atmosphere of dry nitrogen using standard Schlenk and cannula techniques, or in a Saffron Scientific nitrogen-filled glove box, unless otherwise stated. Bulk solvents were purified using an Innovative Technologies SPS facility, except chlorobenzene, which was dried by distillation from calcium hydride. All solvents were degassed prior to use, unless otherwise stated. CD_2Cl_2 , CD_3COCD_3 , PhCl-d_5 , and $\text{C}_6\text{D}_5\text{CD}_3$ were purchased from Goss Scientific while C_6D_6 , and CDCl_3 from Apollo Scientific. Each deuterated solvent was distilled from CaH_2 , degassed and stored under nitrogen. EtAlCl_2 , Et_3Al , MeAlCl_2 , Me_3Al , Me_2AlCl , WCl_6 , TaCl_5 , KBH_4 , NaBH_4 , $\text{NbCl}_3(\text{DME})$ TppNH_2 , TtbpNH_2 , $(n\text{-Oct})_4\text{NBr}$, $(n\text{-Oct})_4\text{NCl}$, Et_4NCl , $\text{Et}_3\text{N}\cdot\text{HCl}$, and $n\text{-BuLi}$ solution (2.5M in hexanes) were purchased from Sigma-Aldrich and used as received. $\text{Mes}^{\text{F}}\text{NH}_2$, and $^i\text{Pr}^{\text{F}}\text{NH}_2$ were purchased from Atlantic research chemicals and Apollo scientific respectively and used as received. TfpNCO , 1,4-diiodobutane and Bu_3SnCl were purchased from Sigma-Aldrich and degassed prior to use. DippNH_2 , $^t\text{BuNH}_2$, 1-Hexene, 1-dodecene, *trans*-3-hexene, 2-methyl-1-pentene, $\text{Ph}^{\text{F}}\text{NCO}$, and 1-pentene were purchased from Sigma-Aldrich, distilled from CaH_2 and degassed prior to use. Cyclopentadiene was obtained *via* reactive distillation from dicyclopentadiene, which was purchased from Sigma-Aldrich. DABCO was purchased from Sigma-Aldrich and sublimed prior to use. Triethylamine was purchased from Sigma-Aldrich, dried over KOH, distilled and degassed prior to use. NbCl_5 , TfpNH_2 , DnpNH_2 , PfpNH_2 , and ZnCl_2 , were purchased from Alfa-Aesar and used as received. DippNCO , TMS_2O , PhNCO , $^t\text{BuNCO}$, EtNCO , $^i\text{PrNCO}$, and TMSCl were purchased from Alfa-Aesar and degassed prior to use. Nonane, MesNH_2 , PhNH_2 , pyridine, $^i\text{PrNH}_2$, and 2,6-lutidine were purchased from Alfa-Aesar, dried over calcium hydride, distilled and degassed prior to use.

The following compounds were all prepared in Durham according to multi-step literature procedures: WO_2Cl_2 ,¹ WOCl_4 ,¹ $\text{W}(\text{NPh}^{\text{F}})\text{Cl}_4(\text{THF})$,² $[\text{W}(\text{NDipp})\text{Cl}_4]_2$,³ $\text{W}(\text{NDipp})\text{Cl}_4(\text{THF})$,³ $\text{W}(\text{NDipp})_2\text{Cl}_2(\text{DME})$,⁴ $\text{W}(\text{NEt})\text{Cl}_4(\text{THF})$,⁵ $[\text{W}(\text{NEt})\text{Cl}_4]_2$,⁵ $\text{W}(\text{N}^i\text{Pr})\text{Cl}_4(\text{THF})$,³ CpSnBu_3 ,⁶ CpNbCl_4 ,⁷ CpTaCl_4 ,⁷ DippNHTMS ,⁸ $\text{CpNb}(\text{NDipp})\text{Cl}_2$,⁹ $\text{CpTa}(\text{NDipp})\text{Cl}_2$,¹⁰ $\text{Nb}(\text{NDipp})\text{Cl}_3(\text{DME})$,¹¹ $\text{Nb}(\text{N}^t\text{Bu})\text{Cl}_3(\text{DME})$,¹¹ $\text{Nb}(\text{NPh})\text{Cl}_3(\text{DME})$,¹¹ $\text{Ta}(\text{NDipp})\text{Cl}_3(\text{DME})$,¹¹ $\text{Ta}(\text{N}^t\text{Bu})\text{Cl}_3(\text{DME})$,¹¹ $\text{Ta}(\text{NPh})\text{Cl}_3(\text{DME})$,¹¹ $[\text{W}(\text{NPh})\text{Cl}_4]_2$,⁵ $\text{W}(\text{NPh})\text{Cl}_4(\text{THF})$,⁵ $\text{W}(\text{NPh})\text{Cl}_2(\text{PMe}_3)_3$,⁵ $\text{CpNb}(\text{NDipp})\text{Cl}_2$,⁹ PMe_3 ,¹² $\text{Ta}(\text{NDipp})\text{Cl}_3(\text{DME})$,¹¹ $^t\text{BuNHTMS}$,¹³ $\text{W}(\text{N}^t\text{Bu})_2\text{Cl}_2\text{py}_2$,¹⁴ $\text{LiCH}_2\text{CH}_2\text{CH}_2\text{CH}_2\text{Li}$,¹⁵ $\text{W}(\text{NDipp})\text{Cl}_2(\text{PMe}_3)_3$,¹⁶ and $\text{W}(\text{NDipp})_2(\text{PMe}_3)_3$.¹⁷

Solution phase NMR spectra were collected on a Varian Mercury 400 or 200, a Varian Inova 500, a Varian VNMR-700 or 600 and a Bruker Advance 400 at ambient probe temperatures (290 K) unless otherwise stated. Chemical shifts were referenced to residual proton impurities in the deuterated solvent (^1H), ^{13}C shift of the solvent (^{13}C) or to external 85% H_3PO_4 aqueous solution (^{31}P). Solvent proton shifts (ppm): CDCl_3 , 7.26 (s); C_6D_6 , 7.16 (s); CD_2Cl_2 , 5.32 (s); THF- d_8 , 3.58 (br), 1.72 (br); $\text{C}_6\text{D}_5\text{CD}_3$, 7.09 (m), 7.01 (s), 6.97 (quin), 2.08 (quin); $\text{C}_6\text{D}_5\text{Cl}$, 7.14 (m), 6.99 (m), 6.96 (m). Solvent

carbon shifts (ppm): CDCl_3 , 77.16 (t); C_6D_6 , 128.06 (t); CD_2Cl_2 , 53.84 (quin); THF- d_8 67.21 (quin), 25.31 (br); $\text{C}_6\text{D}_5\text{CD}_3$, 137.48 (s), 128.87 (t), 127.96 (t), 125.13 (t), 20.43 (sept); $\text{C}_6\text{D}_5\text{Cl}$, 134.19 (s), 129.26 (t), 128.25 (t), 125.96 (t). ^1H and ^{13}C NMR spectra were assigned with the aid of COSY, HSQC and HMBC experiments. Chemical shifts are reported in ppm and coupling constants in Hz.

Mass spectra (ES) were obtained using a Waters TQD mass spectrometer. GC-MS analysis was performed on a Thermo-Finnigan Trace GC-MS mass spectrometric instrument, while ASAP (Atmospheric Solids Analysis Probe) mass spectra were acquired with a Waters Xevo QToF mass spectrometer.

GC-FID analyses were conducted on a Perkin Elmer Clarus 400 GC or an Agilent Technologies 6890N GC instrument both equipped with a PONA column (50 m \times 0.20 mm \times 0.50 μm), and supplied with H_2 as a carrier gas. Hydrogenative GC-FID analysis was performed using an Agilent Technologies 6890N or a Perkin Elmer Clarus 400 GC System equipped an inlet liner packed with hydrogenating catalyst (Pt on Chromosorb W at 200 $^\circ\text{C}$) and PONA column (50 m \times 0.20 mm \times 0.50 μm).¹⁸

DSC analysis of polyethylene was performed on a TA Instruments DSC Q1000. The samples were heated from room temperature to 200 $^\circ\text{C}$ with a heating rate of 10 $^\circ\text{C}/\text{min}$. The temperature of each sample was held constant at 200 $^\circ\text{C}$ for five minutes in order to erase its thermal history and then cooled down to 10 $^\circ\text{C}$ with a cooling rate of 10 $^\circ\text{C}/\text{min}$. The samples were then kept at 10 $^\circ\text{C}$ for five minutes followed by re-heating at 10 $^\circ\text{C}/\text{min}$ to 200 $^\circ\text{C}$. The peak melting temperature and the crystallinity were determined from the final heating cycle¹⁹⁻²¹ while the density of each resin was calculated from the peak melting temperature according to literature procedures.²²

Catalysis experiments with ethylene were performed in 250 mL volume Buchi Miniclaves or in a 1.2 L volume Premex Pinto autoclave equipped with stainless steel vessels with integral thermal-fluid jackets, internal cooling coils and mechanical mixing via gas-entraining stirrers, and were all carried out at Sasol UK Ltd., St. Andrews. Ethylene (Grade 4.5) was supplied by Linde and passed through oxygen and moisture scrubbing columns prior to use; ethylene flow was measured using a Siemens Sitrans F C Massflo system (Mass 6000-Mass 2100) and the data logged. All catalytic tests were allowed to run until ethylene uptake had ceased.

5.2 Synthesis

All procedures described in this section were carried out using standard Schlenk techniques unless otherwise stated. The additions of all reagents were performed with vigorous stirring, which was achieved using a Teflon stirrer bar and a magnetic stirrer hotplate.

5.2.1 Bis-imido tungsten complexes

5.2.1.1 W(NDipp)₂Cl₂(DME) (27) from W(NDipp)Cl₄(THF) (59) and DABCO

W(NDipp)₂Cl₂(DME) (27) was synthesized using the procedure described in section 5.2.1.8 with W(NDipp)Cl₄(THF) (59) (500 mg, 0.87 mmol), DippNH₂ (164 μ L, 0.87 mmol) and DABCO (197 mg, 1.75 mmol). **Unoptimized yield** (425 mg, 70.3%).

5.2.1.2 W(NTfp)₂Cl₂(DME) (28)

W(NTfp)₂Cl₂(DME) (28) was synthesized using a modification of the procedure used for the preparation of W(NDipp)₂Cl₂(DME) (27) as described by Schrock *et al.*,⁴ by suspending WO₂Cl₂ (1.95 g, 6.85 mmol) in DME (2.9 mL) and sequentially adding TMSCl (9.25 mL, 72.5 mmol), 2,6-lutidine (3.27 mL, 28.1 mmol), and TfpNH₂ (2.00 g, 13.6 mmol). The mixture was heated at 80 °C for 7 days resulting in a colour change from pale yellow to dark orange-red along with formation of a precipitate. Following filtration of the mixture the remaining solid was washed with DME until the washings were colourless. The filtrate and washings were combined, condensed and stored at -30 °C for 5 hours during which time a white precipitate formed, which was removed *via* filtration. The filtrate was then dried under reduced pressure resulting in a dark red oil that, after being left standing for 12 hours, yielded crystals of W(NTfp)₂Cl₂(DME) (28). This complex can be further purified by recrystallization from a DCM solution by slow evaporation. **Unoptimized yield** (2.33 g, 54 %).

¹H NMR (700 MHz, C₆D₆) δ = 6.15 (t, ³J_{FF} = 7.2, 2H, H_m), 3.67 (s, 6H, OCH₃), 3.11 (s, 4H, OCH₂). **¹³C NMR** (176 MHz, C₆D₆) δ = 159.86 (dt, ¹J_{CF} = 249.9, ³J_{CF} = 14.1, C_p), 159.38 (ddd, ¹J_{CF} = 253.4, ³J_{CF} = 15.8, ³J_{CF'} = 6.2, C_o), 99.81 (m, C_m), 71.37 (s, OCH₂), 64.77 (s, OCH₃). **¹⁹F NMR** (188 MHz, C₆D₆) = -110.0 (sept, ³J_{HF} = 8.7, ⁴J_{FF} = 4.0, 1F, F_p), -116.3 (m, 2F, F_o).

5.2.1.3 W(NPfp)₂Cl₂(DME) (29)

The title complex was prepared using a procedure analogous to that described for W(NTfp)₂Cl₂(DME) (28) (section 5.2.1.2). WO₂Cl₂ (2.35 g, 8.19 mmol) was treated with TMSCl (11.1 mL, 87.3 mmol), 2,6-lutidine (3.94 mL, 33.8 mmol), and PfpNH₂ (3.00 g, 16.4 mmol) in DME (3.6 mL) to give W(NPfp)₂Cl₂(DME) in the form of orange crystals. **Unoptimized yield** (3.93 g, 68 %).

¹H NMR (600 MHz, C₆D₆) δ = 3.60 (s, 6H, OCH₃), 3.07 (s, 4H, OCH₂). **¹³C NMR** (151 MHz, C₆D₆) δ = 144.52 (dm, ¹J_{CF} = 250.8, C_o), 140.29 (dm, ¹J_{CF} = 257.2, C_o or C_m), 136.94 (dm, ¹J_{CF} = 250.1, C_o or C_m), 71.59 (s, OCH₂), 65.06 (s, OCH₃). **¹⁹F NMR** (564 MHz, C₆D₆) = -149.0 (dd, ³J_{FF} = 21.1, ⁴J_{FF} = 4.4, 2F, F_o), -157.9 (t, ³J_{FF} = 21.9, 1F, F_p), -164.1 (td, ³J_{FF} = 23.3, ⁴J_{FF} = 5.9, 2F, F_m).

5.2.1.4 W(NMes^F)₂Cl₂(DME) (30)

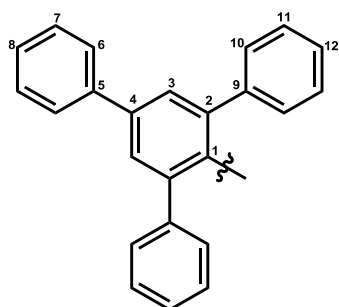
W(Mes^F)₂Cl₂(DME) (**30**) was synthesized using a methodology modified from that used to prepare W(NTfp)₂Cl₂(DME) (section 5.2.1.2). Thus, WO₂Cl₂ (3.52 g, 1.23 mmol) was treated with TMSCl (1.67 mL, 13.1 mmol), 2,6-lutidine (0.59 mL, 5.09 mmol), and Mes^FNH₂ (729 mg, 2.45 mmol) in DME (0.5 mL) to give W(NMes^F)₂Cl₂(DME) in the form of orange crystals. **Unoptimized yield** (661 mg, 58 %).

¹H NMR (600 MHz, C₆D₆) δ = 7.86 (s, br, 2H, H_m), 3.30 (s, 6H, OCH₃), 3.02 (s, 4H, OCH₂). ¹³C NMR (151 MHz, C₆D₆) δ = 153.60 (s, C_{ipso}), 127.26 (s, br, C_m), 126.94 (q, ²J_{CF} = 32.4, C_o), 125.47 (q, ²J_{CF} = 34.5, C_p), 123.10 (q, ¹J_{CF} = 272.4, (CF₃)_o or (CF₃)_m), 122.51 (q, ¹J_{CF} = 274.1, (CF₃)_o or (CF₃)_m), 71.93 (s, OCH₂), 64.18 (s,br, OCH₃). ¹⁹F NMR (564 MHz, C₆D₆) = -58.8 (s, (CF₃)_o), -62.5 (s, (CF₃)_p).

5.2.1.5 W(NTpp)₂Cl₂(DME) (31)

The title complex was prepared *via* a procedure analogous to that described for the synthesis of W(NTfp)₂Cl₂(DME) (**28**) (section 5.2.1.2): WO₂Cl₂ (447 mg, 1.56 mmol) was treated with TMSCl (2.13 mL, 16.7 mmol), 2,6-lutidine (0.75 mL, 6.46 mmol), and TppNH₂ (1.00 g, 3.12 mmol) in DME (0.7 mL). This resulted in a red solution, which was filtered whilst hot to remove a white precipitate. The resulting solid was washed with hot DME until the washings were colourless. The washings were then combined with the filtrate and the resulting solution condensed to half its volume, inducing formation of W(NTpp)₂Cl₂(DME) (**31**) as red crystals that can be further purified by recrystallization from hot DME. **Unoptimized yield** (953 mg, 62 %).

¹H NMR (600 MHz, C₆D₆) δ = 7.60 (s, 4H, H₃), 7.59 (d, ³J_{HH} = 8.5, 8H, H₁₀), 7.43 (m, 4H, H₆), 7.30 (t, ³J_{HH} = 7.7, 8H, H₁₁), 7.22 (m, 4H, H₇), 7.16 (m, 4H, H₁₂), 7.13 (m, 2H, H₈), 2.91 (s, 4H, OCH₂), 2.85 (s, 6H, OCH₃). ¹³C NMR (151 MHz, C₆D₆) δ = 150.95 (s, C₂), 141.07 (s, C₁), 140.37 (s, C₉ or C₅), 140.09 (s, C₉ or C₅), 137.48 (s, C₄), 132.11 (s, C₁₀), 129.07 (s, C₃ or C₇), 129.04 (s, C₃ or C₇), 127.70 (s, C₁₁), 127.57 (s, C₈), 127.50 (s, C₆), 127.18 (s, C₁₂), 71.21 (s, OCH₂), 61.71 (s, OCH₃).



5.2.1.6 W(NDipp)₂Cl₂(PMe₃) (40)

W(NDipp)₂Cl₂(DME) (**27**) (500 mg, 0.72 mmol) was dissolved in toluene (15 mL) and PMe₃ (0.1 mL, 0.97 mmol) subsequently added *via* vacuum transfer. This resulted in a dark red solution, which was left stirring for 20 hours. The solution was then condensed and stored at -78 °C for 24 hours after

which time a yellow powder had formed. The yellow powder was isolated by filtration, dissolved in DCM and layered with pentane yielding pure $W(\text{NDipp})_2\text{Cl}_2(\text{PMe}_3)$ (**40**) in the form of orange crystals, which were isolated by decanting the supernatant solution. **Unoptimized yield** (299 mg, 55 %).

^1H NMR (700 MHz, CD_2Cl_2) δ = 7.18 (d, $^3J_{\text{HH}} = 7.7$, 2H, $\text{Dipp}H_m$), 7.05 (t, $^3J_{\text{HH}} = 7.7$, 1H, $\text{Dipp}H_p$), 3.52 (sept., $^3J_{\text{HH}} = 6.8$, 2H, $\text{CH}(\text{CH}_3)_2$), 1.67 (d, $^2J_{\text{PH}} = 10.6$, 9H, $\text{P}(\text{CH}_3)_3$), 1.14 (d, $^3J_{\text{HH}} = 6.8$, 12H, $\text{CH}(\text{CH}_3)_2$ axial or equatorial), 1.11 (d, $^3J_{\text{HH}} = 6.8$, 12H, $\text{CH}(\text{CH}_3)_2$ axial or equatorial). **^{13}C NMR** (176 MHz, CD_2Cl_2) δ = 151.11 (s, $\text{Dipp}C_{\text{ipso}}$ axial or equatorial), 151.13 (s, $\text{Dipp}C_{\text{ipso}}$ axial or equatorial), 144.98 (s, $\text{Dipp}C_o$ axial or equatorial), 144.97 (s, $\text{Dipp}C_o$ axial or equatorial), 128.07 (s, $\text{Dipp}C_p$), 122.59 (s, $\text{Dipp}C_m$), 28.37 (s, $\text{CH}(\text{CH}_3)_2$), 24.40 (s, $\text{CH}(\text{CH}_3)_2$ axial or equatorial), 24.03 (s, $\text{CH}(\text{CH}_3)_2$ axial or equatorial), 14.14 (d, $^1J_{\text{PC}} = 33.9$). **^{31}P NMR** (283 MHz, CD_2Cl_2) = 11.1 (t, $^1J_{\text{PW}} = 841.1$).

5.2.1.7 $W(\text{NDipp})_2\text{Cl}_2(\text{py})_2$ (**39**)

The title complex was prepared by dissolving $W(\text{NDipp})_2\text{Cl}_2(\text{DME})$ (**27**) (500 mg, 0.72 mmol) in DCM (10 mL) followed by addition of pyridine (230 μL , 2.88 mmol). The dark red solution that formed was stirred for 3 hours and all volatile components removed *in vacuo*. The resulting red solid was washed with hexane and re-dissolved in DCM (3 mL). Addition of hexane to the DCM solution followed by cooling at -78 °C resulted in the precipitation of the product as a fine red powder. Single crystals of $W(\text{NDipp})_2\text{Cl}_2(\text{py})_2$ (**39**) can be obtained from a DCM solution of the compound *via* solvent evaporation. **Conversion** (100 %).

^1H NMR (700 MHz, C_6D_6) δ = 9.04 (d, $^3J_{\text{HH}} = 4.6$, 2H, $\text{py}H_o$), 7.19 (d, $^3J_{\text{HH}} = 7.7$, 2H, $\text{Dipp}H_m$), 6.88 (t, $^3J_{\text{HH}} = 7.6$, 1H, $\text{Dipp}H_p$), 6.81 (t, $^3J_{\text{HH}} = 7.5$, 1H, $\text{py}H_p$), 6.41 (t, $^3J_{\text{HH}} = 6.2$, 2H, $\text{py}H_m$), 4.26 (sept., $^3J_{\text{HH}} = 6.8$, 2H, $\text{CH}(\text{CH}_3)_2$), 1.27 (d, $^3J_{\text{HH}} = 6.8$, 12H, $\text{CH}(\text{CH}_3)_2$). **^{13}C NMR** (176 MHz, C_6D_6) δ = 152.58 (s, $\text{py}C_o$), 151.97 (s, $\text{Dipp}C_{\text{ipso}}$), 144.29 (s, $\text{Dipp}C_o$), 137.71 (s, $\text{py}C_p$), 125.27 (s, $\text{Dipp}C_p$), 123.89 (s, $\text{py}C_m$), 122.78 (s, $\text{Dipp}C_m$), 27.66 (s, $\text{CH}(\text{CH}_3)_2$), 25.03 (s, $\text{CH}(\text{CH}_3)_2$).

5.2.1.8 $W(\text{NDipp})(\text{N}^t\text{Bu})\text{Cl}_2(\text{DME})$ (**33**)

The title complex was synthesised in the following manner: $W(\text{NDipp})\text{Cl}_4(\text{THF})$ (**59**) (1.00 g, 1.75 mmol) was dissolved in DME (10 mL) followed by addition of $^t\text{BuNH}_2$ (184 μL , 1.75 mmol) and DABCO (393 mg, 3.50 mmol). The mixture was stirred for 20 hours during which time a colour change occurred from dark green to orange along with the formation of a white precipitate, which was isolated *via* filtration. The filtrate was then dried under reduced pressure resulting in an orange microcrystalline solid of $W(\text{NDipp})(\text{N}^t\text{Bu})\text{Cl}_2(\text{DME})$. Single crystals of $W(\text{NDipp})(\text{N}^t\text{Bu})\text{Cl}_2(\text{DME})$ (**33**) were grown by storing a solution of $W(\text{NDipp})(\text{N}^t\text{Bu})\text{Cl}_2(\text{DME})$ (**33**) in a DCM/pentane mixture at -30 °C for 24 hours. **Unoptimized yield** (0.77 g, 74.6%).

^1H NMR (400 MHz, C_6D_6) δ = 7.25 (d, $^3J_{\text{HH}} = 7.7$, 2H, H_m), 6.93 (t, $^3J_{\text{HH}} = 7.7$, 1H, H_o), 4.31 (sept., $^3J_{\text{HH}} = 6.7$, 2H, $\text{CH}(\text{CH}_3)_2$), 3.43 (s, 6H, OCH_3), 3.09 (s, 4H, OCH_2), 1.47 (d, $^3J_{\text{HH}} = 6.7$, 12H, $\text{CH}(\text{CH}_3)_2$), 1.30 (s, 9H, $\text{C}(\text{CH}_3)_3$). **^{13}C NMR** (101 MHz, C_6D_6) δ = 152.17 (s, C_{ipso}), 143.75 (s, C_o), 124.87 (s, C_p),

122.89 (s, C_m), 71.15 (s, OCH₃), 70.27 (s, CCH₃) 62.80 (s, OCH₂), 31.10 (s, C(CH₃)₃), 27.84 (s, CH(CH₃)₂), 25.22 (s, CH(CH₃)₂).

5.2.1.9 W(NDipp)(NMe_s)Cl₂(DME) (34)

W(NDipp)(NMe_s)Cl₂(DME) (**34**) was synthesized using the procedure used for the preparation of W(NDipp)(N^tBu)Cl₂(DME) (**33**) (section 5.2.1.8) with W(NDipp)Cl₄(THF) (**59**) (500 mg, 0.87 mmol), Me_sNH₂ (122 μL, 0.87 mmol) and DABCO (197 mg, 1.75 mmol). W(NDipp)(NMe_s)Cl₂(DME) (**34**) can be recrystallized from a DCM/Hexane solution at -30 °C. **Unoptimized yield** (291 mg, 51%).

¹H NMR (600 MHz, C₆D₆) δ = 7.17 (d, ³J_{HH} = 7.7, 2H, DippH_m), 6.88 (t, ³J_{HH} = 7.7, 1H, DippH_o), 6.70 (s, 2H, Me_sH_m), 4.35 (sept, ³J_{HH} = 6.8, 2H, CH(CH₃)₂), 3.46 (s, 6H, OCH₃), 3.10 (s, 4H, OCH₂), 2.72 (s, 6H, Me_sC_oCH₃), 2.17 (s, 3H, Me_sC_pCH₃), 1.33 (d, ³J_{HH} = 6.8, 12H, CH(CH₃)₂). **¹³C NMR** (151 MHz, C₆D₆) δ = 152.00 (s, Me_sC_{ipso}), 151.41 (s, DippC_{ipso}), 145.53 (s, DippC_o), 134.90 (s, Me_sC_p), 134.40 (s, Me_sC_o), 128.35 (s, Me_sC_m), 126.23 (s, DippC_p), 123.01 (s, DippC_m), 71.08 (s, OCH₂), 63.76 (s, OCH₃), 27.64 (s, CH(CH₃)₂), 25.15 (s, CH(CH₃)₂), 20.80 (s, C_pCH₃), 19.01 (s, C_oCH₃).

5.2.1.10 W(NDipp)(NⁱPr)Cl₂(DME) (32)

W(NDipp)(NⁱPr)Cl₂(DME) (**32**) was synthesized in the same way as W(NDipp)(N^tBu)Cl₂(DME) (**33**) (section 5.2.1.8) with W(NDipp)Cl₄(THF) (**59**) (500 mg, 0.87 mmol), ⁱPrNH₂ (71 μL, 0.87 mmol) and DABCO (197 mg, 1.75 mmol). Analytically pure samples can be obtained from a concentrated DCM solution of W(NDipp)(NⁱPr)Cl₂(DME) (**32**) after recrystallization at -30 °C. **Unoptimized yield** (266 mg, 53%).

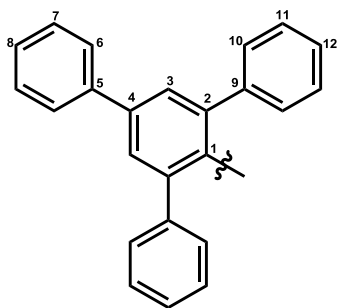
¹H NMR (600 MHz, C₆D₆) δ = 7.21 (d, ³J_{HH} = 7.7, 2H, H_m), 6.91 (t, ³J_{HH} = 7.7, 1H, H_o), 4.97 (sept, ³J_{HH} = 6.4, 1H, NCH(CH₃)₂), 4.28 (sept, ³J_{HH} = 6.9, 2H, DippCH(CH₃)₂), 3.30 (s, 6H, OCH₃), 3.20 (s, 4H, OCH₂), 1.41 (d, ³J_{HH} = 6.9, 12H, DippCH(CH₃)₂), 1.16 (d, 6H, ³J_{HH} = 6.4, NCH(CH₃)₂). **¹³C NMR** (151 MHz, C₆D₆) δ = 151.86 (s, C_{ipso}), 144.00 (s, C_o), 125.02 (s, C_p), 122.81 (s, C_m), 71.97 (s, OCH₃), 65.52 (s, NCH(CH₃)₂), 59.54 (s, OCH₂), 27.72 (s, DippCH(CH₃)₂), 24.99 (s, DippCH(CH₃)₂), 24.41 (s, NCH(CH₃)₂).

5.2.1.11 W(NDipp)(NTpp)Cl₂(DME) (36)

The title complex was prepared in the following manner: W(NDipp)Cl₄(THF) (**59**) (500 mg, 0.87 mmol) was mixed with TppNH₂ (280 mg, 0.87 mmol) and DABCO (196 mg, 1.74 mmol) followed by addition of DME (15 mL). The resulting mixture was stirred for 60 hours at ambient temperature. A colour change occurred from green to orange along with the formation of a white precipitate. The volatile components were removed by application of vacuum resulting in the formation of a yellow residue, which was washed with hexane (3 mL). Extraction of the yellow residue with DME resulted in an orange solution, which after being condensed, yielded fine crystals of W(NDipp)(NTpp)Cl₂(DME) (**36**) that were isolated *via* filtration. Crystals of W(NDipp)(NTpp)Cl₂(DME)

(36) appropriate for a crystallographic analysis were grown by slow evaporation of a DCM solution of W(NDipp)(NTpp)Cl₂(DME) (36). **Unoptimized yield** (300 mg, 41.1 %).

¹H NMR (700 MHz, CD₂Cl₂) δ = 7.61 (d, ³J_{HH} = 7.9, 2H, H⁶), 7.49 (s, 2H, H³), 7.45 (t, ³J_{HH} = 4.2, 4H, H¹¹), 7.41 (t, ³J_{HH} = 7.7, 2H, H⁷), 7.29 (t, ³J_{HH} = 7.4, 1H, H⁸), 7.22 (m, 6H, H¹⁰ and H¹²), 7.13 (d, ³J_{HH} = 7.7, 2H, DippH_m), 6.93 (t, ³J_{HH} = 7.7, 1H, DippH_p), 3.77 (s, 4H, OCH₂), 3.66 (sept., ³J_{HH} = 6.9, 2H, CH(CH₃)₂), 3.64 (s, 6H, OCH₃), 1.07 (d, ³J_{HH} = 6.9, 12H, CH(CH₃)₂). ¹³C NMR (176 MHz, CD₂Cl₂) δ = 151.66 (s, C¹), 150.08 (s, DippC_{ipso}), 145.98 (s, DippC_o), 140.33 (s, TppC_{arom.}), 140.30 (s, TppC_{arom.}), 138.79 (s, TppC_{arom.}), 136.91 (s, TppC_{arom.}), 130.94 (s, C¹¹), 129.09 (s, C⁷), 128.50 (s, TppC_{arom.}), 128.20 (s, TppC_{arom.}), 127.65 (s, C⁸), 127.28 (s, TppC_{arom.}), 127.05 (s, TppC_{arom.}), 126.17 (s, DippC_p), 122.58 (s, DippC_m), 71.87 (s, OCH₂), 64.02 (s, OCH₃), 27.48 (s, CH(CH₃)₂), 25.29 (s, CH(CH₃)₂).



5.2.1.12 W(NDipp)(NTfp)Cl₂(DME) (35)

W(NDipp)(NTfp)Cl₂(DME) (35) was obtained as an orange solid from the reaction of W(NDipp)Cl₄(THF) (59) (500 mg, 0.87 mmol) with TfpNH₂ (128 mg, 0.87 mmol) and DABCO (196 mg, 1.74 mmol) in DME (3 mL). A colour change from green to bright orange was observed after the addition of DABCO in the W(NDipp)Cl₄(THF) (59) /TfpNH₂ solution with simultaneous formation of a white precipitate. The mixture was stirred at ambient temperature for 12 hours and dried *in vacuo*. The residue was then washed with hexane (5 mL) and extracted with DCM. The complex was precipitated out of the DCM solution by addition of hexane as an orange solid. Crystals of the compound appropriate for a crystallographic analysis were grown by slow evaporation of a W(NDipp)(NTfp)Cl₂(DME) (35) solution in DCM. **Unoptimized yield** (307 mg, 53 %).

¹H NMR (700 MHz, C₆D₆) δ = 7.22 (d, ³J_{HH} = 7.7, 2H, DippH_m), 6.92 (t, ³J_{HH} = 7.7, 1H, DippH_p), 6.06 (t, ³J_{HF} = 8.0, 2H, TfpH_m), 4.39 (sept., ³J_{HH} = 6.8, 2H, CH(CH₃)₂), 3.78-3.54 (bs, 3H, OCH₃), 3.53-3.29 (bs, 3H, OCH₃), 3.08 (s, 4H, OCH₂), 1.40 (d, ³J_{HH} = 6.8, 12H, CH(CH₃)₂). ¹³C NMR (176 MHz, C₆D₆) δ = 159.75 (dt, ¹J_{CF} = 249.9, ³J_{CF} = 14.2, TfpC_p), 158.53 (ddd, ¹J_{CF} = 253.4, ³J_{CF} = 15.0, ³J_{CF}' = 6.5, TfpC_o), 150.67 (s, DippC_{ipso}), 146.52 (s, DippC_o), 131.00 (td, ²J_{CF} = 16.4, ⁴J_{CF} = 5.1, TfpC_{ipso}), 126.51 (s, DippC_p), 122.87 (s, DippC_m), 99.69 (m, TfpC_m), 71.21 (s, OCH₂), 64.16 (s, OCH₃), 53.34 (s, OCH₃), 27.91 (s, CH(CH₃)₂), 25.11 (s, CH(CH₃)₂). ¹⁹F NMR (188 MHz, C₆D₆) = -110.6 (sept, ³J_{HF} = 8.8, ⁴J_{FF} = 4.3, 1F, F_p), -115.9 (m, 2F, F_o).

5.2.1.13 W(NDipp)(NDnp)Cl₂(DME) (37)

W(NDipp)(NDnp)Cl₂(DME) (**37**) was obtained from the reaction of W(NDipp)Cl₄(THF) (**59**) (1.00 g, 1.74 mmol) with DnpNH₂ (342 mg, 1.74 mmol) and DABCO (392 mg, 3.48 mmol) in DME (4 mL). A colour change from green to dark red was observed after the addition of DABCO to the W(NDipp)Cl₄(THF) (**59**) /DnpNH₂ solution with simultaneous formation of a precipitate. The mixture was stirred at ambient temperature for 20 hours and then dried *in vacuo*. The residue was washed with hexane (5 mL) and extracted with DCM. The DCM extracts were combined, layered with hexane, and stored at -30 °C for two days. This resulted in the formation of W(NDipp)(NDnp)Cl₂(DME) (**37**) in the form of dark brown crystals, which were isolated by filtration. **Unoptimized yield** (451 mg, 37 %).

¹H NMR (700 MHz, C₆D₆) δ = 7.11 (d, ³J_{HH} = 7.7, 2H, DippH_m), 6.96 (d, ³J_{HH} = 7.7, 2H, DnpH_m), 6.81 (t, ³J_{HH} = 7.7, 1H, DippH_p), 5.86 (t, ³J_{HH} = 8.1, 1H, DnpH_p), 4.20 (sept, ³J_{HH} = 6.8, 2H, CH(CH₃)₂), 3.7-2.9 (m, br 10H, OCH₃ and OCH₂), 1.33 (d, ³J_{HH} = 6.8, 12H, CH(CH₃)₂). ¹³C NMR (176 MHz, C₆D₆) δ = 149.47 (s, DippC_{ipso}), 147.82 (s, DippC_o), 143.70 (s, DnpC_o), 143.38 (s, DnpC_{ipso}), 128.35 (s, DippC_p), 126.01 (s, DnpC_m), 122.97 (s, DippC_m), 121.18 (s, DnpC_p), 71.64 (s, OCH₂), 64.38 (bs, OCH₃), 28.05 (s, CH(CH₃)₂), 25.08 (s, CH(CH₃)₂).

5.2.2 Mono(imido) tungsten complexes

5.2.2.1 [W(NTfp)Cl₄]₂ (52) and W(NTfp)Cl₄(THF) (58)

The title complexes were prepared as follows: WOCl₄ (6.53 g, 19.1 mmol) was suspended in heptane (100 ml) followed by addition of TfpNCO (5.00g, 28.9 mmol). Heating the mixture at reflux for three days resulted in the formation of a dark green solid, which was dried under reduced pressure. The solid was quickly extracted with hot toluene resulting in a hot dark brown solution, which upon cooling to room temperature yielded dark crystals which were isolated by filtration. The isolated crystals were partially re-dissolved in hot DCM and the solution was dried *in vacuo*. This resulted in the formation of pure [W(NTfp)Cl₄]₂ (**52**) as a green powder. **Unoptimized yield** (7.64 g, 85 %). The complex is not sufficiently soluble for an NMR spectroscopic analysis. Nevertheless, its THF adduct can be synthesized and analyzed:

[W(NTfp)Cl₄]₂ (**52**) (2.00 g, 2.12 mmol) was suspended in DCM. THF was added dropwise to the suspension until the solid dissolved to produce a green solution. The green solution was dried *in vacuo* and pure W(NTfp)Cl₄(THF) (**58**) was isolated as a green solid. **Unoptimized yield** (2.19 g, 95 %).

¹H NMR (700 MHz, C₆D₆) δ = 5.79 - 5.75 (m, 2H, H_m), 4.45 - 4.41 (m, 4H, OCH₂CH₂), 1.28 - 1.22 (m, 4H, OCH₂CH₂). ¹³C NMR (176 MHz, C₆D₆) δ = 166.16 (ddd, ¹J_{CF} = 265.7, ³J_{CF} = 15.8, ³J_{CF'} = 5.2, C_o), 165.35 (dt, ¹J_{CF} = 259.6, ³J_{CF} = 13.8, C_p), 99.37 (m, C_m), 74.42 (s, OCH₂CH₂), 25.43 (s,

OCH₂CH₂). ¹⁹F NMR (376 MHz, C₆D₆) δ = -96.7 (p, ³J_{HF} = ⁴J_{FF} = 8.6, 1F, F_p), -108.7 (t, ³J_{HF} = ⁴J_{FF} = 8.3, 2F, F_o).

5.2.2.2 W(NDipp)(H)(Cl)(PMe₃)₃ (62)

W(NDipp)(H)(Cl)(PMe₃)₃ (**62**) was synthesized using a variation of the procedure reported by Nikonov *et al.*²³ with W(NDipp)Cl₂(PMe₃)₃ (**61**) (800 mg, 1.22 mmol) and L-selectride (1.0 M in THF, 1.22 mL, 1.22 mmol) in toluene (40 mL). The complex can be recrystallized from a toluene/pentane solution stored at -30 °C for 24 hours. **Unoptimized yield** (415 mg, 55 %).

¹H NMR (700 MHz, C₆D₆) δ = 7.65 (m, ¹J_{HW} = 56.7, ²J_{HP} = 43.4, ²J_{H2P} = 22.4, 1H, WH), 7.06 (t, ³J_{HH} = 7.7, 1H, H_p), 6.95 (d, ³J_{HH} = 7.7, 2H, H_m), 4.22 (bs, 2H, CH(CH₃)₂), 1.59 (vt, ²J_{HP} = 3.4, 18H, 2P(CH₃)₃), 1.51 (d, ³J_{HP} = 7.0, 9H, P(CH₃)₃), 1.23 (d, ³J_{HH} = 7.0, 12H, CH(CH₃)₂). ¹³C NMR (176 MHz, C₆D₆) δ = 152.08 (s, C_{ipso}), 142.27 (s, C_o), 123.61 (s, C_p), 123.40 (s, C_m), 26.89 (s, CH(CH₃)₂), 24.53 (d, ¹J_{CP} = 20.6, P(CH₃)₃), 24.15 (s, CH(CH₃)₂), 23.26 (vt, ¹J_{CP} = 13.3, 2P(CH₃)₃). ³¹P NMR (283 MHz, C₆D₆) δ = -24.1 (td, ¹J_{PW} = 147, ²J_{PP} = 5.0, 2P, 2PMe₃), -35.6 (tt, ¹J_{PW} = 112, ²J_{PP} = 5.0, 1P, P(CH₃)₃).

5.2.2.3 [[W(NDipp)Cl₂]₂(μ-Cl)₃][Et₄N] (60)

[[W(NDipp)Cl₂]₂(μ-Cl)₃][Et₄N] (**60**) was prepared as follows: a Schlenk was loaded with sodium amalgam (0.4 %, 3.66 mmol Na), DCM (20 mL), W(NDipp)Cl₄(THF) (**59**) (2.00 g, 3.49 mmol), and Et₄NCl (273 mg, 1.65 mmol). The mixture was vigorously stirred for 48 hours and the resulted mixture was filtered via cannula. The brown filtrate was dried *in vacuo* giving [[W(NDipp)Cl₂]₂(μ-Cl)₃][Et₄N] (**60**) in the form of brown crystals. The complex [[W(NDipp)Cl₂]₂(μ-Cl)₃][Et₄N] (**60**) can be recrystallized from a DCM solution *via* solvent evaporation. **Unoptimized yield** (1.03 g, 76 %).

¹H NMR (600 MHz, CD₂Cl₂) δ = 6.99 (bm, 6H, H_{arom}), 3.67 (sept, ³J_{HH} = 6.7, 4H, CH(CH₃)₂), 3.25 (q, ³J_{HH} = 7.2, 8H, NCH₂CH₃), 1.34 (tt, ³J_{HH} = 7.2, ³J_{HN} = 1.9, 12H, NCH₂CH₃), 0.99 (d, ³J_{HH} = 6.8, 24H, CH(CH₃)₂). ¹³C NMR (151 MHz, CD₂Cl₂) δ = 151.30 (s, C_{ipso}), 149.96 (s, C_o), 128.97 (s, C_p), 122.61 (s, C_m), 52.98 (s, NCH₂CH₃), 28.21 (s, CH(CH₃)₂), 23.65 (s, CH(CH₃)₂), 7.70 (s, NCH₂CH₃).

5.2.3 Tantalum and niobium imido complexes

5.2.3.1 Nb(NMes)Cl₃(DME) (71)

Nb(NMes)Cl₃(DME) (**71**) was synthesized using a variation of the procedure used for the preparation of Ta(NPh)Cl₃(DME) (**74**) as described by Korolev *et al.*,¹¹ starting with NbCl₅ (5.00 g, 18.5 mmol). Analytically pure samples can be obtained by layering a concentrated DCM solution of the compound with pentane. **Unoptimized yield** (4.93 g, 63 %).

¹H NMR (700 MHz, CDCl₃) δ = 6.76 (s, 2H, H_m), 4.14 (m, 2H, OCH_{2A}), 4.08 (m, 2H, OCH_{2B}), 3.98 (s, 3H, OCH_{3A}), 3.95 (s, 3H, OCH_{3B}), 2.79 (s, 6H, C_oCH₃), 2.30 (s, 3H, C_pCH₃). ¹³C NMR (176 MHz,

CDCl₃) δ = 151.15 (s, C_{ipso}), 138.21 (s, C_o), 137.04 (s, C_p), 128.15 (s, C_m), 75.67 (s, OCH_{2A}), 70.77 (s, OCH_{2B}), 69.06 (s, OCH_{3A}), 62.53 (s, OCH_{3B}), 21.10 (s, C_pCH₃), 19.36 (s, C_oCH₃).

5.2.3.2 Ta(NMes)Cl₃(DME) (75)

Ta(NMes)Cl₃(DME) (**75**) was synthesized using a variation of procedure for the preparation of Ta(NPh)Cl₃(DME) (**74**) as described by Korolev *et al.*,¹¹ starting with TaCl₅ (5.00 g, 14.0 mmol). Analytically pure samples can be obtained by layering a concentrated DCM solution of the compound with pentane. **Unoptimized yield** (5.13 g, 72 %).

¹H NMR (700 MHz, CDCl₃) δ = 6.85 (s, 2H, H_m), 4.22 (m, 2H, OCH_{2A}), 4.12 (s, 3H, OCH_{3A}), 4.08 (m, 2H, OCH_{2B}), 4.01 (s, 3H, OCH_{3B}), 2.79 (s, 6H, C_oCH₃), 2.40 (s, 3H, C_pCH₃). ¹³C NMR (176 MHz, CDCl₃) δ = 148.85 (s, C_{ipso}), 138.52 (s, C_o), 135.45 (s, C_p), 127.51 (s, C_m), 76.12 (s, OCH_{2A}), 71.00 (s, OCH_{3A}), 70.31 (s, OCH_{2B}), 63.00 (s, OCH_{3B}), 20.71 (s, C_pCH₃), 19.14 (s, C_oCH₃).

5.3 Reactions

All reactions described below were performed in NMR tubes fitted with a J. Youngs tap unless stated otherwise. Eppendorf micro-pipettes were used for the additions of all liquid reagents.

5.3.1 Reactions of aluminum-based reagents

5.3.1.1 Reaction of PhNO₂ with Me₃Al

PhNO₂ (40 μ L, 0.39 mmol) was treated with Me₃Al (37.4 μ L, 0.39 mmol) in C₆D₆ (0.6 mL). An immediate colour change occurred from pale yellow to red. The ¹H NMR spectroscopic analysis of the solution revealed multiple, un-assignable resonances.

5.3.1.2 Reaction of THF with Me₃Al

THF (20.0 μ L, 0.25 mmol) was dissolved in C₆D₆ (0.6 mL) and Me₃Al (5.9 μ L, 0.13 mmol) added. The resulting mixture was subject to a ¹H and ¹³C NMR spectroscopic analysis. The above process of Me₃Al addition was repeated until one equivalent of Me₃Al (23.6 μ L, 0.25 mmol) was added in total. ¹H and ¹³C NMR spectroscopic analyses were carried out in between each addition. Subsequently, one more equivalent of Me₃Al (23.6 μ L, 0.25 mmol) was added to the tube and the mixture was analysed by ¹H and ¹³C NMR spectroscopy. Sequential addition of aliquots of Me₃Al (23.6 μ L, 0.25 mmol) followed until the total amount of Me₃Al added was six equivalents with ¹H and ¹³C NMR spectroscopic analyses being carried out in between each addition.

5.3.1.3 Reaction of THF with AlCl₃

AlCl₃ (60 mg, 0.44 mmol) was suspended in C₆D₆ (0.6 mL) and of 0.25 equivalents of THF (9.0 μ L, 0.11 mmol) added. The solution was then subject to a ¹H NMR spectroscopic analysis. Sequential

additions of Me₃Al (23.6 μL, 0.25 mmol) followed until four equivalents of Me₃Al were added in total with ¹H NMR spectroscopic analyses being carried out in between each addition.

5.3.1.4 Reaction of DME with Me₃Al

The process described in section 5.3.1.2 was repeated by dissolving DME (20.0 μL, 0.192 mmol) in C₆D₆ followed by four and six additions of 0.25 equivalents Me₃Al (4.6 μL, 0.048 mmol) and one equivalent of Me₃Al (18.4 μL, 0.192 mmol), respectively, with ¹H and ¹³C NMR spectroscopic analyses being carried out in between each addition.

5.3.1.5 Reaction of PhCl with Me₃Al and 1-hexene

A mixture of PhCl (40.0 μL, 0.39 mmol), C₆D₆ (0.5 mL) and Me₃Al (37.4 μL, 0.39 mmol) was heated at reflux for 24 hours followed by an NMR spectroscopic analysis which confirmed that no reaction occurred. Following that, 1-hexene (461.8 μL, 3.69 mmol) was added to the solution which was then heated at reflux for another 24 hours. The NMR spectroscopic analysis of the new solution indicated that no reaction occurred. Lastly, W(NDipp)₂Cl₂(DME) (**27**) (23 mg, 0.033 mmol) was added into the tube and the solution was heated at reflux for 12 hours. The ¹H NMR spectroscopic analysis that followed indicated that no reaction took place.

5.3.1.6 Reaction of PhCl with Et₃Al and 1-hexene

The reaction of PhCl, 1-hexene and Et₃Al was performed under the conditions described in section 5.3.1.5 with Et₃Al (55.3 μL, 0.39 mmol) instead of Me₃Al. All of the NMR spectroscopic analyses indicated that no reaction occurred.

5.3.1.7 Reaction of PhCl with MeAlCl₂ and 1-hexene

A mixture of PhCl (40.0 μL, 0.39 mmol), C₆D₆ (0.5 mL) and MeAlCl₂ (44 mg, 0.39 mmol) was heated at reflux for 24 hours followed by an NMR spectroscopic analysis which confirmed that no reaction occurred. Following that, 1-hexene (461.8 μL, 3.69 mmol) was added to the solution which was then heated at reflux for another 24 hours. The NMR spectroscopic analysis of the new solution indicated that no reaction occurred. Lastly, W(NDipp)₂Cl₂(DME) (**27**) (23 mg, 0.033 mmol) was added into the tube and the solution was heated at reflux for 12 hours. Upon cooling to ambient temperature light yellow crystals were formed which were subject to an X-ray crystallographic study and found to be W(NDipp)₂Me₂AlCl₃. Then the volatile components were removed from the NMR tube and the residue was dissolved in C₆D₆. Subsequent ¹H NMR spectroscopic analysis indicated that formation of hexene dimers had taken place.

5.3.1.8 Reaction of PhCl with EtAlCl₂ and 1-hexene

This reaction was performed and behaved in the same way as described in section 5.3.1.7 using EtAlCl₂ (50.9 μL, 0.39 mmol) instead of MeAlCl₂ up to the point where W(NDipp)₂Cl₂(DME) (**27**) (23 mg, 0.033 mmol) was added and the mixture was heated at reflux for 12 hours. The volatile

components were then removed from the NMR tube and the residue was dissolved in C_6D_6 . Subsequent 1H NMR spectroscopic analysis indicated that formation of hexene dimers occurred.

5.3.1.9 Reaction of Et_3N with $AlCl_3$: formation of $Et_3N-AlCl_3$

Et_3N (50.0 μL , 0.36 mmol) was added to a suspension of $AlCl_3$ (48 mg, 0.36 mmol) in C_6D_6 (0.6 mL). The mixture was agitated until the $AlCl_3$ dissolved and the solution at which point the mixture was subject to a 1H , ^{13}C , and ^{27}Al NMR spectroscopic analysis, each of which confirmed formation of $Et_3N-AlCl_3$.

1H NMR (400 MHz, C_6D_6) δ = 2.43 (q, $^3J_{HH}$ = 7.4, 6H, NCH_2CH_3), 0.82 (t, $^3J_{HH}$ = 7.4, 9H, NCH_2CH_3). ^{13}C NMR (101 MHz, C_6D_6) δ = 49.39 (s, NCH_2CH_3), 9.30 (s, NCH_2CH_3). ^{27}Al NMR (104 MHz, C_6D_6) δ = 109.5 (s).

5.3.1.10 Reaction of Et_3N with $EtAlCl_2$: formation of $Et_3N-AlEtCl_2$

The reaction of Et_3N with $EtAlCl_2$ was performed by adding Et_3N (30.7 μL , 0.22 mmol) in a solution of $EtAlCl_2$ (29.9 μL , 0.22 mmol) in C_6D_6 (0.6 mL). Subsequent NMR spectroscopic analysis indicated that $Et_3N-AlEtCl_2$ had formed. A small amount of $Et_3N-AlCl_3$ was also observed in the aluminum spectra (resonating at 109.5 ppm) originating from some $AlCl_3$ impurity in the commercially purchased $EtAlCl_2$.

1H NMR (400 MHz, C_6D_6) δ = 2.36 (q, $^3J_{HH}$ = 7.3, 6H, NCH_2CH_3), 1.36 (t, $^3J_{HH}$ = 8.1, 3H, $AlCH_2CH_3$), 0.77 (t, $^3J_{HH}$ = 7.3, 9H, NCH_2CH_3), 0.27 (q, $^3J_{HH}$ = 8.1, 2H, $AlCH_2CH_3$). ^{13}C NMR (101 MHz, C_6D_6) δ = 48.49 (s, NCH_2CH_3), 9.16 (s, NCH_2CH_3), 9.10 (s, $AlCH_2CH_3$). ^{27}Al NMR (104 MHz, C_6D_6) δ = 134.6 (bs).

5.3.1.11 Reaction of Et_3N with $MeAlCl_2$: formation of $Et_3N-AlMeCl_2$

Et_3N (30.7 μL , 0.22 mmol) and $MeAlCl_2$ (25 mg, 0.22 mmol) were reacted in C_6D_6 (0.6 mL). The final reaction mixture was subject to an NMR spectroscopic analysis, which indicated that formation of $Et_3N-MeAlCl_2$ occurred along with a small quantity of $Et_3N-AlCl_3$ ($AlCl_3$ impurity in the purchased $MeAlCl_2$).

1H NMR (400 MHz, C_6D_6) δ = 2.37 (q, $^3J_{HH}$ = 7.4, 6H, NCH_2CH_3), 0.78 (t, $^3J_{HH}$ = 7.4, 9H, NCH_2CH_3), -0.22 (s, 3H, $AlCH_3$). ^{13}C NMR (101 MHz, C_6D_6) δ = 48.53 (s, NCH_2CH_3), 9.16 (s, NCH_2CH_3). ^{27}Al NMR (104 MHz, C_6D_6) δ = 135.3 (bs).

5.3.1.12 Reaction of $[Et_3NH]Cl$ with $AlCl_3$: formation of $[Et_3NH][AlCl_4]$

$[Et_3NH]Cl$ (30 mg, 0.22 mol) was suspended in C_6D_6 (0.6 mL) followed by addition of $AlCl_3$ (30 mg, 0.22 mmol). The mixture was agitated resulting in the formation of two colourless liquid phases implying formation of an ionic liquid sparingly soluble in C_6D_6 . The NMR spectra of the solution obtained indicated formation of $[Et_3NH][MeAlCl_3]$.

¹H NMR (400 MHz, C₆D₆) δ = 2.16 (dq, ³J_{HH} = 7.3, ³J_{HH'} = 5.2, 6H, NCH₂CH₃), 0.56 (t, ³J_{HH} = 7.3, 9H, NCH₂CH₃). **¹³C NMR** (101 MHz, C₆D₆) δ = 47.32 (s, NCH₂CH₃), 8.64 (s, NCH₂CH₃). **²⁷Al NMR** (104 MHz, C₆D₆) δ = 103.5 (s).

The reaction was repeated in CD₂Cl₂ (0.6 mL), which resulted in a colourless homogeneous solution consisting of [Et₃NH][AlCl₄] as supported by NMR spectroscopic analysis.

¹H NMR (400 MHz, CD₂Cl₂) δ = 6.07 (bt, ¹J_{NH} = 51.6, 1H, NH), 3.29 (dq, ³J_{HH} = 7.3, ³J_{HH'} = 5.2, 6H, NCH₂CH₃), 1.39 (t, ³J_{HH} = 7.3, 9H, NCH₂CH₃). **²⁷Al NMR** (104 MHz, CD₂Cl₂) δ = 102.8 (s).

5.3.1.13 Reaction of [Et₃NH]Cl with Me₃Al: formation of methane and Et₃N-AlMe₂Cl

Et₃NHCl (60 mg, 0.44 mol) and Me₃Al (42.0 μL, 0.44 mmol) were mixed in C₆D₆ (0.6 mL). The mixture was agitated which caused effervescence and formation of a colourless solution consisting of methane and Et₃N-AlMe₂Cl as demonstrated by an NMR spectroscopic analysis. The NMR spectra remained unchanged even after heating the solution at reflux for five days.

¹H NMR (400 MHz, C₆D₆) δ = 2.34 (q, ³J_{HH} = 7.3, 6H, NCH₂CH₃), 0.77 (t, ³J_{HH} = 7.3, 9H, NCH₂CH₃), 0.16 (methane), -0.36 (s, 3H, AlCH₃). **¹³C NMR** (101 MHz, C₆D₆) δ = 48.04 (s, NCH₂CH₃), 9.12 (s, NCH₂CH₃), -4.21 (methane).

5.3.1.14 Reaction of [Et₃NH]Cl with Et₃Al: formation of ethane and Et₃N-AlEt₂Cl

The reaction between [Et₃NH]Cl (30 mg, 0.22 mol) and Et₃Al (30.1 μL, 0.22 mmol) was performed as described in section 5.3.1.13. Subsequent NMR spectroscopic analysis indicated formation of ethane and Et₃N-AlEt₂Cl.

¹H NMR (400 MHz, C₆D₆) δ = 2.29 (q, ³J_{HH} = 7.3, 6H, NCH₂CH₃), 1.43 (t, ³J_{HH} = 8.2, 6H, AlCH₂CH₃), 0.80 (ethane), 0.72 (t, ³J_{HH} = 7.3, 9H, NCH₂CH₃), 0.21 (q, ³J_{HH} = 8.2, 4H, AlCH₂CH₃). **¹³C NMR** (101 MHz, C₆D₆) δ = 47.90 (s, NCH₂CH₃), 9.99 (s, NCH₂CH₃), 9.09 (s, AlCH₂CH₃), 6.94 (ethane). **²⁷Al NMR** (104 MHz, C₆D₆) δ = 156.6 (bs).

5.3.1.15 Reaction of [Et₃NH]Cl with EtAlCl₂: formation of [Et₃NH][EtAlCl₃]

[Et₃NH]Cl (60 mg, 0.44 mol) was suspended in C₆D₆ (0.6 mL) followed by addition of EtAlCl₂ (59.7 μL, 0.44 mmol). The mixture was agitated, which resulted in the formation of a colourless solution consisting of [Et₃NH][EtAlCl₃] as demonstrated by an NMR spectroscopic analysis. Additionally, a small amount of [Et₃NH][AlCl₄] was also observed in the aluminum spectra (resonating at 103.5 ppm) originating from some AlCl₃ impurity in the commercially purchased EtAlCl₂.

¹H NMR (400 MHz, C₆D₆) δ = 5.92 (bt, 1H, NH), 2.42 (dq, ³J_{HH} = 7.3, ³J_{HH'} = 5.2, 6H, NCH₂CH₃), 1.40 (t, ³J_{HH} = 8.1, 3H, AlCH₂CH₃), 0.77 (t, ³J_{HH} = 7.3, 9H, NCH₂CH₃), 0.55 (q, ³J_{HH} = 8.1, 2H, AlCH₂CH₃). **¹³C NMR** (101 MHz, C₆D₆) δ = 47.59 (s, NCH₂CH₃), 9.11 (s, AlCH₂CH₃), 8.91 (s, NCH₂CH₃). **²⁷Al NMR** (104 MHz, C₆D₆) δ = 129.7 (bs).

The above [Et₃NH][EtAlCl₃] solution was heated at reflux for 15 days after which time formation of a mixture of [Et₃NH][EtAlCl₃], ethane and Et₃N-AlCl₃ occurred based on the NMR spectroscopic analysis of the final reaction mixture.

5.3.1.16 Reaction of [Et₃NH]Cl with MeAlCl₂: formation of [Et₃NH][MeAlCl₃]

[Et₃NH]Cl (30 mg, 0.22 mol) was treated with MeAlCl₂ (25 mg, 0.22 mmol) in C₆D₆ (0.6 mL) and the mixture was agitated. Two colourless liquid phases were formed indicating presence of an ionic liquid sparingly soluble to C₆D₆. The NMR spectra of the solution suggested formation of [Et₃NH][MeAlCl₃]. Additionally, a small amount of [Et₃NH][AlCl₄] was also observed in the aluminum spectra (resonating at 103.5 ppm) originating from some AlCl₃ impurity in the commercially purchased EtAlCl₂.

¹H NMR (400 MHz, C₆D₆) δ = 6.52 (bt, 1H, NH), 2.34 (dq, ³J_{HH} = 7.3, ³J_{HH'} = 4.9, 6H, NCH₂CH₃), 0.70 (t, ³J_{HH} = 7.3, 9H, NCH₂CH₃), -0.22 (s, 3H, AlCH₃). **¹³C NMR** (101 MHz, C₆D₆) δ = 47.17 (s, NCH₂CH₃), 8.66 (s, NCH₂CH₃). **²⁷Al NMR** (104 MHz, C₆D₆) δ = 132.6 (bs).

The reaction was repeated in CD₂Cl₂ (0.6 mL), which resulted in a colourless solution consisting of [Et₃NH][MeAlCl₃]; this is supported by the NMR spectroscopic analysis.

¹H NMR (400 MHz, CD₂Cl₂) δ = 6.71 (bt, ¹J_{HN} = 49.6, 1H, NH), 3.26 (dq, ³J_{HH} = 7.3, ³J_{HH'} = 4.9, 6H, NCH₂CH₃), 1.38 (t, ³J_{HH} = 7.3, 9H, NCH₂CH₃), -0.53 (s, 3H, AlCH₃). **¹³C NMR** (101 MHz, CD₂Cl₂) δ = 48.18 (s, NCH₂CH₃), 9.34 (s, NCH₂CH₃). **²⁷Al NMR** (104 MHz, CD₂Cl₂) δ = 129.7 (bs).

Heating the [Et₃NH][MeAlCl₃] solution at reflux in C₆D₆ for 15 days resulted in a colorless solution, the NMR spectroscopic analysis of which indicated formation of a mixture of [Et₃NH][MeAlCl₃], methane and Et₃N-AlCl₃.

5.3.2 Reactions of mono-imido tungsten complexes

5.3.2.1 Reaction of [W(NDipp)Cl₄]₂ (53) with 1-hexene

[W(NDipp)Cl₄]₂ (53) (60 mg, 0.060 mmol) was suspended in C₆D₆ (0.6 mL) followed by addition of 1-hexene (10.1 μL, 0.12 mmol). The mixture was heated at reflux for 24 hours during which time the [W(NDipp)Cl₄]₂ (53) dissolved. Upon cooling to room temperature, dark crystals formed which were re-dissolved by heating the mixture at reflux. Whilst still hot, the mixture was analyzed by ¹H NMR spectroscopy, which indicated that no reaction occurred. The process was repeated in C₆D₅Cl and

the obtained ^1H NMR spectrum indicated that the composition of the mixture again remained unchanged.

5.3.2.2 Reaction of $\text{W}(\text{NDipp})\text{Cl}_4(\text{THF})$ (**59**) or $[\text{W}(\text{NDipp})\text{Cl}_4]_2$ (**53**) with $[\text{Et}_3\text{NH}]\text{Cl}$: formation of $[\text{W}(\text{NDipp})\text{Cl}_5][\text{Et}_3\text{NH}]$ (**66**)

$\text{W}(\text{NDipp})\text{Cl}_4(\text{THF})$ (**59**) (1.00 g, 1.75 mmol) and $[\text{Et}_3\text{NH}]\text{Cl}$ (240 mg, 1.75 mmol) were dissolved in toluene (10 mL) with stirring, resulted in the formation of a green solution. Layering of the green solution with hexane for a period of 24 hours yielded red/green dichroic crystals, which were isolated by filtration. **Unoptimized yield** (879 mg, 79 %).

^1H NMR (400 MHz, C_6D_6) δ = 7.31 (d, $^3J_{\text{HH}}$ = 7.8, 2H, H_m), 6.33 (t, $^3J_{\text{HH}}$ = 7.8, 1H, H_p), 5.22 (sept, $^3J_{\text{HH}}$ = 6.8, 2H, $\text{CH}(\text{CH}_3)_2$), 2.69 (qd, $^3J_{\text{HH}}$ = 7.3, $^2J_{\text{HH}}$ = 4.7, 6H, NCH_2CH_3), 1.46 (d, $^3J_{\text{HH}}$ = 6.8, 12H, $\text{CH}(\text{CH}_3)_2$), 0.92 (t, $^3J_{\text{HH}}$ = 7.3, 9H, NCH_2CH_3). ^{13}C NMR (101 MHz, C_6D_6) δ = 156.50 (s, C_o), 144.07 (s, C_{ipso}), 133.45 (s, C_p), 122.10 (s, C_m), 46.98 (s, NCH_2CH_3), 27.83 (s, $\text{CH}(\text{CH}_3)_2$), 26.76 (s, $\text{CH}(\text{CH}_3)_2$), 8.72 (s, NCH_2CH_3).

The same complex can be synthesized from the reaction of $[\text{W}(\text{NDipp})\text{Cl}_4]_2$ (**53**) with one equivalent of $[\text{Et}_3\text{NH}]\text{Cl}$ in 100% conversion. This was confirmed by comparing the ^1H NMR spectrum of the final reaction mixture of $[\text{W}(\text{NDipp})\text{Cl}_4]_2$ (60 mg, 0.060 mmol) and $[\text{Et}_3\text{NH}]\text{Cl}$ (16.5 mg, 0.120 mmol) in C_6D_6 (0.6 mL) with the ^1H NMR spectrum of isolated $[\text{W}(\text{NDipp})\text{Cl}_5][\text{Et}_3\text{NH}]$ (**66**).

5.3.2.3 Reaction of $[\text{W}(\text{NDipp})\text{Cl}_4]_2$ (**53**) with Et_3Al

Et_3Al (8.2 μL , 0.030) was added to a suspension of $[\text{W}(\text{NDipp})\text{Cl}_4]_2$ (**53**) (30 mg, 0.030 mmol) in C_6D_6 (0.6 mL). This resulted in effervescence and a color change from dark brown to dark orange. The solution was analyzed by ^1H NMR spectroscopy, which indicated formation of ethane along with various un-assignable species.

5.3.2.4 Reaction of $[\text{W}(\text{NDipp})\text{Cl}_4]_2$ (**53**) with MeAlCl_2

$[\text{W}(\text{NDipp})\text{Cl}_4]_2$ (**53**) (60 mg, 0.060 mmol) was suspended in C_6D_6 (0.6 mL). MeAlCl_2 (14 mg, 0.120 mmol) was added and the mixture was agitated until homogeneous. The resulting dark brown solution was analyzed immediately by ^1H NMR spectroscopy, which revealed multiple un-assignable signals. After 24 hours, a dark brown oil was formed, which was isolated and dissolved in CD_2Cl_2 . Again, multiple un-assignable signals were observed in the ^1H NMR spectrum. The reaction was repeated by suspending $[\text{W}(\text{NDipp})\text{Cl}_4]_2$ (**53**) (100 mg, 0.10 mmol) in toluene (20 mL) in a Schlenk loaded with a stirrer bar. The suspension was cooled to $-30\text{ }^\circ\text{C}$ followed by dropwise addition of a solution of MeAlCl_2 (22.5 mg, 0.20 mmol) in toluene (20 mL) under vigorous stirring. After the MeAlCl_2 addition, the mixture was left to slowly warm up to ambient temperature resulting in a dark brown solution which was left stirring for an additional two hours. Removal of the volatile components from the dark brown solution *in vacuo* resulted in the isolation of a dark brown solid the ^1H NMR spectrum of which revealed multiple un-assignable resonances.

5.3.2.5 Reaction of W(NDipp)Cl₄(THF) (59) with one equivalent of MeAlCl₂

W(NDipp)Cl₄(THF) (**59**) (100 mg, 0.175 mmol) was dissolved in C₆D₆ (0.8 mL) followed by addition of MeAlCl₂ (20 mg, 0.177 mmol). This resulted in a brown solution the ¹H NMR spectrum of which revealed a multitude of resonances. The solution was layered with hexane and after 48 hours orange needle like crystals of **65** formed, whose structure was ascertained following an X-ray crystallographic analysis. Attempts to analyze the crystals *via* NMR spectroscopy were unsuccessful due to their low solubility. The liquid part of the mixture was then decanted and the isolated solution was dried. The resulted dark solid was then dissolved in C₆D₆ (0.6 mL) and analyzed by ¹H NMR spectroscopy which revealed multiple broad resonances which could not be assigned to any products.

5.3.2.6 Reaction of [W(NEt)Cl₄]₂ (48) with MeAlCl₂

The reaction between [W(NEt)Cl₄]₂ (**48**) and MeAlCl₂ was performed in an analogous fashion to the one described in section 5.3.2.5 with [W(NEt)Cl₄] (**48**) (60 mg, 0.081 mmol) and MeAlCl₂ (18 mg, 0.160 mmol) in C₆D₆ (0.6 mL). Subsequent ¹H NMR spectroscopic analysis of the final solutions revealed multiple un-assignable signals. The reaction was repeated with three equivalents of MeAlCl₂ (54 mg, 0.48 mmol). A color change from bright red to dark orange occurred with simultaneous formation of a white precipitate. The ¹H NMR spectroscopic analysis of the supernatant solution revealed that formation of W(NEt)Me₃Cl occurred along with some other unidentified by-products.

5.3.2.7 Reaction of [W(NTfp)Cl₄]₂ (52) with MeAlCl₂

The reaction between [W(NTfp)Cl₄]₂ (**52**) and MeAlCl₂ reaction was performed in a way similar to the one described in section 5.3.2.5 with [W(NTfp)Cl₄] (**52**) (60 mg, 0.064 mmol) and MeAlCl₂ (14 mg, 0.127 mmol) in C₆D₆ (0.6 mL). ¹H NMR spectroscopic analysis of the final solutions revealed multiple un-assignable signals.

5.3.2.8 Reaction of [W(NDipp)Cl₄]₂ (59) with Me₃Al: formation of W(NDipp)Me₃Cl·AlCl₃ (64)

[W(NDipp)Cl₄]₂ (**53**) (500 mg, 0.998 mmol) was suspended in DCM (3 mL) in a sample pot loaded with a stirrer bar. Me₃Al (95.7 μL, 0.998 mmol) was added with vigorous stirring resulting in a light brown solution, which was stirred at ambient temperature for three hours. The solvent was evaporated from the light brown solution under a flow of nitrogen resulting in the formation of a dark solid, which was re-dissolved in a minimal amount of DCM. The DCM solution was then layered with hexane and stored at -30 °C for 24 hours during which time brown crystals of W(NDipp)Me₃Cl·AlCl₃ (**64**) formed. The crystals were isolated by filtration, washed with cold hexane and dried. **Unoptimized yield** (324 g, 57 %).

¹H NMR (700 MHz, CD₂Cl₂) δ = 7.39-7.35 (m, 3H, *H_{arom}*), 3.57 (sept, ³*J_{HH}* = 7.0, 2H, CH(CH₃)₂), 1.93 (s, 9H, WCH₃), 1.34 (d, ³*J_{HH}* = 7.0, 12H, CH(CH₃)₂). **¹³C NMR** (176 MHz, C₆D₆) δ = 150.35 (s, C_o), 148.87 (s, C_{ipso}), 131.05 (s, C_p), 123.97 (s, C_m), 67.47 (t, ¹*J_{CW}* = 40.3, WCH₃), 29.60 (s, CH(CH₃)₂), 24.42 (s, CH(CH₃)₂). **²⁷Al NMR** (182 MHz, C₆D₆) δ = 104 (bs).

In order to explore the effect that addition of excess of Me₃Al has on [W(NDipp)Cl₄]₂ (**53**), [W(NDipp)Cl₄]₂ (**53**) (60 mg, 0.060 mmol) was suspended in C₆D₆ (0.6 mL) and Me₃Al (11.5 μL, 0.120 mmol) was added. The mixture was then subject to a ¹H and ¹³C NMR spectroscopic analysis. One more equivalent of Me₃Al was added and the process of Me₃Al addition followed by NMR spectroscopic analyses was repeated until a total of 6 equivalents of Me₃Al were added.

5.3.2.9 Reaction of W(NDipp)Me₃Cl·AlCl₃ (**64**) with Et₄NCl: formation of W(NDipp)Me₃Cl and [Et₄N][AlCl₄]

W(NDipp)Me₃Cl·AlCl₃ (**64**) (76 mg, 0.131 mmol) was dissolved in CD₂Cl₂ (0.6 mL) followed by addition of Et₄NCl (22 mg, 0.131 mmol). After the Et₄NCl dissolved the resulting orange solution was subject to an NMR spectroscopic analysis which indicated formation of W(NDipp)Me₃Cl and [Et₄N][AlCl₄].

¹H NMR (400 MHz, CD₂Cl₂) δ = 7.29 (m, 2H, *H_m*), 7.21 (m, 2H, *H_m*), 3.62 (sept, ³*J_{HH}* = 6.9, 2H, CH(CH₃)₂), 3.25 (q, ³*J_{HH}* = 7.2, 8H, NCH₂CH₃), 1.42 (t, ²*J_{HW}* = 3.2, 9H, WCH₃), 1.35 (tt, ³*J_{HH}* = 7.2, ³*J_{HN}* = 2.0, 12H, NCH₂CH₃), 1.27 (d, ³*J_{HH}* = 6.9, 12H, CH(CH₃)₂). **¹³C NMR** (101 MHz, CD₂Cl₂) δ = 150.66 (s, C_o), 147.04 (s, C_{ipso}), 128.48 (s, C_p), 123.33 (s, C_m), 57.15 (t, ¹*J_{CW}* = 38.9, WCH₃), 53.25 (t, ¹*J_{CN}* = 2.0, NCH₂CH₃), 29.01 (s, CH(CH₃)₂), 24.44 (s, CH(CH₃)₂), 7.90 (s, NCH₂CH₃). **²⁷Al NMR** (104 MHz, C₆D₆) δ = 102.8 (bs).

Addition of one more equivalent of Et₄NCl (22 mg, 0.131 mmol) to the above solution of W(NDipp)Me₃Cl and [Et₄N][AlCl₄] did not result in formation of new products as indicated by the ¹H NMR spectroscopic analysis that followed.

5.3.2.10 Reaction of W(NDipp)Cl₄(THF) (**59**) with Me₃Al: formation of W(NDipp)Me₃Cl

The process described in section 5.3.2.8 was repeated with W(NDipp)Cl₄(THF) (**59**) (60 mg, 0.105 mmol) followed by four additions of one equivalent of Me₃Al (10 μL, 0.105 mmol) with ¹H, ¹³C, and ²⁷Al NMR spectroscopic analyses being carried out in between each addition. Formation of W(NDipp)Me₃Cl was confirmed by comparing the NMR spectra obtained from this reaction to the ones in section 5.3.2.8.

5.3.2.11 Reaction of $[W(\text{NEt})\text{Cl}_4]_2$ (**48**) with Me_3Al : formation of $W(\text{NEt})\text{Me}_3\text{Cl}\cdot\text{AlCl}_3$

$[W(\text{NEt})\text{Cl}_4]$ (**48**) (60 mg, 0.081 mmol) was suspended in C_6D_6 (0.6 mL) followed by addition of Me_3Al (15.6 μL , 0.16 mmol). The mixture was agitated and subject to a ^1H and ^{13}C NMR spectroscopic analysis.

^1H NMR (400 MHz, C_6D_6) δ = 3.66 (q, $^3J_{\text{HH}} = 7.1$, 4H, CH_2), 1.27 (s, 9H, WCH_3), 0.87 (t, $^3J_{\text{HH}} = 7.1$, 3H, CH_3). ^{13}C NMR (101 MHz, C_6D_6) δ = 62.72 (t, $^1J_{\text{CW}} = 40$, WCH_3), 59.75 (s, CH_2), 13.46 (s, CH_3).

The above process of sequential Me_3Al additions was repeated until three equivalents of Me_3Al (46.8 μL , 0.48 mmol) were added in total with ^1H and ^{13}C NMR spectroscopic analyses being carried out in between each addition.

5.3.2.12 Reaction of $[W(\text{NTfp})\text{Cl}_4]_2$ (**52**) with Me_3Al : formation of $W(\text{NTfp})\text{Me}_3\text{Cl}\cdot\text{AlCl}_3$

The process described in section 5.3.2.11 was repeated with $[W(\text{NTfp})\text{Cl}_4]_2$ (**52**) (60 mg, 0.064 mmol) and Me_3Al (12.2 μL , 0.127 mmol) with a ^1H and ^{13}C NMR spectroscopic analyses were carried out in between each addition. The NMR spectra after the first addition are presented below:

^1H NMR (400 MHz, C_6D_6) δ = 5.98 (m, 2H, H_m), 1.52 (s, 9H, WCH_3). ^{13}C NMR (101 MHz, C_6D_6) δ = 161.44 (ddd, $^1J_{\text{CF}} = 257.9$, $^3J_{\text{CF}} = 15.2$, $^3J_{\text{CF}'} = 5.5$, C_o), 161.85 (dt, $^1J_{\text{CF}} = 257.4$, $^3J_{\text{CF}} = 14.4$, C_p), 101.31 (m, C_m), 64.79 (t, $^1J_{\text{CW}} = 37.7$, WCH_3).

5.3.2.13 Reaction of $[W(\text{NDipp})\text{Cl}_4]_2$ (**53**) or $W(\text{NDipp})\text{Cl}_4(\text{THF})$ (**59**) with Et_3N

$[W(\text{NDipp})\text{Cl}_4]_2$ (**53**) (60 mg, 0.060 mmol) was suspended in C_6D_6 followed by addition of Et_3N (8.4 μL , 0.060 mmol). The mixture was agitated resulting in the formation of a dark brown solution along with a small amount of small (~0.5 mm) dark crystals. An X-ray crystallographic analysis of the crystals revealed that formation of **68** had occurred, while the supernatant solution was analysed by ^1H NMR spectroscopy and indicated the presence of two unidentified Dipp environments. The rest of the dark brown solution was filtered and the filtrate was layered with hexane. After two days dark green rectangular crystals and brown-red needle like crystals were formed. The crystals were isolated and an X-Ray crystallographic analysis revealed that the two types of crystals corresponded to $[W(\text{NDipp})\text{Cl}_5][\text{Et}_3\text{NH}]$ (**66**) and $[[W(\text{NDipp})\text{Cl}_2]_2(\mu\text{-Cl})_3][\text{Et}_3\text{NH}]$ (**67**), respectively. The mixture of crystals was dissolved in C_6D_6 and the ^1H NMR spectrum revealed presence of $[W(\text{NDipp})\text{Cl}_5][\text{Et}_3\text{NH}]$ (**66**) along with a second Dipp environment possibly belonging to $[[W(\text{NDipp})\text{Cl}_2]_2(\mu\text{-Cl})_3][\text{Et}_3\text{NH}]$ (**67**). The reaction was repeated with one or two equivalents of Et_3N providing similar results. When $W(\text{NDipp})\text{Cl}_4(\text{THF})$ (**59**) (100 mg, 0.175 mmol) was mixed with Et_3N (24.3, 0.175 mmol) in C_6D_6 (0.6 mL) a gradual color change occurred from green to dark brown which was completed by heating the mixture at reflux for 24 hours. The ^1H NMR spectroscopic analysis of the resulted dark brown

solution revealed broad resonances implying that a paramagnetic species was present in the solution. Thus, the dark brown solution was layered with hexane in the NMR tube. After 3 days a dark brown crystalline material accumulated in the bottom of the tube. The supernatant solution was decanted and the material was washed with hexane and dried. Addition of CD_2Cl_2 (0.6 mL) in the tube containing the brown crystals led to formation of a dark brown solution which was analyzed by ^1H NMR spectroscopy. Once more, broad resonances of low diagnostic value were observed in the ^1H NMR spectrum.

5.3.2.14 Reaction of $[\text{W}(\text{NDipp})\text{Cl}_4]_2$ (53) with $\text{W}(\text{NDipp})\text{Cl}_2(\text{PMe}_3)_3$ (61)

$[\text{W}(\text{NDipp})\text{Cl}_4]_2$ (53) (50 mg, 0.050 mmol) was mixed with $\text{W}(\text{NDipp})\text{Cl}_2(\text{PMe}_3)_3$ (61) (51.5 mg, 0.10 mmol) in CD_2Cl_2 (0.6 mL). Agitating the mixture resulted in the formation of a dark orange solution which was subject to a ^1H NMR spectroscopic analysis. The broad resonances observed in the ^1H NMR spectrum indicated formation of paramagnetic species. Slow evaporation of the paramagnetic solution resulted in the formation of dark orange crystals which were found to be the previously reported paramagnetic complex $\text{W}(\text{NDipp})\text{Cl}_3(\text{PMe}_3)_2$ (61)¹⁶.

5.3.3 Reactions of bis-imido tungsten complexes

5.3.3.1 Reaction of $\text{W}(\text{NDipp})_2\text{Cl}_2(\text{DME})$ (27) with Et_3N

$\text{W}(\text{NDipp})_2\text{Cl}_2(\text{DME})$ (27) (60 mg, 0.086 mmol) was dissolved in C_6D_6 (0.6 mL) followed by addition of Et_3N (24.1 μL , 0.172 mmol). The solution was agitated, heated at reflux for 24 hours and then analyzed using ^1H NMR spectroscopy. No reaction between $\text{W}(\text{NDipp})_2\text{Cl}_2(\text{DME})$ (27) and Et_3N was observed.

5.3.3.2 Conversion of $\text{W}(\text{NDipp})(\text{NTfp})\text{Cl}_2(\text{DME})$ (35) to a mixture of $\text{W}(\text{NDipp})(\text{NTfp})\text{Cl}_2(\text{DME})$ (35), $\text{W}(\text{NDipp})_2\text{Cl}_2(\text{DME})$ (27) and $\text{W}(\text{NTfp})_2\text{Cl}_2(\text{DME})$ (28)

$\text{W}(\text{NDipp})(\text{NTfp})\text{Cl}_2(\text{DME})$ (35) was dissolved in C_6D_6 (0.5 mL) and was heated at reflux for 3 hours. Subsequent ^1H NMR spectroscopic analysis indicated formation of a mixture of $\text{W}(\text{NDipp})(\text{NTfp})\text{Cl}_2(\text{DME})$ (35), $\text{W}(\text{NDipp})_2\text{Cl}_2(\text{DME})$ (27) and $\text{W}(\text{NTfp})_2\text{Cl}_2(\text{DME})$ (28). Similarly, complex $\text{W}(\text{NDipp})(\text{N}^t\text{Bu})(\text{DME})$ (33) formed a mixture of complexes but only after 3 days of heating at reflux.

5.3.3.3 Reaction of $\text{W}(\text{NDipp})_2\text{Cl}_2(\text{DME})$ (27) with one equivalent of Me_2AlCl : Synthesis of $\text{W}(\text{NDipp})_2\text{Me}_2$ (44) and $[\text{AlCl}_2(\text{DME})_2][\text{AlCl}_4]$ (43)

A sample pot was loaded with a stirrer bar, $\text{W}(\text{NDipp})_2\text{Cl}_2(\text{DME})$ (27) (200 mg, 0.288 mmol), and DCM (3 mL) in an N_2 -filled glove box followed by addition of Me_2AlCl (26.7 μL , 0.288 mmol) under

vigorous stirring. The resulting orange solution was stirred for five minutes during which time the colour of the solution changed to dark red. Stirring was stopped and the solution was left to stand with no agitation for 24 hours. This resulted in the formation of colourless crystals of $[\text{AlCl}_2(\text{DME})_2][\text{AlCl}_4]$ (**43**) (37 mg, 76 % yield) as indicated from an X-ray crystallographic analysis which were isolated by filtration. These crystals were found to be soluble only in THF possibly due to the ability of the latter to coordinate to the aluminium.²⁴ Meanwhile the filtrate was dried resulting in the formation of a dark red residue which was extracted with pentane. The dark red pentane extracts were combined, condensed and stored at $-30\text{ }^\circ\text{C}$. After 48 hours red crystals were formed the ^1H NMR and ^{13}C NMR spectra of which were found to be identical to the ones reported by Wright *et al.*,²⁵ confirming the formation of $\text{W}(\text{NDipp})_2\text{Me}_2$ (**44**). No resonances were observed in the ^{27}Al NMR spectrum. **Unoptimized yield** (34 mg, 21 %).

5.3.3.4 Reaction of $\text{W}(\text{NDipp})_2\text{Cl}_2(\text{DME})$ (**27**) with two equivalents of Me_3Al : Synthesis of $\text{W}(\text{NDipp})_2\text{Me}_2\cdot\text{AlClMe}_2$ (**45**).

A sample pot was loaded with a stirrer bar, $\text{W}(\text{NDipp})_2\text{Cl}_2(\text{DME})$ (**27**) (200 mg, 0.288 mmol), and toluene (3 mL) in a N_2 -filled glove box followed by addition of Me_3Al (26.7 μL , 0.288 mmol) under vigorous stirring. The resulted orange solution was stirred for five hours during which time the color of the solution changed to red. The volatile components were removed *in vacuo* resulting in the formation of a red solid, which was extracted with pentane. The red pentane solution was condensed and stored at $-30\text{ }^\circ\text{C}$ for 24 hours. This resulted in the formation of rectangular light yellow crystals, which were isolated by filtration. The ^1H and ^{13}C NMR spectra of the yellow crystals were found to be identical to the spectra reported by Wright *et al.*,²⁵ confirming formation of $\text{W}(\text{NDipp})_2\text{Me}_2\cdot\text{AlClMe}_2$ (**45**) (81 mg, 43 % yield).

5.3.3.5 Reaction of $\text{W}(\text{NDipp})_2\text{Cl}_2(\text{DME})$ (**27**) with two equivalents of MeAlCl_2 : Synthesis of $\text{W}(\text{NDipp})_2\text{Me}_2\cdot\text{AlCl}_3$ (**47**) and $[\text{AlCl}_2(\text{DME})_2][\text{AlCl}_4]$ (**43**).

A sample pot was loaded with a stirrer bar, $\text{W}(\text{NDipp})_2\text{Cl}_2(\text{DME})$ (**27**) (200 mg, 0.288 mmol), and DCM (3 mL) in a N_2 -filled glove box followed by addition of MeAlCl_2 (65 mg, 0.576 mmol) with vigorous stirring. The resulted orange solution was stirred for one minute and then left still. After 24 hours of standing the colour of the solution changed from orange to red along with formation of colourless crystals of $[\text{AlCl}_2(\text{DME})_2][\text{AlCl}_4]$ (**43**) (based on an ^1H NMR spectroscopic analysis) which were separated *via* filtration. Slow evaporation of the filtrate resulted in the formation of orange crystals of $\text{W}(\text{NDipp})_2\text{Me}_2\cdot\text{AlCl}_3$ (**47**) which were isolated by decanting the supernatant solution (94 mg, 47% yield). The NMR spectra of the crystals in C_6D_6 were identical to those reported by Wright *et al.*²⁶

5.3.3.6 Reaction of $W(\text{NDipp})_2\text{Me}_2\cdot\text{AlClMe}_2$ (**45**) with one equivalent of Et_4NCl : formation of $W(\text{NDipp})_2\text{Me}_2$ (**44**)

$W(\text{NDipp})_2\text{Me}_2\cdot\text{AlClMe}_2$ (**45**) (34 mg, 0.046 mmol) was dissolved in CD_2Cl_2 (0.6 mL) followed by addition of $[\text{Et}_4\text{N}]\text{Cl}$ (8.6 mg, 0.046 mmol). A colour change from yellow to red was observed due to formation of $W(\text{NDipp})_2\text{Me}_2$ (**44**) and $[\text{Et}_4\text{N}][\text{Me}_2\text{AlCl}_2]$ as indicated by ^1H NMR spectroscopic analysis.

5.4 Attempted syntheses

5.4.1 $W(\text{NPh}^{\text{F}})(\text{N}^t\text{Bu})\text{Cl}_2(\text{DME})$

$W(\text{NPh}^{\text{F}})\text{Cl}_4(\text{THF})$ (**57**) (500 mg, 0.99 mmol) was dissolved in DME (10 mL) followed by addition of $^t\text{BuNH}_2$ (105 μL , 0.99 mmol) and DABCO (222 mg, 3.5 mmol) with vigorous stirring. The mixture was left stirring for two days during which a colour change was observed from dark green to dark red along with the formation of a precipitate. The mixture was filtered and the filtrate was concentrated. In order to grow crystals, the condensed solution was kept at $-30\text{ }^\circ\text{C}$ for 20h. However, no crystals were formed, thus the solution was dried, re-dissolved in DCM. Addition of pentane in the aforementioned DCM solution resulted in the precipitation of a red solid, which was isolated *via* filtration. Attempts to grow crystals from the filtrate by keeping it at $-78\text{ }^\circ\text{C}$ for 20h failed. The red solid was subject to a ^1H NMR analysis, which was not consistent with that expected for the target molecule (four ^tBu environments were detected), implying formation of more than one species that could not be separated or identified.

5.4.2 $W(\text{NDipp})(\text{NMes}^{\text{F}})\text{Cl}_2(\text{DME})$

The synthesis of $W(\text{NDipp})(\text{NMes}^{\text{F}})\text{Cl}_2(\text{DME})$ was attempted by treating $W(\text{NDipp})\text{Cl}_4(\text{THF})$ (**59**) (500 mg, 0.87 mmol) with $\text{Mes}^{\text{F}}\text{NH}_2$ (258 mg, 0.87 mmol) and DABCO (196 mg, 1.74 mmol) as described in section 5.2.1.8. The filtrate was dried and the dark residue was analyzed *via* ^1H NMR spectroscopy and ASAP mass spectrometry. The desirable product was not detected in either analysis. Subsequently, the dark residue was dissolved in toluene and layered with pentane. After a two-day period, a red powder formed which was removed *via* filtration. The filtrate was condensed under reduced pressure resulting in the formation of a red oil. After two days, red crystals emerged from the oil, which were found to be $W(\text{NDipp})_2\text{Cl}_2(\text{DME})$ (**27**) based on a ^1H NMR spectroscopic analysis.

5.4.3 $W(\text{NDipp})(\text{NPh}^{\text{F}})\text{Cl}_2(\text{DME})$

The synthesis of this compound was attempted in the same way as described in paragraph 5.4.1 by using DippNH_2 (187 μL , 0.99 mmol) instead of $^t\text{BuNH}_2$. This resulted in a dark red solution with a precipitate being formed which was filtered. The filtrate was dried under reduced pressure leaving behind a dark red solid. The ^1H NMR spectroscopic analysis of the red solid indicated the formation of $W(\text{NDipp})_2\text{Cl}_2(\text{DME})$ (**27**) along with other unidentified products.

5.4.4 W(NPh)(N^tBu)Cl₂(DME)

The synthesis of this compound was attempted in the same way as described in paragraph 5.4.1 by using W(NPh)Cl₄(THF) (**56**) (300 mg, 0.61 mmol), ^tBuNH₂ (65 μL, 0.61 mmol) and DABCO (137 mg, 1.22 mmol). The resulting mixture exhibits a similar behaviour to the one described in section 5.4.1 with four ^tBu environments being detected in the ¹H NMR spectrum. In addition, a second experiment was conducted by first adding DABCO and then ^tBuNH₂. Addition of DABCO results in a formation of a dark brown-green mixture with a precipitate formed. Subsequent addition of ^tBuNH₂ results in a colour change of the mixture to brown-yellowish. The ¹H NMR of the suspending solution was identical to the one obtained above when ^tBuNH₂ was added first to the W(NDipp)Cl₄(THF) (**59**) solution. However, the mixture was dried and extracted with acetonitrile. This resulted in a dark red acetonitrile solution, which was dried leaving behind a dark red solid. The ¹H NMR of the red solid was obtained with a multitude of resonances being detected between 1.6 and 0.6 ppm. The red solid was then dissolved in DCM and layered with pentane that resulted in the precipitation of a red powder the ¹H NMR of which was acquired still revealing a multitude of un-attributable resonances.

5.4.5 W(NDipp)(NPh)Cl₂(DME)

The synthesis of this compound was attempted in the same way as described in section 5.4.1 by using W(NPh)Cl₄(THF) (**56**) (0.5 mg, 1.02 mmol), DippNH₂ (192 μL, 1.02 mmol) and DABCO (229 mg, 2.04 mmol). The resulting dark red solution was filtered in order to remove the white precipitate formed, which was characterized as DABCO·HCl by ¹H NMR spectroscopy. The filtrate was dried leaving behind a dark red solid which was analyzed *via* ¹H NMR where two Dipp environments were detected, one being characteristic of W(NDipp)₂Cl₂(DME) (**27**). The red solid was re-dissolved in DCM and layered with pentane in order to isolate a pure crystalline product from the reaction mixture without any success. The experiment was repeated in DCM with addition of TMEDA (153 μL, 1.02 mmol) after DABCO was added. The resulted dark red solution was filtered and kept at -30 °C for 20 h in order to grow crystals without any success. Thus, the dark red solution was dried and the ¹H NMR of the red solid that was left behind was acquired revealing various resonances some of which were characteristic of W(NDipp)₂Cl₂(TMEDA). Single crystals of the red solid suitable for a crystallographic analysis were grown from a DCM/Hexane solution at -30 °C and characterized as W(NDipp)₂Cl₂(TMEDA) which was in agreement with the ¹H NMR. The synthesis of W(NDipp)(NPh)Cl₂(DME) was also attempted by using W(NDipp)Cl₄(THF) (**59**) (500 mg, 0.87 mmol) as a starting material along with PhNH₂ (79 μL, 0.87 mmol) and DABCO (196 mg, 1.75 mmol) according to section 5.4.1. However, the resulting dark red solution behaved in the same way as described above.

5.4.6 W(NPh)₂Cl₂(DME)

The synthesis of this compound was attempted in the same way as described in section 5.4.1 by using W(NPh)Cl₄(THF) (**56**) (0.5 mg, 1.02 mmol), PhNH₂ (93 μL, 1.02 mmol) and DABCO (229 mg, 2.04 mmol). The resulting dark red solution was filtered and dried under reduced pressure. The

remaining dark red solid was subject to a ^1H and ^{13}C NMR spectroscopic analysis, revealing various resonances indicating the presence of impurities. Crystallization of the dark red solid was attempted by dissolving it in a minor amount of DCM and storing it at $-30\text{ }^\circ\text{C}$ for 2 days without any success. Layering with hexane followed, which resulted in the formation of a dark red powder instead of providing single crystals of the compound.

5.4.7 W(NDipp)(NTtbp)Cl₂(DME)

W(NDipp)Cl₄(THF) (**59**) (500 mg, 0.87 mmol), TtbpNH₂ (227 mg, 0.87 mmol) and DABCO (195 mg, 1.74 mmol) were dissolved in DME (15 mL) giving rise to a dark red solution along with formation of a precipitate. The mixture was left stirring for 20 hours followed by filtration and drying of the filtrate under reduced pressure. This resulted in a dark red solid, which was analyzed *via* ^1H NMR spectroscopy where various un-attributable resonances were detected. Therefore, the dark red solid was first extracted with hexane providing a bright orange hexane solution and then with DME providing a dark brown yellow solution. A greenish solid, which was left behind was discarded. Both orange and green solutions were dried resulting in an orange and a green solid respectively which were both found to be mainly TtbpNH₂.

A second attempt to synthesize the compound was made by using lutidine (203 μL , 1.74 mmol) instead of DABCO, but no change in the dark green reaction mixture was observed after all of the reactants were added and left stirring for 20 hours. Thus the mixture was refluxed for 20 hours, but still no change was observed. AlCl₃ (232 mg, 1.74 mmol) was then added to the above reaction mixture, which was then heated at reflux for 20 hours resulting in the formation of a dark red solution. The dark red solution was dried under reduced pressure leaving behind a dark red paste, which was extracted with hexane. The hexane extracts were dried leaving behind a red solid that was analyzed *via* ^1H NMR and was found to consist mainly of TtbpNH₂ along with some impurities.

As a final attempt to synthesize the complex, W(NDipp)Cl₄(THF) (**59**) (500 mg, 0.87 mmol) was dissolved in DME (15 mL) and cooled to $-78\text{ }^\circ\text{C}$. A suspension of TtbpNHLi in DME was also prepared by addition of nBuLi (2.5 M, 0.348 mL, 0.87 mmol) in a DME solution of TtbpNH₂ (227 mg, 0.87 mmol) at $-78\text{ }^\circ\text{C}$. The TtbpNHLi suspension was added dropwise to the cold W(NDipp)Cl₄(THF) (**59**) solution under vigorous stirring. The resulted brown solution was left to react at ambient temperature for 3 hours followed by addition of DABCO (98 mg, 0.87 mmol). The above mixture was then left to react for 2 days giving rise to a brown yellowish solution along with formation of a white precipitate. The volatile components were removed under reduced pressure and the residue was extracted with hexane. The resulting hexane solution was dried and the isolated yellow solid consisted mainly of TtbpNH₂ after being analyzed *via* ^1H NMR.

5.5 Catalysis protocols

5.5.1 Catalysis protocol: 1-hexene dimerisation

Pre-catalyst stock solutions (5.00 mM) were prepared in grease-free ampoules by dissolving the desired complex (0.200 mmol) in PhCl (40.0 mL). Two four-Schlenk arrangements were used. The Schlenks were oven-dried overnight (100 °C) and subsequently allowed to cool (20 mins) under vacuum. Each of the 8 individual Schlenks was then loaded with a Teflon-coated magnetic stirrer bar, PhCl (8.50 mL) and the appropriate pre-catalyst stock solution (4.00 mL, 20.0 μmol) followed by addition of *n*-nonane (1.000 mL, 5.60 mmol) and 1-hexene (12.4 mL, 100 mmol). Stirring was achieved using an IKA stirrer-hotplate set to 1000 rpm and a single silicone oil bath used to heat all the reaction vessels (temperature regulated to 60 °C using an IKA temperature probe). After reaching thermal equilibrium (typically 20 mins), the appropriate quantity (0.60 mL, 300 μmol) of a stock solution of the activator EtAlCl₂ (0.50 M in *n*-heptane) was added to the Schlenk. Subsequently, samples (0.5 mL) from the catalysis mixture were taken under a nitrogen flow *via* syringe at t=30 and t=240 min (after the addition of EtAlCl₂). Each of the samples was then quenched by stirring in a cold 50:50 toluene/HCl_{aq} (10% w/w) mixture (3 mL) and the organic layer was separated, collected, filtered, and subject to GC and hydrogenative GC analysis.

5.5.2 Catalysis protocol: 1-hexene dimerisation in NMR tubes

All of the operations were performed in a nitrogen-filled glove box unless stated otherwise. Eppendorf Reference® micropipettes were used for all solution additions. Pre-catalyst stock solutions (5.00 mM) were prepared in sample pots as follows: each complex (0.188 mmol) was dissolved in PhCl (3.00 mL). The desired pre-catalyst concentration was obtained by diluting an aliquot (400 μL) of the above solution with PhCl (4.60 mL). Stock solutions of the various activators and additives used for catalysis were prepared in a similar way. Catalyst testing was undertaken in standard NMR tubes, which had been oven dried (100 °C) and allowed to cool (1 hour) under vacuum. The NMR tubes were loaded with the appropriate amount (varies depending on the experiment) of pre-catalyst stock solution, followed by PhCl (varies depending on the experiment) and substrate (type and amount varies depending on the experiment). After addition of the substrate, each NMR tube was capped (in order to minimize substrate loss due to evaporation) and agitated. The resulting solutions were heated at 60 °C. Heating was achieved using an IKA stirrer-hotplate (temperature regulated to 60 °C using an IKA temperature probe) equipped with an aluminum heating block able to accommodate 25 NMR tubes. When thermal equilibrium was reached (20 mins) an aliquot (quantity varies depending on the experiment) of activator stock solution was added. Care was taken to ensure that the initiation of the catalytic reaction was performed in exactly the same way for all samples in order to obtain reproducible results. The samples were left in the heating block for 5 hours, after which time they were taken out of the glove box and cooled to -78 °C in order to prevent the evaporation of any residual substrate. Subsequently, d₆-acetone (250 μL), *n*-

nonane (40.0 μL), and *p*-anisaldehyde (97.4 μL) were added under air to each tube. After being allowed to warm to room temperature, an aliquot (~ 0.25 mL) of each solution was collected and diluted with PhCl (~ 0.5 mL). The resulting mixture was filtered and subject to GC and hydrogenative GC analysis. The residual solution in each NMR tube was then analysed by quantitative ^1H NMR spectroscopic analysis. Once NMR spectroscopic analysis was complete, all volatile components were removed from the samples under dynamic vacuum and d_6 -acetone (400 μL) was added to each tube. The resulting solutions were re-analyzed *via* quantitative ^1H NMR spectroscopy.

5.5.3 Catalysis protocol: ethylene

Pre-catalyst stock solutions (5.00 mM) were prepared in grease-free ampoules by dissolving the desired complex (0.200 mmol) in PhCl (40.0 mL). An autoclave was heated to 90°C under vacuum for 1 hour, then cooled to reaction temperature (according to the particular experiment) and back-filled with Ar. The vessel was charged with solvent (amount depends on the particular experiment) and the complex added as a stock solution (4.00 mL, 20.0 μmol). If any additives were to be employed, they were added as a stock solution (amount varies depending on the experiment). Stirring and heating/cooling was achieved using a mechanical stirrer set to 1000 rpm and an automated oil bath, respectively. The vessel was pressurised (40 bar) with ethylene, then vented to 1 bar. The appropriate quantity (0.60 mL, 300 μmol) of a stock solution of the activator EtAlCl_2 (0.50 M in PhCl) was added to initiate catalysis and the vessel was immediately pressurised (pressure depends on the experiment) with ethylene. The ethylene pressure was kept constant throughout the reaction by the continuous addition of gas, which was regulated *via* an automated flow-meter. Once gas uptake had ceased (due to filling of the vessel or catalyst deactivation), the gas supply was closed and the reactor cooled to 4°C . The reactor was carefully vented, with a portion of the vent gas being directly fed to a GC-FID instrument equipped with gas-sampling loop. The reactor contents were treated sequentially with nonane (1000 μL), as internal GC standard), MeOH, and 10% HCl. A sample of the organic phase was taken for GC and hydrogenative GC analysis. Any solid formed was collected, washed with aqueous HCl (10% w/w) and EtOH, then acetone, dried overnight and weighed.

5.6 References

- (1) Gibson, V. C.; Kee, T. P.; Shaw, A. *Polyhedron* **1988**, *7*, 579.
- (2) Bradley, D. C.; Hodge, S. R.; Runnacles, J. D.; Hughes, M.; Mason, J.; Richards, R. L. *Journal of the Chemical Society-Dalton Transactions* **1992**, 1663.
- (3) Leny, J. P.; Osborn, J. A. *Organometallics* **1991**, *10*, 1546.
- (4) Schrock, R. R.; Depue, R. T.; Feldman, J.; Yap, K. B.; Yang, D. C.; Davis, W. M.; Park, L.; Dimare, M.; Schofield, M.; Anhaus, J.; Walborsky, E.; Evitt, E.; Kruger, C.; Betz, P. *Organometallics* **1990**, *9*, 2262.
- (5) Bradley, D. C.; Hursthouse, M. B.; Malik, K. M. A.; Nielson, A. J.; Short, R. L. *Journal of the Chemical Society-Dalton Transactions* **1983**, 2651.
- (6) Reddy, A. C.; Jemmis, E. D.; Scherer, O. J.; Winter, R.; Heckmann, G.; Wolmershauser, G. *Organometallics* **1992**, *11*, 3894.

- (7) Bunker, M. J.; Decian, A.; Green, M. L. H.; Moreau, J. J. E.; Siganporia, N. *Journal of the Chemical Society-Dalton Transactions* **1980**, 2155.
- (8) Chandrasekhar, V.; Boomishankar, R.; Azhakar, R.; Gopal, K.; Steiner, A.; Zacchini, S. *European Journal of Inorganic Chemistry* **2005**, 1880.
- (9) Williams, D. N.; Mitchell, J. P.; Poole, A. D.; Siemeling, U.; Clegg, W.; Hockless, D. C. R.; Oneil, P. A.; Gibson, V. C. *Journal of the Chemical Society-Dalton Transactions* **1992**, 739.
- (10) Nikonov, G. L.; Mountford, P.; Ignatov, S. K.; Green, J. C.; Leech, M. A.; Kuzmina, L. G.; Razuvaev, A. G.; Rees, N. H.; Blake, A. J.; Howard, J. A. K.; Lemenovskii, D. A. *Journal of the Chemical Society-Dalton Transactions* **2001**, 2903.
- (11) Korolev, A. V.; Rheingold, A. L.; Williams, D. S. *Inorganic Chemistry* **1997**, 36, 2647.
- (12) Wolfsber.W; Schmidba.H *Synth. React. Inorganic Met.-Org. Chem.* **1974**, 4, 149.
- (13) Courtois, G.; Miginiac, L. *Journal of Organometallic Chemistry* **1988**, 340, 127.
- (14) Rische, D.; Baunemann, A.; Winter, M.; Fischer, R. A. *Inorganic Chemistry* **2006**, 45, 269.
- (15) Negishi, E.; Swanson, D. R.; Rousset, C. J. *Journal of Organic Chemistry* **1990**, 55, 5406.
- (16) Clark, G. R.; Nielson, A. J.; Rickard, C. E. F. *Journal of the Chemical Society, Dalton Transactions* **1995**, 1907.
- (17) Ignatov, S. K.; Khalimon, A. Y.; Rees, N. H.; Razuvaev, A. G.; Mountford, P.; Nikonov, G. I. *Inorganic Chemistry* **2009**, 48, 9605.
- (18) Kuzmenko, T. E.; Samusenko, A. L.; Uralets, V. P.; Golovnya, R. V. *Journal of High Resolution Chromatography* **1979**, 2, 43.
- (19) Chen, Y.; Credendino, R.; Callens, E.; Atiqullah, M.; Al-Harhi, M. A.; Cavallo, L.; Basset, J.-M. *Acs Catal* **2013**, 1360.
- (20) TA 123-1, T. A. A. B., TA Instruments, New Castle, DE
- (21) Wunderlich, B. *Thermal Analysis of Polymeric Materials*; Springer, 2005.
- (22) Chai, C. K.; Frye, C. J. 2003; Vol. US 6,642,339 B1.
- (23) Peterson, E.; Khalimon, A. Y.; Simionescu, R.; Kuzmina, L. G.; Howard, J. A. K.; Nikonov, G. I. *Journal of the American Chemical Society* **2008**, 131, 908.
- (24) Bury, W.; Chwojnowska, E.; Justyniak, I.; Lewinski, J.; Affek, A.; Zygadlo-Monikowska, E.; Bak, J.; Florjanczyk, Z. *Inorganic Chemistry* **2012**, 51, 737.
- (25) Wright, W. R. H.; Batsanov, A. S.; Howard, J. A. K.; Tooze, R. P.; Hanton, M. J.; Dyer, P. W. *Dalton Transactions* **2010**, 39, 7038.
- (26) Wright, W. R. H., PhD Thesis, Durham University, 2009.

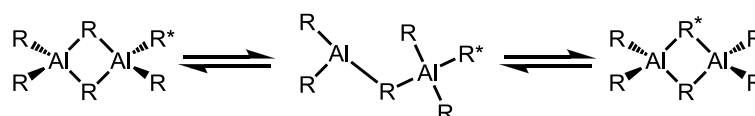
6 Appendices

6.1 Appendix I: exploring the interaction of $R_nAlCl_{(3-n)}$ reagents with DME, THF, and Et_3NHCl

The majority of the catalysis experiments presented in this thesis involve the use of Me_3Al , Et_3Al , $MeAlCl_2$, or $EtAlCl_2$ (referred to as $R_nAlCl_{(3-n)}$ reagents) in the activation step of the oligomerization/polymerization processes and their reactivity probed in a number of stoichiometric reactions described in this thesis (see for example sections 2.4.2.7 and 3.4.1.2). Hence, in this section, the NMR spectroscopic properties of these aluminum alkyls and alkyl chlorides are explored. Additionally, since the majority of the pro-initiators used in the alkene dimerization experiments described contain DME or THF in their coordination sphere, selected stoichiometric reactions of $R_nAlCl_{(3-n)}$ reagents with DME and THF are investigated. Furthermore, it is well-established that the Lewis acidity of various aluminum alkyls differs depending on the number of chloride atoms bound to aluminum.¹³ Hence, in order to assess the Lewis acidity *versus* the alkylation potential of the $R_nAlCl_{(3-n)}$ reagents, their reactions with Et_3NHCl have also been examined, since a strong Lewis acidic character will result in binding of the chloride anion from ammonium salt, while greater alkylating character will be manifest by the production of alkanes following reaction of the acidic ammonium proton.

6.1.1 NMR spectroscopic data for Me_3Al , Et_3Al , Me_2AlCl , $MeAlCl_2$, and $EtAlCl_2$ in C_6D_6

The room temperature 1H , ^{13}C , and ^{27}Al NMR spectroscopic data for Me_3Al , Et_3Al , Me_2AlCl , $MeAlCl_2$, and $EtAlCl_2$ in C_6D_6 are summarized in Table 6.1. As is well established, the simplicity of the room temperature 1H NMR spectra of such $R_nAlCl_{(3-n)}$ compounds implies that the alkyl substituents are equivalent on the NMR timescale, although these species are dimers in solution and in the solid state (exceptions to this are bulky aluminum-alkyls, such as triisobutylaluminum, which are essentially monomeric in solution).¹⁴⁻¹⁶ The observed equivalence of the Al-bound alkyl groups has been attributed to the fast exchange between the terminal and bridging groups of the aluminum compounds, which readily occurs at room temperature (Scheme 6.1).^{14,17}



Scheme 6.1 Terminal/bridging alkyl group exchange processes in aluminum alkyl compounds

These types of terminal-bridging alkyl exchange process for $R_nAlCl_{(3-n)}$ reagents causes broadening of the ^{13}C NMR resonances of the carbon atoms connected to the Al centre, something that is further exacerbated by the quadrupolar nature of the aluminum nucleus.¹⁵ For example, in the NMR spectra obtained, the ^{13}C NMR resonance of the CH_2 moiety of Et_3Al is much broader ($\nu_{1/2} = 5.1$ Hz) than the

resonance observed for the CH₃ fragment ($\nu_{1/2}$ = 0.70 Hz). Furthermore, for systems where the environment around the aluminum atom has low symmetry (e.g. in EtAlCl₂ and MeAlCl₂) the induced quadrupolar relaxation is so intense that the NMR signals of the carbon atoms adjacent to the aluminum broaden to the extent that they cannot be observed in their ¹³C NMR spectra.¹⁸ These types of line broadening are also apparent in the ²⁷Al NMR spectra of all of the aluminum-containing reagents examined in this thesis.

Table 6.1 Experimentally-determined solution state NMR (400 MHz, C₆D₆) spectroscopic data for Me₃Al, Et₃Al, MeAlCl₂, and EtAlCl₂ (concentration of ~ 0.5 M)^a

Al Reagent	Chemical shift (ppm)		
	¹ H NMR	¹³ C NMR	²⁷ Al NMR
Me₃Al	-0.35 (s, 9H)	-7.06 (16.3)	155 (1327)
Et₃Al	0.32 (q, 6H) 1.10 (t, 9H)	0.66 (5.1) 8.89	158 (2553)
Me₂AlCl	-0.33 (s, 6H)	-6.19	175 (2942)
MeAlCl₂^b	-0.42 (s, 3H)	Not observed	134 (1825)
EtAlCl₂^b	0.16 (q, 2H) 0.90 (t, 3H)	Not observed 7.17	131 (2189)

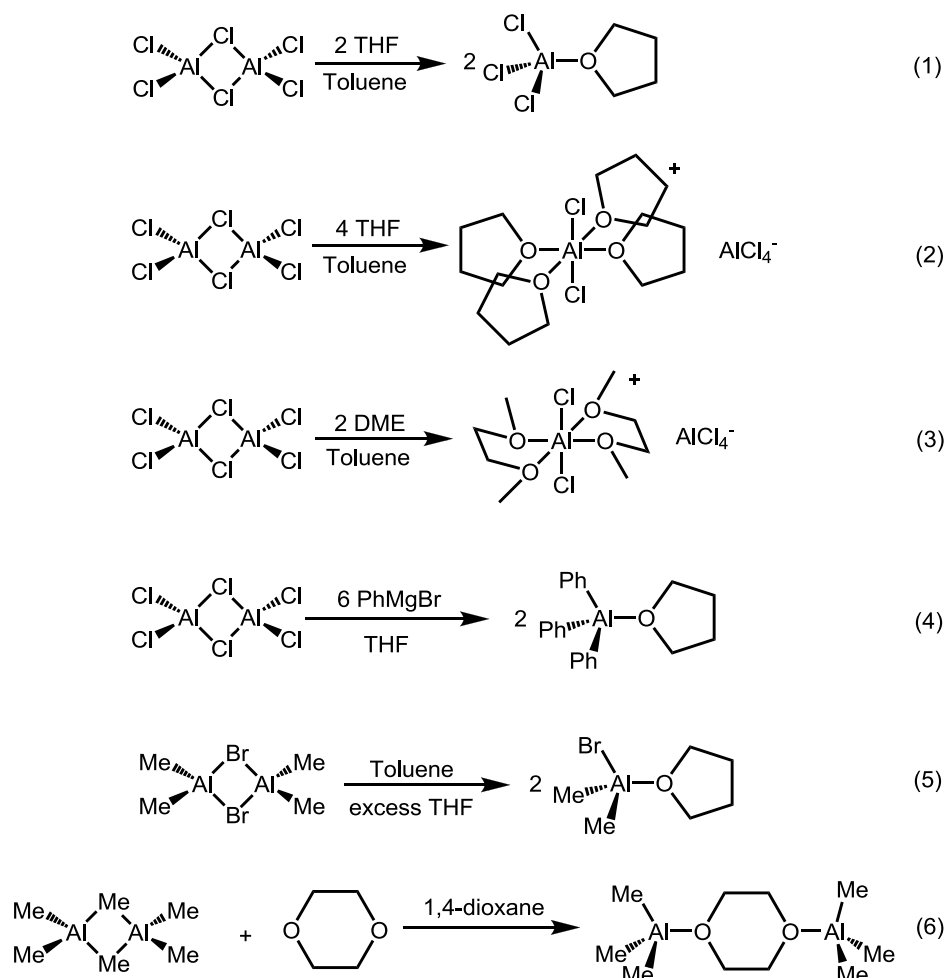
^a The peak widths at half maximum height (in Hz) are included in brackets where resonances are broader than 4 Hz. ^b A secondary broad resonance ($\nu_{1/2}$ = ~600 Hz) in the ²⁷Al NMR spectra was detected at 100 ppm corresponding to ~ 7% of the sample based on the integration of the aluminum signals

It is important to note here that in the commercially obtained MeAlCl₂ and EtAlCl₂ reagents used through this thesis, their ²⁷Al NMR spectra always contained an additional resonance at 100 ppm was detected (Table 6.1), which has been tentatively ascribed to arising from the presence of AlCl₃.^{†††,19}

6.1.2 Reactions of R_nAlCl_(3-n) reagents with DME and THF

Many of the transition metal-based pre-catalysts used in this study have THF or DME present in their primary coordination sphere. Since these systems are then activated with R_nAlCl_(3-n) reagents, using transition metal:aluminium ratios of typically 1:15, there is the possibility that any Lewis acid/base interactions between the ethers and aluminium species could significantly influence subsequent reactivity/catalysis. Consequently, it was of interest to probe the interactions between ethers and aluminum compounds of the general formula R_nAlCl_(3-n) since, somewhat surprisingly, to the best of our knowledge, these have been only explored scarcely in the literature; some of the few known examples are depicted in Scheme 6.2.²⁰⁻²⁵

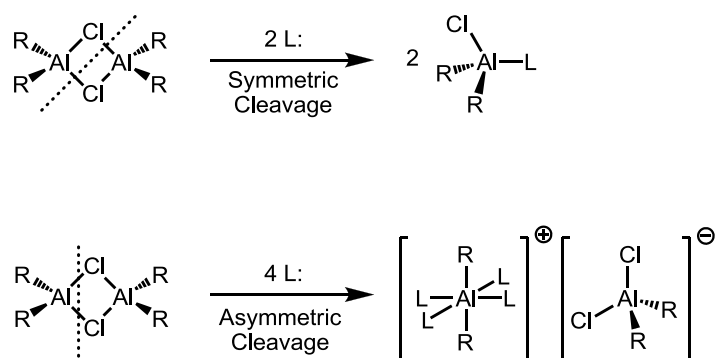
††† The ²⁷Al NMR spectroscopic data for AlCl₃ in such mixtures has not been reported in the literature. Nevertheless, the AlCl₄⁻ anion and the adduct Et₃N-AlCl₃ exhibit sharp singlet resonances in C₆D₆ at 103.5 ppm and 109.5 ppm respectively (see sections 5.3.1.12 and 5.3.1.9). Hence, the presence of AlCl₃ resonating at 100 ppm in the ²⁷Al NMR spectra of the commercially obtained MeAlCl₂ and EtAlCl₂ was confirmed indirectly from the detection of AlCl₄⁻ and Et₃N-AlCl₃ by ²⁷Al NMR spectroscopy in the C₆D₆ solutions that resulted from the reaction between MeAlCl₂ and EtAlCl₂ with Et₃NHCl and Et₃N, respectively (sections 5.3.1.16 and 5.3.1.10).



Scheme 6.2 Previously-reported reactions between $R_n\text{AlCl}_{(3-n)}$ ($R = \text{alkyl}$, $X = \text{halide}$) and THF or DME²⁰⁻²⁵

For example, the reaction between Al_2Cl_6 and THF ($\text{Al}:\text{O} = 1:1$) has been reported to produce $\text{AlCl}_3\cdot\text{THF}$, although no details are provided concerning its structure (Scheme 6.2, eq. 1).²⁰ A more detailed study of products from reactions between Al_2Cl_6 and THF or DME was presented by Means *et al.*, in which formation of $[\text{AlCl}_2(\text{THF})_4][\text{AlCl}_4]$ and $[\text{AlCl}_2(\text{DME})_2][\text{AlCl}_4]$ (**43**), respectively, were observed (Scheme 6.2, eq. 2 and 3).²³ Complex (**43**) was also synthesized by reacting $[(\text{PhCO}_2)\text{AlCl}_2]_2$ with DME, and its structure subsequently confirmed *via* an X-ray crystallographic study.²¹

In contrast to AlCl_3 , alkyl aluminum compounds often have a preference towards formation of 1:1 adducts with Lewis bases *via* the symmetric cleavage of the dimeric aluminum reagent (Scheme 6.3). For example, reaction of Me_2AlBr with THF yields $\text{Me}_2\text{AlBr}\cdot\text{THF}$,²² while reacting AlCl_3 with PhMgBr in THF resulted in formation of $\text{Ph}_3\text{Al}\cdot\text{THF}$ (Scheme 6.2, eq. 4 and 5).²⁴ Similarly, reaction of 1,4-dioxane with Me_3Al ($\text{Al}:\text{O} = 1:1$) gives the bimetallic complex $\text{Me}_3\text{Al}-\text{O}(\text{C}_2\text{H}_4)_2\text{O}-\text{AlMe}_3$ Scheme 6.2, eq. 6. Following X-ray crystallographic characterization of this 1,4-dioxane adduct, it was confirmed that the aluminum atom adopts a tetrahedral geometry.²⁵



Scheme 6.3 Symmetric and asymmetric cleavage of $[R_2AlCl]_2$, $R = \text{alkyl group}$ and $L = \text{Lewis base}$

Since, in the present work, catalytic testing was generally carried out with aluminum-to-transition metal ratios of typically greater than 5:1, it was of interest to study the interaction between an excess of an aluminum alkyl with DME or THF in comparable ratios. To this end, C_6D_6 solutions of THF or DME were prepared and increasing quantities of Me_3Al added; the reactions were explored by 1H NMR spectroscopy after each addition (Figure 6.1 for THF and Figure 6.2 for DME).

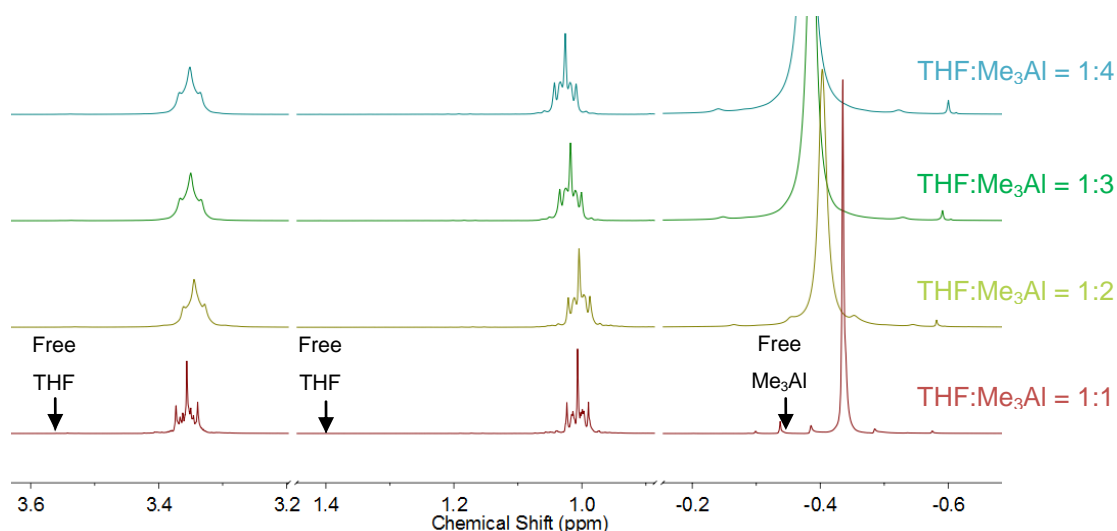
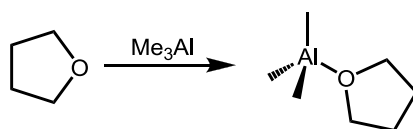


Figure 6.1 1H NMR (400 MHz, C_6D_6) spectroscopic study of the reaction of THF with Me_3Al at ~ 0.4 M in THF (the indicated ratios are expressed in moles)

Me_3Al addition was ceased when no further significant changes could be detected in the NMR spectra. For a Me_3Al :THF ratio of 1:1, the THF proton resonances appear to low frequency shift of those for free THF, consistent with formation of a Lewis acid/base adduct, as described in Scheme 6.4, and in line with the previously-reported reactions presented in Scheme 6.2, eq. 5 and eq. 6.^{22,25} Addition of further equivalents of Me_3Al resulted only in a broadening of the Me_3Al proton resonances, something attributed to exchange of free and bound Me_3Al . This was accompanied by a low frequency shift, as well as a broadening, for the methyl protons of the Me_3Al , something that could be indicative of exchange between free and bound Me_3Al .



Scheme 6.4 Proposed interaction between THF and Me_3Al based on previously characterized complexes.^{22,25}

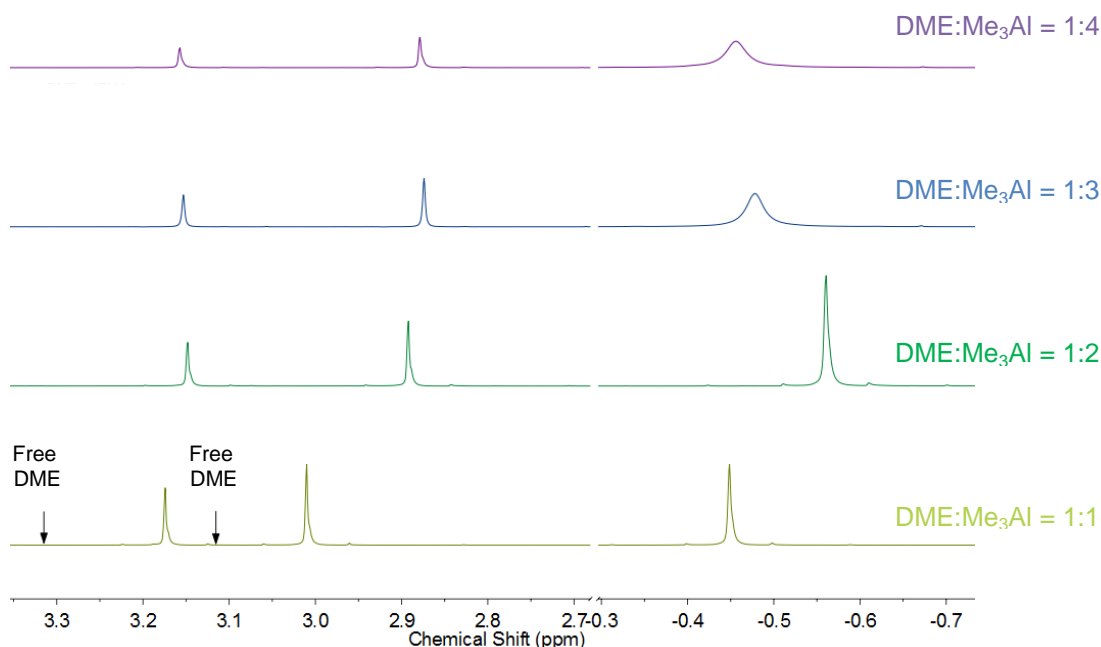
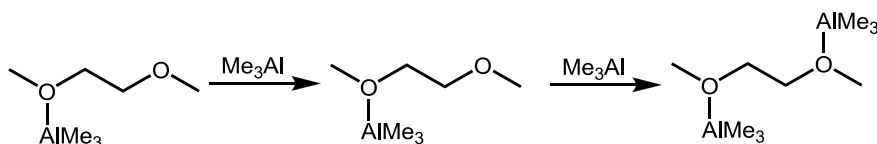


Figure 6.2 ^1H NMR (400 MHz, C_6D_6) spectroscopic study of the reaction of DME with Me_3Al ($\sim 0.4\text{ M}$ in DME) the indicated ratios are expressed in moles.

In contrast to the observations made for THF, addition of both 1 and 2 equivalents of Me_3Al to DME leads to a progressive low frequency shift of the DME resonances (Figure 6.2). Further addition of Me_3Al (>3 equiv.) only results in a broadening of the Me_3Al resonance, but has no additional effect on the chemical shifts associated with the DME fragment. Together, these observations indicate that Me_3Al is able to bind DME in at least two different modes of coordination. Since neither of the species resulting from 1:1 or 2:1 Me_3Al :DME reactions could be crystallised, elucidation of the actual structures was precluded. However, it is suggested that coordination proceeds as shown in Scheme 6.5, resulting in the formation of a bimetallic complex akin to that for the previously-reported 1,4-dioxane complex (Scheme 6.2, eq. 6).



Scheme 6.5 Proposed interactions of DME with Me_3Al

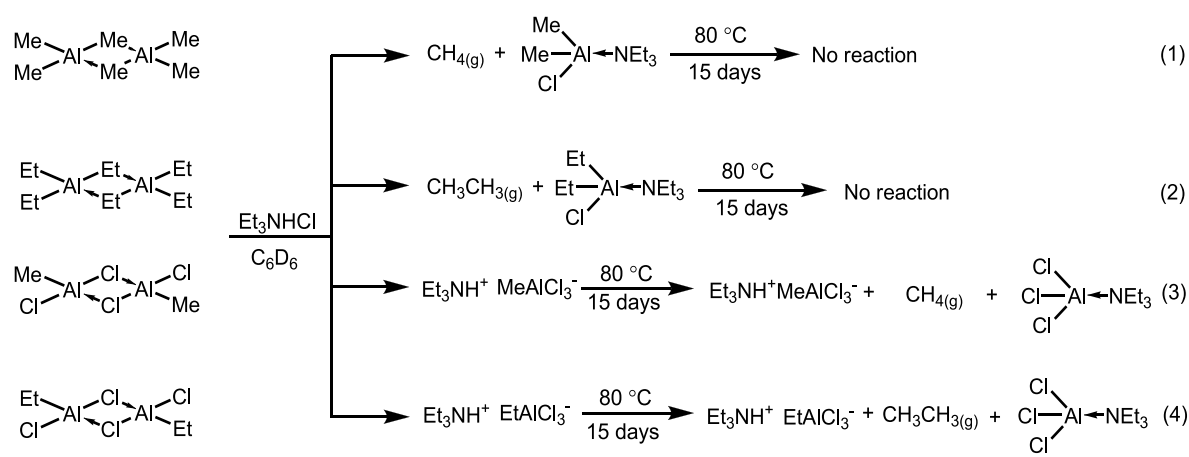
The reactions described in this section of the thesis demonstrate that trialkyl aluminium reagents can, as expected, bind DME and THF forming Lewis acid-Lewis base adducts without any other type of transformation taking place. Since an excess of aluminum alkyls and alkyl chlorides are used to

initiate catalysis in this study, it is reasonable to suggest that the DME and THF originating from the transition metal-based pre-catalysts could become bound to the excess of aluminium-based activator and thus such reactions are unlikely to directly influence the nature of the catalytically active species.

6.1.3 Reactions of aluminum-containing reagents with Et₃NHCl

In section 2.4.1.7 the ability of Et₃NHCl to significantly enhance the catalytic performance of the tungsten imido ethylene dimerization systems was demonstrated. In order to probe this effect, it is of interest to directly explore the interaction between Me₃Al, Et₃Al, MeAlCl₂, and EtAlCl₂ with Et₃NHCl, since it is well established that aluminum compounds of the type R_nAlCl_(3-n) (R = alkyl, X = halide) can act as Lewis acids and/or as alkylating agents.¹⁵

Reactions between Et₃NHCl and the aluminum reagents were performed in C₆D₆ and the resulting solutions were analyzed *via* NMR spectroscopy (see section 5.3.1). Colourless C₆D₆ solutions were obtained from each reaction, apart from with the reaction of Et₃NHCl with one equivalent of MeAlCl₂, which resulted in two immiscible, colourless liquid phases, which implies the formation of an ionic liquid sparingly soluble in C₆D₆.^{†††,26} For both the reactions of Me₃Al and Et₃Al with Et₃NHCl immediate evolution of gas (methane and ethane as identified by ¹H NMR, respectively) was observed. The results from these experiments are summarized in Scheme 6.6.



Scheme 6.6 Reactions of Me₃Al, Et₃Al, MeAlCl₂, and EtAlCl₂ with Et₃NHCl in C₆D₆.

As expected, reaction of Me₃Al or Et₃Al with Et₃NHCl resulted in the protonation of the aluminium alkyl group by the acidic trialkyl ammonium cation, with formation of methane or ethane, respectively, and the appropriate Et₃N-aluminum adduct, with 100% conversions based on the NMR data of the reaction mixtures, Scheme 6.6 eq. 1 and 2 (see also sections 5.3.1.13 and 5.3.1.14). In contrast, addition of MeAlCl₂ or EtAlCl₂ to a suspension of Et₃NHCl in C₆D₆ resulted in the coordination of the Cl⁻ anion to the aluminium, forming [Et₃NH][MeAlCl₃] and [Et₃NH][EtAlCl₃], respectively, according to the NMR spectroscopic analysis of the reaction mixtures that followed (see also sections 5.3.1.15

††† Subsequent evaporation of the volatile components from the reaction mixture of Et₃NHCl with MeAlCl₂ gave a colorless liquid, which was soluble in CD₂Cl₂ allowing its NMR spectroscopic characterization.

and 5.3.1.16). On heating the C₆D₆ solutions of both [Et₃NH][MeAlCl₃] and [Et₃NH][MeAlCl₃] to reflux for 15 days, partial alkyl transfer occurs, with ethane and methane being detected in the ¹H NMR spectra of the reaction mixtures (Scheme 6.6 eq. 3 and 4). These reactions (Scheme 6.6) demonstrate the difference in reactivity between R₃Al (R = Et or Me) derivatives, which are strong alkylating agents, and compounds of the type RAlCl₂ (R = Et or Me), which are weak alkylating agents, but strong Lewis acids, as expected due to the presence of the electronegative halide substituents.

The differences observed here between the reactivity of the trialkyl aluminium and alkyl aluminium dichloride reagents described in this section parallel the differences observed when using each of these types of aluminium reagent as co-initiator in olefin dimerization catalysis experiments (sections 2.4.2.5 and 3.4.2.3). Specifically, it was found that the trialkyl aluminum reagents did not efficiently initiate the dimerization of ethylene or 1-hexene, while in contrast, the alkyl aluminum dichlorides proved very effective dimerization initiators with tungsten imido pro-initiators. Similar observations with regards to the efficiency of various aluminum activators in initiating dimerization have been disclosed for the *in situ* Sasol olefin dimerization system, where Et₃Al and MAO were found to be inactive, while EtAlCl₂, Et₂AlCl, and MeAlCl₂ were all very efficient.⁴ Hence, it appears that an aluminum activator with strong Lewis acidic rather than strong alkylating character is crucial in such catalytic olefin dimerisation reactions.

6.2 Appendix II: definitions used in the analysis of catalysis test data

Following 1-hexene and ethylene catalytic dimerization testing the composition of the resulting organic fractions was analyzed by GC, hydrogenative GC and NMR spectroscopy. Here, the analytical protocols for each method are outlined and, due to the controversial nature of the various expressions used to describe catalytic activity,¹ the catalytic performance parameters (e.g. productivities, activities, etc.) used in this thesis are defined. The following abbreviations are used throughout:

- Heavies = all catalysis products heavier than trimers.
- t = time until the catalytic system becomes deactivated or, in the case of ethylene, the catalysis reaction vessel is filled.
- C₂, 1C₄, C₄, 1C₆, C₆, iC₆, C₁₂, C₁₈ = ethylene, 1-butene, butenes, 1-hexene, hexenes, internal hexenes, dodecenes, and octadecenes, respectively.
- FW_{TM}, FW_{C₂}, FW_{C₄}, FW_{C₆}, FW_{C₁₂}, FW_{C₁₈} = formula weight of the transition metal, ethylene, butenes, hexenes, dodecenes, and octadecenes, respectively.
- m_{C₂}, m_{1C₄}, m_{C₄}, m_{1C₆}, m_{C₆}, m_{iC₆}, m_{C₁₂}, m_{C₁₈}, m_{hev} = the mass (g) of ethylene, 1-butene, butenes, 1-hexene, hexenes, internal hexenes, dodecenes, octadecenes, and heavies at a specific time during the progress of the catalytic reaction, respectively.

- n_{C_2} , n_{1C_4} , n_{C_4} , n_{1C_6} , n_{C_6} , n_{iC_6} , $n_{C_{12}}$, $n_{C_{18}}$, n_{heav} = the moles of ethylene, 1-butene, butenes, 1-hexene, hexenes, internal hexenes, dodecenes, octadecenes, and heavies at a specific time during the progress of the catalytic reaction, respectively.
- $m_{C_6}^{t=0}$ = the mass (g) of 1-hexene before initiation of the catalytic reaction.
- $n_{C_6}^{t=0}$ = the moles of 1-hexene before initiation of the catalytic reaction.
- $m_{C_2}^{used}$ = mass of ethylene consumed at a specific time during an ethylene dimerization run.

6.2.1 Definition of the performance parameters for catalytic ethylene dimerization

In the following section, the parameters used to demonstrate the performance of each catalytic system in the dimerization of ethylene are described.

6.2.1.1 Productivity (TON) and activity

The *productivity (TON)* of the catalytic system is defined as *the number of grams of all products formed per gram of transition metal*. This can be calculated (eqn. 18) by measuring the total mass of the resulting products (dimers, trimers, and heavies).

$$\text{Prod}_g^{C_2} = \frac{m_{\text{products}}}{m_{\text{TM}}} = \frac{m_{C_4} + m_{C_6} + m_{\text{heav}}}{n_{\text{TM}} \times \text{FW}_{\text{TM}}} (\text{g}_{C_2} \times \text{g}_{\text{TM}}^{-1}) \quad (\text{eq. 1})$$

Productivities may also be expressed in moles, eqn. 19:

$$\text{Prod}_{\text{mol}}^{C_2} = \frac{\text{Prod}_g^{C_2} \times \text{FW}_{\text{TM}}}{\text{FW}_{C_2}} (\text{mol}_{C_2} \times \text{mol}_{\text{TM}}^{-1}) \quad (\text{eq. 2})$$

The *activity* of the catalytic system is defined as the *productivity per unit time* (eq. 3):

$$\text{Act}_g = \frac{\text{Prod}_g}{t} (\text{g}_{\text{substrate}} \times \text{g}_{\text{TM}}^{-1} \times \text{h}^{-1}) \text{ or } \text{Act}_{\text{mol}} = \frac{\text{Prod}_{\text{mol}}}{t} (\text{mol}_{\text{substrate}} \times \text{mol}_{\text{TM}}^{-1} \times \text{h}^{-1}) \quad (\text{eq. 3})$$

6.2.1.2 Percentage of liquid and polymer fractions in the catalysis products

The term *liquid%* expresses the mass percentage of the liquid fraction in the catalysis products, while the *polymer%* fraction expresses the mass percentage of any polymeric material formed (eqn. 5):

$$\text{Liquid}\% = \frac{m_{C_4} + m_{C_6} + m_{C_{\text{heav}}}}{m_{C_4} + m_{C_6} + m_{C_{\text{heav}}} + m_{\text{pol}}} \times 100 \quad (\text{eq. 4}),$$

$$\text{Polymer}\% = 100 - \text{Liquid}(\%) \quad (\text{eq. 5})$$

6.2.1.3 Percentage of 1-alkene in corresponding alkene product fraction

The percentages of 1-butene (eq. 6) and 1-hexene (eq. 7) in the corresponding butene and hexene fractions, respectively, are expressed as:

$$1C_4 \text{ in } C_4 (\%) = \frac{m_{1C_4}}{m_{C_4}} \times 100 \quad (\text{eq. 6}), \quad 1C_6 \text{ in } C_6 (\%) = \frac{m_{1C_6}}{m_{C_6}} \times 100 \quad (\text{eq. 7})$$

6.2.1.4 Determination of weight and mole percentage product compositions

The weight (wt%) and mole (mol%) percentages for each component in the catalysis mixture after a specific time are expressed as follows (eqs. 8 to 15):

$$\text{wt}\%_{C_4} = \frac{m_{C_4}}{m_{C_4} + m_{C_6} + m_{\text{hev}}} \times 100 \quad (\text{eq. 8}), \quad \text{mol}\%_{C_4} = \frac{n_{C_4}}{n_{C_4} + n_{C_6} + n_{\text{hev}}} \times 100 \quad (\text{eq. 9})$$

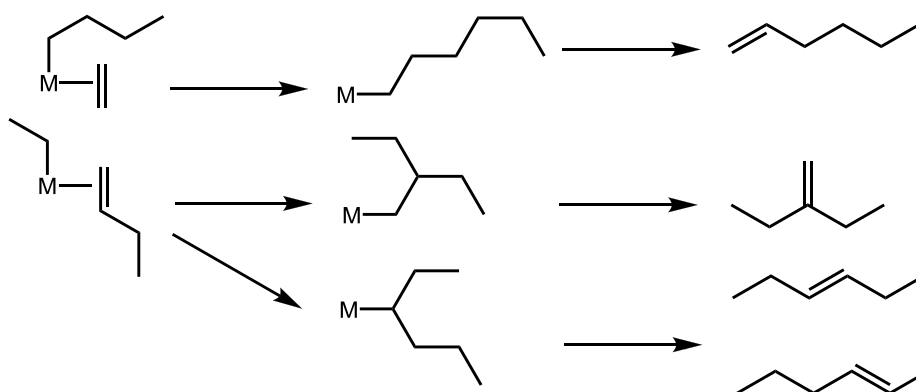
$$\text{wt}\%_{1C_4} = \frac{m_{1C_4}}{m_{C_4} + m_{C_6} + m_{\text{hev}}} \times 100 \quad (\text{eq. 10}), \quad \text{mol}\%_{1C_4} = \frac{n_{1C_4}}{n_{C_4} + n_{C_6} + n_{\text{hev}}} \times 100 \quad (\text{eq. 11})$$

$$\text{wt}\%_{C_6} = \frac{m_{C_6}}{m_{C_4} + m_{C_6} + m_{\text{hev}}} \times 100 \quad (\text{eq. 12}), \quad \text{mol}\%_{C_6} = \frac{n_{C_6}}{n_{C_4} + n_{C_6} + n_{\text{hev}}} \times 100 \quad (\text{eq. 13})$$

$$\text{wt}\%_{C_{\text{hev}}} = \frac{m_{C_{\text{hev}}}}{m_{C_4} + m_{C_6} + m_{\text{hev}}} \times 100 \quad (\text{eq. 14}), \quad \text{mol}\%_{C_{\text{hev}}} = \frac{n_{C_{\text{hev}}}}{n_{C_4} + n_{C_6} + n_{\text{hev}}} \times 100 \quad (\text{eq. 15})$$

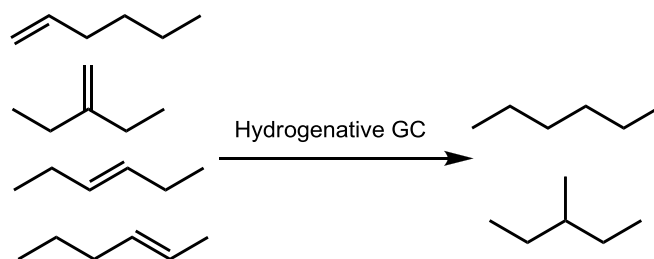
6.2.1.5 Hexenes fraction branching selectivity

During the dimerization of ethylene, hexenes are also formed, as a result of either ethylene trimerization or to coupling of ethylene with 1-butene (itself produced *via* dimerization). The possible hexene isomers derived from the dimerization of 1-butene with ethylene *via* a Cossee-Arlman mechanism are outlined in Scheme 6.7.



Scheme 6.7 Hexene isomers formed as side products during ethylene dimerization

The *branching selectivity* of the catalytic system towards a specific branching pattern is defined as *the percentage of a particular branched isomer as a fraction of all isomers*. In order to determine the branching selectivity in the hexenes fraction, a sample of the catalysis products was analyzed *via* hydrogenative GC,² which results in the formation of hexane and 3-methyl pentane (Scheme 6.8).



Scheme 6.8 Hexanes formed after hydrogenation of trimer side products

The branching selectivity (BrSel%) of a catalyst towards linear hexenes and methyl pentenes in the hexenes fraction can be calculated from the mass of each hexane isomer detected by hydrogenative GC according to eq. (16):

$$\text{BrSel}\%_{\text{branching pattern}} = \frac{m_{\text{alkane}}}{\sum m_{\text{alkanes}}} \times 100 \quad (\text{eq. 16})$$

Hydrogenative GC analysis is important because it produces a more simple/resolved chromatogram for the dimers fraction compared to that of routine GC. This is especially helpful for the identification of the various branching patterns in the dimerization of 1-hexene where a great variety of dodecene isomers is formed (section 6.2.2.6).

6.2.2 Definition of the performance parameters for catalytic 1-hexene dimerization

In the following section, the parameters used to demonstrate the performance of each catalytic system for the 1-hexene dimerization are outlined.

6.2.2.1 Productivity (TON) and activity for the dimers fraction

In a similar manner to those defined previously for ethylene dimerization, the productivity (TON) for the dimer fraction expressed in grams and moles is expressed according to eqs. 17 and 18:

$$\text{Prod}_g^{C_{12}} = \frac{m_{C_{12}}}{m_{TM}} = \frac{m_{C_{12}}}{n_{TM} \times \text{FW}_{TM}} \quad (\text{g}_{C_{12}} \times \text{g}_{TM}^{-1}) \quad (\text{eq. 17})$$

$$\text{Prod}_{\text{mol}}^{C_{12}} = \frac{n_{C_{12}}}{n_{\text{complex}}} = \frac{\text{Prod}_g^{C_{12}} \times \text{FW}_{TM}}{\text{FW}_{C_{12}}} \quad (\text{mol}_{C_{12}} \times \text{mol}_{TM}^{-1}) \quad (\text{eq. 18})$$

The corresponding catalytic activities can be calculated from eq. 3.

It should be noted that in the majority of the 1-hexene dimerization experiments the catalyst became inactive before the substrate was fully converted. Since there is not a convenient way to determine the exact time when catalyst deactivation occurs during a run, all of the 1-hexene dimerization experiments were run past the point where catalyst deactivation occurs (typically 5 h). This means that calculating the catalytic activity of a complex in the 1-hexene dimerization experiments is not possible since the activity is calculated by dividing the productivity by the time that the catalytic system remains active.

6.2.2.2 Productivity and activity

As for ethylene dimerization the catalytic productivities for hexene dimerization may be defined by eqs. 19 and 20:

$$\text{Prod}_g^{C_6} = \frac{m_{C_{12}} + m_{C_{18}} + m_{\text{hev}}}{n_{\text{TM}} \times \text{FW}_{\text{TM}}} (\text{g}_{C_6} \times \text{g}_{\text{TM}}^{-1}) \quad (\text{eq. 19})$$

$$\text{Prod}_{\text{mol}}^{C_6} = \frac{\text{Prod}_g^{C_6} \times \text{FW}_{\text{TM}}}{\text{FW}_{C_6}} (\text{mol}_{C_6} \times \text{mol}_{\text{TM}}^{-1}) \quad (\text{eq. 20})$$

The activities can be calculated using eq. 3.

6.2.2.3 Determination of weight and mole percentage product compositions

In an analogous way to that used for the ethylene testing, the weight (wt%) and mole (mol%) percentages for each component in the catalysis mixture after a specific time are expressed as follows (eqs. 21 to 27):

$$\text{wt}\%_{C_6} = \frac{m_{C_6}}{m_{C_{12}} + m_{C_{18}} + m_{\text{hev}} + m_{C_6}} \times 100 \quad (\text{eq. 21})$$

Similarly for dimers, trimers and heavies:

$$\text{wt}\%_{C_{12}} = \frac{m_{C_{12}}}{m_{C_{12}} + m_{C_{18}} + m_{\text{hev}} + m_{C_6}} \times 100 \quad (\text{eq. 22})$$

$$\text{wt}\%_{C_{18}} = \frac{m_{C_{18}}}{m_{C_{12}} + m_{C_{18}} + m_{\text{hev}} + m_{C_6}} \times 100 \quad (\text{eq. 23})$$

$$\text{wt}\%_{\text{hev}} = \frac{m_{\text{hev}}}{m_{C_{12}} + m_{C_{18}} + m_{\text{hev}} + m_{C_6}} \times 100 \quad (\text{eq. 24})$$

In the product fraction obtained the above quantities become:

$$\text{wt}\%_{C_{12}}^{\text{prod}} = \frac{m_{C_{12}}}{m_{C_{12}} + m_{C_{18}} + m_{\text{hev}}} \times 100 \quad (\text{eq. 25}) \quad \text{wt}\%_{C_{18}}^{\text{prod}} = \frac{m_{C_{18}}}{m_{C_{12}} + m_{C_{18}} + m_{\text{hev}}} \times 100 \quad (\text{eq. 26})$$

$$\text{wt}\%_{\text{hev}}^{\text{prod}} = \frac{m_{\text{hev}}}{m_{C_{12}} + m_{C_{18}} + m_{\text{hev}}} \times 100 \quad (\text{eq. 27})$$

All the above quantities can also be expressed in mol% like in section 6.2.1.2.

6.2.2.4 Percent Conversion (Conv%)

Percent conversion of 1-hexene is defined as the mass% of hexenes converted to products at a specific time during catalysis (eqn. 28):

$$\text{Conv}\% = \frac{m_{C_6}^{t=0} - m_{C_6}}{m_{C_6}^{t=0}} \times 100 = 100 - \frac{m_{C_6}}{m_{C_{12}} + m_{C_{18}} + m_{\text{hev}} + m_{C_6}} \times 100 \quad (\text{eq. 28})$$

Combining with eq. 21, eq. 28 becomes:

$$\text{Conv}\% = 100 - \text{wt}\%_{C_6} \quad (\text{eq. 29})$$

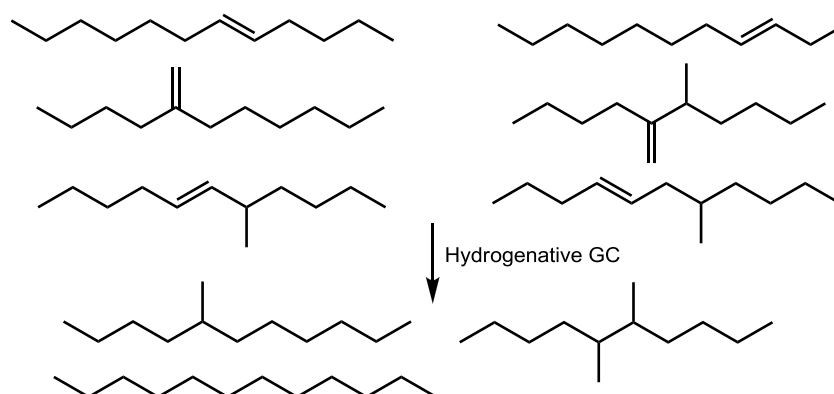
6.2.2.5 Percentage Substrate Isomerized (Isom%)

The percentage of the product that is isomerized (Isom%) is defined as *the fraction of terminal alkene that is isomerized to internal alkenes after a specific amount of time during a run* and is expressed as a percentage:

$$\text{Isom}\% = \frac{m_{iC_6}}{m_{C_6} + m_{C_{12}} + m_{C_{18}} + m_{\text{hev}}} \times 100 \quad (\text{eq. 30})$$

6.2.2.6 Branching selectivity in the dimer fraction

Various dodecene isomers can be formed depending on the orientation with which two 1-hexene molecules are linked during dimerization (Scheme 6.9).



Scheme 6.9 Dodecene isomers formed during 1-hexene dimerization and their hydrogenation products

By analogy with the methodology used in section 6.2.1.5, the branching selectivity in the dimer fraction may be determined for each sample collected from the 1-hexene dimerization experiments using hydrogenative GC (section 6.2.1.5). This *in situ* hydrogenation process results in the formation of alkanes with different branching patterns. The branching selectivity of the catalytic system to the various branching patterns in the dimer fraction is calculated from eq. 16.

6.3 Appendix III: analysis of olefin dimerization products: analytical method validation

In order to calculate the performance parameters of each catalytic system described in sections 2, 3, and 4, the masses of each of the components of the mixtures that result from a particular catalysis experiment must be determined. This can be achieved either by gas chromatography (ethylene and 1-hexene dimerization) or by ^1H NMR spectroscopy (1-hexene dimerization). In this section these two methods are compared and validated.³

6.3.1 Analysis of olefinic hydrocarbons using gas chromatography

The samples collected after each catalytic dimerization experiment were analyzed *via* GC. A PONA (Paraffins, Olefins, Naphthalenes and Aromatics) capillary chromatographic column is required for adequate separation of the components in each sample; detection was achieved with an FID (Flame Ionization Detector). Here, the nature of each catalysis product was determined from its retention time,⁴ while its quantification in the post-catalytic reaction mixture was determined against a suitable internal standard, namely *n*-nonane.

Below, the calculations involved in the quantitation of the alkenes present in each sample are outlined along with an assessment of the accuracy of the technique. The following abbreviations are used throughout:

- i = a component of the catalysis mixture.
- A_i, A_{st} = peak area of component i and internal standard in the gas chromatogram, respectively.
- RF_i, RF_{st} = response factor of the FID for component i and internal standard, respectively.
- FW_i, FW_{st} = formula weight of component i and internal standard, respectively.
- m_i, m_{st} = the mass (g) of component i and internal standard in the catalysis mixture, respectively.
- $n_i, n_i^{col}, n_i^{inj}, n_i^{fid}$ = number of moles of component i in the catalysis mixture, number of moles of component i in the GC column, number of moles of component i injected into the GC, and number of moles of component i reaching the FID, respectively.
- V^{inj}, V^{sam} = the volume of sample injected into the GC and the total volume of the catalysis mixture.
- m, \bar{m} = general mass and average mass

Each component i of the mixture injected into the GC will reach the FID at a specific time giving rise to a peak in the chromatogram. In the FID, eq. 31 applies:

$$A_i = RF_i \times n_i^{\text{fid}} \quad (\text{eq. 31})$$

Also eq. 32 is true:

$$n_i^{\text{fid}} \propto n_i^{\text{col}} \propto n_i^{\text{inj}} \quad (\text{eq. 32})$$

Taking into account that:

$$n_i^{\text{inj}} = \frac{n_i \times V^{\text{inj}}}{V_{\text{sample}}} \quad (\text{eq. 33})$$

eqn. 31 becomes:

$$A_i = RF_i \times \frac{n_i \times V^{\text{inj}}}{V_{\text{sam}}} \quad (\text{eq. 34})$$

Similarly, for the internal standard:

$$A_{\text{st}} = RF_{\text{st}} \times \frac{n_{\text{st}} \times V^{\text{inj}}}{V_{\text{sam}}} \quad (\text{eq. 35})$$

Dividing eq. 34 by eq. 35 results in eq. 36.

$$\frac{A_i}{A_{\text{st}}} = \frac{RF_i \times n_i}{RF_{\text{st}} \times n_{\text{st}}} \quad (\text{eq. 36})$$

Thus, the mass of compound i in the catalysis mixture can be calculated by rearranging eq. 36 to eq. 37:

$$m_i = \frac{RF_{\text{st}}}{RF_i} \times \frac{A_i}{A_{\text{st}}} \times \frac{FW_i}{FW_{\text{st}}} \times m_{\text{st}} \quad (\text{eq. 37})$$

On the right hand side of eq. 37 all values are known, apart from the ratio of the response factors RF_{st}/RF_i (*i.e.* the relative response factor). This ratio can be calculated either by using the analyte's FW as its response factor (section 6.3.1.1) or, by plotting a calibration curve (section 6.3.1.2).

6.3.1.1 Use of the analyte's FW as its response factor

According to various studies, simple hydrocarbons respond within the FID to give a current that is proportional to their molecular weight or to the number of carbon atoms they contain (eqn. 8).⁵⁻⁷ This is due to the way the FID is speculated to operate: as the analyte burns, CHO^+ ions and free electrons are generated, which create the measured current in the detector. In the case of simple hydrocarbons, where C–C bond cleavage is equally easy for all C–C bonds, the amount of CHO^+ fragments generated per molecule of compound will be equal to the amount of carbon atoms of the compound and, thus, the response factor should be equal to the FW of the compound,⁶ *i.e.*,

$$RF_i = FW_i \quad (\text{eq. 38})$$

So, combining eq. 37 and eq. 38 gives:

$$m_i = \frac{A_i}{A_{st}} \times m_{st} \quad (\text{eq. 39})$$

In order to determine whether eq. 39 applies to the gas chromatograph used for the analysis of the catalytic reaction products generated in this thesis, a test mixture comprising *n*-pentane, *n*-hexane, *n*-heptane, *n*-octane, *n*-nonane, *n*-dodecane, *n*-decatetane, and *n*-decapentane (150 μL of each added with a 250 μL microsyringe) diluted with toluene and chlorobenzene (the solvents used during the GC analysis of the 1-hexene dimerization products) was subject to a GC analysis (Table 6.2). Eq. 39 was then used to determine the mass of each alkane against *n*-nonane as the internal standard. The sample was run on two GC instruments: a Perkin Elmer Clarus 400 GC and an Agilent Technologies 6890N GC both equipped with a PONA column (50 m \times 0.20 mm \times 0.50 mm). The results are summarized in Table 6.2, with a characteristic chromatogram presented in Figure 6.3.

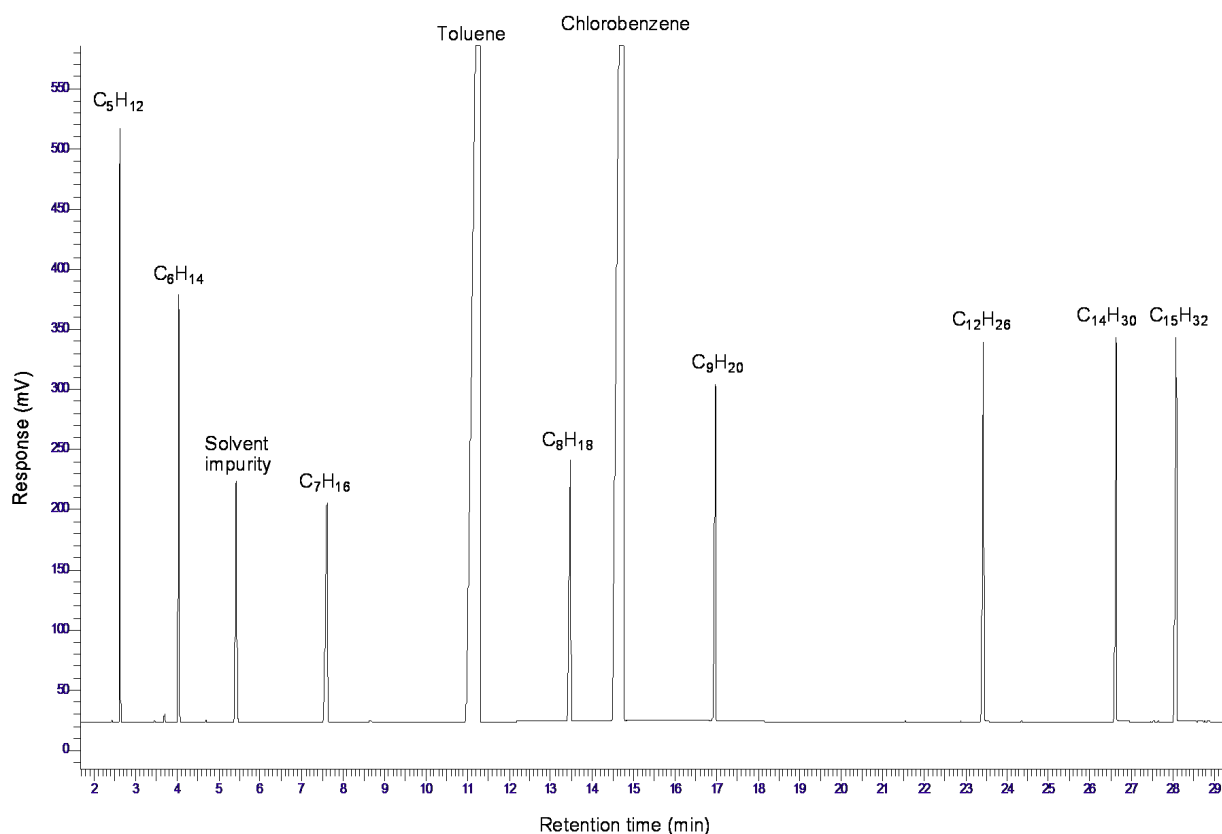


Figure 6.3 GC chromatogram of alkane/solvent test mixture obtained using a Perkin Elmer Clarus 400 GC.

From Table 6.2 it is evident that, in the case of alkanes, the calculation according to eq. 40 is reasonable, but not very accurate, with RSD% up to 16.7. In addition, different average masses are calculated for the same sample by the two different FIDs (Perkin Elmer and Agilent) implying that each system responds to the same compound in a slightly different way. This means that eq. 38 is only an approximation. It should also be noted that the lower the molecular mass of the alkane, compared to that of the internal standard, the more negative the error associated with its determination. The opposite applies for heavier alkanes, where the errors become more positive with

increasing FWs. As expected, the smallest errors are observed for alkanes most similar in structure to the internal standard, such as *n*-octane.

Table 6.2 Quantitative analysis of a known mixture of alkanes by GC

Alkane	Mass added (mg)	Perkin Elmer					Agilent				
		m run1 (mg)	m run2 (mg)	\bar{m} (mg)	Error%	RSD%	m run1 (mg)	m run2 (mg)	\bar{m} (mg)	Error%	RSD%
C₅H₁₂	93.9	89.3	89.1	89.2	-4.7	7.1	83.6	82.1	82.9	-12.0	16.7
C₆H₁₄	98.2	93.6	94.2	93.9	-4.0	6.2	89.9	89.2	89.6	-8.7	12.5
C₇H₁₆	101.9	98.5	99.0	98.8	-3.3	4.4	97.6	97.4	97.5	-4.0	6.1
C₈H₁₈	105.5	103.7	104.1	103.9	-1.3	2.2	103.3	103.3	103.3	-2.0	2.9
C₉H₂₀	107.7	107.7	107.7	107.7	-	-	107.7	107.7	107.7	-	-
C₁₂H₂₆	112.5	115.3	115.4	115.4	+2.7	3.6	117.8	118.0	117.9	+4.7	6.8
C₁₄H₃₀	114.5	122.7	122.4	122.6	+7.3	9.9	123.0	123.7	123.4	+8.0	10.9
C₁₅H₃₂	115.4	124.2	123.7	124.0	+7.3	10.5	123.8	124.7	124.3	+8.0	10.9

6.3.1.2 Determination of the relative response factors *via* a calibration curve.

The use of relative response factors is a well-established method and, in some cases, can provide very accurate results in the quantification of certain analytes by GC.⁸ However, the main limitation to this approach is the availability of the necessary compounds in order to construct the calibration curve. In contrast to 1-hexene, which is readily available, the dodecene isomers resulting from the dimerization of 1-hexene cannot be purchased and their synthesis is either unavailable in the literature or very laborious. Nevertheless, due to their structural similarities it is likely that each dodecene isomer will respond in the same way to the FID something that was confirmed by performing a quantitative GC analysis of a mixture of branched hexenes. This experiment showed that the various branching isomers have the same response factors. As a result, in order to generate a calibration curve for the dodecene isomers formed during the dimerization of 1-hexene, eight standard solutions were prepared from a pure (by distillation) sample of dodecene isomers produced by dimerizing 1-hexene using W(NDipp)₂Cl₂(DME) (**27**) /15 EADC. An appropriate amount of 1-hexene and *n*-nonane (internal standard) was added and each sample was analyzed *via* GC (Figure 6.4).

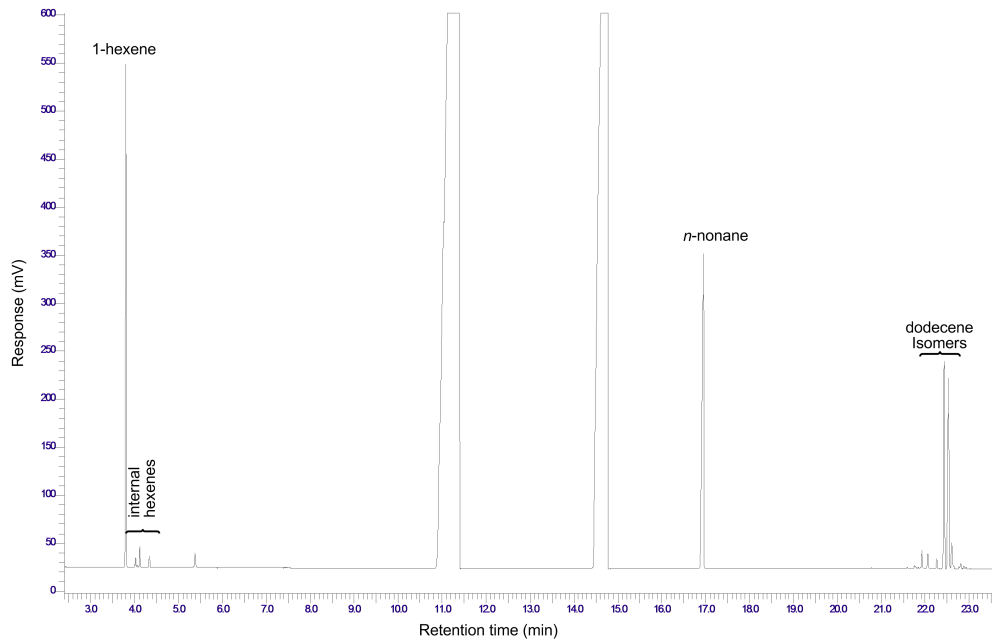


Figure 6.4 An example of a GC spectrum obtained from a sample used for constructing the curves $A_{C_6}/A_{st}=f(m_{C_6}/m_{st})$ and $A_{C_{12}}/A_{st}=f(m_{C_{12}}/m_{st})$.

For each sample eq.37 applies, which can be rearranged to eq. 40:

$$\frac{A_i}{A_{st}} = \frac{RF_i}{RF_{st}} \times \frac{FW_{st}}{FW_i} \times \frac{m_i}{m_{st}} \quad (\text{eq. 40})$$

which in turn can be expressed as eq. 41:

$$\frac{A_i}{A_{st}} = a_{st}^i \times \frac{m_i}{m_{st}} \quad (\text{eq. 41})$$

The constant a_{st}^i is characteristic of the analyte-internal standard couple. Thus, the use of $FW = RF$ (section 6.3.1.1) is a special expression of eq. 41 where $a_{st}^i = 1$. The calibration curves for 1-hexene and dodecenes are obtained by plotting $A_{C_6}/A_{st} = f(m_{C_6}/m_{st})$ and $A_{C_{12}}/A_{st} = f(m_{C_{12}}/m_{st})$, respectively (Table 6.3, Figure 6.5). The intercept was forced to 0 during the regression analysis. It should be noted that commercially available 1-hexene contains traces of internal hexenes (Figure 6.4). These internal hexene isomers have the same response factor as that of 1-hexene (*vide supra*) and thus were treated as if they were 1-hexene.

Table 6.3 Calibration curve calculations for the quantification of 1-hexene and isomeric dodecenes.

Sample	m_{C_6} (mg)	$m_{C_{12}}$ (mg)	m_{st} (mg)	A_{C_6}	$A_{C_{12}}$	A_{st}	m_{C_6}/m_{st}	$m_{C_{12}}/m_{st}$	A_{C_6}/A_{st}	$A_{C_{12}}/A_{st}$
1	50.6	48.7	65.5	235191	249283	323171	0.772	0.744	0.7278	0.7714
2	169.2	79.9	60.3	774021	373096	278816	2.81	1.33	2.7761	1.3381
3	299.5	105.2	57.7	1060031	408318	216238	5.20	1.82	4.9021	1.8883
4	409.3	124.0	54.0	917215	301642	126830	7.58	2.30	7.2318	2.3783
5	527.1	562.6	65.2	1121758	1240686	142050	8.08	8.63	7.8970	8.7342
6	245.0	144.1	18.3	1338710	833337	106650	13.4	7.87	12.552	7.8138
7	92.6	89.1	34.1	1347082	1323356	492753	2.72	2.61	2.7338	2.6856
8	205.1	136.5	22.4	1359030	998519	151465	9.16	6.09	8.9726	6.5924

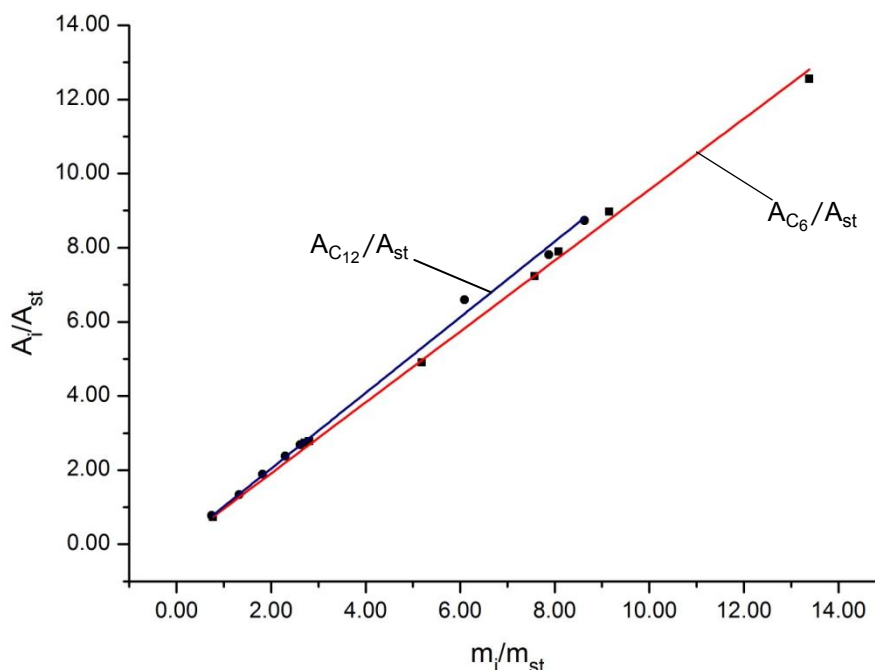


Figure 6.5 Calibration curve for 1-hexene (■) and dodecenes (●) derived using data obtained from a Perkin Elmer Clarus 400 GC system equipped with PONA column.

The parameters for the two calibration curves are presented in Table 6.4. The correlation between the x and y values for both linear regressions is good (adjusted R^2 values >0.99).⁹ In addition, the standard deviation for both gradients is small enough to allow the accurate calculation of $a_{st}^{C_6} = 0.957$ and $a_{st}^{C_{12}} = 1.021$. Since both these two values are close to 1.00, it may be assumed that the approximation that $FW=RF$ is applicable under the specific experimental conditions used here, especially for the analysis of dodecenes.

Table 6.4 Parameters for linear regressions $A_{C_6}/A_{st} = f(m_{C_6}/m_{st})$ and $A_{C_{12}}/A_{st} = f(m_{C_{12}}/m_{st})$

Curve	Slope ($\pm 2\sigma$)	Intercept	Adjusted R^2	Residual sum of squares	Weight
A_{C_6}/A_{st}	0.957 (± 0.015)	0 (-)	0.9995	0.16862	No weighting
$A_{C_{12}}/A_{st}$	1.021 (± 0.024)	0 (-)	0.9989	0.19675	No weighting

The use of the above calibration curves is a more accurate method for the quantification of species present in the GC (according to the calculated standard deviations) compared to using the assumption that RF=FW. However, a calibration curve has the disadvantage that it needs to be verified/replotted regularly in order to maintain its accuracy, which can be laborious. Thus, for the analysis of the post-catalytic dodecenes mixture using the approximation RF=FW is advantageous. This decision can be justified firstly due to the value of $a_{st}^{C_{12}}$ being very close to one, allowing the accurate determination of dodecenes by both methods under the specific experimental setup employed. Secondly, the determination of hexenes (where the RF=FW approximation is not as good) is inherently unreliable due to the relatively high volatility of this olefin (see section 6.3.2). Thus, using a calibration curve here won't make the measurement significantly more accurate. Lastly, the purpose of the above calculations is to determine and compare the catalytic performance parameters of the catalysts examined. Thus, since this is essentially a comparative study, obtaining reproducible results is more important than the accurate determination of absolute values.

6.3.2 Evaluation of the quantification errors resulting from 1-hexene evaporation

All of the catalysis experiments exploring the dimerisation of 1-hexene were performed at 60 °C. In order to initiate the catalytic reaction (addition of aluminium activator) it is necessary to open the reaction vessel while at 60 °C, something that inevitably results in the escape of an amount of 1-hexene *via* evaporation (1-hexene b.p. = 63 °C). The extent of 1-hexene loss during this activation stage can be calculated by running blank samples for each batch of experiments. The accuracy and precision in the determination of evaporated hexenes relies on the ability of the researcher to consistently execute the necessary operations for all experiments in a batch; this can be a very challenging task. For this reason, the calculations of the catalytic performance parameters in sections 2, 3, and 4 are based on the actual amounts of products detected in the final reaction mixture rather than the initial amount of 1-hexene added.

Calculating the catalytic performance parameters based on the products detected in the final reaction mixture assumes that all of the catalysis products can be detected by GC. In the case of 1-hexene dimerization, this is always true apart from two occasions: when ethylene is produced *via* metathesis,¹⁰ and when high molecular weight chlorobenzene-soluble oligomers are formed, which due to their high boiling point, are insufficiently volatile to pass through the GC capillary column. For the case where metathesis occurs, the produced ethylene will probably escape the reaction vessel before the GC analysis, something that will introduce errors in the calculations that follow. However, the corresponding linear decenes formed as the secondary metathesis products can be easily detected. Thus, a catalytic system, which is active for metathesis can be identified through detection of the decenes produced (even though ethylene isn't readily observed). Moreover, all catalysts tested in the dimerization of 1-hexene were also tested for the dimerization of ethylene; for the later, no significant amounts of polymer were formed (see sections 2 and 3). Since none of the catalytic

systems examined gave rise to significant quantities of ethylene polymerization/oligomerisation products, it has been assumed this would also be the case for the bulkier 1-hexene substrate.

Lastly, by calculating the mass balance^{§§§}, it is possible to verify that all catalysis products have been detected and quantified correctly. In order to do this, it was verified that the mass of 1-hexene added to the catalysis vessel (corrected for evaporation from the blank sample runs) was equal to the total mass of detected material at the end of each run.

6.3.3 Gas chromatographic analysis of ethylene dimerization products

The catalytic dimerization of ethylene, along with the analysis of the resulting dimerization products, was performed in the St. Andrews laboratory of Sasol Technology (UK) (section 5.5.3). The masses of the various products produced at the end of each catalysis experiment were determined from GC analysis using the relation $RF=FW$ (section 6.3.1.1). However, it must be borne in mind that due to the volatility of butenes (b.p = $-6\text{ }^{\circ}\text{C}$), their partial loss from the liquid fraction when venting the reactor at the end of each run is inevitable. In order to determine the amount of butenes lost due to such evaporation, a headspace sample from the reactor was collected, at a specific temperature and pressure, and fed directly into an appropriately calibrated GC. This allowed calculation of the mass of butenes present in the collected sample (250 μL of gas at $20\text{ }^{\circ}\text{C}$ and 1 bar). The amount of butenes detected in the GC sample is then reduced to the total volume of the uncompressed reactor headspace, which is calculated using process simulation software (Aspen). Combining the results from the liquid and headspace GC analysis, the total mass of butene can be calculated.

6.3.4 NMR spectroscopic analysis of 1-hexene dimerization products

In order to try and circumvent some of the issues described above for the GC analysis of the products resulting from catalytic 1-hexene dimerization, a second series of tests was carried out in NMR tubes (section 5.5.2). This methodology proved to be the most reliable, efficient, and versatile method of analysis. The advantages of this NMR tube-based approach over that using Schlenks as the reaction vessels are listed below:

- Greater efficiency in the use of starting materials since the reactions are performed at a 50 times smaller scale.
- The obtained results are more accurate and precise (*vide infra*).

^{§§§} The mass balance equation ($m_{C_6}^{t=0} = m_{C_6} + m_{C_{12}} + m_{C_{18}} + m_{\text{hev}}$) results from the law of conservation of mass and expresses that the amount of starting material before the catalysis occurs should be equal to the sum of the masses of the products detected in the reaction mixture at any time during catalysis.

- The method is versatile since the catalysis products can be directly analyzed *via* automated NMR and then, subsequently, readily analysed by GC and hydrogenative GC.
- The calculated mass balances are more accurate (*vide infra*).

The disadvantages/assumptions made when using this method are:

- The method doesn't allow the collection of samples from the catalysis mixture during a run.
- The method is sensitive to the number of alkene C=C double bond protons detected without taking into account whether these protons belong to dimers, trimers or oligomers. Thus, differentiation between dimers and oligomers is not straightforward. This is not a problem for the particular experiments undertaken here since formation of trimers or "heavies" is rare, and occurs in very small amounts. However, at the current stage of development of this NMR spectroscopic method, it has been undertaken alongside GC analysis in order to determine the approximate amount of oligomers formed, if any.

In order to validate this NMR spectroscopic method, 1-dodecene was used in the place of 1-hexene and *trans*-3-hexene in the place of the internal dodecene products. These compounds were selected due to their commercial availability in high purity (>99%).

To analyze the mixtures resulting from the catalytic dimerization of 1-hexene by ^1H NMR spectroscopy there must be adequate separation between the double bond proton resonances of the terminal and internal alkenes. This proved to be the case as shown in the ^1H NMR spectrum of a mixture of 1-dodecene and *trans*-3-hexene in d_6 -acetone (Figure 6.6).

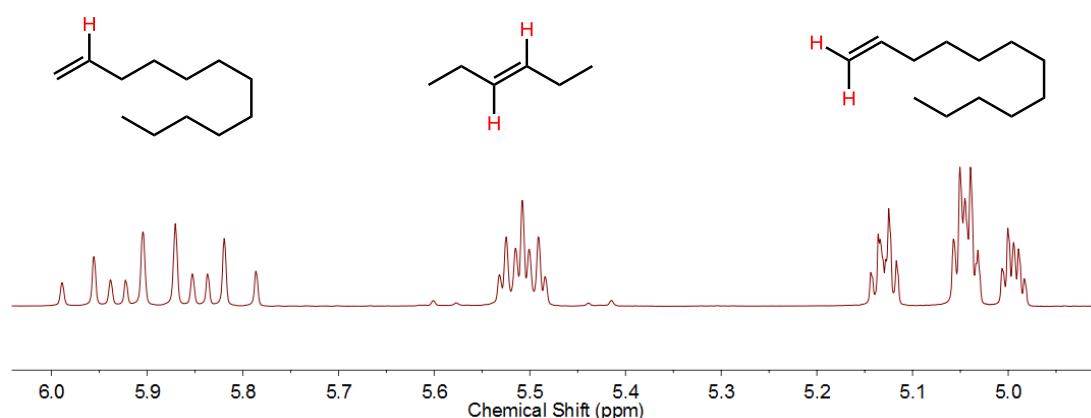


Figure 6.6 ^1H NMR (400 MHz, d_6 -acetone) spectrum of a mixture of *trans*-3-hexene and 1-dodecene in the double C=C bond region.

However, isomerization of 1-hexene to internal hexenes is also observed during catalysis. This means that analysis of the resulting products by ^1H NMR spectroscopy will result in resonances in the 5.4-5.6 ppm region corresponding to dodecenes and internal hexenes. Therefore, in order to calculate the amount of pure dodecenes it is necessary to remove all volatile components from each NMR sample under dynamic vacuum and then re-analyze the sample. In this way, the 1-hexene

remaining after catalysis and its isomers is completely removed without any dodecenes being lost due to their high boiling points (1-dodecene b.p. = 214-216 C).

To ensure accuracy of the quantification process, a suitable internal standard for the NMR analysis must be included, which should:

- Be a liquid so it can be measured and transferred accurately using a micro-pipette.
- Be commercially available in high purity and low cost.
- Exhibit a strong, ideally singlet, resonance in a region of the ^1H NMR spectrum devoid of other resonances.
- Have a boiling point of >210 °C so it will not be removed when the sample is subject to vacuum.
- Have an appropriate GC retention time so its signal will not overlap with other signals in the GC.

p-Anisaldehyde (OMe_3 resonance) was found to conform to all of the above criteria and was therefore chosen as the internal standard for the ^1H NMR spectroscopic analyses.

For an NMR spectrographic analysis to be quantitative there are certain criteria to be met, which are well covered in the literature.¹¹ One of the most important factors in ensuring quantitative peak integration is related to the relaxation time (T_1) of the various resonances of interest and hence, the use of an appropriate relaxation delay during spectral acquisition is essential. Thus, for the studies undertaken here, the relaxation times for the resonances of interest were measured (and found to be approximately 6 sec, depending on the conditions) and, as a result, a relaxation delay of $d1=5*T1-AT$ was used in all analytical experiments, where $d1$, $T1$, and AT refer to the relaxation delay, highest relaxation time observed, and acquisition time, respectively. Furthermore, in order to improve the signal to noise ratio, 128 scans were performed during the analysis of each sample.

Having developed this new NMR spectroscopic method for analyzing the products from 1-hexene dimerization, it was necessary to assess its accuracy and precision. For this purpose, three mixtures of *trans*-3-hexene/1-dodecene were prepared in NMR tubes to mimic three catalysis samples in which 10%, 50%, and 90% conversion of 1-hexene had been achieved (Table 6.5). The resulting ^1H NMR spectrum for the sample mimicking a 50% conversion of 1-hexene is presented in Figure 6.7.

Table 6.5 Composition of standard solutions mimicking catalysis samples.

Component	Volume (μL) / μmoles added for 10% conversion simulation	Volume (μL) / μmoles added for 50% conversion simulation	Volume (μL) / μmoles added for 90% conversion simulation
<i>trans</i> -3-Hexene	12.4/99.7	62.2/500.3	112/901.0
1-Dodecene	400/1801	222/999.7	44.4/199.9
Chlorobenzene	270	270	270
Heptane	12.0	12.0	12.0
<i>d</i> ₆ -Acetone	250	250	250
<i>p</i> -Anisaldehyde	97.4/790.0	97.4/790.0	97.4/790.0
<i>n</i> -Nonane	60.0	40.0	60.0

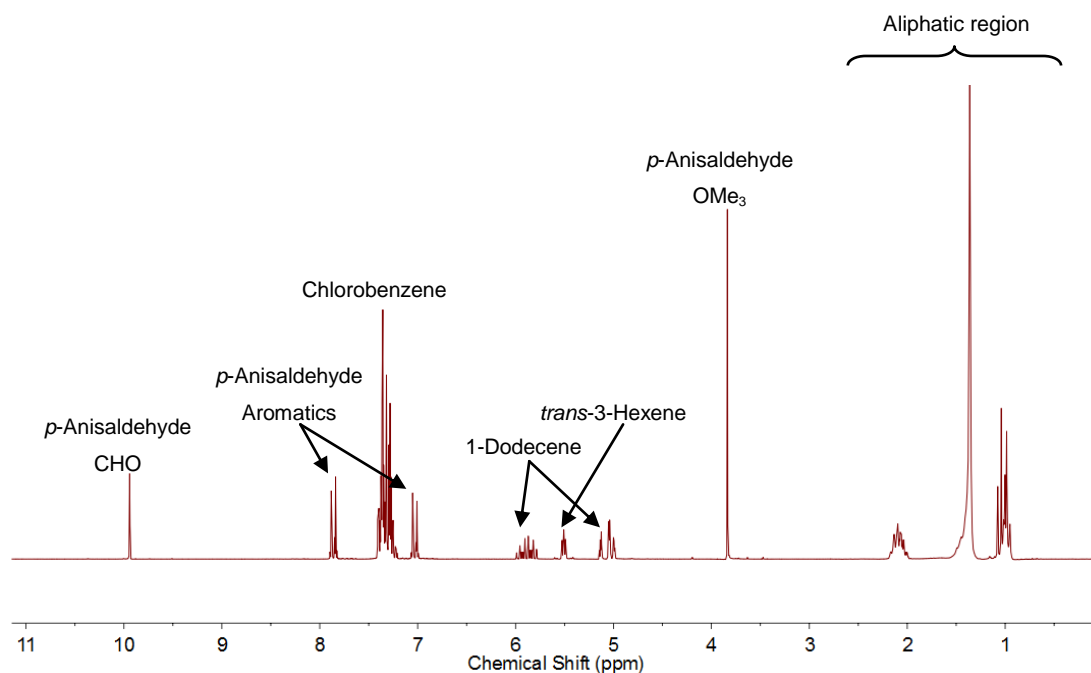


Figure 6.7 ^1H NMR (400 MHz, d_6 -acetone) of a mixture mimicking a catalytic 1-hexene dimerization run where 50% of 1-hexene was converted.

These samples were analyzed by GC and by the new NMR spectroscopic method (Table 6.6). From the errors calculated, it is evident that the quantitative NMR (qNMR) method provides results with a maximum absolute error of 4.3%. In contrast, the errors calculated from the GC analysis of the same samples were at least two times larger with a maximum absolute error of 9.2%. As expected (section 6.3.1), the errors in the GC determination of *trans*-3-hexene (lighter than *n*-nonane) are negative while the opposite applies for the heavier 1-dodecene. In the case of determination *via* qNMR such trends are not observed, which implies that qNMR is not biased.

Table 6.6 Analysis of three mixtures mimicking reaction conversions of 10%, 50% and 90% of 1-hexene (relative to internal dodecenes) by NMR spectroscopy and GC.

Sample	Mass (mg) of compound added		Mass (mg) calculated by Quantitative ^1H NMR analysis (Error%)		Mass (mg) calculated by GC analysis using RF = FW (Error%)	
	<i>trans</i> -3-hexene	1-dodecene	<i>trans</i> -3-hexene	1-dodecene	<i>trans</i> -3-hexene	1-dodecene
10% Conv.	8.39	303.1	8.45 (+ 0.72)	305.3 (+ 0.71)	7.76 (- 7.5)	324.3 (+ 7.0)
50% Conv.	42.1	168.3	42.1 (0.00)	175.6 (+ 4.3)	38.7 (- 7.9)	178.7 (+ 6.2)
90% Conv.	75.8	33.6	73.3 (- 3.5)	33.5 (- 0.37)	70.3 (-7.3)	36.7 (+9.2)

Having confirmed that the accuracy of the qNMR method for analyzing alkenes was satisfactory, it was necessary to examine the precision of the technique as expressed by the reproducibility of the experimental results. Hence, five identical 1-hexene dimerization experiments were performed using the complex $W(\text{NDipp})_2\text{Cl}_2(\text{DME})$ (**27**) as the pre-catalyst and 15 eq. EtAlCl_2 as the initiator in NMR tubes and in Schlenks according to the appropriate catalysis protocols. Two characteristic ^1H NMR spectra, one of the catalysis runs before and one after being subject to vacuum, are presented in Figure 6.8.

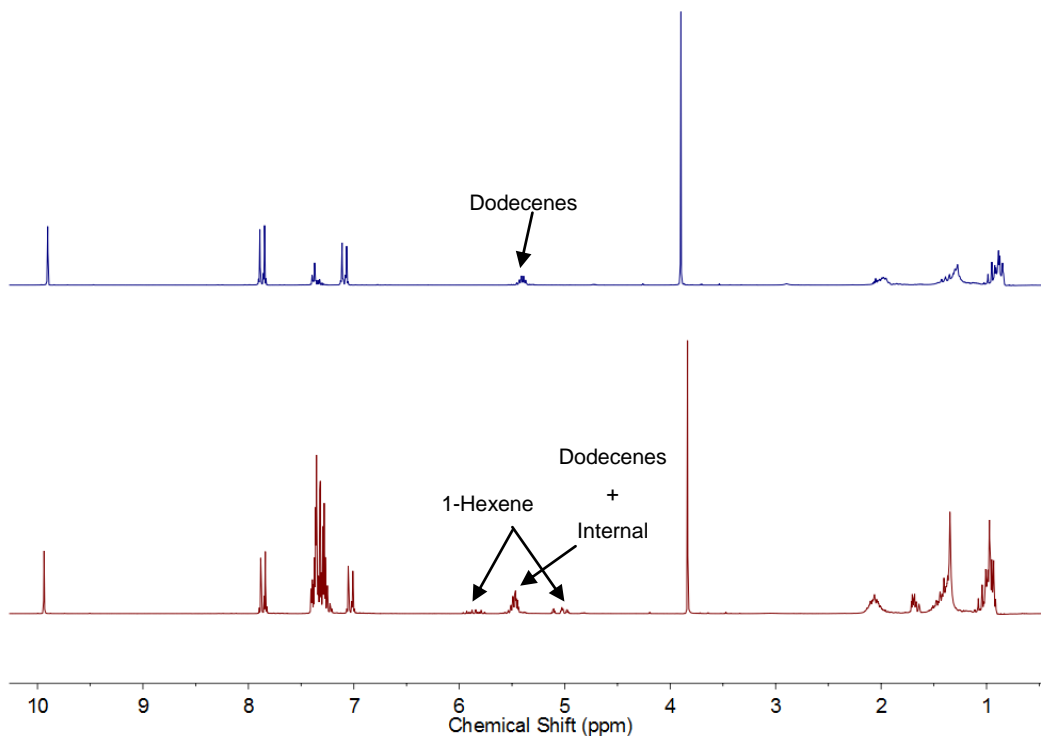


Figure 6.8 ^1H NMR (600 MHz, d_6 -acetone) spectra of a standard 1-hexene dimerization run before (bottom red) and after (top blue) application of vacuum.

In order to assess the amount of 1-hexene evaporated in each run (see section 6.3.2) three blank experiments were performed for both NMR tube and Schlenk methods (Table 6.7). The 1-hexene dimerization products, obtained following tests performed in NMR tubes, were analyzed by qNMR and GC; the products obtained from Schlenk-based tests were analyzed by GC only. The results are summarized in Table 6.8.

Table 6.7 Blank experiments performed to determine the mass of evaporated 1-hexene during a catalytic run.

Run #	NMR Tube		Run #	Schlenk	
	NMR calculation (mg)	GC calculation (mg)		GC calculation at t = 30' (g)	GC calculation at t = 240' (g)
1	153.3	149.5	4	6.78	6.57
2	149.8	137.6	5	7.08	6.70
3	154.2	151.2	6	6.95	6.70
\bar{m}	152.4	144.4	\bar{m}	6.94	6.66
RSD%	1.54	5.13	RSD%	2.17	1.13

Table 6.8 Comparison of analyses of 1-hexene dimerization data from reactions initiated by $W(NDipp)_2Cl_2(DME)$ (**27**) /15 $EtAlCl_2$ performed in NMR tubes and Schlenks.

NMR tube catalysis protocol							Schlenk catalysis protocol			
Run #	Calculation by NMR			Calculation by GC			Run #	Calculation by GC		
	m_{C_6} (mg)	$m_{C_{12}}$ (mg)	Mass balance (mg)	m_{C_6} (mg)	$m_{C_{12}}$ (mg)	Mass balance (mg)		m_{C_6} (g)	$m_{C_{12}}$ (g)	Mass balance (g)
1	69.8	69.6	9.9	61.8	96.1	-17.0	6	3.36	3.44	-0.33
2	69.8	70.0	12.3	63.7	89.6	-9.1	7	3.45	2.95	0.09
3	70.0	68.5	10.7	60.5	88.1	-7.9	8	2.68	2.86	1.12
4	77.9	71.4	-0.5	72.3	83.7	-15.5	9	2.47	4.57	-0.58
5	65.8	80.6	1.9	62.2	94.3	-16.6				
\bar{m}	70.7	72.0	6.9	64.1	90.4	-13.2	\bar{m}	2.99	3.46	0.075
RSD%	6.2	6.8	83.9	7.4	5.5	-33.0	RSD%	16.3	22.7	999
Means conversion%	51.3			59.4			Means conversion%	54.3		

From the RSD% values shown in Table 6.8 it is clear that the use of NMR tubes as the catalytic 1-hexene dimerization reaction vessels provides more precise results compared to the use of Schlenks. Also, it should be noted that the conversions calculated in Table 6.8 don't vary significantly when the catalytic reaction is scaled down for reactions undertaken in NMR tubes instead of Schlenks. Together, these observations further validate the use of NMR-scale reactions as a reliable method for the exploration of the catalytic dimerization of 1-hexene.

The mass balances derived from the GC analyses are always negative due to the lower and higher response of the FID detector towards 1-hexene and dodecenes, respectively, which makes the calculated total mass of products higher than the mass of the initially added hexene even after evaporation is accounted for (from blank experiments). On the other hand, the mass balances calculated *via* qNMR are usually positive or slightly negative implying that some 1-hexene is lost during the reaction, which can be attributed to evaporation or to random experimental errors, especially so when the slightly negative values are obtained. Taking into account the practical difficulties in performing the catalytic experiments in exactly the same way each time, mass balances of between -1 mg and +9 mg from the qNMR analyses are considered reasonable.

Lastly, the use of qNMR for the analysis of the 1-hexene dimerization products can provide some additional information on the alkene double bond environment of the resulting dodecenes. This is demonstrated in the 1H NMR spectrum of a mixture of alkenes with different double bond environments such as those for 1-dodecene (1° terminal α -olefin), 2-methyl-2-butene (3° internal olefin), 2-methyl-1-pentene (2° terminal α -olefin), 2-methyl-3-heptene (2° internal olefin), and *trans*-3-hexene (2° internal olefin) (Figure 6.9).

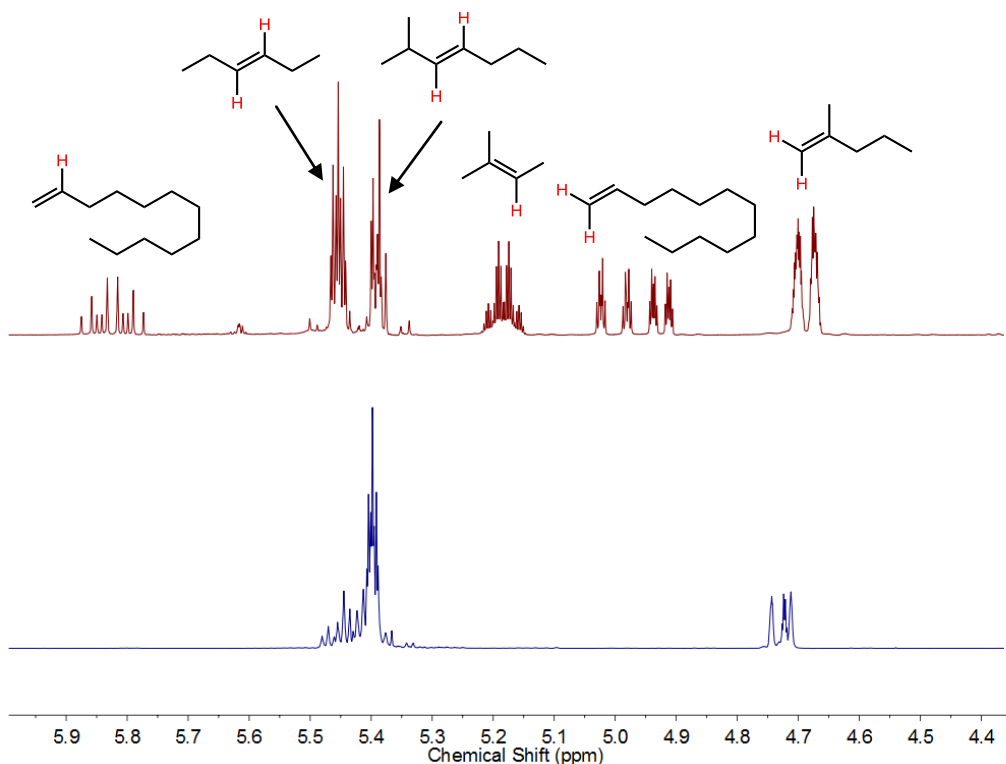


Figure 6.9 ^1H NMR (400 MHz, d_6 -acetone) spectra of a mixture of 1-dodecene, *t*-3-hexene, 2-methyl-3-heptene, 2-methyl-2-butene, and 2-methyl-1-pentene (top, red) and a mixture of dodecenes produced from the catalytic dimerization of 1-hexene over $W(\text{N}^i\text{Bu})_2\text{Cl}_2\text{py}_2$ (**41**)/ 15 EtAlCl_2 (bottom, blue).

From the top red spectrum of Figure 6.9, good separation between the C=C double-bond proton environments is apparent for the specific mixture of alkenes. Unfortunately, the spectrum of an actual mixture of dodecenes produced *via* catalytic dimerization of 1-hexene is more complex, (bottom, blue spectrum in Figure 6.9, especially in the region of 5.5 to 5.3 ppm. Nevertheless, three pieces of important information regarding the product double bond environments can still be obtained. Firstly, 3° internal olefins can be easily detected since they resonate in a region of the spectrum that is devoid of other resonances, which allows differentiation between 3° and 2° internal olefins. Secondly, the detection and quantification of 1-dodecene is easily achieved (resonance at 5.8 ppm). Lastly, the detection and quantification of 2° terminal α -olefins is also easy since they resonate at ~ 4.7 ppm (Figure 6.9). Thus, the bottom blue spectrum of Figure 6.9, it can clearly be concluded that formation of 1-dodecene or dodecenes with a single double bond proton did not occur. On the other hand, a reasonable amount of 2° terminal α -dodecenes are formed (that can be quantified), while the bulk of the sample is most likely to consist of 2° internal dodecenes. Complete assignment of the double bond environments of the olefins obtained from the catalytic dimerization of 1-hexene is difficult, but not impossible. From a qualitative perspective the ^{13}C NMR spectra of these olefinic mixtures can be obtained where the resolution is higher due to the absence of coupling to other nuclei.¹² Alternatively, the ^1H NMR spectra can be proton decoupled increasing their resolution. However, such studies were beyond the scope of this work.

6.4 Appendix IV: crystallographic data

Single-crystal X-ray diffraction experiments were carried out on Bruker 3-circle CCD area detector diffractometers SMART 1000 or SMART 6000, using graphite-monochromated Mo- K_{α} radiation ($\lambda=0.71073$ Å) and Cryostream (Oxford Cryosystems) open-flow N₂ cryostats. The structures were solved by direct methods and refined by full-matrix least squares on F^2 of all data, using SHELXTL 6.12²⁷ and OLEX2 software. Non-hydrogen atoms were refined with anisotropic displacement parameters, H atoms as 'riding' in idealised positions. Full crystallographic data, excluding structure factors, have been deposited at the Cambridge Crystallographic Data Centre.

Compound	Nb(NMes)Cl ₃ (DME)	Nb(NPh)Cl ₃ (DME)	Ta(NPh)Cl ₃ (DME)
Empirical formula	C ₁₃ H ₂₁ NO ₂ Cl ₃ Nb	C ₁₀ H ₁₅ NO ₂ Cl ₃ Nb	C ₁₀ H ₁₅ NO ₂ Cl ₃ Ta
Formula weight	422.57	380.49	468.53
Temperature/K	120(2)	120.15	120(2)
Crystal system	monoclinic	monoclinic	monoclinic
Space group	P2 ₁ /c	P2 ₁ /n	P2 ₁ /c
a/Å	12.0313(4)	8.6294(7)	7.1963(5)
b/Å	12.1595(4)	16.3091(13)	31.241(2)
c/Å	24.7836(10)	10.3060(8)	20.1701(12)
α /°	90.00	90	90
β /°	92.752(8)	90.772(13)	98.719(9)
γ /°	90.00	90	90
Volume/Å ³	3621.5(2)	1450.3(2)	4482.2(5)
Z	8	4	12
ρ_{calc} /mg/mm ³	1.550	1.743	2.083
m/mm ⁻¹	1.107	1.372	7.883
F(000)	1712	760	2664
Crystal size/mm ³	0.18 × 0.16 × 0.13	0.18 × 0.1 × 0.07	0.36 × 0.14 × 0.1
Theta range for data collection	3.3 to 59.98°	4.68 to 59.94°	4.08 to 59.98°
Index ranges	-16 ≤ h ≤ 16, -17 ≤ k ≤ 17, -34 ≤ l ≤ 34	-12 ≤ h ≤ 12, -22 ≤ k ≤ 22, -14 ≤ l ≤ 14	-10 ≤ h ≤ 10, -43 ≤ k ≤ 43, -28 ≤ l ≤ 28
Reflections collected	64159	19342	80871
Independent reflections	10526[R(int) = 0.0649]	4218[R(int) = 0.0889]	13055[R(int) = 0.0747]
Data/restraints/parameters	10526/0/381	4218/0/158	13055/0/472
Goodness-of-fit on F^2	0.994	0.984	1.014
Final R indexes [$I > 2\sigma(I)$]	R ₁ = 0.0307, wR ₂ = 0.0694	R ₁ = 0.0274, wR ₂ = 0.0576	R ₁ = 0.0396, wR ₂ = 0.0845
Final R indexes [all data]	R ₁ = 0.0493, wR ₂ = 0.0742	R ₁ = 0.0414, wR ₂ = 0.0614	R ₁ = 0.0557, wR ₂ = 0.0899
Largest diff. peak/hole / e Å ⁻³	0.749/-0.336	0.580/-0.712	4.323/-1.762

Compound	Ta(NMes)Cl ₃ (DME)	Ta(N ⁱ Bu)Cl ₃ (DME)	[W(NDipp)Cl ₄] ₂
Empirical formula	C ₁₃ H ₂₁ NO ₂ Cl ₃ Ta	C ₈ H ₁₉ Cl ₃ NO ₂ Ta	C ₂₄ H ₃₄ N ₂ Cl ₈ W ₂
Formula weight	510.61	448.54	1001.83
Temperature/K	120(2)	120	120
Crystal system	tetragonal	monoclinic	triclinic
Space group	P4 ₃	P2 ₁ /n	P-1
a/Å	12.7504(12)	6.6997(3)	9.6082(6)
b/Å	12.7504(12)	18.3393(10)	9.7882(7)
c/Å	11.0324(11)	11.9461(6)	10.2905(6)
α/°	90	90	106.301(8)
β/°	90	90.968(7)	106.481(8)
γ/°	90	90	110.355(8)
Volume/Å ³	1793.6(3)	1467.58(13)	788.82(9)
Z	4	4	1
ρ _{calc} /mg/mm ³	1.891	2.03	2.109
m/mm ⁻¹	6.575	8.019	7.982
F(000)	984	856	476
Crystal size/mm ³	0.35 × 0.05 × 0.05	0.32 × 0.15 × 0.12	0.26 × 0.17 × 0.14
Theta range for data collection	3.2 to 59.98°	4.07 to 69.982°	4.56 to 69.96°
Index ranges	-17 ≤ h ≤ 17, -17 ≤ k ≤ 17, -15 ≤ l ≤ 15	-10 ≤ h ≤ 10, -28 ≤ k ≤ 28, -18 ≤ l ≤ 18	-15 ≤ h ≤ 14, -15 ≤ k ≤ 15, -16 ≤ l ≤ 16
Reflections collected	32645	33807	22919
Independent reflections	5216[R(int) = 0.0469]	6276[R(int) = 0.0348]	6611[R(int) = 0.0265]
Data/restraints/parameters	5216/1/191	6276/0/146	6611/0/167
Goodness-of-fit on F ²	1.07	1.091	1.239
Final R indexes [I > 2σ (I)]	R ₁ = 0.0239, wR ₂ = 0.0521	R ₁ = 0.0289, wR ₂ = 0.0597	R ₁ = 0.0246, wR ₂ = 0.0633
Final R indexes [all data]	R ₁ = 0.0282, wR ₂ = 0.0536	R ₁ = 0.0374, wR ₂ = 0.0626	R ₁ = 0.0269, wR ₂ = 0.0638
Largest diff. peak/hole / e Å ⁻³	1.948/-0.833	4.12/-1.53	1.46/-1.85

Compound	[W(NTfp)Cl ₄] ₂	W(NDipp)Me ₃ Cl·AlCl ₃	[W(NDipp)Cl ₅][Et ₃ NH]
Empirical formula	C ₁₃ H ₁₀ Cl ₄ F ₃ NW	C ₁₅ H ₂₆ AlCl ₄ NW	C ₂₄ H ₃₈ Cl ₅ N ₂ W
Formula weight	562.87	573	716.67
Temperature/K	120	120	120
Crystal system	triclinic	monoclinic	monoclinic
Space group	P-1	P2 ₁ /c	P2 ₁ /c
a/Å	7.1984(5)	10.0824(5)	13.0112(14)
b/Å	9.6255(6)	16.3429(10)	11.7214(13)
c/Å	12.8058(8)	13.3029(7)	19.807(2)
α/°	68.524(16)	90	90
β/°	86.291(18)	96.616(6)	97.5712(10)
γ/°	81.137(18)	90	90
Volume/Å ³	815.80(13)	2177.4(2)	2994.4(6)
Z	2	4	4
ρ _{calc} /mg/mm ³	2.291	1.748	1.59
m/mm ⁻¹	7.757	5.833	4.319
F(000)	528	1112	1424
Crystal size/mm ³	0.243 × 0.215 × 0.048	0.36 × 0.33 × 0.25	0.1953 × 0.1673 × 0.07
Theta range for data collection	5.728 to 71.136°	3.964 to 69.964°	5.3 to 64.48°
Index ranges	-11 ≤ h ≤ 11, -15 ≤ k ≤ 14, -20 ≤ l ≤ 20	-16 ≤ h ≤ 15, -25 ≤ k ≤ 25, -21 ≤ l ≤ 20	-19 ≤ h ≤ 19, -16 ≤ k ≤ 17, -29 ≤ l ≤ 28
Reflections collected	16041	50007	47094
Independent reflections	6780[R(int) = 0.0314]	= 9270[R(int) = 0.0224]	9904[R(int) = 0.0451]
Data/restraints/parameters	6780/0/200	9270/0/212	9904/0/303
Goodness-of-fit on F ²	1.051	1.032	1.057
Final R indexes [I > 2σ (I)]	R ₁ = 0.0240, wR ₂ = 0.0560	R ₁ = 0.0161, wR ₂ = 0.0341	R ₁ = 0.0247, wR ₂ = 0.0435
Final R indexes [all data]	R ₁ = 0.0286, wR ₂ = 0.0580	R ₁ = 0.0198, wR ₂ = 0.0350	R ₁ = 0.0341, wR ₂ = 0.0466
Largest diff. peak/hole / e Å ⁻³	1.90/-1.75	1.50/-0.70	0.70/-0.75

Compound	W(NPfp) ₂ Cl ₂ (DME)	W(NMes ^F) ₂ Cl ₂ (DME)	W(N ⁱ Pr)(NDipp)Cl ₂ (DME)
Empirical formula	C ₁₆ H ₁₀ N ₂ O ₂ F ₁₀ Cl ₂ W	C ₂₂ H ₁₄ Cl ₂ F ₁₈ N ₂ O ₂ W	C ₁₉ H ₃₄ N ₂ O ₂ Cl ₂ W
Formula weight	707.01	935.1	577.23
Temperature/K	120	120	120(2)
Crystal system	triclinic	monoclinic	monoclinic
Space group	P-1	P2 ₁ /c	P2 ₁ /n
a/Å	7.3379(3)	12.5254(6)	13.4052(6)
b/Å	7.8387(4)	27.3985(15)	9.8029(6)
c/Å	17.8616(8)	9.0867(5)	18.7197(9)
α/°	87.953(7)	90	90
β/°	81.828(7)	105.516(5)	109.016(8)
γ/°	87.079(7)	90	90
Volume/Å ³	1015.22(8)	3004.7(3)	2325.7(2)
Z	2	4	4
ρ _{calc} /mg/mm ³	2.313	2.067	1.649
m/mm ⁻¹	6.061	4.16	5.211
F(000)	668	1784	1144
Crystal size/mm ³	0.11 × 0.1 × 0.1	0.24 × 0.22 × 0.21	0.33 × 0.2 × 0.15
Theta range for data collection	2.3 to 69.92°	2.972 to 66.25°	4.6 to 60°
Index ranges	-11 ≤ h ≤ 11, -12 ≤ k ≤ 12, -28 ≤ l ≤ 28	-18 ≤ h ≤ 18, -42 ≤ k ≤ 40, -13 ≤ l ≤ 13	-18 ≤ h ≤ 18, -13 ≤ k ≤ 13, -26 ≤ l ≤ 26
Reflections collected	23707	56012	42406
Independent reflections	8443[R(int) = 0.0233]	10835[R(int) = 0.0293]	6782[R(int) = 0.0345]
Data/restraints/parameters	8443/0/302	10835/51/475	6782/0/251
Goodness-of-fit on F ²	1.035	1.121	1.092
Final R indexes [I > 2σ (I)]	R1 = 0.0200, wR2 = 0.0450	R1 = 0.0228, wR2 = 0.0479	R1 = 0.0250, wR2 = 0.0550
Final R indexes [all data]	R1 = 0.0247, wR2 = 0.0464	R1 = 0.0265, wR2 = 0.0490	R1 = 0.0301, wR2 = 0.0574
Largest diff. peak/hole / e Å ⁻³	1.29/-1.18	1.06/-0.66	3.532/-1.106

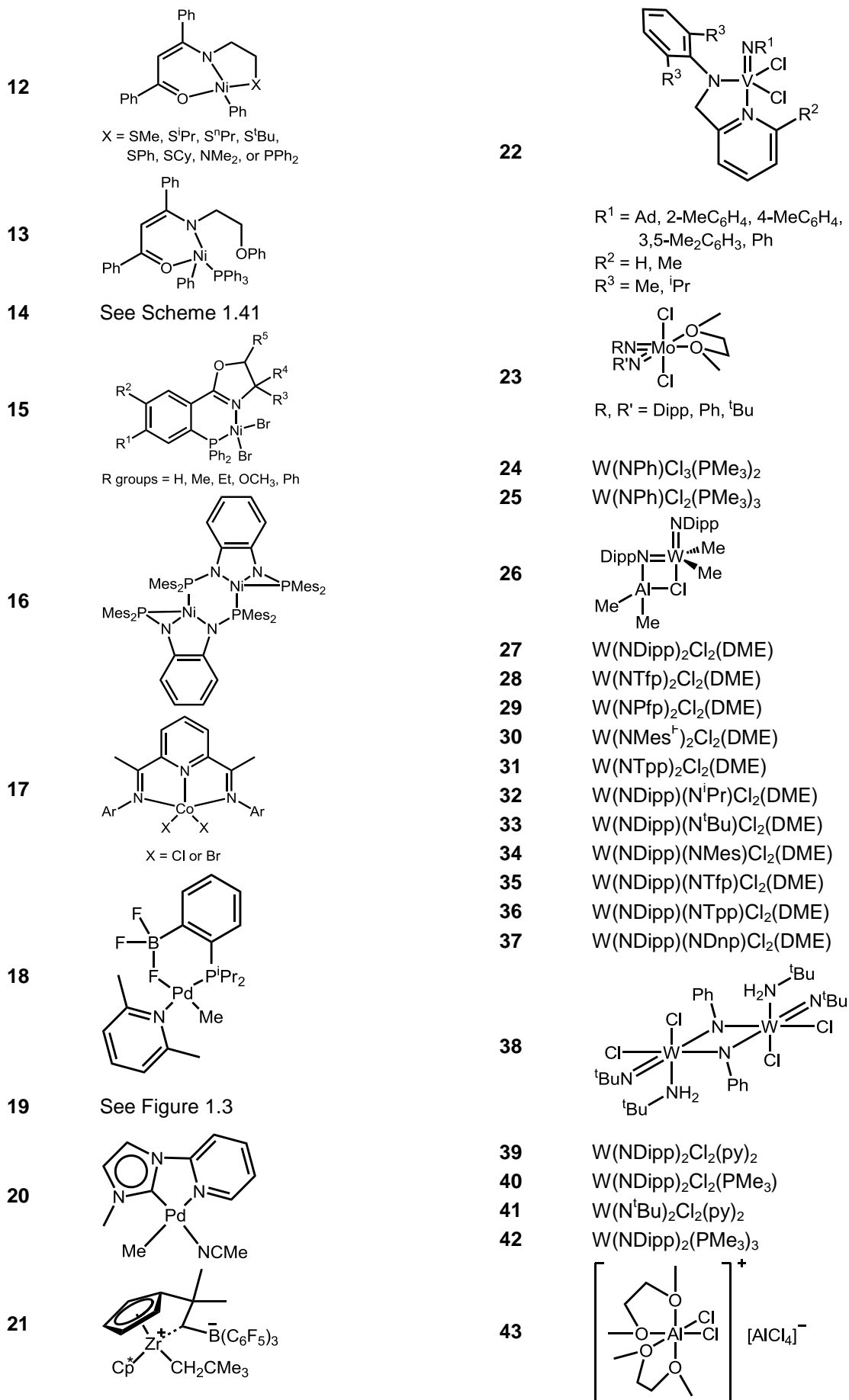
Compound	W(N ^t Bu)(NDipp)Cl ₂ (DME)	W(NMes)(NDipp)Cl ₂ (DME)	W(NTfp)(NDipp)Cl ₂ (DME)
Empirical formula	C ₂₀ H ₃₆ N ₂ O ₂ Cl ₂ W	C ₂₅ H ₃₈ N ₂ O ₂ Cl ₂ W ^{1/4} CH ₂ Cl ₂ 3/8 C ₆ H ₁₄	C ₂₂ H ₂₉ N ₂ O ₂ F ₃ Cl ₂ W
Formula weight	591.26	706.87	665.22
Temperature/K	120(2)	120(2)	120(2)
Crystal system	triclinic	triclinic	triclinic
Space group	P-1	P-1	P-1
a/Å	9.8343(6)	9.0974(5)	8.8303(5)
b/Å	9.9604(6)	12.8175(8)	11.5526(6)
c/Å	13.7645(8)	14.1008(10)	12.8453(7)
α/°	70.528(8)	112.357(9)	77.061(6)
β/°	85.509(8)	90.965(9)	85.454(6)
γ/°	71.846(8)	99.035(9)	74.916(6)
Volume/Å ³	1207.40(13)	1496.49(16)	1232.81(12)
Z	2	2	2
ρ _{calc} /mg/mm ³	1.626	1.569	1.792
m/mm ⁻¹	5.021	4.109	4.946
F(000)	588	711	652
Crystal size/mm ³	0.19 × 0.18 × 0.09	0.18 × 0.15 × 0.05	0.14 × 0.11 × 0.05
Theta range for data collection	3.14 to 60°	3.14 to 60°	3.26 to 69.98°
Index ranges	-13 ≤ h ≤ 13, -14 ≤ k ≤ 14, - 19 ≤ l ≤ 19	-12 ≤ h ≤ 12, -18 ≤ k ≤ 18, - 19 ≤ l ≤ 19	-14 ≤ h ≤ 14, -18 ≤ k ≤ 18, -20 ≤ l ≤ 20
Reflections collected	21874	27439	28833
Independent reflections	7040[R(int) = 0.0362]	8717[R(int) = 0.0344]	10307[R(int) = 0.0286]
Data/restraints/parameters	7040/0/265	8717/0/351	10307/0/301
Goodness-of-fit on F ²	1.03	1.047	1.017
Final R indexes [$I > 2\sigma(I)$]	R ₁ = 0.0258, wR ₂ = 0.0651	R ₁ = 0.0248, wR ₂ = 0.0576	R ₁ = 0.0229, wR ₂ = 0.0468
Final R indexes [all data]	R ₁ = 0.0297, wR ₂ = 0.0678	R ₁ = 0.0300, wR ₂ = 0.0595	R ₁ = 0.0295, wR ₂ = 0.0487
Largest diff. peak/hole / e Å ⁻³	2.192/-1.686	2.693/-1.111	2.342/-1.064

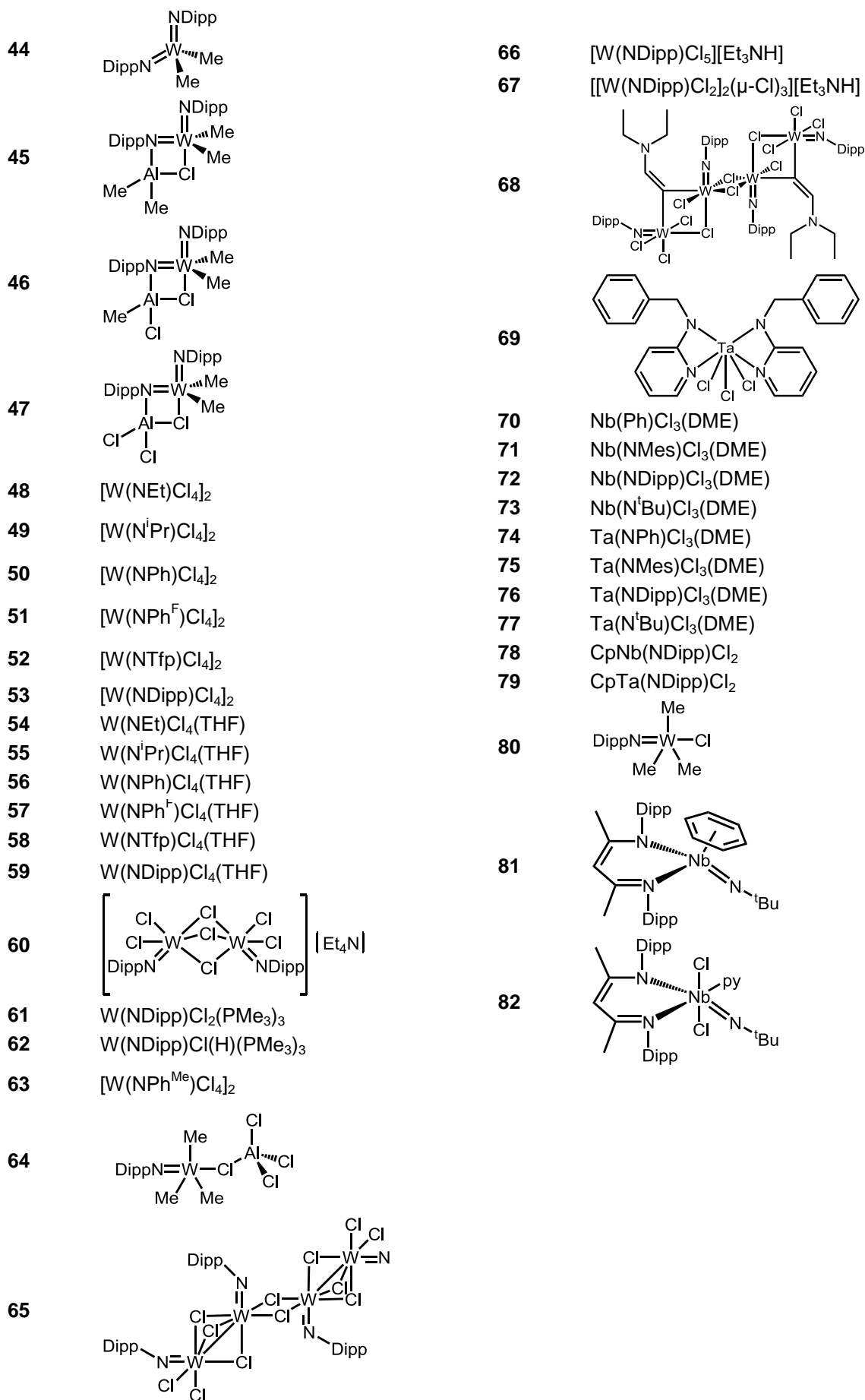
Compound	W(NTpp)(NDipp)Cl ₂ (DME)	W(NDnp)(NDipp)Cl ₂ (DME)	W(NTfp) ₂ Cl ₂ (DME)
Empirical formula	C ₄₀ H ₄₄ Cl ₂ N ₂ O ₂ W	C ₂₃ H ₃₂ Cl ₄ N ₄ O ₆ W	C ₁₆ H ₁₄ ClF ₆ N ₂ O ₂ W
Formula weight	839.52	786.18	599.59
Temperature/K	120(2)	120(2)	120(2)
Crystal system	monoclinic	orthorhombic	orthorhombic
Space group	P2 ₁ /n	Pca2 ₁	P2 ₁ 2 ₁ 2 ₁
a/Å	16.2309(9)	16.4344(6)	12.0005(5)
b/Å	10.3469(7)	10.2454(3)	12.4893(5)
c/Å	22.3012(13)	17.7291(7)	13.5857(6)
α/°	90	90	90
β/°	103.618(11)	90	90
γ/°	90	90	90
Volume/Å ³	3640.0(4)	2985.17(18)	2036.20(15)
Z	4	4	4
ρ _{calc} /mg/mm ³	1.532	1.749	1.956
m/mm ⁻¹	3.357	4.27	5.871
F(000)	1688	1552	1140
Crystal size/mm ³	0.13 × 0.07 × 0.05	0.25 × 0.22 × 0.04	0.22 × 0.15 × 0.13
Theta range for data collection	2.82 to 65°	3.98 to 59.98°	4.43 to 55.07°
Index ranges	-24 ≤ h ≤ 24, -15 ≤ k ≤ 15, -33 ≤ l ≤ 33	-23 ≤ h ≤ 23, -14 ≤ k ≤ 14, -24 ≤ l ≤ 24	0 ≤ h ≤ 15, 0 ≤ k ≤ 16, 0 ≤ l ≤ 17
Reflections collected	85660	52310	4711
Independent reflections	13177[R(int) = 0.0737]	8673[R(int) = 0.0465]	4711[R(int) = ?]
Data/restraints/parameters	13177/0/430	8673/1/355	4711/21/260
Goodness-of-fit on F ²	0.913	1.053	1.099
Final R indexes [I>2σ (I)]	R ₁ = 0.0307, wR ₂ = 0.0550	R ₁ = 0.0266, wR ₂ = 0.0581	R ₁ = 0.0513, wR ₂ = 0.1565
Final R indexes [all data]	R ₁ = 0.0578, wR ₂ = 0.0608	R ₁ = 0.0332, wR ₂ = 0.0609	R ₁ = 0.0546, wR ₂ = 0.1646
Largest diff. peak/hole / e Å ⁻³	1.58/-1.28	3.73/-1.22	2.98/-1.18

Compound	W(NTpp) ₂ Cl ₂ (DME)	W(NDipp) ₂ Cl ₂ (PMe ₃)	W(NDipp) ₂ Cl ₂ (py) ₂
Empirical formula	C ₅₂ H ₄₄ Cl ₂ N ₂ O ₂ W	C ₂₇ H ₄₃ Cl ₂ N ₂ PW	C ₃₄ H ₄₄ Cl ₂ N ₄ W
Formula weight	983.64	681.35	763.48
Temperature/K	120(2)	120(2)	120(2)
Crystal system	trigonal	orthorhombic	orthorhombic
Space group	R-3	P2 ₁ 2 ₁ 2 ₁	P2 ₁ 2 ₁ 2 ₁
a/Å	32.8492(7)	10.5486(9)	9.8592(4)
b/Å	32.8492(7)	16.4202(14)	17.5673(6)
c/Å	20.7376(4)	17.0860(13)	19.3518(7)
α/°	90	90	90
β/°	90	90	90
γ/°	120	90	90
Volume/Å ³	19379.3(9)	2959.5(4)	3351.7(2)
Z	18	4	4
ρ _{calc} /mg/mm ³	1.517	1.529	1.513
m/mm ⁻¹	2.85	4.155	3.634
F(000)	8892	1368	1536
Crystal size/mm ³	0.16 × 0.09 × 0.07	0.4 × 0.08 × 0.07	0.2 × 0.09 × 0.01
Theta range for data collection	2.43 to 55.01°	3.44 to 69.98°	3.132 to 54.974°
Index ranges	-42 ≤ h ≤ 42, -42 ≤ k ≤ 42, -26 ≤ l ≤ 26	-16 ≤ h ≤ 16, -25 ≤ k ≤ 25, -27 ≤ l ≤ 27	-9 ≤ h ≤ 12, -22 ≤ k ≤ 22, -24 ≤ l ≤ 25
Reflections collected	80646	68981	26858
Independent reflections	9910[R(int) = 0.0958]	12654[R(int) = 0.0516]	7675[R(int) = 0.0888]
Data/restraints/parameters	9910/34/438	12654/0/320	7675/0/383
Goodness-of-fit on F ²	1.145	1.093	0.963
Final R indexes [<i>I</i> > 2σ (<i>I</i>)]	R ₁ = 0.0469, wR ₂ = 0.1006	R ₁ = 0.0334, wR ₂ = 0.0712	R ₁ = 0.0351, wR ₂ = 0.0681
Final R indexes [all data]	R ₁ = 0.0811, wR ₂ = 0.1080	R ₁ = 0.0393, wR ₂ = 0.0731	R ₁ = 0.0450, wR ₂ = 0.0705
Largest diff. peak/hole / e Å ⁻³	1.13/-1.74	4.336/-1.352	1.53/-1.17

6.5 Appendix V: numbering scheme for compounds referred to in the text

Compound number	Compound formula
1	
2	 Z = NH, O, S R ¹ , R ² = Me, H, Ph, ^t Bu
3	 R ¹ , R ² = Me, H, Ph, ^t Bu
4	
5	
6	 R = ⁿ Bu or H R' = H, Me, or Ph
7	 R, R ¹ , R ² = H, Me, Et, ⁱ Pr, CHPh ₂ M = Ni, Co, Fe
8	 R, R ¹ , R ² = H, Me, Et, ⁱ Pr, CHPh ₂
9	 Z = S or O R = Me, Et or ⁱ Pr X = Cl or Br
10	 R, R ¹ = Me, Et, ⁱ Pr M = Ni, Co, Fe
11	See Scheme 1.38





6.6 References

- (1) Kozuch, S.; Martin, J. M. L. *Acs Catal* **2012**, *2*, 2787.
- (2) Kuzmenko, T. E.; Samusenko, A. L.; Uralets, V. P.; Golovnya, R. V. *Journal of High Resolution Chromatography* **1979**, *2*, 43.
- (3) Bressolle, F.; BrometPetit, M.; Audran, M. *J. Chromatogr. B-Biomed. Appl.* **1996**, *686*, 3.
- (4) Hanton, M. J.; Daubney, L.; Lebl, T.; Polas, S.; Smith, D. M.; Willemse, A. *Dalton Trans* **2010**, *39*, 7025.
- (5) Dietz, W. A. *Journal of Gas Chromatography* **1967**, *5*, 68.
- (6) Huang, Y. R.; Ou, Q. Y.; Yu, W. L. *Analytical Chemistry* **1990**, *62*, 2063.
- (7) Tong, H. Y.; Karasek, F. W. *Analytical Chemistry* **1984**, *56*, 2124.
- (8) Harvey, D. *Modern Analytical Chemistry*; 1st ed.; McGraw-Hill, 2000.
- (9) Pontes, H.; Guedes de Pinho, P.; Casal, S.; Carmo, H.; Santos, A.; Magalhães, T.; Remião, F.; Carvalho, F.; Bastos, M. L. *Journal of Chromatographic Science* **2009**, *47*, 272.
- (10) Menapace, H. R.; Maly, N. A.; Wang, J. L.; Wideman, L. G. *Journal of Organic Chemistry* **1975**, *40*, 2983.
- (11) Pauli, G. F.; Jaki, B. U.; Lankin, D. C. *J Nat Prod* **2005**, *68*, 133.
- (12) Aguilar, J. A.; Nilsson, M.; Morris, G. A. *Angewandte Chemie-International Edition* **2011**, *50*, 9716.
- (13) Murtuza, S.; Harkins, S. B.; Long, G. S.; Sen, A. *Journal of the American Chemical Society* **2000**, *122*, 1867.
- (14) Petrakis, L.; Dickson, F. E. *Applied Spectroscopy Reviews* **1970**, *4*, 1.
- (15) Greenwood, N. N.; Earnshaw, A. *Chemistry of the elements*; 2nd ed.; Butterworth Heinemann, 1997.
- (16) Benn, R.; Janssen, E.; Lehmkuhl, H.; Rufinska, A. *Journal of Organometallic Chemistry* **1987**, *333*, 155.
- (17) Ramey, K. C.; O'Brien, J. F.; Hasegawa, I.; Borchert, A. E. *The Journal of Physical Chemistry* **1965**, *69*, 3418.
- (18) Balaban, R. S.; Knepper, M. A. *Am. J. Physiol.* **1983**, *245*, C439.
- (19) Bream, R. N.; Hulcoop, D. G.; Gooding, S. J.; Watson, S. A.; Blore, C. *Organic Process Research & Development* **2012**, *16*, 2043.
- (20) Bryliakov, K. P.; Babushkin, D. E.; Talsi, E. P.; Voskoboynikov, A. Z.; Gritzo, H.; Schröder, L.; Damrau, H.-R. H.; Wieser, U.; Schaper, F.; Brintzinger, H. H. *Organometallics* **2005**, *24*, 894.
- (21) Bury, W.; Chwojnowska, E.; Justyniak, I.; Lewinski, J.; Affek, A.; Zygadlo-Monikowska, E.; Bak, J.; Florjanczyk, Z. *Inorganic Chemistry* **2012**, *51*, 737.
- (22) Jegier, J. A.; Atwood, D. A. *Inorganic Chemistry* **1997**, *36*, 2034
- (23) Means, N. C.; Means, C. M.; Bott, S. G.; Atwood, J. L. *Inorganic Chemistry* **1987**, *26*, 1466.
- (24) Pour, N.; Gofer, Y.; Major, D. T.; Aurbach, D. *Journal of the American Chemical Society* **2011**, *133*, 6270
- (25) Atwood, J. L.; Stucky, G. D. *Journal of the American Chemical Society* **1967**, *89*, 5362.
- (26) Zhang, J.; Huang, C.; Chen, B.; Ren, P.; Pu, M. *Journal of Catalysis* **2007**, *249*, 261